

## Flow Rates of Polymer Solutions through Porous Disks as a Function of Solute. I. Method

FRED W. ROWLAND\* and FREDERICK R. EIRICH, *Polytechnic Institute of Brooklyn, Brooklyn, New York*

### Synopsis

A method for studying the thickness of adsorbed polymer films, based on the reduction in effective cross section for liquid flow caused by the deposition of such a film on the interior of a capillary, is described. A sintered disk is used instead of a single capillary to raise the flow rate to an easily measured level, to avoid the difficulties of obtaining or fabricating the extremely fine capillaries which would be required, and to eliminate the extreme precautions needed to prevent plugging of a single capillary. Techniques for characterizing the sintered disks are presented. When applied to benzene solutions of stearic acid and of polystyrene, film thicknesses of 30 and 312 Å., respectively, were obtained. This is in good agreement with present knowledge of fatty acid adsorption, and suggests that the polymer is adsorbed in a highly extended configuration. The application of this method to solutions of poly(vinyl acetate), poly(methyl methacrylate), and polystyrene in several solvents at various temperatures is described in a following paper.

For a Newtonian liquid flowing through a capillary of a length sufficient that end effects may be neglected, the product of flow rate times viscosity is proportional to the fourth power of the capillary radius. Deviations occur at large Reynolds numbers when turbulence sets in and, in some cases, when a very narrow capillary is used. An apparent slowing down of flow has been observed repeatedly with solutions of high polymers and has been attributed to macromolecular adsorption on the capillary walls which decreases the effective cross section for flow.<sup>1-3</sup> On this basis, estimates of the thickness of the adsorbed layers have been made for a number of polymer-solvent systems, but a technique suitable to the systematic study of the adsorbed material has never been developed. In this paper such a technique is described, and its application to several vinyl polymer solutions will be given in a following paper.<sup>4</sup>

### THEORETICAL

The rate of flow of liquids in capillaries of the fineness required to observe the effects of adsorbed layers is extremely small and difficult to measure, nor are such capillaries readily obtained or easily prepared. Still more im-

\* Present address: Carothers Research Laboratory, E. I. du Pont de Nemours and Company, Inc., Wilmington, Delaware.

portant, one will wish to compare the thickness of the adsorbed layers with the amounts adsorbed, so that adsorption isotherms are needed whose determination is simplified by using large surface areas. For these reasons a packed column of the adsorbent, rather than a single capillary, was used. The geometry of the system was fixed by using columns in which the adsorbent particles were bonded to one another, i.e., sintered glass filter disks.

The flow rate of a polymer solution through such a disk which is in adsorption equilibrium with the solution is less than that of the solvent through the clean disk, but the difference is considerably greater than can be accounted for by the viscosity difference alone. If one assumes that the discrepancy is due to a reduction in the average conduit radius by adsorbed polymer, one may write from Poiseuille's law

$$\eta_{rel}(f/f_0) = \|r - \Delta r\|^4 / \|r\|^4 \quad (1)$$

where  $\eta_{rel}$  is the viscosity of the solution divided by that of the solvent,  $f$  and  $f_0$  are the flow rates (at the same pressure differential) of the solution and the solvent, respectively,  $r$  is the conduit radius, and  $\Delta r$  is the effective thickness of the adsorbed layer. The symbol  $\|r\|$  refers to the root-mean-fourth average appropriate in this case and is defined as

$$\|r\| = \left( \frac{1}{N} \sum_1^N r_i^4 \right)^{1/4} \quad (2)$$

where  $N$  is the number of conduits. If the flow rate increases linearly with pressure, the ratio  $f/f_0$  may be replaced by the more easily measured  $m/m_0$ , where  $m$  and  $m_0$  are the slopes of flow rate versus pressure curves for the solution and the solvent, respectively.

Expanding eq. (1) and making the substitution

$$X = \Delta r / \|r\|$$

we find

$$\eta_{rel} \left( \frac{m}{m_0} \right) = 1 - 4X \left[ \frac{\langle r^3 \rangle}{\|r\|^3} - \frac{3}{2} \frac{\langle r^2 \rangle}{\|r\|^2} X + \frac{\langle r \rangle}{\|r\|} X^2 - \frac{1}{4} X^3 \right] \quad (3)$$

where

$$\langle r^n \rangle = \frac{1}{N} \sum_1^N r_i^n = \frac{1}{N} \int_0^{r_{max}} r^n f(r) dr \quad (4)$$

The quantities  $\langle r^n \rangle / \|r\|^n$  may be evaluated if  $f(r)$ , the conduit size distribution, is known. In the study reported here it was found that this had a very sharp cutoff as  $r$  increased, and was well represented by a function of the form.

$$f(r) = N \frac{\exp \{ ar \}}{\exp \{ ar_{max} \} - 1} \quad (5)$$

where  $a = d \log f(r) / dr$  and is obtained graphically.

Using this function the size ratios in eq. (3) may be written

$$\frac{\langle r^n \rangle}{\|r\|^n} = \left( \frac{a}{\exp \{ar_{\max}\} - 1} \right)^{1-n/4} \frac{\int_0^{r_{\max}} r^n \exp \{ar\} dr}{\left( \int_0^{r_{\max}} r^4 \exp \{ar\} dr \right)^{n/4}} \quad (6)$$

These integrations can be performed and the size ratios evaluated.

The function  $f(r)$  cannot be used to obtain  $\|r\|$  since  $N$  is not known, except that its value is very large, therefore an independent measure of  $\|r\|$  is required. In compressible fluid flow through a porous disk a plot of the specific flow rate (in milliliters STP/second/millimeter Hg) against the fluid density yields a straight line<sup>5</sup> whose slope is a function of the thickness, cross-sectional area, and porosity of the disk, the viscosity and temperature of the fluid, and  $\|r\|$ . Since all but the last of these quantities are readily measured,  $\|r\|$  may be determined for each disk and used, together with eq. (3), to obtain the thickness  $\Delta r$  of an adsorbed polymer layer.

## EXPERIMENTAL

### Characterization of Filter Disks

Thicknesses were measured by using a dial indicator with rounded anvil and plunger. Disks showing appreciable nonuniformity were rejected. Since part of the sintered disk is fused while attaching glass connecting tubes, the effective area for fluid flow was obtained by forcing a dye solution through the disk, washing off excess surface dye, drying, and photographing the disk face together with a millimeter scale. The stained area was measured on a planimeter.

An Aminco-Winslow mercury intrusion porosimeter<sup>6,7</sup> was used to obtain  $f(r)$ , the conduit size distribution, as well as the total porosity. These distributions were found to be well represented by an exponential function with a well-defined largest conduit radius,  $r_{\max}$ . Because of this, the size ratios in eq. (6) were within 5% of unity for all disks.

The average conduit radius  $\|r\|$  was obtained by using nitrogen gas as the working fluid. The density was varied by changing the mean pressure (arithmetic average of the supply and receiver pressures) in the measuring system. The nitrogen was supplied from a gas buret attached to a pressure regulator which controlled the admission of mercury to the buret. The receiver was a 10-liter vessel maintained at the desired pressure by an intermittent leak to vacuum. Linear plots of the specific flow rate (volume at STP/time/pressure differential) against mean pressure were obtained, from whose slopes  $\|r\|$  was calculated for each disk.

### Solution and Solvent Viscosities

Ubbelohde suspended-level viscometers were used for all relative viscosity determinations. Instruments giving flow times exceeding 100 sec. were chosen; kinetic energy and shear rate corrections were made when

necessary. The capillaries were sufficiently wide so that the effects of an adsorbed layer were far below the limits of accuracy; this was checked by repeating several measurements in smaller capillaries than those finally selected and obtaining identical results.

### Flow Rates in the Sintered Disks

The quantities  $m$  and  $m_0$  of eq. (3) were obtained with the flow cell shown in Figure 1. This consisted of solution reservoirs I and II so arranged that, by applying nitrogen pressure to one reservoir with the other open to the atmosphere, the solution or solvent could be forced from one to the other. When moving from I to II it passed through the sintered disk, and the trailing meniscus was timed as it moved through the horizontal graduated tube. In the reverse direction a check valve provided for rapid return of the liquid to reservoir I. Liquids were added or removed using a long needle inserted through one of the stopcocks A or B which, like C which was used to remove trapped air, had Teflon plugs to avoid contamination by grease. The entire assembly was thermostatted.

The normal procedure for the determination of  $m$  and  $m_0$  was as follows. Reservoir I was charged with pure solvent and a series of flow times measured at pressure differentials in the range 15–600 mm. Hg. It was experimentally convenient to begin at the lower pressure, and measurements were made at intervals of approximately 50 mm. Hg. Flow rates were plotted against applied gas pressure (because of the geometry of the system no liquid pressure head was involved), and the slope of the resulting straight line was taken as  $m_0$ . The solvent was aspirated from the cell

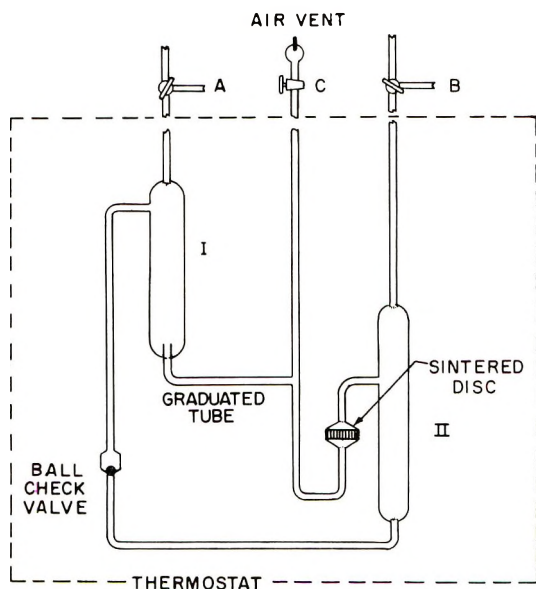


Fig. 1. Porous disk flow apparatus: (I), (II) solution reservoirs; (A), (B) stopcocks with Teflon plugs for sample addition or removal; (C) stopcock for air venting.



with a long needle extending to the bottom of II, and drying was completed with a nitrogen gas stream. The polymer solution was then placed in I and circulated through the disk under a pressure of 10–20 mm. Hg for 3 hr. to achieve adsorption equilibrium. Thorough mixing occurred during the several transfers from II to I required during this period. Flow rates and the value of  $m$  were obtained as described above. After taking a sample of solution to determine the equilibrium concentration, the sintered disk with attached glass tubing was cut out and flushed with hot solvent. It was cleaned with hot nitric acid–sulfuric acid mixture, rinsed thoroughly, and dried. After resealing to the cell a determination of  $m_c$  was made for a sample of benzene which was set aside for this use. If this did not duplicate  $m_0$  as measured with the new disk within 1%, the cleaning procedure was repeated.

### RESULTS AND DISCUSSION

The procedure described above provides a method whereby the thicknesses of adsorbed polymer layers may be studied and compared. This is not an absolute method; however, the results are reproducible from disk to disk and are internally consistent, so that the changes in  $\Delta r$  as a function of molecular weight, polymer composition, solvent, and temperature may be considered significant.

A major cause of the uncertainty as to absolute scaling lies in the nature of  $f(r)$ , the conduit size distribution. The mercury intrusion method measures the volume of nonwetting liquid which is forced into a system of pores against the resistance of surface tension as the applied pressure is increased. What is measured then is not the distribution of the effective conduit radii (in the Poiseuille law sense) in terms of radii as desired, but rather the distribution of effective conduit radii in terms of the cavity volumes to which they provide access. These are not equivalent, but may differ considerably depending on the precise internal geometry of a given sample. Unfortunately, no better method is available, and the utility of a more sophisticated technique is doubtful, since the theoretical treatment of porous solids is still in a state of considerable uncertainty. In the present study the determination of the conduit size distribution has served mainly to ensure that all of the disks had similar geometries, although the details of those geometries were not accessible.

For the same reasons, the disks have been treated in eq. (1) as systems of capillaries adequately described by Poiseuille's law. More elaborate descriptions of the Kozeny<sup>8</sup> or Scheidegger<sup>9</sup> type offer no advantages for the present purpose, since they either involve arbitrary constants or are vague regarding the underlying model. The parallel capillary model offers the important advantages of unambiguous values for the average conduit size and its changes, permitting the ranking of adsorbed film thicknesses though admittedly on an arbitrary scale.

The average conduit radius  $\|r\|$  has been obtained with the use of gas, rather than liquid, flow. This is essentially the extrapolation procedure

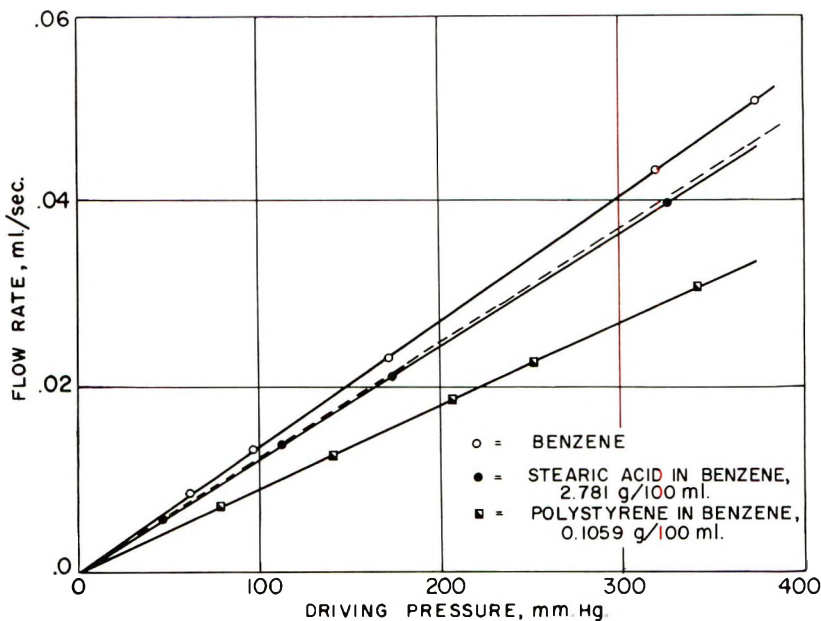


Fig. 2. Flow rate as a function of driving pressure: (O) benzene control; (●) stearic acid in benzene,  $\eta_{rel} = 1.091$ ; (■) polystyrene in benzene,  $\eta_{rel} = 1.092$ ; (- -) solution flow line calculated from the relative viscosity.

of Klinkenberg,<sup>10</sup> who demonstrated that measurements employing a gas may be used to calculate an average conduit size suitable to liquid flow. The equations incorporate a constant which has been evaluated empirically for a wide variety of conduit shapes and sizes.<sup>11</sup>

Turbulent flow within the sintered disks would introduce an element of uncertainty large enough to outweigh the errors from all other sources. This possibility may be ruled out on several counts. First, the curves of fluid flow rate versus applied pressure are quite linear. Second, the actual rate of advance of the fluid front through the disks was obtained by injecting a dye close to the upstream face and measuring the time of its appearance on the opposite side. The Reynolds numbers estimated from these data were of the order of  $10^{-4}$ . Considering the conduits as cavities connected by bottlenecks, as would result from close packing of spheres, one would expect a low critical value for turbulence due to the rapid intermittent widening of the conduits. Thus, presumably, the critical Reynolds number should not be very far from that normally assigned to the motion of spheres, which is approximately unity. Third, by collecting and weighing the effluent during the dye experiment the tortuosity of the conduits within the disk could be calculated. This was approximately 1.6, as compared with a theoretical value for close-packed spheres of 1.4. In view of the compression and sintering which occurs during manufacture this is considered satisfactory agreement. Finally, the viscosities of three solvents, diethyl ether, cyclohexane, and isopropanol, relative to benzene were de-

terminated in Ubbelohde viscometers and from flow rates in the sintered disk cell. These were compared with handbook values and agreed within 4% for diethyl ether and 1% for the other two liquids. This last result also justifies the use of the Ubbelohde viscometer (of sufficiently large capillary size) for the relative viscosity term of eq. (3).

As a final check on the validity and utility of this method, solutions of polystyrene (unfractionated,  $\bar{M}_v$  in toluene 154,000) and of stearic acid in benzene having the same relative viscosities (polystyrene 0.1059 g./100 ml.,  $\eta_{rel} = 1.092$ ; stearic acid 2.781 g./100 ml.,  $\eta_{rel} = 1.091$ ) were prepared and flow rates determined in the same sintered disk, after allowing time for equilibration. The results are shown in Figure 2, where the dashed line indicates the position of the solution curves had they been altered by viscosity alone. It is evident that the flow rate is diminished by the solute to a greater degree than can be accounted for on that basis alone. It is also clear that the nature of the solute is involved, with the polymer having much greater effect than the stearic acid. From the slopes of these curves the adsorbed film thicknesses are calculated to be 30 Å. for stearic acid and 312 Å. for polystyrene. This is quite compatible with our knowledge of fatty acid monolayers and a polymer chain strongly swollen by solvent.

In conclusion, we believe we have shown that a measure of the thickness of adsorbed polymer layers can be obtained from the apparent reduction of conduit size in a filter disk through which the polymer solution flows. The value obtained is the hydrodynamic equivalent of a radius change. It depends upon the validity of the assumptions made in the calculation, such as the applicability of Poiseuille's law, smallness of corrections, appropriate averaging, etc. but even in a single, well-defined capillary  $\Delta r$  must be a function of the extent of adsorption, structure of the adsorbed layer, and of shear rate. Of these, the last does not seem to be operative, since no effect of flow rate on  $\Delta r$  was observed. The extent of adsorption and the structure of the adsorbate do affect  $\Delta r$ , as will be shown in Part II.<sup>4</sup>

Finally, it was found that  $\Delta r$  varied with the nature of the solvent from which the polymer was adsorbed in almost exactly the same way as the polymer coil dimensions varied in solution as a function of the solvent. This indicates that the adsorbed polymer is at least partly pervaded by the solvent, and that  $\Delta r$  might be likened to the change in clearance to liquid flow through a tube caused by the deposition of cilia on the inner wall.

Taken from a dissertation submitted by F. W. R. in partial fulfillment of the requirements for the degree of Doctor of Philosophy (Chemistry) at the Polytechnic Institute of Brooklyn.

Support by the United States Air Force Office of Scientific Research is gratefully acknowledged.

## References

1. O. E. Ohrn, *J. Polymer Sci.*, **17**, 137 (1955).
2. M. Takeda and R. Endo, *J. Phys. Chem.*, **60**, 1202 (1956).
3. C. A. F. Tuijnman and J. J. Hermans, *J. Polymer Sci.*, **25**, 385 (1957).
4. F. W. Rowland and F. R. Eirich, *J. Polymer Sci. A-1*, in press.

5. F. A. Schwertz, *J. Appl. Phys.*, **20**, 1070 (1949).
6. N. Winslow and J. Shapiro, *ASTM Bull.*, No. **236**, 39 (1959).
7. Porosimeter Instruction Manual No. 597, American Instrument Co., Silver Springs, Md., 1960.
8. J. Kozeny, *Sitzber. Wiener Acad., Abt. IIa*, **136**, 271 (1927).
9. A. E. Scheidegger, *Producers Monthly*, **17**, No. 10, 17 (1953).
10. L. J. Klinkenberg, *API Drill. Prod. Pract.*, **1941**, 200.
11. P. C. Carman, *Trans. J. Soc. Chem. Ind.*, **57**, 225 (1938).

### Résumé

Une méthode d'étude de l'épaisseur de films polymériques adsorbés basée sur la réduction de la section transversale effective à l'écoulement liquide causé par la déposition d'un tel film à l'intérieur d'un capillaire est décrite. Un disque en verre fritté est utilisé au lieu d'un simple capillaire pour augmenter la vitesse d'écoulement jusqu'à un niveau facilement mesurable pour éviter les difficultés à obtenir ou fabriquer des capillaires extrêmement fins qui seraient indispensables et en vue d'éliminer les précautions extrêmes nécessaires à prévenir l'obstruction d'un simple capillaire. Les techniques pour caractériser les disques en verre fritté sont présentées. Appliquée à des solutions benzéniques d'acide stéarique et de polystyrène on a déterminé par cette méthode une épaisseur de film de 30 et de 312 Å respectivement. Ceci est en bon accord avec notre connaissance actuelle de l'adsorption des acides gras et suggère que le polymère est adsorbé en une configuration fortement étendue. L'application de cette méthode aux solutions d'acétate de polyvinyle et de polyméthacrylate de méthyle et de polystyrène dans de nombreux solvants à des températures variables est décrite dans le manuscrit suivant.

### Zusammenfassung

Eine Methode zur Untersuchung der Dicke von adsorbierten Polymerfilmen auf Grundlage der Herabsetzung des effektiven Querschnitts für das Fließen von Flüssigkeiten durch die Ablagerung eines solchen Films auf die innere Wand einer Kapillare wird beschrieben. An Stelle einer einzelnen Kapillare wird eine Sinterplatte benutzt, um die Fließgeschwindigkeit auf eine leicht messbare Grösse zu bringen, um die Schwierigkeiten bei der Herstellung der erforderlichen extrem reinen Kapillaren zu vermeiden und um die extremen, zur Vermeidung des Verstopfens einer einfachen Kapillare notwendigen Vorsichtsmaßnahmen auszuschalten. Verfahren zur Charakterisierung der Sinterplatte werden angegeben. Mit Benzollösungen von Stearinsäure und von Polystyrol wurden Filmdicken von 30 bzw. 312 Å erhalten. Dies steht in guter Übereinstimmung mit unsere gegenwärtigen Kenntnis der Adsorption von Fettsäuren und zeigt, dass das Polymere in einer hochgradig gestreckten Konfiguration adsorbiert wird. Die Anwendung der Methode auf Lösungen von Poly(vinylacetat), Poly(methylmethacrylat) und Polystyrol in mehreren Lösungsmitteln bei verschiedenen Temperaturen wird in einer folgenden Arbeit beschrieben.

Received December 16, 1965  
Prod. No. 5031A



## Study of the Mechanism of Formation of Transparent Polyacrylonitrile

N. SHAVIT, A. OPLATKA, and M. LEVY, *Polymer Department,  
The Weizmann Institute of Science, Rehovoth, Israel*

### Synopsis

The kinetics of bulk polymerization of acrylonitrile, leading to a transparent polymer, was studied. The reaction was followed by a dilatometer specially designed for high degrees of conversion and for continuous supply of monomer during the reaction. The last stages of polymerization were followed by density determinations. It was found that the kinetic scheme did not show any irregularities, and that the major condition for obtaining a transparent polymer is a continuous supply of monomer to fill up the gaps formed by the contraction during the polymerization process.

It was discovered lately by Shavit et al.<sup>1-4</sup> that under proper conditions acrylonitrile (AN) can be polymerized to give a transparent, colorless polymer. The polymerization was carried out in bulk, and a large variety of catalysts were used, including the usual radical initiators such as benzoyl peroxide and azobisisobutyronitrile and unconventional systems such as sulfinic acid-hydrogen peroxide and various metal salts. It was observed that in all cases a powdery white polymer precipitated first and at a later stage of the reaction the hard white polymer gradually turned into a transparent body with the exact shape of the reaction flask. In order to elucidate the mechanism of the formation of transparent PAN it was necessary to carry out a detailed kinetic study of the process.

From the finding that various catalysts could yield transparent PAN, it was apparent that transparency was not dependent on the type of initiation but on the conditions of polymerization. We decided therefore to concentrate our studies on a simple and well-investigated initiating system, namely, azobisisobutyronitrile (AZO) under high vacuum conditions. The kinetics of bulk polymerization of AN with such catalysts were thoroughly investigated by Thomas,<sup>5</sup> Bamford,<sup>6</sup> and others. However, most workers were interested in the initial steps of the polymerization and in the radicals occluded in the precipitated polymer. Only a few experiments were carried out at high degrees of conversion. The study of the high conversions is rather difficult, as the resulting solid hard mass is insoluble in most solvents and dissolves only in hot dimethylformamide. Therefore, special techniques had to be applied for high conversion studies.



### Experimental and Results

We started out by repeating some of the experiments which were carried out by Thomas, using exactly the same procedure. AZO catalyst (0.5 g./l.) was introduced into a tube 5 mm. in diameter. After degassing AN was distilled into the tube from another container. The tube was then sealed off *in vacuo* and introduced into a 50°C. constant-temperature bath. Polymerization started immediately, and a hard white, nontransparent solid resulted. Another sample was prepared in exactly the same way but only the lower half of the tube was introduced into the bath, the upper half remaining at room temperature. Polymer began precipitating immediately, and after 1 hr. the lower half solidified to a white mass while the upper part was still mostly liquid monomer. After about 2 hr. the polymer started showing signs of transparency, and in 3 hr. a transparent body was obtained at the lower half, while the top one was still liquid. This experiment verified the conclusion which we derived from our previous experience with different catalysts, that one necessary condition for obtaining transparent PAN is to have a continuous supply of monomer to fill up the gaps formed by the contraction due to the polymerization.

This brought us to the conclusion that in order to study the phenomenon we have to devise a proper method for following the reaction to high degrees of conversion under conditions of continuous monomer supply. For this purpose we built the dilatometer described in Figure 1. The dilatometer

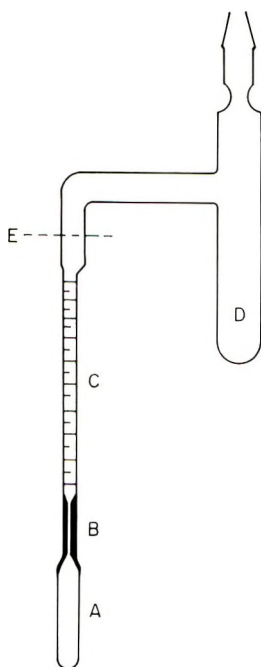


Fig. 1. Schematic diagram of the dilatometer.

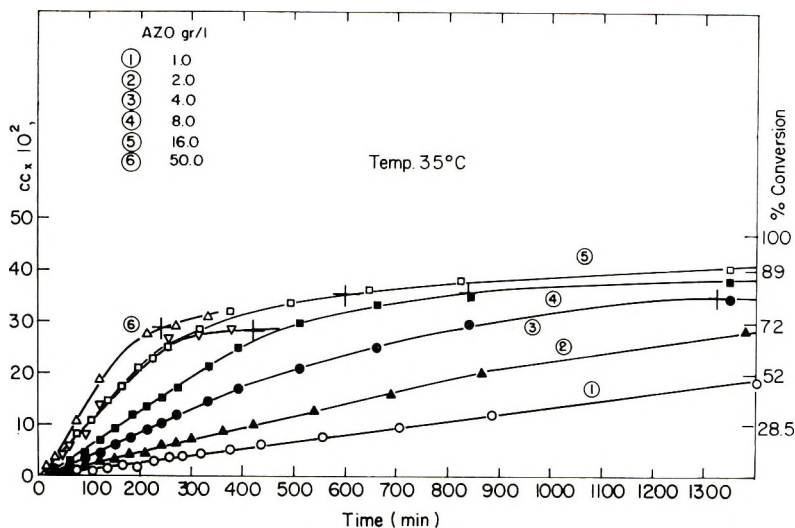


Fig. 2. Volume contraction and per cent conversion vs. time at 35°C.

consists of a small tube A (5 mm. diameter), a capillary B (0.1 mm. diameter, 2 cm. length) and a calibrated tube C. This is sealed onto a tube D equipped with a ground joint and a constriction. The tube D is filled up with monomer containing the required amount of catalyst. It is degassed under high vacuum and the tube is sealed off at the constriction. The whole solution is then poured into the reaction tube. The glass is cut open at the mark E. The reaction tube is heated to the required temperature and the excess solution in the calibrated tube is poured out. The calibrated tube is rinsed carefully with monomer, filled to the upper mark with pure monomer, and sealed with a rubber stopper. The whole dilatometer is placed in a constant-temperature bath, and the level of the monomer in the calibrated tube is read as a function of the time of the reaction. A large contraction takes place as a result of the polymerization, and monomer flows very rapidly through the narrow capillary so that no catalyst can diffuse against the direction of flow into the calibrated tube and no polymerization occurs there. It is assumed that the volume contraction resulting from polymerization sucks in the equivalent volume of the monomer which flows from the calibrated upper tube through the capillary into the reaction tube A. This assumption was checked by carrying out the reaction until the whole reaction tube was filled with transparent PAN. The weight and the specific gravity of the PAN were measured. The per cent polymerization calculated from the specific gravity (as discussed below) agreed with the per cent polymerization calculated from the amount of monomer that flowed in.

The results are presented graphically by plotting  $v$  (the volume contraction divided by the volume of the reaction tube A) versus time. The per cent conversion was calculated by taking the specific gravity of the mon-

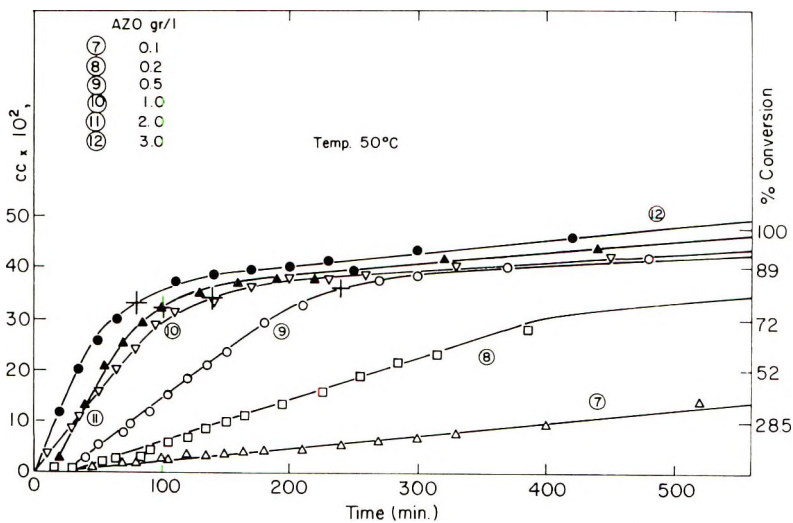


Fig. 3. Volume contraction and per cent conversion vs. time at 50°C.

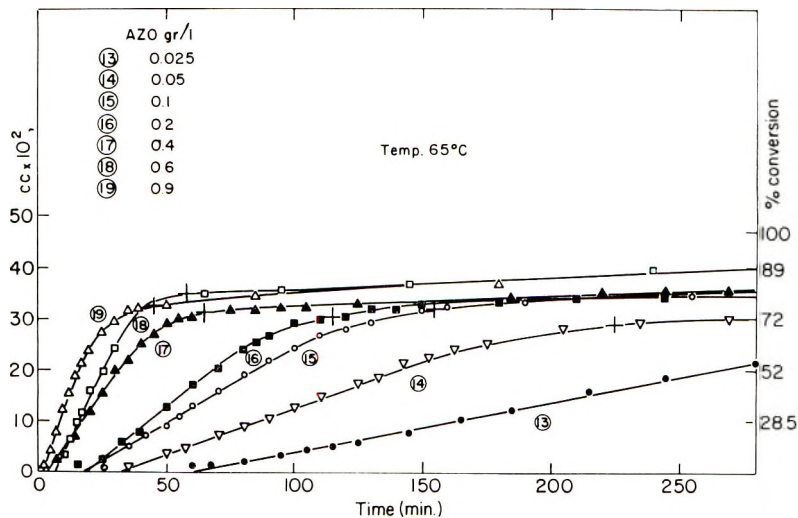


Fig. 4. Volume contraction and per cent conversion vs. time at 65°C.

omer and of the polymer as 0.8 and 1.18 g./cc., respectively. The volume contraction for the polymerization of 1 g. monomer is then  $(1/0.8) - (1/1.18) = 0.4$  cc., and

$$\% \text{ conversion} = \frac{v/0.4}{(1+v)0.8} = \frac{3.1v}{(1+v)}$$

Notice that the per cent conversion calculated in this way takes into consideration the monomer added during the reaction and is thus different from the regular polymerization experiments. Figures 2, 3, and 4 represent

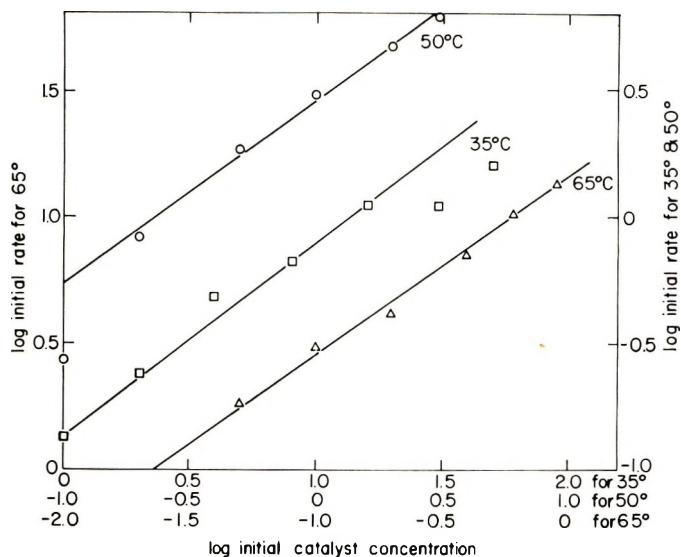


Fig. 5. Log initial rate of polymerization vs. initial catalyst concentration at 35, 50, and 65°C.

the data obtained at 35, 50, and 65°C., respectively. The volume contraction and the per cent conversion are plotted versus time. One can see that in all cases the first part of the curves is almost linear as observed by other workers,\* and then the reaction slows down very sharply.

The initial slopes of these curves give the initial rates of polymerization. The logarithm of these initial rates were plotted in Figure 5 versus the logarithm of initial catalyst concentrations. From this figure we can obtain the reaction order with respect to the catalyst concentration. It was found to be 0.75. The calculated overall activation energy was 36 kcal./mole. Both values are in good agreement with those obtained by Thomas. The times needed for the initial appearance of transparency,  $t_{\text{initial}}$  are marked by crosses on Figures 2-4. The reciprocals of these values are plotted in Figure 6 against the catalyst concentration to power 0.75, giving straight lines. The interpretation of this result could be sought in the fact that transparency appears always between 70 and 80% conversion, and the reaction may be described by the equation

$$n_{M_0} - n_{M_t} = k[M][C]^{0.75}t$$

In this equation  $n_{M_0}$  represents the number of moles of monomer at zero time and  $n_{M_t}$  the number of moles of monomer at time  $t$ . As the polymer precipitates during the polymerization, the monomer concentration  $[M]$  in the liquid phase can be taken as constant, and the catalyst concentration,

\* There is a short autoacceleration period in the very beginning of the reaction. This was not taken into consideration in the evaluation of the initial slopes, and only the linear portion was considered.

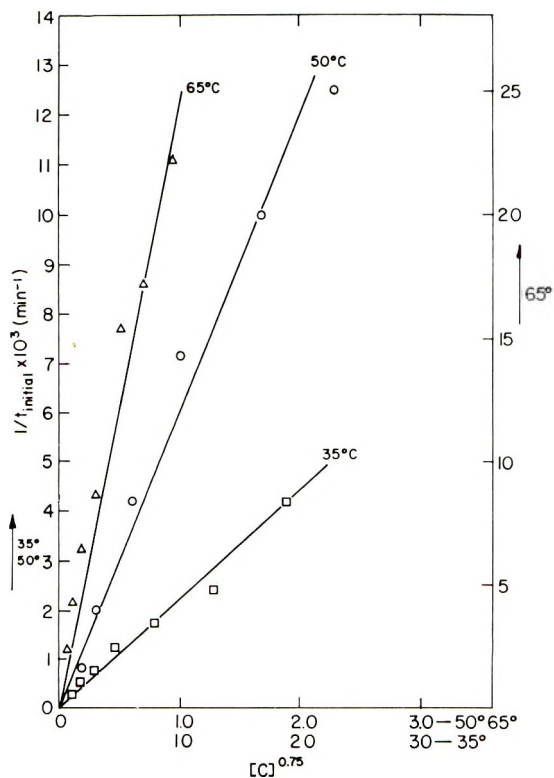


Fig. 6. Plot of the reciprocal of  $t_{\text{initial}}$  (time needed for the initial appearance of transparency) vs.  $[\text{catalyst}]^{0.75}$ .

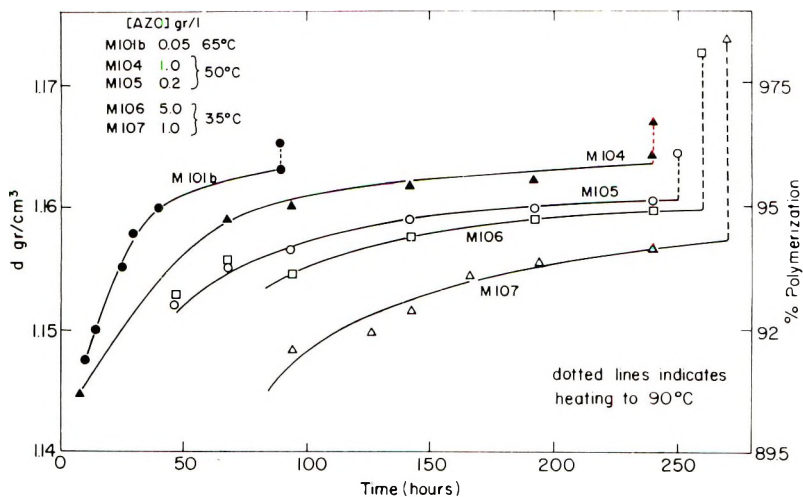


Fig. 7. Density and per cent polymerization vs. time for 35, 50, and 64°C.



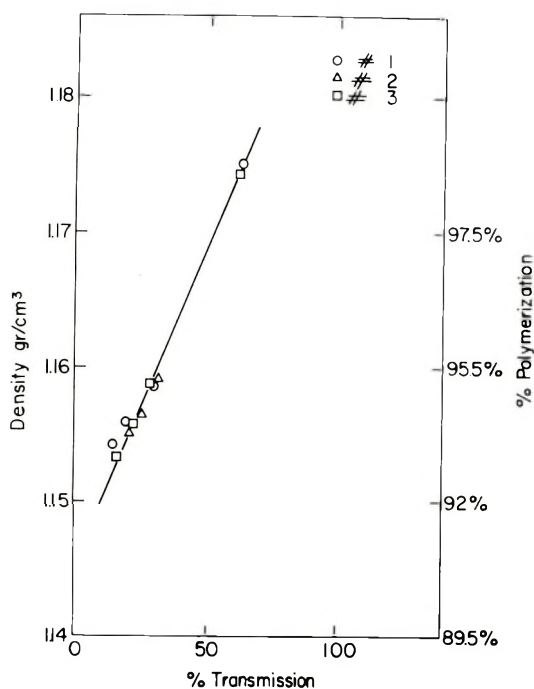


Fig. 8. Density and per cent polymerization vs. per cent transmission of light.

although not constant, could be expected to change in a parallel way in all experiments, and thus the product  $[C]^{0.75}t$  should be constant for a given degree of conversion.

In all our experiments we could observe that transparency always appeared at the bottom of the reaction tube and the transparent zone gradually spread up the tube. At the appearance of transparency the solid body detaches itself from the glass tube, leaving a void into which monomer cannot flow. Therefore, further polymerization is not correctly reflected by the lowering of the meniscus in the calibrated tube, and another method had to be used to follow the reaction at higher degrees of conversion.

It occurred to us that, as there is such a large difference between the densities of the monomer and the polymer, the polymerization at high degrees of conversion could be followed by density measurements. This is possible because the polymer formed is a hard solid with a glassy surface and is almost impermeable to water or other liquids. Assuming that the polymer consists of monomer and polymer only (without voids or air) one could calculate the per cent conversion from the density  $\rho$

$$\% \text{ conversion} = 100 \left( \frac{\rho - 0.8}{1.18 - 0.8} \right) = 100 \left( \frac{\rho - 0.8}{0.38} \right)$$

To check this point all samples were heated, at the end of the experiment, to 90°C. for 1/2 hr. in order to complete the reaction. In most cases the

ห้องสมุด กรมวิทยาศาสตร์

calculated per cent conversion rose to more than 96%; in experiments where polymerization could not be completed by heating, presumably either the catalyst was exhausted or the monomer had evaporated. The results are shown in Figure 7. It can be seen that the polymerization for the last stages is very slow at temperatures of 35–65°C. This is probably due to the fact that the whole body is a solid mass and both monomer flow and contraction due to polymerization has to proceed in the solid phase. When, however, the polymer is heated to 90°C. there is loosening of the structure, and almost complete polymerization proceeds, giving a perfectly transparent body (colored yellow).

Finally, measurements of the light transmission were carried out on transparent samples. The samples were cylindrical, rather than flat, and the measurements were intended for comparison and not as absolute values. It can be seen from Figure 8 that the light transmission increases with increase in density, which means also with increase in per cent conversion. The increase in the degree of transparency with time indicates that the process of formation of a transparent body is a rate process. Due to the difference in index of refraction of monomer and polymer, one would expect the monomer globules dispersed in the polymer phase to scatter light and thus yield a lower degree of transparency. As the polymerization proceeds, the monomer disappears, and the per cent transmission increases accordingly.

### Conclusions

From the above results we conclude that the bulk polymerization process leading to transparent PAN seems to follow a kinetic scheme which does not differ from the polymerization kinetics studied previously. When the polymerization is allowed to proceed to a high conversion and with proper supply of monomer so that no voids are formed, transparency begins to appear. The degree of transparency depends directly on the per cent conversion. The rate of the reaction does not affect the results as long as the reaction tube is of the proper size (to avoid run away). Satisfactory results can be obtained with times as short as 20 min. or as long as a few days, provided the monomer is properly supplied to the polymerizing mixture.

### References

1. N. Shavit, M. Konigsbuch, and A. Oplatka, Israeli Pat. 14,410; Brit. Pat. 964,533; French Pat. 1,398,711; Japan. Pat. 439,511.
2. A. Oplatka, M. Konigsbuch, and N. Shavit, paper presented at International Symposium on Macromolecular Chemistry, Prague, 1965, *Preprints*, p. 333.
3. N. Shavit, M. Konigsbuch, and A. Oplatka, paper presented at International Symposium on Macromolecular Chemistry, Prague 1965, *Preprints*, p. 546.
4. N. Shavit and M. Konigsbuch, paper presented at International Symposium on Macromolecular Chemistry, Prague 1965, *Preprints*, p. 619.
5. W. M. Thomas, *Fortschr. Hochpolymer. Forsch.*, **2**, 401 (1961).
6. C. H. Bamford, *Proc. Roy. Soc. (London)*, **A216**, 515 (1953).

### Résumé

La cinétique de polymérisation en bloc de l'acrylonitrile en vue d'obtenir un polymère transparent a été étudiée. La réaction a été suivie au moyen d'un dilatomètre spécialement construit pour des degrés de conversion élevés et permettant un apport constant en monomère au cours de la réaction. Les dernières étapes de la polymérisation ont été suivies par détermination de la densité. On a trouvé que les schémas cinétiques ne manifestent aucune irrégularité et que la condition principale d'obtention d'un polymère transparent est l'apport continu de monomère de façon à remplir les vides résultant de la contraction en cours de polymérisation.

### Zusammenfassung

Die Kinetik der zu einem transparenten Polymeren führenden Polymerisation von Acrylnitril in Substanz wurde untersucht. Die Reaktion wurde in einem speziell für hohe Umsätze und für kontinuierliche Nachführung des Monomeren während der Reaktion konstruierten Dilatometer verfolgt. Die letzte Polymerisationsphase wurde durch Dichtebestimmungen verfolgt. Das kinetische Schema zeigte keinerlei Unregelmässigkeiten; Hauptbedingung für die Bildung eines transparenten Polymeren ist eine kontinuierliche Nachführung des Monomeren, um den durch Kontraktion während des Polymerisationsprozesses gebildeten Hohlraum aufzufüllen.

Received December 14, 1965

Prod. No. 5037A

## Radiochemical Determination of Low Un saturations in Polyisobutene

R. McGUCHAN and I. C. McNEILL, *Chemistry Department,  
University of Glasgow, Glasgow, Scotland*

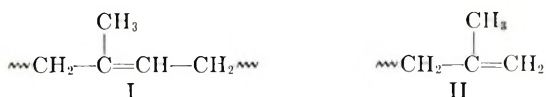
### Synopsis

A radiochemical technique involving the use of  $^{36}\text{Cl}$  has been described previously for the measurement of butyl rubber unsaturations. This method has now been applied to the estimation of the much lower concentration of double bonds present in polyisobutene prepared by the cationic polymerization of isobutene at a low temperature. The nature of the reaction of polyisobutene with radiochlorine in the absence of air is examined, and the experimental results are discussed in relation to present theories of the mechanisms of chain termination in cationic polymerization.

### INTRODUCTION

In polymers which have been prepared by a cationic mechanism, the end-group problem has evoked considerable speculation and discussion, and most mechanistic schemes in the literature stipulate a terminally unsaturated polymer chain. Apart from a few qualitative investigations,<sup>1,2</sup> however, very little work has been done on the nature of the endgroups. In high polymers the very small concentration of endgroups defies normal methods of analysis. Pepper and Reilly<sup>3</sup> have measured terminal unsaturation in polystyrene, but their hydrogenation technique was limited to oligomers which have a relatively high mole per cent unsaturation. The same restriction would apply to the use of conventional techniques<sup>4,5</sup> which have been successfully employed for butyl rubbers having unsaturations in the range 0.5–5.0 mole-%. A radiochemical technique has been described by McNeill,<sup>6</sup> in which butyl rubbers with unsaturations from 0.5 to 2.0 mole-% were reacted with radiochlorine ( $^{36}\text{Cl}$ ). The unsaturation values obtained were in agreement with those found by other procedures. This paper examines the extension of the radiochlorine method to the determination of lower unsaturations, of the order of 0.1–0.01 mole-%, in samples of polyisobutene.

Polyisobutene was selected for this investigation for two reasons. Firstly, the unsaturated centers in polyisobutene should be similar structurally to the double bonds in butyl rubber. This is illustrated by the structure I in butyl rubber and the probable end structure II in polyisobutene (see following page):



The nature of the reaction of olefins with chlorine depends to some extent on the structure of the olefin.<sup>7</sup> Structures I and II both have an allylic methyl group and would be expected to behave similarly with chlorine. Secondly, the polymerization of isobutene by Friedel-Crafts type catalysts, on which a considerable volume of work has already been carried out, can be regarded as a "typical" cationic system. Because of the crowding of the methyl substituents in the chain structure, isobutene polymerizes without the abnormalities of many systems.<sup>8</sup>

## EXPERIMENTAL

### Preparation of Polyisobutene

Isobutene (50 ml., I.C.I. Ltd., Billingham) was distilled from a cylinder into a graduated tube and thence into a 1-liter reaction vessel containing redistilled methylene chloride (450 ml.) and granular calcium chloride (20 g.) at  $-78^\circ\text{C}$ . The purpose of the calcium chloride was to ensure a fairly reproducible water content in the various polymerizations carried out, since water is the cocatalyst under the conditions used. The reaction vessel was equipped with an alcohol thermometer, which read from 20 to  $-120^\circ\text{C}$ ., a stirrer, a drying tube, and a nitrogen inlet by means of which a nitrogen atmosphere was maintained above the solution. Stannic chloride (1 ml., B.D.H. Ltd.) was introduced by use of a microsyringe. As polymerization proceeded, a slow rise in temperature was observed, and a sludge of polymer precipitated out of solution. The polymerization was quenched with methanol after 3 hr., and the polymer reprecipitated twice in ethanol (B.D.H. Ltd.) from *n*-hexane solution. The polymer was dried in a vacuum oven at  $60^\circ\text{C}$ . Four samples of polyisobutene were prepared in this manner.

The number-average molecular weights of the polymers were obtained from osmotic pressure measurements in toluene with a Mechrolab Model 501 high speed osmometer with Sylvania 300 grade or Ultracella "allerfeinst" cellophane membranes. Three samples had similar molecular weights ( $\bar{M}_n = 45,000$ ) and the fourth a higher molecular weight ( $\bar{M}_n = 100,000$ ). The high molecular weight sample was fractionated by use of a fractional precipitation technique<sup>9</sup> to give five fractions with a molecular weight range of  $\bar{M}_n = 30,000$  to  $\bar{M}_n = 380,000$ .

### The Radiochlorine Vacuum Apparatus

The design of the apparatus for the quantitative handling of radiochlorine is illustrated in Figure 1. Stopcocks 1, 2, and 3 are greaseless stopcocks (G. Springham and Co. Ltd.) with Viton A fluorocarbon diaphragms. All traces of air and moisture are removed from the system by evacuation. Radiochlorine, prepared by the decomposition of palladous



chloride ( $\text{Pd}^{36}\text{Cl}_2$ ) *in vacuo*,<sup>10</sup> is introduced into the apparatus at E and distilled into the reservoir A, the volume of which was approximately 3 liters. The radiochlorine was diluted with ordinary chlorine from a cylinder if quantities exceeding 100 mg. were required for a series of chlorinations. The transfer of known amounts of chlorine from the reservoir to reaction tubes D can be accomplished in two ways.

(a) The chlorine is allowed to expand from volume  $A$  into the volume  $A + B$  by opening stopcock 1. The weight of chlorine in  $B$  is a definite fraction, which may be called the "delivery fraction," of the original weight of chlorine in  $A$ , i.e.,

$$\text{Delivery fraction } F = B/(A + B)$$

The delivery fraction can be determined by the methods used by McNeill<sup>6</sup> or by using the Geiger counter (C) to count successive fractions taken from the reservoir. The counting tube is a liquid-counting tube (Mullard G. M. tube, type MX124/01) which has been fused to the vacuum apparatus and functions as a gas counter. The ratio of successive count rates, after correction for background and dead-time errors, obeys the equation,

$$R = A/(A + B)$$

The "delivery fraction" is obtained by subtracting this ratio from unity. The results for a series of experiments are given in Table I.

From Table I a mean value  $\bar{R} = 0.932$  and therefore  $\bar{F} = 0.068$  is obtained. This value of the delivery fraction  $F$  was in good agreement with the value ( $F = 0.069$ ) obtained from titration experiments in which successive fractions of chlorine were condensed into solutions of potassium iodide, the liberated iodine was titrated against standard sodium thiosulfate solution, and the delivery fraction calculated from the mean ratio of successive titers.

(b) If the specific activity of the radiochlorine in the gas phase is known, the weight of chlorine can be found by counting. The specific activity (S.A.) is found for the chlorine supply by counting a fraction and condensing

TABLE I  
Determination of the Delivery Fraction by Chlorine Counting

Fraction number ( $n$ )	Observed count rate, counts/min.	Corrected count rate, counts/min.	Ratio $n/n + 1$
1	7632	7911	—
2	7237	7452	0.942
3	6795	6965	0.934
4	6287	6408	0.920
5	5926	6017	0.939
6	5564	5627	0.935
7	5154	5187	0.922
8	4829	4837	0.932

it into a solution of potassium iodide. The weight of chlorine is found by the titration procedure described above:

$$1 \text{ ml. } 0.1N \text{ Na}_2\text{S}_2\text{O}_3 = 3.55 \text{ mg. chlorine.}$$

$$\text{S. A. (gas phase)} = \text{Corrected count rate of fraction/titer} \times 3.55 \\ \text{counts/min. per mg. Cl.}$$

The weight of chlorine in other fractions is obtained by dividing the count rate in the gas phase by the S.A. (gas phase). This method is useful in that large or small fractions can be withdrawn as desired, independently of the total weight of chlorine in the reservoir.

### Solution Counting

Solutions were counted in an open G.M. tube in conjunction with a G.M. sealing unit (Type 121 A, Ericsson Telephones Ltd.) and a probe unit (Type 110 A, Bendix Ericsson Ltd.). The amount of chlorine which has reacted with the polymer is found by counting a 10 ml. portion of the solution of the chlorinated polymer in carbon tetrachloride. The corrected count rate is divided by the specific activity of the radiochlorine in carbon tetrachloride. The S.A. ( $\text{CCl}_4$ ) is found by condensing a known weight of chlorine into a 5% (v/v) styrene in carbon tetrachloride solution and making the solution up to a standard volume for counting.

### Reaction of Polyisobutene with Radiochlorine

Polyisobutene samples (250 mg.) were dissolved in 10 ml. AR carbon tetrachloride and the solutions transferred to reaction tubes *D* (Figure 1). The solutions were made up to 15 ml., the reaction tubes sealed at *E*, the solutions thoroughly degassed, and suitable amounts of chlorine transferred into the reaction tubes as previously described. The reaction tubes were

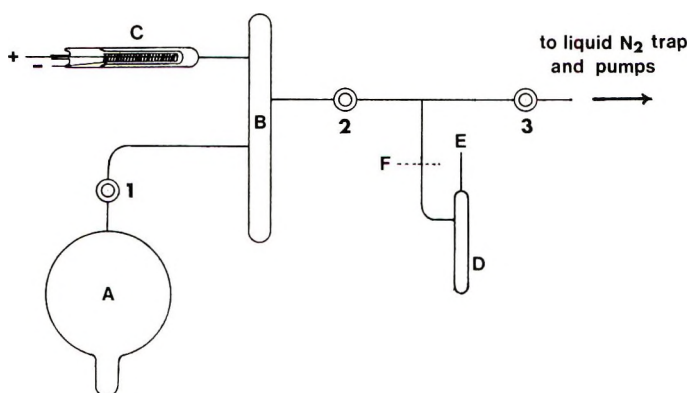


Fig. 1. Design of the radiochlorine apparatus: (A) chlorine reservoir; (B) chlorine delivery tube; (C) Geiger tube for gas counting radiochlorine; (D) reaction tube containing polymer solution; (E), (F) points at which reaction tube can be sealed off; (1), (2), (3), greaseless stopcocks.

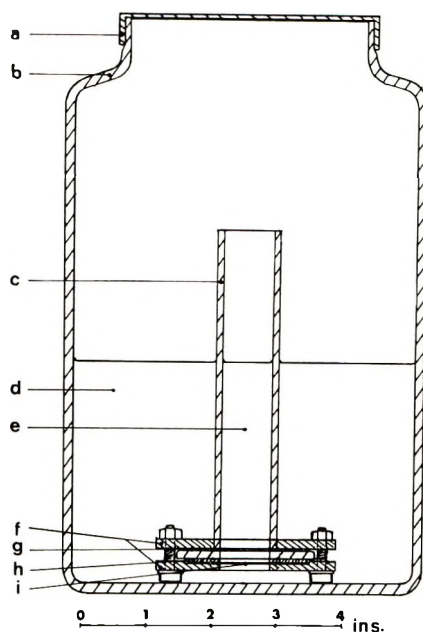


Fig. 2. Apparatus used for dialysis: (a) lid of jar; (b) jar; (c) Quickfit F.G.25 flange; (d) solvent; (e) polymer solution; (f) brass plates clamping membrane to flange; (g) upper Teflon washer; (h) lower Teflon washer; (i) membrane.

sealed off at  $F$  and placed in a thermostat at  $25^{\circ}\text{C}$ . for 3 hr.; dark glass containers were used to exclude light from the reaction vessels. When the tubes were opened, the solutions were shaken with an excess of powdered sodium thiosulfate to remove excess chlorine, filtered, and the remaining low molecular weight radioactive impurities removed by dialyzing the solutions for 14 days. A diagram of the dialyzing apparatus is shown in Figure 2. The outside solvent was renewed frequently and dialysis continued until a constant count rate was observed for the polymer solution. Sylvania 300 grade gel cellophane membranes were normally used in the dialysers but they were replaced by Ultracella filter "allerfeinst" membranes (Membranfilter-Gesellschaft, Göttingen) for low molecular weight samples,  $\bar{M}_n < 40,000$ . All membranes were conditioned to carbon tetrachloride by a method similar to that used by McNeill.<sup>11</sup> The 10-ml. portions of the solutions were counted as described above.

## RESULTS

The results obtained for the unfractionated polyisobutenes are tabulated in Table II. A graph was drawn of weight per cent Cl in the polymer versus weight per cent Cl in the reaction mixture for each polymer. The shape of the curves obtained is illustrated in Figure 3. Points on the rising part of the curve correspond to samples which have not reacted completely with chlorine in the time of the experiment. As the chlorine content of the

TABLE II  
 Reaction of Unfractionated Polyisobutenes with Radiochlorine

Polymer no.	Cl in reaction mixture, wt.-%	Count rate, counts/min. per 10 ml. solution	Wt. polymer, mg. per 10 ml. solution	S.A. (CCl <sub>4</sub> ) of Cl supply, counts/min. per mg. Cl	Wt. Cl in polymer, mg.	Cl in polymer, wt.-%
1	6.71	239.0	100	2320	0.103	0.103
	5.40	126.8	150	814	0.157	0.104
	4.45	107.3	150	814	0.132	0.088
	3.72	114.0	150	814	0.140	0.093
	3.40	85.0	166	570	0.149	0.090
	2.18	92.3	150	814	0.113	0.076
	1.43	80.3	150	814	0.099	0.066
	0.92	158.5	166	2575	0.062	0.037
2	7.12	101.2	164	517	0.196	0.119
	5.82	84.1	164	517	0.163	0.099
	5.63	80.5	164	517	0.156	0.095
	4.29	74.0	164	517	0.143	0.087
	3.70	73.6	164	517	0.142	0.086
	3.32	71.6	164	517	0.139	0.085
	3.00	82.8	164	517	0.160	0.097
	2.28	74.5	164	517	0.144	0.087
	1.58	59.9	164	517	0.116	0.070
	1.12	66.3	164	517	0.128	0.078
	0.67	56.5	164	517	0.109	0.066
	0.62	54.6	164	517	0.106	0.064
3	3.24	85.5	164	517	0.165	0.100
	2.46	76.4	164	517	0.148	0.090
	1.46	62.9	164	517	0.121	0.074
	0.94	53.9	164	517	0.104	0.063
	0.45	42.1	164	517	0.081	0.049
4	6.36	103.5	168	814	0.127	0.076
	5.15	100.3	168	814	0.123	0.074
	4.10	64.8	168	563	0.115	0.068
	3.85	60.8	166	563	0.108	0.065
	3.62	63.3	168	569	0.111	0.066
	2.83	78.9	168	814	0.097	0.058
	1.99	80.1	168	814	0.098	0.059
	0.65	22.0	168	563	0.039	0.024
	0.24	14.7	162	563	0.026	0.016

mixture is increased, a situation is reached where further excess of chlorine produces little further increase in the amount of chlorine incorporated into the polymer; it is concluded that for the samples giving points on this linear portion of the curve all the double bonds present have reacted completely, and the slight increase in the amount of chlorine incorporated in the polymer at high chlorine contents is attributed to side reactions. The

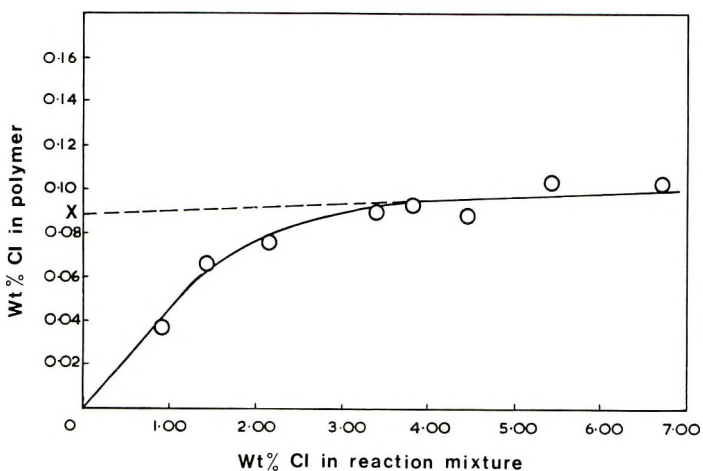


Fig. 3. Reaction of radiochlorine with polyisobutene, no. 1.

intercept  $X$ , which is derived by extrapolation of the linear part of the curve, is a measure of the unsaturation, and may be called the weight per cent unsaturation ( $U_w$ ). Since the plateau regions of the graphs were almost horizontal, an accurate extrapolation to the vertical axis was feasible.

The mole per cent unsaturation ( $U_M$ ) is calculated from the weight per cent unsaturation by assuming that one mole of chlorine enters the polymer

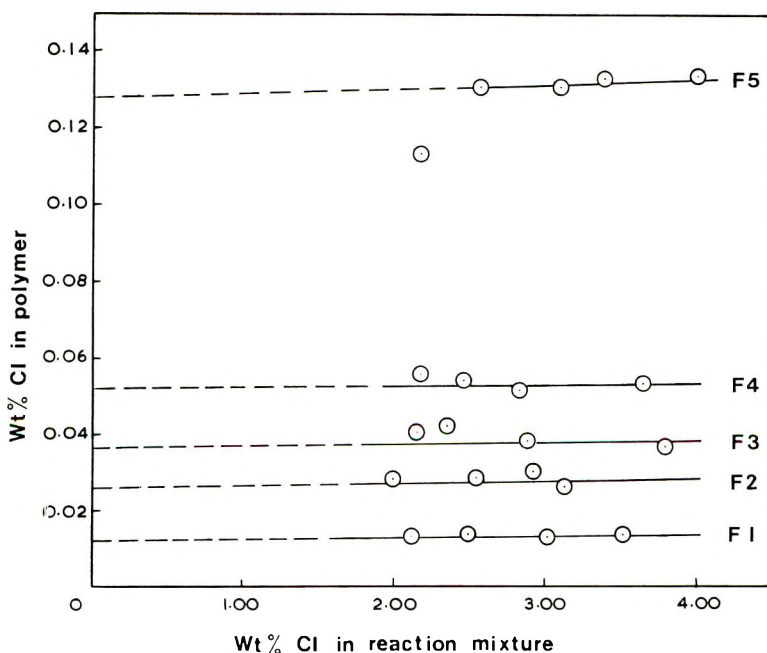


Fig. 4. Reaction of radiochlorine with polyisobutene fractions.



TABLE III  
 Un saturations of Unfractionated Polyisobutenes

Polymer no.	Molecular weight ( $\bar{M}_n$ )	$10^5 \bar{M}_n$	$U_w$	$U_M$	$U'_M$	Double bonds per molecule
1	45,700	2.19	0.090	0.070	0.125	0.56
2	49,100	2.04	0.083	0.065	0.118	0.55
3	40,500	2.47	0.095	0.075	0.142	0.53
4	100,000	1.00	0.049	0.040	0.058	0.69

 TABLE IV  
 Chlorination of Fractionated Polyisobutenes

Polyisobutene fraction	Cl in reaction mixture, wt.-%	Count rate of solution, counts/min. per 10 ml.	Wt. polymer in solution, mg. per 10 ml.	Wt. Cl in polymer, mg.	Cl in polymer, wt.-%
S.A. of Cl = 814 counts/min. per mg. Cl in CCl <sub>4</sub> solution					
F1	3.52	18.4	164	0.0226	0.0138
	2.90	17.9	168	0.0220	0.0132
	2.49	19.1	168	0.0234	0.0139
	2.12	17.7	164	0.0219	0.0132
S.A. of Cl = 406 counts/min. per mg. Cl in CCl <sub>4</sub> solution					
F2	3.25	17.7	165	0.0439	0.0264
	2.93	21.4	168	0.0527	0.0312
	2.55	20.1	172	0.0495	0.0289
	1.99	19.4	168	0.0478	0.0285
F3	3.80	25.5	169	0.0628	0.0372
	2.88	26.1	166	0.0643	0.0388
	2.36	16.4	95	0.0406	0.0426
	2.15	28.1	169	0.0692	0.0410
F4	3.67	36.2	166	0.0894	0.0538
	2.84	34.6	165	0.0854	0.0517
	2.47	36.6	166	0.0902	0.0546
	2.18	38.1	168	0.0940	0.0560
F5	4.01	90.8	167	0.224	0.134
	3.40	90.9	168	0.224	0.133
	3.10	88.0	166	0.217	0.131
	2.57	90.1	169	0.222	0.131
	2.18	76.2	166	0.188	0.113

per double bond.\* The mole per cent unsaturation is given by the expression,

$$U_M = U_w (\text{M.W. of monomer}/\text{M.W. of chlorine})$$

\* Note added in proof: The validity of this assumption is currently being investigated in detail.

The experimental unsaturations can be compared to the unsaturations ( $U'_M$ ) which would be measured in polymers having one double bond per molecule. The ratio  $U_M/U'_M$  gives the unsaturation in terms of double bonds per molecule. The values of unsaturation exhibited by the unfractionated polymers are given in Table III.

The results of chlorination for the fractionated polyisobutenes are given in Table IV and illustrated graphically in Figure 4. Once the general shape of the chlorination curve had been established, four points in the plateau region were considered sufficient for each determination. The calculated unsaturations are tabulated in Table V.

TABLE V  
Unsaturation of Fractionated Polyisobutenes

Polymer fraction	Molecular weight ( $\bar{M}_n$ )	$10^5/\bar{M}_n$	$U_W$	$U_M$	$U'_M$	Double bonds per molecule
F1	376,000	0.266	0.012	0.009	0.015	0.60
F2	190,000	0.526	0.026	0.020	0.030	0.67
F3	125,000	0.800	0.036	0.028	0.046	0.61
F4	77,000	1.299	0.052	0.041	0.075	0.55
F5	32,000	3.120	0.128	0.101	0.181	0.56

## DISCUSSION

The chlorination data for the fractionated polyisobutenes clearly indicate that the mole per cent unsaturation is inversely proportional to the

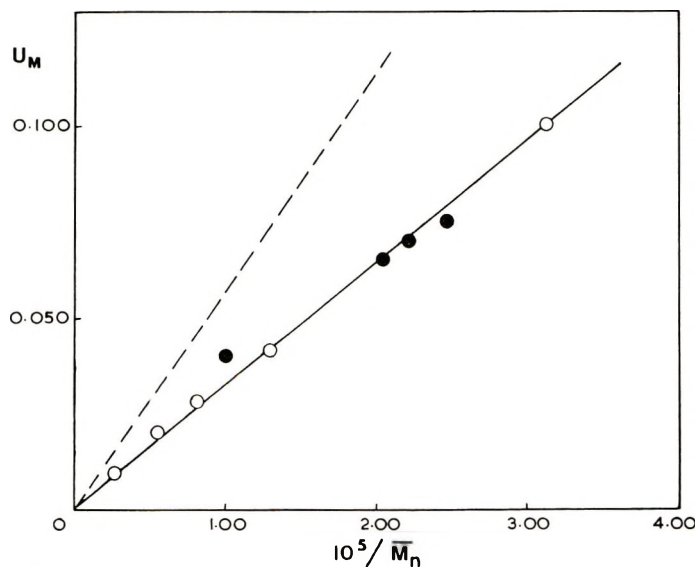


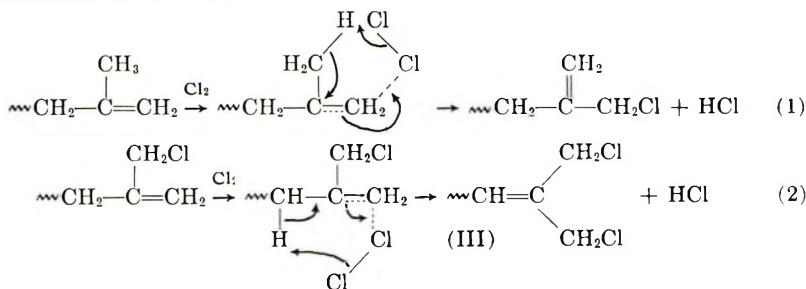
Fig. 5. Relationship between unsaturation of polyisobutenes and molecular weight: (●) unfractionated polymers; (○) fractionated polymers; (--) behavior expected for polymers having one terminal double bond per chain.

molecular weight. This is illustrated in Figure 5. The points for the unfractionated samples are also shown in the figure. The two sets of results are in good agreement. It can be concluded from Figure 5 that the unsaturation is terminal: this quantitative proof is consistent with spectroscopic evidence<sup>1,2</sup> which indicates the predominance of methylenic unsaturation in oligomers and low molecular polymers of isobutene prepared by other catalysts. This result is as expected for a linear polyisobutene chain with regular head-to-tail linkages.

### Nature of Chlorination

In order to derive mole per cent unsaturations from the chlorination results, the incorporation of 1 mole Cl per double bond was postulated.\* This assumption is supported by the available evidence concerning the reaction between chlorine and polyisobutene. Neither main-chain chlorination nor replacement of saturated endgroups, e.g., hydroxyl chain ends, is significant in this reaction under the conditions used; this was established by studying the reaction between chlorine and tertiary amyl alcohol, a suitable model compound for hydroxyl chain and structures. No reaction was observed under the same conditions used in the polymer experiments. The chlorination is induced by the double bond, but it is not a typical addition, since butyl rubbers chlorinated in a similar manner retain unsaturation.<sup>6,12</sup> Moreover, in butyl rubbers the introduction of two chlorine atoms at each unsaturated center was conclusively established. The reaction of chlorine with isobutene and related branched olefins has been shown to be one of allylic substitution.<sup>13</sup> Using equimolar ratios of olefin to halogen, Groll et al.<sup>13</sup> found monosubstitution to be predominant, although small amounts of disubstituted products were also observed. It is probable, therefore, that disubstitution will occur when chlorine is present in excess. The reaction is not free-radical by nature as in photochemical chlorinations. It is of interest that a more extensive reaction between chlorine and polymer, presumably a free-radical reaction, is observed when small quantities of air are present in the reaction mixture. This potential source of error is eliminated by rigorously degassing the reaction mixtures prior to the addition of chlorine.

From this discussion, the chlorination is deduced to proceed by the mechanism shown in eqs. (1) and (2).

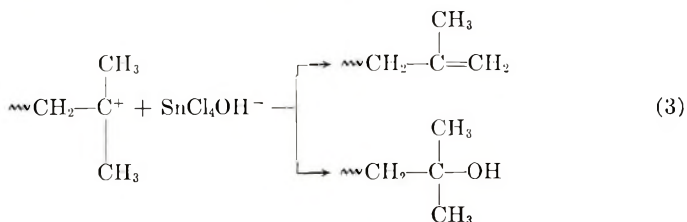


\* See footnote to p. 2058.

Products which are isomeric with III could be derived by similar mechanisms. It is suggested that further substitution is suppressed by the steric hindrance of the two chlorine atoms shielding the ethylenic linkage. The chlorination graphs (Figs. 3 and 4) are in accordance with this mechanism. The rising part of the curve corresponds to the introduction of chlorine; stage (1) and stage (2) are not distinguished, but the slight gradient of the plateau region indicates that further substitution or main-chain chlorination are negligible under the reaction conditions employed.

### Degree of Unsaturation

When the mole per cent unsaturations of polyisobutenes samples having one double bond per chain are plotted against reciprocal molecular weight, the dotted line in Figure 5 is obtained. The experimental line corresponds to approximately 0.6 double bonds per chain. The possibility of diffusion of low molecular weight polymer during dialysis, which could cause the apparent unsaturations to be lower than the true ones, was not supported by molecular weight measurements taken before and after dialysis. Therefore, there must be at least one other transfer or termination reaction which can compete favorably with the proton expulsion process during polymerization. Kinetic investigations<sup>14</sup> of this system show that transfer reactions are unimportant and that the main chain-breaking process is a bimolecular collision involving the cation and the anionic catalyst residue. It may be concluded, therefore, that the termination step in this polymerization involves the two reactions shown in eq. (3).



Hydroxyl endgroups have been observed in oligomeric isobutene prepared by a titanium tetrachloride-water catalyst<sup>2,15</sup> and in oligomers prepared by a boron fluoride-water catalyst.<sup>1</sup> The ratio of saturated to unsaturated endgroups would be expected to vary with the conditions of polymerization, but the double bonds can be analyzed quantitatively by this method.

The authors are indebted to Messrs. R. Smith and G. Perrit for the measurement of molecular weights, and to the Science Research Council for a research studentship grant (R.McG.) during the tenure of which this work was carried out.

### References

1. F. S. Dainton and G. B. B. M. Sutherland, *J. Polymer Sci.*, **4**, 37 (1949).
2. M. St. C. Flett and P. H. Plesch, *J. Chem. Soc.*, **1952**, 3355.
3. D. C. Pepper and P. J. Reilly, *Proc. Chem. Soc.*, **1961**, 460.
4. S. G. Gallo, H. K. Weise, and J. F. Nelson, *Ind. Eng. Chem.*, **40**, 1277 (1948).
5. T. S. Lee, I. M. Kolthoff, and E. Johnson, *Anal. Chem.*, **22**, 995 (1950).

6. I. C. McNeill, *Polymer*, **4**, 15 (1963).
7. G. Mayer, J. C. Kuriacose, and F. Eschard, *Bull. Soc. Chim. France*, **1961**, 624.
8. P. H. Plesch, ed., *The Chemistry of Cationic Polymerisation*, Pergamon, London, 1963, pp. 143-146.
9. P. J. Flory and T. G. Fox, *J. Am. Chem. Soc.*, **70**, 2384 (1948).
10. I. C. McNeill, *J. Chem. Soc.*, **1961**, 639.
11. I. C. McNeill, *Polymer*, **4**, 247 (1963).
12. F. P. Baldwin, D. J. Buckley, I. Kuntz, and S. B. Robinson, *Rubber Plastics Age*, **42**, 500 (1961).
13. J. Burgin, W. Engs, H. P. A. Groll, and H. Hearne, *Ind. Eng. Chem.*, **31**, 1413 (1939).
14. R. G. W. Norrish and K. E. Russel, *Trans. Faraday Soc.*, **48**, 91 (1952).
15. R. H. Biddulph, P. H. Plesch, and P. P. Rutherford, *J. Chem. Soc.*, **1965**, 275.

### Résumé

Une technique radiochimique utilisant le chlore-36 a été décrite précédemment pour mesurer l'insaturation du caoutchouc butylique. Cette méthode a maintenant été appliquée en vue d'estimer la concentration beaucoup plus faible en double soudure qui se présente dans le polyisobutylène préparé par polymérisation cationique de l'isobutène à basse température. La nature de la réaction du polyisobutène avec le chlore radioactif en absence d'air a été examinée et les résultats expérimentaux sont discutés en rapport avec les théories actuelles des mécanismes de terminaison de chaîne en cours de polymérisation cationique.

### Zusammenfassung

Ein radiochemisches Verfahren unter Verwendung von Chlor-36 zur Bestimmung der Doppelbindungen in Butylakutschuk wurde schon beschrieben. Diese Methode wurde nun zur Bestimmung der viel niedrigeren Doppelbindungskonzentration in Polyisobuten verwendet, welches durch kationische Polymerisation von Isobuten dargestellt worden war. Die Natur der Reaktion von Polyisobuten mit Radiochlor in Abwesenheit von Luft wurde untersucht und die Versuchsergebnisse werden in Zusammenhang mit der heutigen Theorien des Mechanismus des Kettenabbruchs bei der kationischen Polymerisation diskutiert.

Received November 17, 1965

Revised December 21, 1965

Prod. No. 5041A



## Radiation-Induced Copolymerization of Formaldehyde and Styrene

Y. P. CASTILLE\* and V. STANNETT, *Camille Dreyfus Laboratory,  
Research Triangle Institute, Durham, North Carolina*

### Synopsis

The radiation-induced copolymerization of styrene with liquid formaldehyde in bulk and in solution has been studied at low temperatures. In bulk and in methylene chloride solution copolymerization took place, whereas in diethyl ether solution only homopolymerization of the formaldehyde was found. At  $-78^{\circ}\text{C}$ ., in bulk and in methylene chloride solution, no evidence of polystyrene blocks could be found, whereas at  $-30^{\circ}\text{C}$ . in bulk about 30% of the styrene content of the copolymer was in the form of high molecular weight blocks. The rate of copolymerization in methylene chloride solution was found to be first-order with respect to dose rate and third-order with respect to formaldehyde concentration similar to results reported for formaldehyde in toluene solution. The thermal stabilities of the copolymers were found to be intermediate between those of pure polyoxymethylene and commercially stabilized polymers. Since the latter were of higher molecular weight and contain added stabilizers, the increased thermal stabilities of the copolymers were considered to be particularly significant.

### INTRODUCTION

The radiation-induced polymerization of formaldehyde in the liquid state, both in bulk and in solution, and in the solid state, has been reported by a number of investigators.<sup>1-5</sup> Although early indications<sup>1</sup> were that the liquid-phase reaction might be free-radical in nature, later work<sup>2-4</sup> clearly indicated that an ionic mechanism was operating.

The radiation-induced copolymerization of formaldehyde was first carried out to clarify the mechanism of polymerization of pure formaldehyde. The rates of copolymerization in bulk and methylene chloride solution have been reported to decrease as follows:  $\alpha$ -methylstyrene > styrene > methyl methacrylate > acrylonitrile > ethylene oxide.<sup>2,3</sup>

Although the polyoxymethylenes obtained by polymerizing formaldehyde, both as monomer or as cyclic trimer, were polymers of considerable commercial interest with excellent mechanical properties, their thermal stability was not satisfactory. This property has been greatly improved by modification of the endgroups of the polymer or by the inclusion of C—C bonds which would stop the "unzipping" of the polymer. The catalytic copolymerization of formaldehyde with various monomers has been described by a number of authors, but only very few satisfactory results

\* Present address: E. I. du Pont de Nemours & Co., Inc., Wilmington, Delaware.

have been reported in regard to the improvement of stability of polyoxymethylene toward heat, acidolysis, and hydrolysis.<sup>6-9</sup>

This work on the radiation-induced copolymerization of formaldehyde and styrene, although incomplete, describes a study of copolymerization of styrene with formaldehyde and of the thermal stability of copolymers containing increasing proportions of styrene.

## EXPERIMENTAL

### Materials

Styrene monomer was first purified by conventional distillation under nitrogen stream at reduced pressure. The monomer was stored over calcium hydride for several weeks at low temperature. Before use, the monomer was distilled over fresh calcium hydride under high vacuum and finally degassed and distilled from sodium and benzophenone directly into the reaction chamber (Fig. 2). The glass walls of the reaction vessel were cleaned by condensing and transferring small portions of reagent back and forth several times between the reactor chamber and the sodium benzophenone solution. This procedure, apparently dislodging impurities from the glass and destroying them, led to the simultaneous purification of the reagent and the glassware. Methylene chloride was dried over calcium hydride for several weeks at low temperature and distilled before use over fresh calcium hydride under high vacuum.

Analytical grade anhydrous absolute diethyl ether was obtained commercially and was used without further purification.

Toluene was purified by fractional distillation under nitrogen stream, dried by refluxing over metallic sodium and, before use, distilled over metallic sodium under a stream of nitrogen.

### Formaldehyde and Monomer Mixtures

When small quantities of formaldehyde were needed for each individual reaction tube, the monomer was prepared following the method of Spence and Wild.<sup>10</sup> Formaldehyde was prepared under reduced pressure by the pyrolysis of commercial paraformaldehyde, using the apparatus shown in Figure 1. Prior to use, paraformaldehyde was dried for several weeks in vacuum over phosphorus pentoxide, and the apparatus was flamed twice. The monomeric formaldehyde was purified by passing over phosphorus pentoxide contained in the three traps, which were maintained at  $-78^{\circ}\text{C}$ ., in order to eliminate moisture and other impurities. Formaldehyde was condensed at liquid nitrogen temperature in the graduated tube (B). The first fraction of monomer was discarded. After melting at  $-78^{\circ}\text{C}$ ., the monomer was distilled from B into the reaction tube (D) maintained at  $-196^{\circ}\text{C}$ .. The prepurified styrene monomer contained in C at  $-78^{\circ}\text{C}$ ., was then distilled into the reaction vessel (D) over the solid formaldehyde. In many cases we observed that the condensation of formaldehyde over the purified styrene led to considerable prepolymerization of the formal-

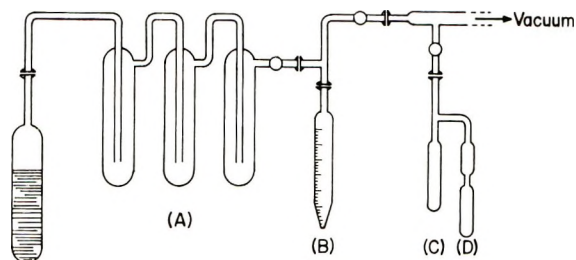


Fig. 1. Apparatus used for the preparation of formaldehyde-styrene mixtures in small quantities for single-tube experiments.

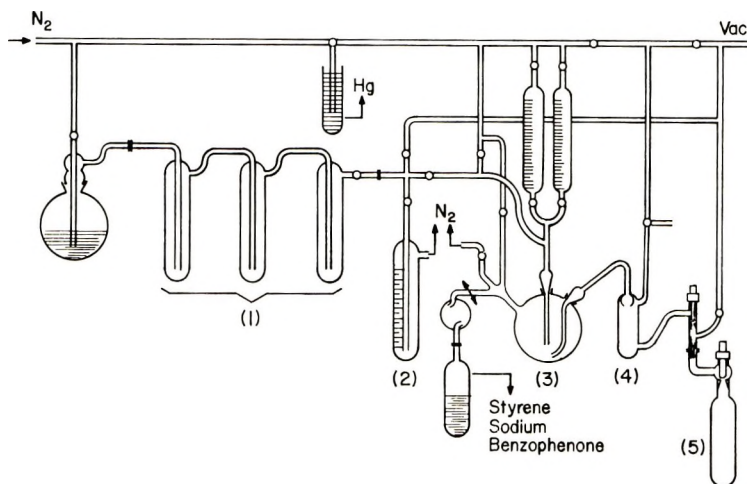


Fig. 2. Apparatus used for the preparation of formaldehyde-styrene mixtures in larger quantities for multiple-tube experiments.

dehyde, and so the reverse procedure was always used. It was interesting that when prepolymerization did occur in the presence of styrene no copolymer was formed but only pure polyoxymethylene.

When a larger quantity of formaldehyde had to be prepared, the method of Spence and Wild was found less effective than that of Walker,<sup>11</sup> which is described below.

The apparatus, shown in Figure 2, was developed in order to obtain enough monomeric mixture to run a complete set of polymerizations with the same starting monomeric mixture. Because of the varying amounts of prepolymerization of formaldehyde, it proved difficult to reproduce the exact starting monomeric material.

Prior to use, the commercial paraformaldehyde was dried for several weeks over phosphorus pentoxide in vacuum. The apparatus was flamed twice and the mixing vessel (3) was finally cleaned by using the sodium benzophenone procedure, as stated previously. During this procedure the desired amount of styrene was introduced into the mixing flask (3), which was then maintained at the chosen temperature.

Formaldehyde was prepared by pyrolysis of paraformaldehyde in a dry nitrogen stream and purified by passing through the three traps (1) maintained at  $-20^{\circ}\text{C}$ . The first fraction of gaseous formaldehyde was introduced into the trap (2) ( $-78^{\circ}\text{C}$ .) and discarded. The monomeric mixture was then formed by introducing formaldehyde into the styrene (bulk or solution) contained in vessel 3. The mixture thus obtained was pushed with nitrogen pressure into the graduated tube (4), and the exact amount of solution could then be pulled by vacuum into the reaction vessel (5), which was closed with a greaseless needle valve.

### Irradiation

The irradiations were carried out in sealed tubes in a 1500-c.  $^{60}\text{Co}$  room-type source.

### Treatment of the Polymers

The polymers were soluble in dimethylformamide (DMF) containing 2%  $\alpha$ -pinene at  $140^{\circ}\text{C}$ . or in *p*-chlorophenol containing 2%  $\alpha$ -pinene at  $60^{\circ}\text{C}$ . Viscometric studies of both solutions showed a faster decomposition of the polyoxymethylene in the DMF solution, and so the latter solvent was always used. Fractionation of the copolymers was effected by the progressive addition of  $\alpha$ -pinene to the solution in *p*-chlorophenol at  $60^{\circ}\text{C}$ . containing 3% of  $\alpha$ -pinene as stabilizer. The first fraction was obtained by adding 30%  $\alpha$ -pinene to the solution followed by filtration at  $60^{\circ}\text{C}$ . In some cases we observed that the filtrate led to a second precipitation by cooling to room temperature. The last fractions showing polyoxymethylene were isolated by pouring the filtrate in methyl ethyl ketone. The last fraction, which was found to be homopolystyrene, was precipitated from the filtrate by pouring into methanol. Each of these fractions was dried at  $30^{\circ}\text{C}$ . *in vacuo* for several days and analyzed by infrared spectroscopy. When copolymers were formed there was always a small proportion of homopolystyrene isolated, but no pure polyoxymethylene could be detected, i.e., all the fractions contained styrene.

### Physical Measurements

Viscosity studies were carried out with an Ostwald-Cannon-Fenske viscometer, starting with 0.6% solutions of polymer in *p*-chlorophenol containing 3%  $\alpha$ -pinene at  $60^{\circ}\text{C}$ .

Infrared analysis was carried out by use of a Perkin-Elmer spectrophotometer, Model 237. Weight ratios of both monomers contained in the polymer were determined by comparing the oxymethylene bands at  $9\ \mu$  and  $10.5\text{--}11\ \mu$  with those of styrene at  $13.1\ \mu$  and  $14.2\ \mu$ . Infrared spectra were obtained from potassium bromide pellets containing 0.5–1% of polymer. Several verification tests have shown that these analyses could be carried out within an accuracy of 2%.

Thermal gravimetric and differential thermal analyses were carried out by Mr. T. Tarim of North Carolina State University at  $2.5$  and  $10^{\circ}\text{C}/\text{min}$ .



## RESULTS

The study of the radiation-induced copolymerization of formaldehyde and styrene has been carried out in bulk and in ethyl ether and methylene chloride solutions. For most of the kinetic studies, the percentage conversion was kept to under 5% in order to avoid the effects due to the precipitation of polymers and to work in a homogeneous system.

In the solution polymerization, with diethyl ether as solvent, only polyoxymethylene and no trace of copolymer could be found. As shown in Figure 3, the polymerization proceeded after an induction period, the length of which was found to be roughly inversely proportional to dose rate. As in most catalytic polymerizations, the existence of this induction period is most probably due to a slight amount of impurities, which are more rapidly consumed at higher concentrations of catalyst, or, in our case, at higher radiation dose rates. The effect of dose rate on the rate of polymerization was found to be essentially first-order, as shown by the results presented in Figure 4. The formaldehyde concentration was only 3.3 mole/l., and the rates are about three times higher than those reported<sup>3</sup> for pure formaldehyde in diethyl ether after a first-order correction for the difference in formaldehyde content. Similar increases were reported<sup>3</sup> for the addition of acrylonitrile and methyl methacrylate to formaldehyde in diethyl ether, whereas the addition of isobutylene caused a decrease in rate. If the reaction is anionic, as suggested by Yamaoka et al.,<sup>3</sup> the styrene could be functioning as an electron acceptor, leading to more initiating

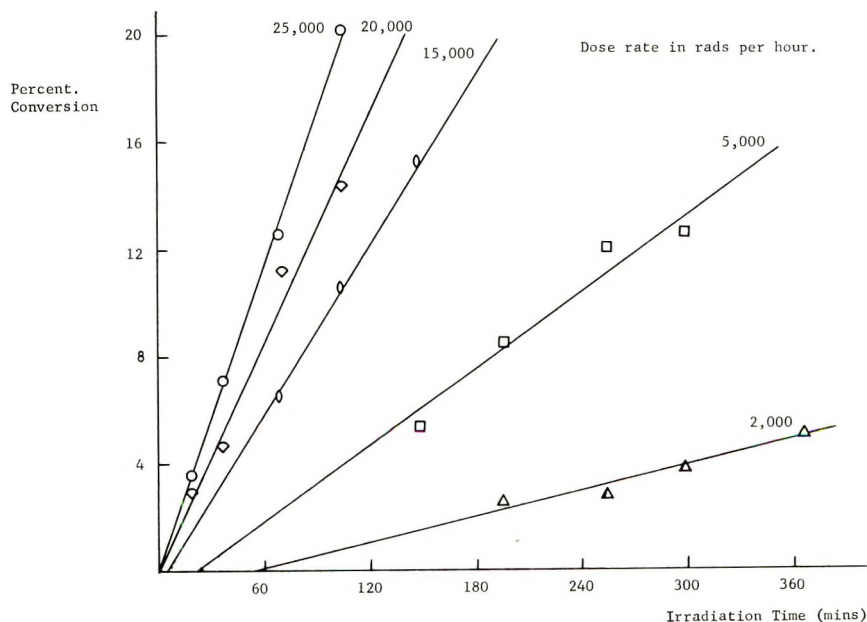


Fig. 3. Polymerization of formaldehyde-styrene in diethyl ether at  $-78^{\circ}\text{C}$ . Formaldehyde-styrene molar ratio 56.3/43.7, 40% solution by volume.



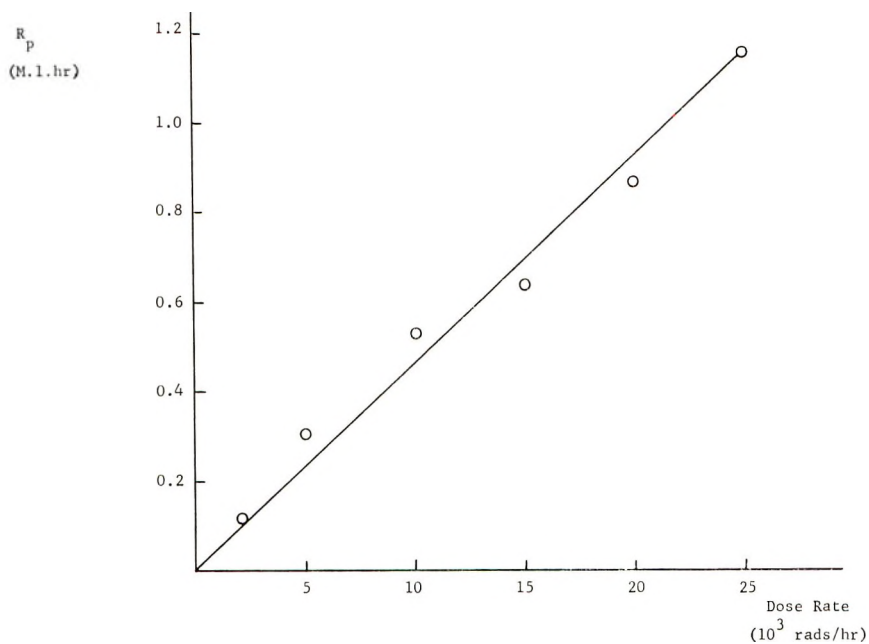


Fig. 4. Effect of dose rate on rate of polymerization of formaldehyde and styrene in diethyl ether. Conditions as in Fig. 3.

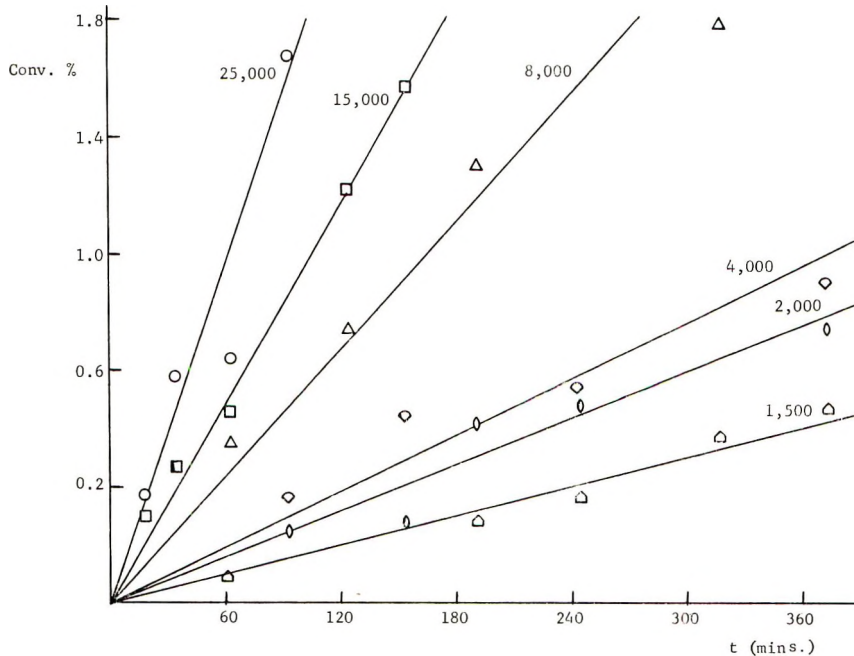


Fig. 5. Copolymerization of styrene and formaldehyde in methylene chloride at  $-78^{\circ}\text{C}$ . Formaldehyde-styrene ratio, 65.5/34.5/34.5, 50% solution by volume. Dose rates given on curves in rads per hour.  $[\text{CH}_2\text{O}] = 4.58$  mole/l.,  $[\text{styrene}] = 2.41$  mole/l.

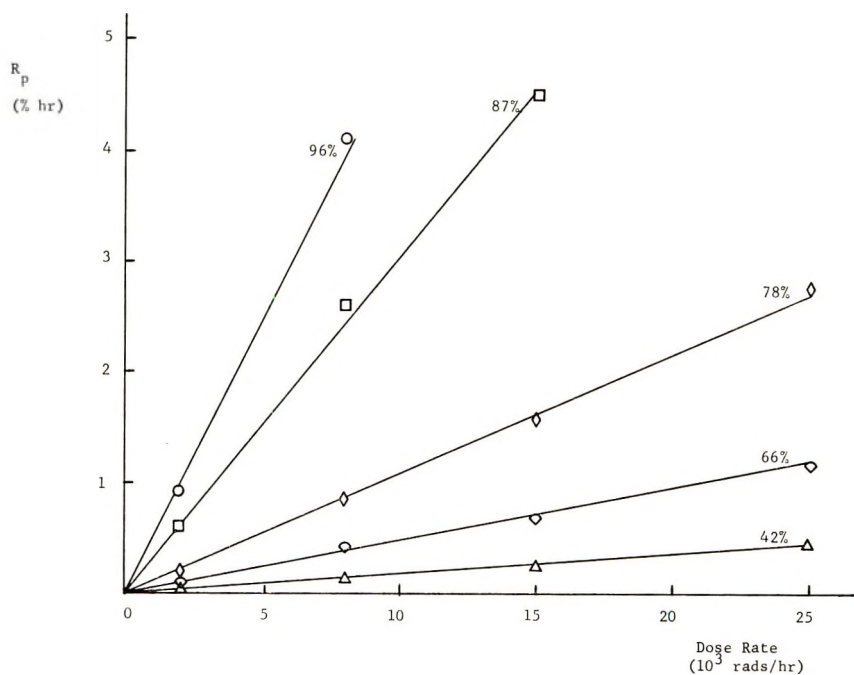


Fig. 6. Effect of dose rate on rate of copolymerization of formaldehyde and styrene in methylene chloride at  $-78^\circ\text{C}$ . Molar per cent of formaldehyde in monomer mixture given on curves (see also Table I).

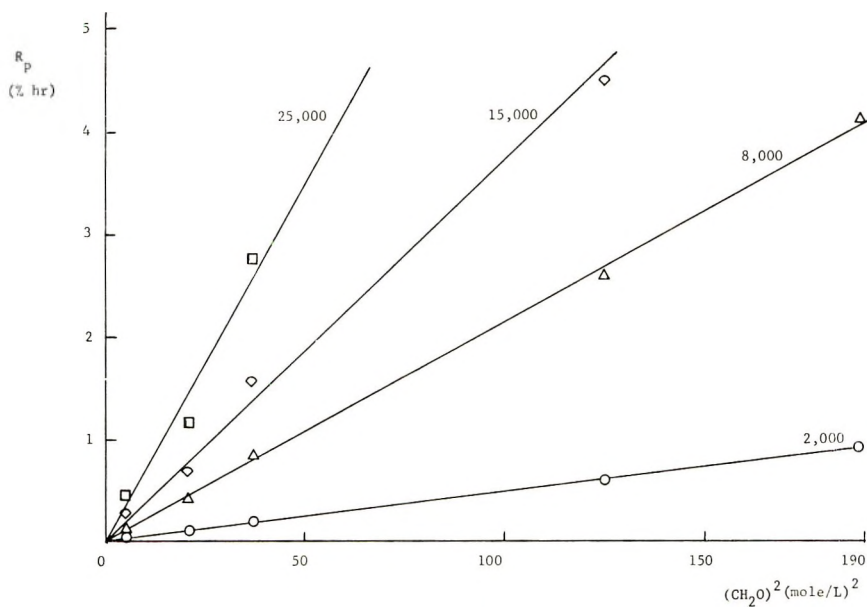


Fig. 7. Effect of formaldehyde concentration on rate of copolymerization of styrene and formaldehyde in methylene chloride solution (50% by volume) at  $-78^\circ\text{C}$ .

sites as suggested for the other two monomers. Since no copolymerization took place in diethyl ether, no further studies were conducted with this system.

A series of experiments was conducted at  $-78^{\circ}\text{C}$ . with methylene chloride as the solvent. In this case styrene-formaldehyde copolymers were formed. Typical conversion curves are presented in Figure 5, and the rate data are given in Table I for various dose rates. It can be seen that no induction periods were found with this system. The dose rate dependences are presented in Figure 6 for a number of different formaldehyde concentrations; a first-order dependence was observed at all the formaldehyde concentrations. The dependence of the rate on the formaldehyde concentration is shown in Figure 7. The rates are presented for convenience in per cent per hour and can be seen to be proportional to the square of the formaldehyde concentration, i.e., the kinetic rates are proportional to the formaldehyde concentration to the third power.

The effect of the styrene monomer concentration on the rate of copolymerization with formaldehyde and on the copolymer composition is shown in Table I and Figure 8. It can be seen that the rate of copolymerization decreased sharply with the addition of styrene in the monomer mixture. This is in marked contrast to the effect of styrene on the polymerization of formaldehyde in diethyl ether, again indicating a different mechanism of polymerization. The rates of copolymerization were found to be much lower than the rates of polymerization in diethyl ether, whereas pure formaldehyde polymerizes faster in methylene chloride solution. A similar reduction of the polymerization rate was observed by Yamaoka et al.<sup>3</sup> when  $\alpha$ -methylstyrene was added to formaldehyde in toluene solution.

Because of the partial crystallization in the monomer mixtures containing higher proportions of styrene, further studies of this system could not be carried out. It should be pointed out that the mixture containing 23% of formaldehyde has already to be diluted with 60% methylene chloride to avoid the crystallization of styrene. Although the determination of the monomer reactivity ratios was subject to limitations due to the limited range of these results, the values, calculated by using the method of Pine-

TABLE I  
Rates of Copolymerization of Formaldehyde and Styrene<sup>a</sup>

Formaldehyde in monomer mixture		CH <sub>2</sub> O in copolymer, mole-%	Rate of copolymerization, % hr.			
mole/l.	mole-%		$2 \times 10^3$ rad/hr.	$8 \times 10^3$ rad/hr.	$15 \times 10^3$ rad/hr.	$25 \times 10^3$ rad/hr.
1.17	23	97.5	0.01	0.03	0.06	0.09
2.3	42	98.5	0.04	0.14	0.26	0.46
4.58	66	99	0.10	0.41	0.69	1.18
6.1	78	99.5	0.20	0.85	1.58	2.77
11.2	87	99.8	0.60	2.60	4.5	>5%
13.7	96	99.8	0.94	4.12	>5%	>5%

<sup>a</sup> Solvent: methylene chloride (50%);  $-78^{\circ}\text{C}$ .

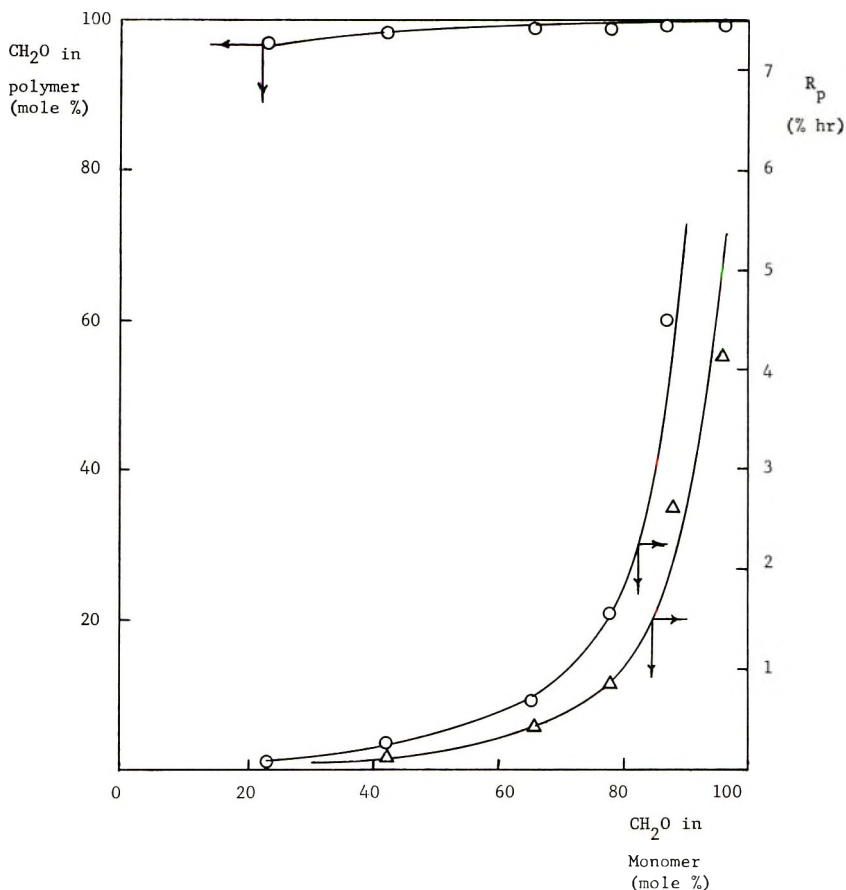


Fig. 8. Copolymerization of styrene and formaldehyde in methylene chloride at  $-78^{\circ}\text{C}$ . Copolymer composition curve and rates of polymerization. (O) dose rate, 15,000 rad/hr.; ( $\Delta$ ) dose rate, 8,000 rad/hr.

man and Ross,<sup>14</sup> were found to be  $r_1 \cong 52$ ;  $r_2 \cong 0$ , where  $M_1$  is formaldehyde.

It can be seen that most of these kinetic results are similar to the data reported in the Japanese literature on the radiation-induced polymerization of liquid formaldehyde. The rate of polymerization was found to be proportional to first order of dose rate, both in ethyl ether and methylene chloride solution. This relationship indicates an ionic mechanism for the copolymerization, and many investigators have reported the same proportionality for radiation-induced ionic polymerizations.<sup>16,17,20</sup> The high, third-order dependence of the rate on the formaldehyde content is also characteristic of many ionic polymerizations and agrees with that found by Nakashio et al.<sup>4</sup> with toluene as the solvent rather than the second-order dependence reported in the earlier work of Yamaoka<sup>3</sup> with both toluene and methylene chloride. It should be pointed out, however, that the systems

are not completely comparable, since, with our copolymerization system, the styrene content was also changed and the methylene chloride kept constant. Furthermore, the formation of a copolymer has been found in the systems using methylene chloride as solvent, whereas the mixtures with ethyl ether as solvent gave only pure polyoxymethylene. These results indicate a pronounced effect of solvents, which not only support the existence of an ionic mechanism of polymerization but also indicate that the mechanism of polymerization is different in each of these solvents. The tremendous retarding effect of the styrene (and  $\alpha$ -methylstyrene<sup>3</sup>) on the polymerization of formaldehyde compared with its accelerating effect in diethyl ether appears to be much greater than could be explained by an energy-transfer process, since toluene exerts comparatively little retarding effect when used as a solvent. If the reaction is cationic, these monomers which have high electron affinities could also act as mobile terminators, as suggested by Dainton<sup>12</sup> to explain the inhibiting effect of oxygen on the radiation-induced polymerization of isobutylene and later shown with other additives of high electron affinity.<sup>13</sup> Fragmentary results concerning the effect of oxygen also show evidence of an inhibiting effect.

Many investigators<sup>16-19</sup> have reported that the radiation-induced polymerization of styrene proceeds, at low temperature, following a cationic mechanism. Furthermore, it is known that methylene chloride is a suitable solvent for the promotion of cationic polymerization, particularly in the case of radiation-induced polymerizations, whereas diethyl ether is a retarding solvent for cationic polymerizations.<sup>20</sup>

The correlation between the data obtained from the literature and our results, as well as the successful copolymerization of formaldehyde and styrene in methylene chloride at low temperature, strongly indicate that the radiation-induced copolymerization of styrene and formaldehyde proceeds by a cationic mechanism.

It has been reported in a previous paper<sup>15</sup> that the <sup>60</sup>Co  $\gamma$ -ray irradiation of bulk mixtures of formaldehyde and styrene led to the formation of copolymer. Pure liquid formaldehyde irradiated at  $-78^\circ\text{C}$ . up to 10 Mrad, led to complete conversion to polyoxymethylene, whereas pure styrene yielded only 1.14% polystyrene at the same temperature. Mixtures of both monomers containing less than 70% formaldehyde consisted, at  $-78^\circ\text{C}$ ., of a paste of styrene crystals in a saturated solution of styrene in formaldehyde. So, in varying the concentration of both monomers, below 70% formaldehyde, the same saturated liquid monomer mixture was always found but contained more or less styrene crystals. At higher ratios of formaldehyde the monomer mixture remains liquid. For monomer mixtures containing less than the 70% (weight) formaldehyde, the total yield of polymer was found to be proportional to the initial quantity of formaldehyde, and the copolymer showed a constant molar composition of about 97% oxymethylene and 3% styrene. The irradiation of mixtures of monomer containing higher concentrations of monomeric formaldehyde



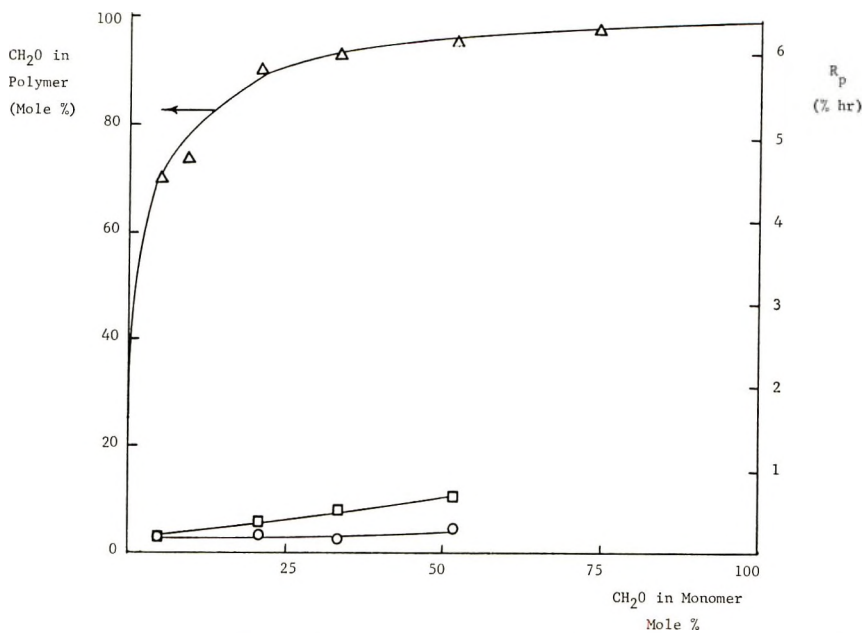


Fig. 9. Copolymerization of styrene and formaldehyde in bulk at  $-30^{\circ}\text{C}$ .: ( $\Delta$ ) experimental copolymer composition curve, solid curve calculated for  $r_1 = 30$ ,  $r_2 = 0$ ; ( $\square$ ) rate of copolymer formation; ( $\circ$ ) rate of polystyrene formation.

led to higher yield in polymer, and the copolymer showed increasing proportions of oxymethylene. These results showed that only the saturated liquid solution, containing a constant proportion of styrene and formaldehyde, participated in the copolymerization.

In order to study the radiation-induced copolymerization of bulk mixtures of formaldehyde and styrene in homogeneous liquid phase over the entire range of concentrations, we irradiated the reaction mixtures at higher temperatures ( $-30^{\circ}\text{C}$ ). As shown in Figure 9, the rate of copolymerization was found to be slightly higher than the rates observed for the copolymerization in methylene chloride solution at  $-78^{\circ}\text{C}$ . The effect of formaldehyde concentration on the molar composition of the copolymer is shown in Figure 9, together with the theoretical curve based on values of the monomer reactivity ratios, calculated by using the method of Fineman and Ross,<sup>14</sup> as  $r_1 \approx 30$ ;  $r_2 \approx 0$  where  $M_1$  is formaldehyde. Further details of the copolymerization experiments are given in Table II. The  $G$  (monomer) values are comparatively low, in the range of 400–8700; however, no attempts have been made to optimize the rates of polymerization. The molecular weights of all the copolymers and the homopolyoxymethylene are low and show some evidence of radiation-induced degradation. The intrinsic viscosities are in good agreement with those found with pure formaldehyde by Yamaoka for methylene chloride. Pure polyoxymethylene produced in bulk and in toluene at  $-78^{\circ}\text{C}$ . was found to be somewhat higher.<sup>3,4</sup> Further work is needed to elucidate the mechanism of chain

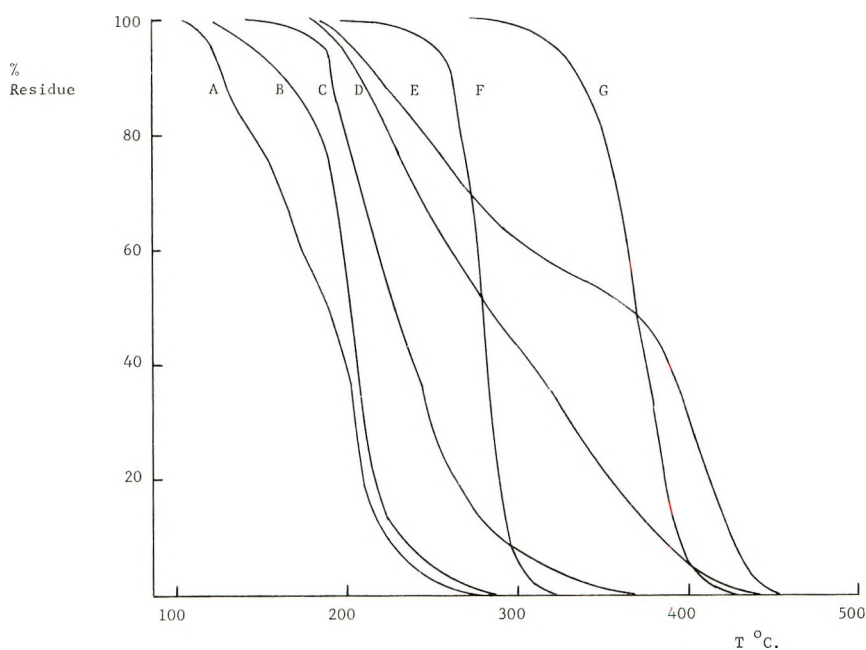


Fig. 10. Thermogravimetric analyses of various polymers measured at 2.5°C./min.: (A) pure polyoxymethylene; (B) copolymer 2-1; (C) copolymer 2-14; (D) copolymers 2-11, 2-12, 2-13 mixed; (E) copolymer 2-10; (F) commercial stabilized polymer; (G) polystyrene. The numbers refer to Table II.

termination. The independence of the molecular weight on dose rate and monomer concentration with formaldehyde in toluene at  $-78^{\circ}\text{C}$ . found by Nakashio et al.<sup>4</sup> indicates also that concurrent degradation may be accompanying the polymerization process as found, for example, with isobutylene.<sup>13</sup>

TABLE II  
Copolymerization of Formaldehyde and Styrene

No.	CH <sub>2</sub> O in monomer, mole-%	CH <sub>2</sub> -Cl <sub>2</sub> vol.-%	CH <sub>2</sub> O in copolymer, mole-%	Dose rates, rad/hr.	Irradiation dose, rad	Temp., °C.	[ $\eta$ ]	$\bar{G}(M)$
1	50	50	97	$2.8 \times 10^5$	$2 \times 10^6$	-78	0.39	2300
2	50	50	97	$3.8 \times 10^5$	$4 \times 10^6$	-78	0.51	1500
3	50	50	97	$3.8 \times 10^5$	$6 \times 10^6$	-78	0.22	900
4	50	50	97	$3.8 \times 10^5$	$8 \times 10^6$	-78	0.09	400
5	50	50	97	$3.8 \times 10^5$	$10 \times 10^6$	-78	0.13	—
6	100	50	(100)	$3.8 \times 10^5$	$10 \times 10^6$	-78	0.09	—
10	4.5	0	70	$2.5 \times 10^4$	$4.5 \times 10^5$	-30	—	2700
11	20	0	91	$2.5 \times 10^4$	$4.5 \times 10^5$	-30	0.39	5400
12	33	0	93	$2.5 \times 10^4$	$4.5 \times 10^5$	-30	0.41	6500
13	51.5	0	95	$2.5 \times 10^4$	$4.5 \times 10^5$	-30	0.31	8700
14	90	0	97	$3.8 \times 10^4$	$10 \times 10^5$	-78	0.09	—

### Thermal Stability of the Copolymers

Thermal gravimetric analysis was used to examine the thermal stability of the copolymers. In Figure 10 the results are shown for polyoxymethylene of low molecular weight prepared by irradiation in bulk, a commercial, stabilized polyoxymethylene, polystyrene, and a number of the styrene-formaldehyde copolymers. It can be seen that catastrophic degradation begins at about 105°C. for the pure polyoxymethylene, at 230°C. for the commercial, stabilized polymers, and at 330°C. for polystyrene. The copolymers obtained at -78°C. in bulk and in methylene chloride solution started to degrade at 120 and 160°C., respectively, although both contained about 3 mole-% of styrene and the bulk material had a considerably lower molecular weight. The copolymers obtained by irradiation in bulk

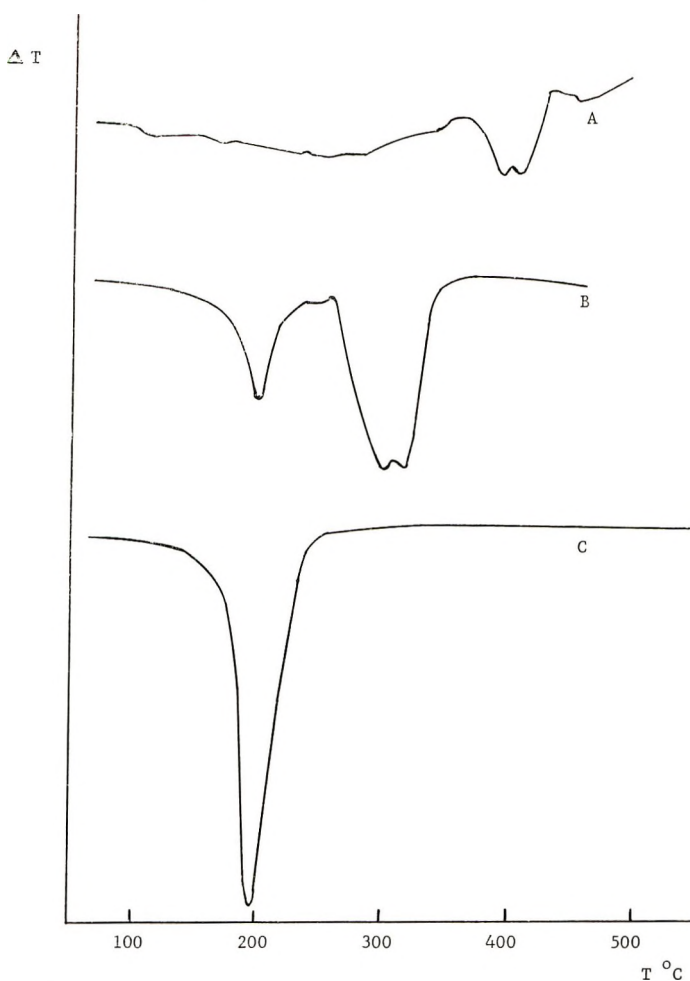


Fig. 11. Differential thermal analysis: (A) polystyrene; (B) commercial stabilized polyoxymethylene; (C) pure polyoxymethylene.

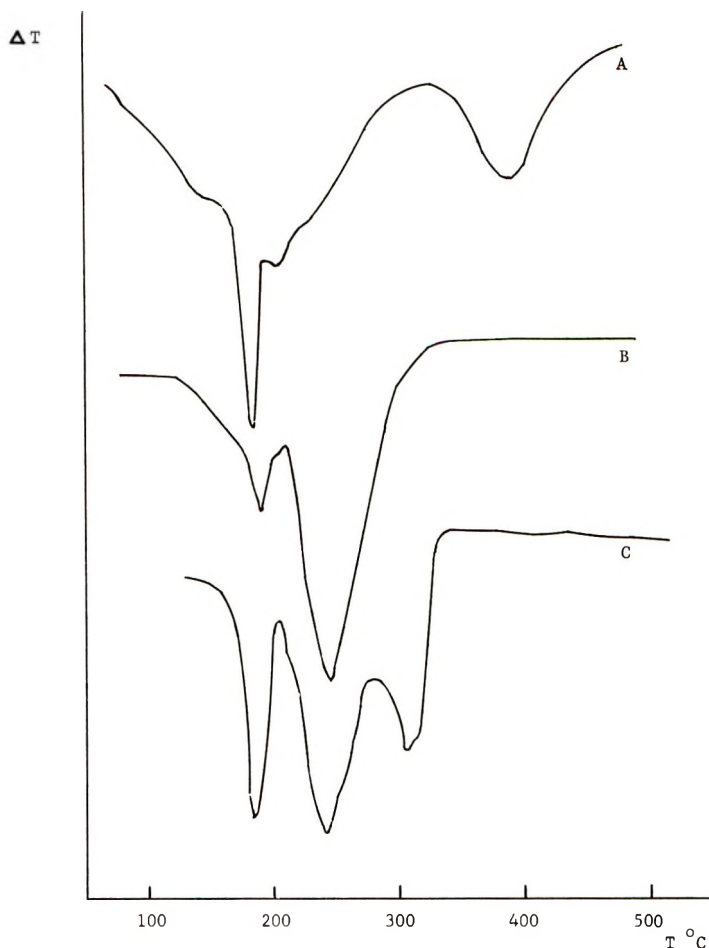


Fig. 12. Differential thermal analysis: (A) physical mixture of 90% polyoxymethylene plus 10% polystyrene; (B) copolymer 2-1; (C) copolymer 2-14.

at  $-30^{\circ}\text{C}$ . started to degrade at about  $190^{\circ}\text{C}$ . and at a lower rate of degradation. The copolymer containing 30 mole-% of styrene showed a distinct two-step degradation curve which suggested the presence of polystyrene blocks in the copolymer. Careful refractionation of this copolymer failed to isolate any additional amount of homopolystyrene.

Differential thermal analysis was also carried out on the various polymers and copolymers to try to detect differences in their structure. The thermograms of pure polyoxymethylene, polystyrene, and a commercial, stabilized polyoxymethylene are shown in Figure 11. Marked endotherms are found at  $200^{\circ}\text{C}$ . and close to  $400^{\circ}\text{C}$ . for polyoxymethylene and polystyrene, whereas the commercial polyoxymethylene shows the pure polyoxymethylene endotherm plus a larger endotherm at about  $300^{\circ}\text{C}$ . In Figure 12 the thermograms of copolymers prepared at  $-78^{\circ}\text{C}$ . in bulk and in methylene

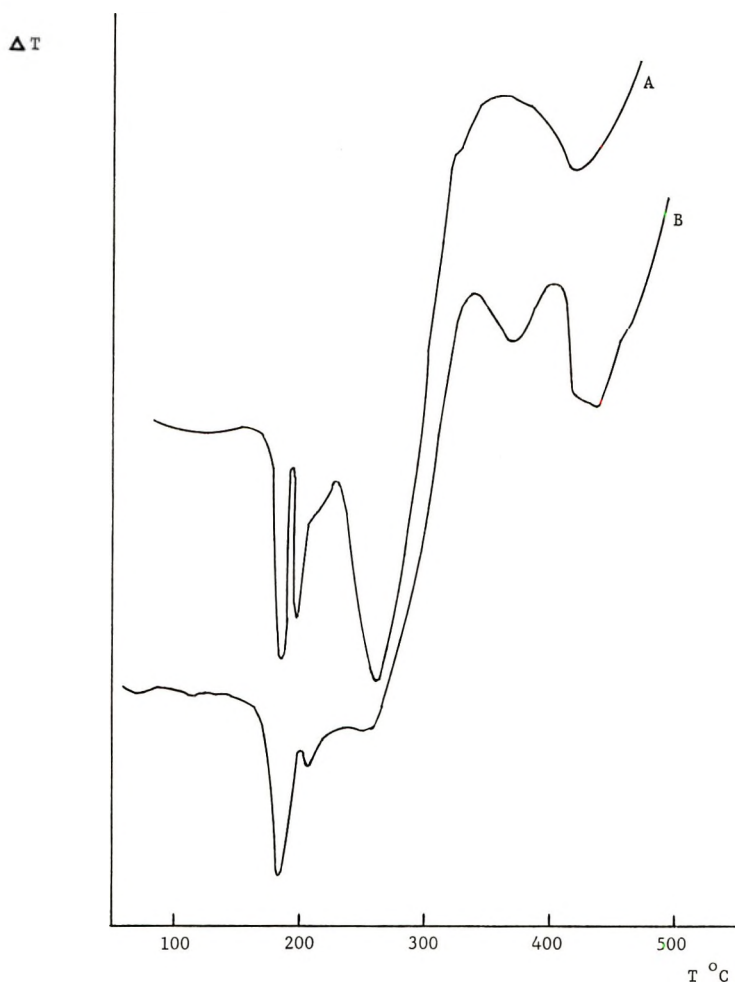


Fig. 13. Differential thermal analysis: (A) 70:30 copolymer 2-10; (B) 93:7 copolymer 2-12.

chloride solution and of a physical mixture of polyoxymethylene and polystyrene are shown. No endotherm corresponding to polystyrene is shown in the copolymers although very apparent with the physical mixture. In Figure 13, on the other hand, where the thermograms of two copolymers prepared at  $-30^{\circ}\text{C}$ . are shown, there is a clear indication of a polystyrene endotherm at about  $400^{\circ}\text{C}$ . An intermediate endotherm can be seen for all the copolymers examined.

The copolymer prepared at  $-30^{\circ}\text{C}$ . which contained 30 mole-% of styrene was degraded by treatment with strong acid. A small amount of polystyrene was isolated comprising about 30% of the total styrene content. The molecular weight was about 200,000, quite similar to that obtained by the radiation polymerization of pure styrene at  $-30^{\circ}\text{C}$ .



Since polyoxymethylene copolymer forms much faster than polystyrene at  $-30^{\circ}\text{C}$ . it was suspected that polystyrene may be grafted on to the polymer either at broken chain ends or as side chains. To investigate this possibility, finely powdered polyoxymethylene was irradiated at  $-30^{\circ}\text{C}$ . in styrene monomer. Although a small amount of polystyrene was formed, no styrene was found to be incorporated into the polyoxymethylene after its isolation in benzene. However, little swelling occurred under these conditions, and so the experiments were not conclusive. It seems clear, however, that a few long polystyrene blocks are formed during the radiation polymerization at  $-30^{\circ}\text{C}$ ., probably by a different mechanism to that causing the formation of random copolymer. The absence of blocks at  $-78^{\circ}\text{C}$ . suggests that a radical mechanism may be responsible for the formation of the blocks at  $-30^{\circ}\text{C}$ .

The copolymers formed were of low molecular weight and contained no added stabilizer. The increased thermal stability was therefore quite gratifying. Further details of the radiation-induced copolymerization of styrene and other monomers with formaldehyde are presently being investigated, and the results will be the subject of another communication.

We would like to thank Mr. T. Tarim of N. C. State University for carrying out the thermogravimetric and differential thermal analyses. This investigation was made possible through the generous support of the Division of Isotopes Development, U. S. Atomic Energy Commission.

### References

1. C. Chachaty, M. Magat, and L. Ter Minassian, *J. Polymer Sci.*, **48**, 139 (1960).
2. K. Hayashi, H. Yamaoka, K. Fujiwara, M. Sakamoto, S. Mori, T. Natori, H. Yoshida, and S. Okamura, *Industrial Uses of Large Radiation Sources*, I.A.E.A., Vienna, 1963, pp. 219-332.
3. H. Yamaoka, K. Hayashi, and S. Okamura, *Makromol. Chem.*, **76**, 196 (1964).
4. S. Nakashio, M. Ueda, and K. Takahashi, *Makromol. Chem.*, **83**, 23 (1965).
5. Y. Tsuda, *J. Polymer Sci.*, **49**, 369 (1961).
6. G. Natta, F. Pregaglia, G. Mazzanti, V. Zamboni, and M. Binaghi, *European Polymer J.*, **1**, 25 (1965).
7. K. Nord, H. Kawazura, T. Moriyama, and S. Yoshioka, *Makromol. Chem.*, **83**, 35 (1965).
8. Du Pont, Brit. Pat. 911,960 (1961).
9. W. Fukuda and H. Wakiuchi, *Kogyo Kagaku Zasshi*, **67**, 1965 (1964).
10. R. Spence and W. Wild, *J. Chem. Soc.*, **1935**, 338.
11. J. F. Walker, *Formaldehyde*, 3rd Ed., Reinhold, New York, 1964, p. 47.
12. E. Collinson, F. S. Dainton, and H. A. Gillis, *J. Phys. Chem.*, **63**, 909 (1959).
13. V. Stannett, F. C. Bahstetter, J. A. Meyer, and M. Szwarc, *Int. J. Appl. Rad. Isotopes*, **15**, 747 (1964).
14. M. Fineman and S. D. Ross, *J. Polymer Sci.*, **5**, 259 (1950).
15. Y. P. Castille and V. Stannett, *J. Polymer Sci. B*, **2**, 1097 (1964).
16. H. Sobue and Y. Tabata, *J. Polymer Sci.*, **43**, 459 (1960).
17. C. S. H. Chen and R. F. Stamm, *J. Polymer Sci.*, **58**, 369 (1962).
18. A. Chapiro and V. Stannett, *J. Chim. Phys.*, **56**, 830 (1959).
19. Y. Tsuda, *J. Polymer Sci.*, **54**, 193 (1961).
20. P. H. Plesch, Ed., *The Chemistry of Cationic Polymerization*, Macmillan, New York, 1963, Chap. 3, p. 132, and Chap. 17.

### Résumé

La copolymérisation induite par irradiation du styrène avec le formaldéhyde liquide, en bloc et en solution a été étudié à basse température. En bloc et en solution dans le chlorure de méthylène, la copolymérisation se passe tandis qu'en solution dans l'éther diéthylique uniquement l'homopolymérisation du formaldéhyde a été observée. A  $-78^{\circ}\text{C}$ , en bloc et en solution dans le chlorure de méthylène, on ne trouve aucune preuve de la formation de blocs de polystyrène, tandis qu'à  $-30^{\circ}\text{C}$ , en bloc, environ 30% du styrène du copolymère se présente sous la forme de blocs de poids moléculaire élevé. La vitesse de copolymérisation dans une solution de chlorure de méthylène est du premier ordre par rapport à la vitesse de la dose et de troisième ordre par rapport à la concentration en formaldéhyde, ce qui est similaire au résultat rapporté pour le formaldéhyde en solution poluénique. Les stabilités thermiques des polymères ont été trouvées intermédiaires entre celles du polyoxyméthylène pur et des polymères commerciaux stabilisés. Étant donné que ces derniers étaient de poids moléculaire plus élevé et contiennent des stabilisants additifs, on admet que les stabilités thermiques accrues des xopolymères obtenus sont particulièrement significatives.

### Zusammenfassung

Die strahlungsinduzierte Kopolymerisation von Styrol und flüssigem Formaldehyd in Substanz und in Lösung wurde bei tiefen Temperaturen untersucht. In Substanz und in Methylenchloridlösung trat Kopolymerisation ein, während in Diäthylätherlösungen nur eine Homopolymerisation des Formaldehyds festgestellt werden konnte. Bei  $-78^{\circ}\text{C}$  konnte in Substanz und in Methylenchloridlösung kein Hinweis auf die Bildung von Polystyrolblöcken gefunden werden, während bei  $-30^{\circ}\text{C}$  in Substanz etwa 30% des Styrolgehalts des Kopolymeren durch hochmolekulare Blöcke gebildet wurde. Die Kopolymerisationsgeschwindigkeit war, ähnlich wie bei den früher für Formaldehyd in Toluollösung erhaltenen Ergebnissen, von erster Ordnung in Bezug auf die Dosisleistung und von dritter Ordnung in Bezug auf die Formaldehydkonzentration. Die thermische Stabilität der Kopolymeren lag zwischen derjenigen von reinem Polyoxymethylen und von handelsüblichen stabilisierten Polymeren. Das letztere ein höheres Molekulargewicht besaßen und zugesetzte Stabilisatoren enthielten, erscheint die erhöhte thermische Stabilität der Kopolymeren als besonders signifikant.

Received November 12, 1965

Revised December 20, 1965

Prod. No. 5046A

## Preparation of Crystalline Polyamides by the Alternating Copolymerization of Aziridines and Cyclic Imides

TSUTOMU KAGIYA, SHIZUO NARISAWA, KUNIYOSHI MANABE, MIKIO KOBATA, and KENICHI FUKUI, *Faculty of Engineering, Kyoto University, Kyoto, Japan*

### Synopsis

The copolymerization of aziridines and cyclic imides was studied. Aziridines copolymerized alternately with cyclic imides to give crystalline polyamides. Ethylenimine and succinimide copolymerized to nylon 2,4, melting near 300°C., without any catalyst. Similarly, the corresponding crystalline polyamides were obtained from the systems of 1,2-propylenimine-succinimide, ethylenimine-glutarimide, and ethylenimine-phthalimide. The copolymerization of aziridine and cyclic imides in the presence of  $\text{BF}_3\text{OEt}_2$  gave a copolymer which was rich in aziridine units, whereas, the addition of triethylamine had no influence on the copolymer composition. A mechanism of copolymerization was proposed based on the facts that *N*-tetramethylenesuccinamide was obtained by the reaction of pyrrolidine and succinimide, *N*-acetyethylenimine reacted with acetamide to yield *N,N'*-diacetyethylenediamine and that the rate of this copolymerization was dependent on the electrophilicity of imide.

### INTRODUCTION

In recent years, investigations have been carried out on the copolymerization of aziridines with cyclic compounds, such as anhydrides,<sup>1</sup> carbonates,<sup>2</sup> ethers,<sup>3,4</sup> and esters.<sup>5</sup>

As a part of the investigation of the copolymerization of aziridines with various kinds of cyclic compounds containing a carbonyl group<sup>6,7</sup> the copolymerization of aziridines and cyclic imides was studied. Aziridines copolymerized alternately with cyclic imides, which are unable to homopolymerize by the scission of imide ring<sup>8</sup> and yielded crystalline polyamides.

### EXPERIMENTAL

#### Materials

Ethylenimine was obtained commercially. 1,2-Propylenimine<sup>9</sup> and *N*-ethylethylenimine<sup>10</sup> were prepared according to the literature. The aziridines were dried over potassium hydroxide pellets and sodium hydride, and then fractionated before use. Physical constants were: ethylen-

imine, b.p. 55.5–56°C.; 1,2-propylenimine, b.p. 65.7–66°C. (reported<sup>9</sup> b.p. 66–67°C.); *N*-ethylethylenimine, b.p. 51.0–51.1°C. (reported<sup>10</sup> b.p. 51°C.).

Succinimide was obtained commercially, recrystallized from acetone, and dried *in vacuo*, m.p. 125–126°C. Phthalimide was obtained commercially, purified by sublimation, m.p. 238°C. *N*-Methylsuccinimide was prepared from succinic anhydride and methylamine, recrystallized from acetone–diethyl ether, and dried *in vacuo*, m.p. 70–71°C. (reported<sup>11</sup> m.p. 66°C.).

ANAL. Calcd. for  $C_5H_7NO_2$ : C, 53.09%; H, 6.24%; N, 12.38%. Found: C, 53.36%; H, 6.47%; N, 12.70%.

Glutarimide was prepared from glutaric acid and formamide, recrystallized from acetone, and dried *in vacuo*, m.p. 156°C. (reported<sup>12</sup> m.p. 150–152°C.).

ANAL. Calcd. for  $C_5H_7NO_2$ : C, 53.09%; H, 6.24%; N, 12.38%. Found: C, 53.33%; H, 6.39%; N, 12.08%.

Maleimide was prepared via *N*-carbamylmaleimide from maleic anhydride and urea, recrystallized from ethyl acetate, and dried *in vacuo*, m.p. 93°C. (reported<sup>13</sup> m.p. 92–94°C.).

ANAL. Calcd. for  $C_4H_3NO_2$ : C, 49.49%; H, 3.12%; N, 14.43%. Found: C, 49.21%; H, 3.63%; N, 14.99%.

Solvents for the copolymerization reaction were purified by the usual method.<sup>14</sup> Triethylamine was distilled over potassium hydroxide pellets, b.p. 89–90°C.  $BF_3OEt_2$  was purified by distillation, b.p. 126°C.

### Copolymerization Procedure

Measured amounts of cyclic imide and solvent were placed in a glass ampule under nitrogen atmosphere, and aziridine and catalyst were added to this system under cooling with Dry Ice–methanol. The ampule was then sealed and kept at a constant temperature for a definite period. The reaction products of aziridine with succinimide, glutarimide, or *N*-methylsuccinimide were washed repeatedly with methanol, acetone, and diethyl ether, except for the reaction products of aziridine with phthalimide or maleimide, which were washed with methanol and diethyl ether, and then dried *in vacuo*.

The composition of the copolymer was determined from the contents of carbon, hydrogen, and nitrogen by elementary analysis. The melting point of the copolymer was measured visually in a nitrogen atmosphere in a capillary with an electric heater. The reduced viscosity of the copolymer was calculated from the viscosity measurement of 0.25% solution of formic acid at 35°C. Infrared spectrum obtained by the use of the potassium bromide pellet technique on a Shimadzu infrared spectrophotometer, Model IR-27, with sodium chloride prism. The x-ray diffraction diagram was recorded by the use of standard techniques with a powder camera on a Shimadzu x-ray diffractometer, Model GX-3B, employing Ni-filtered  $CuK\alpha$  radiation. A differential thermogram was obtained using sand-

wiches in powdery  $\alpha$ -alumina as a diluent on a Rigaku Denki differential thermal apparatus, Model VTP-32, with nickel cell.

### Hydrolysis of the Copolymer

A 10-g. portion of the copolymer of ethylenimine and succinimide was hydrolyzed by refluxing in 50 ml. of 20% hydrochloric acid for 10 hr. and then filtered. The filtrate was made alkaline with 30% aqueous solution of sodium hydroxide and distilled. The distillate, being positive (purple) in the ninhydrin reaction, was neutralized with hydrochloric acid with the use of phenolphthalein as an indicator and evaporated *in vacuo*; a colorless solid was obtained. The infrared spectrum of this material was identical with that of authentic ethylenediamine dihydrochloride and displayed characteristic peaks of amine salt at near 3000, 1602, 1508, and 803  $\text{cm}^{-1}$ . A chloride of this material was titrated with 0.1N  $\text{AgNO}_3$  by Mohr's method<sup>15</sup> and results compared with those for authentic ethylenediamine dihydrochloride.

Calcd. for  $\text{C}_2\text{H}_{10}\text{N}_2\text{Cl}_2$ : Cl, 53.30%. Found: Cl, 53.37%. Found for authentic sample of ethylenediamine dihydrochloride: Cl, 53.34%.

In view of the above fact, it is considered that the copolymer of ethylenimine and succinimide contains a polyamide having the structure



### Reaction of Pyrrolidine with Succinimide

A mixture of 6.40 g. of pyrrolidine and 2.97 g. of succinimide was heated at 70°C. for 2 hr. in a glass ampule. The crystals obtained were washed with diethyl ether and recrystallized from ethanol-diethyl ether to yield 4.87 g. (95.5%) of colorless plates, *N*-tetramethylenesuccinamide, m.p. 109.5–110°C.

ANAL. Calcd. for  $\text{C}_8\text{H}_{14}\text{N}_2\text{O}_2$ : C, 56.45%; H, 8.29%; N, 16.46%. Found: C, 56.20%; H, 8.57%; N, 16.72%. The infrared spectrum (KBr) showed peaks at 3370, 3180 (NH), 1657, 1641, and 1633  $\text{cm}^{-1}$  (C=O).

### *N,N'*-Diacetylenediamine

A mixture of 2.5 g. of ethylenediamine and 7.4 g. of ethyl acetate was refluxed for 46 hr. The crystals formed were filtered and recrystallized from ethanol-ethyl acetate, giving 3.03 g. (50.5%) of colorless needles, m.p. 173–174°C. (reported<sup>16</sup> m.p. 173–173.5°C.). The infrared spectrum (KBr) showed characteristic peaks of secondary amide<sup>17</sup> at 3310, 3070, 1647, and 1555  $\text{cm}^{-1}$ .

### Reaction of *N*-Acetythylenimine with Acetamide

A solution of 4.25 g. of *N*-acetythylenimine, 2.95 g. of acetamide, and 20 ml. of dimethylformamide was heated in a sealed glass ampule at 150°C. for 8 hr., and then the most of solvent and unreacted materials was removed under reduced pressure. After the residue was washed with acetone, the crystals were recrystallized from ethanol-ethyl acetate to yield colorless



needles (0.912 g., 12.7%), m.p. 173–174°C., which were identified by the mixed melting point test and by comparison of the infrared spectrum with that of *N,N'*-diacetylenediamine.

ANAL. Calcd. for  $C_6H_{12}N_2O_2$ : C, 49.98%; H, 8.39%; N, 19.43%. Found: C, 50.05%; H, 8.31%; N, 19.56%.

## RESULTS AND DISCUSSION

### Copolymerization of Ethylenimine and Succinimide

The results of the copolymerization of ethylenimine and succinimide are shown in Table I.

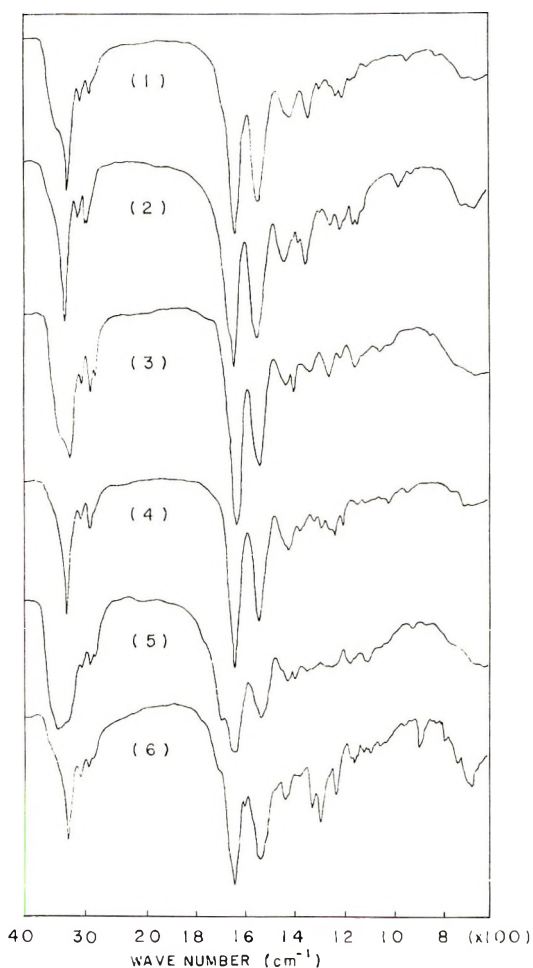


Fig. 1. Infrared spectra of the copolymers of aziridines and cyclic imides: (1) copolymer of ethylenimine and succinimide; (2) copolymer of 1,2-propylenimine and succinimide; (3) copolymer of ethylenimine and *N*-methylsuccinimide; (4) copolymer of ethylenimine and glutarimide; (5) copolymer of ethylenimine and maleimide; (6) copolymer of ethylenimine and phthalimide.

TABLE I  
Copolymerization of Ethylenimine and Succinimide<sup>a</sup>

Expt. no.	Monomers, g. (mole)		Catalyst, mole $\times 10^4$	Solvent	Yield, g.	$\eta_{sp}/c$ , dl./g.	M.p., °C.	Copolymer composition <sup>b</sup>	
	C <sub>2</sub> H <sub>5</sub> N	C <sub>4</sub> H <sub>5</sub> NO <sub>2</sub>						C <sub>2</sub> H <sub>5</sub> N, mole-%	C <sub>4</sub> H <sub>5</sub> NO <sub>2</sub> , mole-%
1	3.876 (0.09)	2.973 (0.03)	—	—	2.660	0.33	294-301 304 <sup>c</sup>	50.0	50.0
2	3.876 (0.09)	2.973 (0.03)	—	Toluene	0.572	0.15	280-306	51.8	48.2
3	3.876 (0.09)	2.973 (0.03)	—	Anisole	0.237	0.13	297-307	49.6	50.4
4	3.876 (0.09)	2.973 (0.03)	—	Dimethyl-formamide	0.850	0.15	293-299	57.6	42.4
5	2.584 (0.06)	2.973 (0.03)	—	Toluene	0.282	0.16	291-304	49.6	50.4
6	1.292 (0.03)	2.973 (0.03)	—	Toluene	0.429	0.09	277-310	55.0	45.0
7	1.292 (0.03)	5.946 (0.06)	—	Toluene	0.583	0.10	284-304	50.4	49.6
8	3.876 (0.09)	2.973 (0.03)	NEt <sub>3</sub> , 50	Toluene	0.869	0.11	300-306	54.3	45.7
9	3.876 (0.09)	2.973 (0.03)	NEt <sub>3</sub> , 100	Toluene	1.162	0.11	300-306	49.6	50.4
10	3.876 (0.09)	2.973 (0.03)	BF <sub>3</sub> OEt <sub>2</sub> , 5	Toluene	2.259	— <sup>d</sup>	354 (dec.)	67.4	32.6
11	3.876 (0.09)	2.973 (0.03)	BF <sub>3</sub> OEt <sub>2</sub> , 10	Toluene	3.054	— <sup>d</sup>	345 (dec.)	73.9	26.1

<sup>a</sup> Solvent: 20 ml., temp.: 70°C., time: 15 hr., except for expt. 1 (polymerized for 1 hr.).

<sup>b</sup> Composition determined by elementary analysis.

<sup>c</sup> Melting point determined by differential thermal analysis.

<sup>d</sup> The copolymer obtained was insoluble in formic acid.

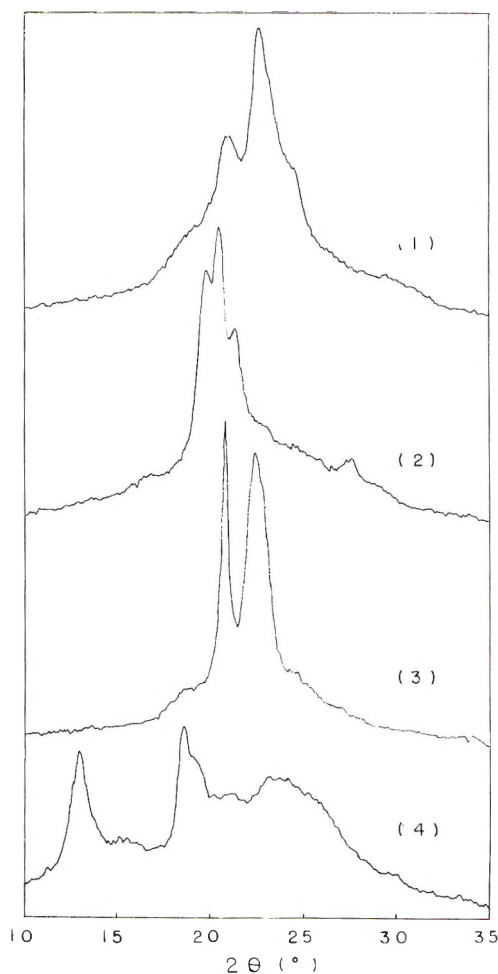


Fig. 2. X-ray diffraction diagrams of the copolymers of aziridines and cyclic imides: (1) copolymer of ethylenimine and succinimide; (2) copolymer of 1,2-propylenimine and succinimide; (3) copolymer of ethylenimine and glutarimide; (4) copolymer of ethylenimine and phthalimide.

Succinimide, being unable to homopolymerize,<sup>8</sup> was allowed to copolymerize with ethylenimine in the absence of any catalyst to give a white or light yellow powdery polymer. The melting point of the copolymer of ethylenimine and succinimide was observed at near 300°C. (Fig. 3), which was identical with that of the polymer obtained by the polyaddition reaction of *N,N'*ethylenedisuccinimide and ethylenediamine.<sup>18</sup> This value lies between that for nylon 3 (320–330°C.)<sup>19a</sup> and that for nylon 4 (265°C.).<sup>19b</sup> The copolymer of ethylenimine and succinimide, excepting the copolymer obtained with  $\text{BF}_3\text{OEt}_2$  catalyst, was soluble in hot water, formic acid, and *m*-cresol, and insoluble in ethyl ether, acetone, ethanol, chloroform, dimethylformamide, and toluene.

As shown in Table I, the molar ratio of ethylenimine and succinimide units in the copolymer did not depend on the composition of monomers, but was almost unity in this copolymerization. The infrared spectrum of the copolymer (Fig. 1) was identical with that of nylon 24 obtained by the polyaddition reaction of *N,N'*-ethylenedisuccinimide and ethylenediamine, and displayed the characteristic peaks of polyamide at 3290, 3070, 1640, and 1550  $\text{cm}^{-1}$ . The copolymer was confirmed to be crystalline from the x-ray diffraction diagram (Fig. 2). Further, hydrolysis of the copolymer yielded ethylenediamine. From these results, it is considered that the copolymerization of ethylenimine and succinimide took place alternately to give a polyamide having the unit structure  $\text{-(NHCH}_2\text{CH}_2\text{NHCO-CH}_2\text{CH}_2\text{CO)-}$ .

In this copolymerization, triethylamine acted as a catalyst and had a negligible effect on such properties of the copolymer as melting point, solubility, infrared spectrum, x-ray diagram, and composition.  $\text{BF}_3\text{OEt}_2$ , on the other hand, accelerated the rate of copolymerization markedly and gave an amorphous polymer which was very hygroscopic, insoluble in formic acid, decomposed over 350°C. without melting, and rich in ethylenimine units.

### Copolymerization of Various Kinds of Aziridines and Cyclic Imides

The results of the copolymerization of various kinds of aziridines and cyclic imides are shown in Table II.

1,2-Propylenimine was less reactive in copolymerization with succinimide than ethylenimine. The propylenimine-succinimide reaction, however, yielded a white powdery polymer which melted at 243°C. (Fig. 3) and was soluble in hot water, formic acid, and *m*-cresol. The copolymer displayed the characteristic peaks of polyamide in the infrared spectrum (Fig. 1) and was proved to be crystalline from x-ray diagram (Fig. 2). From the results of the elementary analysis, infrared spectrum, and x-ray diagram, it is considered that 1,2-propylenimine and succinimide copolymerized alternately to polyamide.

In the copolymerization of *N*-ethylethylenimine and succinimide no polymer was obtained under the condition mentioned in Table II. The copolymerization of ethylenimine and *N*-methylsuccinimide took place less easily than that of ethylenimine and succinimide and gave a polymer displaying the characteristic peaks of polyamide (Fig. 1). The copolymer obtained with the use of  $\text{BF}_3\text{OEt}_2$  catalyst was amorphous, insoluble in formic acid, and had a large ethylenimine content.

The copolymerization of glutarimide with ethylenimine was slower than the case of succinimide, and gave a crystalline copolymer (Fig. 2) which melted at near 236°C. (Fig. 3) and displayed the characteristic peaks of polyamide (Fig. 1). The copolymer obtained in run 17 at high temperature was amorphous, however, and the nature of the copolymer was similar to that of the copolymer obtained with the use of  $\text{BF}_3\text{OEt}_2$ .

TABLE II  
Copolymerization of Aziridines and Cyclic Imides

Expt. no.	Monomers, g. (mole) <sup>a</sup>		Solvent <sup>b</sup>	Temp., °C.	Time, hr.	Yield, g.	$\eta_{sp}/c$ , dl./g.	M.p., °C.	Composition <sup>c</sup>	
	Imine	Imide							Imine, mole-%	Imide, mole-%
12	PI, 3.426 (0.06)	SI, 2.973 (0.03)	Toluene	150	25	0.605	0.11	230-240 243 <sup>d</sup>	50.4	49.6
13	EEL, 4.267 (0.06)	SI, 2.973 (0.03)	Toluene	150	125	0	—	—	—	—
14	EL, 0.431 (0.01)	MSI, 1.131 (0.01)	Anisole	150	45	0.015	— <sup>e</sup>	—	—	—
15 <sup>f</sup>	EL, 0.431 (0.01)	MSI, 1.131 (0.01)	Anisole	150	5	0.562	— <sup>e</sup>	346 (dec.)	73.6	26.4
16	EL, 3.876 (0.09)	GI, 3.394 (0.03)	—	70	17	0.559	0.18	238-251 234 <sup>e</sup>	57.25	42.75
17	EL, 3.876 (0.09)	GI, 3.394 (0.03)	Anisole	150	5	1.373	— <sup>e</sup>	360 (dec.)	74.0	26.0
18	EL, 3.876 (0.09)	MI, 2.912 (0.03)	Toluene	70	4	1.115	— <sup>e</sup>	255-344 (dec.)	60.8	39.2
19	EL, 3.876 (0.09)	PhI, 4.414 (0.03)	Anisole	70	5	0.341	— <sup>e</sup>	281-284 291 <sup>d</sup>	52.5	47.5

<sup>a</sup> Monomers: SI = succinimide, MSI = *N*-methylsuccinimide, GI = glutarimide, MI = maleimide, PhI = phthalimide, EI = ethylenimine, EEL = *N*-ethylethylenimine, PI = 1,2-propylenimine.

<sup>b</sup> Solvent: 20 ml., except for expts. 3 and 4, in which 3 ml. of solvent was used.

<sup>c</sup> The composition was determined by elementary analysis.

<sup>d</sup> The melting point was determined by the differential thermal analysis.

<sup>e</sup> The copolymer obtained was insoluble in formic acid.

<sup>f</sup>  $\text{BF}_3\text{OEt}_2$ ,  $2 \times 10^{-4}$  mole, was added as a catalyst.



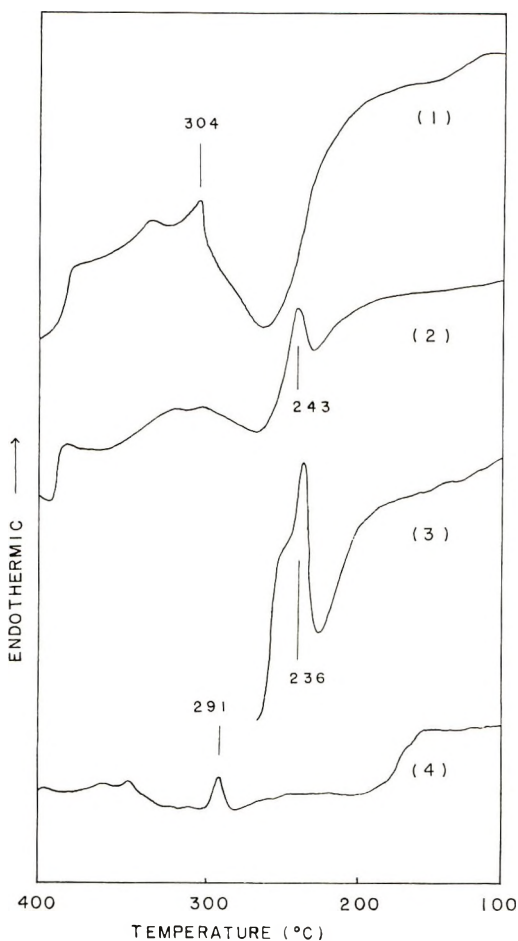
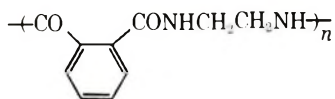


Fig. 3. Differential thermal analysis diagrams of the copolymers of aziridines and cyclic imides (1) copolymer of ethylenimine and succinimide; (2) copolymer of 1,2-propylenimine and succinimide; (3) copolymer of ethylenimine and glutarimide; (4) copolymer of ethylenimine and phthalimide.

Maleimide copolymerized with ethylenimine quite easily in comparison with succinimide to yield an amorphous copolymer which displayed the characteristic peaks of polyamide (Fig. 1) and was insoluble in formic acid.

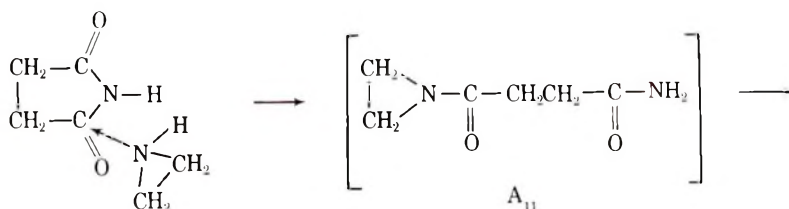
Phthalimide and ethylenimine copolymerized relatively rapidly to yield a crystalline copolymer (Fig. 2) which melted at about 291°C. (Fig. 3), contained a portion insoluble in formic acid. It is considered that the copolymer obtained from ethylenimine and phthalimide had the structure



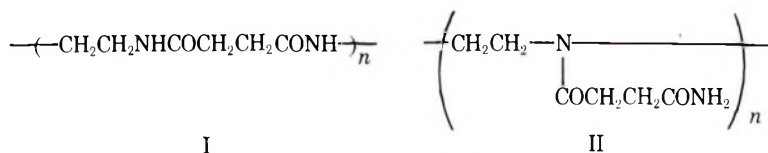
which is similar to that of the polymer obtained, for instance, by the interfacial polycondensation of phthaloyl chloride and ethylenediamine.<sup>20</sup>

### Mechanism of Copolymerization

It may be reasonable to consider that the copolymerization of aziridine and cyclic imide is a kind of acid-base reaction to form an adduct. In view of the fact that *N*-tetramethylenesuccinamide was obtained by the reaction of pyrrolidine and succinimide, *N*-ethylenesuccinamide ( $A_{11}$ ) is considered to form first in the copolymerization of ethylenimine and succinimide.

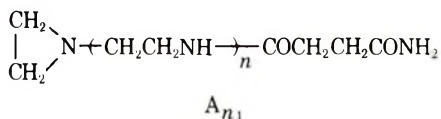


The melting points, infrared spectra, x-ray diagrams, and hydrolysis data indicate that the polymer formed by the scission of aziridine ring of  $A_{11}$  is not likely to have the structure of polyethylenimine derivative (II)



but is most likely a polyamide (I). This result is in accord with the fact that *N*-acetyethylenimine reacted with acetamide to yield *N,N'*-diacetyethylenediamine. These results are attributed to the fact that the reactivity of carbonium ion formed by the scission of aziridine ring of  $A_{11}$  is much larger toward the primary nitrogen atom than the tertiary nitrogen of  $A_{11}$ . This consideration is consistent with the tendency of  $\pi$ -electron density of the nitrogen atom ( $q_N$ ) in acetamides, as calculated by the simple LCAO MO method,<sup>21</sup> i.e.,  $\text{CH}_3\text{CONH}_2 > \text{CH}_3\text{CONHCH}_3 > \text{CH}_3\text{CON}(\text{CH}_3)_2$ , for which  $q_N$  is, respectively, 1.750, 1.742, and 1.610.

The presence of  $\text{BF}_3\text{OEt}_2$  in the copolymerization of ethylenimine and succinimide brought about an increase of ethylenimine content in the polymer. This may be attributable to the formation of a poly-imine linkage,  $A_{n1}$  from the *N*-substituted aziridine compound and production of an amorphous polymer by the scission of aziridine ring of  $A_{n1}$ .



Similarly, it is believed that other aziridines and cyclic imides also copolymerized by the mechanism mentioned above.

The reactivity of copolymerization of ethylenimine and cyclic imides decreased in the following order; maleimide > phthalimide > succinimide > glutarimide > *N*-methylsuccinimide. This order agrees with the order of the rate (in liters/mole-second) of alkaline hydrolysis of the imides:<sup>22</sup> succinimide (3.16) > glutarimide (0.63) > *N*-methylsuccinimide (0.15), and with the acidity ( $pK_a$ ) of cyclic imides:<sup>23,24</sup> phthalimide (8.3) > succinimide (9.656) > glutarimide (11.43). In the hydrolysis of imide, the rate-determining step is considered to be the reaction of a hydroxide ion with an un-ionized molecule.<sup>25</sup> The cause of the relation between  $pK_a$  of imide and rate of copolymerization is not clear, but these facts suggest that the electrophilic reaction of imide in either initiation or propagation process is the rate-determining step of this copolymerization.

More detailed study of this copolymerization will be reported in a subsequent paper.

### References

1. Brit. Pat. 784,059 (1957); U. S. Pat. 3,036,974 (1962).
2. U. S. Pat. 2,824,857 (1958).
3. Brit. Pat. 466,344 (1937).
4. C. G. Overberger and M. Tobkes, *J. Polymer Sci. A*, **2**, 2481 (1964).
5. T. Kagiya, S. Narisawa, K. Manabe, and K. Fukui, *J. Polymer Sci. B*, **3**, 617 (1965); *Kogyo Kagaku Zasshi*, **68**, 1741 (1965).
6. T. Kagiya, S. Narisawa, and K. Fukui, paper presented at 13th Symposium on High Polymer Chemistry, Tokyo, November 1964.
7. T. Kagiya, S. Narisawa, T. Ichida, K. Fukui, H. Yokota, and M. Kondo, *J. Polymer Sci. A-1*, **4**, 293 (1966).
8. H. K. Hall, Jr., and A. K. Schneider, *J. Am. Chem. Soc.*, **80**, 6409 (1958).
9. Y. Minoura, M. Takebayashi, and C. C. Price, *J. Am. Chem. Soc.*, **81**, 4689 (1957).
10. R. C. Elderfield and H. A. Hageman, *J. Org. Chem.*, **14**, 605 (1949).
11. J. Brecht and W. Boeddinghaus, *Ann.*, **251**, 320 (1889).
12. S. Sugawara and H. Shigehara, *J. Pharm. Soc. Japan*, **62**, 531 (1942).
13. P. O. Towney, R. H. Snyder, C. E. Bryan, R. P. Conger, F. S. Dovell, R. J. Kelly, and C. H. Stiteler, *J. Org. Chem.*, **25**, 56 (1960).
14. A. Weissberger et al., *Organic Solvents*, (*Technique of Organic Chemistry*, Vol. VII) Interscience, New York, 1955.
15. I. M. Kolthoff and V. A. Stenger, *Volumetric Analysis*, Vol. II, Interscience, New York, 1947, p. 256.
16. N. B. Tucker, *J. Am. Chem. Soc.*, **57**, 1989 (1935).
17. L. J. Bellamy, *The Infra-red Spectra of Complex Molecules*, Methuen, London; Wiley, New York, 1958, pp. 203.
18. T. Kagiya, M. Izu, S. Kawai, T. Matsuda, and K. Fukui, *J. Polymer Sci. A-1*, in press.
19. W. R. Sorenson and T. W. Campbell, *Preparative Methods of Polymer Chemistry*, Interscience, New York, 1961, (a) p. 90; (b) p. 239.
20. M. Katz, *J. Polymer Sci.*, **40**, 337 (1959).
21. S. Yoneda, I. Morishima, K. Fukui, and Z. Yoshida, *Kogyo Kagaku Zasshi*, **68**, 1074 (1965).

22. H. K. Hall, Jr., M. K. Brandt, and R. M. Mason, *J. Am. Chem. Soc.*, **80**, 6420 (1958).
23. G. Schwarzenbach and K. Lutz, *Helv. Chim. Acta*, **23**, 1162 (1940).
24. P. E. Stecher et al., *The Merck Index of Chemicals and Drugs*, 7th Ed., Merck & Co., Inc., 1960, p. 813.
25. J. T. Edward and K. A. Terry, *J. Chem. Soc.*, **1957**, 3527.

### Résumé

La copolymérisation des aziridines et des imides cycliques a été étudiée. Les aziridines copolymérisaient alternativement avec les imides cycliques pour former des polyamides cristallins. L'éthylènimine et le succinimide copolymérisaient pour former des nylons-2,4 fondant vers 300°C sans aucun catalyseur. Similairement des polyamides cristallins correspondant ont été obtenus au départ de systèmes de 1,2-propylènimine-succinimide, éthylènimine-glutarimide et éthylènimine-phthalimide. La copolymérisation d'aziridines et d'amides cycliques en présence de  $\text{BF}_3\text{OEt}_2$  donne un copolymère qui était riche en unités aziridiniques, tandis que l'addition de triéthylamine n'exerce aucune influence sur la composition du copolymère. Considérant que le *N*-tétraméthylène-succinimide, était obtenu par réaction de la pyrrolidine et de la succinimide, la *N*-acétyléthylènimine réagit avec l'acétamide pour former la *N,N'*-diacétyléthylènimine, et la vitesse de cette copolymérisation dépendait du caractère électrophile de l'imide; un mécanisme de copolymérisation a été proposé.

### Zusammenfassung

Die Copolymerisation von Aziridinen und zyklischen Imiden wurde untersucht. Aziridine zeigten mit zyklischen Imiden eine alternierende Copolymerisation unter Bildung kristalliner Polyamide. Äthylenimin und Succinimid copolymerisierten ohne jeden Katalysator zu 2,4-Nylon mit einem Schmelzpunkt bei 300°C. In ähnlicher Weise wurden die entsprechenden kristallinen Polyamide aus 1,2-Propylenimin-Succinimid, Äthylenimin-Glutarimid und Äthylenimin-Phthalimid erhalten. Die Copolymerisation von Aziridinen und zyklischen Imiden in Gegenwart von  $\text{BF}_3\text{OEt}_2$  liefert ein an Aziridineinheiten reiches Copolymeres, während der Zusatz von Triäthylamin keinen Einfluss auf die Copolymerzusammensetzung hatte. Auf Grund der Befunde, dass durch die Reaktion von Pyrrolidin und Succinimid *N*-Tetramethylensuccinamid erhalten wurde, dass *N*-Acetyläthylenimin mit Acetamid unter Bildung von *N,N'*-Diacetyläthylediamin reagierte und die Geschwindigkeit dieser Copolymerisation von der Elektrophilität des Imids abhängt, wurde ein Copolymerisationsmechanismus aufgestellt.

Received November 30, 1965

Revised December 28, 1965

Prod. No. 5051A

## New High-Temperature Polymers. II. Ordered Aromatic Copolyamides Containing Fused and Multiple Ring Systems\*

FRANK DOBINSON and J. PRESTON, *Chemstrand Research Center, Inc., Durham, North Carolina*

### Synopsis

Symmetrical diamines, containing preformed carbonamide linkages, were prepared by reacting nitrobenzoyl chlorides with aromatic diamines and reducing the dinitro intermediates. The diamines were polymerized with aromatic diacid chlorides to give wholly aromatic ordered copolyamides of exceptionally high thermal stability. Ordered diamines were prepared containing only phenylene units as the aromatic portion, and others containing phenylene and naphthylene or biphenylene groups. Low-temperature solution polymerization of these diamines with isophthaloyl chloride, 4,4'-bibenzoyl chloride, or 2,6-naphthalenedicarbonyl chloride, gave thirteen ordered copolyamides, each containing a naphthylene and/or biphenylene group in its repeating unit. Differential thermal analyses and thermogravimetric analyses showed these polymers to have melting points or decomposition temperatures of from 420 to over 500°C. Films of one of the polymers had a breakdown voltage of 3000 v./mil at 180°C. Fibers of the same composition had tenacities of up to 8 g/den.; a 5.5 g/den. sample retained 85% of its tenacity after 17 hr. at 300°C. and 21% after 9 days.

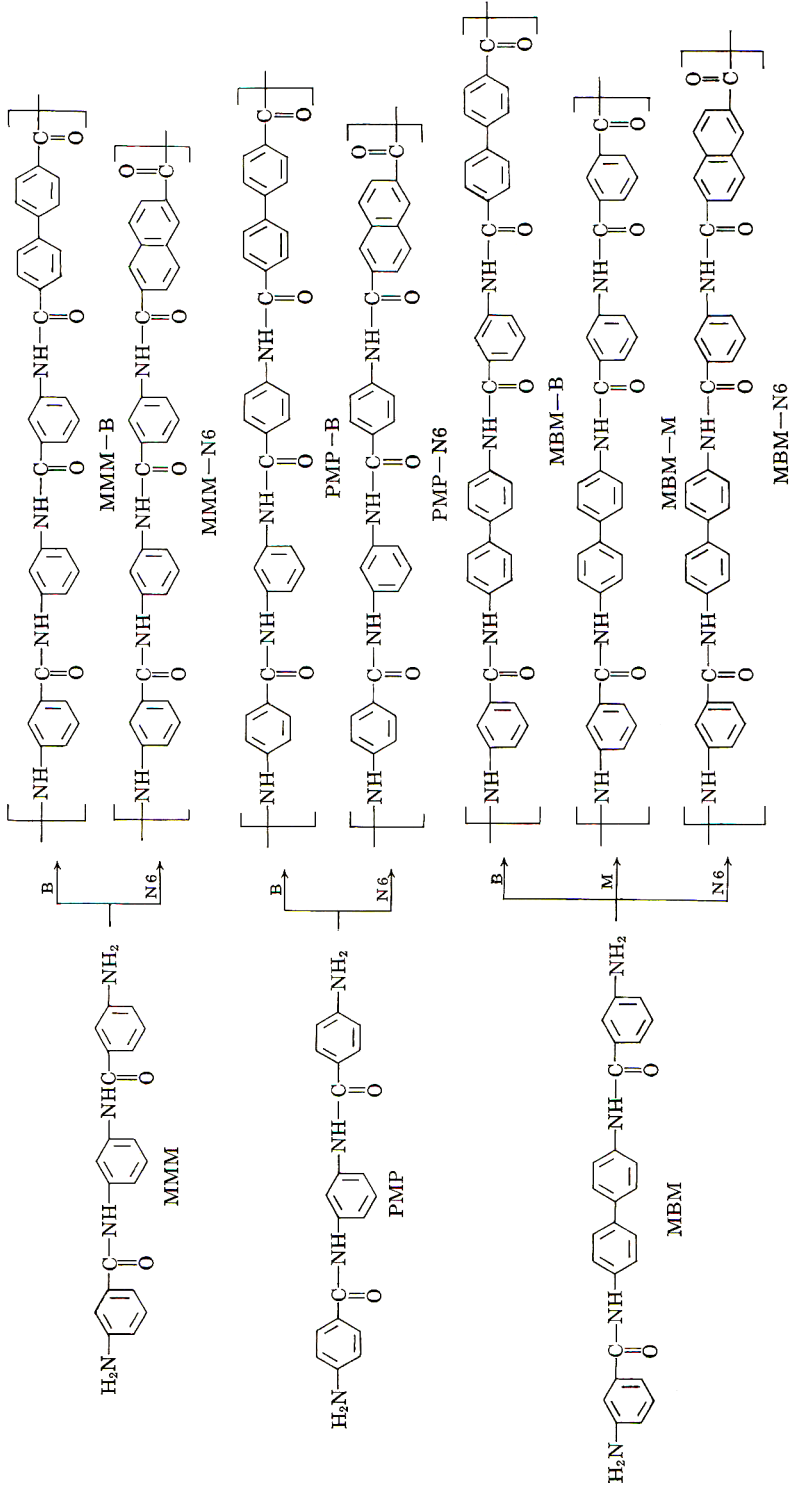
### INTRODUCTION

One of the results of the accelerating rate of technological progress has been the necessity to develop fiber- and film-forming polymers that have exceptional stability at temperatures where conventional fibers are useless. The aromatic polyamides fulfil many of the technical and practical requirements for such a polymer: they possess high thermal stability, due to intermolecular bonding, chain stiffness, and the inherent stability of aromatic structures; and they can be prepared as highly viscous solutions that can be spun to fibers or made into films by conventional techniques.

Until recently, two general types of aromatic polyamide had been described. One was produced by the self-condensation of an aromatic amino acid, such as *m*-aminobenzoic acid<sup>1-4</sup> to give polymers with the repeating unit —NH—X—CO—. Polymers of the second class were formed by the polycondensation of aromatic diamines such as *m*-phenylenediamine with aromatic diacid halides such as isophthaloyl chloride,<sup>5-7</sup> the polymers

\* Presented at the Symposium on High Temperature Polymers—Synthesis and Degradation, ACS Western Regional Meeting, Los Angeles, California, November, 1965.





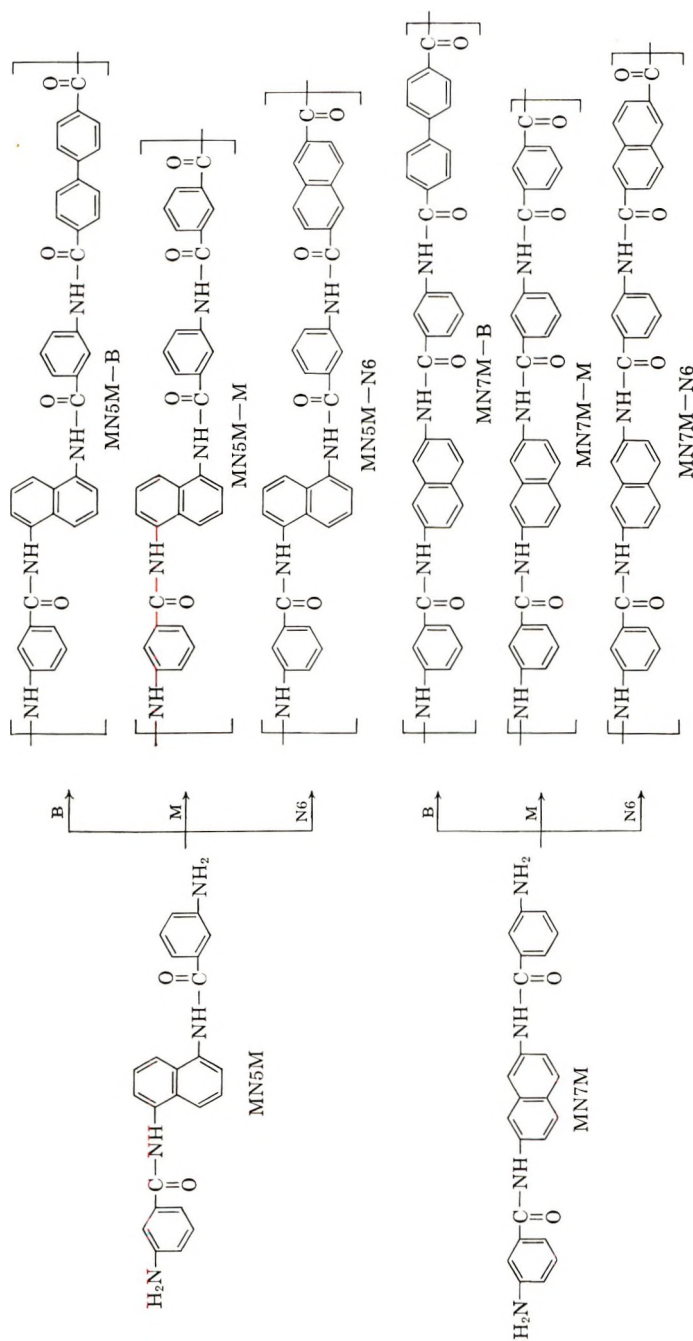


Fig. 1. Ordered diamines and ordered copolyamides. M: isophthaloyl chloride; B: 4,4'-biphenoyl chloride; N6: 2,6-naphthalenedicarbonyl chloride.

having the repeating unit  $\text{—NH—X—NH—CO—Y—CO}$ , where X and Y are arylene groups. A third type of wholly aromatic polyamide has recently been reported;<sup>8,9</sup> polymers of this type were made by polymerizing diacid chlorides with aromatic diamines that contained preformed carbonamide linkages. The first paper<sup>9</sup> in this series described aromatic polyamides containing aromatic structures derived from benzene.

The present paper describes the preparation of high molecular weight polyamides of this third type, containing naphthalene and/or biphenyl ring structures<sup>10</sup> in their repeating units, in addition to simple benzene rings. The regular order of these fiber- and film-forming polyamides is achieved by using complex diamines containing preformed carbonamide linkages; the diamines<sup>11,12</sup> used in this work are shown in the left-hand column of Figure 1. The diamines were polymerized with isophthaloyl chloride, 4,4'-bibenzoyl chloride, and 2,6-naphthalenedicarbonyl chloride, to give the ordered copolyamides shown in the right-hand column of Figure 1.

## EXPERIMENTAL

Differential thermal analysis (DTA) was used to determine the polymer melt temperatures; thermogravimetric analysis (TGA) gave the temperature of onset of rapid weight-loss, which was taken as the decomposition temperature. Inherent viscosities ( $\eta_{inh}$ ) were measured at 30°C. on solutions of 0.5 g. of polymer dissolved in 100 ml. of *N,N*-dimethylacetamide (DMAc) containing 5% dissolved lithium chloride.

The code system used in this paper simplifies the writing of structures. The ordered copolyamides were prepared from two moles of nitrobenzoyl chloride and one mole of an aromatic diamine, the nitro groups of the intermediate product being reduced to amine groups (preparations detailed below). Three symbols are therefore used for the diamine: in the first symbol, M or P refers to a *meta* or *para* aminobenzoyl group; in the second symbol, representing the central portion of the symmetrical ordered diamine, M refers to the residue from *m*-phenylenediamine, B to that from benzidine, N5 to that from 1,5-diaminonaphthalene, and N7 to that from 2,7-diaminonaphthalene; the third symbol of the code for the ordered diamines is the same as the first. Thus the simplest ordered diamine, derived from two moles of *m*-nitrobenzoyl chloride and one mole of *m*-phenylenediamine, is coded MMM.

These diamines were polymerized with diacid chlorides. The resulting polymers are coded with four symbols, the first three representing the diamine, the last symbol being that for the acid chloride: M for isophthaloyl chloride, B for 4,4'-bibenzoyl chloride, and N6 for 2,6-naphthalenedicarbonyl chloride. Thus the polymer from MMM and 4,4'-bibenzoyl chloride is coded MMM-B.

The polyamide from *m*-phenylenediamine and isophthaloyl chloride, used as a basis for comparison in some of this work, is coded M-M.

The diacid chlorides were prepared and purified by conventional methods.

### Preparation of the Ordered Diamines

In a typical preparation, a solution of 0.2 mole of *m*-nitrobenzoyl chloride in 40 ml. tetrahydrofuran was poured all at once into a vigorously agitated slurry of 0.1 mole of recrystallized 1,5-diaminonaphthalene in 200 ml. ice water containing 0.2 mole of sodium hydroxide. The reaction was complete within a few minutes. The dinitro intermediate was washed successively with water, dilute hydrochloric acid, water, dilute sodium hydroxide solution, and finally with hot water.

Alternatively, the condensation could be carried out entirely in dry DMAc. In one experiment, 0.1 mole of benzidine dihydrochloride was dissolved in 1 liter of DMAc in a 2-liter stirred flask. *m*-Nitrobenzoyl chloride, 0.2 mole, was added as a saturated solution in DMAc. The reaction solution was stirred for 15 min., then poured into a larger volume of water to precipitate the dinitro intermediate.

The dinitro intermediates prepared are listed in Table I. The yields were essentially quantitative. In order to obtain pure ordered diamines, it was advantageous to recrystallize the dinitro intermediates from hot *N,N*-dimethylformamide. Diamines were obtained by reduction with

TABLE I  
*N,N'*-Arylenebis(nitrobenzamides)

Compound	Melting point, °C. (uncor.)
<i>N,N'</i> - <i>m</i> -Phenylenebis( <i>m</i> -nitrobenzamide) <sup>a</sup>	269–271
<i>N,N'</i> - <i>m</i> -Phenylenebis( <i>p</i> -nitrobenzamide) <sup>a</sup>	279–281
<i>N,N'</i> -4,4'-Biphenylenebis( <i>m</i> -nitrobenzamide)	357–362
<i>N,N'</i> -1,5-Naphthylenebis( <i>m</i> -nitrobenzamide)	304–306
<i>N,N'</i> -2,7-Naphthylenebis( <i>m</i> -nitrobenzamide)	360–362

<sup>a</sup> Data of Preston.<sup>9</sup>

TABLE II  
*N,N'*-Arylenebis(aminobenzamides)

Compound	Code	Melting point, °C. (uncor.)	N, %	
			Calcd.	Found
<i>N,N'</i> - <i>m</i> -Phenylenebis( <i>m</i> -aminobenzamide) <sup>a,b</sup>	MMM	213–214	16.14	16.13, 16.08
<i>N,N'</i> - <i>m</i> -Phenylenebis( <i>p</i> -aminobenzamide) <sup>a,b</sup>	PMP	227–228	16.14	15.93, 15.89
<i>N,N'</i> -4,4'-Biphenylenebis- ( <i>m</i> -aminobenzamide)	MBM	332–334	13.27	13.32, 13.36
<i>N,N'</i> -1,5-Naphthylenebis- ( <i>m</i> -aminobenzamide)	MN5M	232–234	14.14	14.26, 14.07
<i>N,N'</i> -2,7-Naphthylenebis- ( <i>m</i> -aminobenzamide)	MN7M	298–300	14.14	14.14, 14.33

<sup>a</sup> Data of Preston.<sup>9</sup>

<sup>b</sup> Reported,<sup>13</sup> but no physical properties quoted.

stannous chloride, or by catalytic hydrogenation (Raney nickel) of solutions of the dinitro-intermediates in DMAc. The diamines (Table II) were essentially white and were stable toward the effects of light, moisture, and air.

### Polymerization

All the polyamides were prepared by solution polymerization at low temperatures,<sup>14</sup> which gives higher inherent viscosities for this type of polymer<sup>9</sup> than interfacial polymerization.<sup>15</sup> The low temperature polymerizations were carried out by dissolving or dispersing the ordered diamine in a suitable solvent that also served as acid acceptor, and adding to the cooled ( $-20$  to  $0^{\circ}\text{C}.$ ) solution or dispersion an equimolar quantity of diacid chloride. The temperature of the cooling bath was maintained at roughly  $-20$  to  $0^{\circ}\text{C}.$  for 30 min. Suitable solvents include DMAc, DMAc containing 5% dissolved lithium or calcium chloride, hexamethylphosphoramide, and *N*-methylpyrrolidone. The solutions were usually neutralized with lithium hydroxide or calcium hydroxide before being cast as films or spun into fibers. Polymer solutions that had been neutralized using calcium or lithium hydroxide could be heated for several hours at  $140^{\circ}\text{C}.$  without noticeable precipitation (microscopic examination of film of polymer solution on a hot-stage).

Carboxyl endgroups were determined for several samples of MMM-N6 by potentiometric titration; amine endgroups were measured colorimetrically. (Methods will be published elsewhere.<sup>16</sup>)

## RESULTS AND DISCUSSION

### Thermal Properties of Polymers

Five diamines, containing preformed carbonamide linkages, were used to make fifteen wholly aromatic copolyamides, two of which (MMM-M and PMP-M), reported in Part I of this series,<sup>9</sup> are included here for comparison. The polymers made are listed in Table III together with data on their thermal stability.

In general, it is clear that replacing a *m*-phenylene moiety by a 4,4'-biphenylene group gives a more thermally stable polymer, and that structures containing 2,6-naphthylene are yet more thermally stable. This can be seen in the three series of polymers formed by polymerizing the diamines MMM, PMP, and MBM, with isophthaloyl chloride, 4,4'-bibenzoyl chloride, and 2,6-naphthalenedicarboxyl chloride.

This stability is illustrated in Figure 2, which shows programmed differential thermal analysis (DTA) curves for MMM-M, MMM-B, and MMM-N6. Thermogravimetric analysis also demonstrated this increase of stability when biphenyl or naphthalene ring systems replaced the *m*-phenylene moieties of MMM-M; this is shown in Figure 3.

These trends in thermal stability were not always clearcut as is demonstrated by the polymer melting temperatures and approximate decomposi-



TABLE III  
Wholly Aromatic Ordered Copolyamides

Polymer	$\eta_{inh}^a$	PMT, °C. <sup>b</sup>	Decom- position temp., °C. <sup>c</sup>	
MMM-M <sup>d</sup>	1.48	410	450	Strong films, excellent crystalline fibers
MMM-B	2.38	420	490	Strong films, excellent crystalline fibers
MMM-N6	2.42	430	490	Strong films, excellent crystalline fibers
PMP-M <sup>d</sup>	1.27	475	485	Strong films, excellent crystalline fibers
PMP-B	1.20	490	490	Strong films
PMP-N6	1.38	>500	500	Strong films
MBM-M	0.58	470	500	
MBM-B	0.60	480	>600	
MBM-N6	0.57	>500	500	
MN5M-M	0.72	>500	>600	
MN5M-B	1.13	400	430	
MN5M-N6	0.99	>500	480	
MN7M-M	0.62	>500	490	
MN7M-B	0.85	>500	450	
MN7M-N6	0.75	475	475	

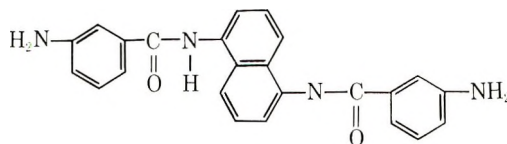
<sup>a</sup> Inherent viscosity, 0.5% solution in 5% lithium chloride in DMAc at 30°C.

<sup>b</sup> Polymer melting temperature observed by DTA.

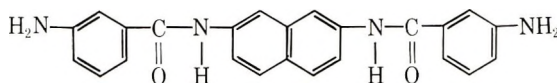
<sup>c</sup> Approximate decomposition temperature observed by TGA.

<sup>d</sup> Data of Preston.<sup>9</sup>

tion temperatures of ordered aromatic polyamides derived from the two diamines MN5M and MN7M.



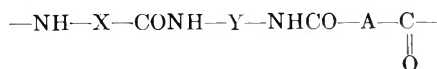
MN5M



MN7M

The polymer MN7M-B was thermally more stable than MN5M-B (data in Table III); but in the case of polymers from these diamines and 2,6-naphthalenedicarbonyl chloride, the situation was reversed, and MN5M-N6 was more stable than MN7M-N6. These differences must be at least in part ascribed to packing.

In isomeric polyamides of this type, the relative positions of the aromatic structures in the general repeating unit:



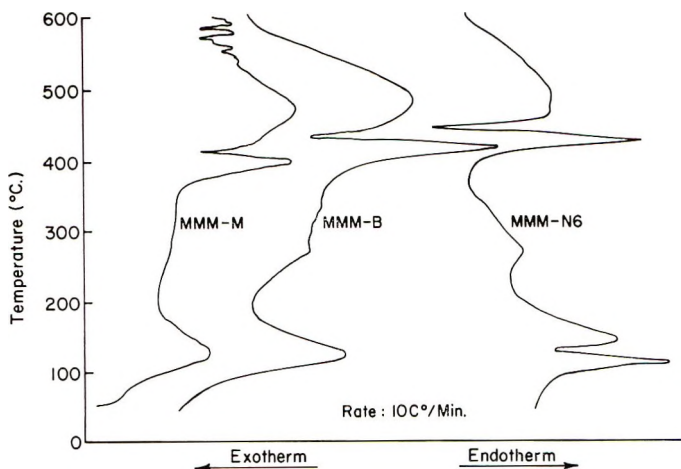


Fig. 2. Programmed DTA (in nitrogen) of fibers of wholly aromatic ordered copolyamides.

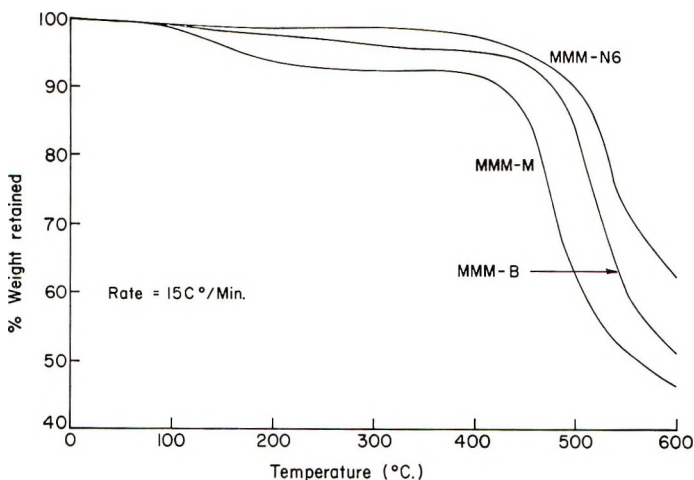


Fig. 3. Programmed TGA (in nitrogen) of wholly aromatic ordered copolyamides.

appear to have an effect on the thermal stability. For example, MBM-M was more thermally stable than its isomer MMM-B (Table III). Data in Part I of this series<sup>9</sup> showed a similar trend: polymer MPM-M had a polymer melt temperature of 460°C., whereas the value for MMM-P was 450°C.

### Preparation of Polymers

Thirteen ordered aromatic polyamides containing phenylene groups and biphenylene and/or naphthylene groups were prepared by solution polymerization, with inherent viscosities as high as 2.4 (Table III). Endgroup analyses (carboxyl and amine) indicated number-average molecular

TABLE IV  
 Endgroup Analyses and Molecular Weight ( $\bar{M}_n$ ) of MMM-N6

Endgroups, $\mu\text{equiv./g.}$		$\bar{M}_n$ (calculated)
—NH <sub>2</sub>	COOH	
100-150	84-88	8,400-10,900
28-42	88-94	14,700-18,900
5.5-8.5	33-37	44,000-51,900
6.5-9.5	28-32	48,200-58,000

weights in the range 8,000-60,000 (Table IV). Two of these thirteen polymers (MMM-B and MMM-N6) were spun to excellent fibers, and the same compositions together with PMP-B and PMP-N6 were cast to strong flexible films.

The polymers, fibers, and films of these compositions were insoluble in the more common organic solvents, including DMAc. For example, fibers of MMM-N6 retained 99.5% cent of their tenacity after soaking in stirred DMAc at 21°C. for 11 days. Clear polymer solutions were obtained for all the compositions when the polymer was prepared in DMAc or, in some cases, in DMAc already containing a dissolved inorganic salt. In a few cases, particularly polymers with a high *p*-phenylene content,<sup>9</sup> polymers isolated from the reaction solutions would not redissolve in DMAc containing a dissolved inorganic salt.

### Film Properties

Films of MMM-B, MMM-N6, PMP-B, and PMP-N6 could be prepared by baking out the solvent from an evenly spread film of polymer solution, and soaking the film in distilled water in the case of solutions that still contained the chloride made by neutralizing the HCl formed during polymerization. The films were clear and tough.

The dielectric constant of MMM-N6 films was  $2.5 \pm 0.2$  at 130,000 cps.

The breakdown voltages of commercial polyethylene film and a film of MMM-N6 were measured according to ASTM-D149-55: the polyethylene film had a breakdown voltage of 900 v./mil; the figure for MMM-N6 was 3000 v./p mil.

The breakdown voltages of MMM-N6 films and films of nylon 66 and polytetrafluoroethylene were measured at elevated temperatures (results in

 TABLE V  
 Breakdown Voltage of MMM-N6 Films at Elevated Temperatures

Composition	Temperature, °C.	Breakdown voltage, v./mil
MMM-N6	180	3000
Polytetrafluoroethylene	150	2250
Nylon 66	150	120

Table V). Finally, small hand-wound condensers made from films of MMM-N6 film and strips of aluminum foil and having capacitances of roughly  $0.25 \mu\text{F}$ . were tested at  $180^\circ\text{C}$ . along with commercial condensers made of metal foil and poly(ethylene terephthalate). All the commercial condensers failed within 20 min. The condensers made from MMM-N6 had not failed at the end of 4 hr.

### Fiber Properties

Solutions of MMM-B and MMM-N6 were spun to excellent crystalline fibers that had a high degree of orientation. Data for these fibers are compared in Table VI with data for the simple aromatic polyamide, poly(*m*-phenylene isophthalamide), coded M-M.

TABLE VI  
Fiber Properties of Wholly Aromatic Polyamides<sup>a</sup>

Property	M-M	MMM-B	MMM-N6
Tenacity, g./den.	6.0	5.9	8.0
Elongation, %	16	16	13
Initial modulus, g./den.	136	93	154
Moisture regain, % <sup>b</sup>	5.1	n.d. <sup>c</sup>	4.5
Density, g./cc.	1.39	n.d. <sup>c</sup>	1.35

<sup>a</sup> Fiber properties are for unboiled-off samples.

<sup>b</sup> Equilibrium moisture at  $70^\circ\text{F}$ . and 65% R.H.

<sup>c</sup> Not determined.

All three compositions had excellent tenacities. The aromatic structures would be expected to impart a high degree of rigidity to the polymer molecules; and this effect, together with intermolecular forces, particularly hydrogen bonding, probably accounts for the high initial moduli.

Conventional polymers like nylon 66 and poly(ethylene terephthalate) begin to lose their useful fiber properties below  $200^\circ\text{C}$ . Figure 4 shows the

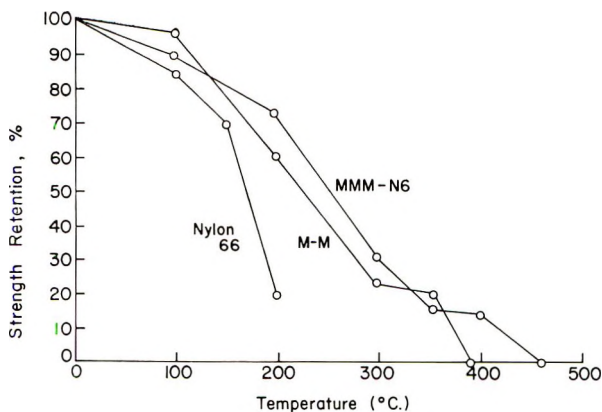


Fig. 4. Fiber properties of M-M and MMM-N6 tested at elevated temperatures. Exposure time: 5 min.

retention of tenacity at elevated temperatures for one of the wholly aromatic ordered copolyamides, MMM-N6, compared with the simpler aromatic polyamide M-M and the aliphatic polyamide, nylon 66. Thus, M-M retained 22% of its original breaking strength at 300 to 330°C., but rapidly lost strength from 370 to 390°C. MMM-N6 retained roughly 12% of its original tenacity at 425°C., rapidly losing strength at temperatures greater than 450°C.

The effect of prolonged exposure of MMM-N6 to dry heat in air at 300°C. was measured. Drawn fibers of this composition were heated in air at 300°C. for a total of 9 days. Discoloration and embrittlement occurred, but the fibers nevertheless retained 85% of their tenacity after 17 hr. exposure and 21% after 9 days, as is shown in Table VII.

The chemical resistance of drawn fibers of MMM-N6 was, in general, excellent. The retention of initial strength after different chemical treatments for compositions MMM-P and MMM-N6 is listed in Table VIII.

Fibers of the wholly ordered aromatic copolyamides showed excellent stability to  $\gamma$ -radiation ( $^{60}\text{Co}$  source); fibers of MMM-N6 actually in-

TABLE VII  
Effect on Fiber Properties of MMM-N6 of Prolonged Exposure in Air at 300°C.<sup>a</sup>

Property	Exposure time		
	0	17 hr.	9 days
Tenacity, g./den.	5.5	4.6	1.2
Elongation, %	25	n.d. <sup>b</sup>	2.5
Initial modulus, g./den.	90	n.d. <sup>b</sup>	53

<sup>a</sup> Data of Morgan.<sup>17</sup>

<sup>b</sup> Not determined.

TABLE VIII  
Chemical Resistance of Fibers of Aromatic Ordered Copolyamides

Reagent	Strength	Temp., °C	Time, hr.	Strength retained, %	
				MMM-P	MMM-N6
Dimethylacetamide	100%	21	264	81	99.5
Sodium hypochlorite	0.5%	21	8	96	89
			264	55	44
Sodium hydroxide	16N	21	8	100	84
			264	71	74
			8	33	38
			22	— <sup>a</sup>	19
Sulfuric acid	20N	21	8	95	70
			264	76	70
			8	51	51
			96	— <sup>b</sup>	— <sup>c</sup>

<sup>a</sup> Too weak to test.

<sup>b</sup> Disintegrated.

<sup>c</sup> Weak, but still in fiber form.



creased in tenacity by about 12% after 10 hr. exposure at  $2.92 \times 10^5$  rad/hr. and fibers of MMM-P by about 9% after the same exposure. This contrasts markedly with the reported behavior of the polyesters of terephthalic acid and 2,6-naphthalenedicarboxylic acid with ethylene glycol.<sup>18</sup> The latter polyester's viscosity increased with increased radiation, indicating cross linking. With poly(ethylene terephthalate), the main effect of gamma radiation was chain rupture.

M-M and MMM-N6 had roughly the same stability to ultraviolet light, fibers of each retaining 45% of their original tenacity after 80 hr. standard Fade-Ometer exposure; MMM-P fibers retained 19% of their tenacity.

The authors wish to record their appreciation of the excellent technical assistance of Mr. C. E. Widen and Mr. R. R. Thomas. They are particularly grateful to Mr. H. S. Morgan who provided certain fiber and radiation data, to Mr. L. C. Garrett, who determined some of the electrical properties, and to Mr. E. L. Ringwald and Dr. W. B. Black for their suggestions and criticisms.

### References

1. C. W. Stephens, Brit. Pat. 901,159 (1962).
2. W. A. H. Huffman, R. W. Smith, and W. T. Dye, Jr., U. S. Pat. 3,203,933 (1965).
3. J. Preston and R. W. Smith, Belg. Pat. 637,260 (1964).
4. J. Cologne and E. Fichet, *Bull. Soc. Chim. France*, **1955**, 412 (1955).
5. M. Katz, Belg. Pat. 569,760 (1958).
6. H. F. Mark, S. M. Atlas, and N. Ogata, *J. Polymer Sci.*, **61**, S49 (1962).
7. R. A. Dine-Hart, B. J. C. Moore, and W. W. Right, *J. Polymer Sci. B*, **2**, 369 (1964).
8. J. Preston and F. Dobinson, *J. Polymer Sci. B*, **2**, 1171 (1964).
9. J. Preston, *J. Polymer Sci. A-1*, **4**, 529 (1966).
10. J. Preston and F. Dobinson, Brit. Pat. 980, 907 (1965).
11. J. Preston and F. Dobinson, Belg. Pat. 637,257 (1964).
12. J. Preston, Belg. Pat. 637,258 (1964).
13. G. M. Bower and L. W. Frost, *J. Polymer Sci. A*, **1**, 3135 (1963).
14. P. W. Morgan, in *Macromolecular Chemistry (J. Polymer Sci. C, 4)*, M. Magat, Ed., Interscience, New York, 1963, p. 1075.
15. E. L. Wittbecker and P. W. Morgan, *J. Polymer Sci.*, **40**, 289 (1959).
16. R. G. Garmon, in preparation.
17. H. S. Morgan, Chemstrand Research Center, Inc., private communication.
18. *Chem. Eng. News*, **43**, 38 (May 17, 1965).

### Résumé

Les diamines symétriques contenant des liaisons carbonamides préformées, ont été préparées par réaction de chlorures de nitrobenzoyle avec des diamines aromatiques et réduction des intermédiaires dinitrés. Les diamines ont été polymérisées avec des chlorures de diacides aromatiques en vue de former des copolyamides aromatiques de stabilité thermique exceptionnellement élevée. Des diamines contenant uniquement des unités phénylènes ont été préparées comme partie aromatique; et d'autres contenaient des groupes phénylènes et naphthylènes ou biphénylènes. Elles ont été condensées à basse température avec le chlorure d'isophthaloyle, le chlorure de 4,4'-bibenzoyle, ou le chlorure de 2,6-naphthalène dicarboxylique; on obtient ainsi 13 copolyamides ordonnés, contenant un groupe naphthylène et/ou biphénylène dans l'unité périodique. L'analyse

thermique différentielle et les analyses thermogravimétriques ont montré que ces polymères avaient un point de fusion et des températures de décomposition variant de 420° à 500°C. Des films de l'un des polymères ont un voltage de rupture de 300 Volts/mil à 180°C. Des fibres de même composition ont des tenacités atteignant jusqu'à 8 gr/den.; un échantillon à 5,5g r/den. gardait 85% de sa tenacité après chauffage durant 17 heures à 300°C et 21% après 9 jours.

### Zusammenfassung

Symmetrische Diamine mit präformierten Carbonamidbindungen wurden durch Reaktion von Nitrobenzoylchloriden mit aromatischen Diaminen und Reduktion der intermediären Dinitroverbindungen dargestellt. Die Diamine wurden mit aromatischen Dicarbonsäurechloriden unter Bildung rein aromatischer geordneter Copolyamide mit aussergewöhnlich hoher thermischer Stabilität polymerisiert. Es wurden solche geordnete Diamine dargestellt, die nur Phenylbausteine als aromatischen Teil enthielten und andere mit Phenyl- und Naphthyl- oder Biphenylgruppen. Tieftemperatur-lösungspolymerisation dieser Diamine mit Isophthaloylchlorid, 4,4'-Bibenzoylchlorid oder 2,6-Naphthalindicarbonylchlorid lieferte 13 geordnete Copolyamide mit einer Naphthyl- oder Biphenylgruppe im Baustein. Differentialthermoanalyse und thermogravimetrische Analyse zeigte, dass diese Polymeren Schmelzpunkte oder Zersetzungstemperaturen von 420 bis über 500°C besitzen. Filme aus einem dieser Polymeren besaßen Durchschlagspannungen von 3000 V/Mil bei 180°C. Fasern der gleichen Zusammensetzung besaßen Festigkeiten bis zu 8 g/den; eine Probe mit 5,5 g/den behielt 85% ihrer Festigkeit nach 17 Stunden bei 300°C und 21% nach neun Tagen

Received November 3, 1965

Prod. No. 5050A

## Quantum Efficiency of the 2537 Å. Photolysis of a Mixed Phenyl-Methyl Polysiloxane

SEYMOUR SIEGEL, ROBERT J. CHAMPETIER, and A. R. CALLOWAY, *Aerospace Corporation, El Segundo, California*

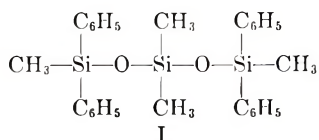
### Synopsis

The ultraviolet ( $\lambda = 2537 \text{ \AA.}$ ) photolysis of a degassed mixed phenyl and methyl polysiloxane liquid is examined in terms of gas and crosslinking yields. Results are compared to the published values obtained by ionizing irradiation of this type of molecule. It is shown that ultraviolet radiation is less efficient by two orders of magnitude in producing decomposition (i.e., gaseous products) than is ionizing radiation. The comparisons for crosslinking efficiencies are less certain, but the yields seem to have much more similar values in this case based on a spectroscopic estimation of crosslinking (i.e., analysis for substituted phenylcyclohexadiene formation). The gas quantum yields were  $\phi_{\text{H}_2} = 2.6 \times 10^{-5}$ ,  $\phi_{\text{CH}_4} = 0.63 \times 10^{-5}$ ,  $\phi_{\text{C}_2\text{H}_6} \approx 0.12 \times 10^{-5}$ , and  $\phi_{\text{C}_2\text{H}_2} \approx 0.06 \times 10^{-5}$ .

### INTRODUCTION

It has been demonstrated in many places that the presence of phenyl groups increases the stability of polysiloxanes with respect to the effects of ionizing radiation.<sup>1-3</sup> The gas evolution and crosslinking yields are decreased by a factor of 10 (or more) when phenyl groups are present compared to the yields observed when pure polydimethylsiloxanes are irradiated. Presumably, the presence of the highly conjugated phenyl groups increases the ability of the molecule to harmlessly dissipate the absorbed energy into nonchemical energy modes (i.e., heat). However, the exact mechanism by which the phenyl group accomplishes this protection is uncertain. Whether the energy is absorbed directly into the phenyl group during an initial highly energetic collective excitation step involving all the electrons of the molecule (or perhaps many molecules) or whether the energy migrates into the phenyl group after one or more preliminary localization steps cannot be answered at this time from the experimental data. The study presented in this paper gives some quantitative results on the efficiency of energy dissipation under conditions where the phenyl group electrons are directly excited as an initial step.

In the present study, a low molecular weight (M.W. = 480) mixed methyl-phenyl polysiloxane was excited with 2537 Å. radiation. The siloxane studied has the structure I (see following page)



and is denoted MPS in the rest of the paper. Absorption by this molecule at 2537 Å. is in the benzoid  ${}^1L_b$  band. Therefore, the region of the molecule where the initial excitation takes place is reasonably well characterized—namely, the phenyl groups. Detailed studies of the gas and cross-linking yields were made to determine the manner and efficiency of chemical dissipation of the selectively absorbed energy in the pure material.

## EXPERIMENTAL

### Material

The siloxane oil was received as a sharply fractionated sample from the Dow Corning Corporation. Further purification of the as-received sample was limited to vacuum distillation; the higher boiling fraction was used for the photolysis studies. The molecular structure of MPS was verified by, first, determination of molecular weight and, second, analysis of its nuclear magnetic resonance and ultraviolet absorption spectra.<sup>4,5</sup>

### Radiation Source

The radiation source used was a Hanovia, flat spiral, low-pressure mercury arc with a Corning No. 9-54 filter between the irradiation cell and the lamp. Besides the 2537-Å. line, the lamp output contains the 1849-Å. line as well as approximately 15% of the radiation at wavelengths corresponding to the mercury lines above 3000 Å. The Corning No. 9-54 filter was used to remove the 1849-Å. radiation. Therefore, because MPS does not absorb appreciably above 3000 Å. (Fig. 1), the effective excitation radiation is essentially all at 2537 Å. With the sample sizes used, all the latter radiation was absorbed by the MPS samples.

The total 2537-Å. radiation flux at the sample was determined by uranyl oxalate actinometry<sup>6</sup> as  $2.3 \times 10^{16}$  photons/sec. or  $8.3 \times 10^{19}$  photons/hr. All of the incident 2537-Å. radiation was absorbed by the sample; therefore, because at this wavelength there is a 4.9 e.v./photon, the absorbed energy flux becomes  $1.1 \times 10^{17}$  e.v./sec. or  $4.0 \times 10^{20}$  e.v./hr. On assuming all the energy is absorbed by 1 g. of material, the latter energy flux is equivalent to a dose rate of 6.7 Mrad/hr. (using the conversion 1 Mrad =  $6 \times 10^{19}$  e.v./g.). The results given in this paper are presented as either the yield per photon absorbed (quantum yield) or the yield per 100 e.v. of energy absorbed ( $G$  value), or both ways.

### Vacuum Manifold and Irradiation Cell

The irradiation cell was constructed out of stainless steel, and the manifold and vacuum valves were made of either brass or copper. A schematic

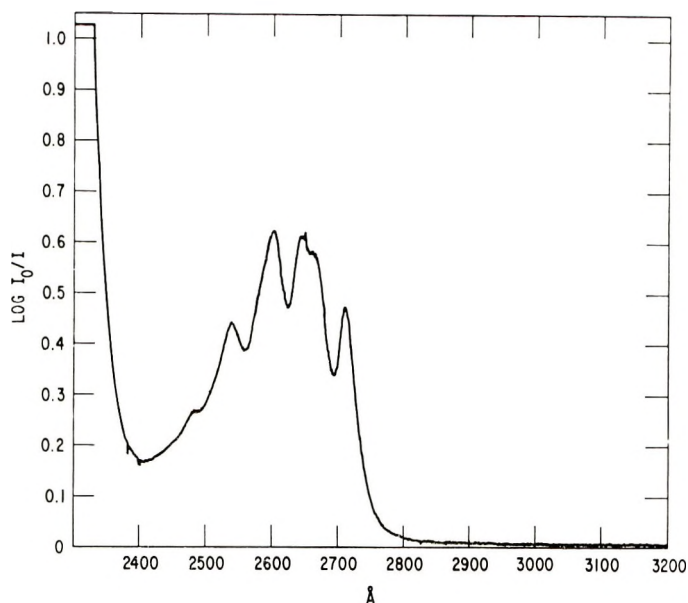


Fig. 1. Electronic absorption spectrum of unirradiated MPS (0.313 g. MPS in 100 g. hexane vs. hexane blank); cell size 1 mm.

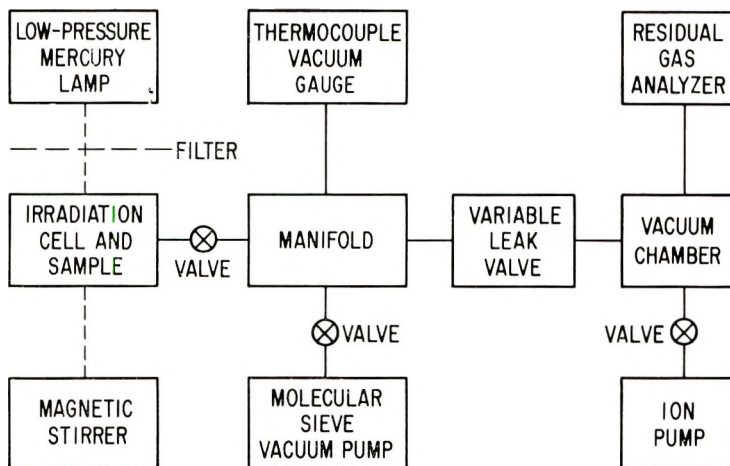


Fig. 2. Schematic of experimental apparatus.

of the experimental arrangement is given in Figure 2. The irradiation cell is illustrated in Figure 3. Samples of MPS were placed on the bottom of the cell with a syringe. The volume of the sample varied between 1.5 and 0.4 ml.; since the area of the bottom of the cell was approximately 10 cm.<sup>2</sup>, the depth of the sample ranged from 150 to 40  $\mu$ . A magnetic stirrer was employed continuously during the irradiation and the outgassing procedures. Before irradiation, the radiation cell containing the sample was degassed by continuous pumping overnight, using the molecular sieve



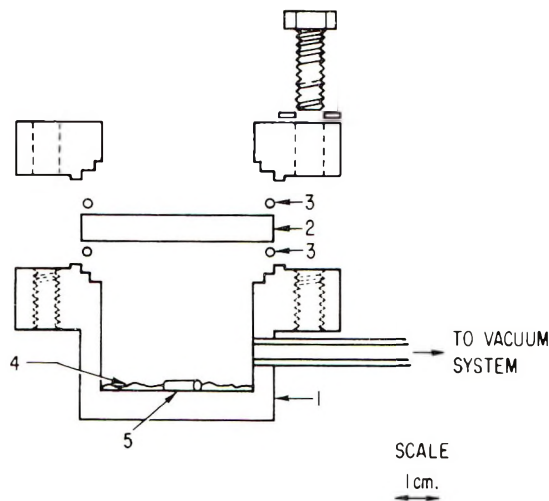


Fig. 3. Irradiation cell: (1) stainless steel cell; (2) Suprasil quartz window; (3) soft alloy gasket (95% Sn, 5% Ag); (4) sample; (5) magnetic stirrer.

pump, to less than  $1 \mu$  pressure (the limit of thermocouple gage readout). All irradiations were carried out at room temperature.

### Gas Analysis

The total gas yields were determined by using a calibrated thermocouple as shown in Figure 2. During the irradiation, the metal valve connecting the cell and manifold was usually closed; the valve was then opened to make the pressure readings. Gas yield versus irradiation time curves were usually obtained by using different samples for different irradiation times. Pressure yield data were converted to molecular yields by determining the total volume of the irradiation cell and manifold ( $\sim 40 \text{ cm.}^3$ ) and using the ideal gas equation. After the total gas yield was measured, the variable leak was opened to a preset value, and the mass spectra of the gaseous products were observed by using a residual gas analyzer (CEC model No. 21-613). Since the major products were  $\text{H}_2$  and  $\text{CH}_4$ , the spectrometer and the manifold were pressure-calibrated for these gases with the use of known samples. The sum of the  $\text{H}_2$  and  $\text{CH}_4$  yields determined in the latter manner agreed, in most cases, to within 20% with the gas yields determined from the calibrated thermocouple readings. Small  $\text{H}_2$  and  $\text{CH}_4$  yields were also found upon irradiating the empty cell which may be due to the nature of ion pumped vacuum systems. Corrections were made for this background in the tables given in this paper. Since most of the light is absorbed by the liquid and some of the gases produced in the empty cell arise from the photo-desorption of the walls, the corrections made are overcorrections, so that the reported values are somewhat too low; however, the errors produced by this procedure are probably smaller than experimental error ( $\sim 20\%$ ). (Because of the fact that an ion pump system was used, it was found that

appreciable CO, A, and H<sub>2</sub>O peaks were always present in the mass spectra; for clarity of presentation, the magnitude of these peaks is not reported in the paper.)

### Ultraviolet and Infrared Absorption Spectra

All ultraviolet spectra were obtained with a Cary-15 spectrometer. The form of the absorption curve of the photoproduct was determined by differential absorption analyses against an essentially equal weight concentration solution of unirradiated MPS as a blank. Spectroscopically pure hexane was used as the solvent for the solution runs and 1-mm. path length matched quartz cells were used as containers. Matched cells with Suprasil quartz windows and variable thickness spacers were used for examining the spectra of the pure material.

The infrared spectra were obtained with the use of a Perkin-Elmer 21 infrared spectrometer. Sample cells consisted of sodium chloride windows separated by metal spacers ranging in width from 0.0006 to 0.040 in. (1 mm). The spectrum of the photoproduct (or products) was synthesized by examining each spectral region with the appropriately sized spacer so that all the absorption lines were on scale. The spectra of the irradiated and unirradiated MPS were taken separately in the same cell and with air as a reference; then a point-by-point comparison was made of the two spectra and a difference spectrum synthesized. All the separate difference spectra were normalized to a constant spacer thickness for presentation purposes.

## RESULTS

### Gas Yields

The quantum yield of total gas produced was very small ( $\phi$  total gas  $\approx 3.3 \times 10^{-3}$ ), illustrating the extreme photostability of this molecule with respect to photodecomposition. Hydrogen was the major component of the photoproduct gas, methane being the next largest component. Analysis of the mass spectra indicates that ethane and acetylene are also produced, but in considerably smaller yields than those of hydrogen and methane. Benzene was produced in only trace quantities (i.e., less than 1 to 2% of the total gas yields). The relative concentrations of the gaseous products H<sub>2</sub>:CH<sub>4</sub>:C<sub>2</sub>H<sub>6</sub>:C<sub>2</sub>H<sub>2</sub> are approximately 4:1:0.2:0.1. Because the total gas yields were so small, the experimental uncertainties in the relative concentrations of C<sub>2</sub>H<sub>6</sub> and C<sub>2</sub>H<sub>2</sub> are 30–50%.

The buildup with increasing irradiation time of hydrogen and methane as well as of the total gas yield is illustrated in Figure 4. In the range of irradiation times shown in this figure, the gas yields are essentially linear with irradiation time (or total dosage) to within the experimental error. However, examination of the data points indicates a possible falloff in the rate of gas production at the longer irradiation times. The latter trend was confirmed by examining the gas yields at considerably longer irradiation

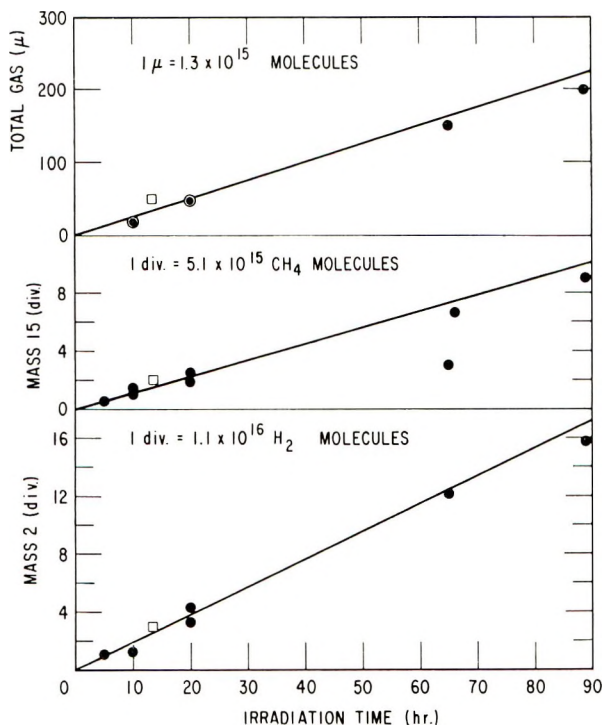


Fig. 4. Absolute gas yields as function of irradiation time (or total dosage). Most points taken at same dose rate; however some points ( $\square$ ) taken with a dose rate smaller by a factor of five (these points were plotted by reducing the actual exposure time by a factor of five).

tion times ( $\sim 300$  hr.). The initial quantum yields of the photoproduced gases are given in Table I.

The rate of gas production has a first-order dependence upon the incident intensity. This conclusion is based on the results shown in Figure 4; i.e., the amount of gas produced with an 80% reduction in incident intensity can be predicted from the normal gas production curve by using a corresponding linear reduction in irradiation time; therefore, the linear reciprocity law is valid in this case.

TABLE I  
Quantum and  $G$  Yields for Gases

Molecule	$\phi \times 10^6$ , molecules/photon	$G \times 10^4$ , molecules/100 e. v.
H <sub>2</sub>	2.6 <sup>a</sup>	5.3 <sup>a</sup>
CH <sub>4</sub>	0.63 <sup>a</sup>	1.3 <sup>a</sup>
C <sub>2</sub> H <sub>6</sub>	$\sim 0.12^b$	$\sim 0.26^b$
C <sub>2</sub> H <sub>2</sub>	$\sim 0.06^b$	$\sim 0.13^b$

<sup>a</sup> Accuracy is estimated as  $\pm 20\%$ .

<sup>b</sup> Accuracy is estimated as  $\pm 50\%$ .

## Spectral Changes

The electronic absorption spectrum of MPS is given in Figure 1 (at 2537 Å. the molar extinction coefficient  $\epsilon \approx 850$ ). With increasing photolysis time, another spectrum appears (Fig. 5) which has a maximum at  $\sim 255$   $m\mu$ . The variation in the intensity of the latter spectrum with irradiation time is given in Figure 6. At the longer irradiation times, the formation rate is dramatically reduced. The inhibition in production of the latter species is much greater than that found for the gas production.

The quantitative determination of the rate of production of the species responsible for the 255- $m\mu$  peak requires determining a value for its absorption coefficient at this wavelength. The shape of the spectrum resembles

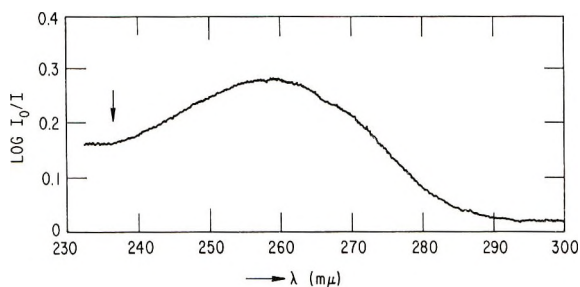


Fig. 5. Differential ultraviolet absorption curve of solution of 1.61 g. irradiated (50 hr.) MPS in 100 g. hexane against solution of 1.61 g. unirradiated MPS in 100 g. hexane. Path length of the cells was 1 mm. The arrow corresponds to the wavelength at which the spectrometer no longer responds because of absorption of blank.

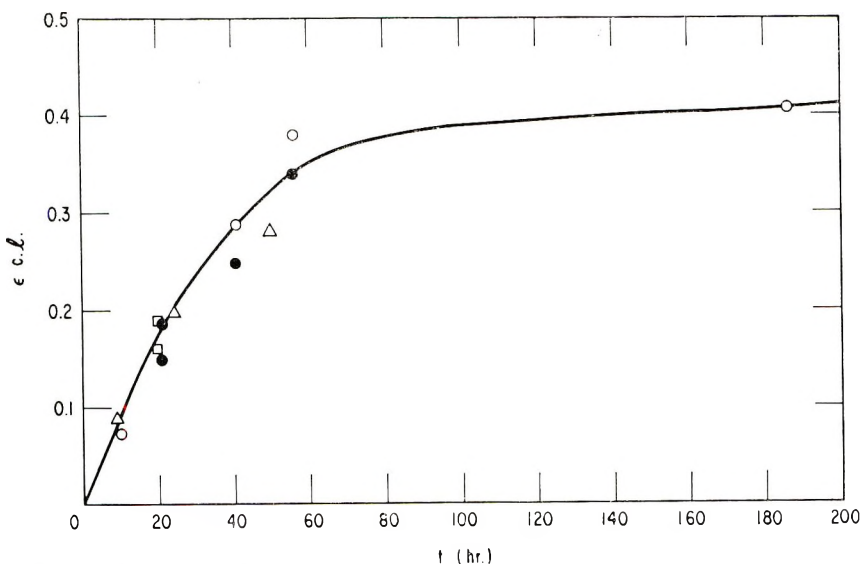
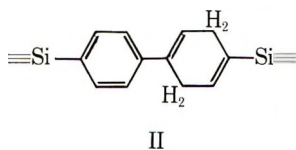


Fig. 6. Intensity of 257  $m\mu$  peak of differential absorption spectrum against total dose or irradiation time at constant dose rate. Some points ( $\square$ ) obtained by using dose rate smaller by a factor of five and dividing actual exposure time by factor of five.

that of either the biphenyl molecule or the cyclohexadiene molecule.<sup>7</sup> Both types of molecules have maximum values of  $\epsilon \approx 10^4$ . Therefore, on assuming this value for the value of  $\epsilon$  for the photoproducted species, the initial slope in Figure 6 corresponds to a production rate of 0.04%/hr. of the MPS molecules present. For a 1.5-g. sample of liquid, the latter rate corresponds to a production rate of  $7.3 \times 10^{17}$  molecules/hr. The corresponding quantum yield is  $8.8 \times 10^{-3}$  (and  $G = 0.18$ ). Obviously, the photoproducted spectrum does not result from a biphenyl-type molecule formed by the elimination of a molecule of hydrogen; the difference between the latter quantum yield and  $\phi_H$ , is three orders of magnitude. The peak at  $255 m\mu$  is probably caused by a product of the type II,



i.e., a disubstituted phenylcyclohexadiene. The exact arrangement of the two double bonds in the diene ring is uncertain; it is possible that the quinoid arrangement is present.

The incident intensity dependence for the production of the diene was also found to obey the linear reciprocity law. Therefore, the effective kinetic rate expression governing the production of this species contains only first-order terms. Since the diene also absorbs strongly at 2537A., part of the falloff of its production rate can be ascribed to competition between MPS and diene for the available light. However, the fraction of light absorbed by the diene was never appreciably greater than 25%; there-

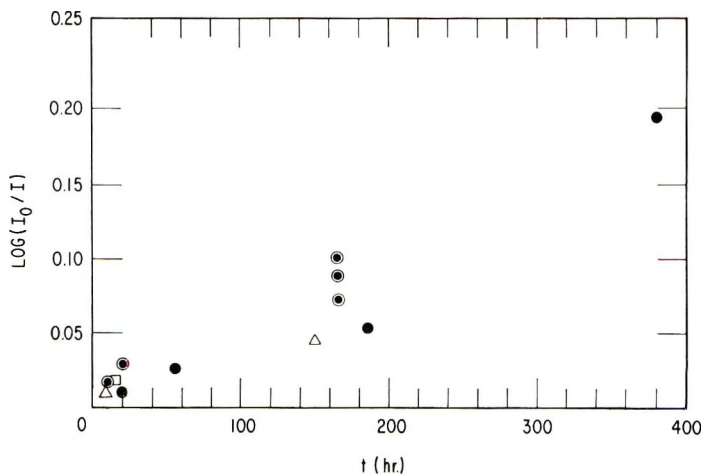


Fig. 7. Intensity of differential absorption at  $\lambda = 4100$  A. against exposure time at constant dose rate (or total dosage). Points obtained with 100% MPS and use of 0.2-mm. spacers. One point ( $\square$ ) obtained by using a dose rate smaller by a factor of five and dividing actual exposure time by a factor of five.



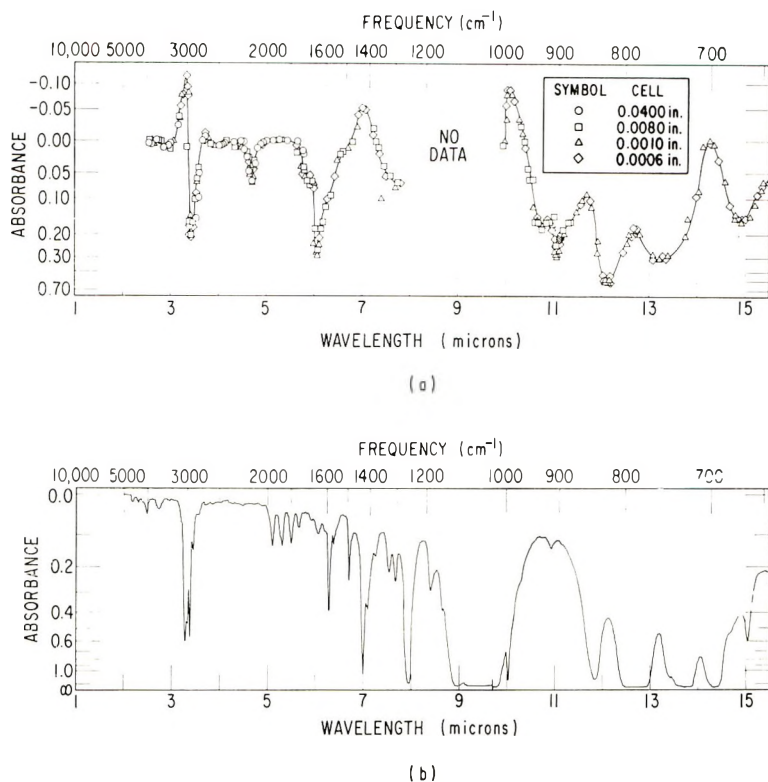


Fig. 8. Infrared spectra: (a) synthesized infrared difference spectrum of a sample of MPS irradiated more than 100 hr. in vacuum (results from the various spacers normalized to 0.040 in., air was used as a reference for both the irradiated and unirradiated MPS spectra used in constructing the difference spectrum, and neat liquids were used in all cases); (b) infrared spectrum of neat unirradiated MPS against air as a reference (a 0.001-in. spacer was used).

fore, the very rapid change in curvature shown in Figure 6 must arise from other mechanisms.

The spectrum shown in Figure 5 arises from two separate species. The diene band with a maximum at 255–260  $\text{m}\mu$  is readily distinguishable. However, the shape of the spectrum indicates that there is also a broad underlying spectrum present which exhibits a long high-wavelength tail (extending to 500  $\text{m}\mu$ ). The presence of the long-wavelength tail gives the irradiated liquid a distinctive yellow color. The fact that two species are produced by the photolysis can be seen by comparing the dependence upon dosage of the long-wavelength tail, given in Figure 7, with that of the maximum of 255  $\text{m}\mu$  in Figure 6. The scatter is appreciable in Figure 7; however, the trend is sufficiently marked to indicate that there is no fast fall-off with time at  $\sim 100$  hr.

The synthesized infrared difference spectrum of a MPS sample irradiated more than 100 hr. is given in Figure 8a for a 0.04 in. (1 mm.) spacer.

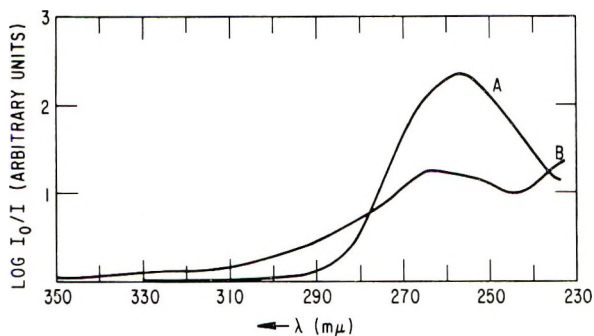


Fig. 9. Differential ultraviolet absorption curves: (a) solution of MPS irradiated 24 hr. in vacuum; (b) solution of MPS irradiated 24 hr. in presence of  $O_2$ . Concentrations of solutions approximately 1.4 g. MPS in 100 g. hexane; solution of unirradiated MPS used as blank; cell size 1 mm.

Note the derivative line shapes of the bands at  $\sim 3000$  and  $\sim 1600$   $cm^{-1}$ . These line shapes are due to (1) the loss of spectral intensity at  $3150$   $cm^{-1}$  and the gain of spectral intensity at  $2940$   $cm^{-1}$  and (2) the loss of spectral intensity at  $1400$   $cm^{-1}$  and the gain of spectral intensity at  $1650$   $cm^{-1}$ . This result supports the suggestion that the photoproduct is a phenylcyclohexadiene, since the change at  $3000$   $cm^{-1}$  indicates a conversion of aromatic CH hydrogens to an aliphatic  $CH_2$  group.<sup>8</sup> Also, the shift to higher frequency of the phenyl vibrations indicates the production of an intense band due to a *para*-substituted phenyl group where one of the substituents is conjugated to the ring.<sup>8</sup> The bands below  $1000$   $cm^{-1}$  are broad and not well defined, and the problem of loss and gain in spectral intensities renders the problem of assigning these bands to structural characteristics of the photoproduct very difficult. The region between  $1300$  and  $1000$   $cm^{-1}$  contains bands of MPS which are too strong to keep on scale with the neat liquid, even when a  $0.0006$ -in. spacer is used. However, when a 20% solution in  $CS_2$  was used together with the  $0.0006$ -in. spacer, there were no spectral differences outside of experimental error which could be found in the  $1300$ – $1000$   $cm^{-1}$  region. The band at  $2140$   $cm^{-1}$  could be assigned to the SiH group; however, it could also be an overtone of one of the stronger bands; the low yield of  $CH_4$  would tend to support the latter assignment. A spectrum of unirradiated MPS is also included (Fig. 8b); however, the spacer size in this case was  $0.001$  in.

A possible origin of the yellow species might be inferred from the results obtained when an oxygen-saturated MPS sample was photolyzed. The effect of the presence of oxygen is shown in Figure 9. Oxygen increases the concentration of yellow species at the expense of the diene. Examination of the infrared spectrum of a MPS sample irradiated in air showed added strong absorption at  $1740$  and  $3540$   $cm^{-1}$ . These new bands can be assigned to the C=O and OH groups, respectively. A close study of the spectrum in Figure 8a reveals the presence of a shoulder at  $1740$   $cm^{-1}$  and a weak band at  $2500$   $cm^{-1}$ . As the sample is kept exposed to air these

bands grow in intensity, indicating that the photoproduct slowly reacts with air. Therefore, it is possible that the yellow color observed in degassed samples arises from the presence of residual oxygen that was not removed during the degassing process.

### Crosslinking

Molecular weight determinations were made by the freezing point depression method.<sup>9</sup> The precision of the method was better than 2%. To within the experimental precision, there were no changes in number-average molecular weight observed over 116 hr. of irradiation of a 1.5-g. sample when the sample was stirred continuously. However, when no stirring was employed during irradiation, so that all the light was absorbed in a very small effective volume, a gel-like film was formed on the surface of the liquid, indicating that crosslinking does take place. Using the precision of the freezing point depression method as an upper bound for the change in molecular weight present in the stirred sample, one can estimate a quantum yield for crosslinking ( $\phi_{cl}$ ). Therefore, for a 1.5-g. sample, a change in  $\bar{M}_n$  after 116 hr. of irradiation of  $\leq 2\%$  corresponds to  $\phi_{cl} \leq 3.9 \times 10^{-4}$  ( $G \leq 7.8 \times 10^{-3}$ ). The latter quantum yield is considerably smaller than that previously estimated for diene formation. However, if crosslink formation is related to diene formation, then the drastic falloff found for the diene formation should result in a similar inhibition in the former case. Consequently, the value of  $\phi_{cl}$  given for the 116-hr. run may be in error by as much as a factor of four or more when considering initial quantum yields. Also, an underestimation of the value of  $\epsilon$  for the diene by a factor of two would result in a corresponding overestimation of the diene quantum yield. At this point, the absence of a definite molecular weight change does not allow any quantitative statements to be made concerning the value of  $\phi_{cl}$ . The best that can be done is to use the initial yield of diene as an estimate for the latter quantum yield.

### DISCUSSION

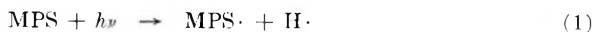
The gas yield per 100 e.v. of energy deposited for MPS subjected to  $\gamma$ -irradiation has been reported<sup>2</sup> as  $G_{\text{gas}} = 0.047$ , of which 75% was noncondensable at 77°K. Another study<sup>1</sup> of the 1.5 Me.v. electron radiolysis of a related phenyl-methyl polysiloxane gave  $G_{\text{gas}} = 0.061$ . The latter study also reported a value of  $G_{\text{gas}} \approx 0.015$  (mostly H<sub>2</sub>) for a cyclic polydiphenylsiloxane. The  $G$  values are approximately one to two orders of magnitude larger than the total gas yields found in this study for ultraviolet photolysis (i.e.,  $G_{\text{gas}} = 7 \times 10^{-4}$ ). The dose rate for the  $\gamma$ -irradiation study was 0.1–0.5 Mrad/hr., while in the electron study a dose rate of 1200 Mrad/hr. was used. Since the ultraviolet radiation dose rate used in this study was approximately 7 Mrad/hr., a dose rate effect cannot be used to explain the differences in gas yield.

The relatively low efficiency of 2537-A. radiation in causing photodecomposition of MPS molecules compared to that found for ionizing radia-

tion leads to the conclusion that the lowest excited state is not predominantly involved in the latter case. With 2537-Å light, only the lowest singlet state (and, via intersystem crossing, the lowest triplet state) is excited. Therefore, the active state leading to decomposition during ionizing irradiation must be higher than the first excited states in both singlet and triplet manifolds. The possibility that the decomposition observed in the ultraviolet photolysis also arises from a higher excited state, which is populated by a triplet-triplet or singlet-singlet energy transfer process or by an absorption of a photon by a metastable triplet state, can be discounted because of the observed first-order dependence on incident light intensity.

For MPS,  $3 \times 10^4$  photons are required to produce one gas molecule. The gas yield found in this study had a hydrogen: methane ratio of approximately 4:1; if the  $C_2H_6$  yield is considered, the ratio would be 3:1. Methane can only arise from the dissociation of a  $\equiv Si-CH_3$  bond followed by a hydrogen abstraction reaction from  $H_3CSi\equiv$  by  $CH_3$ . Hydrogen, however, can arise from a  $\equiv SiCH_2-H$  dissociation and from a  $\equiv SiC_6H_4-H$  dissociation. The relative efficiencies of the two dissociation reactions cannot be unambiguously determined from the available data. For polydimethylsiloxane, the observed  $H_2:CH_4$  ratio under ionizing radiation<sup>1,2</sup> is  $\sim 1:2$ ; however, with increasing phenyl content, the ratio reverses because of the contribution of  $H_2$  from the phenyl groups. Also, it has been suggested<sup>1</sup> that the protection of phenyl groups toward decomposition under ionizing radiation is greater toward  $\equiv Si-CH_3$  dissociations than toward  $\equiv SiCH_2-H$  dissociations leading to the larger value of the gas ratio in the presence of phenyl groups. Correspondingly, it is possible for ultraviolet irradiation, where the energy must "leak out" of the phenyl group (as opposed to ionizing radiation where the phenyl group acts as a sink), that  $\equiv SiCH_2-H$  dissociations are preferred. This latter possibility cannot be unambiguously proved; however, an examination of the EPR spectra of MPS irradiated at 77°K. showed a larger  $\equiv SiCH_2$  radical yield than a  $CH_3$  radical yield. While uncertainties arise from extrapolation of 77°K. results to room temperature, the EPR results serve as some support for the hypothesis that the  $\equiv SiCH_2-H$  dissociation is preferred.

Using the initial yield of diene formation as an estimate of crosslinking efficiency (i.e.,  $G \approx 0.1$ ), one concludes that the phenyl group can utilize the absorbed ultraviolet energy more efficiently for crosslinking than for gas production. This conclusion on the efficiency of energy conversion has also been reached in studies on the radiolysis of benzene<sup>10,11</sup> as well as on the radiolysis of methyl-phenyl siloxanes.<sup>1</sup> The value for  $G_{e1}$  obtained with the use of electrons for a related molecule is 0.25,<sup>1</sup> which is close to the value found here for MPS. Because the diene is formed by a process that is first-order in incident light intensity, such radical reactions as those shown in eqs. (1)–(3)







can be eliminated, since they would have a second-order dependence on incident intensity. The observed first-order intensity dependence suggests a reaction sequence such as shown in eqs. (4) and (5)



as the mechanism of diene formation (a cage effect involving the former radical mechanism so that only nearest neighbors reacted could not be distinguished from the excited molecule reaction).

Data are not available to ascertain whether the excited state is a triplet or a singlet state. In general, oxygen that quenches the triplet-state concentration can be used to make the latter distinction. However, in this case another product is formed as well as the diene formation being reduced. The fact that the diene formation rate is affected by oxygen suggests that the triplet state of MPS is an intermediate, but more evidence is needed before a definitive conclusion can be reached.

As discussed previously, competition between MPS and the photoproduced diene for the available radiation cannot be invoked to explain the rapid falloff in diene formation with total dosage. Another possibility is that the absorbed energy is channeled into the diene via energy transfer steps. However, if the latter mechanism is correct then the probability of gas formation via excitation of MPS or diene must be essentially equal. The latter requirement is imposed because the gas yields exhibit a more gradual falloff with a total dosage, rather than a rapid falloff.

The obvious missing key to complete elucidation of the photochemistry of the MPS polymer is the isolation of the very small yields of photoproduced products. Preliminary attempts in this direction with the use of molecular sieves have not proved successful; however, it is expected that further work to isolate the products will be continued in the future.

This work was supported by the U. S. Air Force under contract AF 04(695)-469.

The authors wish to thank R. Rennick for his valuable assistance in obtaining the IR spectra as well as other experimental details.

### References

1. A. A. Miller, *Ind. Eng. Chem. Prod. Res. Develop.*, **3**, 252 (1964).
2. J. F. Zack, Jr., E. L. Warrick, and G. Knoll, *J. Chem. Eng. Data*, **6**, 279 (1961).
3. M. Koike and A. Danno, *J. Phys. Soc. Japan*, **15**, 1501 (1960).
4. T. Uriu and T. Hakamada, *Kogyo Kagaku Zasshi*, **62**, 1421 (1959).
5. V. S. Fikhlgol'ts and R. V. Zolotareva, *Zh. Fiz. Khim.*, **35**, 78 (1961).
6. C. R. Masson, V. Boekelheide, and W. A. Noyes, Jr., in *Catalytic, Photochemical, and Electrolytic Reactions (Techniques of Organic Chemistry, Vol. II)*, A. Weissberger, Ed., Interscience, New York, 1956, 2nd Ed., p. 294.
7. Yu. P. Egorov, E. P. Kaplan, Z. I. Letina, V. A. Shliapochnikov, and A. D. Petrov, *J. Gen. Chem. USSR (Engl. Transl.)* **28**, 3258 (1958).



8. L. J. Bellamy, *The Infra-Red Spectra of Complex Molecules*, Wiley, New York, 1954.

9. E. L. Skau, J. C. Arthur, Jr., and H. Wakeham, in *Physical Methods of Organic Chemistry (Techniques of Organic Chemistry, Vol. I)*, Interscience, New York, 1959, 3rd Ed., p. 338.

10. S. Gordon, A. R. Van Dyken, and T. F. Doumani, *J. Phys. Chem.*, **62**, 20 (1958).

11. W. G. Burns and C. R. V. Reed, *Trans. Faraday Soc.*, **59**, 101 (1963).

### Résumé

La photolyse à l'ultraviolet ( $\lambda = 2537 \text{ \AA}$ ) d'un mélange dégazé de polysiloxane phényl-méthylrique liquide a été examinée du point de vue des gaz et du rendement en pontage. Les résultats sont comparés aux valeurs publiées obtenues par irradiation ionisante du même type de molécule. On a montré que la radiation ultraviolette est moins efficace de deux ordres de grandeurs en ce qui concerne la décomposition du produit (des produits gazeux) que ne l'est la radiation ionisante. Les comparaisons en ce qui concerne l'efficacité de pontage sont moins certaines, mais le rendement semble indiquer des valeurs beaucoup plus similaires dans ce cas sur la base d'une estimation spectroscopique du pontage (c.a.d. l'analyse du point de vue de la formation de phénylcyclohexadiène substitué). Le rendement quantique en gaz était  $\phi_{\text{H}_2} = 2.6 \times 10^{-5}$ ,  $\phi_{\text{CH}_4} = 0.63 \times 10^{-5}$ ,  $\phi_{\text{C}_2\text{H}_6} \approx 0.12 \times 10^{-5}$  et  $\phi_{\text{C}_2\text{H}_2} \approx 0.06 \times 10^{-5}$ .

### Zusammenfassung

Die Ultravioletphotolyse ( $\lambda = 2537 \text{ \AA}$ ) eines entgasten, flüssigen Phenyl-Methylpolysiloxangemisches wird hinsichtlich der Gas- und Vernetzungsausbeute untersucht. Die Ergebnisse werden mit den für die bei Einwirkung ionisierender Strahlung auf diesen Molekültyp erhaltenen Literaturwerten verglichen. Es wird gezeigt, dass die Ultravioletstrahlung bei der Hervorrufung der Zersetzung (d.h. gasförmige Produkte) um zwei Größenordnungen weniger wirksam ist als die ionisierende Strahlung. Der Vergleich der Vernetzungsausbeute ist weniger sicher, doch scheinen die Ausbeuten in diesem Fall aufgrund der spektroskopischen Bestimmung der Vernetzung (d.h. Analyse auf Bildung von substituiertem Phenylcyclohexandien) viel ähnlicher zu sein. Die Quantenausbeute für die Gasbildung war  $\phi_{\text{H}_2} = 2,6 \cdot 10^{-5}$ ,  $\phi_{\text{CH}_4} = 0,63 \cdot 10^{-5}$ ,  $\phi_{\text{C}_2\text{H}_6} \approx 0,12 \cdot 10^{-5}$  und  $\phi_{\text{C}_2\text{H}_2} \approx 0,06 \cdot 10^{-5}$ .

Received September 20, 1965

Revised January 11, 1966

Prod. No. 5054A

## Correlation of Cationic Copolymerization Parameters of Cyclic Ethers, Formals, and Esters

YUYA YAMASHITA, TETSUO TSUDA, MASAHIKO OKADA, and SHOUJI IWATSUKI, *Department of Synthetic Chemistry, Faculty of Engineering, Nagoya University, Furo-cho, Chikusa-ku, Nagoya, Japan*

### Synopsis

Carefully determined cationic copolymerization parameters of cyclic ethers, formals, and esters are collected. Relative reactivity correlates with basicity and free energy. Further correlations of the copolymerization parameters for styrene, the effect of promoters, and the known mechanism of hydrolysis permitted a decision between the carbonium ion (including acylium ion) or the oxonium ion as the active intermediate of the propagation. Structural features which promote depropagation are identified. Equations describing these possibilities were derived and briefly discussed. Catalyst and solvent effects limited the correlation possibilities.

### Copolymerization Parameters and Basicity

Cationic copolymerization of cyclic ethers, formals, and esters has been studied in recent years, and now sufficient copolymerization parameters are available. In previous communications we indicated that the basicity of the monomers is a factor in the cationic copolymerization of cyclic ethers;<sup>1-3</sup> the plot of  $\log 1/r_1$  (relative reactivity) versus  $pK_b$  for monomer  $M_2$  gave a straight line in the copolymerization of 1,3-dioxolane.<sup>2</sup> Reexamining the existing monomer reactivity ratios for the cationic copolymerization of cyclic ethers, formals, and esters in relation to the basicity of monomers, we can obtain valuable information about the reactivity of the cyclic compounds and some factors affecting the propagation of cationic polymerization.

The monomer reactivity ratios are summarized in Table I. Only reliable values which were determined from the Fineman-Ross plot or from the line intersection method were chosen from the literature or from our own experiments. It must be mentioned that in ionic polymerizations random copolymerization is disproved in some cases, and the meaning of the monomer reactivity ratios might be rather obscure. Tada, Saegusa, and Furukawa<sup>10</sup> succeeded in the quantitative analysis of the sequence, distribution of cationic copolymers obtained from 3,3-bis(chloromethyl)oxetane and  $\beta$ -propiolactone, and proved that the polymer has some block character and does not therefore obey the copolymer statistics. Block

TABLE I  
 Monomer Reactivity Ratios in Cationic Copolymerization

M <sub>1</sub>	M <sub>2</sub>	Catalyst	Solvent	Temperature, °C.	r <sub>1</sub>	r <sub>2</sub>	Ref.
3,3-Bischloromethyl- oxetane	γ-Butyrolactone	BF <sub>3</sub> ·Et <sub>2</sub> O	C <sub>7</sub> H <sub>8</sub>	0	1.4	0.04	4
	ε-Caprolactone	BF <sub>3</sub> ·Et <sub>2</sub> O	C <sub>7</sub> H <sub>8</sub>	0	0.24	0.44	4
	4-Chloromethyl-1,3-dioxane	BF <sub>3</sub> ·Et <sub>2</sub> O	CH <sub>2</sub> Cl <sub>2</sub>	0	13	0	5
	β-Dimethyl-β-propiolactone	BF <sub>3</sub> ·Et <sub>2</sub> O	C <sub>7</sub> H <sub>8</sub>	0	7.24 ± 0.32	1.42 ± 0.10	6
	1,3-Dioxane	BF <sub>3</sub> ·Et <sub>2</sub> O	CH <sub>2</sub> Cl <sub>2</sub>	0	13	0	5
	1,4-Dioxane	BF <sub>3</sub> ·Et <sub>2</sub> O	—	0	2.12	0	7
	1,4-Dioxane	BF <sub>3</sub> ·Et <sub>2</sub> O	CH <sub>2</sub> Cl <sub>2</sub>	0	7	0	5
	1,3-Dioxolane	BF <sub>3</sub> ·Et <sub>2</sub> O	C <sub>7</sub> H <sub>8</sub>	0	1.5 ± 0.1	0.65 ± 0.05	2
	Epichlorohydrin	BF <sub>3</sub> ·Et <sub>2</sub> O	CH <sub>2</sub> Cl <sub>2</sub>	0	3-2	0.3-0.5	8
	4-Methyl-1,3-dioxane	BF <sub>3</sub> ·Et <sub>2</sub> O	CH <sub>2</sub> Cl <sub>2</sub>	0	13	0	5
	4-Methyl-1,3-dioxolane	BF <sub>3</sub> ·Et <sub>2</sub> O	—	0	3.02	—	7
	β-Methyl-β-propiolactone	BF <sub>3</sub> ·Et <sub>2</sub> O	C <sub>7</sub> H <sub>8</sub>	0	11.9 ± 0.2	0.13 ± 0.02	6
	2-Methyltetrahydrofuran	BF <sub>3</sub> ·Et <sub>2</sub> O	—	0	1.29	—	7
	2-Methyltetrahydrofuran	BF <sub>3</sub> ·Et <sub>2</sub> O	—	0	2.7 ± 0.25	0.05 ± 0.01	9
	4-Phenyl 1,3-dioxane	BF <sub>3</sub> ·Et <sub>2</sub> O	—	0	13	—	7
	4-Phenyl 1,3-dioxane	BF <sub>3</sub> ·Et <sub>2</sub> O	CH <sub>2</sub> Cl <sub>2</sub>	0	46	0	5
	β-Propiolactone	BF <sub>3</sub> ·Et <sub>2</sub> O	C <sub>7</sub> H <sub>8</sub>	0	16.7 ± 0.5	0.15 ± 0.01	6
	β-Propiolactone	BF <sub>3</sub> ·Et <sub>2</sub> O	CH <sub>2</sub> Cl <sub>2</sub>	0	38	0.06	10
	β-Propiolactone	BF <sub>3</sub> ·Et <sub>2</sub> O	CH <sub>2</sub> Cl <sub>2</sub>	0	16	0.05	10
	β-Propiolactone	AlEt <sub>3</sub> -H <sub>2</sub> O	CH <sub>2</sub> Cl <sub>2</sub>	-50	30	0.1	10
	β-Propiolactone	AlEt <sub>3</sub> -H <sub>2</sub> O	CH <sub>2</sub> Cl <sub>2</sub>	-50	30	0.04	10
	Propylene oxide	BF <sub>3</sub> ·Et <sub>2</sub> O	CH <sub>2</sub> Cl <sub>2</sub>	0	0.3	0.65	8
	Styrene oxide	BF <sub>3</sub> ·Et <sub>2</sub> O	CH <sub>2</sub> Cl <sub>2</sub>	0	0.8	0.8	8
	Tetrahydrofuran	BF <sub>3</sub> ·Et <sub>2</sub> O	C <sub>7</sub> H <sub>8</sub>	0	0.82 ± 0.05	1.00 ± 0.05	11
	Tetrahydrofuran	AlEt <sub>3</sub> -H <sub>2</sub> O-ECH <sup>a</sup>	CH <sub>2</sub> Cl <sub>2</sub>	0	0.00	1.50 ± 0.20	12 <sup>a</sup>
	Tetrahydrofuran	AlEt <sub>3</sub> -ECH <sup>a</sup>	CH <sub>2</sub> Cl <sub>2</sub>	0	0.01 ± 0.01	1.80 ± 0.01	12 <sup>a</sup>

4-Chloromethyl-1,3-dioxolane	Tetrahydropyran	BF <sub>3</sub> ·Et <sub>2</sub> O	0	1.66	0	0	7
	δ-Valerolactone	BF <sub>3</sub> ·Et <sub>2</sub> O	30	0.20	0	0	14
	1,3-Dioxolane	BF <sub>3</sub> ·Et <sub>2</sub> O	0	0.18 ± 0.10	10.7 ± 0.3	2	2
	1,3-Dioxolane	BF <sub>3</sub> ·Et <sub>2</sub> O	0	0.12 ± 1.0	12.0 ± 1.0	15	15
	1,3-Dioxolane	BF <sub>3</sub> ·Et <sub>2</sub> O	0	0.37 ± 0.10	21 ± 2	15	15
	1,3-Dioxolane	SnCl <sub>4</sub>	0	0.14 ± 0.08	20 ± 5	15	15
	1,3-Dioxolane	SnCl <sub>4</sub>	0	0.07 ± 0.05	9.3 ± 1.0	15	15
	1,3-Dioxolane	SnCl <sub>4</sub>	0	0.23 ± 0.15	23.0 ± 6.0	15	15
	1,3-Dioxolane	HClO <sub>4</sub> -Ac <sub>2</sub> O	0	0.15 ± 0.05	1.8 ± 0.2	2	2
	1,3-Dioxolane	HClO <sub>4</sub> -Ac <sub>2</sub> O	0	0.13 ± 0.04	13.3 ± 1.3	15	15
	1,3-Dioxolane	HClO <sub>4</sub> -Ac <sub>2</sub> O	0	0.30 ± 0.20	28 ± 10	15	15
	1,3-Dioxolane	HClO <sub>4</sub> -Ac <sub>2</sub> O	0	0.08 ± 0.04	4.5 ± 1.0	15	15
	1,3-Dioxolane	HClO <sub>4</sub> -Ac <sub>2</sub> O	0	0.09 ± 0.04	14.0 ± 2.0	15	15
	1,3-Dioxolane	BF <sub>3</sub> ·Et <sub>2</sub> O	0	0.45 ± 0.08	3.3 ± 0.4	16	16
	4-Methyl 1,3-dioxolane	BF <sub>3</sub> ·Et <sub>2</sub> O	0	0.12 ± 0.05	14.2 ± 1.5	16	16
1,3-Dioxolane	Tetramethylene formal	BF <sub>3</sub> ·Et <sub>2</sub> O	0	0.08 ± 0.02	75 ± 0.02	16	16
	Trioxocane	BF <sub>3</sub> ·Et <sub>2</sub> O	0	0.65 ± 0.05	1.5 ± 0.1	2	2
	3,3-Bischloromethylloxetane	BF <sub>3</sub> ·Et <sub>2</sub> O	0	10.7 ± 0.3	0.18 ± 0.10	2	2
	4-Chloromethyl 1,3-dioxolane	BF <sub>3</sub> ·Et <sub>2</sub> O	0	12.0 ± 1.0	0.12 ± 0.03	15	15
	"	BF <sub>3</sub> ·Et <sub>2</sub> O	0	21 ± 2	0.37 ± 0.10	15	15
	"	BF <sub>3</sub> ·Et <sub>2</sub> O	0	20 ± 5	0.14 ± 0.08	15	15
	"	SnCl <sub>4</sub>	0	9.3 ± 1.0	0.07 ± 0.05	15	15
	"	SnCl <sub>4</sub>	0	23.0 ± 6.0	0.25 ± 0.15	15	15
	"	HClO <sub>4</sub> -Ac <sub>2</sub> O	0	1.8 ± 0.2	0.15 ± 0.05	2	2
	"	HClO <sub>4</sub> -Ac <sub>2</sub> O	0	13.3 ± 1.3	0.13 ± 0.04	15	15
	"	HClO <sub>4</sub> -Ac <sub>2</sub> O	0	28 ± 1.0	0.30 ± 0.20	15	15
	"	HClO <sub>4</sub> -Ac <sub>2</sub> O	0	4.5 ± 1.0	0.08 ± 0.04	15	15
	"	HClO <sub>4</sub> -Ac <sub>2</sub> O	0	14.0 ± 2.0	0.09 ± 0.04	15	15
	Epichlorohydrin	BF <sub>3</sub> ·Et <sub>2</sub> O	0	0.08	1.2	15	15
	Oxetane	BF <sub>3</sub> ·Et <sub>2</sub> O	0	0.0125	165	15	15
"	SnCl <sub>4</sub>	0	0.03	100	15	15	
"	SnCl <sub>4</sub>	0	0.01	90	15	15	

(continued)

TABLE I (continued)

$M_1$	$M_2$	Catalyst	Solvent	Temperature, °C.	$r_1$	$r_2$	Ref.
	Tetrahydrofuran	$\text{BF}_3 \cdot \text{Et}_2\text{O}$	—	0	$0.25 \pm 0.05$	$28 \pm 4$	2
	"	$\text{BF}_3 \cdot \text{Et}_2\text{O}$	$\text{C}_7\text{H}_8$	0	$0.71 \pm 0.10$	$25 \pm 3$	15
	"	$\text{SnCl}_4$	$\text{C}_7\text{H}_8$	0	$0.24 \pm 0.03$	$195 \pm 10$	15
	"	$\text{SnCl}_4$	$\text{CH}_2\text{Cl}_2$	0	0.245	40	15
	Trioxane	$\text{SiHSO}_4$	—	70	1.75	0.57	17
	3,3-Bischloromethylloxetane	$\text{BF}_3 \cdot \text{Et}_2\text{O}$	$\text{CH}_2\text{Cl}_2$	0	—	3	8
Epichlorohydrin	1,3-Dioxolane	$\text{BF}_3 \cdot \text{Et}_2\text{O}$	—	0	1.2	0.08	15
	2-Methyltetrahydrofuran	$\text{BF}_3 \cdot \text{Et}_2\text{O}$	—	0	$0.04 \pm 0.05$	$0.27 \pm 0.05$	9
	Tetrahydrofuran	$\text{BF}_3 \cdot \text{Et}_2\text{O}$	—	0	$0.00 \pm 0.05$	$3.85 \pm 0.05$	9
	"	$\text{AlEt}_3\text{-H}_2\text{O}$	—	0	$0.5 \pm 0.3$	$20 \pm 5$	12
	3,3-Bischloromethylloxetane	$\text{BF}_3 \cdot \text{Et}_2\text{O}$	$\text{C}_7\text{H}_8$	0	$0.15 \pm 0.01$	$16.7 \pm 0.5$	6
$\beta$ -Propiolactone	"	$\text{BF}_3 \cdot \text{Et}_2\text{O}$	$\text{CH}_2\text{Cl}_2$	0	0.06	38	10
	"	$\text{BF}_3 \cdot \text{Et}_2\text{O}$	$\text{CH}_2\text{Cl}_2$	-50	0.05	16	10
	"	$\text{AlEt}_3\text{-H}_2\text{O}$	$\text{CH}_2\text{Cl}_2$	0	0.1	30	10

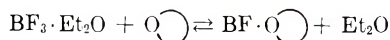


	"	AlEt <sub>3</sub> -H <sub>2</sub> O	CH <sub>2</sub> Cl <sub>2</sub>	-50	0.04	30	10
	γ-Butyrolactone	AlEt <sub>3</sub> -H <sub>2</sub> O	CH <sub>2</sub> Cl <sub>2</sub>	0	18 ± 2	0.36 ± 0.10	18
	Tetrahydrofuran	BF <sub>3</sub> ·Et <sub>2</sub> O	—	0	0.4 ± 0.2	2.9 ± 0.5	19
	"	AlEt <sub>3</sub> -H <sub>2</sub> O	—	0	0.1 ± 0.1	5.5 ± 0.1	19
Styrene oxide	3,3-Bischloromethylloxetane	BF <sub>3</sub> ·Et <sub>2</sub> O	CH <sub>2</sub> Cl <sub>2</sub>	0	—	0.9	8
	p-Chlorostyrene oxide	BF <sub>3</sub> ·Et <sub>2</sub> O	C <sub>7</sub> H <sub>8</sub>	-20	1.1 + 0.2	0.4 ± 0.15	20
	p-Methylstyrene oxide	BF <sub>3</sub> ·Et <sub>2</sub> O	C <sub>7</sub> H <sub>8</sub>	-20	0.65 ± 0.10	1.2 ± 0.2	20
	3,3-Bischloromethylloxetane	BF <sub>3</sub> ·Et <sub>2</sub> O	C <sub>7</sub> H <sub>8</sub>	0	1.00 ± 0.05	0.82 ± 0.05	11
Tetrahydrofuran	"	AlEt <sub>3</sub> -H <sub>2</sub> O-ECH	CH <sub>2</sub> Cl	0	1.50 ± 0.20	0.00	12
	"	AlEt <sub>3</sub> -ECH	CH <sub>2</sub> Cl <sub>2</sub>	0	1.80 ± 0.01	0.01 ± 0.01	12
	Epichlorohydrin	BF <sub>3</sub> ·Et <sub>2</sub> O	—	0	3.85 ± 0.05	0.00 ± 0.05	9
	"	AlEt <sub>3</sub> -H <sub>2</sub> O	—	0	20 ± 5	0.5 ± 0.3	12
	Ethylene oxide	BF <sub>3</sub>	—	0	2.2	0.08	21
	1,3-Dioxolane	BF <sub>3</sub> ·Et <sub>2</sub> O	—	0	28 ± 4	0.25 ± 0.05	2
	"	BF <sub>3</sub> ·Et <sub>2</sub> O	C <sub>7</sub> H <sub>8</sub>	0	25 ± 3	0.71 ± 0.10	15
	"	SnCl <sub>4</sub>	C <sub>7</sub> H <sub>8</sub>	0	195 ± 10	0.24 ± 0.03	15
	"	SnCl <sub>4</sub>	CH <sub>2</sub> Cl <sub>2</sub>	0	40	0.245	15
	β-Propiolactone	BF <sub>3</sub> ·Et <sub>2</sub> O	—	0	2.9	0.4	19
	"	AlEt <sub>3</sub> -H <sub>2</sub> O	—	0	5.5	0.1	19

<sup>a</sup> Epichlorohydrin, promotor.

copolymers were also obtained in the case of  $\beta$ -propiolactone with epichlorohydrin or propylene oxide,<sup>19</sup> and of tetrahydrofuran with epichlorohydrin.<sup>9</sup> In some cases, as in the copolymerization of trioxane with 1,3-dioxolane,<sup>17</sup> a significant amount of homopolymer was formed. However, the tabulated copolymerization parameters were calculated for the case of an almost random copolymers, and the correlation of these parameters will be discussed.

We have measured the infrared absorption spectra of cyclic compounds in the presence of 0.1 mole/l. methanol-*d*, and the basicity of the monomers was calculated (Table II) from the shift value of the O-D stretching band by the Gordy equation<sup>22</sup> as in our previous reports.<sup>1,3</sup> The consistency of these values with data obtained by other methods<sup>23</sup> is sufficient to permit them to be used as a measure of basicity. We reported that the equilibrium constant for the reaction



is also parallel to the basicity of cyclic compounds, as shown in Table II.<sup>24,25</sup>

Some characteristic features of these results are worthy of mention. The basicity of cyclic monomers is affected by the chemical structure, ring size, and substituents. In the case of cyclic ethers, the basicity order is affected by the ring size as follows:  $4 > 5 > 6 > 3$ , but in the case of cyclic formals the order is  $7 > 5 > 6$  and in the case of lactones  $6 > 7 > 5 > 4$ . If we compare the basicity of compounds of the same ring size the basicity order is ether  $>$  lactone  $>$  formal in five-membered compounds and lactone  $>$  ether  $>$  formal in six-membered compounds. In every case methyl substitution increases the basicity and chloromethyl substitution decreases the basicity, as expected.

When we consider the propagation reaction of copolymerization,  $1/r_1 = k_{12}/k_{11}$  represents the relative reactivity of monomer  $M_2$  toward  $M_1$ . The plot of  $\log 1/r_1$  versus  $pK_b$  of monomer  $M_2$  is shown in Figure 1 for the 3,3-bischloromethyloxetane cation end  $M_1^+$ . It is apparent that the relative reactivity is not dependent on the basicity alone, and considerable scattering is observed.

The propagating steps of cationic copolymerization are shown in eqs. (1)–(4).



The rate constants of these reactions are supposed to depend mainly on the reactivity of the chain end and the nucleophilicity of the attacking monomer. The linear plot of  $1/r_1$  versus  $pK_b$  means that the proton affinity or

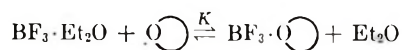
TABLE II  
 Basicity of Cyclic Monomers

No.	Monomer	Infrared		$K^c$
		$\nu_{OD}$ cm. <sup>-1a</sup>	$pK_b^b$	
1.	Oxetane	2565	3.13	
2.	2-Methyltetrahydrofuran	2578	4.56	14 ± 4
3.	Tetrahydrofuran	2582	5.00	34 ± 9
4.	$\delta$ -Valerolactone	2584	5.10	1.1 ± 0
5.	$\epsilon$ -Caprolactone	2586	5.31	0.41 ± 0.05
6.	Tetrahydropyran	2587	5.42	12 ± 0
7.	3,3-Bischloromethyloxetane	2589	5.65	
8.	Trioxocane	2589	5.65	
9.	1,4-Dioxane	2590	5.71	1.9 ± 0.8
10.	4-Phenyl-1,3-dioxane	2591	5.78	
11.	Tetramethylene formal	2594	6.12	
12.	$\gamma$ -Butyrolactone	2594	6.12	0.16 ± 0.02
13.	Propylene oxide	2602	6.94	
14.	2-Methyl-1,3-dioxolane	2605	7.21	0.59 ± 0.07
15.	1,3-Dioxolane	2608	7.55	
16.	4-Methyl-1,3-dioxolane	2609	7.62	0.34 ± 0.1
17.	Styrene oxide	2616	8.30	
18.	Epichlorohydrin	2621	8.84	
19.	4-Chloromethyl 1,3-dioxolane	2623	9.05	(4.5 ± 0.9) × 10 <sup>-3</sup>
20.	$\beta$ -Dimethyl- $\beta$ -propiolactone	2625	9.53	
21.	$\beta$ -Methyl- $\beta$ -propiolactone	2629	9.59	
22.	Trioxane	2633	10.00	
23.	$\beta$ -Propiolactone	2634	10.06	

<sup>a</sup> IR, methanol-*d* 0.1 mole/l.

<sup>b</sup> Calculated by the Gordy equation  $\Delta\mu = 0.0147 \log K_b + 0.194$ , where  $\Delta\mu$  represents the shift value of  $\nu_{OD}$  in millimicrons from the  $\nu_{OD}$  of methanol-*d* in benzene (2666 cm.<sup>-1</sup>).

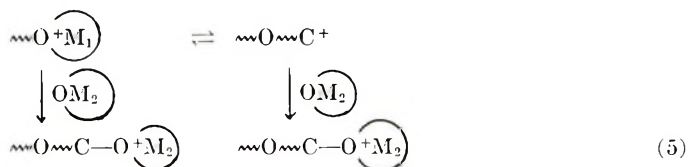
<sup>c</sup> Equilibrium constant measured by NMR for the reaction:



basicity toward the Lewis acid is a measure of carbonium ion affinity. The slope of the plot shows the selectivity of the chain end.<sup>2</sup>

### Propagating Species of Cationic Polymerization

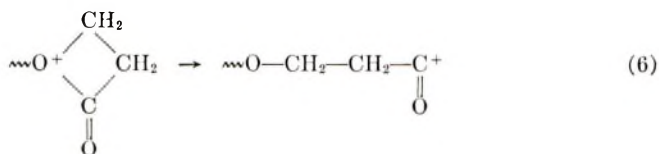
There is some question as to the propagating species of cationic polymerization of cyclic compounds. The trialkyloxonium ion is believed to be more stable than the carbonium ion derived by the ring opening of the oxonium ion, except for the resonance-stabilized carbonium ion. So we assume an oxonium ion as the predominant species in the propagation, but the active species may be an oxonium ion or a carbonium ion in the rate-determining step. Irrespective of either ion pair or free ion, we assume the scheme shown in eq. (5) for the propagation reaction.

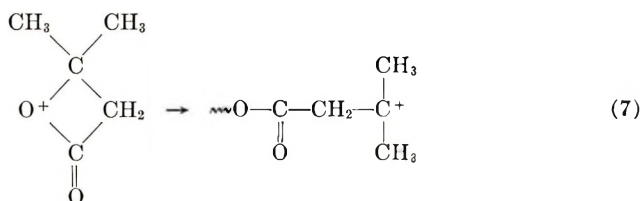


In the case of oxetane and tetrahydrofuran, the propagating species of cationic polymerization is assumed to be an oxonium ion, and  $S_N2$  attack is suggested from kinetic evidence.<sup>24-31</sup> Also the *trans* opening of 7-oxabicyclo[2.2.1]heptane<sup>32</sup> and 2,3-butylene oxide<sup>33,34</sup> is in favor of an oxonium ion. On the other hand, Eastham suggested that  $S_N1$  opening of the oxonium ion is the rate-determining step in the cationic polymerization of ethylene oxide.<sup>35</sup> The propagating species of cationic polymerization of trioxane was assumed to be a carbonium ion from kinetic investigation<sup>36,37</sup> and chain transfer studies.<sup>38</sup>

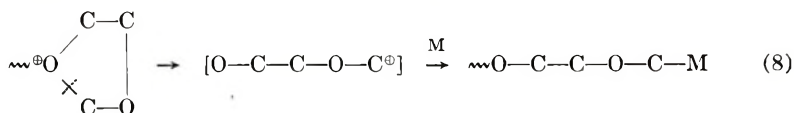
The propagating species can be examined from the copolymerization behavior of cyclic compounds with styrene. Random copolymerization with styrene indicates that the propagating species of cyclic compounds are similar to the styryl cation, that is, a carbonium ion from the  $S_N1$  opening of the oxonium ion. On the other hand, the oxonium ion is rather stable and is difficult to react with styrene, and a homopolymer mixture may result in the attempted copolymerization of styrene with  $S_N2$  opening of cyclic compounds.

The failure of cross propagation with combinations of monomers of different polarities is often reported, and O'Driscoll deduced an equation based on the assumption of negligible cross propagation.<sup>39</sup> The cationic copolymerization of 3,3-bischloromethyloxetane or tetrahydrofuran with styrene yields homopolymer mixtures.<sup>40</sup> This is further evidence for the oxonium ion structure in these cases. On the other hand, we reported an almost random copolymerization of 1,3-dioxolane<sup>26</sup> or related formals with styrene,<sup>27</sup> and a true copolymer is reported to be obtained in the case of epichlorohydrin, styrene oxide, or trioxane with styrene.<sup>41,42</sup> Ease of  $S_N1$  opening of an oxonium ion to a carbonium ion is explained from the existing ring strain in epoxides or from the resonance stabilization of the carbonium ion structure of  $\sim\text{O}-\text{CH}_2^+ \leftrightarrow \text{O}^+ = \text{CH}_2$  in cyclic formals. In the case of  $\beta$ -lactones, acyl-oxygen fission of the oxonium ion to give the acyl carbonium ion is suggested with  $\beta$ -propiolactone [eq. (6)], and alkyl-oxygen fission of the oxonium ion to give the more stable tertiary carbonium is suggested with  $\beta$ -dimethyl- $\beta$ -propiolactone [eq. (7)] from the copolymerization behavior of  $\beta$ -lactones with 3,3-bischloromethyloxetane or with styrene.<sup>4,6</sup>

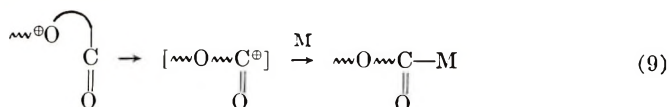




Some comments must be added on the ring scission of cyclic formals and esters. From the decrease of the formal unit corresponding to the monomer unit in the copolymerization of 1,3-dioxolane and related formals with styrene, we concluded the mode of fission<sup>26,27</sup> shown in eq. (8).

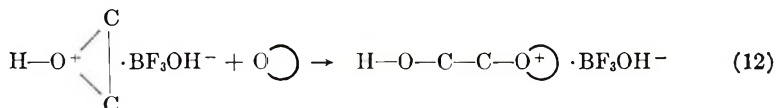
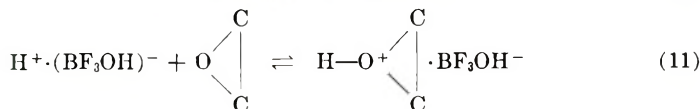


Also in the cationic polymerization of lactones, the scheme shown in eq. (9) was established from the copolymerization with styrene.<sup>4,6</sup>



The basicity of lactones involves carbonyl oxygen rather than ether oxygen,<sup>14</sup> so that the relation between reactivity and basicity might be modified in these systems. However, the apparent existence of some relationship indicates that the attack of the chain end by ether oxygen may be an equilibrated reaction, with the attack by carbonyl oxygen leading to the propagating oxonium ion at the ether oxygen.

The polymerization of 3,3-bis(chloromethyl)oxetane and tetrahydrofuran with  $\text{BF}_3 \cdot \text{Et}_2\text{O}$  is greatly accelerated by promoters such as epichlorohydrin and propylene oxide, but less by 1,3-dioxolane and  $\beta$ -propiolactone.<sup>43,44</sup> The rate increase was ascribed to the formation of a trialkyl-oxonium ion by the easy  $S_N1$  opening of promoters [eqs. (10)–(12)].



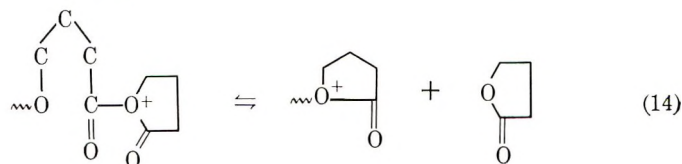
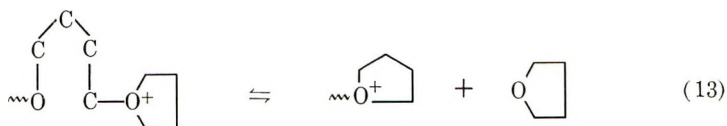
These discussions are in good accord with the mechanism of acid-catalyzed hydrolyses. The mechanism of hydrolyses are characterized by their entropies of activation. For the case of  $\gamma$ -<sup>45</sup> and  $\delta$ -lactones<sup>46</sup> the  $S_N2$  mechanism was established, and for the case of  $\beta$ -lactones,<sup>47,48</sup> epoxides,<sup>49</sup> and cyclic acetals a  $S_N1$  mechanism was concluded.



Therefore,  $S_N1$  character is assumed to increase in the following order:  $\beta$ -lactones  $<$  1,3-dioxolane  $<$  epoxides; pure  $S_N2$  character is assumed with tetrahydrofuran and  $\gamma$ - and  $\delta$ -lactones.

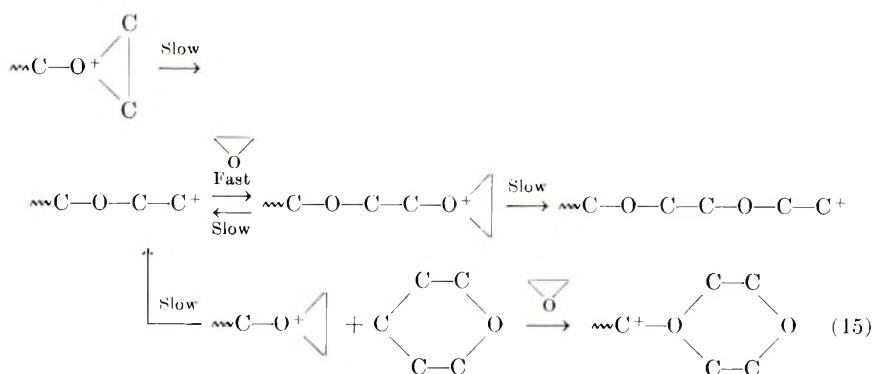
### Depropagation Reaction

In cationic polymerization, five- or six-membered cyclic ethers and esters are less reactive and do not yield polymers in any significant amount; these are also less reactive in copolymerization. Some examples are 2-methyltetrahydrofuran, tetrahydropyran, 1,4-dioxane,  $\gamma$ -butyrolactone, ethylene carbonate, and succinic anhydride. These monomers do yield copolymers with 3,3-bis(chloromethyl)oxetane,<sup>4,5,7</sup>  $\beta$ -propiolactone,<sup>18</sup> or alkylene oxide<sup>9</sup> but not with tetrahydrofuran or 1,3-dioxolane. These facts are explained by the equilibrium of propagation and depropagation. From acid-catalyzed hydrolysis of  $\gamma$ -lactones, the equilibrium is in favor of the ring,<sup>46</sup> and the equilibrium of propagation and depropagation is also supposed in favor of monomers, due to the stability of the oxonium ion. The trialkyloxonium ion is supposed to be very stable with five- or six-membered monomers, from the stability of  $BF_3$  complexes<sup>25</sup> and from the effect of promoters in the polymerization of these monomers.<sup>43,44</sup>

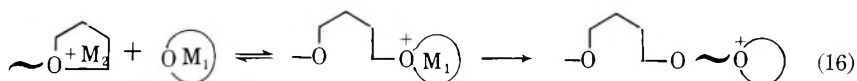


The ceiling temperature of tetrahydrofuran is shown to lie near the room temperature,<sup>50</sup> and substituted tetrahydrofuran cannot be polymerized.<sup>51</sup> Dainton revealed that, from the thermodynamic point of view, the free energy decrease due to polymerization is very small or even negative, especially when the five- or six-membered monomer has some substituents.<sup>52</sup>

The depropagation reaction was observed with tetrahydrofuran by Meerwein,<sup>31</sup> Bawn,<sup>53</sup> and Tobolsky,<sup>54</sup> with trioxane by Kern,<sup>36</sup> and with ethylene oxide by Eastham.<sup>35</sup> The formation of 1,4-dioxane in the cationic polymerization of ethylene oxide shows that the six-membered oxonium ion is so stable as to be able to establish the depropagation equilibrium [eqs. (15)].



The copolymerization of these five- and six membered monomers ( $M_2$ ) is possible if the produced oxonium ion is so unstable as that the propagation reaction proceeds before the depropagation occurs [eq. (16)].



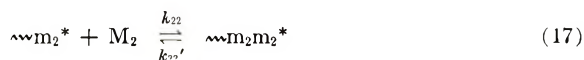
This is the case with epoxides, oxetanes, and  $\beta$ -lactones.

We have observed considerable reactivity decrease of tetrahydrofuran near the ceiling temperature in the copolymerization with 3,3-bischloromethyloxetane, thus proving the participation of depropagation in the copolymerization of tetrahydrofuran.<sup>15</sup>

### Relative Reactivity of Cyclic Compounds

Inspecting the scatter observed in Figure 1 we notice the upperward deviation of three-membered ethers and the downward deviation of five- or six-membered ethers. This can be related to the strain in the ring or to the free energy of polymerization.

Nucleophilic attack of monomer  $M_2$  on the  $M_1$  oxonium end by the  $S_N2$  mechanism leads to an ordinary second-order propagation rate equation, and the Mayo-Lewis equation results. In these cases the relative reactivity should be dependent on the basicity alone. If we consider the depropagation reaction, however, the kinetic scheme must be modified as shown in eqs. (17) and (18) if only the oxonium end with penultimate  $M_2$  unit can depropagate.



We can derive a copolymerization equation by Lowry's method.<sup>55</sup> The equation including  $k_{22}/k'_{22}$  and  $k_{21}/k'_{21}$  is not so straightforward, but at least qualitatively we can say that the  $M_2$  content of the copolymer decreases from the basicity predictions by the participation of depropagation, which is significant in the case of five- or six-membered compounds.

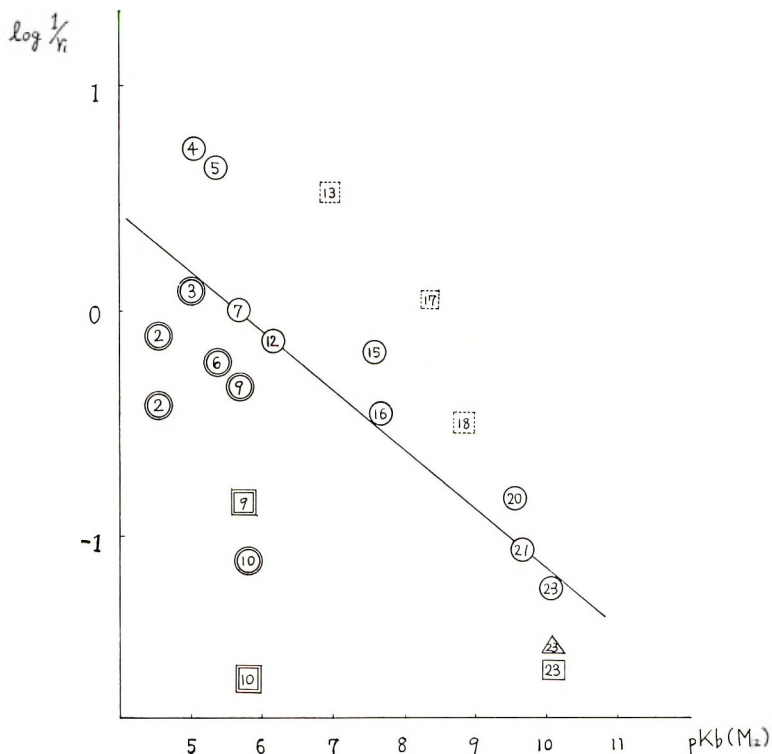
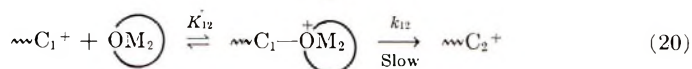
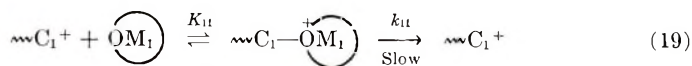


Fig. 1. Relative reactivity toward 3,3-bis(chloromethyloxy)ethane cation end  $M_1^+$ . (○)  $\text{BF}_3 \cdot \text{Et}_2\text{O}$  bulk or in  $\text{C}_7\text{H}_8$ ; (□)  $\text{BF}_3 \cdot \text{Et}_2\text{O}$  in  $\text{CH}_2\text{Cl}_2$ ; (△)  $\text{AlEt}_3\text{-H}_2\text{O}$  in  $\text{CH}_2\text{Cl}_2$ ; (⊠) three-membered ethers; (⊙), (⊞) five- or six-membered ethers. Numbers in symbols refer to Table II.

On the other hand, the  $S_N1$  propagation leads to the scheme shown in eqs. (19) and (20).



The existence of the first equilibrium was suggested in the copolymerization of styrene with cyclic ethers, formals, and esters<sup>6</sup> or in the  $S_N1$  solvolysis of tosylates in aqueous ethers. The rate of reactions (19) and (20) is expressed as

$$\frac{k_{11}K_{11}[\text{C}_1^+][\text{M}_1]}{1 + K_{11}[\text{M}_1] + K_{12}[\text{M}_2]}$$

and

$$\frac{k_{12}K_{12}[\text{C}_1^+][\text{M}_2]}{1 + K_{11}[\text{M}_1] + K_{12}[\text{M}_2]}$$

respectively. The copolymerization equation reduces to the ordinary Mayo-Lewis equation if  $r_1$  and  $r_2$  are expressed as

$$\frac{d[M_1]}{d[M_2]} = \frac{[M_1]}{[M_2]} \frac{r_1[M_1] + [M_2]}{[M_1] + r_2[M_2]}$$

where  $r_1 = k_{11}K_{11}/k_{12}K_{12}$  and  $r_2 = k_{22}K_{22}/k_{21}K_{21}$ . The copolymerization parameters should therefore include  $k$  and  $K$ .  $K$  should be proportional to the basicity, but  $k$  is the rate of  $S_N1$  opening of the derived oxonium ion. The relative reactivity of monomer  $M_2$  estimated from the  $1/r_1$  value thus includes the rate of ring opening in addition to basicity. Thus we can explain the larger reactivity of epoxides.

Thus the basicity and the free energy of polymerization participate in these copolymerization kinetically and/or thermodynamically as the case may be.

In ionic copolymerizations, monomer reactivity ratios are significantly affected by solvent and catalyst, and systematic interpretation is difficult even in the simplest cases.<sup>56</sup> At least two explanations are possible with these effects. By the first explanation, the stronger the catalyst (i.e., the more stable the counter-anion) and more polar the solvent, the larger the ionic character of the chain end and the smaller the selectivity. But these factors also affect the course of the propagation steps, and  $S_N1$  character may have advantages in polar solvents with stronger Lewis acids, and the depropagation equilibrium may be affected by counteranion and solvent polarities. It is therefore very difficult to interpret these effects quantitatively in such complicated systems. In the copolymerization of trioxane in nitrobenzene, Kern et al.<sup>13</sup> obtained very unusual copolymerization parameters which these values do not fit our prediction from the basicities. The use of a polar solvent may have made the participation of the depropagation equilibrium very significant, and the incorporation of comonomers might have been affected by thermodynamic equilibrium rather than by kinetic control.

By the second explanation, Overberger<sup>57</sup> proposed preferential solvation of cation end by the more basic monomers in nonpolar solvents. This might be the case, but again the possibility of participation of these factors cannot be determined in these systems.

We are much indebted to Dr. S. Sakai of the Nagoya University, Dr. S. Aoki of the Osaka City University, and Dr. V. Jaacks of the Mainz University for valuable discussions and for offering their data.

### References

1. S. Iwatsuki, N. Takikawa, M. Okada, Y. Yamashita, and Y. Ishii, *J. Polymer Sci. B*, **2**, 549 (1964).
2. M. Okada, N. Takikawa, S. Iwatsuki, Y. Yamashita, and Y. Ishii, *Makromol. Chem.*, **82**, 16 (1965).
3. S. Iwatsuki, N. Takikawa, M. Okada, Y. Yamashita, and Y. Ishii, *Kogyo Kagaku Zasshi*, **67**, 1236 (1964).

4. T. Tsuda, T. Shimizu, and Y. Yamashita, *Kogyo Kagaku Zasshi*, **67**, 2145 (1964); *Makromol. Chem.*, **86**, 304 (1965).
5. S. Aoki, T. Otsu, and M. Imoto, *Kogyo Kagaku Zasshi*, **67**, 1958 (1964).
6. T. Tsuda, T. Shimizu, and Y. Yamashita, *Kogyo Kagaku Zasshi*, **67**, 1661 (1964).
7. T. Tsuda, T. Nomura, and Y. Yamashita, *Makromol. Chem.*, **86**, 301 (1965).
8. S. Aoki, K. Fujisawa, T. Otsu, and M. Imoto, *Kogyo Kagaku Zasshi*, **69**, 131 (1966).
9. A. Ishigaki, T. Shono, and Y. Hachihama, *Makromol. Chem.*, **79**, 170 (1964).
10. K. Tada, T. Saegusa, and J. Furukawa, *Makromol. Chem.*, **71**, 71 (1964).
11. T. Saegusa, H. Imai, and J. Furukawa, *Makromol. Chem.*, **56**, 55 (1962).
12. T. Saegusa, T. Ueshima, H. Imai, and J. Furukawa, *Makromol. Chem.*, **79**, 22 (1964).
13. V. Jaacks, G. E. Ham, and W. Kern, in *Copolymerization*, G. E. Ham, Ed., Interscience, New York, 1964, p. 803; also private communication.
14. T. Tsuda, T. Shimizu, and Y. Yamashita, *Kogyo Kagaku Zasshi*, **68**, 2473 (1965).
15. M. Okada and Y. Yamashita, unpublished work.
16. M. Okada, S. Iwatsuki, and Y. Yamashita, *Kogyo Kagaku Zasshi*, **68**, 2466 (1965).
17. M. Kučera and J. Pichler, *Polymer*, **5**, 371 (1964).
18. K. Tada, Y. Numata, T. Saegusa, and J. Furukawa, *Makromol. Chem.*, **77**, 220 (1964).
19. K. Tada, T. Saegusa, and J. Furukawa, *Kogyo Kagaku Zasshi*, **66**, 996, 1501 (1964).
20. M. Okada, K. Suyama, Y. Yamashita, and Y. Ishii, *Kogyo Kagaku Zasshi*, **68**, 546 (1964).
21. W. J. Murbach and A. Adicoff, *Ind. Eng. Chem.*, **52**, 772 (1960).
22. W. Gordy and S. C. Stanford, *J. Chem. Phys.*, **7**, 93 (1939); *ibid.*, **8**, 170 (1940); *ibid.*, **10**, 204, 215 (1941).
23. E. M. Arnett, *Progr. Phys. Org. Chem.*, **1**, 1 (1964).
24. M. Okada, K. Suyama, and Y. Yamashita, *Tetrahedron Letters*, **1965**, 2329.
25. M. Okada, K. Suyama, and Y. Yamashita, *Kogyo Kagaku Zasshi*, **68**, 1431 (1965).
26. M. Okada, Y. Yamashita, and Y. Ishii, *Kogyo Kagaku Zasshi*, **68**, 364 (1965); **69**, 506 (1966).
27. M. Okada, Y. Yamashita, and Y. Ishii, *Makromol. Chem.*, **80**, 196 (1964) and papers in press.
28. F. S. Dainton, T. R. E. Delvin, and P. A. Small, *Trans. Faraday Soc.*, **51**, 1710, 1717 (1955).
29. I. Penczek and St. Penczek, *Makromol. Chem.*, **67**, 203 (1963).
30. J. B. Rose, *J. Chem. Soc.*, **1956**, 542, 547.
31. H. Meerwein, D. Delfs, and H. Marshel, *Angew. Chem.*, **72**, 927 (1960).
32. E. L. Wittbecker, H. K. Hall, Jr., and T. W. Campbell, *J. Am. Chem. Soc.*, **82**, 1218 (1960).
33. E. J. Vandenberg, *J. Am. Chem. Soc.*, **83**, 3538 (1961).
34. E. J. Vandenberg, *J. Polymer Sci. B*, **2**, 1085 (1964).
35. A. M. Eastham, D. J. Worsfold, G. A. Latremouille, and G. T. Merrall, *J. Am. Chem. Soc.*, **79**, 897, 900 (1957); **82**, 120 (1960).
36. W. Kern and V. Jaacks, *J. Polymer Sci.*, **48**, 399 (1960).
37. S. Okamura, T. Higashimura, and M. Tomikawa, *Kogyo Kagaku Zasshi*, **65**, 712 (1962).
38. V. Jaacks, H. Baader, and W. Kern, *Makromol. Chem.*, **83**, 56 (1965).
39. K. F. O'Driscoll, *J. Polymer Sci.*, **57**, 721 (1962).
40. S. Aoki, Y. Harita, T. Otsu, and M. Imoto, *Polymer*, in press; *Bull. Chem. Soc. Japan*, **38**, 1922 (1965).
41. S. Aoki, K. Fujisawa, T. Otsu, and M. Imoto, *Bull. Chem. Soc. Japan*, **39**, 729 (1966).
42. L. Höhr, H. Cherdron, and W. Kern, *Makromol. Chem.*, **52**, 59 (1962).



43. T. Saegusa, H. Imai, and J. Furukawa, *Makromol. Chem.*, **54**, 218 (1962).
44. T. Saegusa, H. Imai, and J. Furukawa, *Kogyo Kagaku Zasshi*, **66**, 474 (1963).
45. E. A. Long, F. B. Dunkle, and W. F. McDevit, *J. Phys. Chem.*, **55**, 829 (1951).
46. O. H. Wheeler, *J. Org. Chem.*, **29**, 1227 (1964); *ibid.*, **26**, 3221 (1961).
47. F. A. Long and M. Purchase, *J. Am. Chem. Soc.*, **72**, 3267 (1950).
48. H. T. Liang and P. D. Bartlett, *J. Am. Chem. Soc.*, **80**, 3585 (1958).
49. J. G. Pritchard and F. A. Long, *J. Am. Chem. Soc.*, **78**, 2667, 6008 (1956); *ibid.* **79**, 2362 (1957).
50. P. A. Small, *Trans. Faraday Soc.*, **51**, 1717 (1955).
51. C. L. Hamermesh and V. E. Hary, *J. Org. Chem.*, **26**, 4748 (1961).
52. F. S. Dainton and K. J. Ivin, *Quart. Rev.*, **12**, 61 (1958).
53. C. E. H. Bawn, *Polymer*, **6**, 95 (1965).
54. D. Vofsi and A. V. Tobolsky, *J. Polymer Sci. A*, **3**, 3261 (1965).
55. G. G. Lowry, *J. Polymer Sci.*, **42**, 463 (1960).
56. B. D. Phillips, T. L. Hanlon, and A. V. Tobolsky, *J. Polymer Sci. A*, **2**, 4231 (1964).
57. C. G. Overberger and V. G. Kamath, *J. Am. Chem. Soc.*, **85**, 446 (1963).

### Résumé

On a réuni les paramètres de copolymérisation cationique, établis avec soin pour les éthers cycliques, les formales et les esters. La réactivité relative relie la basicité à l'énergie libre. Il a été possible de décider si c'était l'ion carbonium (y compris l'ion acylium) ou si c'était l'ion oxonium qui était l'intermédiaire actif au cours de la propagation. Ceci a été effectué en reliant les paramètres de copolymérisation du styrène à l'effet des promoteurs et au mécanisme bien connu d'hydrolyse. Des données structurales qui favorisent la dépropagation ont été identifiées. Les équations décrivant ces possibilités ont été dérivées et brièvement discutées. Les effets des catalyseurs et solvants limitaient les possibilités de corrélation.

### Zusammenfassung

Sorgfältig bestimmte kationische Copolymerisationsparameter von zyklischen Äthern, Formalen und Estern werden zusammengestellt. Die relative Reaktivität steht in Korrelation zur Basizität und zur freien Energie. Die Entscheidung zwischen Carboniumion (einschliesslich Acyliumion) oder Oxoniumion als aktivem Zwischenstoff beim Wachstum konnte getroffen werden. Es geschah dies durch eine weitere Korrelation der Copolymerisationsparameter für Styrol, des Einflusses von Promotoren und des bekannten Hydrolysemechanismus. Strukturmerkmale, welche die Depropagation förderlich werden identifiziert. Gleichungen zur Beschreibung dieser Möglichkeiten werden abgeleitet und kurz diskutiert. Katalysator- und Lösungsmiteleinflüsse bilden eine Grenze für die mögliche Korrelation.

Received September 13, 1965

Revised January 14, 1966

Prod. No. 5055A

## Studies in Some New Initiator Systems for Vinyl Polymerization. Part I. Molecular Halogens or Halates as One Component

MIHIR K. SAHA,\* MANASI SEN, and DINABANDHU PRAMANICK, *Indian Association for the Cultivation of Science, Jadavpur, Calcutta, India*

### Synopsis

Several new initiating systems involving a molecular halogen, halates, or perhalate as one of the components and a reducing metal salt, ammonia, an amine or an organic compound as the other component, have been introduced for the aqueous (and in a few cases the non-aqueous) polymerization of methyl methacrylate. Some of the resulting polymers have been subjected to endgroup analysis by the application of the ultra-sensitive dye techniques recently developed in our laboratory. Reducing metal salt-halogen-initiated polymers are found to incorporate hydroxyl and halogen endgroups, while polymers initiated by amine-halogen systems incorporate hydroxyl and halogen as well as amino endgroups. However, in the ammonia-halogen system polymers incorporate only halogen endgroups. On the basis of the results of the endgroup analysis of the polymers an attempt has been made to explain the probable initiation mechanism with regard to the nature and identity of the initiating species involved in such processes.

### INTRODUCTION

Although numerous initiator systems<sup>1-6</sup> have been used for vinyl polymerization, the use of molecular halogens ( $\text{Cl}_2$ ,  $\text{Br}_2$ , and  $\text{I}_2$ ) as one component is not reported in the literature. However, some studies have been reported in which  $\text{ClO}_3^-$  was used as the oxidant and  $\text{SO}_3^{=}$  and  $\text{HSO}_3^-$  as the reductants.<sup>7,8</sup> Also Uri<sup>6</sup> indicated that the Br atom liberated from the  $\text{Fe}^{++}\text{-Br}_2$  system might initiate polymerization. The present work has been undertaken to study molecular halogens, halates, or perhalates as one of the components in the initiator system for the polymerization of methyl methacrylate in combination with metal salts, ammonia, amines and organic compounds, both in aqueous and in nonaqueous media. Also, to get some idea about the nature and identity of the initiating species, endgroup analysis has been carried out on the resulting polymers by the ultrasensitive dye techniques recently developed in our laboratory.<sup>9,10</sup> The present paper reports some of our preliminary results on the ability of the various systems to initiate the polymerization of methyl methacrylate and the endgroup analysis data for some of the resulting polymers.

\* Present address: Chemistry Department, University of Notre Dame, Notre Dame, Indiana.

## EXPERIMENTAL

### Materials

Purified methyl methacrylate (MMA) was used as the monomer. Chlorine was generated by the reduction of A. R. HCl with potassium permanganate and purified by passing through distilled water. All other reagents used were of analytical grade.

### Polymerization

Aqueous polymerization of purified MMA was carried out at room temperature ( $\approx 30^\circ\text{C}$ .) under nitrogen in conical Pyrex flasks in the dark. The polymers obtained in a coarse precipitated form were filtered, washed with distilled water, dried in an air oven at  $45^\circ\text{C}$ . and then purified by the usual procedure.<sup>11</sup> The monomer concentration was kept at 0.094 mole/l., and the experiments were conducted in the dark in all but a few cases. Nonaqueous polymerization was carried out in benzene under nitrogen in sealed tubes at  $60^\circ\text{C}$ . for a period of about 3–5 hr.

### Endgroup Analysis

The purified polymers after proper treatments were subjected to the appropriate dye tests for hydroxyl,<sup>12</sup> sulfate,<sup>13</sup> halogen,<sup>14</sup> and amino<sup>15</sup> endgroups. For the determination of halogen endgroup (in the case of polymers containing both amino and halogen endgroups) a blank experiment was done with the polymer in benzene solution for each set. From the difference between the optical density of the original polymer solution and that of the quaternized polymer solution, the halogen endgroup was calculated.

## RESULTS AND DISCUSSION

A series of initiator systems involving molecular halogens, halates, and perhalates as one of the components were used for the polymerization of MMA; results are presented in Tables I and II. A few suitable initiator systems were selected and determinations of the endgroups incorporated in the resulting polymers obtained with these initiators carried out.

### Ferrous Ion–Halogen Initiator System

With chlorine and bromine as one of the components, polymerization started almost instantaneously. The rate of polymerization was slow, but the yield of polymer was fairly good. In the case of the  $\text{Fe}^{++}-\text{I}_2$  system no polymerization took place in the dark; polymerization proceeded rather slowly only on exposure to ultraviolet light. This is probably due to the strong inhibiting effect of iodine. The polymers obtained were found to contain predominantly hydroxyl endgroups, i.e., about 1.4–2.1 OH groups per chain; halogen endgroups were present to a very limited extent i.e., about 0.1–0.6 per chain (Table III).

TABLE I  
Initiator Systems Involving Molecular Halogens for  
Polymerization of Methyl Methacrylate

Initiator system		Induction period min.	Polymer yield <sup>a</sup>	Endgroups found
Halogen component	Other component			
Aqueous polymerization				
Cl <sub>2</sub>	Fe <sup>+2</sup>	0	++	OH, Cl
Cl <sub>2</sub>	Ti <sup>+3</sup>	10	+++	
Cl <sub>2</sub>	Ag <sup>+</sup>	30	++	
Cl <sub>2</sub>	NH <sub>3</sub>	0	+++	Cl
Cl <sub>2</sub>	MEA	20	+++	OH, Cl, NR <sub>2</sub>
Cl <sub>2</sub>	DEA	40	+++	OH, Cl, NR <sub>2</sub>
Cl <sub>2</sub>	TEA	60	+++	OH, Cl, NR <sub>2</sub>
Br <sub>2</sub>	Fe <sup>+2</sup>	0	+++	OH, Br
Br <sub>2</sub>	Ti <sup>+3</sup>	60	+	
Br <sub>2</sub>	Ag <sup>+</sup>	—	—	
Br <sub>2</sub>	NH <sub>3</sub>	60	++	
Br <sub>2</sub>	MEA	40	+++	OH, Br, NR <sub>2</sub>
Br <sub>2</sub>	DEA	60	+++	OH, Br, NR <sub>2</sub>
Br <sub>2</sub>	TEA	90	+++	OH, Br, NR <sub>2</sub>
I <sub>2</sub>	Fe <sup>+2</sup>	60	++ <sup>b</sup>	OH, I
I <sub>2</sub>	Ti <sup>+3</sup>	—	—	
I <sub>2</sub>	Ag <sup>+</sup>	—	—	
I <sub>2</sub>	NH <sub>3</sub>	—	—	
I <sub>2</sub>	MEA	—	—	
I <sub>2</sub>	DEA	—	—	
I <sub>2</sub>	TEA	—	—	
Nonaqueous polymerization				
Cl <sub>2</sub>	Diaminoethane	60	+++	Cl, NR <sub>2</sub>
Cl <sub>2</sub>	DEA	30	+++	Cl, NR <sub>2</sub>
Cl <sub>2</sub>	TEA	120	+	
Cl <sub>2</sub>	<i>n</i> -Butylamine	120	+++	Cl, NR <sub>2</sub>
Cl <sub>2</sub>	<i>n</i> -Dodecylamine	60	+++	Cl, NR <sub>2</sub>
Cl <sub>2</sub>	Cetyldimethylamine	90	+++	Cl, NR <sub>2</sub>
Br <sub>2</sub>	Diaminoethane	60	+++	Br, NR <sub>2</sub>
Br <sub>2</sub>	DEA	30	+++	
Br <sub>2</sub>	TEA	120	+	
Br <sub>2</sub>	<i>n</i> -Butylamine	180	+	
Br <sub>2</sub>	<i>n</i> -Dodecylamine	60	++	
Br <sub>2</sub>	Cetyldimethylamine	180	+	Br, NR <sub>2</sub>
I <sub>2</sub>	Diaminoethane	240	+	
I <sub>2</sub>	DEA	210	+	
I <sub>2</sub>	TEA	240	+	
I <sub>2</sub>	<i>n</i> -Butylamine	—	—	
I <sub>2</sub>	<i>n</i> -Dodecylamine	—	—	
I <sub>2</sub>	Cetyldimethylamine	—	—	

<sup>a</sup> Yield in 3 hr.: (+++) ~60%; (++) ~40%; (+) <10%; (—) no polymerization.

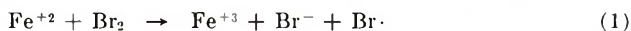
<sup>b</sup> Polymerization proceeds in presence of ultraviolet light only.

TABLE II  
Initiator Systems Involving Halates ( $\text{XO}_3^-$ ) and Perhalates ( $\text{XO}_4^-$ )  
for the Aqueous Polymerization of Methyl Methacrylate

Initiator system		Induction period, min.	Yield <sup>a</sup>
Halate or perhalate	Other component		
$\text{ClO}_3^-$	$\text{Fe}^{+2}$	0	+++
$\text{ClO}_3^-$	$\text{Ti}^{+3}$	0	+++
$\text{ClO}_3^-$	$\text{Ag}^+$	20	++
$\text{ClO}_3^-$	Oxalic acid	—	—
$\text{ClO}_3^-$	Tartaric acid	180	+
$\text{ClO}_3^-$	Citric acid	—	—
$\text{ClO}_3^-$	Glucose (acidified)	60	+
$\text{ClO}_3^-$	$\text{HCHO}$ (acidified)	—	—
$\text{BrO}_3^-$	$\text{Fe}^{+2}$	0	+++
$\text{BrO}_3^-$	$\text{Ti}^{+3}$	0	+++
$\text{BrO}_3^-$	$\text{Ag}^+$	—	—
$\text{BrO}_3^-$	Oxalic acid	60	+++
$\text{BrO}_3^-$	Tartaric acid	240	++
$\text{BrO}_3^-$	Citric acid	—	—
$\text{BrO}_3^-$	Glucose (acidified)	—	—
$\text{BrO}_3^-$	$\text{HCHO}$ (acidified)	20	+++
$\text{IO}_3^-$	$\text{Fe}^{+2}$	0	+++
$\text{IO}_3^-$	$\text{Ti}^{+3}$	0	+++
$\text{IO}_3^-$	$\text{Ag}^+$	—	—
$\text{IO}_3^-$	Oxalic acid	300	+
$\text{IO}_3^-$	Tartaric acid	—	—
$\text{IO}_3^-$	Citric acid	300-360	+
$\text{IO}_3^-$	Glucose (acidified)	—	—
$\text{IO}_3^-$	$\text{HCHO}$ (acidified)	—	—
$\text{ClO}_4^-$	$\text{Fe}^{+2}$	0	+++
$\text{ClO}_4^-$	$\text{Ti}^{+3}$	0	++
$\text{ClO}_4^-$	$\text{Ag}^+$	—	—
$\text{ClO}_4^-$	Oxalic acid	60	+
$\text{ClO}_4^-$	Tartaric acid	240	+++
$\text{ClO}_4^-$	Citric acid	—	—
$\text{ClO}_4^-$	Glucose (acidified)	—	—
$\text{ClO}_4^-$	$\text{HCHO}$ (acidified)	40	+
$\text{IO}_4^-$	$\text{Fe}^{+2}$	0	+++
$\text{IO}_4^-$	$\text{Ti}^{+3}$	0	+++
$\text{IO}_4^-$	$\text{Ag}^+$	30	+
$\text{IO}_4^-$	Oxalic acid	360	++
$\text{IO}_4^-$	Tartaric acid	360	+
$\text{IO}_4^-$	Citric acid	360	++
$\text{IO}_4^-$	Glucose (acidified)	180	+
$\text{IO}_4^-$	$\text{HCHO}$ (acidified)	—	—

<sup>a</sup> See Table I.

It was indicated by Uri<sup>6</sup> that Br atom liberated by the reaction (1)



may initiate vinyl polymerization. If this is the only reaction, the resulting polymers should contain only halogen endgroups. As the polymers ob-



TABLE III  
Endgroup Study of Poly(methyl Methacrylate) Obtained by Using  
Ferrous Ion/Halogen as Initiator in Aqueous Medium

Halogen	Halogen concn., mole/l.	Fe <sup>+2</sup> concn., mole/l.	[ $\eta$ ] <sup>a</sup>	OH/ chain	Halogen/ chain	Total end- groups/ chain
Chlorine	$1.37 \times 10^{-3}$	$1 \times 10^{-4}$ $1 \times 10^{-3}$	1.80-1.30	1.83-1.69	0.36-0.25	2.22-1.96
Bromine	$2.21 \times 10^{-3}$	$5 \times 10^{-5}$ $1 \times 10^{-3}$	1.40-0.81	2.14-1.50	0.47-0.12	2.29-1.97
Iodine	0.088-0.90	$5 \times 10^{-4}$ $1 \times 10^{-3}$	2.50-0.80	2.09-1.41	0.58-0.13	2.22-1.99

<sup>a</sup> Intrinsic viscosity was determined by the usual extrapolation method and the number-average molecular weight,  $\bar{M}_n$ , was calculated from the equation,<sup>16</sup>  $\bar{M}_n = 2.81 \times 10^5 [\eta]^{1.32}$  for PMMA in benzene.

tained have been found to incorporate mostly hydroxyl endgroups and less halogen, it appears that most of the halogen atoms liberated in the primary step react with water to give OH radicals, which in turn initiate the chains [eq. (2)].



It is also known that in aqueous solution of halogens, hypohalous acid is formed by the reaction shown in eq. (3):



Ferrous ion may react with HOX as shown in eqs. (4) and (5)



to give halogen and OH radicals. Evans, et al.<sup>17</sup> have indicated, however, that in the Fe<sup>+2</sup>-HOBr system polymerization is predominantly due to free bromine atom liberated by reaction (4). In whatever way ferrous ion and halogen may react, it has been conclusively demonstrated on the basis of the endgroup results that hydroxyl radicals are the predominantly chain-initiating species.

### Amines and Ammonia-Halogen Initiator System

Mono-, di-, and triethanolamines (MEA, DEA, and TEA, respectively) were found to form very efficient initiating systems with chlorine and bromine. For polymerization with chlorine as one of the components the induction period varied between 10 and 60 min. in the ethanolamine series. With bromine the induction period increased in the same order from 30 to 90 min. In combination with the same amines, iodine failed to initiate the polymerization even when exposed to ultraviolet light. Chlorine-amine-initiated polymers gave an average of 2.40-1.50 hydroxyl endgroups per chain, and halogen endgroup content varied between 0.17 and

TABLE IV  
Endgroup Study of Polymers: Polymerization Initiated by Halogen and Amine or Ammonia Systems

Halogen	Halogen concn., mole/l.	Amine	Amine concn., mole/l.	$[\eta]$	OH/chain	Halogen/chain	O.D. at 630 m $\mu$ <sup>a</sup>
Cl <sub>2</sub>	$4.05 \times 10^{-3}$	MEA	$1.27 \times 10^{-1}$	1.16-0.56	2.41-1.61	0.103-0.234	0.279-0.342 <sup>b</sup>
Cl <sub>2</sub>	$4.05 \times 10^{-3}$	DEA	$5.2 \times 10^{-2}$	1.37-0.67	2.33-1.57	0.113-0.227	0.370-0.609 <sup>b</sup>
Cl <sub>2</sub>	$4.05 \times 10^{-2}$	TEA	$1.89 \times 10^{-2}$	1.54-0.96	2.03-1.41	0.119-0.239	0.501-0.606 <sup>b</sup>
Cl <sub>2</sub>	$3.49 \times 10^{-4}$	NH <sub>3</sub>	$1.379 \times 10^{-1}$	1.19-0.74	—	0.20-0.23	—
Br <sub>2</sub>	$1.32 \times 10^{-2}$	MEA	$1.25 \times 10^{-1}$	0.46-0.16	2.62-1.57	0.116-0.262	0.367-0.780 <sup>c</sup>
Br <sub>2</sub>	$1.32 \times 10^{-2}$	DEA	$1.04 \times 10^{-1}$	0.74-0.44	2.08-0.98	0.108-0.233	0.442-0.757 <sup>c</sup>
Br <sub>2</sub>	$1.32 \times 10^{-2}$	TEA	$5.66 \times 10^{-2}$	1.63-0.96	1.97-0.78	0.124-0.208	0.525-0.632 <sup>c</sup>

<sup>a</sup> Optical density of the chloroform solution of the purified polymer with disulfine blue reagent was measured for amino endgroup.

<sup>b</sup> 0.1% solution.

<sup>c</sup> 0.025% solution.

0.24 per chain. In case of the bromine-amine-initiated polymers, the hydroxyl endgroups content was between 2.62 and 0.78 per chain and halogen endgroup content was about 0.2 per chain. Quantitative determinations of the amino endgroup have not yet been done. From the optical density value (Table IV) a comparative idea of the extent of the amino endgroup incorporated may be obtained.

With the ammonia-chlorine initiator system polymerization started immediately, having practically no induction period. The yield of polymer was low. With bromine as one component, the polymer obtained was of very low molecular weight; and the yield was also very low, and the polymer could not be further investigated for endgroups. The ammonia-iodine system could not initiate the polymerization even when exposed to ultraviolet light. For the ammonia-chlorine-initiated polymers response for hydroxyl and amino endgroups was negative, and only a slight response (about 0.2 per chain) for halogen endgroup was obtained (Table IV).

From the results of endgroup analysis of the amine-halogen-initiated polymers it is apparent that both amino and halogen radicals are involved and have been formed in some stages of the reaction. The results suggest that many of the systems employed may involve a redox mechanism through the formation of radicals or ion-radicals, but without further work the possibility of nonradical reactions can not be completely ruled out. However, the incorporation of hydroxyl endgroups in the amine-halogen-initiated polymers may be due to the presence of hydroxyl groups in the ethanolamines or due to the reaction of amino or halogen radicals with water. The endgroup picture of the polymers obtained with ammonia-halogen system was, however, somewhat different from that obtained with the amine-halogen system. This may be due to some substitution effect of the amines.

Further work on endgroups and kinetics is in progress to explain the reaction mechanism of the above systems.

Thanks are due to Prof. Santi R. Palit, for his encouragements. Thanks are also due to Dr. U. S. Nandi for valuable discussion. Financial assistance from National Bureau of Standards (USA) is gratefully acknowledged.

### References

1. J. H. Baxendale, M. G. Evans, and G. S. Park, *Trans. Faraday Soc.*, **42**, 155, 668, 675 (1946).
2. I. M. Kolthoff, A. I. Medalin, and H. P. Raaen, *J. Am. Chem. Soc.*, **73**, 1733 (1951).
3. P. Davies, M. G. Evans, and W. C. E. Higginson, *J. Chem. Soc.*, **1951**, 2563.
4. S. R. Palit and R. S. Konar, *J. Polymer Sci.*, **57**, 609 (1962).
5. R. S. Konar and S. R. Palit, *J. Indian Chem. Soc.*, **38**, 481 (1961).
6. N. Uri, *Chem. Rev.*, **50**, 375 (1952).
7. W. M. Thomas, E. H. Gleason, and G. Mino, *J. Polymer Sci.*, **24**, 43 (1957).
8. F. H. Firsching and I. Rosen, *J. Polymer Sci.*, **36**, 305 (1959).
9. S. R. Palit, *Chem. Ind. (London)*, **1960**, 1531.
10. S. R. Palit, *Makromol. Chem.*, **36**, 89 (1959); *ibid.*, **38**, 96 (1960).

11. S. R. Palit and P. Ghosh, *J. Polymer Sci.*, **58**, 1225 (1962).
12. P. Ghosh, P. K. Sengupta, and A. Pramanick, *J. Polymer Sci. A*, **3**, 1725 (1965).
13. P. Ghosh, S. C. Chadha, A. R. Mukherjee, and S. R. Palit, *J. Polymer Sci. A*, **2**, 4433 (1964).
14. M. K. Saha, P. Ghosh, and S. R. Palit, *J. Polymer Sci. A*, **2**, 1365 (1964).
15. S. Maiti and M. K. Saha, *Sci. Cult. (Calcutta)*, in press.
16. J. H. Baxendale, S. Bywater, and M. G. Evans, *J. Polymer Sci.*, **1**, 237 (1946).
17. M. G. Evans, J. H. Baxendale, and D. J. Cowling, *Discussions Faraday Soc.*, **2**, 206 (1947).

### Résumé

De nombreux nouveaux systèmes initiateurs comprenant les halogènes moléculaires, les halogénates et perhalogénates comme un des composants et un sel métallique réducteur, l'ammoniac, une amine ou un composé organique comme autre composant ont été introduits en vue de provoquer une polymérisation du polyméthacrylate de méthyle en milieu aqueux et dans certains cas en milieu non-aqueux. Certains des polymères résultants ont été soumis à une analyse de groupes terminaux par application de méthodes ultrasensibles à base de colorants développées récemment dans nos laboratoires. Les polymères initiés au moyen d'un sel métallique réducteur et des halogènes contiennent des groupes terminaux hydroxylés et halogènes, tandis que les polymères initiés par les systèmes amines-halogènes contiennent des groupes terminaux hydroxylés de même que des groupes aminés terminaux. Toutefois, les polymères initiés au moyen d'un système ammoniac-halogène ont uniquement des groupes halogènes terminaux. Sur la base de l'analyse des groupes terminaux et de ces résultats, on essaie d'expliquer le mécanisme probable d'initiation en ce qui concerne la nature et l'identité des espèces initiatrices présentes dans ces procédés.

### Zusammenfassung

Einige neue Startersysteme mit molekularem Halogen, Halogenat oder Perhalogenat als die eine Komponente und einem reduzierenden Metallsalz, Ammoniak, einem Amin oder einer organischen Verbindung als andere Komponente wurden zur Polymerisation von Methylmethacrylat in wässrigem und in einigen Fällen im nicht wässrigen System verwendet. Einige der erhaltenen Polymeren wurden einer Endgruppenanalyse nach dem ultraempfindlichen, im Laboratorium der Verfasser entwickelten Anfarbungsverfahren unterzogen. In die durch reduzierendes Metallsalz-Halogen gestarteten Polymeren werden Hydroxyl- und Halogenendgruppen eingebaut, während die durch Amin-Halogen-System gestarteten Polymeren Hydroxyl-, Halogen- und auch Aminoendgruppen enthalten. Im Ammoniak-Halogen-System werden jedoch nur Halogenendgruppen in die Polymeren eingebaut. Auf Grundlage der Ergebnisse der Endgruppenanalyse der Polymeren wurde versucht, den in Bezug auf Natur und Identität der startenden Spezies bei solchen Prozessen wahrscheinlichsten Startmechanismus aufzustellen.

Received September 27, 1965

Revised January 18, 1966

Prod. No. 5057A

## Ferrocene-Containing Polymers. XIII. Polymeric Compounds Possessing Carboxyphenyl Side Groups

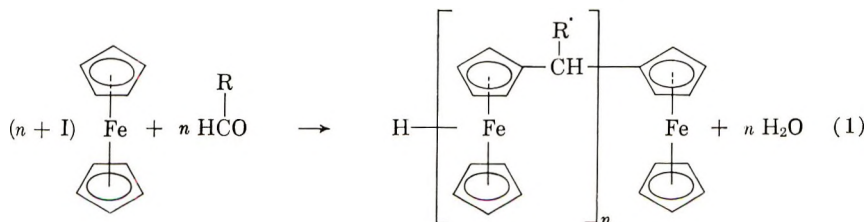
EBERHARD W. NEUSE and KAZUKO KODA, *Polymer Laboratory, Missile & Space Systems Division, Douglas Aircraft Company, Inc., Santa Monica, California*

### Synopsis

As an extension of earlier work on the condensation of ferrocene with aldehydes, the polycondensation of ferrocene with *p*- and *o*-carboxybenzaldehyde is described. While, in the former case, regular polycondensation occurs giving rise to a polymer composed of ferrocenylene and 4-carboxybenzal units, a deviation from this route is observed in the *o*-carboxybenzaldehyde case, where a polymer containing both carboxybenzal and 3,3-phthalide bridging units between the ferrocenylene groups is formed instead. This unexpected behavior can be accounted for by a hydride abstraction mechanism. In support of the polymer structure proposed, 3-ferrocenylphthalide and 3,3-diferrocenylphthalide are isolated as intermediates or by-products. In both polymer series, number-average molecular weights up to 3000 (unsubfractionated) are measured. The polymers are soluble in a number of organic solvents and can be cured with epoxides.

### INTRODUCTION

As part of a study comprising the polycondensation of ferrocene with aldehydes<sup>1-4</sup> according to the general reaction path of eq. (1), the present work describes the reaction of ferrocene with *p*-carboxybenzaldehyde (4-formylbenzoic acid) and *o*-carboxybenzaldehyde (phthalaldehydic acid).



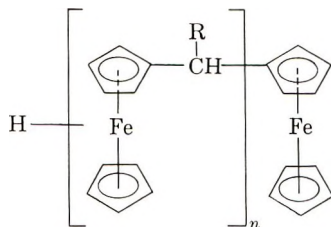
### RESULTS AND DISCUSSION

#### Polycondensation of Ferrocene with *p*-Carboxybenzaldehyde

By employing the general melt phase technique described in preceding communications,<sup>1,3</sup> ferrocene was reacted with *p*-carboxybenzaldehyde to give polymer I. Based on earlier experience with Lewis acids in ferrocene



polycondensations, zinc chloride was used as catalyst to minimize undesired side reactions such as cleavage of the ferrocene system. The high reactivity of the aldehydic component permitted reduction of the catalyst concentration to a 4–10% level (by weight of ferrocene). The high melting points of the reactants called for melt temperatures as high as 170°C. to ensure homogeneous fusing. Under these conditions, on the other hand, the reaction was rapid enough to result in solidification of the melt within approximately 1 hr. or less, and yields in soluble polymer amounted to 55–70%. After removal of catalyst and unreacted aldehyde by suitable extraction processes, the crude polycondensation products were worked up by a procedure combining selective extraction and reprecipitation in such a manner as to prevent oxidation of the ferrocene system as well as involvement of the carboxyl side groups through salt formation or complexation with the solvent. In each case, the soluble, but infusible polymer was collected as two fractions, a higher molecular weight portion termed "1st fraction", and a lower molecular-weight portion, generally the major part, labeled "2nd fraction."



- I, R = 4-carboxyphenyl  
 II, R = 4-cyanophenyl  
 III, R = 2-carboxyphenyl

For seven representative condensations of ferrocene with *p*-carboxybenzaldehyde, experimental variables and analytical results for the first and second fractions are summarized in Tables I and II. The tabulations show that consistency of the elemental analytical data with the composition of I is best for the first four experiments listed, in which the ferrocene component was employed in an excess larger than 10% over equimolarity. It can also be seen that, for these four experiments, despite the rather wide range of reactant ratios covered, there is no apparent compositional change that would point to a clear-cut correlation between the elemental composition and the molar reactant ratio employed. On the other hand, the analytical data for runs 5, 6, and, most strikingly, 7 demonstrate that a reduction of the ferrocene concentration below the level indicated (molar ferrocene/aldehyde ratio  $\leq 1.1$ ) resulted in increased incorporation of *p*-carboxybenzal groups into the polymer, probably in the form of bridging units both between vicinal ferrocene nuclei (double-bridge formation<sup>1</sup>) and ferrocene units of different polymer chains (crosslinking). In agreement with these analytical findings is the increase in insoluble matter in experiments 6 and 7, coupled with the higher molecular weights found for these

TABLE I

Expt. no.	Aldehydic reactant	Molar ratio ferrocene/aldehyde	Concentration of ZnCl <sub>2</sub> , wt.-% based on ferrocene	Temperature, °C.	Time, hr.	Total yield of soluble polymer, % <sup>a</sup>
1	<i>p</i> -Carboxybenzaldehyde	3.0	10 <sup>b</sup>	160	0.9	70.8
2		2.0	10 <sup>c</sup>	170	0.4	63.9
3		1.5	10 <sup>c</sup>	170	0.4	66.4
4		1.2	10	170	0.5	63.1
5		1.1	10 <sup>c</sup>	170	0.4	54.6
6		1.0	10	170	0.5	56.7
7		0.9	10	170	0.5	52.1
8	<i>o</i> -Carboxybenzaldehyde	2.5 <sup>d</sup>	5	115	1.7	69.9
9		1.7 <sup>e</sup>	5 <sup>f</sup>	115	1.6	78.1
10		1.3	5	115	1.5	76.7
11		1.1	5 <sup>g</sup>	115	1.5	67.2
12 <sup>h</sup>		1.0	5 <sup>h</sup>	115	1.5	57.4

<sup>a</sup> Combined yield of 1st and 2nd fractions. Insoluble polymer yield 5-7% in runs 5-7, 11, 12; <5% in all other cases.

<sup>b</sup> With AlCl<sub>3</sub> in lieu of ZnCl<sub>2</sub>: yield, 53.3%; Fe, 14.82; insolubles, 9.4%.

<sup>c</sup> With 5% ZnCl<sub>2</sub> at 0.7 hr., nearly same yield and composition, slightly increased  $\bar{M}_n$ .

<sup>d</sup> Practically same results at molar ratio 2.0.

<sup>e</sup> Similar results but slightly higher  $\bar{M}_n$  at molar ratio 1.5.

<sup>f</sup> Similar results with 10% ZnCl<sub>2</sub> at 115°C., 0.5 hr., or with 5% ZnCl<sub>2</sub> at 105°C., 2.4 hr.

<sup>g</sup> Higher yields (75-77%), but lower iron contents and molecular weights (Fe, 12-13%;  $\bar{M}_n$  of 1st fraction, 1900-2100) with 30% ZnCl<sub>2</sub> at 90°C., 0.5 hr., and with 10% ZnCl<sub>2</sub> at 130°C., 0.3 hr.

<sup>h</sup> Similar results with 3-ethoxyphthalide in lieu of the carboxybenzaldehyde. Decreased  $\bar{M}_n$  and low total polymer yield, (10.8%) with 3-ethoxyphthalide in lieu of the carboxybenzaldehyde and 20% HCl in lieu of ZnCl<sub>2</sub> at 115°C., 15 hr.

reaction products and the relative yield increase of the limitedly soluble 1st fractions at the expense of the well-soluble 2nd fractions.

These phenomena are somewhat in contrast to the furfural condensation case discussed earlier<sup>3</sup> and may be explained by the fact that excess aldehyde functions as a reactant giving rise to the formation of additional bridging units, whereas any significant excess of ferrocene can only act as a diluent. Such a diluting effect, while relevant in the furfural example insofar as it suppresses intermolecular Diels-Alder addition,<sup>3</sup> is certainly of minor significance in the present case. (Herewith in accord, infrared spectroscopy failed to evidence any structures that might arise from interaction of carboxyphenyl groups, e.g., anhydride formation or acylation of the phenyl nucleus.)

A comparison of the molecular weight and yield data in Table II with the corresponding figures for the earlier ferrocene-benzaldehyde<sup>1</sup> and ferrocene-furfural polymers<sup>3</sup> reveals a comparatively low average degree of polymerization. The high melting points of the reactants and the infusi-

TABLE II

Expt. no.	Fraction	$\bar{M}_n^a$	Yield, % <sup>b</sup>	Anal. calcd. <sup>c</sup>				Anal. found <sup>d</sup>			
				C, %	H, %	Fe, %	COOH, %	C, %	H, %	Fe, %	COOH, %
1	1st	1930	14.5	67.63	4.53	18.76	12.8	67.05	5.13	18.03	12.7
	2nd	790	56.3	67.16	4.67	20.47	10.8	66.66	4.89	20.12	10.7
2	1st	2440	19.7	67.69	4.51	18.51	13.1	66.64	4.46	17.85	13.3
	2nd	930	44.2	67.27	4.64	20.08	11.3	66.83	4.54	20.02	11.1
3	1st	2560	16.2	67.70	4.51	18.46	13.1	66.71	4.66	17.96	13.4
	2nd	810	50.2	67.17	4.66	21.40	10.9	67.08	4.60	19.81	11.0
4	1st	2010	21.3	67.64	4.53	18.71	12.8	66.38	4.78	18.06	13.1
	2nd	840	41.8	67.20	4.66	20.32	11.0	67.39	4.97	19.49	11.3
5	1st	2340	25.5	67.68	4.51	18.55	13.0	66.54	4.58	17.41	13.6
	2nd	970	29.1	67.30	4.63	19.98	11.4	67.15	4.65	19.55	12.2
6	1st	2950	28.6	67.74	4.50	18.34	13.2	66.93	4.53	17.22	13.6
	2nd	950	28.1	67.73	4.63	20.02	11.4	66.90	4.69	18.72	12.3
7	1st	2830 <sup>e</sup>	36.2	67.41	4.50	18.35	13.2	67.09	4.60	16.83	13.7 <sup>g</sup>
	2nd	1160	15.9	67.76	4.60	19.55	11.9	66.59	4.58	18.79	12.9
8	1st	1610	30.3	67.76	4.28	19.04	6.3	67.98	4.22	14.91	6.7
	2nd	640	39.6	67.35 <sup>f</sup>	4.42	20.42	5.5	68.60	4.23	16.90	6.3
9	1st	1780	35.4	67.70	4.27	18.91	6.3	67.55	4.27	15.39	7.3
	2nd	690	42.7	67.35 <sup>f</sup>	4.42	20.42	5.5	67.17	4.42	17.68	6.8
10	1st	1830	35.1	67.80	4.27	18.87	6.3	67.06	4.19	14.93	7.2
	2nd	730	41.6	67.35 <sup>f</sup>	4.42	20.42	5.5	67.35	4.21	16.55	6.0
11	1st <sup>g</sup>	2260	38.7	67.87	4.24	18.65	6.5	67.71	4.45	13.88	9.0
	2nd	740	28.5	67.35 <sup>f</sup>	4.42	20.42	5.5	68.14	4.33	14.21	7.1
12	1st <sup>g</sup>	2850	33.3	67.92	4.22	18.46	6.6	65.69	4.04	12.22	8.2
	2nd	800	24.1	67.35 <sup>f</sup>	4.42	20.42	5.5	67.31	4.39	13.88	7.0

<sup>a</sup> Mean values of duplicate runs in pyridine solution; <sup>b</sup> In per cent of theory, based on aldehyde in experiments 1-4 and 8-10 and on ferrocene in 5-7 and 11, 12; <sup>c</sup> For I (and III) in runs 1-7, for IV (with  $m = n$ ) in runs 8-12; <sup>d</sup> Mean values of duplicate determinations. Fe values up to 0.8% low on higher molecular fractions; <sup>e</sup> Traces insoluble in pyridine; <sup>f</sup> Calculated for IV, where  $m = n = 1$ ; <sup>g</sup> Incompletely soluble in cyclohexanone.

bility of the polycondensation products may account for the low  $\bar{M}_n$  values found, with premature solidification of the melt precluding further propagation. Such premature melt solidification may also explain the reduced yields in experiments 5-7 lacking the diluting and melting range-depressing effects of excess ferrocene.

The molecular weights listed were obtained by using pyridine as solvent, for which, in contrast to such other solvents as dibromomethane or cyclohexanone,  $\bar{M}_n$  determinations at different solute concentrations were found to remain constant within the range of experimental error, thus indicating essential lack of dissociation or dimerization. This was confirmed by the absence of any significant dimer absorption in the region of 3.5-4.0  $\mu$  in the infrared spectrum of I dissolved in pyridine in concentrations comparable to those used for  $\bar{M}_n$  determinations. Additional indication of the absence of dissociation or association effects resulted from  $\bar{M}_n$  measurements conducted at various concentrations in pyridine solutions of the lowest member of I, 4-carboxyphenyl-diferrocenylmethane. This derivative was isolated chromatographically from lower-molecular reaction products, and its structural assignment was corroborated by proton magnetic resonance spectroscopy (phenyl/methine proton ratio 4.0:1.2 in dimethylsulfoxide) as well as by its independent preparation via hydrolysis of 4-cyanophenyl-diferrocenylmethane (II, with  $n = 1$ ), which in turn was collected as a by-product in the polycondensation of ferrocene with *p*-cyanobenzaldehyde leading to polymer II. Irrespective of the concentrations applied, the  $\bar{M}_n$  values found were well in agreement with the calculated molecular weight.

Further structural evidence for I was obtained from infrared data (recorded on KBr pellets). All spectra, including that of the dinuclear compound, 4-carboxyphenyl-diferrocenylmethane, showed the characteristic absorption patterns of the substituted ferrocene system and the *p*-phenylene group. The 6.22  $\mu$  phenyl C=C stretching vibration was strongly enhanced by conjugation with the acid carbonyl, and the two bands appearing near 9 and 10  $\mu$  were suggestive of some homoannular bonding on ferrocene.<sup>5</sup> While a quantitative evaluation<sup>1,6</sup> of the last-named two bands was impossible because of superposition by strong carboxyl and phenyl absorption, a qualitative comparison suggests an extent of homoannularity similar to that observed earlier<sup>1</sup> with ferrocene-benzaldehyde polymers (I, R = phenyl), the trend of decreasing homoannularity with increasing molecular weight again indicating some branching. Polymeric samples exhibited a broad shoulder near 2.9  $\mu$  (in addition to the common carboxyl absorption between 3 and 4  $\mu$ ), which indicates the carboxyl groups to occur partially in the nonbonded state.\* The multiplicity observed for the C=O stretching absorption (strong principal peaks at 5.77, 5.84, and 5.90  $\mu$  in the polymers; doublets at 5.90-5.95  $\mu$  in the dimerized dinuclear compound) may have arisen from coupling effects with C-O stretching modes. Analogous coupling vibrations of C-O

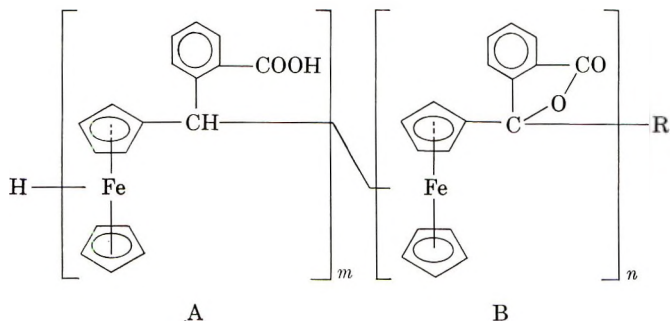
\* In contrast, the dinuclear compound, likely to exist almost entirely in the associated, i.e., dimeric form, failed to show any significant absorption in the vicinity of 2.9  $\mu$ .



with O—H in-plane deformation modes<sup>8</sup> are likely to have given rise to the two additional carboxyl bands observed at  $7.05 \mu$  and in the broad range  $7.9$ – $8.1 \mu$ .

### Polycondensation of Ferrocene with *o*-Carboxybenzaldehyde

The polycondensation reactions of ferrocene with *o*-carboxybenzaldehyde (phthalaldehydic acid) were carried out by much the same technique as employed in the preceding *p*-carboxybenzaldehyde case, except that considerably lower reaction temperatures could be applied owing to the low melting point ( $96$ – $97^\circ\text{C}$ .) of the phthalaldehydic acid. Soluble polymers were obtained in yields up to nearly  $80\%$ . The experimental conditions for five typical polycondensation reactions of ferrocene with *o*-carboxybenzaldehyde are summarized in Table I (runs 8–12), and the corresponding analytical data for the 1st and 2nd fractions of the resulting polymers are collected in Table II. These fractions were obtained by reprecipitation of the crude polycondensation products in much the same manner as in the preceding case, except that a single solvent proved sufficient for the purpose, and admixed ferrocene was removed by vacuum sublimation. Again, as before, the molecular weights listed were measured in pyridine solution to avoid errors resulting from dissociation or association effects.



- IV, R = ferrocenyl  
 V, R = hydrogen  
 VI, R = ferrocenyl,  $m = 0$

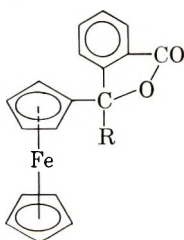
The analytical data tabulated show the polymer compositions to deviate from that of the structure III expected for a reaction following the regular path of eq. (1) (R = 2-carboxyphenyl). The analyses rather suggest a composition essentially of the idealized type IV, with the two different recurring units A and B alternating randomly along the polymer backbone. (Hence, the units in brackets do not depict block polymer segments.) Best agreement of the analytical data with structure IV is manifest in those experiments where the ferrocene/aldehyde molar ratios exceeded 1.1–1.3 (runs 8–10). Here, polymer compositions were essentially consistent with a ratio of the population of units A to that of B equal to, or slightly above, unity. However, the somewhat low iron contents even at these relatively



high reactant ratios indicate the incorporation of *o*-carboxybenzal and 3,3-phthalide bridging units in excess over the stoichiometry of IV, i.e., about one such additional bridge for every three ferrocene units. In reactions employing ferrocene/aldehyde ratios of below 1.1 (runs 11, 12), the further decreased iron contents in the polymer products point to a still higher number of additional bridging units in the molecule. Probably, as in the case of polymer I and also in the earlier reported polymer systems,<sup>1-3,6</sup> these bridges are mainly of the intrachain type, giving rise to double-bridged segments. Yet some interchain bridging may also have resulted, especially at lower ferrocene/aldehyde ratios, as is indicated by the decreased cyclohexanone solubility of the 1st fractions of runs 11 and 12 and the increase in insoluble matter in these two experiments.

The existence of units B in IV, indicated by the low hydrogen and carboxyl percentages found (Table II), was confirmed by infrared spectroscopy. The spectra of all polymer fractions IV, while similar to those of I, showing the typical ferrocene and carboxyl absorptions, exhibited the characteristic carbonyl stretching multiplet of the five-membered lactone ring<sup>9</sup> at 5.70  $\mu$ , partially merged with carboxyl C=O stretching absorption at 5.80-5.85  $\mu$ .<sup>\*</sup> In addition, there was shown a strong ester band at 7.80  $\mu$ ,<sup>10</sup> coupled with two bands due to asymmetric and symmetric C—O—C vibrations<sup>9</sup> at 9.45 and 10.65  $\mu$ , as similarly exhibited by the related lactone, 3-phenylphthalide. It is of interest to note that the 10- $\mu$  ferrocene band indicative of the presence of an unsubstituted  $\pi$ -cyclopentadienyl ring<sup>5</sup> was considerably reduced in intensity as compared to the *p*-carboxyphenyl analog, which suggests a rather high degree of heteroannularity. Steric factors are likely to be responsible for this substitution orientation.

In order to isolate defined intermediates that might provide further evidence in support of the rather unexpected structure IV, low molecular 2nd fractions (Table II) were chromatographed on alumina. It was possible to separate in yields up to 5% the two monomeric lactones, VII (3-



VII, R = hydrogen

VIII, R = ferrocenyl

ferrocenylphthalide) and VIII (3,3-diferrocenylphthalide), whose structures were established on the basis of elemental analyses, molecular weight

\* The position of this carboxyl band, in conjunction with the strong  $\nu_{\text{O-H}}$  at 2.90  $\mu$ , suggests still less carboxyl association than in I, probably as a result of diminished steric accessibility.

determinations, and spectroscopic evidence.\* The infrared spectra of both compounds showed the aforementioned typical lactone absorption (with some minor shifts occurring in the C—O—C regions), and the mononuclear lactone VII exhibited the expected  $3.42 \mu$  stretching band of the *tert*-CH group, whereas no such methine absorption appeared in the spectrum of VIII. The proton magnetic resonance spectrum of VII, taken in deuterio-chloroform solution, was characterized by a phenyl proton multiplet in the  $\tau$  range of 2.0–2.7, a methine proton singlet at  $\tau = 3.74$ , and a ferrocene proton singlet at  $\tau = 5.82$ , with integrated intensities in the expected ratio 4:1:9. Analogously, VIII gave multiplet signals in both the phenyl proton region at  $\tau = 1.9$ –2.7 and the ferrocene proton region at  $\tau = 5.7$ –6.2 in the exact 4:18 area ratio, thus attesting to the absence of a tertiary hydrogen atom.†

The formation of polymer IV may be rationalized in terms of an ionic mechanism which involves the two intermediary metallocarbonium species IX and X (Fig. 1), both competing in propagation reactions that lead to units A and B via the various substitution steps proposed earlier.<sup>1,6</sup> While cation IX arises in the regular fashion<sup>1</sup> from the primary adduct XI or immediately from lactone VII, a mechanism involving hydride ion abstraction from the tertiary  $\alpha$ -carbon of VII may account for the generation of cation X. Such hydride transfer possibly involves proton<sup>11,12</sup> rather than carbonium ion participation ( $R^+ = H^+$  in Fig. 1), because the only cation, other than a proton, potentially available for hydride abstraction would be IX (or higher homologs), in which case a benzylic species would be produced for every ion X generated (disproportionation). The absence of such benzylic groupings, however, is clearly indicated on the basis of the elemental analytical and spectroscopic data. The postulated hydride transfer mechanism finds additional support in the observation that further condensation of VII, either *per se* or with ferrocene (see below), can be accomplished not only by Lewis acids as catalysts, but even by Brønsted acids, such as hydrochloric acid. Lactone VII occurring as intermediate in the above reaction scheme may arise from the transitory carbinol XI through dehydration or, more probably, may result directly from condensation of the ring-tautomeric (lactol) form<sup>9</sup> of phthalaldehydic acid with ferrocene (Fig. 1). The latter path is substantiated by the observation that VII could also be isolated in condensations with the use of 3-ethoxyphthalide in lieu of phthalaldehydic acid.

In support of the various steps proposed in the reaction scheme of Figure 1, it was possible to: (1) isolate lactone VII not only from final, but even

\* 3-Ferrocenylphthalide had earlier been described in the Russian literature,<sup>7</sup> but the reported data did not permit an unambiguous identification in the present case.

† It is of interest to note the resolution in the ferrocene proton region, giving rise to singlet signals at  $\tau = 5.72$ , 5.87, and 6.13 in the ratio 2:6:10. This pattern suggests the existence of a preferred conformation with both freely rotating unsubstituted ferrocene rings oriented so as to reside in the shielding cones of the sterically fixed phenyl or carbonyl groups.

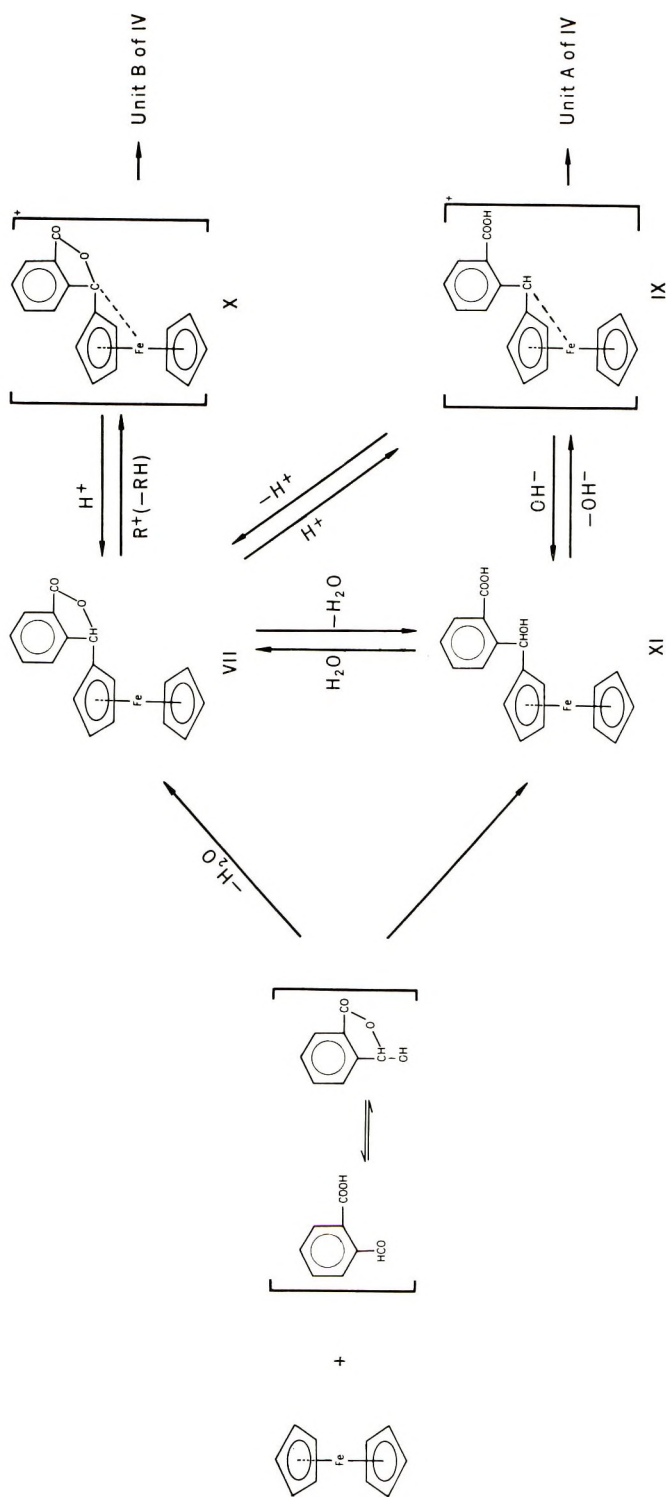
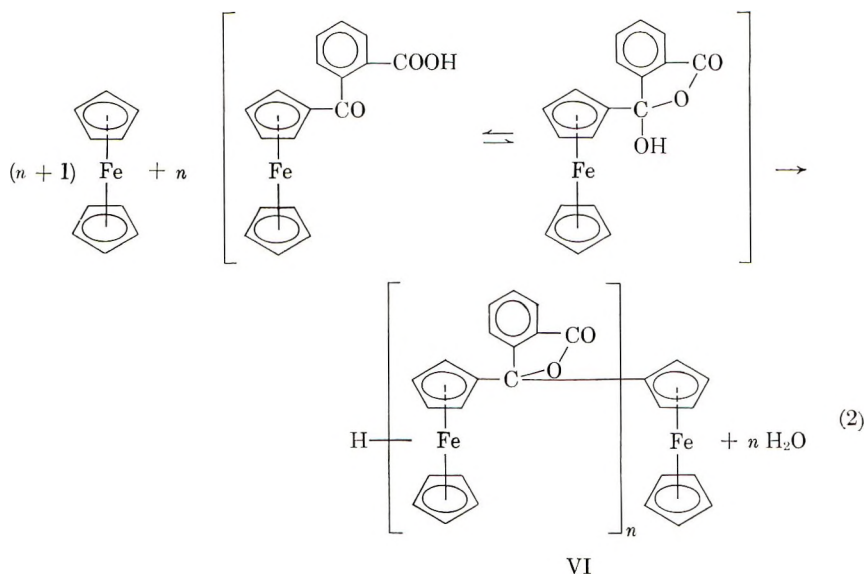


Figure 1.

from the very initial stages of condensations of ferrocene with phthalaldehydic acid (or 3-ethoxyphthalide); (2) condense this lactone with ferrocene in the presence of zinc chloride or hydrochloric acid to give the dinuclear phthalide VIII in addition to polymer IV; (3) submit VII to an acid-catalyzed self-addition reaction to yield polymer of the idealized structure V (infrared spectrum practically identical with that of IV); (4) prepare, by zinc chloride-catalyzed polycondensation of ferrocene with *o*-ferrocenoylbenzoic acid<sup>13</sup> [eq. (2)], a polymer for which elemental and spectroscopic analyses were essentially consistent with structure VI; (5) isolate VIII (identical with VI, where  $n = 1$ ) from polycondensation reactions of the preceding type.



The polymers discussed, those containing *p*-carboxyphenyl groups (I) as well as those possessing the *o*-carboxyphenyl moiety (IV, V), lend themselves to curing reactions involving the carboxyl function, with di- or polyepoxy compounds being especially suitable as co-reactants. For instance, I was cured with resorcinol diglycidyl ether, whereas oligomeric and polymeric IV and V were crosslinked by using the glycidyl ethers of, e.g., bis(hydroxyphenyl)propane or phenolic novolacs. The cured products are of interest in applications requiring heat and radiation resistance.

## EXPERIMENTAL

### Analyses, Materials

Elemental and instrumental analyses were conducted as described earlier.<sup>3</sup> The carboxyl content, expressed in per cent COOH, was determined by potentiometric titration in pyridine solution with 0.1*N* ethanolic KOH and with the use of a blank in the usual manner. Dioxane was freed

from peroxides by means of  $\text{FeSO}_4$ . Other solvents, zinc chloride and ferrocene, all commercially available, were purified as described.<sup>3</sup> *p*-Carboxy-, *o*-carboxy- and *p*-cyanobenzaldehyde were also obtained from commercial sources; the latter two compounds were recrystallized from water to give products with m.p. 96–97 and 98–100°C., respectively. 3-Ethoxyphthalide was prepared as described by Wheeler et al.;<sup>9</sup> m.p. 64–66°C. *o*-Ferrocenoylbenzoic acid was synthesized from ferrocene, phthalic anhydride, and anhydrous aluminum chloride in methylene chloride solution (1:1:2 molar ratio, 1.0 hr. at 0°C., then 4.0 hr. at room temperature, 1.5 hr. at reflux, usual work-up; crude yield, 10.1%). The orange-pink compound, after repeated recrystallization from ether, had m.p. 189–191°C. dec. (lit.:<sup>13</sup> m.p. 183–184°C.).

ANAL. Calcd. for  $\text{C}_{18}\text{H}_{14}\text{FeO}_3$ : C, 64.67%; H, 4.19%; Fe, 16.77; COOH, 13.47; mol. wt., 334. Found: C, 64.51%; H, 4.31%; Fe, 16.99%; COOH, 13.3%; mol. wt., 350 (pyridine).

### Polycondensation Reactions

**Polymer I from Ferrocene and *p*-Carboxybenzaldehyde.** By employing the equipment and technique described previously,<sup>1,6</sup> the well-ground mixture of ferrocene, *p*-carboxybenzaldehyde, and anhydrous zinc chloride was heated under nitrogen in the molar proportions and under the reaction conditions listed in Table I (experiments 1–7). Heating was generally discontinued after the reaction mixture had become so viscous as to prevent further stirring. The solidified melt was extracted with warm water for removal of catalyst and unreacted aldehyde, followed by Soxhlet extraction with pentane to remove admixed ferrocene. Exhaustive extraction of the crude polymer with glacial acetic acid, precipitation of the dissolved polymer portion (usually the major part) by excess water and thorough drying (10 days at room temperature over  $\text{P}_2\text{O}_5$  *in vacuo*) of the precipitated, water-washed solid furnished light-brown, polymeric I of lower molecular weight, which was designated 2nd fraction. The polymer portion insoluble in acetic acid was dissolved in a 80:20 (by volume) mixture of pyridine and glacial acetic acid. From this solution, weakly acidified with hydrochloric acid (pH 4–5) and filtered from some insoluble residue mainly containing crosslinked resin, a higher molecular fraction of I was precipitated by excess acidified water (pH 4–5) containing a trace of  $\text{NaHSO}_3$ . Washing and drying as above furnished a dark-brown solid designated 1st fraction. Both fractions were infusible up to 300°C., showed solubility in pyridine, *N,N*-dimethylformamide, and dimethyl sulfoxide, and were insoluble in water and aliphatic hydrocarbons. The 2nd fraction also dissolved in glacial acetic acid and cyclohexanone and largely so in warm aqueous alkali. Both fractions could be cast from organic solutions into brittle, transparent films. The 1st fraction, when precipitated in the absence of mineral acid and reducing agent, showed diminished solubility in pyridine.

Yields, analytical data and found  $\bar{M}_n$  values for the 1st and 2nd fractions are collected in Table II. The  $\bar{M}_n$  values listed were determined on pyridine



solutions. The invariance of  $\bar{M}_n$  with concentration is seen from the values below, measured on the 2nd fraction of No. 1 at five different concentrations (concentrations, in grams of solute per 100 ml. of solution, given in parenthesis): 763 (4.12), 765 (10.48), 751 (20.58), 768 (57.70), 801 (86.65); the value given in Table II was obtained as the mean of the first four figures listed. With dibromomethane as solvent, typical  $\bar{M}_n$  values were: 1420 (1.21), 1680 (2.57); cyclohexanone solvent gave: 540 (1.30), 570 (1.60). From the chloroform-soluble, low-molecular constituents of the 2nd fraction, the lowest member of I, 4-carboxyphenyl-diferrocenylmethane, was isolated in several cases by chromatography of the chloroform extracts on partially deactivated alumina (Alcoa grade F-20, exposed for 150 hr. to air of 40% R.H.), followed by recrystallization from chloroform-hexane of the products crystallizing from the concentrated first eluate. The orange-yellow compound, collected in yields up to 3.8% in experiments 1-3, showed the solubility behavior of polymeric I and, in addition, was soluble in dioxane and chlorinated hydrocarbons; it did not melt up to 300°C.

ANAL. Calcd. for  $C_{28}H_{24}Fe_2O_2$ : C, 66.70%; H, 4.80%; Fe, 22.15%; mol. wt., 504. Found: C, 66.72%; H, 4.99%; Fe, 22.08%; mol. wt. 510 (pyridine, mean value from two runs); 1060 (dibromomethane, 1.80 g./100 ml).

**Polymer II from Ferrocene and *p*-Cyanobenzaldehyde.** The reactants, ferrocene and *p*-cyanobenzaldehyde (molar ratio 1.8), were heated with zinc chloride (3.5 wt.-% of ferrocene) for 10 hr. at 150°C. in the manner described for polymer I. The solidified melt, after water extraction and drying, was taken up in warm *N,N*-dimethylformamide. From the solution, filtered under nitrogen, a higher molecular portion of II was precipitated by excess isopropanol; it was briefly digested with 0.5*N* hydrochloric acid in the presence of a little  $SnCl_2$  to remove coordinated solvents, thoroughly washed with water, and dried for 10 days at 50°C. *in vacuo*. This polymer portion, collected as a brown, infusible solid in 34.7% yield, was designated 1st fraction.

ANAL. Calcd. for II: C, 71.64%; H, 4.46%; Fe, 19.60%; N, 4.30%. Found: C, 71.10%; H, 4.55%; Fe, 18.83%; N, 4.68%; COOH, 0.9% (indicating partial hydrolysis).

From the mother liquor, excess water precipitated an additional fraction which, after acid treatment as above and removal of admixed ferrocene by vacuum sublimation, was obtained in 35.9% yield as a brown-yellow solid melting in the range 70-85°C.; it was designated 2nd fraction. Both fractions, while insoluble in water, dissolved readily in pyridine, *N,N*-dimethylformamide, cyclohexanone, and halo hydrocarbons.

ANAL. Calcd. for II: C, 70.44%; H, 4.63%; Fe, 21.36%; N, 3.57%. Found: C 69.97%; H, 4.54%; Fe, 21.07%; N, 3.92%.

The molecular weights for both fractions, 2310 and 760, respectively, were obtained in pyridine solution. No significant deviations from these values were found in dibromomethane solution at various concentrations.

Chromatography of the benzene extract of the 2nd fraction on alumina (partially deactivated by 8-hr. exposure to air of 40% R.H.), with benzene as eluent, furnished in 10.6% yield 4-cyanophenyl-diferrocenylmethane (II,  $n = 1$ ) as orange crystals, which, after repeated recrystallization from isopropanol, melted at 178–180°C. (sealed), homoannularity,<sup>6</sup> 98.2%.

ANAL. Calcd. for  $C_{28}H_{23}Fe_2N$ : C, 69.31%; H, 4.78%; Fe, 23.02%; N, 2.89%; mol. wt., 485. Found: C, 69.05%; H, 4.76%; Fe, 22.80%; N, 2.96%; mol. wt., 480 (pyridine); 490 (benzene).

From the subsequent chromatographic zone, there was isolated in 4.3% yield the heteroannular trinuclear homolog of II, 1,1'-bis( $\alpha$ -ferrocenyl-4-cyanobenzyl)ferrocene, m.p. 92–94°C. (from cyclohexane–hexane), homoannularity,<sup>6</sup> 62.6%.

ANAL. Calcd. for II ( $n = 2$ ): C, 70.44%; H, 4.63%; Fe, 21.36%; N, 3.57%; mol. wt., 784. Found: C, 70.91%; H, 4.85%; Fe, 20.98%; N, 3.53%; mol. wt., 730 (pyridine); 740 (benzene).

The dinuclear compound (II,  $n = 1$ ), when refluxed for 6 hr. with a 5% solution of KOH in an 85% water–ethanol mixture, was hydrolyzed to 4-carboxyphenyl-diferrocenylmethane (I,  $n = 1$ ), whose identity was established by elemental analysis,  $\bar{M}_n$  determination, infrared spectra and x-ray diffractograms. Similarly, hydrolysis of polymeric II under somewhat more severe conditions led to polymeric I.

**Polymer IV from Ferrocene and *o*-Carboxybenzaldehyde.** The mixture of ferrocene, *o*-carboxybenzaldehyde and zinc chloride was treated as described above for polymer I, at the reactant ratios and experimental conditions listed in Table I (runs 8–12). Work-up of the crude reaction product, after water extraction, was accomplished by reprecipitation much in the same manner as described for polymer II, except that the solvent was dioxane. Both fractions were reprecipitated from trifluoroacetic acid by water. Analytical data, yield, and  $\bar{M}_n$  for the 1st and 2nd fractions thus obtained are collected in Table II. While the 1st fraction was infusible up to 300°C., the 2nd fraction melted partially in the 110–150°C. range. Both fractions showed the solubility behavior of polymer I and in addition, owing to the reduced carboxyl content, dissolved readily in dioxane, cyclohexanone, and halohydrocarbons. With strongly branched or slightly crosslinked products (runs 11, 12), solubility in cyclohexanone was reduced. All fractions could be cast from solution into brittle, transparent films. As with polymer I, solvents other than pyridine used for  $\bar{M}_n$  measurements gave erratic results owing to association and dissociation. Thus, dibromomethane solvent led to  $\bar{M}_n$  in the 3000–6000 range for the 1st fractions, and in the 1800–4000 range for the 2nd fractions.

By chromatography of the cyclohexane-soluble constituents of the 2nd fraction on alumina (partially deactivated by 60-hr. air exposure, 40% R.H.), the two lactones VIII and VII were isolated by elution with 90:10 hexane–ether from two distinctly separated yellow-orange zones in the order given (order reversed with benzene as eluent). Yields in experiments

8, 9, and 11 were, respectively, 5.0, 3.4, and 0.9% for VII, and 3.4, 3.1, and 0.08% for VIII. With heating time in run 11 reduced to 4 min. and catalyst concentration increased to 10%, yields in VII and VIII were 3.1 and 0.6%, respectively. The corresponding figures for 30% ZnCl<sub>2</sub> (2 min.) were 4.7 and 0.5%. Lactone VII crystallized as two modifications, both melting at 138–140°C. (lit.<sup>7</sup> 137°C.), but giving different x-ray diffractograms.

ANAL. Calcd. for C<sub>18</sub>H<sub>14</sub>FeO<sub>2</sub>: C, 67.95%; H, 4.44%; Fe, 17.55%; mol. wt., 318  
Found: C, 68.12%; H, 4.39%; Fe, 17.96%; (COOH, 0.0); mol. wt. 330 (benzene); 325 (pyridine).

Lactone VIII formed orange prisms (from hexane or ether–hexane), m.p. 173–175° (sealed). Occasionally, an allotropic modification (different x-ray diffractogram), m.p. 184–186°C. (sealed), was observed if the compound was allowed to crystallize from hexane–benzene. Both modifications showed identical spectroscopic behavior in solution.

ANAL. Calcd. for C<sub>28</sub>H<sub>22</sub>Fe<sub>2</sub>O<sub>2</sub>: C, 66.97%; H, 4.42%; Fe, 22.24%; mol. wt., 502.  
Found: C, 66.72%; H, 4.60%; Fe, 22.68%; (COOH, 0.0); mol. wt., 495 (benzene); 500 (pyridine).

**Polymer IV from Ferrocene and 3-Ethoxyphthalide.** All experiments conducted with 3-ethoxyphthalide in place of *o*-carboxybenzaldehyde under the conditions of Table I, except that heating times were generally extended by 30–50%, gave reaction products comparable to runs 8–12 listed in Table II. The HCl catalyst in the experiment summarized in footnote h, Table I, was added as 2*N* hydrochloric acid in three portions over the first 10 hr.

**Lactone VIII and Polymer IV from Ferrocene and 3-Ferrocenylphthalide (VII).** The mixture of ferrocene and lactone VII (molar ratio 2:1) was heated with zinc chloride (12 wt.-% of VII) for 10 min. at 170°C. following the conventional procedure. The product, after washing with water and drying as before, was reprecipitated from dioxane solution by excess 95% aqueous isopropanol. The first fraction of IV was collected in 3.3% yield (C, 67.92%; H, 4.22%;  $\bar{M}_n$ , 1870). Excess water precipitated the balance of products, from which unreacted ferrocene as well as lactones VII and VIII were removed by hexane extraction. The hexane-insoluble portion was reprecipitated from trifluoroacetic acid by water to give oligomeric IV (C, 67.55%; H, 4.41%; Fe, 16.93%;  $\bar{M}_n$ , 810) in 31.8% yield. Chromatographic work-up of the hexane extract as described above, gave unreacted ferrocene, lactones VII (25% recovery) and VIII (17.5% yield), both identified by x-ray diffractograms and mixed melting points.

An experiment conducted as above, except that the ferrocene/lactone ratio was 3:1 and the heating time was reduced to 1 min., gave low molecular IV in 5.1% yield (C, 67.53%; H, 4.46%; melting range, 100–130°C.), while the yield in VIII and the recovery of VII were 6.7% and 58%, respectively.

**Polymer V from 3-Ferrocenylphthalide (VII).** Lactone VII was heated with 5 wt.-% of anhydrous zinc chloride for 20 min. at 145°C. under nitrogen. The solidified melt was worked up in the conventional manner giving, in 67.1% overall yield, two fractions of V as yellow-tan solids that showed the solubility behavior of IV. From the 2nd fraction, admixed starting material was removed by extraction with hexane. While the 1st fraction was infusible up to 300°C., the 2nd fraction had the melting range 120–140°C.

ANAL. Calcd. for V ( $m = n$ ) (2nd fraction in parentheses): C, 68.13% (68.02%); H, 4.19% (4.33%); Fe, 17.60% (17.57%); COOH, 7.1% (7.1%). Found: C, 66.55% (67.71%); H, 4.22% (4.40%); Fe, 17.01% (17.28%); COOH, 7.2% (6.3%);  $\bar{M}_w$ , 3200 (900) (pyridine).

Similar results were obtained with the use of 12 wt.-% HCl as catalyst at an overall reaction time of 12 hr. at 115°C. The catalyst was added as 2*N* hydrochloric acid in small portions over the first 6 hr.

**Polymer VI and Lactone VIII from Ferrocene and *o*-Ferrocenoylbenzoic Acid.** The mixture of ferrocene and *o*-ferrocenoylbenzoic acid (molar ratio 6:1) was fused with anhydrous zinc chloride (10 wt.-% of ferrocene) for 0.5 hr. at 170°C. in the conventional manner. After removal of catalyst and unreacted acid by extraction with hot water, the low molecular constituents were extracted with cyclohexane. Chromatography of the concentrated extract as described above gave lactone VIII in 11.0% yield in addition to unreacted ferrocene. From the cyclohexane-insoluble portion, VI was extracted with trifluoroacetic acid and was precipitated as a single fraction by excess water; yield, 51.2%. The presence of broad absorption near 2.9  $\mu$ , coupled with a shoulder at 5.80  $\mu$ , in the infrared spectrum indicates partial hydrolysis of the lactone rings.

ANAL. Calcd. for VI: C, 67.90%; H, 4.03%; Fe, 19.25%. Found: C, 67.52%; H, 4.24%; Fe, 18.73%.

If, in the above experiment, the ferrocene/acid molar ratio was changed to 2:1 and the heating time reduced to 10 min., yields in VI and VIII were 42.0 and 10.2%, respectively.

This work was performed by the Missile & Space Systems Division, Douglas Aircraft Company, Inc., under company-sponsored research and development funds. The authors are indebted to Dr. R. H. Boschan for many stimulating discussions, and to Mrs. E. Carter and Mr. E. Quo for contributing to the experimental and analytical work.

## References

1. E. W. Neuse and D. S. Trifan, paper presented at the 148th National Meeting, American Chemical Society, Chicago, September 1964; *Abstracts of Papers*, p. 5-S.
2. E. W. Neuse, *Nature*, **204**, 179 (1964).
3. E. W. Neuse, K. Koda, and E. Carter, *Makromol. Chem.*, **84**, 213 (1965).
4. E. W. Neuse and K. Koda, *J. Organometal. Chem.*, **4**, 475 (1965).
5. M. Rosenblum, Ph.D. Thesis, Harvard University, 1953.
6. E. W. Neuse and D. S. Trifan, *J. Am. Chem. Soc.*, **85**, 1952 (1963).



7. A. N. Nesmeyanov, V. D. Vilchevskaya, and N. S. Kochetkova, *Dokl. Akad. Nauk SSSR*, **138**, 390 (1961).
8. D. Hadzi and U. Sheppard, *Proc. Roy. Soc. (London)*, **A216**, 247 (1953).
9. D. D. Wheeler, D. C. Young, and D. S. Erley, *J. Org. Chem.*, **22**, 547 (1957).
10. J. K. Wilmshurst, *Spectrochim. Acta*, **6**, 95 (1954).
11. H. S. Bloch, H. Pines, and L. Schmerling, *J. Am. Chem. Soc.*, **68**, 153 (1946).
12. C. D. Nenitzescu, M. Avrau, and B. Sliam, *Bull. Soc. Chim. France*, **1955**, 1266.
13. A. N. Nesmeyanov, N. A. Voikenau, and V. D. Vilchevskaya, *Dokl. Akad. Nauk SSSR*, **118**, 512 (1958).

### Résumé

En vue d'étendre un travail antérieur sur la condensation du ferrocène avec les aldéhydes, on décrit la polycondensation du ferrocène avec le para- et orthocarboxybenzaldehyde. Tandis que dans le premier cas, la polycondensation régulière se passe donnant naissance à un polymère composé de ferrocénylène et d'unité 4-carboxybenzylidénique une déviation de cette voie est observée dans le cas l'*o*-carboxybenzaldehyde, tandis que le polymère contenant à la fois des unités carboxy benzylidéniques et 3,3-phthalides entre les groupes ferrocényléniques est formée. Ce comportement inattendu peut être expliqué par un mécanisme d'abstraction d'hydrure. En vue de confirmer la structure proposée de ce polymère, on a pu isoler comme intermédiaire ou comme sous-produit le 3-ferrocénylphthalide et le 3,3-diferrocénylphthalide. Dans les deux séries de polymères, des poids moléculaires en nombre jusque 3.000 ont été mesurés (échantillon nonfractionné). Les polymères sont solubles dans un nombre de solvants organiques et peuvent être insolubilisés par traitement aux époxydes.

### Zusammenfassung

In Erweiterung einer früheren Arbeit über die Kondensation von Ferrocen mit Aldehyden wird die Polykondensation von Ferrocen mit *p*- und *o*-Carboxybenzaldehyd beschrieben. Während im früheren Fall eine reguläre Polykondensation unter Bildung eines aus Ferrocenyl- und 4-Carboxybenzaleinheiten aufgebauten Polymeren eintritt, wird im Fall des *o*-Carboxybenzaldehyd eine Abweichung von diesem Weg beobachtet und ein Polymeres mit Carboxybenzal- und 3,3-Phthalid-Brückenbausteinen zwischen den Ferrocenylgruppen gebildet. Dieses unerwartete Verhalten kann durch einen Hydridabstraktionsmechanismus erklärt werden. Die vorgeschlagene Polymerstruktur wird durch die Isolierung von 3-Ferrocénylphthalid und 3,3-Diferrocénylphthalid als Zwischen- und Nebenprodukt gestützt. In beiden Polymerreihen werden Zahlenmittelmolekulargewichte bis zu 3000 (unfraktioniert) gemessen. Die Polymeren sind in einer Reihe organischer Lösungsmittel löslich und können mit Epoxyden gehärtet werden.

Received November 4, 1965

Revised December 27, 1965

Prod. No. 5063A



## Irradiation of Some Polysiloxanes in Various Gases

ROBERT K. JENKINS,\* *Northrop Space Laboratories, Hawthorne, California*

### Synopsis

The changes produced by  $\gamma$ -irradiations on two polysiloxanes in several gaseous atmospheres were studied by both sequential and parallel exposures with an *in-situ* vibrating reed technique. Irradiation in atmospheres of  $N_2O$ , He, air, and a mixture of 20%  $NO_2$  and 80%  $N_2$ , caused reduction in the crosslinking rates of the polymers as compared to vacuum. Marked discolorations of the samples occurred when irradiations were conducted in air,  $N_2O$ , and 20%  $NO_2$ -80%  $N_2$ . Similarities in crosslinking rates and color changes were obtained when the polymers were irradiated in either air or the gas mixture.

### INTRODUCTION

Irradiation of polymers in air and vacuum have been extensively reported in the literature with the conclusions that crosslinking rates are enhanced in vacuum and depressed in air.<sup>1-6</sup> Okada<sup>7-10</sup> has published results of the effects of various gases on the irradiation crosslinking rates of polyethylene and concluded that several gases, most notably  $N_2O$ , accelerated the crosslinking rate, as compared to his vacuum control. Okada suggested that some type of radiolytic intermediate from  $N_2O$  was responsible for the apparent rate increase. Lyons and Dole<sup>11</sup> examined the radiation chemistry of polyethylene in the presence of the gases  $N_2O$  and  $NO$  and postulated two mechanisms for the accelerating rate effects of  $N_2O$  observed by Okada. Both postulations were dependent upon hydrogen abstraction by either O or OH with the subsequent formation of  $H_2O$  to account for the apparent rate increase.

Considering that the final radiolytic products from  $N_2O$  are  $N_2$ ,  $O_2$ , and  $NO_2$ <sup>12</sup> and that the latter two gases are known to depress the crosslinking rates in ionizing radiation while  $N_2$  yields a crosslinking rate analogous to a vacuum exposure,<sup>13</sup> it seemed worthwhile to investigate the crosslinking rates of two siloxane polymers by the *in-situ* vibrating reed technique<sup>14</sup> in air,  $N_2O$ , He, vacuum, and a gas mixture of 20%  $NO_2$ -80%  $N_2$ , by weight, to determine if analogous rate accelerations would occur. Two polysiloxane polymers were chosen, principally due to their low glass transition temperatures  $T_g$ , low crystalline melting points  $T_m$ , and high gas permeability in the bulk form.

\* Present address: 6061 Sydney Drive, Huntington Beach, California.

The kinetic theory of elasticity that relates the stress elongation-temperature dependency of polymers in their rubbery plateau region offers a convenient equation to follow the change of modulus with changes in either the effective elastic chains in the polymer network ( $\nu$ ) or with temperature changes, providing the strain is small.<sup>9</sup> The force  $f$  per unit area on the sample is

$$f = \nu RT [(L/L_0)^2 - (L_0/L)] \quad (1)$$

where  $\nu$  is the number of moles of effective elastic chains per unit volume of polymer,  $R$  is the gas constant,  $T$  is the absolute temperature,  $L_0$  is the unstretched length of the polymer sample, and  $L$  is the stretched length.

Equation (1) may be written as:

$$E'_{\text{dyn}} = 3\phi RT\nu \quad (2)$$

where  $E'_{\text{dyn}}$  is the real part of the dynamic modulus of elasticity and  $\phi$  is a front factor that takes into consideration both the nonequilibrium type testing and the contribution of internal energy.<sup>15,16</sup> Comparison of  $\nu$  values obtained by both the dynamic modulus and swelling techniques on identically  $\gamma$ -crosslinked siloxane samples yields a  $\phi$  value of about 3.3.<sup>17</sup>

The principal interest of this investigation was to determine the effects of various gases on the rate at which the modulus changes with  $\gamma$ -exposure; therefore, eq. (2) may be written

$$[dE'_{\text{dyn}}/d(\text{Mr})]_{\text{gas}} = k \quad (3)$$

where  $dE'_{\text{dyn}}/d(\text{Mr})$  is the change in modulus per megarentgen  $\gamma$ -exposure.

The dynamic modulus allows one to follow the overall effects of both crosslinking and scissioning events which occur simultaneously during the irradiation of the polysiloxanes but does not allow assignments of individual rates for either process.

## APPARATUS AND EXPERIMENTAL TECHNIQUE

The apparatus consisted of a miniaturized vibrating reed fabricated to fit inside a stainless steel canister equipped with a heating unit and the capability of either low or high pressures. A more detailed description of the vibrating reed has been published previously.<sup>14</sup>

The polymers examined were gum products of polydimethylsiloxane (PDMS) and polydimethyldiphenylsiloxane (PDMDPS) containing about 7 mole-% diphenyl units. Prior to this study, the two gums were lightly crosslinked into sheet forms ( $1/8$  in. thick) by about 5.5 Mr of  $\gamma$ -radiation from a 5000-c. cobalt source. The lightly crosslinked sheets of polymers were then cut into reeds  $5/16$  in. wide and about 2 in. long and stored at 5°C.

Reeds (one each of PDMS and PDMDPS) were mounted in the vibrating reed apparatus and the dynamic modulus of each determined. The temperature was held constant at 38°C. by use of a heating element controlled by a thermocouple embedded in a control polymer sample located between

the two reeds. Vacuum was obtained by using a 15-cfm mechanical pump connected directly to the canister. A dynamic vacuum system was preferred over a static system to prevent any possible back reaction that might be caused by gaseous radiolytic by-products. Prior to irradiation, the system was pumped down and held at about  $1.0 \mu$  for a period of 4 hr. to remove  $O_2$  from the system and the polymers. Following the degassing period, the various gases\* were admitted into the system and the canister lowered into a  $\gamma$  flux of  $2.6 \times 10^5$  r./hr., or, in the case of a vacuum environment, the canister was lowered directly into the radiation field. The change in dynamic moduli of the two reeds was determined by following the change of the fundamental frequencies of vibrations at the desired time intervals by sweeping the reeds through a small frequency range of 20–100 cps. Once the polymers had become sufficiently crosslinked to reduce their  $\tan \delta$  to small values it was possible to find the first and, occasionally, the second overtones.

When the crosslinking rate in the specific environment had been well established, the samples were either removed from the source for visual and infrared inspection or the canister was reevacuated and flushed several times with the gas in which the next experiment was to be conducted.

## RESULTS AND DISCUSSION

### Parallel Exposure

Figure 1 depicts the changes of the dynamic moduli,  $E'_{dyn}$ , as a function of  $\gamma$  exposure for the PDMS and PDMDPS polymers in environments of  $N_2O$ , air, and vacuum at a temperature of  $38^\circ C$ . The change of moduli is a linear function of exposure time under vacuum and air conditions, except for a brief initiation period of approximately 26 hr. On utilizing this linear relationship of modulus to exposure time, a crosslinking rate  $k$ , is introduced, defined as the change in modulus per megareöntgen exposure  $dE'_{dyn}/d(Mr)$ . The values calculated for the vacuum and air exposures are  $22.2 \times 10^4$  and  $9.25 \times 10^4$  dynes/cm.<sup>2</sup>-Mr, respectively. Radiation of the polymer under an atmosphere of  $N_2O$  produced a complex behavior. Rapid scissioning of the siloxane main chain was observed in the initial exposure as evidenced by the decrease in modulus from 0 to 26 hr. Continued radiation produced a rapid modulus increase that gradually lessened until a steady crosslinking rate was observed from about 110 hr. to the end of the experiment. The value of  $k$ , was found to be  $11.9 \times 10^4$  for the linear portion of this curve. The ratios  $(k_{gas}/k_{vacuum}) \times 100$ , which define the efficiency factor  $E$ , with the presumption that  $k_{vacuum}$  represents the optimum environment for crosslinking, are presented in Table I. It is seen that  $E_{air}$  is 42%, while  $E_{N_2O}$  is 53.5%. The results obtained from irradiation in  $N_2O$  were lower than anticipated, as Okada<sup>7-10</sup> previously had

\* The  $NO_2$  gas mixture was maintained at a pressure of 1.5 atm. to insure that the number of  $NO_2$  moles was about equal to the number of  $O_2$  moles in air at 1 atm.

TABLE I  
Property Changes of Some Siloxane Polymers Irradiated in Various Gases

Polymer	Property	Environment					
		Air	Vacuum	N <sub>2</sub> O	He	80% N <sub>2</sub> + 20% NO <sub>2</sub>	
PDMS	Crosslinking rate $k = dE'_{\text{dyn}}/d(\text{Mr})$ , dyne/cm. <sup>2</sup> Mr,	$9.25 \pm 0.8 \times 10^{1a}$	$22.2 \pm 1.6 \times 10^{1a}$	$11.9 \times 10^{1b}$	$20.2 \times 10^1$	$9.22 \times 10^1$	
	Color development	Lt. yellow, dose-depend- <sup>ent</sup> $3.58 \times 10^{-7}$ 42	Clear, no change	Orange	—	Lt. yellow	
PDDMPS	$d_p/d(\text{Mr})$ $E = k_{\text{gas}}/k_{\text{vacuum}}$ , %	$3.3 \pm 0.6 \times 10^{1a}$	$8.6 \times 10^{-7}$ 100	$4.61 \times 10^{-7}$ 53.5	$7.83 \times 10^{-7}$ 91	$3.57 \times 10^{-7}$ 42	
	Crosslinking rate $k = dE'_{\text{dyn}}/d(\text{Mr})$ , dyne/cm. <sup>2</sup> Mr		$15.6 \pm 0.6 \times 10^{1a}$	$7.1 \pm 0.5 \times 10^{1b}$	$9.6 \times 10^1$	$5.4 \times 10^1$	
	Color development	Red-brown	V. lt. yellow	Red-brown	—	Orange	
	$d_p/d(\text{Mr})$ $E = k_{\text{gas}}/k_{\text{vacuum}}$ , %	$1.28 \times 10^{-7}$ 21	$6.04 \times 10^{-7}$ 100	$2.75 \times 10^{-7}$ 46	$3.72 \times 10^{-7}$ 62	$2.09 \times 10^{-7}$ 35	

<sup>a</sup> Average of three runs.

<sup>b</sup> Average of two runs.

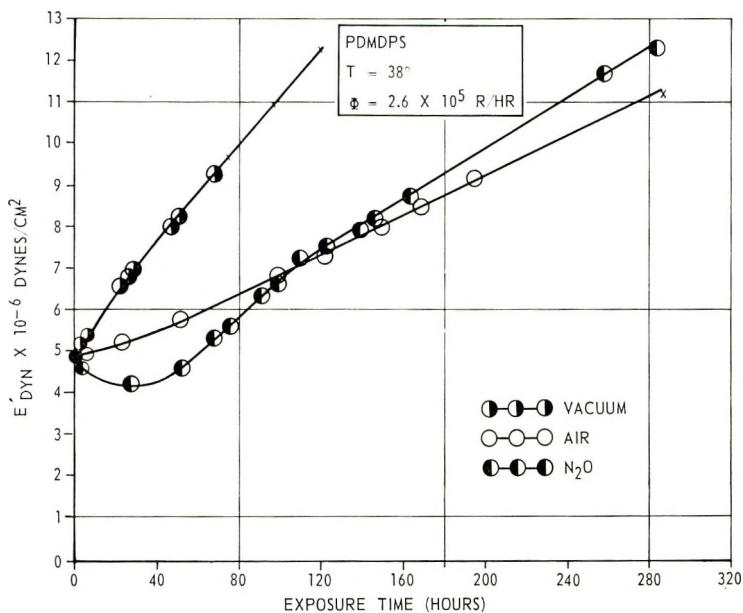


Fig. 1. Change of dynamic modulus with  $\gamma$  exposure of PDMS in several atmospheric environments. Parallel exposure.

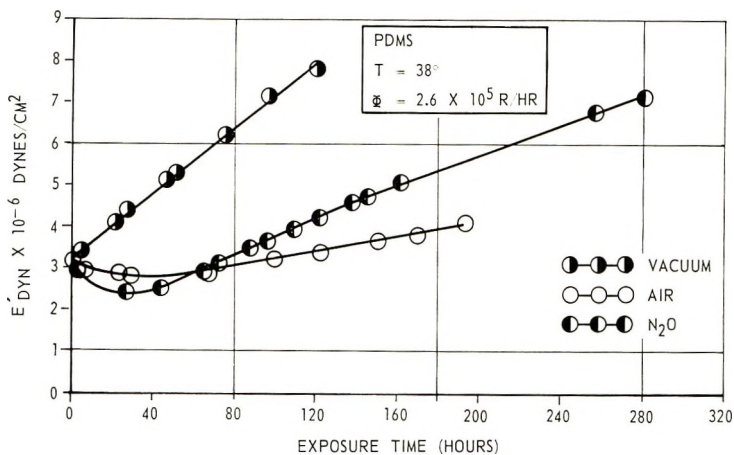


Fig. 2. Change of dynamic modulus with  $\gamma$  exposure of PDMDPS in several atmospheric environments. Parallel exposure.

shown a greater crosslinking rate for polyethylene when irradiated under an  $N_2O$  atmosphere as compared to his vacuum control. The differences in experimental results obtained by Okada and in this investigation prompted a repetition of the  $N_2O$  irradiation with subsequent identical results.

The final radiolytic products of  $N_2O$  are  $N_2$ ,  $O_2$ , and  $NO_2$ .<sup>12</sup> The latter two gases depress the crosslinking rates of polymers, whereas  $N_2$  yields a



crosslinking rate equivalent to irradiation in vacuum. The results obtained from the irradiation of PDMS in  $N_2O$  suggest that the crosslinking rate is probably dependent on the concentration of final radiolytic products and not on a radiolytic intermediate. Secondly, the physical state of the polymer during irradiation largely controls the observed crosslinking rates and prevents a direct comparison of semicrystalline polyethylene and amorphous siloxane polymers. Finally, the increased crosslinking rate of polyethylene over PDMS may possibly be explained by the relative ease of hydrogen abstraction from the methylene group, as compared to the methyl group of PDMS.

Figure 2 depicts the change in moduli as a function of exposure time for the PDMDPS polymer in environments of  $N_2O$ , air, and vacuum. Comparison of the  $k_{\text{vacuum}}$  rates obtained for both polymers demonstrates the effectiveness of the phenyl group to act as an energy sink, thus inhibiting the formation of active sites available for crosslinking.<sup>19,20</sup> The crosslinking efficiencies  $E$  were lower than the values obtained for the PDMS polymer, thus indicating a possible synergistic effect between the phenyl group and irradiation atmosphere that may provide increased protection against crosslinking. The maximum crosslinking efficiency was obtained in vacuum followed by  $N_2O$  and then air. These results were analogous to that obtained from the irradiation of PDMS.

### Sequential Exposure

**Vacuum,  $NO_2$ .** Once the crosslinking rates of the polymers had been established in  $N_2O$ , it was considered important to determine the effects of  $NO_2$  on the reaction rates. A gas mixture consisting of 20%  $NO_2$  and 80%  $N_2$ , on a weight basis, was employed in this portion of the experiment, principally to determine if the effects of  $O_2$ , as present in air, and  $NO_2$  in the gas mixture were basically the same, as measured by the mechanical method. The irradiation of the polymers in the gas mixture was conducted at 1.5 atm., thus providing essentially equal molar quantities of  $NO_2$  in  $N_2$  as  $O_2$  in air. Figure 3 presents the change in dynamic modulus of both PDMS and PDMDPS while in the gas mixture before and during  $\gamma$ -irradiation. Prior to irradiation, the samples were exposed to the gas mixture for a period of about 24 hr. This exposure resulted in a decrease of modulus, apparently caused by scissioning of the main siloxane chain. As a result of this scissioning, the loss factor,  $\tan \delta$ , of the polymer had reached a level from which it was difficult to discern the fundamental frequency of vibration; therefore, the canister was evacuated to a pressure of about  $10 \mu$  and placed into the radiation well. The polymers were irradiated in vacuum for a period of 71 hr. with an increase in modulus and decrease in  $\tan \delta$  which provided an adequate signal response. The gas mixture was reintroduced into the canister and the experiment continued. The introduction of the gas into the canister caused a drop in modulus followed by a steady crosslinking rate of  $9.22 \times 10^4$  and  $5.4 \times 10^4$  dyne/cm.<sup>2</sup>-Mr for the PDMS and PDMDPS polymers, respectively. The drop

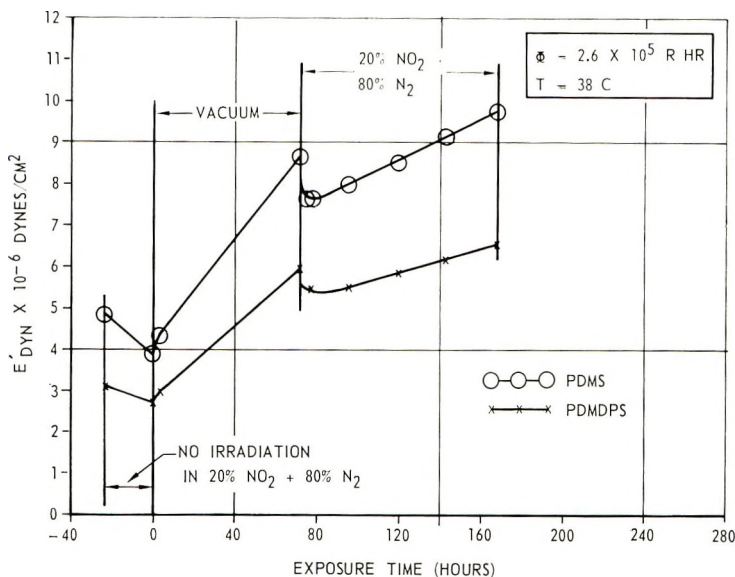


Fig. 3. Change of dynamic modulus with exposure time in several atmospheres. Sequential exposure.

in modulus that occurred when the system was changed from vacuum to gas is due to a rapid scissioning reaction and is not the result of gas pressure on the fundamental frequency of vibration of the polymeric reeds.

The crosslinking rate for the PDMS in the gas mixture was identical to the rate found when the polymer was irradiated in air. This correspondence of rates suggests that the mechanism for crosslinking is the same in air and the NO<sub>2</sub> gas mixture. Miller<sup>18</sup> proposed that both the  $\equiv\text{SiCH}_2$  and  $\equiv\text{Si}^\cdot$  radicals react with O<sub>2</sub> to form peroxy radicals. Subsequently, the  $\equiv\text{SiCH}_2\text{OO}^\cdot$  radical is oxidized to  $\equiv\text{SiCOOH}$ , whereas  $\equiv\text{SiOO}^\cdot$  is an intermediate that forms a residual crosslink. However, it is unlikely that NO<sub>2</sub> should form a free-radical intermediate leading to crosslinking but, rather, that it should cause complete termination of the free-radical species.

The crosslinking rate of the PDMDPS was found to be slightly higher in the gas mixture than in air, but again, the additional variable (phenyl group) may, and apparently does, react differently in the presence of NO<sub>2</sub> and O<sub>2</sub>.

**Vacuum, Air, Helium.** The dynamic modulus behavior as a function of irradiation time are presented in Figure 4 for both polymers. A linear dependency of modulus with exposure time was observed under each condition studied except for the PDMDPS polymer in air. As seen in Figure 2, the PDMDPS polymer requires 70-80 hr. of irradiation before a steady crosslinking rate is obtained.

The introduction of air into the system after 121 hr. of irradiation caused a sharp decrease in the modulus of the samples as previously noted in the NO<sub>2</sub>-N<sub>2</sub> irradiation section. Following the air irradiation, the canister

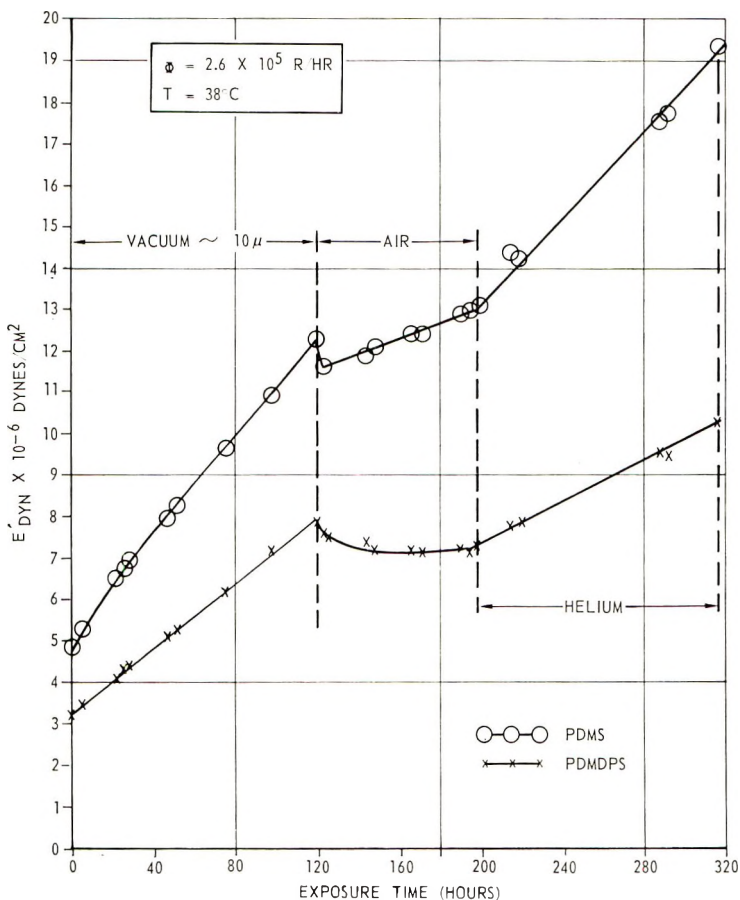


Fig. 4. Change of dynamic modulus with exposure time in several atmospheres. Sequential exposure.

was flushed several times with helium and then held at a slight positive helium pressure. The modulus change as a function of exposure time was found to increase and to remain linear. The  $k_{He}$  values were found to be  $20.2 \times 10^4$  and  $9.6 \times 10^4$  dyne/cm.<sup>2</sup>-Mr for the PDMS and PDMDPS polymers, respectively.

#### Discoloration of Polymer Samples

It was observed during the course of this investigation and in previous work that irradiations of the siloxane polymers in air and other gases produced a discoloration. The intensity and hue developed in the polymers were dependent upon the length of  $\gamma$  exposure and the gas employed. Irradiation of the polymers in vacuum produced a very slight discoloration in the PDMDPS, whereas the PDMS remained clear; therefore, it would appear that the development of chromophores in the polymers is somehow dependent upon the structural use of  $O_2$  and  $NO_2$ . Heating the irradiated

samples to a temperature of about 150°C. intensified the discoloration slightly, with subsequent prolonged heating producing no further changes. The color intensity of the PDMDPS was always greater than that of the PDMS which suggests that the phenyl group plays a role in the discoloration mechanism. Discoloration of polymers during irradiations is not unique and various reactions and structures have been proposed to explain the mechanisms. The discoloration of polysiloxanes is somewhat difficult to explain in that the structures do not readily lend themselves to unsaturation, or other chromophoric groups. Infrared spectra of the irradiated polymers compared against a nonirradiated control has not been particularly fruitful with the KBr disk technique; but preliminary results utilizing the differential KBr disk technique do show some promise.

### CONCLUSIONS

(1) The crosslinking rate  $k$  of PDMS is dependent upon the irradiation atmosphere employed. The order of rates for PDMS was found to be  $k_{\text{vacuum}} \geq k_{\text{He}} > k_{\text{N}_2\text{O}} > k_{\text{air}} = k_{\text{NO}_2 + \text{N}_2}$ , and for PDMDPS  $k_{\text{vacuum}} > k_{\text{He}} > k_{\text{N}_2\text{O}} > k_{\text{NO}_2 + \text{N}_2} > k_{\text{air}}$ .

(2) A simulated air atmosphere consisting of 20%  $\text{NO}_2$  and 80%  $\text{N}_2$ , by weight, yielded identical reaction rates and color development at equivalent  $\gamma$  exposure for the PDMS polymer, as in air.

(3) Both polymers discolored when irradiated in air,  $\text{N}_2\text{O}$ , and the gas mixture. PDMDPS, at equivalent radiation exposures, was found to discolor more than PDMS. The mechanism that results in the discoloration is not known.

(4) The irradiation mechanisms of the polymers in  $\text{N}_2\text{O}$  is complex. The crosslinking rate is apparently controlled by the concentration of  $\text{N}_2\text{O}$  and the radiolytic by-products of  $\text{N}_2$ ,  $\text{O}_2$ , and  $\text{NO}_2$ .

The author expresses his appreciation to the Northrop Corporation for permission to publish this article and to L. Brown who fabricated most of the apparatus. In addition, the infrared work by L. Karre is appreciated.

### References

1. F. A. Bovey, *The Effects of Ionizing Radiation on Natural and Synthetic High Polymers*, Interscience, New York, 1958, pp. 55-56.
2. R. O. Bolt and J. G. Carroll, *Radiation Effects on Organic Materials*, Academic Press, New York, 1963, pp. 171-172.
3. A. Chapiro, *Radiation Chemistry of Polymeric Systems*, Interscience, New York, 1962, pp. 360-361.
4. A. Charlesby and P. G. Garratt, *Proc. Roy. Soc. (London)*, **A273**, 117 (1963).
5. P. Alexander and D. Toms, *J. Polymer Sci.*, **22**, 343 (1956).
6. R. G. Bauman and J. W. Born, *J. Appl. Polymer Sci.*, **1**, 351 (1959).
7. Y. Okada and A. Amemiya, *J. Polymer Sci.*, **50**, S22 (1961).
8. Y. Okada, *J. Appl. Polymer Sci.*, **7**, 695 (1963).
9. Y. Okada, *J. Appl. Polymer Sci.*, **7**, 703 (1963).
10. Y. Okada, *J. Appl. Polymer Sci.*, **7**, 1153 (1963).
11. B. J. Lyons and M. Dole, *J. Phys. Chem.*, **68**, 526 (1964).

12. S. Dondes, *Proc. Intern. Conf. Peaceful Uses Atomic Energy*, **14**, 176 (1956).
13. P. Alexander and D. Toms, *J. Polymer Sci.*, **22**, 343 (1956).
14. R. K. Jenkins, *J. Polymer Sci. B*, **2**, 999 (1964).
15. A. V. Tobolsky, *Properties and Structures of Polymers*, Wiley, New York, 1960.
16. M. C. Shen, paper presented at the Pacific Southwest Regional Meeting, American Chemical Society, Costa Mesa, California, December 5, 1965.
17. R. K. Jenkins, *J. Polymer Sci. A-2*, **4**, 41 (1966).
18. A. A. Miller, *J. Am. Chem. Soc.*, **83**, 31 (1961).
19. M. Koike and A. Danno, *J. Phys. Soc. Japan*, **15**, 1501 (1960).
20. M. Koike, *J. Phys. Soc. Japan*, **18**, 387 (1963).

### Résumé

Les changements produits par irradiation  $\gamma$  sur deux polysiloxanes dans de nombreuses atmosphères gazeuses ont été étudiées à la fois dans des expositions consécutives ou parallèles au moyen d'une technique de vibration *in situ*. L'irradiation dans des atmosphères de  $N_2O$ , He, d'air et dans un mélange de 20%  $NO_2$  et 80%  $N_2$  provoque une réduction dans les vitesses de pontage des polymères si on les compare à cette même vitesse sous vide. Des colorations marquées des échantillons se marquent lorsque des irradiations sont conduites à l'air,  $N_2O$  et dans le mélange 20%  $NO_2$ -80%  $N_2$ . Des similitudes de vitesses de pontage et de couleurs ont été obtenues lorsque les polymères sont irradiés dans l'air soit dans le mélange gazeux.

### Zusammenfassung

Die durch  $\gamma$ -Bestrahlung bei zwei Polysiloxanproben in verschiedener Gasatmosphäre hervorgerufenen Veränderungen wurden bei aufeinanderfolgender und paralleler Exposition mit einem Vibrations-Stäbchenverfahren *in situ* untersucht. Bestrahlung in  $N_2O$ -, He-, Luft- und einer gemischten (20%  $NO_2$  und 80%  $N_2$ )-Atmosphäre verursacht im Vergleich zum Vakuum eine Herabsetzung der Vernetzungsgeschwindigkeit der Polymeren. Bei Bestrahlung unter Luft,  $N_2O$  und (20%  $NO_2$ -80%  $N_2$ ) trat eine merkliche Verfärbung der Proben auf. Ähnliche Vernetzungsgeschwindigkeiten und Farbänderungen wurden bei Bestrahlung der Polymeren unter Luft oder in der Gasmischung erhalten.

Received December 1, 1965

Revised January 3, 1966

Prod. No. 5064A



## Influence of Addition of Ethylene on the $\gamma$ -Ray-Induced Alternating Copolymerization of Ethylenimine and Carbon Monoxide\*

TSUTOMU KAGIYA, SHIZUO NARISAWA, TAIZO ICHIDA,  
and KENICHI FUKUI, *Faculty of Engineering, Kyoto University, Kyoto,*  
*Japan,* and HISAO YOKOTA, *Sumitomo Atomic Energy Industries, Ltd.,*  
*Osaka, Japan*

### Synopsis

The influence of the addition of ethylene on the  $\gamma$ -ray-induced alternating copolymerization of ethylenimine and carbon monoxide was investigated. A mixture of ethylenimine, carbon monoxide, and ethylene was irradiated to produce a polymer containing these monomeric units. The infrared spectrum of the copolymer showed the characteristic absorption peaks of the secondary amide and ketone bond and was different from that of the reaction product of polyketone with ethylenimine and that of the  $\gamma$ -ray irradiation product of ethylene and poly- $\beta$ -alanine. The x-ray diffraction diagram of the copolymer was different from those of poly- $\beta$ -alanine and polyketone and exhibited an amorphous structure. Paper chromatographic analysis showed that the hydrolysis product of the copolymer contained  $\beta$ -alanine and  $\delta$ -aminovaleric acid. These results indicate that terpolymerization of ethylenimine, carbon monoxide, and ethylene took place under  $\gamma$ -ray irradiation and gave an amorphous polymer containing the units  $\text{-(CH}_2\text{CH}_2\text{NHCO)-}$ ,  $\text{-(CH}_2\text{CH}_2\text{CO)-}$ , and  $\text{-(CH}_2\text{CH}_2\text{CH}_2\text{CH}_2\text{NHCO)-}$ .

### INTRODUCTION

In recent years, the copolymerization of ethylene and carbon monoxide by radical initiators<sup>1,2</sup> and by  $\gamma$ -ray irradiation<sup>3-6</sup> has been studied. Little attention, however, has been paid to the influence of various additives on this copolymerization.

During the course of an investigation on the copolymerization of aziridines and various kinds of cyclic compounds,<sup>7,8</sup> it was found that aziridines and carbon monoxide copolymerize alternately to poly- $\beta$ -alanines under  $\gamma$ -ray irradiation.<sup>9</sup>

The present investigation was undertaken to determine the influence of addition of ethylene on this novel alternating copolymerizing system of aziridines and carbon monoxide.

\* Presented at the 14th Annual Meeting of the Society of Polymer Science, Japan, Tokyo, May 1965.

## EXPERIMENTAL

### Materials and Polymerization

Ethylene (99.9% purity, oxygen content less than 5 ppm) and carbon monoxide (99.2% purity) were obtained commercially. Ethylenimine obtained commercially was dried over KOH pellets and NaH and then fractionated at 55.5–56°C. before use.

The  $\gamma$ -ray-induced copolymerizations were carried out as follows. A measured amount of ethylenimine was placed into a stainless steel high-pressure reaction vessel. The vessel was degassed twice *in vacuo* under cooling with liquid nitrogen bath. Then, measured amounts of ethylene and carbon monoxide were fed into the vessel from each reservoir. All irradiations were performed with  $\gamma$ -rays from a  $^{60}\text{Co}$  (5000) source without agitation. The polymer formed was washed with methanol and ethyl ether and then dried *in vacuo* and weighed.

### Chemical Analysis of the Copolymer

The composition of the polymer was determined from the contents of carbon, hydrogen, and nitrogen by elemental analysis.

In order to determine the structure of copolymer, the hydrolysis product of the copolymer obtained in expts. 7, 10, and 11 was analyzed by a paper chromatographic method.<sup>9</sup> The hydrolysis products were compared with commercial  $\beta$ -alanine and  $\delta$ -aminovaleric acid by the usual one-way ascending chromatography for amino acid.<sup>12</sup> Both samples were developed on Toyo Roshi No. 50 paper for chromatography with *n*-butanol–glacial acetic acid–water (4:1:5) and also with phenol–water (7:3) as solvents. Both spots were detected by using a *n*-butanol solution of ninhydrin.  $R_f$  values of the hydrolysis product were: 0.37 ( $\beta$ -alanine) and 0.50 ( $\delta$ -aminovaleric acid) in the *n*-butanol–glacial acetic acid–water (4:1:5) system, and 0.69 ( $\beta$ -alanine) and 0.88 ( $\delta$ -aminovaleric acid) in the phenol–water (7:3) system.

### Physical Analysis of the Copolymer

The melting point of the polymer was determined visually in a nitrogen atmosphere in a capillary with an electric heater. The infrared spectrum was obtained by using a KBr pellet technique with NaCl prism. The x-ray diffraction diagram was recorded by employing Ni-filtered  $\text{CuK}\alpha$  radiation with a powder camera.

### Reaction of Ethylenimine and Polyketone

In order to further elucidate the mode of ethylenimine incorporation in the polymer, the reaction of ethylenimine and polyketone was studied.

Polyketone (57.8 mole-% ethylene, 42.2 mole-% carbon monoxide; m.p. 356–358°C.) was prepared by the  $\gamma$ -ray-induced copolymerization of ethylene and carbon monoxide under the following conditions: reaction vessel, 200 ml.; ethylene, 12.9 g.; carbon monoxide, 14.0 g.; polymeriza-

tion temperature, 11°C.; polymerization time, 116 hr.; dose rate,  $2.85 \times 10^5$  rad/hr., polymer yield; 14.35 g.

ANAL. Calcd.: C, 67.60%; H, 8.31%. Found: C, 68.40%; H, 8.41%.

A mixture of 0.1 g. of polyketone and 1.0 ml. of ethylenimine was subjected to  $\gamma$ -rays from a  $^{60}\text{Co}$  source at a dose rate of  $4.5 \times 10^5$  rad/hr. for 24 hr. at 17°C. in a glass tube without agitation. The product was washed with a large amount of methanol and ethyl ether, and then dried *in vacuo*; a brown-yellowish powdery product was obtained in 0.107 g. yield. It melted at 354–359°C. and was amorphous from x-ray diffraction diagram. The results of elemental analysis indicate that ethylenimine was incorporated in the product at a mole ratio of  $\text{C}_2\text{H}_5\text{N}/\text{CO} = 0.595$ .

ANAL. Calcd.: N, 9.06%. Found: N, 9.05%.

In the same procedure without irradiation, a mixture of 0.1 g. of polyketone and 3 ml. of ethylenimine produced 0.88 g. of a red-brown powdery solid (m.p. 372–374°C., amorphous). The product contained ethylenimine at a mole ratio of  $\text{C}_2\text{H}_5\text{N}/\text{CO} = 0.635$ .

ANAL. Calcd.: N, 9.49%. Found: N, 9.48%.

## RESULTS AND DISCUSSION

The results of the  $\gamma$ -ray-induced alternating copolymerization of ethylenimine and carbon monoxide in the presence of ethylene are shown in Table I.

Ethylenimine did not readily polymerize on  $\gamma$ -ray irradiation, while it does copolymerize alternately with carbon monoxide to poly- $\beta$ -alanine as already reported.<sup>9</sup> As shown in Table I, in the case of addition of ethylene to the mixture of ethylenimine and carbon monoxide (expt. 6), polymer containing ethylene was obtained. Increasing ethylene content in the monomers (expts. 8–11) gave rise to increased ethylene content in the polymer. The remarkable increase in ratio of carbon monoxide to ethylenimine in the polymer with increasing ethylene content (expts. 8 and 11) is due to the formation of the polyketone structure mentioned below.

On the other hand, it is well known that ethylene not only homopolymerizes<sup>10,11</sup> but also copolymerizes with carbon monoxide on  $\gamma$ -ray irradiation.<sup>3–6</sup> With a small amount of ethylenimine in the mixture of ethylene and carbon monoxide (expt. 8), the polymer obtained contained a remarkable amount of ethylenimine. No polymer was obtained with the use of the mixture of ethylene and ethylenimine without carbon monoxide (expt. 4, Table I). However, even with a small amount of carbon monoxide (expt. 7), a considerable powdery polymer containing a good amount of carbon monoxide was obtained. From these results, it is presumed that  $\gamma$ -radiation-induced terpolymerization of these monomers took place in this system.

As stated above, the hydrolysis products of the copolymers obtained in expts. 7, 10, and 11 were analyzed by paper chromatography with two

TABLE I  
Influence of Ethylene on the  $\gamma$ -Ray-Induced Copolymerization of Ethylenimine and Carbon Monoxides<sup>a</sup>

Expt. no.	Monomers in feed				Temp., °C.	Yield, g.	Melting point, °C.	Polymer composition				Elemental analysis					
	C <sub>2</sub> H <sub>5</sub> N, g.	CO, g.	C <sub>2</sub> H <sub>4</sub> , g.	C <sub>2</sub> H <sub>6</sub> , g.				C <sub>2</sub> H <sub>5</sub> N, mole ratio	CO, mole ratio	Found			Calculated				
										C, %	H, %	N, %	C, %	H, %	N, %		
1	1.10	—	—	—	17	0	—	—	—	—	—	—	—	—	—	—	—
2	—	—	3.0	—	17	0.284	110	—	—	—	—	—	—	—	—	—	—
3	4.6	3.5	—	—	26	0.584	324-330	1.0	0.94	—	—	48.83	7.90	19.35	50.88	7.26	20.18
4	4.6	—	3.2	—	26	0	—	—	—	—	—	—	—	—	—	—	—
5	—	3.5	3.2	—	17	1.780	349-353 (dec.)	—	0.74	—	—	67.33	8.26	—	67.45	8.27	—
6	4.6	3.5	0.3	—	26	0.388	320-325	1.0	1.02	0.04	—	49.70	8.09	18.82	51.17	7.15	19.25
7	4.6	0.3	3.2	—	26	0.409	350 (dec.)	1.0	1.04	0.90	—	59.26	8.83	14.30	59.65	8.90	14.37
8	0.4	3.5	3.1	—	26	0.990	365 (dec.)	1.0	3.11	2.60	—	60.72	8.06	6.86	60.96	7.64	6.90
9	4.6	3.5	3.2	—	17	0.663	339-346	1.0	0.6	0.6	—	52.56	8.50	16.22	53.29	7.20	16.45
10	2.31	4.5	1.5	—	17	0.750	354-356	1.0	0.86	0.44	—	55.38	8.40	17.20	56.50	8.57	17.62
11	2.20	2.8	4.3	—	17	1.350	345 (dec.)	1.0	1.6	0.9	—	56.87	8.67	12.38	57.33	7.66	12.38

<sup>a</sup> Time, 47 hr.; dose rate,  $4.5 \times 10^6$  rad/hr.; total dose,  $2.11 \times 10^7$  rad. A 40-ml. autoclave was used, except for expts. 2, 5, and 9, in which a 30-ml. autoclave was used.

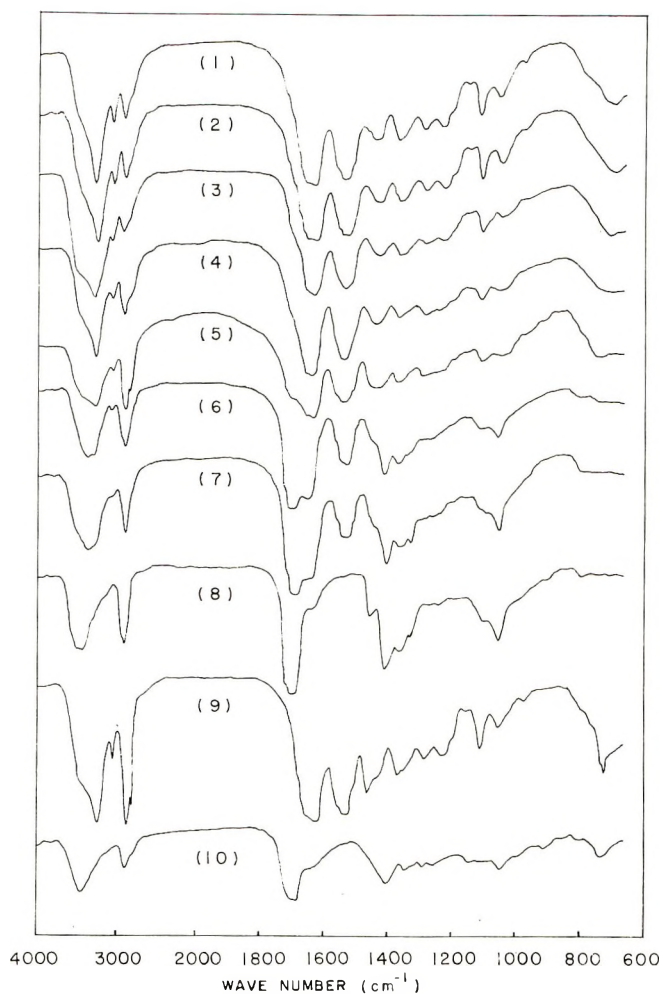


Fig. 1. Infrared spectra of: (1) poly- $\beta$ -alanine obtained in expt. 3; (2) copolymer obtained in expt. 6; (3) copolymer obtained in expt. 9; (4) copolymer obtained in expt. 10; (5) copolymer obtained in expt. 7; (6) copolymer obtained in expt. 11; (7) copolymer obtained in expt. 8; (8) polyketone obtained in expt. 5; (9) product obtained from  $\gamma$ -irradiation of poly- $\beta$ -alanine and ethylene; (10) product obtained from  $\gamma$ -irradiation of polyketone and ethylenimine.

kinds of solvents. The  $R_f$  values of the hydrolysis product in these solvent systems agreed closely with those of commercial  $\beta$ -alanine and  $\delta$ -aminovaleric acid. From these results, it is concluded that the copolymers contained unit structures of poly- $\beta$ -alanine  $+\text{CH}_2\text{CH}_2\text{NHCO}+$  and poly- $\delta$ -valeramide  $+\text{CH}_2\text{CH}_2\text{CH}_2\text{CH}_2\text{NHCO}+$ .

As shown in expts. 9 and 10, elemental analysis of the polymer showed the ethylenimine content to be larger than that of carbon monoxide in the polymer. On the other hand, the results of the reaction of ethylenimine and polyketone show that the polyketone reacts with ethylenimine in any



case. Then, the fact that ethylenimine content was larger than that of carbon monoxide in the copolymer may be attributable to the reaction of ethylenimine and ketone bond in the copolymer.

### Infrared Spectra of the Copolymers

Figure 1 shows the infrared spectra of the copolymers obtained by the  $\gamma$ -ray-induced copolymerization of ethylenimine, carbon monoxide, and ethylene in comparison with those of polyketone and poly- $\beta$ -alanine.

All of the copolymers displayed major absorption peaks assigned to secondary amide at near 3300, 3080, 1635, and 1540  $\text{cm}^{-1}$ . The infrared spectrum of the copolymer obtained in expt. 6 with the use of a small amount of ethylene was similar to that of poly- $\beta$ -alanine, and no peak of ketone at 1700  $\text{cm}^{-1}$  was observed. However, with increasing ethylene content in the monomers, the copolymer produced showed a small shoulder characteristic of ketone at 1700  $\text{cm}^{-1}$ , and the copolymer obtained in expts. 8 and 11, in which ethylene content in the monomer feed was larger than ethylenimine, exhibited a marked polyketone peak as well as those assigned to the secondary amide bond. The infrared spectra of the copolymers were different from that of the product obtained by the  $\gamma$ -irradiation of a mixture of ethylene and poly- $\beta$ -alanine which exhibited peaks characteristic of polyethylene near 2900, 1460, and 720  $\text{cm}^{-1}$ , and that of the  $\gamma$ -irradiation product of polyketone and ethylenimine which did not display the peaks characteristic of the secondary amide.

These results lead to the consideration that the ethylenimine-carbon monoxide-ethylene copolymer may be a mixture or block copolymer of polyamide and polyketone.

### X-Ray Diffraction Diagrams of the Copolymers

The x-ray diffraction diagrams of the copolymers, polyketone, and poly- $\beta$ -alanine were determined.

As shown in Figure 2, the x-ray diagrams of the copolymers were quite different from those of polyketone and poly- $\beta$ -alanine, and showed that the copolymers, except for the products of expts. 6, 8, and 11, were amorphous. From this result, it may be presumed that the copolymer is not a mixture of polyketone and poly- $\beta$ -alanine but a terpolymer of three monomers. The x-ray diagram of the copolymer obtained in expt. 6 was similar to that of the poly- $\beta$ -alanine obtained from ethylenimine and carbon monoxide by  $\gamma$ -irradiation and showed the copolymer was crystalline. Since the x-ray results are in accord with those of the infrared spectrum and of elemental analysis, it is concluded that the copolymer obtained by the  $\gamma$ -ray-induced copolymerization in the presence of a small amount of ethylene in the monomers consisted mainly of poly- $\beta$ -alanine. The x-ray diagrams of the copolymers obtained in expts. 8 and 11, with a larger content of carbon monoxide than ethylenimine in the monomer feed, were similar to that of polyketone and indicated a crystalline product. This result leads to the conclusion that the copolymers contained the terpolymer and polyketone, and this conclusion is consistent with the results of ele-

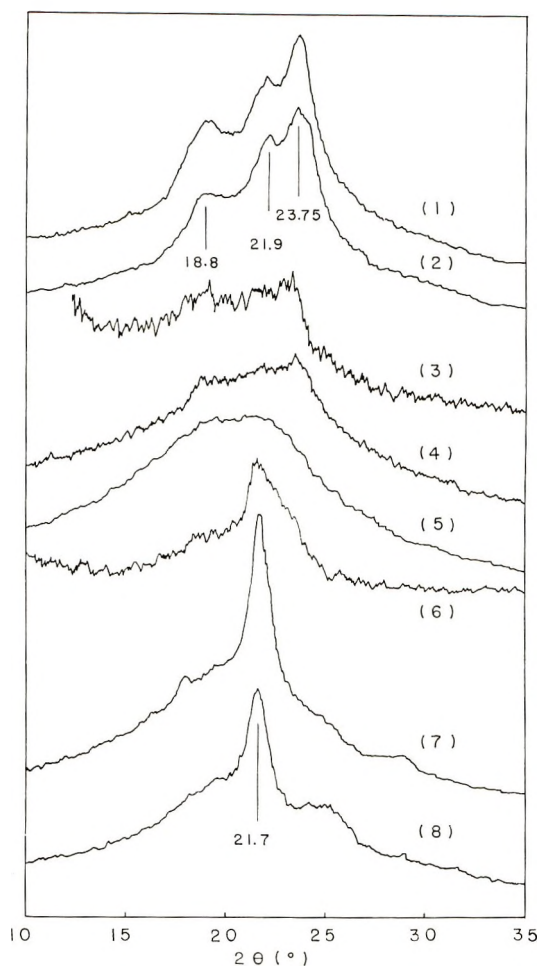


Fig. 2. The x-ray diffraction diagrams of: (1) poly- $\beta$ -alanine obtained in expt. 3; (2) copolymer obtained in expt. 6; (3) copolymer obtained in expt. 9; (4) copolymer obtained in expt. 10; (5) copolymer obtained in expt. 7; (6) copolymer obtained in expt. 11; (7) copolymer obtained in expt. 8; (8) polyketone obtained in expt. 5.

mental analysis, paper chromatography, and infrared spectra as mentioned above.

In view of the results of elemental analysis, paper chromatography, infrared spectrum, x-ray diffraction diagram, it seemed reasonable to assume that the terpolymerization of ethylenimine, carbon monoxide, and ethylene took place on  $\gamma$ -irradiation and gave a polymer containing the units  $+\text{CH}_2\text{CH}_2\text{NHCO}+$ ,  $+\text{CH}_2\text{CH}_2\text{CO}+$ , and  $+\text{CH}_2\text{CH}_2\text{CH}_2\text{CH}_2\text{NHCO}+$ .

### References

1. M. M. Brubaker, D. D. Coffman, and H. H. Hoehn, *J. Am. Chem. Soc.*, **74**, 1509 (1952).
2. D. D. Coffman, P. S. Pinkney, F. T. Wall, W. H. Wood, and H. S. Young, *J. Am. Chem. Soc.*, **74**, 3391 (1952).

3. R. Roberts and S. J. Skinner, Brit. Pat. 778,225 (1957).
4. Y. Chatani, T. Takizawa, S. Murahashi, Y. Sakata, and Y. Nishimura, *J. Polymer Sci.*, **55**, 811 (1961).
5. P. Colombo, M. Steinberg, and J. Fontana, *J. Polymer Sci., B*, **1**, 447 (1963).
6. Ye. Ye. Braudo and A. I. Dintsès, *Petrol. Chem. USSR*, **4**, 19 (1965).
7. T. Kagiya, S. Narisawa, and K. Fukui, paper presented at 13th Symposium of the Society of Polymer Science, Japan, Tokyo, November 1964.
8. T. Kagiya, S. Narisawa, K. Manabe, and K. Fukui, *J. Polymer Sci. B*, **3**, 617 (1965).
9. T. Kagiya, S. Narisawa, T. Ichida, K. Fukui, H. Yokota, and M. Kondo, *J. Polymer Sci. A-1*, **4**, 293 (1966).
10. J. C. Hayward, Jr., and R. H. Bretton, *Chem. Eng. Progr. Symp. Ser.*, **50** (13), 73 (1954).
11. S. Machi, M. Hagiwara, M. Gotoda, and T. Kagiya, *J. Polymer Sci. B*, **2**, 765 (1964).
12. M. Shibata, *Experimental Methods of Paper Chromatography (Paper Chromatography—Hō no Jissai)*, Kyoritsu, Tokyo, 1960.

### Résumé

L'influence de l'addition d'éthylène à la copolymérisation alternante d'éthylènimine et de monoxyde de carbone a été étudiée. Un mélange d'éthylènimine et de monoxyde de carbone et d'éthylène a été irradié en vue d'obtenir un polymère contenant ces unités monomériques. Le spectre infrarouge du copolymère montrait des pics d'absorption d'amines secondaires et de groupes cétoniques, qui étaient différents de ceux du produit de réaction d'une polycétone avec l'éthylènimine et de celui du produit d'irradiation de rayons  $\gamma$  sur l'éthylène et la poly- $\beta$ -alanine. Le diagramme de diffraction aux rayons-X était différent de ceux des poly- $\beta$ -alanines et des polycétones, et montrait une structure amorphe. L'analyse chromatographique sur papier montrait que le produit d'hydrolyse du copolymère contenait de la  $\beta$ -alanine et de l'acide aminovalériannique. Au départ de ces résultats on conclut que la terpolymérisation de l'éthylènimine, du monoxyde de carbone et de l'éthylène se passe sous l'influence de l'irradiation aux rayons- $\gamma$  pour former un polymère amorphe contenant les unités de  $\text{-(CH}_2\text{CH}_2\text{NHCO)-}$ ,  $\text{-(CH}_2\text{CH}_2\text{CO)-}$  et  $\text{-(CH}_2\text{CH}_2\text{CH}_2\text{CH}_2\text{NHCO)-}$ .

### Zusammenfassung

Der Einfluss eines Äthylenzusatzes auf die  $\gamma$ -strahlinduzierte alternierende Copolymerisation von Äthylenimin und Kohlenmonoxyd wurde untersucht. Eine Mischung von Äthylenimin, Kohlenmonoxyd und Äthylen wurde bestrahlt, um ein Polymeres mit diesen Polymerbausteinen zu erzeugen. Das Infrarotspektrum des Copolymeren zeigte die für sekundäres Amid und Keton charakteristischen Absorptionsmaxima und war von denjenigen des Reaktionsprodukts von Polyketon mit Äthylenimin und demjenigen des  $\gamma$ -Strahlenprodukts von Äthylen und Poly- $\beta$ -alanin verschieden. Das Röntgenbeugungsdiagramm des Copolymeren unterschied sich von demjenigen von Poly- $\beta$ -alanin und Polyketon und liess eine amorphe Struktur erkennen. Eine papierchromatographische Analyse zeigte, dass das Hydrolysenprodukt des Copolymeren  $\beta$ -Alanin und  $\delta$ -Aminovaleriansäure enthält. Aus den Ergebnissen wird geschlossen, dass durch  $\gamma$ -Bestrahlung eine Terpolymérisation von Äthylenimin, Kohlenmonoxyd und Äthylen stattfindet und ein amorphes Polymeres mit  $\text{-(CH}_2\text{CH}_2\text{NHCO)-}$ ,  $\text{-(CH}_2\text{CH}_2\text{CO)-}$  und  $\text{-(CH}_2\text{CH}_2\text{CH}_2\text{CH}_2\text{NHCO)-}$  als Bausteinen gebildet wurde.

Received November 4, 1965

Revised December 27, 1965

Prod. No. 5065A

## ***p*-Chlorophenyldiazonium Hexafluorophosphate as a Catalyst in the Polymerization of Tetrahydrofuran and Other Cyclic Ethers\***

M. P. DREYFUSS† and P. DREYFUSS,† *Department of Inorganic, Physical, and Industrial Chemistry, University of Liverpool, Liverpool, England*

### **Synopsis**

*p*-Chlorophenyldiazonium hexafluorophosphate is shown to be a convenient and effective catalyst for initiating the polymerization of tetrahydrofuran (THF) and other cyclic ethers. The polymerizations apparently proceed without any significant termination or transfer reactions (i.e., "living" polymers result), and materials of very high molecular weight can be obtained. A mobile monomer-polymer equilibrium for THF was obtained during polymerization and equilibrium conversions were determined at a number of temperatures. The ceiling temperature derived from these data was 84°C., the heat of polymerization was -4.58 kcal./mole and the corresponding entropy change was -17.7 cal./°C.-mole. Hydrocarbons are suitable inert solvents for these polymerizations, but concentrated solutions must be used at ambient temperatures in order to stay above the required equilibrium monomer concentration and also to dissolve the catalyst which is insoluble in hydrocarbons. It was shown that acyclic ethers act as transfer agents in these polymerizations and that transfer with consequent reduction of molecular weight continues even after monomer-polymer equilibrium is reached. Cyclic ethers do not act as transfer agents but only copolymerize. Trimethyl orthoformate was shown to be a particularly effective transfer agent; it resulted in a polymer with methoxy endgroups and produced methyl formate as a by-product. The data obtained are consistent with a mechanism involving initiation by hydrogen abstraction and polymerization via tertiary oxonium ions associated with PF<sub>6</sub><sup>-</sup> gegenions. This gegenion is thought to be responsible for the "living" nature of the system.

### **INTRODUCTION**

It is only within the past twenty years that four- and five-membered cyclic ethers have been reported to polymerize. The initiators employed for these polymerizations are all of the typical cationic class such as strong acids and Friedel-Crafts halides.<sup>3,4</sup> The polymerization of tetrahydrofuran (THF) is among the earliest recorded.<sup>5</sup> A variety of Friedel-Crafts catalysts such as perchloric acid, BF<sub>3</sub>, FeCl<sub>3</sub>, or AlCl<sub>3</sub> in combination with a reactive alkyl halide as cocatalyst, and SbCl<sub>5</sub> alone were found to be effective initiators.

\* Preliminary reports of parts of this work appeared previously.<sup>1,2</sup>

† Present address: B. F. Goodrich Company, Research Center, Brecksville, Ohio.



At about the same time Gresham<sup>6</sup> reported the polymerization of the cyclic formal, 1,3-dioxolane, using  $\text{BF}_3$ ,  $\text{AlCl}_3$ , sulfuric acid and the like to initiate polymerization.

Similar catalysts are also effective initiators for the polymerization of oxetanes. For instance, Farthing<sup>7</sup> and Hercules<sup>8</sup> have exploited the use of  $\text{BF}_3$  or  $\text{BF}_3$  etherate for the polymerization of a variety of 3,3-disubstituted oxetanes.

More recently, complex ions such as  $(\text{C}_6\text{H}_5)_3\text{CSbCl}_6$ <sup>9-12</sup> and triethyl-oxonium fluoroborate and hexachloroantimonate generated *in situ*<sup>13-16</sup> have been shown to be effective catalysts for the polymerization of THF.

However, none of the above catalysts readily gave high molecular weight polytetrahydrofurans. It was not until the use of  $\text{PF}_5$  was reported, that this was accomplished.<sup>17</sup> Recent studies<sup>18,19</sup> have verified the above work with  $\text{PF}_5$  and in addition kinetic evidence suggested that  $\text{PF}_5$ -catalyzed polymerizations may proceed without termination.

These results with  $\text{PF}_5$  suggested to us that a system employing the  $\text{PF}_6^-$  gegenion might lead to a cationic polymerization that proceeded without termination or transfer. The subsequent discovery by us<sup>1</sup> that *p*-chlorophenyldiazonium hexafluorophosphate is itself a catalyst for THF polymerizations seemed to open the way for a study of the effect of  $\text{PF}_6^-$  gegenion on the cationic polymerization of cyclic ethers. The results of our study with  $4\text{-ClC}_6\text{H}_4\text{N}_2\text{PF}_6$  as a catalyst are reported below.

## EXPERIMENTAL

### Materials

***p*-Chlorophenyldiazonium Hexafluorophosphate.** The crude material, a red brown powder, was obtained as Phosfluorogen A\* from Ozark Mahoning Company, Tulsa, Oklahoma, and was purified by recrystallization from water.<sup>20</sup> In a typical case, 10 g. of Phosfluorogen A was dissolved in 650 ml. of water by stirring at temperatures of 28-32° C. for 1 hr. The solution was filtered to remove the remaining dark solids, and the clear, colorless filtrate was cooled in ice water for 2 hr. to effect crystallization. After drying in a vacuum oven at 25°C., 4.9 g. of glistening white plates, m.p. 152-154° (dec.), was obtained. Recovery was generally in the range of 40-50%. The material so obtained appeared to be stable to air and atmospheric moisture. Nevertheless, it was stored over  $\text{P}_2\text{O}_5$  in a desiccator; no change in color or catalytic behavior was noted for periods of 6 months or more.

**Monomers and Solvents.** Tetrahydrofuran (THF), 2-methyltetrahydrofuran, dioxane, and 1,2-dimethoxyethane were refluxed over and

\* In our preliminary communication<sup>1</sup> we suggested that Phosfluorogen A was the unsubstituted benzenediazonium hexafluorophosphate and the calculations therein were made on this assumption. We have since learned that Phosfluorogen A is in fact the more stable *p*-chloro isomer.



distilled from sodium or potassium, and a center cut was stored *in vacuo* in the presence of sodium naphthalene complex.

Benzene, cumene, methylecyclohexane, and methylene chloride were refluxed over and distilled from calcium hydride and a center cut was stored *in vacuo* over fresh calcium hydride.

Ethyl ether, diisopropyl ether, dioxolane, and trimethylorthoformate were refluxed over and distilled from potassium, and a center cut was stored *in vacuo* over lithium aluminum hydride.

3,3-Bis(chloromethyl)oxetane was distilled, and a center cut of m.p. 19°C. was distilled *in vacuo* before use.

**3,3-Bis(methoxymethyl)oxetane.** Potassium (101 g., 2.6 mole) was dissolved in 600 ml. of absolute methanol, and 118 g. (0.76 mole) of 3,3-bis(chloromethyl)oxetane was added. After 22 hr. reflux, the mixture was cooled and the precipitated KCl was removed by filtration. Most of the methanol was removed under vacuum, ether was added to the remaining semisolid mass, and the solids were removed by filtration. Distillation after removal of ether yielded 91 g. (61%) 3,3-bis(methoxymethyl)oxetane, b.p. 65–66° C./9 mm.,  $n_D^{19}$  1.4318, f.p. approximately –24°C.

ANAL. Calcd. for  $C_7H_{14}O_3$ : C, 57.51%; H, 9.65%. Found: C, 57.40%; H, 9.55%.

### Procedure

All polymerizations were carried out under an air pressure of approximately  $10^{-4}$  mm. of mercury by using conventional vacuum procedures. Monomers and solvents were generally distilled into breakseals and weighed. The catalyst was weighed in small Pyrex glass cups, which were transferred to the apparatus just prior to final evacuation. After addition of the materials in the breakseals to the catalyst, the polymerization ampule was separated from the apparatus and placed in a 50°C. bath for 20–30 min. before transferring to a bath at 25°C. for the required period. For polymerizations conducted at 50°C. or above, the preliminary heating was omitted.

Polymers of intrinsic viscosity 2–3 or greater were isolated by removing the red-brown polymer mass from the polymerization ampule, dissolving by stirring in crude THF containing 10% acetic acid, precipitating in water, and drying overnight *in vacuo* at 25°C.

In order to avoid loss of low molecular weight fractions it was found necessary to isolate polymers of lower intrinsic viscosity by evaporation of the polymer cement obtained after dissolving the polymer mass in the THF–acetic acid.

### Characterization

Intrinsic viscosities were determined in benzene at 25°C. in a dilution viscometer designed by Hartley and co-workers.<sup>21</sup>

Molecular weights were determined in benzene at 25°C. in Fuoss Mead osmometers fitted with regenerated cellulose membranes, type 300 supplied by American Viscose Corporation.

Infrared spectra were taken on a Unicam SP200 spectrophotometer equipped with NaCl optics.

NMR spectra were obtained on a Varian Associates Model A-60 NMR spectrophotometer.

Analyses were carried out by the microanalytical laboratories of the Department of Organic Chemistry of the University of Liverpool.

### Addition Experiments

In these experiments part of the solution of known concentration of THF, solvent, and catalyst was poured into a side ampule and removed before polymerization. Additional weighed amounts of monomer or catalyst were added through an attached breakseal. Otherwise the procedure was unchanged.

### Ceiling Temperature Measurements

Equilibrium monomer-polymer concentrations of bulk THF polymerizations were obtained from the yield of polymer at the various temperatures, after the equilibrium was approached from monomer or monomer-polymer mixtures equilibrated at a higher or lower temperature. Temperatures of 25 and 50°C. were controlled by means of a thermostated water bath. Other temperatures were maintained by boiling an appropriate pure compound and suspending the polymerization ampule either in an air bath heated by this liquid or directly in the vapor.

### Kinetic Studies

A solution of known concentration of THF, additive, and catalyst was prepared as previously described and was added by means of a breakseal to an evacuated manifold with the required number of ampules. After appropriately dividing the solution among the ampules, the ampules were removed, and the polymerizations were conducted as previously described. The weight of solution in each ampule was obtained by weighing the ampule before and after the removal of the polymer mass.

### Polymerization of THF in 40% Trimethylorthoformate

As in the method for polymerization described above, 24.0 g. (0.333 mole) of THF and 17.4 g. (0.164 mole) of trimethylorthoformate were added from breakseals to 0.627 g. ( $2.2 \times 10^{-4}$  mole) of *p*-chlorophenyldiazonium hexafluorophosphate. After 18 hr. at 25°C. the solution was bright yellow and slightly viscous. On further standing the mixture became fluid again. After 14 days at 25°C. the ampule was opened and the reaction was terminated with 0.5 ml. of methyl alcohol containing 0.01 g. of dissolved sodium. The mixture was fractionally distilled through a 12-in. Vigreux column fitted with a partial reflux takeoff head to give 0.7

g. of fraction 1, b.p. < 25°C.; 6.7 g. of fraction 2, b.p. 31–33°C.; 10.0 g. of fraction 3, b.p. 60–70°C.; 9.3 g. of fraction 4, b.p. 45–57°C./50 mm.,  $n_D^{24}$  1.3940; 4.6 g. of fraction 5, b.p. 95–96°C./6 mm.,  $n_D^{24}$  1.4214; and 7.6 g. of residue,  $n_D^{24}$  1.4395.

Fraction 1 was identified as dimethyl ether by comparing its infrared spectrum with that reported.<sup>22</sup>

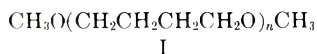
Fraction 2 was identified as methyl formate by comparison of the infrared and NMR spectra with those obtained from a known material.

Fraction 3 was shown from its infrared spectrum to be largely THF containing some methanol.

Fraction 4 was redistilled to give a center cut boiling at 126–127°C.,  $n_D^{22}$  1.3979. Its NMR spectrum consisted of only two multiplets, one at 6.75  $\tau$  with a relative area of 18.5 and the other at 8.45  $\tau$  with a relative area of 7.5. This is consistent with 1,4-dimethoxybutane, for which b.p. 132–133°C.,  $n_D^{15}$  1.4031 is reported,<sup>23</sup> and for which the ratio of protons on the C<sub>2</sub> and C<sub>3</sub> (8.45  $\tau$ ) to the protons  $\alpha$  to oxygen (6.76  $\tau$ ) is 10/4 (2.5). This ratio compares well with the observed ratio 18.5/7.5 (2.46).

Fraction 5 was consistent with 4,4'-dimethoxydi-*n*-butyl ether, for which b.p. 67°C./0.55 mm.,  $n_D^{25}$  1.4219 is reported.<sup>24</sup> The NMR spectrum consisted of only two multiplets, one at 6.76  $\tau$  with an area of 17.2 and the other at 8.45  $\tau$  with an area of 9. The ratio of these areas (1.9) compares well with that expected (1.75) but is probably high due to the presence of some of the 1,4-dimethoxybutane.

Fraction 6 had a similar NMR spectrum. The ratios of the areas of the 6.75  $\tau$  multiplet to the 8.43  $\tau$  multiplet was 20/14 (1.43). From this ratio an average  $n$  of 3.5 in the structure I was calculated.



In another similar experiment the product was isolated by evaporation as with higher polymers. The oil obtained in this way was found to have a molecular weight of 241 (cryoscopic in benzene) and an NMR spectrum similar to those described above with a ratio of the area of the 6.75  $\tau$  multiplet to the 8.45  $\tau$  multiplet of 1.59 or an average  $n$  in I of 2.54.

ANAL. Calcd. for I,  $n = 2.5$ , C<sub>12</sub>H<sub>26</sub>O<sub>3.5</sub>: C, 63.7%, H 11.5%, M.W. 226.3. Found: C, 64.54%; H, 11.76%.

### Reactions of *p*-ClC<sub>6</sub>H<sub>4</sub>N<sub>2</sub>PF<sub>6</sub> with Various Ethers

**Bulk THF.** THF (102.6 g.) was added to 0.4029 g. *p*-chlorophenyldiazonium hexafluorophosphate ([cat.] = 1.2 × 10<sup>-2</sup>*M*) in an evacuated vessel attached to a mercury U-tube manometer. The mixture was magnetically stirred and allowed to come to 19°C. The pressure in the system was observed to increase slowly over a period of 3 hr., suggesting evolution of nitrogen.

**2-Methyltetrahydrofuran.** 2-Methyltetrahydrofuran (5 ml.) was added to 0.997 g. 4-ClC<sub>6</sub>H<sub>4</sub>N<sub>2</sub>PF<sub>6</sub> in a nitrogen-purged round-bottomed flask fitted

with a reflux condenser leading to a trap and an inverted graduated cylinder filled with mineral oil. The mixture was magnetically stirred and brought to reflux. In the course of 2 hr. reflux an inert gas (presumably nitrogen) collected in the cylinder. The volatiles were vacuum-stripped, leaving a resinous residue. In addition to 2-methyltetrahydrofuran, the volatiles were shown by infrared spectroscopy to contain chlorobenzene and to be free of 4-chlorofluorobenzene.

A similar experiment with 1,2-dimethoxyethane carried out under vacuum and at 25°C. gave an inert gas and chlorobenzene. Again no evidence for 4-chlorofluorobenzene was obtained.

**Trimethylorthoformate.** Trimethylorthoformate (4.21 g., 0.04 mole) was added to 1.007 g. of 4-ClC<sub>6</sub>H<sub>4</sub>N<sub>2</sub>PF<sub>6</sub> under vacuum. The resulting solution gradually became bright yellow and was allowed to stand for 3 days at 25°C. A solution of 0.1 g. of sodium in 2 ml. of methanol was added through a breakseal to the now orange-brown solution. The apparatus was cooled in liquid nitrogen, opened, and vented through a Dry Ice-cooled trap as it warmed to room temperature. In this way 1.8 g. of a low-boiling liquid, b.p. approximately -22°C., was collected. This liquid was identified as largely dimethyl ether (0.039 mole) by means of the infrared spectrum of its gas and by its trimethyloxonium hexachloroantimonate derivative, m.p. 156°C. (dec.), reported m.p. 158°C. (dec.).<sup>25</sup>

On further heating of the reaction vessel 2.3 g. of a liquid, b.p. 30-32°C., was obtained and identified as methyl formate (0.038 mole) by means of the infrared spectrum of its gas and its hydrazide derivative, m.p. 55-57°C., reported m.p. 54°C.<sup>26</sup>

## RESULTS

### Bulk THF Polymerizations

*p*-Chlorophenyldiazonium hexafluorophosphate has proved to be a very active initiator for the polymerization of THF in bulk and has led to tough crystalline polymers. This material initiates polymerization of THF with the use of only crude precautions (nitrogen atmosphere in a test tube), but in order to insure reproducible results high-vacuum techniques were employed throughout.

As we studied this catalyst it soon became evident, as shown in Figure 1, that the intrinsic viscosity after polymerization to equilibrium conversion at 25°C. increased as the catalyst concentration decreased. Above concentrations of about  $20 \times 10^{-3}M$  no further decrease in intrinsic viscosity was observed because *p*-ClC<sub>6</sub>H<sub>4</sub>N<sub>2</sub>PF<sub>6</sub> has a limited solubility in THF.

As has been previously reported,<sup>5, 9-12, 18, 19</sup> the polymerization does not proceed to 100% conversion at ordinary temperatures but instead reaches a monomer-polymer equilibrium. In the presence of PF<sub>6</sub><sup>-</sup> gegenions this equilibrium is very mobile and the polymerization can readily be reversed. This is dramatically demonstrated by the data in Table I. Propagation or depropagation in the direction required to attain monomer-polymer

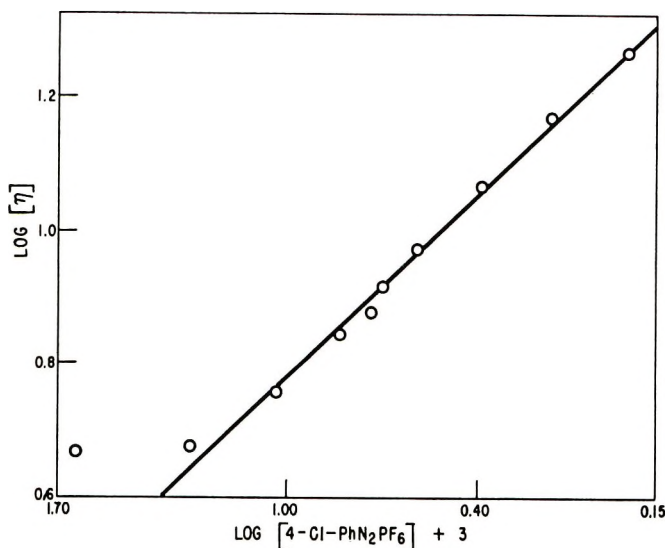


Fig. 1. Effect of catalyst concentration on intrinsic viscosity in bulk THF polymerizations at 25°C. for 24–48 hr.

equilibrium at a given temperature occurs as dictated by temperature changes.

Since monomer–polymer equilibrium could be approached either by propagation or depropagation, a very convenient system was at hand for determining the ceiling temperature of THF in bulk polymerizations. When equilibrium conversions at various temperatures are plotted against temperatures (Fig. 2), extrapolation gives a ceiling temperature of 84°C.

TABLE I  
Bulk THF Polymerization<sup>a</sup>

Conditions			
Hours at $T_1$ , °C.	Hours at $T_2$ , °C.	Hours at $T_1$ , °C.	Conversion, %
24–25	—	—	76.3
24–50	24–25	—	75.9
24–25	24–50	24–25	75.8
48–50	—	—	56.6
192–50	—	—	55.8
24–25	24–50	—	56.9
24–50	24–25	24–50	55.6
18–80	—	—	13.4
18–50	9–80	—	12.6
24–25	4–80	48–25	75.2
4–77 <sup>b</sup>	—	—	17.9
72–25 <sup>b</sup>	4–77	—	18.2

<sup>a</sup> [cat] =  $5.5 \times 10^{-3}M$  unless otherwise noted.

<sup>b</sup> [cat] =  $4.1 \times 10^{-3}M$ .



It is interesting to note that even at 82.4°C., 3.9% of polymer of intrinsic viscosity 0.3 dl./g. was obtained when a catalyst charge of  $5.1 \times 10^{-3}M$  was used. Our value for the ceiling temperature is in good agreement with the value of 83°C. reported by Sims,<sup>18</sup> but it is considerably higher

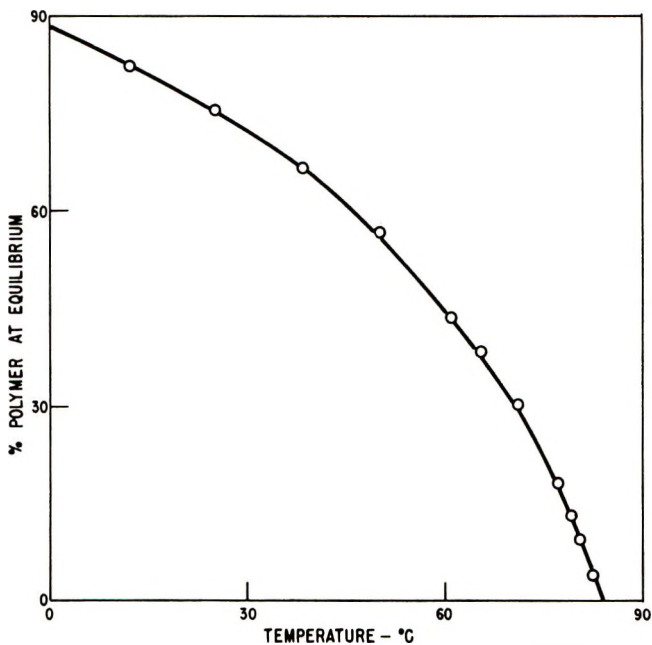


Fig. 2. Ceiling temperature in THF polymerization.

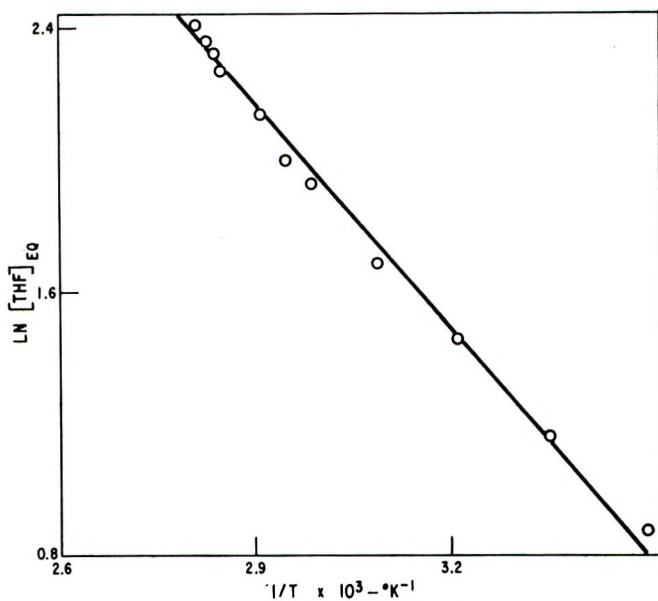


Fig. 3. Equilibrium monomer concentration as a function of temperature.

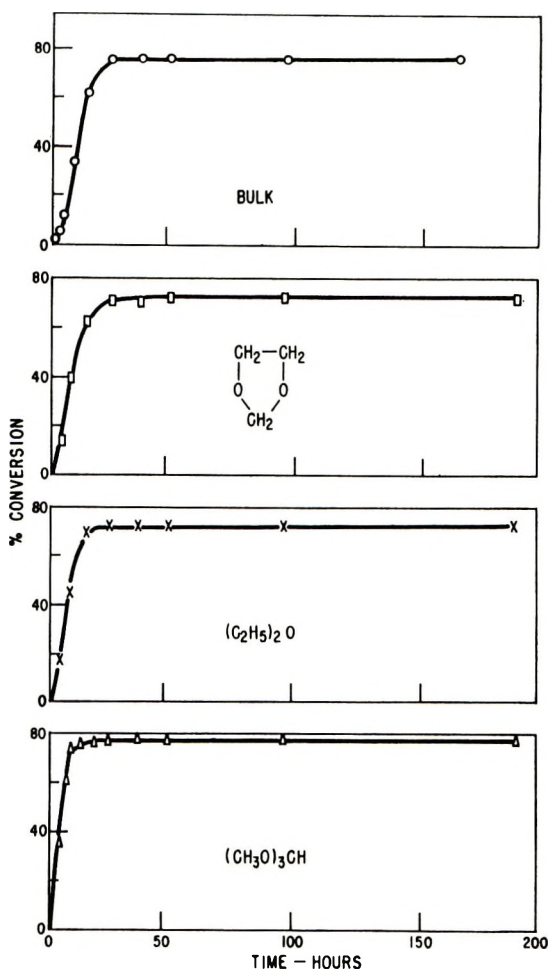


Fig. 4. Conversions in THF polymerizations at 25°C. as a function of time at various additive and catalyst concentrations (O) bulk,  $5.1 \times 10^{-3}M$  THF; ( $\square$ ) dioxolane, 5.6%,  $5.5 \times 10^{-3}M$  THF; ( $\times$ ) ether, 8.7%,  $5.5 \times 10^{-3}M$  THF; ( $\Delta$ ) trimethylorthoformate, 1.0%,  $5.3 \times 10^{-3}M$  THF.

than the value of 60–70°C. reported by Bawn et al.<sup>11</sup> and of 73°C. reported by Rozenberg et al.<sup>13</sup> When the data are plotted according to the equation of Dainton and Ivin<sup>27</sup> in the form

$$\ln [\text{THF}]_{e,q} = (1/T)(\Delta H_x/R - \Delta S_x^\circ/R)$$

as shown in Figure 3,\* the heat of polymerization  $\Delta H_x$  calculated is  $-4.58$

\* The values of  $[\text{THF}]_{e,q}$  were calculated from the equilibrium conversion. The densities used in the calculations were obtained by plotting the densities reported in the literature, for THF<sup>28,29</sup> and polytetrahydrofuran in THF<sup>10</sup> as a function of temperature and reading the appropriate values from the curve. Ideal solution was assumed in the calculations.

TABLE II  
Molecular Weights Determined by Osmometry

$[\eta]$ , dl./g.	$\bar{M}_n \times 10^3$ , g.-mole
1.6	76
2.1	85
2.9	154
4.4	296
4.5	270
7.0	490
7.9	600

kcal./mole and the corresponding entropy change  $\Delta S_x^\circ$  is  $-17.7$  cal./ $^\circ\text{C}$ .-mole, in good agreement with previous reports.<sup>11,13</sup> It is interesting to note that on this plot the temperature at which the concentration of THF is that of pure monomer, the ceiling temperature, is  $85^\circ\text{C}$ ., showing the good agreement it should with the value of  $84^\circ\text{C}$ . derived from the conversion versus temperature plot.

Existing equations relating intrinsic viscosity and number-average molecular weight<sup>9,13,19,30-33</sup> have been derived for polytetrahydrofurans with an intrinsic viscosity which is generally less than one. Hence it was felt necessary to measure the molecular weight of some of our polymers directly. The values obtained are given in Table II.

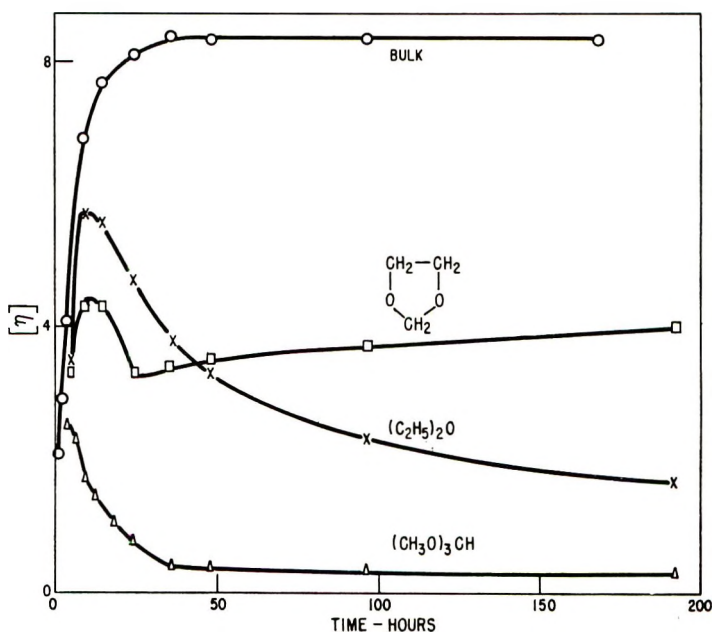


Fig. 5. Comparison of the effect of additives on the intrinsic viscosity of poly(THF) as a function of time. Symbols have the same meaning as in Fig. 4.

Values of  $\bar{M}_n$  for the polymers in Figure 1 calculated on the basis of these data are four to five times greater than would be predicted from the amount of catalyst charged for their preparation and suggest a low catalyst efficiency. Similar calculations for polymers from the bulk THF polymerization in Figures 4 and 5 show that initiation is slow but apparently complete before equilibrium is reached. The molecular weight distribution of these polymers was not determined and, in fact, may or may not be rather broad.<sup>34</sup> Thus a generally applicable intrinsic viscosity-molecular weight relationship was not derived from these data.

### Addition Experiments

Polymerizations that proceed without termination or transfer should be capable of continued polymerization leading to higher molecular weight polymers on the addition of more monomer. Several examples of continued growth are shown in Table III.

TABLE III  
Addition Experiments

Expt. no.	[Catalyst], $M$ THF $\times 10^3$		Conversion, %		Reaction time, days		$[\eta]$ , dl./g.	
	Initial	Final	Initial	Final	Before addn.	After addn.	Before addn.	After addn.
1 <sup>a</sup>	26.0	8.9	75	75	1	1	4.8	5.9
2 <sup>b</sup>	4.0	1.6	9.4	25.6	5	2	7.2	13.0
3 <sup>c</sup>	3.4	5.0	12.1	12.9	3	2	5.7	3.9
4 <sup>d</sup>	3.4	—	—	85	3	2	—	—

<sup>a</sup> THF added to THF polymerized in bulk.

<sup>b</sup> THF added to THF polymerized in 40.3% (w/w) solution in benzene.

<sup>c</sup> Catalyst added to THF polymerized in 42.3% (w/w) solution in benzene.

<sup>d</sup> 3,3-Bis(chloromethyl)oxetane (6.93 g.) added to THF (9.33 g.) polymerized to equilibrium in 56.1% (w/w) solution in benzene.

### Polymerizations of THF in Solvents

It is always more convenient to study polymerizations in solvent if possible. However, since in the case of THF the concentration of monomer remaining at equilibrium is large,\* and the conversion drops rapidly with increasing dilution, any study of the effect of chemical composition of solvent needs to be made in fairly concentrated solutions. We have studied the effect of ten different additives. Our results are summarized in Table IV. It can be seen that all the compounds in group A were inert and had only the expected effect of slightly lowering the percent conversion compared to the bulk. However, the compounds in group B all markedly lowered the intrinsic viscosity of the resulting polymers. Apparently,

\* Our data suggest that at 25°C. in 40-60% benzene the molar concentration of monomer remaining at equilibrium is approximately 4.5.

TABLE IV  
 Polymerization of THF in the Presence of Additives<sup>a</sup>

Additive	$[\eta]$ , dl./g.	Conversion, %
Group A		
None	7.8	75.5
C <sub>6</sub> H <sub>6</sub>	7.7	71.8
C <sub>6</sub> H <sub>5</sub> CH(CH <sub>3</sub> ) <sub>2</sub>	8.1	73.0
(C <sub>6</sub> H <sub>5</sub> ) <sub>3</sub> CH	7.2	72.3
$\text{CH}_2(\text{CH}_2)_4\text{CHCH}_3$	8.1	73.3
CH <sub>2</sub> Cl <sub>2</sub>	7.5	69.9
Group B		
$\text{CH}_2\text{CH}_2\text{CH}_2\text{OCH}(\text{CH}_3)$	4.5	74.9
(CH <sub>3</sub> ) <sub>2</sub> CHOCH(CH <sub>3</sub> ) <sub>2</sub>	5.5	72.7
CH <sub>3</sub> CH <sub>2</sub> OCH <sub>2</sub> CH <sub>3</sub>	3.7	72.6
(CH <sub>3</sub> O) <sub>3</sub> CH	0.4	72.6
$\text{CH}_2\text{CH}_2\text{OCH}_2\text{O}$	2.8	77.9

<sup>a</sup> [Catalyst] =  $5.4\text{--}5.5 \times 10^{-3}M$ ; 48 hr.; Additive = 8.4–9.1% by volume; 25°C.

the presence of an ether oxygen exerted a marked influence on the course of the polymerization.

The manner in which the ether oxygen may bring about this marked effect became clearer when the time dependence of conversion and intrinsic viscosity of THF polymerization in the presence of three of these additives was studied. As shown in Figure 4, the conversion increased smoothly with time until equilibrium conversion was reached, just as it does in the absence of additives. About 24 hr. was required to reach equilibrium in all cases, except the trimethylorthoformate one, which required about 12 hr.

The corresponding time dependence of the intrinsic viscosity of the polymers isolated is shown in Figure 5. As is seen from the curve, in bulk polymerizations the viscosity of 8.3 did not change after equilibrium conversion was reached. In the presence of 8.7% ether, the viscosity reached a maximum of 5.7, considerably below that attained in the bulk experiment and then decreased with time to 1.6 after 8 days. This behavior was even

 TABLE V  
 Products of Polymerization of THF in 40% Trimethylorthoformate

Compound isolated	Amt. from total charge of 41.4 g., g.
CH <sub>3</sub> O(CH <sub>2</sub> CH <sub>2</sub> CH <sub>2</sub> CH <sub>2</sub> O) <sub>n</sub> CH <sub>3</sub>	
<i>n</i> = 1	9.3
<i>n</i> = 2	4.6
<i>n</i> > 2	7.6
HCOOCH <sub>3</sub>	6.7
THF	10.0
CH <sub>3</sub> OCH <sub>3</sub>	0.7



more marked with trimethylorthoformate. In the presence of only 1% additive, a very much lower maximum of 2.5 was reached and a very rapid decrease to 0.4 after 36 hr. was observed. In the presence of 5.6% dioxolane, a lower maximum than in the bulk polymerization was reached but there was no decrease of the intrinsic viscosity of about 3.7 after equilibrium was attained.

The remarkable effectiveness of trimethylorthoformate in reducing the intrinsic viscosity was further demonstrated when THF was polymerized in the presence of 40% by volume trimethylorthoformate for 14 days at 25°C. As shown in Table V, only oligomers were isolated.

### Scope of Catalyst

*p*-Chlorophenyldiazonium hexafluorophosphate is also effective for initiating the polymerization of cyclic ethers other than THF. For example, 1,3-dioxolane is rapidly and exothermally converted in high yields to a highly crystalline white polymer. 3,3-Bis(chloromethyl)oxetane can be polymerized in bulk. The latter can also be polymerized in 30% benzene solution at 50°C. to give an 85% yield of white powder. 3,3-Bis(methoxymethyl)oxetane is also very readily polymerized in benzene solution. At 25°C. a 50% benzene solution yielded 82% of a very soluble, white crystalline polymer.

In contrast, the catalyst does not seem to be very effective for epoxides. After 7 days at 50°C. only 58% of a dark yellow viscous oil was obtained from an attempted bulk polymerization of propylene oxide. Nor does the catalyst seem to initiate the polymerization of styrene, in which it is not soluble. When styrene was added to a THF polymerization, no evidence of styrene polymerization or copolymerization was obtained.

In agreement with all previous reports, and the prediction made by Dainton and Ivin<sup>27</sup> based on thermodynamic considerations, 2-methyltetrahydrofuran did not form polymer at temperatures from -10 to 79°C.

As would be expected, copolymerizations are also readily possible. Thus, 3,3-bis(chloromethyl)oxetane copolymerizes with THF in high yield. Experiment 4 in Table III is one example; in another example a 90% conversion to copolymer resulted. In both cases the copolymer was a rubbery material, in agreement with the report of Furukawa.<sup>35</sup>

When THF was polymerized in 50% 2-methyltetrahydrofuran, a 37% yield of a soft, noncrystalline polymer was obtained, while in 12% 2-methyltetrahydrofuran a 65% yield of a rubbery, noncrystallizing polymer resulted. The nature of the polymer obtained here was so different from that of polytetrahydrofuran that the products almost certainly were THF-2-methyltetrahydrofuran copolymers.

When 3,3-bis(chloromethyl)oxetane was polymerized in 70% 1,4-dioxane a 72% yield of a soluble (dioxane and acetone), soft polymer was obtained. The characteristics of this polymer are very different from the insoluble homopolymer of the oxetane and furthermore the chlorine analysis

(40.86% Cl) suggested that a copolymer containing approximately 11% dioxane had formed.

## DISCUSSION

### Lack of Termination

In any polymerization process, successive additions of monomer units to a growing polymer chain (propagation) will continue either until a termination reaction takes place or until the supply of monomer is exhausted. Szwarc<sup>36</sup> has given the name "living" to polymers in which the second of these criteria is important, and the polymerizations are free of termination reactions. It is only since Szwarc discovered the "living" nature of styrene polymerization catalyzed by sodium naphthalene<sup>37,38</sup> that very much progress has been made toward understanding the far-reaching consequences of this type of polymerization.

One important consequence is that the molecular weight of a polymer isolated from a "living" system depends only on the number of growing centers and the amount of monomer available for polymerization. Several experimental verifications of this consequence are now available.<sup>39-41</sup> It follows that, if there is a direct relationship between the amount of catalyst charged and the number of growing centers formed, and the system is "living" there also is a linear relationship between  $\log [\eta]$  and  $\log [\text{catalyst}]$ . We have shown that the latter relationship exists in the case of THF polymerizations initiated with *p*-chlorophenyldiazonium hexafluorophosphate over a fiftyfold range in catalyst concentration (cf. Fig. 1).

Another consequence of a "living" system is that eventually a steady state is attained where the "living" polymers are in equilibrium with their monomer, and the rate of propagation becomes equal to the rate of depropagation.<sup>27</sup> In the case of styrene the amount of monomer in equilibrium with polymer under normal polymerization conditions is very small ( $10^{-6}$ – $10^{-5}M$ ),<sup>42</sup> while in the case of  $\alpha$ -methylstyrene the amount of monomer in equilibrium with polymer is much more significant (0.75 and 7.5M at 0 and 60°C., respectively).<sup>43</sup> About the same amount of THF monomer remains at equilibrium at the temperatures normally used in tetrahydrofuran polymerizations as in the  $\alpha$ -methylstyrene case. Thus THF appears to be the cationic counterpart of the anionic  $\alpha$ -methylstyrene case.

Of course, the exact amount of monomer at equilibrium varies with temperature and it varies in a predictable manner.<sup>27</sup> If a system containing "living" polymers is at equilibrium at one temperature and the temperature is then altered, the steady state is destroyed, and polymerization or depolymerization will occur as required until a new steady state is established. This situation has been nicely demonstrated in the anionic polymerization of  $\alpha$ -methylstyrene,<sup>42</sup> and it can be equally well demonstrated by the cationic polymerization of THF initiated by *p*-ClC<sub>6</sub>H<sub>4</sub>N<sub>2</sub>PF<sub>6</sub>. We have shown (Table I) that these THF polymerizations are readily reversible and that a given sample can be polymerized and depolymerized repeatedly.

Furthermore, the values we derive for the equilibrium monomer concentration lead to a linear relationship between  $1/T$  and  $\ln[\text{THF}]_{\text{eq}}$  (Fig. 3) as required by the theory for equilibrium polymerization developed by Dainton.<sup>27</sup> Thus we see, that although all the monomer has not been consumed in the THF polymerizations, all the monomer available for polymerization has been consumed, if thermodynamic considerations are taken into account.

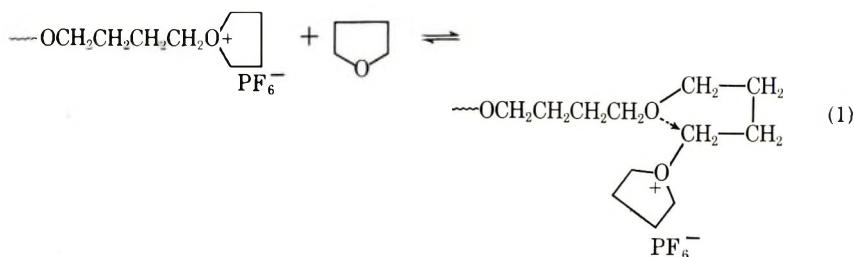
Still another consequence of a "living" system is that upon addition of further monomer to a polymerization at equilibrium, polymerization will continue on the existing chains until an equilibrium is again reached at a higher molecular weight. If another monomer is added, polymerization again continues, and a block copolymer is formed. Conversely, if additional growing centers are introduced to a polymerization at equilibrium, propagation of the new chains occurs only at the expense of depropagation of the existing chains and a lower molecular weight polymer results. As shown in Table III, all of these phenomena take place in THF polymerizations catalyzed by  $p\text{-ClC}_6\text{H}_4\text{N}_2\text{PF}_6$ .

### Transfer

Sometimes in the course of a polymerization the growing center reacts in such a way that a new reactive center is formed and the old one is destroyed by interaction with a chain transfer agent. The presence of a chain transfer agent in a "living" system where a significant amount of monomer is in equilibrium with its polymer has important and interesting consequences, which do not seem to have been considered previously.

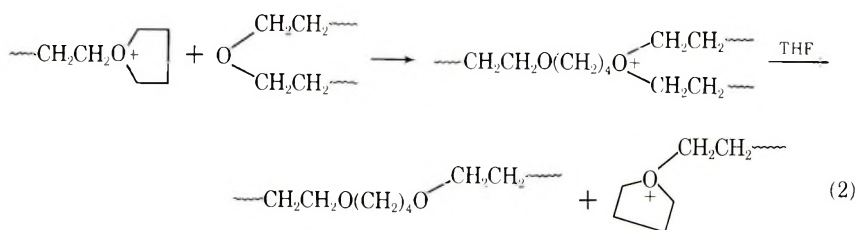
For instance in THF polymerizations with  $\text{PF}_6^-$  gegenions the presence of ether oxygens has a marked effect and this effect is very dependent upon the structure of the ether added. The ultimate conversion is not markedly affected as shown in Figure 4 but the time dependence of the intrinsic viscosity shows significant effects (Fig. 5).

It is possible to come to a reasonable understanding of the above results and to gain some insight into their significance by considering the polymerization mechanism. The cationic polymerization of THF is generally regarded<sup>3,9-12</sup> to proceed through tertiary oxonium ions where addition of monomer occurs by nucleophilic attack at the  $\alpha$ -carbon atoms of these ions [eq. (1)].



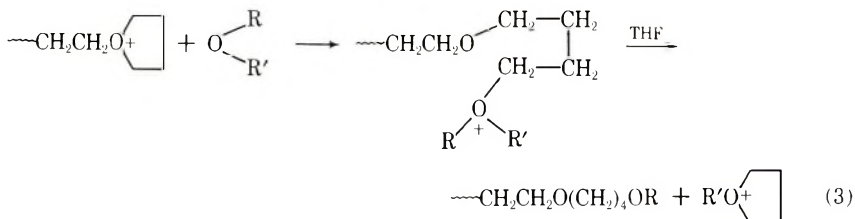
The depropagation reaction would occur by a similar nucleophilic attack by the penultimate oxygen atom (as shown by the dotted arrow) followed by the expulsion of monomer. At monomer-polymer equilibrium the rates of propagation and of depropagation become equal and, as has been shown above, both appear to be of some consequence, and must always be considered.

In addition to reaction with monomer oxygen and penultimate polymer chain oxygen, the oxonium ion should also be capable of reacting with other ether oxygens. Let us examine the possibilities. Polymer ether oxygens are always present and the possibility of intermolecular reaction exists [eq. (2)].



An analysis of the consequences of this reaction reveals that the only result is an alteration of the molecular weight distribution.

If an acyclic ether is present the analogous reaction [eq. (3)]

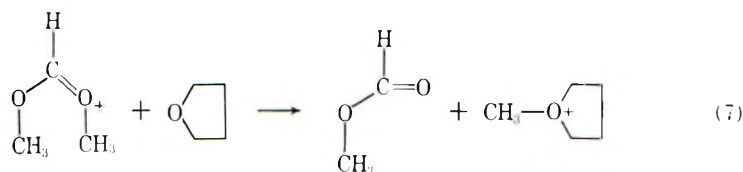


leads to chain transfer and the formation of new short chains. These new short chains can be formed even at equilibrium. They will enter into the propagation-depropagation reaction and they can also react with polymer oxygen. Both of these reactions will lead to a decrease in overall molecular weight; the first results in growth of the new chains at the expense of longer ones and the second brings about chain cleavage.

If another cyclic ether, such as 1,3-dioxolane, is present, its reaction with oxonium ion can lead only to copolymerization and the reaction with polymer oxygen is now the same as in the case of bulk tetrahydrofuran and leads to redistribution. Since there is no possible mechanism for the production of new short chains, there should be and indeed there was no fall in intrinsic viscosity at equilibrium. The intrinsic viscosity hump observed in this case before equilibrium conversion was reached is probably due to changes in the copolymer composition during approach to equilibrium. The incorporation of 2-methyltetrahydrofuran and dioxane in the copolymers reported above most probably occurred by this mechanism.



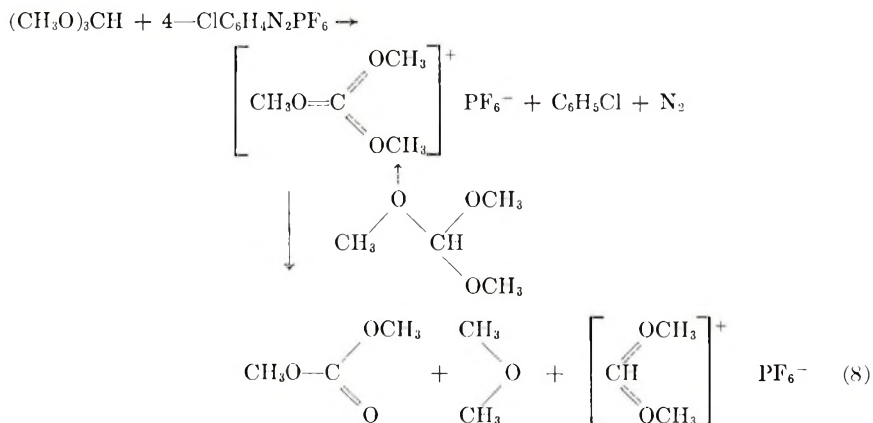




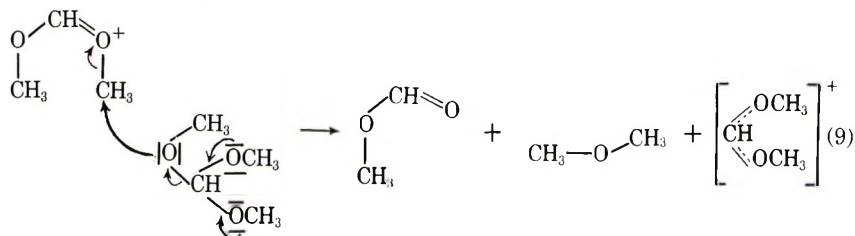
methoxy group at the beginning of the chain is produced in addition to the observed methyl formate.

The high degree of effectiveness of trimethylorthoformate as a transfer agent is undoubtedly due to its ability to form a resonance-stabilized oxonium ion.

The small amount of dimethyl ether observed in the polymerization of THF in the presence of 40% trimethylorthoformate is due to a side reaction in which the dimethyl formate oxonium ion reacts with trimethylorthoformate. This was demonstrated in the nearly quantitative *p*-ClC<sub>6</sub>H<sub>4</sub>N<sub>2</sub>PF<sub>6</sub>-catalyzed decomposition of trimethylorthoformate to dimethyl ether and methyl formate. Apparently a hydrogen abstraction occurs initially, followed by further reaction with trimethylorthoformate to give the same resonance-stabilized dimethyl formate oxonium ion as above [eq. (8)]



In the absence of THF this oxonium ion undergoes a chain reaction [eq. (9)] with trimethylorthoformate to yield the observed products. THF



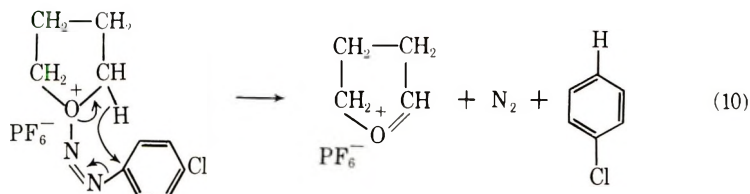
effectively competes in this chain reaction in spite of the resultant loss of the resonance stabilized oxonium ion. It may be that the nucleophilicity of

the THF oxygen is sufficiently greater than that of the trimethylorthoformate oxygens as a result of the steric environment of the trimethylorthoformate oxygens to compensate for the loss of resonance energy of the dimethyl formate oxonium ion.

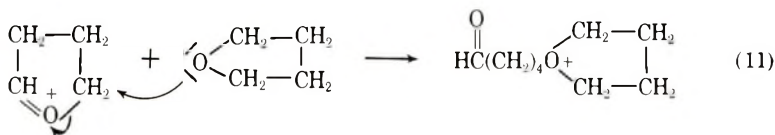
It is interesting to note that in the case of the additive trimethylorthoformate the rate of formation of polymer was about two times as great as that observed in bulk polymerization at the same catalyst concentration (Fig. 4). Apparently more growing polymer centers were present. This suggests that the hydrogen abstraction that apparently precedes the formation of the primary oxonium ion is easier in the presence of trimethylorthoformate.

Further evidence that hydrogen abstraction is the primary mode of initiation in polymerizations catalyzed by  $p\text{-ClC}_6\text{H}_4\text{N}_2\text{PF}_6$  was gained in the experiments with 2-methyltetrahydrofuran and 1,2-dimethoxyethane, where the isolation of chlorobenzene and the absence of 4-chlorofluorobenzene demonstrated that chlorophenyl cation abstracted hydrogen from the system rather than fluorine from  $\text{PF}_6^-$  as in the thermal decomposition.

It seems likely that in ethereal solvents this hydrogen abstraction is not made by a free chlorophenyl cation, but that instead the solvated diazonium salt decomposes in a concerted fashion as illustrated in eq. (10) with THF.\*



On further reaction of this initially formed oxonium ion with THF, by analogy with the mechanism proposed above for transfer with trimethylorthoformate, we would predict attack at the  $\text{CH}_2$  carbon as shown in eq. (11).



Thus a hydrogen abstraction mechanism operating in bulk THF polymerization should lead directly to an aldehyde group at the beginning of the chain and not to the cyclic acetal suggested by others.<sup>9-12</sup> In fact, carbonyl-type compounds have been isolated from reactions of this kind; specifically, reactions of 2-substituted-1,3-dioxolenium fluoroborate ions with mildly nucleophilic reagents have been reported<sup>46</sup> to occur on  $\text{C}_2$  of the dioxolane ring.

\* 1,5-Hydride ion transfer in decomposition of diazonium compounds has been previously proposed and shown to take place.<sup>44,45</sup>

The support of Imperial Chemical Industries (I.C.I. Postdoctoral Fellowship, M.P.D.) and of the American Association of University Women (Marie Curie Fellowship, P.D.) is gratefully acknowledged.

### References

1. M. P. Dreyfuss and P. Dreyfuss, *Polymer*, **6**, 93 (1965).
2. M. P. Dreyfuss and P. Dreyfuss, paper presented at the 150th Meeting, American Chemical Society, Atlantic City, N.J., September 1965; *Abstracts*, p. 7W; *Polymer Preprints*, **6**, 608 (1965).
3. P. H. Plesch, *The Chemistry of Cationic Polymerization*, Pergamon, Oxford, 1963, p. 431.
4. J. Furukawa and T. Saegusa, *Polymerization of Aldehydes and Oxides*, Interscience, New York, 1963, p. 225.
5. H. Meerwein, D. Delfs, and H. Morschel, *Angew. Chem.*, **72**, 927 (1960); cf. first report, H. Meerwein, *ibid.*, **59**, 168 (1947).
6. W. F. Gresham, U.S. Pat. 2,394,910 (1946).
7. A. C. Farthing, *J. Chem. Soc.*, **1955**, 3648.
8. Hercules Powder Co., Brit. Pat. 758,450 (1957).
9. C. E. H. Bawn, R. Bell, and A. Ledwith, paper presented at Chem. Soc. Anniversary Mtg., Cardiff (1963).
10. R. Bell, Ph.D. Thesis, University of Liverpool (1963).
11. C. E. H. Bawn, R. Bell, and A. Ledwith, *Polymer*, **6**, 95 (1965).
12. C. E. H. Bawn, R. M. Bell, C. Fitzsimmons, and A. Ledwith, paper presented at 150th Meeting, American Chemical Society, Atlantic City, N.J., September 1965; *Abstracts*, p. 3W.
13. B. A. Rozenberg, O. M. Chekhuta, E. B. Lyudvig, A. R. Gantmakher, and S. S. Medvedev, *Vysokomolekul. Soedin.*, **6**, 2030 (1964).
14. B. A. Rozenberg, E. B. Lyudvig, A. R. Gantmakher, and S. S. Medvedev, *Vysokomolekul. Soedin.*, **6**, 2035 (1964).
15. N. V. Makletsova, I. V. Epel'baum, B. A. Rozenberg, and E. B. Lyudvig, *Vysokomolekul. Soedin.*, **7**, 70 (1965).
16. E. B. Lyudvig, B. A. Rozenberg, T. M. Zvereva, A. R. Gantmakher, and S. S. Medvedev, *Vysokomolekul. Soedin.*, **7**, 269 (1965).
17. E. L. Muetterties, U.S. Pat. 2,856,370 (1958).
18. D. Sims, *J. Chem. Soc.*, **1964**, 864.
19. D. Sims, personal communication.
20. W. Lange and E. Müller, *Ber.*, **63**, 1058 (1930).
21. F. D. Hartley, private communication.
22. R. H. Pierson, A. N. Fletcher, and E. St. Clair Gantz, *Anal. Chem.*, **28**, 1218 (1956).
23. *Beilstein's Handbuch der Organischen Chemie*, Vol. I, F. R. Richter, Ed., 1st suppl., Springer-Verlag, Berlin, 1928, p. 249.
24. K. Alexander and L. E. Schniepp, *J. Am. Chem. Soc.*, **70**, 1839 (1948).
25. H. Meerwein, E. Battenberg, H. Gold, E. Pfeil, and G. Willfang, *J. Pract. Chem.*, **154**, 112 (1940).
26. P. P. T. Sah, *Rec. Trav. Chim.*, **59**, 1036 (1940).
27. F. S. Dainton, and K. Ivin, *Quart. Rev.*, **12**, 61 (1958).
28. E. I. du Pont de Nemours, *Technical Information on THF*.
29. D. J. Worsfold and S. Bywater, *J. Polymer Sci.*, **26**, 299 (1957).
30. R. C. Burrows and B. F. Crowe, *J. Appl. Polymer Sci.*, **6**, 465 (1962).
31. S. M. Ali and M. B. Huglin, *Makromol. Chem.*, **84**, 117 (1965).
32. E. A. Ofstead, paper presented at 150th Meeting, American Chemical Society, Atlantic City, N.J., September 1965; *Abstracts*, p. 11W; *Polymer Preprints*, **6**, 674 (1965).

33. P. R. Johnston, *J. Appl. Polymer Sci.*, **9**, 461 (1965).
34. A. Miyake and W. H. Stockmayer, *Polymer Preprints*, **6**, 273 (1965).
35. T. Saegusa, H. Inui, S. Hirai, and J. Furukawa, *Kogyo Kagaku Zasshi*, **65**, 699 (1962).
36. M. Szwarc, *Fortschr. Hochpolymer. Forsch.*, **2**, 275 (1960).
37. M. Szwarc, M. Levy, and R. Milkovich, *J. Am. Chem. Soc.*, **78**, 2656 (1956).
38. M. Szwarc, *Nature*, **178**, 1168 (1956).
39. R. Waack, A. Rembraun, J. D. Coombes, and M. Szwarc, *J. Am. Chem. Soc.*, **79**, 2026 (1957).
40. H. Brody, M. Ladacki, R. Milkovich, and M. Szwarc, *J. Polymer Sci.*, **25**, 221 (1957).
41. H. W. McCormick, *J. Polymer Sci.*, **36**, 341 (1959); *ibid.*, **41**, 327 (1959).
42. S. Bywater, and D. J. Worsfold, *J. Polymer Sci.*, **58**, 571 (1962).
43. H. W. McCormick, *J. Polymer Sci.*, **25**, 488 (1957).
44. T. Cohen and J. Lipowitz, *J. Am. Chem. Soc.*, **86**, 2514 (1964).
45. T. Cohen, A. H. Dinwoodie, and L. D. McKeever, *J. Org. Chem.*, **27**, 3385 (1962).
46. H. Meerwein, K. Bodenbenner, P. Borner, F. Kunert, and K. Wunderlich, *Ann.*, **632**, 38 (1960).

### Résumé

L'hexafluorophosphate de *p*-chlorophényldiazonium est un catalyseur efficace pour initié la polymérisation du tétrahydrofuranne (THF) et d'autres éthers cycliques. Les polymérisations progressent sans terminaisons appréciables ni réactions de transfert (c.à.d. il se forme des polymères vivants) et les matériaux peuvent être obtenus avec des poids moléculaires très élevés. Un équilibre mobile monomère-polymère pour THF a été obtenu au cours de la polymérisation et les conversions à l'équilibre ont été déterminées à diverses températures. Au départ de ces résultats, on trouve une température pland de 84°C, une chaleur de polymérisation de -4.58 Kcal/mole et une variation correspondante d'entropie de -17.7 cal/deg-mole. Les hydrocarbures sont des solvants inertes, adaptés à de telles polymérisations et les solutions concentrées doivent être utilisées à température ambiante afin d'être conservées au-dessus de la concentration en monomères requise par l'équilibre et aussi afin de dissoudre le catalyseur qui est insoluble dans les hydrocarbures. On a montré que les éthers acycliques agissent comme agents de transfert au cours de ces polymérisations et que ces transferts avec réduction conséquente du poids moléculaire continuent même après que l'équilibre monomère-polymère ait été atteint. Les éthers cycliques n'agissent pas comme agents de transfert mais copolymérisent uniquement. L'orthoformite de triméthyle est un agent de transfert particulièrement efficace; il en résulte des polymères avec des groupes terminaux méthoxylés et formation de formiate de méthyle comme produit secondaire. Les résultats obtenus sont en accord avec un mécanisme comprenant une initiation par abstraction d'hydrogène et une polymérisation via des oxonium tertiaires associés avec des ions de signes contraires  $\text{PF}_6^-$ . Cet ion de signe contraire est responsable de la nature vivante du système.

### Zusammenfassung

Es wird gezeigt, dass *p*-Chlorphenyldiazoniumhexafluorphosphat ein brauchbarer und wirksamer Katalysator für die Polymerisation von Tetrahydrofuran (THF) und anderen zyklischen Äthern ist. Die Polymerisation verläuft offenbar ohne merkliche Abbruchs- oder Übertragungsreaktionen (d.h. es entstehen "lebende" Polymere) und es können sehr hochmolekulare Stoffe erhalten werden. Ein dynamisches Monomer-Polymer-Gleichgewicht wurde für THF während der Polymerisation erhalten und der Gleichgewichtsumsatz wurde bei einer Reihe von Temperaturen bestimmt. Die aus diesen Daten abgeleitete ceiling-Temperatur betrug 84°C, die Polymerisationswärme -4,58 kcal/Mol und die entsprechende Entropieänderung -17,7 cal/°Mol. Kohlen-

wasserstoffe sind für diese Polymerisation als inerte Lösungsmittel geeignet, es müssen aber bei Raumtemperatur konzentrierte Lösungen verwendet werden, um oberhalb der erforderlichen Gleichgewichtskonzentration des Monomeren zu liegen und zugleich den Katalysator zu lösen, der in Kohlenwasserstoffen unlöslich ist. Es wurde gezeigt, dass azyklische Äther bei dieser Polymerisation als Kettenüberträger wirken und dass die Übertragung mit der dadurch bedingten Herabsetzung des Molekulargewichts auch nach Einstellung des Monomer-Polymergleichgewichts stattfindet. Zyklische Äther wirken nicht als Kettenüberträger, sondern bilden bloss Kopolymere. Trimethylorthoformiat erwies sich als besonders wirksamer Kettenüberträger. Es führte zu Polymeren mit Methoxyendgruppen und lieferte Methylformiat als Nebenprodukt. Die erhaltenen Ergebnisse lassen sich durch einen Mechanismus mit Start durch Wasserstoffabstraktion und Polymerisation über tertiäre, mit  $\text{PF}_6^-$ -Gegenionen assoziierte Oxoniumionen erklären. Dieses Gegenion scheint für die das Verhalten des Systems als "lebendes" Polymeres verantwortlich zu sein.

Received January 27, 1966

Prod. No. 5069A



## Polymerization Kinetics in Highly Viscous Media

F. DE SCHRIJVER and G. SMETS, *Laboratoire de Chimie  
Macromoléculaire, University of Louvain, Belgium*

### Synopsis

The influence of the viscosity of the reaction medium on the rate of polymerization of styrene has been examined by adding different amounts of inert polystyrene to pure monomer and its solutions in benzene. Azobisisobutyronitrile was decomposed photochemically ( $\lambda = 365 \text{ m}\mu$ ) at  $25^\circ\text{C}$ . or thermally at  $70^\circ\text{C}$ .; its rate of decomposition was followed by ultraviolet spectrometry. The rate of formation of dimethyl-*N*-cyanoisopropylketenimine (DKI) was followed by infrared spectrometry ( $2020 \text{ cm}^{-1}$ ). The initiation efficiency was determined by the scintillation method with the use of a  $^{14}\text{C}$ -labeled initiator. The rate of polymerization was followed dilatometrically. An increase of viscosity does not affect the rate of decomposition of the initiator; on the contrary, during the photochemical decomposition, it causes an increase of DKI concentration and an appreciable decrease of efficiency (from 0.51 to 0.30). From the point of view of the rate of photopolymerization, an increase of viscosity causes a decrease in the order of the reaction with respect to the initiator (from 0.5 to 0.3) and an increase with respect to monomer from 1.5 to 2. These results are interpreted on the basis of a decrease of termination rate constant between two growing chains in favor of a termination reaction between a growing chain and a primary radical. These effects, due to an increase of the viscosity of the solution, on the initiation and termination reactions influence the rate of polymerization in opposite direction and compensate each other to approximately 25%.

When graft polymerizations are initiated by photochemical or thermal decomposition of groups attached to a polymeric chain, primary radicals are produced in high viscous medium and their recombination must be appreciably enhanced. Therefore, the first question that arises is whether the efficiency of these radicals is affected by the viscosity of the reaction medium. Secondly, the decreasing mobility of the growing chains must impede the chain termination reactions considerably, so that the rate of termination may become diffusion-controlled; in this case,<sup>1,2</sup> the termination rate constant will be proportional to the viscosity of the solution.<sup>3-7</sup> Consequently the chain propagation is favored.

It is evident that both effects due to the high viscosity of the medium must influence the total rate of polymerization in opposite directions, and it is difficult to predict to what extent one effect will prevail over the other one. It must be pointed out, however, that an increasing viscosity can also improve chain termination processes between primary radicals and growing chains as well as termination by radical occlusion.<sup>8-13</sup>

It is the purpose of the present paper to examine a particularly simple

case, that of the polymerization of styrene initiated by 2,2'-azobisisobutyronitrile (AIBN) in the presence of varying amounts of inert polystyrene. Considering that AIBN does not undergo induced decomposition, it is evident that a difference in the relative amounts of decomposition products will reflect a change in cage recombination. On the other hand, the rate of polymerization will give an indication of the relative importance of both initiation and termination processes.

Recently the influence of the viscosity of the medium on the reaction products has been examined in the case of acetyl peroxide, and it was shown that an increase in importance of cage recombination accompanies the increase of viscosity.<sup>14,15</sup>

## EXPERIMENTAL

### Materials

$\alpha,\alpha'$ -Azobisisobutyronitrile (AIBN) was purified by crystallization three times from ethanol below 35°C.

The <sup>14</sup>C-labeled AIBN (Saclay, France) was used without further purification; before use it was mixed with conventional AIBN by freeze-drying of a solution of both active and inactive initiators in benzene.

Tetramethylsuccinodinitrile was prepared by thermal decomposition at 80°C. of AIBN in benzene solution for 48 hr. White crystals precipitate on cooling and were recrystallized from benzene, m.p. 166–167°C.

1,1'-Dimethylethylisopropyl keteneimine (DKI) was prepared by the method of Smith.<sup>16,17</sup> The physical properties of these compounds (ultra-violet, infrared, and NMR spectra and melting point) correspond closely to the literature data.

High molecular weight polystyrene was prepared in emulsion. After precipitation with methanol from butanone, the polymer was fractionated roughly in order to isolate a product with a molecular weight of about 10<sup>6</sup>. Therefore it was dissolved in a mixture of butanone and *n*-butanol, and the solvent progressively evaporated in a thermostat at 25°C. The intrinsic viscosity of this polymer remains unchanged before and after irradiation with light of 365 m $\mu$  wavelength; consequently it undergoes no chain degradation during the photopolymerization experiments described further.

### Rate of Decomposition of $\alpha,\alpha'$ -Azobisisobutyronitrile

The decomposition of AIBN was carried out in high vacuum; before sealing, the solution was degassed several times by freezing and thawing successively. The light source (Hanau S81,350 w. tube) was immersed in a thermostatic bath (25°C.) located 20 cm. from a 1-cm. diameter Pyrex cell containing the solution. The light was selected with an interference filter with a transmittance maximum at 365 m $\mu$ . The decrease of absorbance at 365 m $\mu$  was followed as a function of time by using a Beckman DU 16.100 spectrophotometer.

The rate of formation of DKI was followed by infrared spectrometry

(Perkin-Elmer Model 21) by measuring the increase of absorbance at 2020  $\text{cm}^{-1}$ , the molar extinction coefficient being 544 mole/l.-cm. Preliminary experiments showed that under our irradiation conditions ( $\lambda = 365 \text{ m}\mu$ ) DKI is stable and undergoes no induced decomposition.<sup>18</sup>

### Initiation Efficiency

The initiation efficiency was determined by measuring the radioactivity of the polymer by the scintillation method with 2,5-diphenyl oxazole and 2,2'-*p*-phenylenebis(5-phenyloxazole). The polymer was purified by re-precipitation three times from toluene with methanol.

### Rate of Polymerization

Polymerization experiments were carried out in a specially devised mushroom dilatometer, as described by Burnett.<sup>19</sup> The volume contraction was followed in a capillary tube filled with a mercury column directly in contact with the polymerization mixture; 1 cm. of the capillary tube corresponded to 0.027 ml. The dilatometer was immersed in a thermostat at 25°C. and irradiated with a Philips 1000-w. ultraviolet lamp through an interference filter (365  $\text{m}\mu$ ).

### Viscosity Determination

The viscosity of the polymer solution in benzene and in styrene was determined at 25°C. in a Höppler viscometer; at polymer concentrations greater than 2% the high viscosity values are practically independent of the nature of the solvent (Table I).

TABLE I

Polymer concn., %	Viscosity, poise
3	0.29
4	0.6
5	1.06
10	7.9
14	12.5
17	20.3

## EXPERIMENTAL RESULTS AND DISCUSSION

### Influence of Viscosity on Initiation with Azobisisobutyronitrile

An increase of viscosity of the reaction medium can affect the rate of initiation by increasing the importance of cage effects, i.e., by improving the recombination of the primary radicals. If the radicals recombine back to an original initiator molecule



the result is a decrease of rate of decomposition of the initiator. If they recombine only after losing nitrogen, inactive species as dimethyl-*N*-

cyanoisopropyl keteneimine (DKI) and tetramethylsuccinodinitrile (TMS) are formed; in this case the initiation efficiency will be affected.



Therefore, in order to determine the influence of the viscosity, the rate of the photolytic and thermal decomposition of AIBN has been determined under high vacuum in benzene solution in the presence of various amounts of high molecular weight polystyrenes. The photolysis was carried out at 25°C. under irradiation with light of wavelength of 365 m $\mu$ , while the thermal decomposition was at 70°C. in the presence of only 5 and 7% polystyrene. Figure 1 shows that the first-order rate constant of decomposition of the initiator is independent of the viscosity of the reaction medium.

With respect to the reaction products of the photolysis (365 m $\mu$ ), the increase of the concentration of DKI was followed as a function of the time by infrared spectrometry (2020 cm.<sup>-1</sup>); the ratio of concentration of DKI to that of decomposed AIBN was determined at different viscosities in benzene as well as in the presence of styrene monomer. The data are summarized in Table II.

The results of series B show that an increase of viscosity favors strongly the formation of DKI, which represents more than 90% of the decomposed AIBN in a highly viscous medium. On the contrary, in the presence of monomer (series A), the formation of DKI decreases linearly with increasing monomer concentration on account of the initiation of polymerization itself. Nevertheless at the same monomer concentration (8.73 mole/l.)

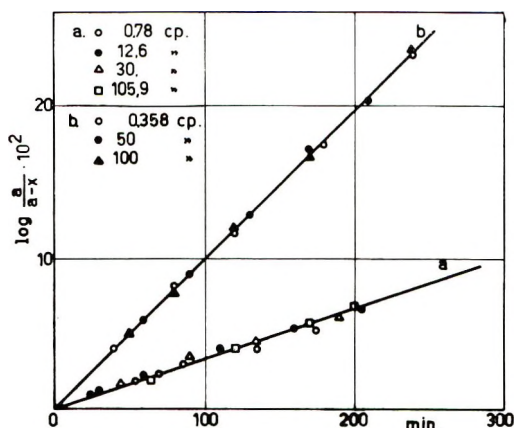


Fig. 1. Influence of the viscosity of the medium on (a) photochemical decomposition (25°C.) and (b) thermal decomposition (70°C.) of azobisisobutyronitrile.  $[\text{AIBN}]_0 = 0.5 \times 10^{-2}$  mole/l.

TABLE II  
Influence of the Monomer Concentration (Series A) and of the  
Viscosity (Series B) on the Ratio Diketeneimine/Decomposed AIBN<sup>a</sup>

Series	$\eta$ , cp.	[DKI], mole/l. $\times 10^3$	$\frac{[\text{DKI}]}{[\text{AIBN}]_{\text{dec}}}$	[Styrene], mole/l.
Series A	0.61	4.9	0.58	—
	0.66	4.25	0.505	2.9
	0.7	3.98	0.47	4.35
	0.78	3.32	0.39	8.73 <sup>b</sup>
Series B	19.2	4.24	0.505	8.73 <sup>b</sup>
	105.9	4.26	0.545	8.73 <sup>b</sup>
	12.6	5.3	0.74	— <sup>c</sup>
	29.2	5.6	0.78	— <sup>c</sup>
	60.3	6.45	0.9	— <sup>c</sup>
	209.0	6.7	0.93	— <sup>c</sup>

<sup>a</sup> [AIBN] = 0.305 mole/l.; temperature, 25°C.; time, 5 hr.;  $\lambda$ , 365 m $\mu$ ; solvent, benzene.

<sup>b</sup> Bulk.

<sup>c</sup> Pure benzene.

the same trend of increasing ratio [DKI]/[AIBN]<sub>dec</sub> with increasing viscosity is found.

It is assumed that in the cyanoisopropyl radical the unpaired electron is strongly delocalized<sup>20</sup> and that in the excited state the contribution of the (CH<sub>3</sub>)<sub>2</sub>C=C=N\* forms becomes more important.<sup>21</sup> Indeed, in a highly viscous medium the number of collisions with solvent molecules is markedly diminished; consequently primary radicals recombine in their excited state, giving rise mainly to DKI instead of tetramethylsuccinodinitrile. The influence of the viscosity on the initiation efficiency has been examined

TABLE III  
Influence of the Monomer Concentration and of the Viscosity on the Initiation Efficiency  
in Photopolymerization of Styrene<sup>a</sup>

$\eta$ , cp.	$\frac{[\text{DKI}]}{[\text{AIBN}]_{\text{dec}}}$	Efficiency	[Styrene], mole/l.
0.66	0.505	0.29	2.9
0.7	0.47	0.32	4.35
30.0		0.28	—
0.74		0.44	7.0
0.78	0.39	0.51	8.73 (bulk)
		0.52	"
12.6		0.425	"
		0.47	"
19.2	0.505	0.4	"
		0.36	"
43.5		0.36	"
		0.315	"
105.9	0.545	0.315	"
		0.29	"

<sup>a</sup> Temperature, 25°C.; solvent, benzene;  $\lambda$  = 365 m $\mu$ .



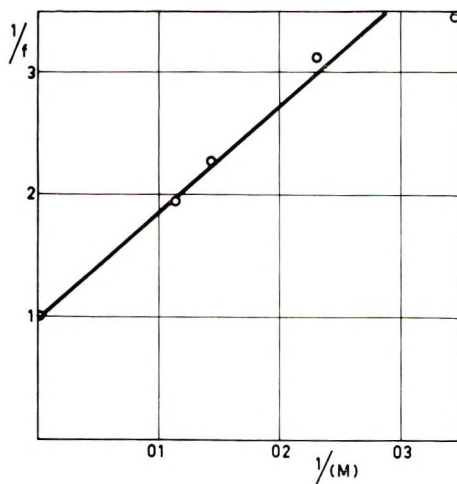


Fig. 2. Influence of the monomer concentration on the initiation efficiency.

by using  $^{14}\text{C}$  azobisisobutyronitrile as initiator, the efficiency being equal to the ratio of the amount of AIBN incorporated in the polymer to that of total decomposed AIBN (Table III).

These data show evidently that if the efficiency increases with the monomer concentration, it decreases strongly with an increase of viscosity of the reaction medium. In pure styrene, the decrease of efficiency is compensated by an increase of the ratio  $[\text{DKI}]/(\text{AIBN})_{\text{dec}}$  in such a manner that the sum remains practically constant and amounts about 0.86–0.90, the residue being tetramethylsuccinodinitrile.

As can be seen from Figure 2, a linear relationship is found between the reciprocal of the efficiency  $f$  and the reciprocal of the monomer concentration except for the highest monomer concentration; it corresponds to the usual expression

$$1/f = 1 + (k_r/k_a)1/[M]$$

where  $k_r$  is the pseudo-first order "cage" recombination rate constant of primary radicals, and  $k_a$  the monomer addition rate constant.

#### Influence of the Viscosity on the Photopolymerization of Styrene

The influence of the viscosity on the order of reaction with respect to the monomer and initiator concentration as well as on the total rate of polymerization has been examined and compared to the corresponding results for a nonviscous medium.

The rate dependence from the initiator concentration and the viscosity of the reaction medium is illustrated by the data of Table IV.

The decrease of styrene concentration in the first column is due to the presence of polystyrene added in order to increase the viscosity of the solution, e.g., the series of samples with viscosities of 106 and 1900 cp. correspond to samples containing 5 and 16% polymer, respectively. It is

TABLE IV  
Rate Dependence of AIBN Concentration on the Photopolymerization of Styrene and Influence of the Viscosity of the Medium

[Styrene], mole/l.	$\eta$ , cp.	[AIBN] $\times 10^2$ , mole/l.	$R_p \times 10^5$ , mole/l.-sec.	$\log R_p / \log$ [AIBN]
8.73 <sup>a</sup>	0.78	2.3	4.62	0.5
		1.75	4.27	
		1.25	3.03	
		0.7	2.78	
		0.35	1.83	
8.56	12.6	0.984	4.55	0.33
		0.687	4.07	
		0.324	3.14	
8.35	106	0.664	3.65	0.25
		0.332	3.00	
		0.166	2.63	
		0.053	1.93	
8.20	316	0.941	3.89	0.27
		0.659	3.48	
		0.283	2.81	
7.7	1900	0.62	4.16	0.34
		0.292	3.12	
		0.2	2.82	

<sup>a</sup> Bulk

worthwhile to notice that the apparent order of reaction with respect to the initiator concentration (fifth column of Table IV) diminishes progressively from 0.5 to 0.25 and then again rises slowly to about 0.30 at very

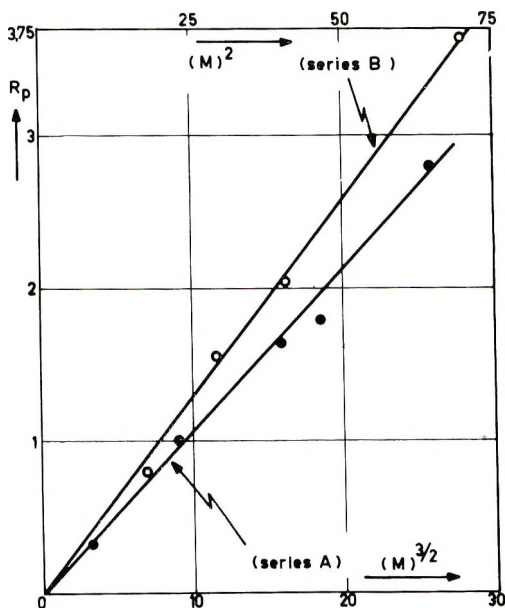


Fig. 3. Rate dependence on the monomer concentration: (series A) pure styrene; (series B) styrene with 5 wt.-% polystyrene.

TABLE V  
Rate Dependence of the Photopolymerization of Styrene on the Monomer Concentration and Influence of the Viscosity of the Medium<sup>a</sup>

Series	[AIBN], $\times 10^2$ , mole/l.	[Styrene], mole/l.	$R_p \times 10^5$ , mole/l.-sec.	$\frac{\Delta \log R_p}{\Delta \log [M]}$
Series A	0.7	8.73	2.8	1.5
		6.98	1.8	
		6.32	1.65	
		4.35	1.0	
		2.18	0.33	
Series B <sup>b</sup>	0.664	8.35	3.64	2.0
		6.36	2.04	
		5.38	1.55	
		4.16	0.8	

<sup>a</sup> Temperature, 25°C.; solvent, benzene.

<sup>b</sup> Polystyrene = 5 wt.-%;  $\eta = 106$  cp.

high viscosities. The decrease of initiator efficiency, as indicated in the first part, is insufficient to account for this pronounced decrease. Therefore chain termination between primary radicals and growing polystyrene chains to some extent must be considered to occur.

At low photosensitizer concentration, the total rate is lowest for pure styrene in the absence of dissolved polymer by a factor of about 1.7. Since it was shown that the efficiency decreases with increasing polymer concentration, the rate increase must therefore be interpreted mainly in the sense of a decrease of the rate of termination. The apparent order of reaction with respect to the monomer concentration has also been considered. As expected, in nonviscous medium, the rate is proportional to the  $3/2$  power of the monomer concentration at constant initiator concentration. In the presence of 5 wt.-% polymer (106 cp.) this value increases to 2. The data are given in Table V; the corresponding plots of  $R_p$

TABLE VI  
Rate of Bulk Polymerization of Styrene at 25°C. and Influence of the Viscosity

[Styrene], mole/l.	[AIBN] $\times 10^2$ , mole/l.	$R_p \times 10^4$ , mole/l.-sec.	$\eta$ , poise	Polymer, wt.-%
8.73	0.7	0.44	0.0078	—
8.56	0.687	0.410	0.126	—
8.42	0.676	0.380	0.605	4
8.35	0.664	0.360	1.059	5
8.20	0.659	0.336	3.16	5
8.16	0.655	0.344	6.2	5
8.02	0.643	0.346	7.9	10
7.88	0.634	0.363	9	10
7.75	0.623	0.408	12.5	14
7.59	0.609	0.455	20.3	17
7.52	0.604	0.470	33	17
7.40	0.595	0.570	42	17

versus  $[M]^{3/2}$  and  $[M]^2$  are shown in Figure 3, and both pass through the origin.

The influence of the viscosity on the rate of polymerization of styrene in bulk was also examined by adding increasing amounts of polystyrene. The data are summarized in Table VI. The decrease of initiation efficiency with increasing viscosity can easily account for the initial 25% decrease of rate. At still higher viscosities the Tromsdorff effect, due to a decrease of termination rate constant, becomes prevalent; the rate increases progressively and becomes then higher than that in pure styrene monomer.

### CONCLUSIONS

The initiation efficiency of azobisisobutyronitrile in the photopolymerization of styrene can decrease by about 50% on increasing the viscosity of the reaction medium; concomitantly the ratio of diketeneimine to AIBN decomposed increases.

An apparent order of reaction with respect to the initiator concentration equal to about 0.30 at high viscosities must be related to the decrease of initiation efficiency and chain termination between growing chains and primary radicals. Simultaneously the order of reaction with respect to the monomer increases from 1.5 to 2.

As a consequence of these effects in opposite directions on the chain initiation and termination reactions, the overall rate of polymerization decreases initially, then increases again with increasing viscosity of the medium, so that, in first approximation, the effects balance each other.

The authors are indebted to the I.W.O.N.L. for a fellowship to one of them (F. D. S.) and to the Centrum voor Hoog Polymeren, Gevaert-Agfa N.V. for supporting this research.

### References

1. E. Tromsdorff, H. Kohle, and P. Lagally, *Makromol. Chem.*, **1**, 169 (1947).
2. P. Allen and G. R. Patrick, *Makromol. Chem.*, **47**, 154 (1961); *ibid.*, **72**, 106 (1964).
3. H. F. Vaughan, *Trans. Faraday Soc.*, **48**, 576 (1952).
4. S. W. Benson and A. M. North, *J. Am. Chem. Soc.*, **84**, 935 (1962).
5. A. N. North and G. A. Reed, *J. Polymer Sci. A*, **1**, 1311 (1963).
6. A. M. North and G. A. Reed, *Trans. Faraday Soc.*, **57**, 859 (1961).
7. A. T. Guertin, *J. Polymer Sci. B*, **1**, 477 (1963).
8. G. Burnett and L. Loan, *Collection Czechoslov. Chem. Commun.*, **22**, 113 (1957).
9. S. Fujii, *Bull. Chem. Soc. Japan*, **27**, 216, 238 (1954).
10. N. G. Baldwin, *J. Polymer Sci. A*, **1**, 3209 (1963).
11. P. Hayden and H. W. Melville, *J. Polymer Sci.*, **43**, 201 (1960).
12. G. Burnett and G. Duncan, *Makromol. Chem.*, **51**, 154, 171 (1962).
13. P. E. Allen and C. R. Patrick, *Makromol. Chem.*, **48**, 89 (1961).
14. F. R. Eirich, W. Braun, and L. Ragbenbach, *J. Phys. Chem.*, **66**, 1591 (1962).
15. W. Braun, Ph.D. Dissertation, Polytechnic Institute of Brooklyn, 1964.
16. R. Back and C. Sivertz, *Can. J. Chem.*, **32**, 1061 (1954).
17. P. Smith and A. Rosenberg, *J. Am. Chem. Soc.*, **81**, 2037 (1959).
18. C. S. Hammond, C. S. Wu, O. D. Trapp, J. Warkentin, and R. T. Keys, *J. Am. Chem. Soc.*, **82**, 5394 (1960).

19. G. B. Burnett: *Trans. Faraday Soc.*, **40**, 771 (1950).
20. I. Vichutinskii and P. Prokofiev, *Zh. Fiz. Khim.*, **38**, 938 (1964).
21. H. E. Zimmerman, *J. Am. Chem. Soc.*, **85**, 922 (1963).

### Résumé

L'influence de la viscosité du milieu de réaction sur la vitesse de polymérisation du styrène a été examinée en additionnant des quantités variables de polystyrène inerte à des solutions benzéniques de monomère, soit au monomère pur. L'azobis-isobutyronitrile était décomposé photochimiquement ( $\lambda = 365 \text{ m}\mu$ ) à  $25^\circ\text{C}$ , soit thermiquement (à  $70^\circ\text{C}$ ); la vitesse de décomposition de l'initiateur était suivie par spectrophotométrie ultraviolette. La vitesse de formation de diméthyl-*N*-cyano-isopropyl-cétène-imine (DKI) était suivie par spectrométrie infra-rouge ( $2020 \text{ cm}^{-1}$ ). L'efficacité d'initiation était déterminée par la méthode de scintillation, au moyen d'initiateur marqué au carbone-14. La vitesse de polymérisation était suivie par dilatométrie. Une augmentation de viscosité n'affecte pas la vitesse de décomposition de l'initiateur; par contre, au cours de la décomposition photochimique, elle entraîne une augmentation de la concentration en DKI de même qu'une diminution appréciable d'efficacité (de 0.51 à 0.30). Du point de vue de la vitesse de photopolymérisation, l'augmentation de viscosité provoque une diminution de l'ordre par rapport à l'initiateur (de 0.5 à 0.3), tandis que l'ordre par rapport au monomère croît de 1.5 à 2. Ces résultats sont interprétés sur la base d'une diminution de la constante de vitesse de terminaison entre deux chaînes en croissance au profit d'une terminaison avec un radical primaire. Les effets causés par une augmentation de viscosité de la solution sur les réactions d'initiation et de terminaison s'exercent en sens opposé et se compensent en première approximation à 25% près.

### Zusammenfassung

Der Einfluss der Viskosität des Reaktionsmediums auf die Polymerisationsgeschwindigkeit von Styrol wurde durch Zusatz verschiedener Mengen von inertem Polystyrol zu reinem Monomeren und seinen Lösungen in Benzol untersucht. Azobisisobutyronitrile wurde photochemisch ( $\lambda = 365 \text{ m}\mu$ ) bei  $25^\circ\text{C}$  oder thermisch bei  $70^\circ\text{C}$  zersetzt; seine Zersetzungsgeschwindigkeit wurde durch UV-Spektrometrie verfolgt. Die Geschwindigkeit der Bildung von Dimethyl-*N*-cyan-isopropyl-ketenimin (DKI) wurde infrarotspektroskopisch ( $2020 \text{ cm}^{-1}$ ) gemessen. Die Starterausbeute wurde mit einem  $\text{C}^{14}$ -Starter nach der Szintillationsmethode bestimmt. Die Polymerisationsgeschwindigkeit wurde dilatometrisch gemessen. Eine Viskositätserhöhung beeinflusst die Zersetzungsgeschwindigkeit des Starters nicht; im Gegensatz dazu verursacht eine Zunahme der DKI-Konzentration während der photochemischen Zersetzung eine beträchtliche Herabsetzung der Starterausbeute (von 0,51 auf 0,30). Hinsichtlich der Geschwindigkeit der Photopolymerisation verursacht eine Viskositätszunahme eine Abnahme der Reaktionsordnung in bezug auf den Starter (von 0,5 auf 0,3), während die Ordnung in bezug auf das Monomere von 1,5 auf 2 zunimmt. Diese Ergebnisse werden auf der Grundlage einer Abnahme der Abbruchgeschwindigkeitskonstanten zwischen zwei wachsenden Ketten gegenüber der Wachstumsreaktion zwischen einer wachsenden Kette und einem Primärradikal interpretiert. Diese auf der Viskositätszunahme beruhenden Effekte bei der Start- und Abbruchreaktion beeinflussen die Polymerisationsgeschwindigkeit in entgegengesetzter Richtung und kompensieren sich gegenseitig etwa zu 25%.

Received January 26, 1966  
Prod. No. 5071A



## Studies on Anionic Polymerization of Lactams. Part II. Effect of Cocatalysts on the Polymerization of Pyrrolidone\*

S. BARZAKAY, M. LEVY, and D. VOFSI, *Plastics Research Laboratory,  
Polymer Department, The Weizmann Institute of Science, Rehovoth, Israel*

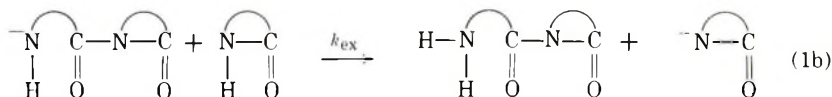
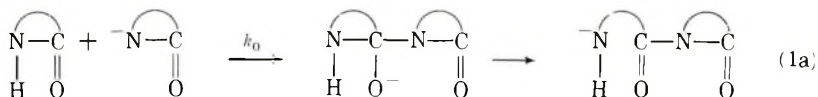
### Synopsis

The rates of addition of pyrrolidone magnesium bromide (PyMgBr) to *N*-benzoyl-, *N*-acetyl-, and *N*-methylpyrrolidone were measured in solution in tetrahydrofuran (THF). The values found for the rate constants at 25°C. were  $9.5 \times 10^{-2}$ ,  $2.8 \times 10^{-2}$ , and  $5 \times 10^{-4}$  l./mole-sec., respectively. The rate constant for addition of PyMgBr to pyrrolidone was also measured and found to be  $3 \times 10^{-9}$  l./mole-sec. Possible causes for the large difference between the values of these constants are discussed.

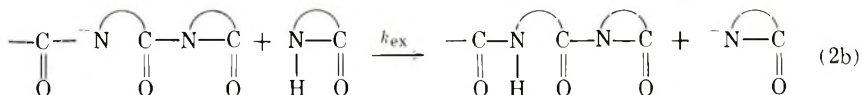
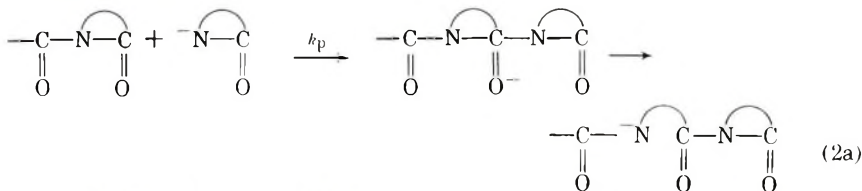
### INTRODUCTION

The mechanism of anionic polymerization of lactams involves initiation and propagation reactions, each consisting of an addition [eqs. (1a), (2a)] and a protonation step [eqs. (1b), (2b)].

Initiation:



Propagation:



\* Paper presented at the IUPAC Symposium of Macromolecular Chemistry, Prague, August 1965. For Part I see Barzakay et. al.<sup>1</sup>

Here

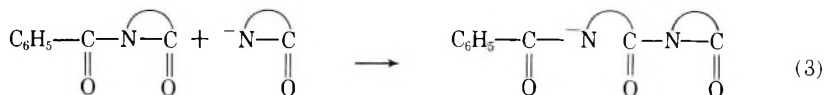


is a general representation of a lactam.

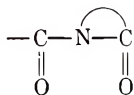
The protonation reaction of both the initiation and the propagation steps was assumed to be very fast. This was verified<sup>1</sup> by studying the sharpening of the NMR line of the N—H hydrogen in pyrrolidone in the presence of its potassium salt. From these changes it was possible to estimate a value of  $k_{ex} = 10^5$  l./mole-sec. for the exchange reaction. Thus it can be safely assumed that the rate-determining steps of both the initiation and the propagation are the addition reactions, followed by the ring opening.

The lactam polymerization has been the subject of numerous studies, but most of them have been concerned with the qualitative aspects of the problem. From the data given by Wichterle et al.<sup>3,4</sup> it can be seen that the propagation of caprolactam is tremendously accelerated by addition of such cocatalysts as acetyl caprolactam. Thus initiation rate by reaction (1a) is by many orders of magnitude slower than the propagation. This was reaffirmed by Sarenson et al.,<sup>5</sup> who claim that no polymer is formed by allowing caprolactam and its sodium salt to stand for a few hours at 139°C. Graf et al.<sup>6</sup> studied the polymerization of 4,4-dimethylazetidione ( $\beta$ -lactam) in dimethyl sulfoxide. Here too, the polymerization is very slow when only the anion is used as catalyst but is greatly accelerated by a cocatalyst such as oxalypyrrolidone.

Sekiguchi<sup>7</sup> measured the rates of polymerization of pyrrolidone in bulk at 30°C. using with potassium pyrrolidonate as catalyst and benzoylpyrrolidone as cocatalyst. From his data we calculated a value for  $k_p = 8$  l./mole-sec. He also measured spectroscopically the rate of disappearance of benzoyl-pyrrolidone from solution. From his few results we could calculate a value for the reaction constant  $k = 10$  l./mole-sec. This shows that the rate of the reaction (3)



is quite close to the propagation rate as it involves the same structure,



All these data indicate that there is a very large difference between  $k_p$  and  $k_0$ , although a very similar addition reaction is involved in both cases. The difference was attributed<sup>8,9</sup> to the inductive effect of the carbonyl group in the imide structure. As the disparity between these two constants seemed to us rather too large to be explained by an inductive effect we decided to carry out a more direct study of the problem. The rates of addition of *N*-benzoylpyrrolidone, *N*-acetylpyrrolidone, *N*-methyl-

pyrrolidone and pyrrolidone to pyrrolidonate MgBr were measured in tetrahydrofuran solution, and the results are discussed below.

## RESULTS

The reaction of benzoylpyrrolidone and pyrrolidone-MgBr in THF leads to an addition compound. This was shown by isolation of the dimer, m.p. 121°C., in good agreement with Sekiguchi.<sup>13</sup> The addition reaction was shown to be second order by plotting  $[(1/c) - (1/c_0)]$  versus time (Fig. 1). In these experiments, the benzoylpyrrolidone and the pyrrolidonate were taken in a ratio of 1:1 and the initial concentrations were  $4.5 \times 10^{-2}$ ,  $9.0 \times 10^{-2}$ , and  $2.1 \times 10^{-2}$  mole/l. The second-order plot was linear up to 90% conversion, and the rate constant at 25°C. was  $9.5 \times 10^{-2}$  l./mole-sec.

Experiments with a ratio of benzoylpyrrolidone to pyrrolidonate ion equal to 2 or 0.5 showed that a 1:1 addition product was formed, the excess of the other component remaining in solution.

It should be noted that a precipitate is formed a short while after mixing of the reactants. Apparently the dimeric species is not soluble in THF. This should not, however, interfere with our results, as both reacting components remain in solution. It could mask the backward reaction if the reaction is reversible. The precipitate formed even when the initial

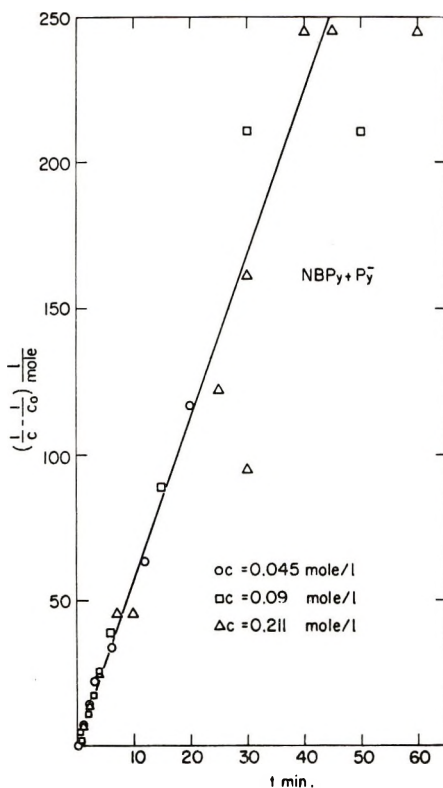


Fig. 1. Second-order plot of the addition reaction of *N*-benzoylpyrrolidone to pyrrolidonate MgBr.

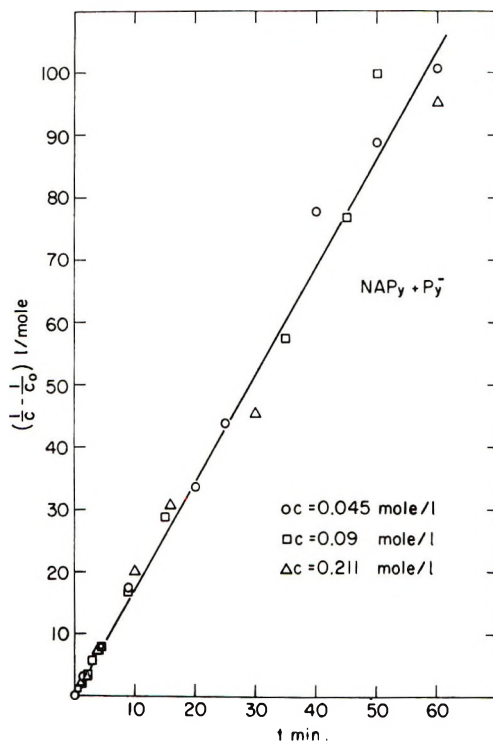


Fig. 2. Second-order plot of the addition reaction of *N*-acetylpyrrolidone to pyrrolidionate MgBr.

concentration was as low as  $10^{-2}M$ . For technical reasons we could not go to lower concentrations, as impurities began to interfere with the reaction. The same precipitation phenomenon was also observed by Graf et al.<sup>6</sup> They worked with *N*-tosyldimethylazetidione and the Na salt of the lactam in dimethyl sulfoxide solution. They claim that a precipitate of the Na salt of the dimer was formed after a few minutes.

The same procedure was followed for the addition of acetylpyrrolidone to PyMgBr. Here, too, the reaction follows a second-order equation, as shown in Figure 2. The value of the rate constant  $k$  was  $2.8 \times 10^{-2}$  l./mole-sec. ( $25^{\circ}C.$ ).

The situation with *N*-methylpyrrolidone is quite different. The reaction does not go to completion, and an equilibrium is attained after a few hours. The equilibrium constant  $K$  was calculated for different ratios of NMePy/Py<sup>-</sup> and was found to be 10 l./mole. The reaction rate data were, therefore, plotted as an equilibrium reaction (Fig. 3), and the forward rate constant  $k$  was found to be  $5 \times 10^{-4}$  l./mole-sec. Thus, the backward reaction constant can be calculated as  $5 \times 10^{-5}$  sec.<sup>-1</sup>.

In order to determine the rate of reaction of pyrrolidone with PyMgBr, equal concentrations of both reactants were mixed and allowed to react for different periods. It was found that no reaction occurred after 7 hr. but in an experiment left for 9 days there was 10% conversion from an initial pyrrolidone concentration of 0.13M, and in another experiment 5%

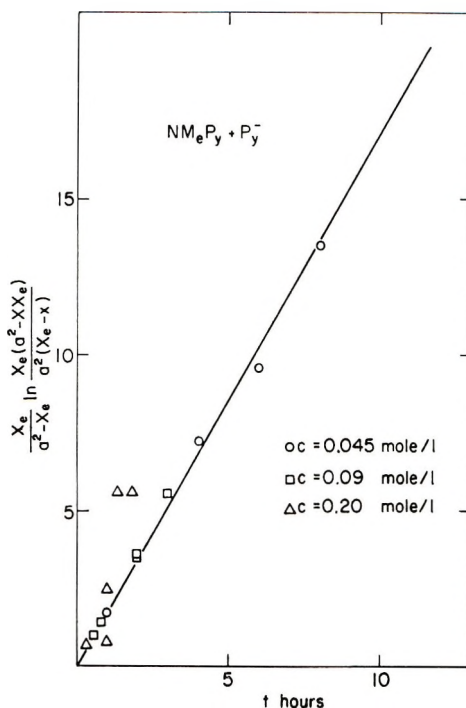


Fig. 3. Plot of the reversible reaction between *N*-methylpyrrolidone and pyrrolidionate ion.

conversion was attained after 8 days from an initial concentration of 0.08*M*.

In order to calculate  $k_0$  we can assume a constant rate of initiation for low conversions:

$$d[I]/dt = k_0[\text{Py}^-][\text{PyH}] = k_0a^2$$

where  $a = [\text{Py}^-] = [\text{PyH}]_0$ , I is the dimeric initiation species. Then

$$[I] = k_0a^2t$$

and the rate of polymerization will be

$$d[\text{P}]/dt = k_p [I][\text{Py}^-] = k_pk_0a^3t$$

$$[\text{Py}] = 1/2k_0k_pa^3t^2$$

From this we can estimate  $k_0 = 3 \times 10^{-9}$  l./mole-sec.

## DISCUSSION

The reaction of addition of *N*-benzoyl- and *N*-acetylpyrrolidone is equivalent to step (2a) in the polymerization mechanism. We actually measure the addition step and we assume that the ring-opening step is faster, as it gives rise to an anion which is stabilized by resonance with the carboxyl group [eq. (4)].







## EXPERIMENTAL

After a long search for a homogeneous system we found that THF could be used as a solvent, provided that pyrrolidone MgBr was used as catalyst instead of the alkali salts. It was known<sup>10</sup> that Grignard reagents can bring about polymerization of lactams, but the lactam salt itself in an inert solvent was not studied before.

### Preparation of Pyrrolidone MgBr

THF was first purified rigorously by continuous reflux over Na benzophenone followed by distillation. Pyrrolidone was dried over Na pyrrolidone and distilled in a high vacuum.

Butylmagnesium bromide was freshly prepared in dry THF. It was then added dropwise, under fast mixing and cooling to an equimolar dilute solution of pyrrolidone in THF. Under these conditions only a Zerevitinov reaction on the amide hydrogen took place. The reaction was complete, as no butane gas was formed by addition of water to an aliquot of the reaction mixture. There was no unreacted pyrrolidone left as shown by chromatographic analysis. The catalyst was kept under dry nitrogen in a flask with a self-sealing stopper, and the required amounts were withdrawn by a syringe.

### Pyrrolidones

*N*-Benzoylpyrrolidone was prepared according to Sekiguchi.<sup>11</sup> Needle-form crystalline *N*-benzoylpyrrolidone melted at 92.5°C. A solution injected into the gas chromatograph showed a single peak. It was kept in a desiccator over P<sub>2</sub>O<sub>5</sub>.

*N*-Acetylpyrrolidone was prepared according to Hall et al.<sup>12</sup> The product boiled at 99°C./4 mm. Hg, and its purity was checked by gas chromatography.

*N*-Methylpyrrolidone from General Aniline and Film Corporation was rigorously purified by vacuum distillation (b.p. 78°C./10 mm. Hg).

### Chromatographic Analysis

The analysis was performed by injecting the reaction mixture into a gas chromatograph (F & M Model 500) with a hot wire detector and a column packed with diethylene glycol polyester adipate (IAC-2-R-466, Cambridge, Ind.) and 2% H<sub>3</sub>PO<sub>4</sub> on Chromosorb W (25:100 by weight), 30-60 mesh. Column temperature was 220°C. The block and injector were kept at 270°C. For every analysis 10 μl. was used. A standard solution was added for calibration before every analysis, and the concentrations were determined in reference to the standard solution.

A measured volume of a solution of the cocatalyst and pyrrolidone was injected into a small reaction flask under dry nitrogen. The calculated amount of the pyrrolidone MgBr was then injected and mixed quickly. After the specified period, the reaction was stopped by injecting glacial acetic acid to the mixture. The solution was then analyzed chromatographically. In most cases only the cocatalyst concentration was fol-

lowed, but in some control experiments the pyrrolidone liberated by the acetic acid was also analyzed. All the experiments were carried out at 25°C.

This paper is taken in part from the Ph.D. thesis of S. Barzakay.

### References

1. S. Barzakay, M. Levy, and D. Vofsi, *J. Polymer Sci. B*, **3**, 601 (1965).
2. G. Champetier and H. Sekiguchi, *J. Polymer Sci.*, **48**, 309 (1960).
3. J. Sebenda and J. Kralicek; *IUPAC Symposium on Macromolecular Chemistry, 1959, Weisbaden* (Weinheim, Short Communications, III-C-6 Verlag Chemie).
4. O. Wichterle, J. Sebenda, and J. Kralicek; *Fortschr. Hochpolymer. Forsch.*, **2**, 578 (1961).
5. W. Sorenson and T. W. Campbell, *Preparative Methods of Polymer Chemistry*, Interscience, New York, 1961, p. 238.
6. R. Graf, G. Lohaus, K. Borner, E. Schmidt, and H. Bestian, *Angew. Chem. Intern. Ed.*, **1**, 481 (1962).
7. H. Sekiguchi, *Bull. Soc. Chim. France*, **1960**, 1831.
8. H. Sekiguchi, *J. Polymer Sci. A*, **1**, 1627 (1963).
9. R. P. Scelia, S. E. Schonfeld, and L. G. Donaruma, *J. Appl. Polymer Sci.*, **8**, 1363 (1964).
10. W. Griell and S. Schaaf, *Makromol. Chem.*, **32**, 170 (1959).
11. H. Sekiguchi, *Bull. Soc. Chim. France*, **1960**, 1827.
12. H. K. Hall, Jr., M. K. Brandt, and R. M. Mason; *J. Am. Chem. Soc.*, **80**, 6420 (1958).
13. H. Sekiguchi, *Bull. Soc. Chim. France*, 1960, 1835.
14. M. Tsuboi, *Bull. Chem. Soc. Japan*, **22**, 215, 255 (1949).
15. N. V. Mikhailov, M. V. Shoblygin, and A. V. Volokhim; *Vysokomolekule. Soedin.*, **5**, 1756 (1963).
16. C. M. Lee, and W. D. Kumler, *J. Am. Chem. Soc.*, **83**, 4593 (1961).
17. C. M. Lee and W. D. Kumler, *J. Am. Chem. Soc.*, **84**, 571 (1962).
18. R. Janssen, *Proceedings of the International Meeting on Molecular Spectroscopy, 4th Meeting Bologna, 1959*, Vol. 2, Pergamon Press, London, 1962, p. 820.

### Résumé

Les vitesses d'addition de bromure de pyrrolidonate magnésium (PyMgBr) à la *N*-benzoyl, *N*-acétyl, et *N*-méthyl pyrrolidone ont été mesurées en solution dans le tétrahydrofurane (THF). La valeur trouvée pour les constantes de vitesse était  $9.5 \times 10^{-2}$ ,  $2.8 \times 10^{-2}$  et  $5 \times 10^{-4} \text{ l}^{-1} \text{ mole}^{-1} \text{ sec}^{-1}$ , respectivement. La constante de vitesse pour l'addition de PyMgBr à la pyrrolidone a également été mesurée et trouvée être égale à  $3 \times 10^{-9} \text{ l/mole}^{-1} \text{ sec}^{-1}$ . Les causes possible pour cette grande différence entre les valeurs de ces constantes sont soumises à discussion.

### Zusammenfassung

Die Additions geschwindigkeit von Pyrrolidonatmagnesiumbromid (PyMgBr) an *N*-Benzoyl-, *N*-Acetyl- und *N*-Methylpyrrolidon wurde in Tetrahydrofuranlösung (THF) gemessen. Für die Geschwindigkeitskonstanten wurden die Werte  $9,5 \cdot 10^{-2}$ ,  $2,8 \cdot 10^{-2}$  und  $5 \cdot 10^{-4} \text{ l/Molsec}$  gefunden. Weiters wurde die Geschwindigkeitskonstante für die Addition von PyMgBr an Pyrrolidon gemessen und zu  $3 \cdot 10^{-9} \text{ l/molsec}$  bestimmt. Die möglichen Ursachen für die grossen Unterschiede zwischen den Werten dieser Konstanten werden diskutiert.

Received January 6, 1966

Revised February 6, 1966

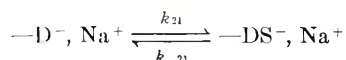
Prod. No. 5076A

## Anionic Copolymerization of Styrene and 1,1-Diphenylethylene

E. URETA, J. SMID, and M. SZWARC,  
*Department of Chemistry, State University College of Forestry at  
 Syracuse University, Syracuse, New York*

### Synopsis

Kinetics of anionic copolymerization of styrene (S) and 1,1-diphenylethylene (D) were investigated in THF. The rate constant of addition of D to living polystyrene was found to be  $k_{1,2\pm} = 250$  l./mole-sec. for  $\sim\sim\text{S}^-$ ,  $\text{Na}^+$  ion-pair, and that for the free  $\sim\sim\text{S}^-$  ion is  $k_{1,2} \sim 400,000$  l./mole-sec. Both values refer to 25°C. The addition of styrene to  $-\text{D}^-$ ,  $\text{Na}^+$  was found to be reversible:



and  $k_{2,1}$  was determined by three different methods to be  $\sim 0.5$ – $0.7$  l./mole-sec. Studies performed in a stirred-flow reactor led to  $k_{-21} = 13$  sec.<sup>-1</sup> and  $K_{21} \sim 5 \times 10^{-2}$  l./mole. An alternating copolymer is obtained in the presence of a large excess of 1,1-diphenylethylene.

Anionic copolymerization of 1,1-diphenylethylene (D) and styrene (S) in THF was thoroughly investigated in our laboratory.<sup>1</sup> Although the system is complex, much information was obtained about the rates of individual steps. These are reported in this paper.

### Addition of 1,1-Diphenylethylene to Living Sodium Polystyrene

The addition of 1,1-diphenylethylene to living polystyrene in THF was found to be very rapid, and the reaction was therefore studied by a capillary-flow method<sup>2</sup> at high rates of flow. The total concentration of active ends was determined by allowing the mixture to flow into a solution of THF containing methyl iodide and titrating the resulting sodium iodide. The flow time was varied by adjusting the nitrogen pressure over the reacting solutions. The mixture was terminated in wet THF and the concentration of the residual 1,1-diphenylethylene was determined by vapor-phase chromatography with the use of an ionization-hydrogen flame detector using biphenyl as an internal standard. A typical run is shown in Figure 1, and the second-order rate constants, calculated on the assumption of a plug flow,<sup>2,3</sup> are reported in Table I.

The apparent second-order rate constant appears to increase substantially as the  $\sim\sim\text{S}^-$ ,  $\text{Na}^+$  concentration is decreased. This phenomenon has

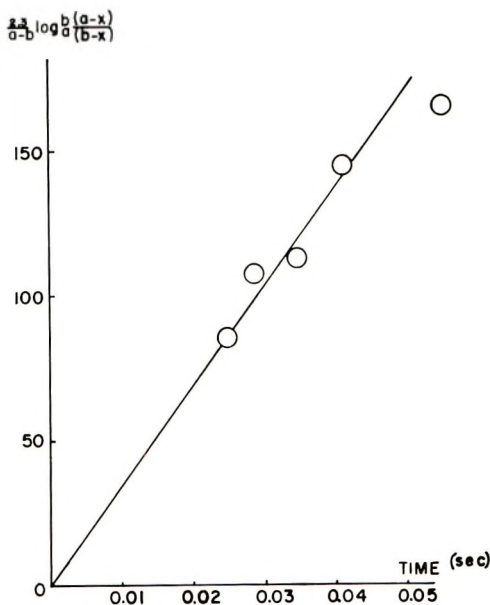


Figure 1.

been observed in nearly all anionic homopolymerization and copolymerization processes carried out in tetrahydrofuran.<sup>2-4</sup> A quantitative investigation<sup>5</sup> of the anionic homopolymerization of styrene in THF has shown that formation of very reactive free  $\sim\text{S}^-$  ions is responsible for the increase in the apparent rate constant on lowering the concentration of active ends. The reactivity of the free  $\sim\text{S}^-$  ion was found to be about 800 times higher than that of the  $\sim\text{S}^-, \text{Na}^+$  ion pair. Addition of sodium tetraphenylboron suppresses the dissociation and decreases the apparent rate constant.<sup>5,6</sup>

In a copolymerization, the reacting ion pair is replaced by a new ion pair which may have a different degree of dissociation. For example, in THF at 25°C. the dissociation constant of  $\sim\text{S}^-, \text{Na}^+$  is  $K_d = 1.5 \times 10^{-7}$  mole/l.,<sup>5-7</sup> while for  $-\text{D}^-, \text{Na}^+$ ,  $K_d \approx 8 \times 10^{-7}$  mole/l.<sup>8</sup> Formation of  $\sim\text{D}^-$ ,

TABLE I  
Addition of 1,1-Diphenylethylene to  $\sim\text{S}^-, \text{Na}^+$  in THF at 25°C.

$[\sim\text{S}^-, \text{Na}^+]_0$ $\times 10^3$ , mole/l.	$[\text{D}]_0 \times 10^3$ , mole/l.	$k_{12}$ , l./mole-sec.
1.8	0.6	4300
2.0	1.7	3600
3.9	3.2	2200
10.6	2.5	1920
11.4	4.7	1600
15.9	19.5	1220
16.0	13.0	1500
16.5	11.1	1430



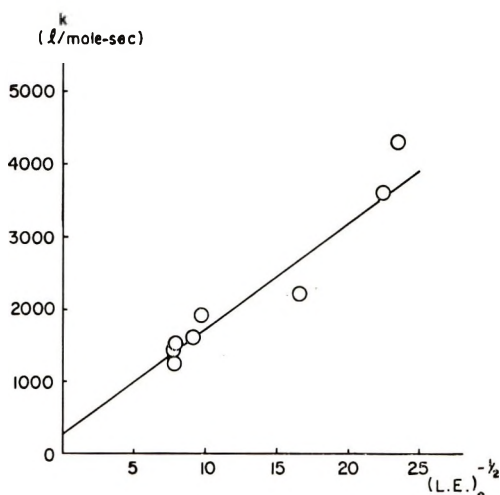


Figure 2.

$\text{Na}^+$  suppresses, therefore, the dissociation of  $\sim\text{S}^-$ ,  $\text{Na}^+$  causing a slow-down of the addition of D to  $\sim\text{S}^-$ ,  $\text{Na}^+$ . On the other hand, a decrease in  $\sim\text{S}^-$ ,  $\text{Na}^+$  concentration, due to its conversion into  $\sim\text{D}^-$ ,  $\text{Na}^+$ , increases the fraction of  $\sim\text{S}^-$ ,  $\text{Na}^+$  dissociation, thus partially counterbalancing the buffering effect of  $\sim\text{D}^-$ ,  $\text{Na}^+$ . Nevertheless, one should expect some gradual decrease of the rate over and above that expected in a bimolecular reaction, and, therefore, a curvature in the second-order plot. This indeed was observed in many runs. The curvature may be minimized by working with as low as possible initial concentrations of the 1,1-diphenylethylene and by keeping the conversion low. The quoted  $k_{1,2}$  values are derived from the initial slopes, if a curvature was observed, and hence they are only slightly affected by the complicating factors discussed above.

A plot of  $k_{1,2}$  versus  $1/[\text{liv. polystyrene}]^{1/2}$  is shown in Figure 2. The intercept gives  $k_{1,2 \pm}$  for the  $\sim\text{S}^-$ ,  $\text{Na}^+$  ion pair, viz.,  $250 \pm 50$  l./mole-sec.; the slope, which is equal to 150, gives  $k_{1,2-} K_d^{1/2}$ . Hence, the rate constant of D addition to  $\sim\text{S}^-$  ion is about 400,000 l./mole-sec. These two constants should be compared with the corresponding rate constants of homopolymerization of styrene in THF, viz.,  $k_{11 \pm} = 80$  l./mole-sec. and  $k_{11-} = 65,000$  l./mole-sec. In both reactions 1,1-diphenylethylene is substantially more reactive than styrene.

#### Addition of Styrene to the Sodium Dimer of 1,1-Diphenylethylene, $\text{Na}^+$ , $-\text{DD}^-$ , $\text{Na}^+$

The addition of styrene to the sodium dimer of 1,1-diphenylethylene was studied by a variety of techniques. In the first method,  $\text{Na}^+$ ,  $-\text{DD}^-$ ,  $\text{Na}^+$  and styrene, both in THF, were mixed in about 1 sec. and the reaction allowed to proceed to completion. The initial and final concentrations of  $-\text{D}^-$ ,  $\text{Na}^+$  ends were determined spectrophotometrically by using the 470-

$m\mu$  peak of  $-D^-$ ,  $Na^+$  ( $\epsilon = 26,000$ ) and correcting it for the contribution of the  $-S^-$ ,  $Na^+$  formed ( $\epsilon$  of the latter at  $470 m\mu$  is 2060).

It was shown<sup>9</sup> that the ratio  $k_{11}/k_{21}$  may be calculated from the equation,

$$[S]_0/[D^-]_0 = f - (k_{11}/k_{21})[\ln(1 - f) + f] \quad (1)$$

where  $[S]_0$  and  $[D^-]_0$  denote the initial concentrations of styrene and  $-D^-$ ,  $Na^+$  respectively, and  $f$  is the fraction of  $-D^-$ ,  $Na^+$  ends converted into  $-S^-$ ,  $Na^+$ , viz.,  $f = ([D^-]_0 - [D^-]_\infty)/[D^-]_0$ .

Table II summarizes the results of a series of experiments performed at 20, 0, and  $-20^\circ C$ . with widely varying  $[S]_0/[D^-]_0$  ratios, and the respective values of  $k_{11}/k_{21}$  are listed in the last column of the table. In spite of the sixfold variation in  $[S]_0/[D^-]_0$ ,  $k_{11}/k_{21}$  is reasonably constant. This may be somewhat surprising in view of the oversimplification of the kinetic scheme. For example, the small fraction of free ions present in the solution (both  $-D^-$  and  $-S^-$ ) affects the respective rate constants  $k_{21}$  and  $k_{11}$ , but this is not considered in the kinetic scheme leading to eq. (1). Fortunately, the buffering effect of  $-D^-$ ,  $Na^+ \rightleftharpoons D^- + Na^+$  depresses the changes in  $k_{11}$  and this justifies, at least partially, the validity of the proposed kinetics. Calculations show that under our experimental conditions  $k_{11}$  varies only from 250 l./mole-sec. to 350 l./mole-sec., and hence  $k_{21} \approx 0.5$  l./mole-sec. This value represents some average of  $k_{2,1\pm}$  and  $k_{2,1-}$ .

It is reassuring that analogous experiments performed with  $HC(C_6H_5)_2^-$ ,  $Na^+$  led to similar values of  $k_{11}/k_{21}'$  (see Table III). This should be expected, because  $-D^-$ ,  $Na^+$  and  $HC(C_6H_5)_2^-$ ,  $Na^+$  are structurally similar.

Alternatively, the reaction  $-D^-$ ,  $Na^+ + S \rightarrow -D.S^-$ ,  $Na^+$  was investigated by a stop-flow technique,<sup>10</sup> in which the disappearance of the  $470\text{-}m\mu$  peak on addition of styrene was followed. The reactants were

TABLE II  
Addition of Styrene to  $Na^+$ ,  $-DD^-$ ,  $Na^+$  in THF

Temp., $^\circ C$ .	$2[-DD^-]_0$ $\times 10^3$ , mole/l.	$[S]_0$ $\times 10^3$ , mole/l.	$[S]_0/$ $2[-DD^-]_0$	$f$	$k_{11}/k_{21}$	Avg. $\frac{k_{11}}{k_{21}}$
25	5.85	1810	309	0.733	510	540 $\pm 25$
25	7.00	1520	217	0.613	640	
25	3.67	690	188	0.658	450	
25	4.14	699	169	0.623	480	
25	3.54	345	97	0.503	500	
25	3.71	348	94	0.488	510	
25	5.56	278	50	0.351	630	
25	5.50	283	51	0.358	600	575 $\pm 90$
0	4.10	704	172	0.613	510	
0	4.10	528	129	0.539	550	
0	4.13	349	84	0.466	580	
$-20$	2.60	822	316	0.578	1100	1240 $\pm 30$
$-20$	2.58	482	187	0.459	1200	
$-20$	2.63	482	183	0.430	1400	
$-20$	2.50	340	136	0.394	1300	

TABLE III  
Addition of Styrene to  $\text{HC}(\text{C}_6\text{H}_5)_2^-$ ,  $\text{Na}^+$  in THF at 25°C.

$[\text{C}^-, \text{Na}^+]_0$ $\times 10^3$ , mole/l.	$[\text{S}]_0 \times 10^3$ , mole/l.	$[\text{S}]_0/[\text{C}^-, \text{Na}^+]_0$	$f$	$k_{11}/k_{21}'$
2.49	94.2	37.8	0.389	360
2.47	94.6	38.3	0.349	460
1.70	71.9	42.3	0.366	470
1.70	76.3	45.0	0.438	320
3.86	297.0	77.0	0.398	700
1.08	91.3	84.5	0.552	340
3.67	412.0	112.	0.517	540
3.67	515.0	140.	0.515	680
3.42	557.0	163.	0.581	570
1.17	339.0	289.	0.767	420
0.98	333.0	340.	0.699	680
1.04	360.0	344.	0.743	600
0.91	420.0	464.	0.838	470
1.44	740.0	515.	0.834	530
1.37	760.0	553.	0.840	560

rapidly mixed in a T-shaped Teflon stopcock, and the reaction mixture then flowed through an optical cell, the time elapsing between mixing of the reagents and their reaching the cell being about 0.1 sec. After a short time, the flow was stopped and the change of optical density at 470  $\mu$  with time was recorded with a Cary spectrophotometer. The initial slope of the recorder tracing was used to calculate the rate constant  $k_{21}$ .

Two experiments were performed by applying this technique and the results are listed in Table IV. The slopes are rather steep and reliable only to about 20%. It is gratifying to see that the value for  $k_{21} = 0.7$  l./mole.-sec. is close to that obtained by the first method ( $\sim 0.5$  l./mole.-sec.).

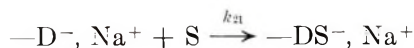
The most detailed information about the reaction  $-\text{D}^-, \text{Na}^+ + \text{S} \rightleftharpoons -\text{DS}^-, \text{Na}^+$ , was obtained by applying the stirred-flow technique.<sup>11,12</sup> This method proved to be useful in some previous studies accomplished in this laboratory;<sup>13,14</sup> a detailed description of the experimental technique is given elsewhere.<sup>13</sup>

TABLE IV  
Determination of  $k_{21}$  by the Stop-Flow Technique

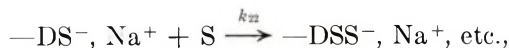
$2[\text{Na}^+,$ $-\text{DD}^-, \text{Na}^+]_0$ $\times 10^3$ , mole/l.	$[\text{S}]_0 \times 10^3$ , mole/l.	$-\frac{d(\text{OD at } 470 \text{ m}\mu)}{dt}$	$k_{21}$ , l./mole-sec. <sup>a</sup>
1.18	356	0.22	0.64
0.85	324	0.18	0.78

<sup>a</sup>  $k_{21}$  is the apparent rate constant.  $k_{21}$  for the free  $-\text{D}^-$  ion cannot be larger than 25 l./mole-sec. The value of  $k_{21}$  is not affected by the reversibility of the addition, i.e., by the reaction  $-\text{DS}^-, \text{Na}^+ \rightarrow -\text{D}^-, \text{Na}^+ + \text{S}$ , because the excess of styrene is so large.

If the reactions



and



suffice to describe the process, then the following balance equations apply to the reaction in a stirred-flow reactor,

$$\{k_{21}[-D^-, Na^+][S] + k_{11}[-S^-, Na^+][S]\} t = [S]_0 - [S] \quad (2)$$

$$\{k_{21}[-D^-, Na^+][S]\} t = [-D^-, Na^+]_0 - [-D^-, Na^+] \quad (3)$$

$t$  denotes the residence time while  $[-D^-, Na^+]$  and  $[S]$  are the stationary concentrations of the respective reagents, which, for the sake of brevity, are denoted by  $D^-$  and  $S$ . Since  $[S^-] = [D^-]_0 - [D^-]$  and  $k_{11} \gg k_{21}$ , the results may be approximated by the equation

$$[D^-]_0 - [D^-] = ([S]_0 - [S])/k_{11}[S]t \quad (4)$$

leading to

$$([S]_0 - [S])/[S]^2[D^-] = k_{11} k_{21} t^2 \quad (5)$$

$[S]_0$ ,  $[S]$ , and  $[D^-]_0$  are obtained from experimental data, but unfortunately our apparatus did not allow us to determine  $[D^-]$ . However,  $[D^-]$  may be calculated from eq. (4) if  $k_{11}$  is estimated from the experimental conditions maintained in the runs, using the known values of  $k_{11\pm}$  and  $k_{11-}$ . Thus, one finds that  $k_{11}$  is not smaller than 350 l./mole-sec. and not greater than 440 l./mole-sec. We shall use, therefore, the value of  $k_{11} = 400$  l./mole-sec. for all subsequent calculations of  $[D^-]$ .

It follows from eq. (5) that a plot of  $([S]_0 - [S])/[S]^2[D^-]$  versus  $t^2$  should give a straight line with a slope of  $k_{11} k_{21}$ , and such plots are indeed linear, but, as shown in Table V, they do not have a constant slope. This indicates that the proposed mechanism is not yet completed.

The steric hindrance encountered in the addition of styrene to  $-D^-$ ,  $Na^+$  suggests that the addition may be reversible, viz.,

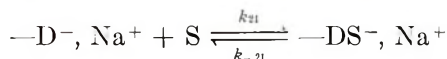


TABLE V  
Values of  $k_{11}k_{21}$  Obtained from the Slope of Plots of  $([S]_0 - [S])/[S]^2[D^-]$  Versus  $t^2$

$[-D^-]_0 \times 10^3$ , mole/l.	$[S]_0 \times 10^3$ , mole/l.	$k_{11}k_{21}$
2.0	5.0	30
1.8	8.8	44
1.1	16.0	100
1.7	35.0	128

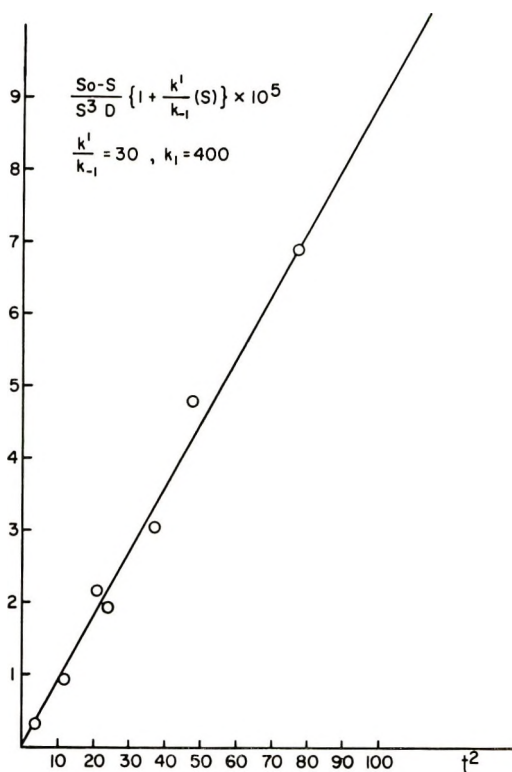


Figure 3.

Assuming reversibility of the addition of the first styrene unit to  $-D^-$ , we derive then the following balance equations:

$$[S_0] - [S] = \{k_{21}[D^-][S] - k_{-21}[X] + k_{11}([D^-]_0 - [D^-])[S]\}t \quad (6)$$

$$[D]_0 - [D^-] = \{k_{21}[D^-][S] - k_{-21}[X]\}t \quad (7)$$

$$[X] = \{k_{21}[D^-][S] - k_{-21}[X] - k_{11}[X][S]\}t \quad (8)$$

where  $[X]$  denotes the stationary concentration of  $-DS^-$ ,  $Na^+$ . These equations lead to

$$[S]_0 - [S] = k_{21}[D^-][S](1 + k_{11}[S]t)^2 / (1/t + k_{-21} + k_{11}[S]) \quad (9)$$

and

$$[D^-]_0 - [D^-] = ([S]_0 - [S]) / (1 + k_{11}[S]t) \quad (10)$$

It should be noticed, however, that under our experimental conditions,  $1/t \ll k_{-21} + k_{11}[S]$  and  $k_{11}[S]t \gg 1$ ; hence, eq. (9) may be approximated by eq. (11),

$$\{([S]_0 - [S]) / [S]^3 [D^-]\} \{1 + (k_{11}/k_{-21})[S]\} = K_{21}k_{11}^2 t^2 \quad (11)$$



where  $K_{21} = k_{21}/k_{-21}$ . Therefore, a plot of the left-hand side of eq. (11) versus  $t^2$  should give a straight line with a constant slope  $K_{21}k_{11}^2$ . We estimated the  $k_{11}$  value to be 400 l./mole.-sec. (see the preceding discussion), and hence we calculate  $[D^-]$  from eq. (10). By applying a method of successive approximations, we find  $K_{21}$  and  $k_{11}/k_{-21}$  from plots representing eq. (11), while  $k_{21}$  has been derived from the stop-flow experiments (see Table IV). For the sake of illustration, a plot of the left-hand side of eq. (11) versus  $t^2$  is shown in Figure 3. The final results are given in Table VI and show that  $K_{21}k_{11}^2$  is now constant if  $k_{11}/k_{-21} = 30$ . Hence,  $K_{21} = 5.5 \times 10^{-2}$  l./mole and  $k_{-21} = 13$  sec.<sup>-1</sup>.

TABLE VI  
Values of  $K_{21}k_{11}^2$  Obtained from the Slopes of Plots of  
 $\{([S]_0 - [S])/[S]^2[D^-]\}(1 + k_{11}[S]/k_{-21})$  Versus  $t^2$

$[-D^-]_0$ $\times 10^3$ , mole/l.	$[S]_0$ $\times 10^3$ , mole/l.	Range of S conversion, %	$K_{21}k_{11}^2$ , l. <sup>3</sup> /mole <sup>2</sup> -sec.
2.0	5.0	1-25	8,500
1.8	8.0	1-25	8,000
1.1	16.0	5-22	11,000
1.7	35.0	3-28	9,000
			Avg. 9,100 $\pm$ 500

One should inquire to what extent the reversibility of reaction (2,1) affects the results given in Tables II and III. The inclusion of the reaction (-2,1) into the pertinent kinetic scheme modifies the original differential equation. Assuming stationary concentration of  $-DS^-$  we find

$$\frac{d[S]}{d[D^-]} = 1 + \frac{k_{11}([D^-]_0 - [D^-])}{k_{21}[D^-]} (1 - \gamma)^{-1}$$

$$\gamma = (1 + k_{11}[S]/k_{-21})^{-1}$$

instead of

$$\frac{d[S]}{d[D^-]} = 1 + \frac{k_{11}([D^-]_0 - [D^-])}{k_{21}[D^-]}$$

Inspection of Table II shows that  $\gamma \ll 1$  when  $[S]_0$  is large, and hence, under these conditions, the results are not much affected by the reversibility of (2,1).

Finally, it was expected that  $k_{21}$  may be derived from kinetic studies of the copolymerization of styrene and 1,1-diphenylethylene in the presence of an excess of the latter. It was believed that the step,



would be rate-determining, whereas the reaction



would be very fast, thus preventing the addition of styrene, i.e.,



or the reverse of (21). Therefore, one expects in such a reaction the formation of an alternating copolymer,  $\sim\text{DSDS}$ , etc., which has been recently reported by Yuki et al.<sup>15</sup> However, although the reaction conforms with this scheme at higher concentration of living ends, there are deviations at lower living ends concentration even when the 1:1 composition of the copolymer is maintained.

This study was supported by the National Science Foundation.

### References

1. E. Ureta, Ph.D. Thesis, Syracuse, N.Y., July 1963.
2. C. Geacintov, J. Smid, and M. Szwarc, *J. Am. Chem. Soc.*, **84**, 2508 (1962).
3. D. N. Bhattacharyya, C. L. Lee, J. Smid, and M. Szwarc, *J. Am. Chem. Soc.*, **85**, 533 (1963).
4. M. Shima, D. N. Bhattacharyya, J. Smid, and M. Szwarc, *J. Am. Chem. Soc.*, **85**, 1306 (1963).
5. D. N. Bhattacharyya, C. L. Lee, J. Smid, and M. Szwarc, *Polymer*, **5**, 54 (1964); *J. Phys. Chem.*, **69**, 612 (1965).
6. H. Hostalka, R. V. Figini, and G. V. Schulz, *Makromol. Chem.*, **69**, 138 (1964).
7. D. J. Worsfold and S. Bywater; *J. Chem. Soc.*, **1960**, 5234.
8. D. N. Bhattacharyya, unpublished result.
9. M. Szwarc, *Makromol. Chem.*, **35**, 132 (1960).
10. J. Jagur, M. Levy, M. Feld, and M. Szwarc, *Trans. Faraday Soc.*, **58**, 2168 (1962).
11. K. G. Denbigh and F. M. Page, *Discussions Faraday Soc.*, **17**, 145 (1954).
12. B. Stead, F. M. Page, and K. G. Denbigh, *Discussions Faraday Soc.*, **2**, 263 (1947).
13. C. L. Lee, J. Smid, and M. Szwarc, *J. Am. Chem. Soc.*, **85**, 912 (1963).
14. J. Stearne, J. Smid, and M. Szwarc, *Trans. Faraday Soc.*, **60**, 2054 (1964).
15. H. Yuki, K. Kosai, S. Murahashi, and J. Hotta; *J. Polymer Sci. B*, **2**, 1121 (1964).

### Résumé

La cinétique de copolymérisation anionique du styrène (S) et du 1,1 diphényl (D) a été étudiée dans le tétrahydrofuranne. La constante de vitesse d'addition de D au polystyrène vivant a été trouvée être égale à  $k_{1,2\pm} = 250 \text{ l/mole}^{-1} \text{ sec}^{-1}$  pour  $\sim\text{S}^-$ ,  $\text{Na}^+$  comme paire d'ions et la constante de vitesse pour l'ion libre  $\sim\text{S}^-$  est  $k_{1,2-} = 400.000 \text{ l/mole}^{-1} \text{ sec}^{-1}$ . Ces deux valeurs se rapportent à 25°C. L'addition de styrène à  $-\text{D}^-$ ,  $\text{Na}^+$  est réversible et  $k_{2,1}$  a été déterminé par trois méthodes différentes et était égal à de 0.5 à 0.7  $\text{l/mole}^{-1} \text{ sec}^{-1}$ . Des études effectuées dans un réacteur à écoulement sous agitation amène à une valeur de  $k_{-2,1} = 13 \text{ sec}^{-1}$  et  $k_{2,1} \sim 5.10^{-2} \text{ l/mole}$ . Un copolymère alternant est obtenu en présence d'un grand excès de 1,1-diphényléthylène.

### Zusammenfassung

Die Kinetik der anionischen Copolymerisation von Styrol (S) und 1,1-Diphenyläthylen (D) in THF wurde untersucht. Die Geschwindigkeitskonstante der Addition von D an lebendes Polystyrol wurde zu  $k_{1,2\pm} = 250 \text{ l. Mol}^{-1} \text{ sec}^{-1}$  für das  $\text{S}^-$ ,  $\text{Na}^+$ -Ionenpaar und zu  $k_{1,2-} \sim 400.000 \text{ l. Mol}^{-1} \text{ sec}^{-1}$  für das freie  $\text{S}^-$ -Ion bestimmt. Beide

Werte gelten für 25°C. Die Addition von Styrol an  $D^-$ ,  $Na^+$  erwies sich als reversibel (s. englische Zusammenfassung) und  $k_{2,1}$  wurde nach drei verschiedenen Methoden zu  $\sim 0,5$  bis  $0,7$  l. Mol $^{-1}$  sec $^{-1}$  bestimmt. Untersuchungen in einem gerührten Fließreaktor führten zu  $k_{-2,1} = 13$  sec $^{-1}$  und  $k_{2,1} \sim 5 \cdot 10^{-2}$  l. Mol $^{-1}$ . In Gegenwart eines grossen Überschusses von 1,1-Diphenyläthylen wird ein alternierendes Copolymeres erhalten.

Received February 1, 1966

Prod. No. 5077A

## Radiation-Induced Polymerization of Hexafluoropropylene at High Temperature and Pressure

R. E. LOWRY, D. W. BROWN, and L. A. WALL, *National Bureau of Standards, Washington, D.C.*

### Synopsis

The radiation-induced polymerization of hexafluoropropylene was studied in the pressure and temperature ranges of 4,500–15,000 atm. and 100–230°C., respectively. Retardation was a serious problem; data thought to apply to the unretarded polymerization are summarized below. At 1,500 rad/hr. the polymerization rate was 15%/hr. at 230°C. and 15,000 atm. The activation enthalpy and volume are 9.5 kcal./mole and  $-10$  cc./mole, respectively. The rate varies as the square root of the radiation intensity. The largest intrinsic viscosity of the polymer is 2.0 dl./g.; values increase with temperature and pressure. At 130°C. and 10,000 atm. the intrinsic viscosity was the same at two radiation intensities.

### INTRODUCTION

Hexafluoropropylene polymerizes to high polymer when the reaction is initiated at pressures of several thousand atmospheres.<sup>1,2</sup> High-boiling liquids have been produced in radiation-induced polymerizations at low pressure.<sup>3,4</sup> The polymerization kinetics have not been reported previously. The onset of thermal dimerization<sup>5</sup> produces an upper temperature limit to polymerization studies of about 250°C. This paper describes the effect of variations in temperature and pressure on the kinetics of the  $\gamma$ -ray-induced polymerization.

### EXPERIMENTAL

The piston-type pressure vessels have been described.<sup>6</sup> Vacuum loading techniques and methods for achieving the desired pressures and temperatures within the bomb are similar to those described for the polymerization of propylene at high pressure.<sup>7</sup>

Hexafluoropropylene was obtained from two commercial sources. The designations, tank I and tank II, indicate monomer from the Columbia Organic Chemical Co., Columbia, S. Carolina, and Peninsular Chem-Research, Gainesville, Fla., respectively. Analyses of the monomer from the mass spectra could not be made because of lack of a pattern for pure hexafluoropropylene. However, no ions occurred at mass numbers incon-

sistent with perfluoropropylene in the spectrum of monomer from tank I. The spectrum of monomer from tank II contained small ion currents at mass numbers normally associated with unsaturated hydrocarbons containing three or less carbon atoms. The quantities of these ions are too small to allow an identification of the specific compounds present but their approximate concentration based on their percentage of the total ion current is 0.1 mole-%. The infrared spectra of monomer from both tanks were identical and showed no bands not present in published spectra.

Since samples from both tanks appeared extremely pure from their mass spectra, they were used initially without further purification, although they were flash distilled and thoroughly degassed. Relatively self-consistent results were obtained with monomer from tank I. Tank II monomer behaved more erratically on polymerization unless purified by passage over silica gel at  $-15^{\circ}\text{C}$ . or through a preparative-scale vapor-phase chromatograph.

Depending on the molecular weight of the polymer, it was in solution, suspension, or swollen with monomer on opening the bomb at  $-60^{\circ}\text{C}$ . Unconverted monomer was recovered and measured volumetrically on a vacuum line or by passing it through a wet test meter. Both vacuum line and meter were calibrated with weighed monomer. Polymer was either recovered with monomer and isolated on a vacuum line or dissolved from the bomb with hexafluorobenzene. Separated polymer was combined in hexafluorobenzene and isolated by pumping off the solvent under vacuum.

Most conversions were below 5%, and the maximum was 17%. Conversion divided by irradiation time was assumed to represent the polymerization rate. The vessel was irradiated by  $^{60}\text{Co}$ , and dose rates inside the vessel were known.

Solution viscosities were measured in Fluorochemical FC-75, obtained from Minnesota Mining and Mfg. Co., St. Paul, Minn. Molecular weight measurements were made with a vapor-pressure osmometer with the use of hexafluorobenzene as solvent.

The uncertainties in temperature and pressure are  $1^{\circ}\text{C}$ . and 400 atm., respectively; pressure differences of about 100 atm. can be detected and are significant. Reported values of the degree of polymerization  $\text{DP}_n$  and the intrinsic viscosity  $[\eta]$  are uncertain by about 5%.

## RESULTS

Preliminary studies were carried out only with monomer from tank I. Polymerization rates were determined for experiments performed at temperatures between 100 and  $160^{\circ}\text{C}$ . and pressures between 4,500 and 15,000 atm. These results are represented by the symbols in Figure 1 that are open or shaded on the left side. This figure contains three sets of isobaric data plotted in the form  $\log 10^5 R_p - \frac{1}{2} \log T$  versus  $10^3/T$ , where  $R_p$  is the fractional hourly polymerization rate and  $T$  is the absolute



temperature. The open symbols are results obtained at 47,000 rad/hr. The symbols shaded on the left side represent results calculated to 47,000 rad/hr. from other intensities by assuming that  $R_p$  is proportional to the square root of intensity.

Radiation-induced polymerization rates at 47,000 rad/hr. at 150°C. and 15,000 and 4,500 atm. were about 200 times the corresponding thermal polymerization rates. Dimerization was negligible in all these experiments.

When tank I was exhausted, monomer from tank II was used. Subsequently, the temperature range of the experiments was expanded to 100–230°C. The results are represented in Figure 1 by symbols that are

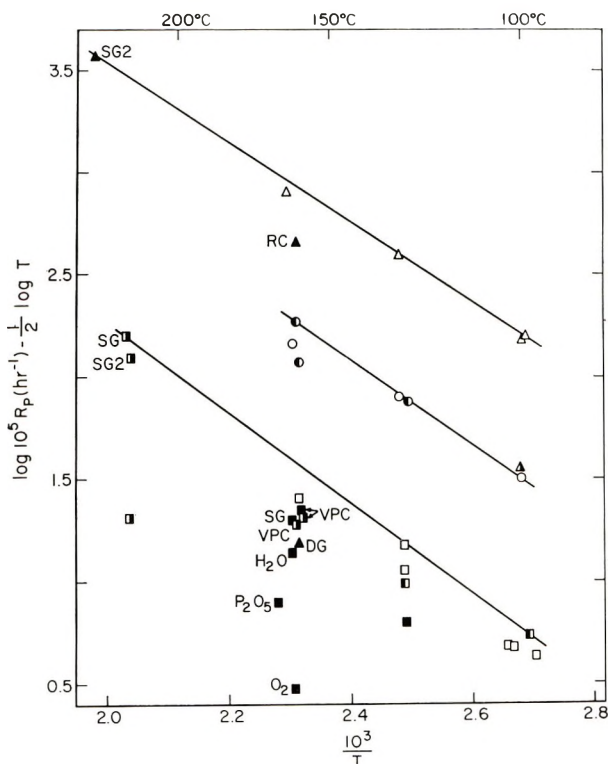


Fig. 1. Polymerization rates at high pressure of perfluoropropylene induced by  $\gamma$ -rays: For 15,000 atm. pressure, ( $\Delta$ ) tank I monomer, 47,000 rad/hr., ( $\blacktriangle$ ) tank II monomer 47,000 rad/hr., ( $\triangle$ ) tank II monomer, calculated for 47,000 rad/hr. from other dose rates; for 10,000 atm. pressure, ( $\circ$ ) tank I monomer 47,000 rad/hr., ( $\bullet$ ) tank I monomer calculated for 47,000 rad/hr. from other dose rates; for 4,500 atm.-pressure, ( $\square$ ) tank I monomer 47,000 rad/hr., ( $\blacksquare$ ) tank I monomer, calculated for 47,000 rad/hr. from other dose rates, ( $\blacksquare$ ) tank II monomer, 47,000 rad/hr., ( $\blacksquare$ ) tank II monomer, calculated for 47,000 rad/hr. from other dose rates; ( $\text{O}_2$ ) 13 parts per million oxygen added; ( $\text{H}_2\text{O}$ ) saturated with water at  $-40^\circ\text{C}$ .; ( $\text{P}_2\text{O}_5$ ) condensed on  $\text{P}_2\text{O}_5$  before final transfer; (DG) more thoroughly outgassed than normal; (RC) recovered monomer; (SG) passed over activated silica gel at  $-15^\circ\text{C}$ .; (SG2) passed twice over activated silica gel at  $-15^\circ\text{C}$ .; (VPC) purified on a preparative-scale vapor-phase chromatograph.

opaque or shaded on the right side. With untreated monomer from this tank, the results were very erratic and always lower than those from tank I. Various treatments, in addition to increasing the temperature range, were tried in attempting to alleviate this problem. Unsuccessful ones were: purposely adding water, drying over  $P_2O_5$ , adding oxygen, performing additional degassing operations, and reusing monomer that had been partially polymerized. Symbols used in Figure 1 to indicate results of these experiments are:  $H_2O$ ,  $P_2O_5$ ,  $O_2$ , DG, and RC, respectively. Results much more comparable to those observed with tank I monomer were obtained by passing the tank II monomer over activated silica gel maintained at about  $-15^\circ C.$  or by purifying the monomer on a preparative-scale vapor-phase chromatograph and then passing it over silica gel at  $25^\circ C.$  Symbols used to indicate these results in Figure 1 are SG and VPC, respectively.

Unsuccessful attempts were made to identify the removable retarder. Vapor-phase chromatograms indicated an impurity level of about 0.1% in the Tank II monomer. The mass spectrogram contained very small peaks characteristic of hydrogen-containing olefins.

In Table I are listed values of the degrees of polymerization ( $DP_n$ ) or intrinsic viscosity of polymers and the corresponding polymerization rates for several replicate experiments. It is seen that values of  $DP_n$  or  $[\eta]$  change in the same direction as  $R_p$ .

In Table II are listed values of  $DP_n$ ,  $[\eta]$ , and  $10^3 R_p$  that were obtained at several temperatures at each reaction pressure. The values chosen are from experiments that gave results most consistent with the isobars drawn in Figure 1. The last two columns in Table II are discussed below.

Certain observations suggest that the polymer samples were slowly attacked by air. A sample of original intrinsic viscosity 0.12 dl./g. was found to have an intrinsic viscosity of 0.10 dl./g. about 6 months later. The difference between these values is only about twice that regarded as significant; in the absence of any other observation one would tend to ignore this decrease. However, acrid gases accumulated above samples stored in air. Peculiar solubility behavior was observed. Solutions of the polymer

TABLE I  
Data from Replicate Experiments at 4,500 atm. Pressure

Temperature, $^\circ C.$	$[\eta]$ , dl./g.	$DP_n$	$R_p \times 10^3$ , hr. $^{-1}$
130		83	3.1
130		65	2.3
160		60	7.1
160		31	5.0
160		14	2.7
220	0.270		34.6
220	0.188		27.2
220	(liquid)		4.5

TABLE II  
Characterization of Polymers Formed at Rates on the Isobars of Figure 1<sup>a</sup>

Conditions		Dose rate, rad/hr. $\times 10^{-3}$	$R_p$ , hr. <sup>-1</sup>	DP <sub>n<sub>a</sub></sub>	[ $\eta$ ], dl./g.	DP <sub>n<sub>b</sub></sub>	$10^{10}R_p$ 4.7 T
$P$ , atm. $\times 10^{-3}$	$T$ , °C.						
4.5	100	140	0.0018	18	0.03	20	27
4.5	130	47	0.0031	83	0.07	94	103
4.5	220	47	0.035	100	0.19	560	1,600
10	100	47	0.0061	62	0.10	180	270
10	130	47	0.016	46	0.12	250	730
10	128	140	0.027		0.14	320	410
10	160	140	0.066		0.24	850	1,020
15	100	47	0.030		0.33	1,500	1,400
15	130	47	0.079		0.59	4,400	3,600
15	160	47	0.173		0.72	6,300	7,900
15	230	1.5	0.152		2.0	38,000	220,000

<sup>a</sup> DP<sub>n<sub>a</sub></sub> is from measurements with a vapor pressure osmometer; DP<sub>n<sub>b</sub></sub> is calculated from a relation determined for fractions of poly-3,3,3-trifluoropropene in acetone, [ $\eta$ ] =  $3.8 \times 10^{-4}$  (96 DP<sub>n</sub>)<sup>0.65</sup>, where [ $\eta$ ] is the intrinsic viscosity at 29.6°C. and DP<sub>n</sub> is the viscosity-average degree of polymerization. It is assumed that DP<sub>n</sub> is 1.5 times DP<sub>n<sub>a</sub></sub>.

in FC-75 were often cloudy. These were cleared by filtration; the fraction of polymer that did not pass the filter was less than one percent. One of our samples appeared initially to be insoluble in FC-75. It dissolved readily in hexafluorobenzene; after being recovered from solution it did dissolve in FC-75. This sample had been removed from the pressure vessel in the form of a solid piece. A sheet of polyperfluoropropylene received several years ago from E. I. DuPont Co. behaved in the same fashion as the solid piece. The intrinsic viscosity of this material in FC-75 was 0.65 dl./g.

TABLE III  
PVT Data for Perfluoropropylene

Pressure, atm. $\times 10^{-3}$	Specific volume, cc./g.		
	100°C.	130°C.	160°C.
2	0.618	0.634	0.642
3	0.583	0.595	0.600
4	0.560	0.568	0.574
5	0.541	0.549	0.556
6	0.527	0.531	0.538
7	0.515	0.518	0.523
8	0.502	0.505	0.513
9	0.491	0.497	0.502
10	0.482	0.487	0.492
11	0.474	0.479	0.484
12	0.467	0.473	0.477
13	0.460	0.467	0.469

These peculiar solubility effects would result if the polymer surface that had been attacked by air became insoluble in FC-75 but remained soluble in hexafluorobenzene. Thus, in FC-75 the surface would become a cage which could pass solvent but not polymer molecules (because of their size). Once dispersed by solution in hexafluorobenzene the original surface would no longer interfere with solution of the bulk of the recovered polymer. Polymer crystallinity is not an explanation of these effects because polyhexafluoropropylene is amorphous.<sup>2</sup>

Dimer was detected in the vapor-phase chromatogram of the monomer recovered from an experiment at 15,000 atm. and 230°C. The dimerization rate is estimated to be about 2%/hr. under these conditions.

In Table III are listed values of pressure and specific volume of hexafluoropropylene at three temperatures. The maximum error in the specific volumes is 0.01 cc./g. but they are precise to 0.002 cc./g. The compressibility and coefficient of thermal expansion decrease with pressure in normal fashion.

## DISCUSSION

### Mechanism

Scattered rate data such as found here indicate that varying amounts of retarder or radiation sensitizer are present. The presence of thermal initiators is ruled out by the low thermal rates. Retardation is indicated rather than sensitization because purification resulted in increased rates rather than decreased rates and because the rate was nearly proportional to the degree of polymerization in replicate experiments (Table I). This is characteristic of retardation under some conditions whereas rate increases due to an increased initiation rate result in lower degrees of polymerization.

It seems likely that some retardation often occurred with tank I monomer as well as purified tank II monomer. With such samples discrepancies between rates in replicate experiments were as much as 50%. In work with propylene, 3,3,3-trifluoropropene, and perfluoropentadiene-1,4, the maximum discrepancy between replicate runs was 10%. The much larger maximum discrepancy encountered with our better hexafluoropropylene probably is not due to a residue of the material removed in the purification, because a sample given two silica gel treatments (point SG2, Fig. 1) did not polymerize faster than a replicate sample given one treatment. We have no firm opinion concerning the source of the difficulty. Certainly the monomer is very sensitive to the presence of oxygen (point O<sub>2</sub>, Fig. 1) but a sample thought to be more thoroughly degassed than our normal standard polymerized rather slowly (point DG, Fig. 1). It is possible that oxygen is more readily dissolved in perfluoropropylene than in nonfluorinated monomers. There is some literature to the effect that some gases, including oxygen, are somewhat more soluble in fluorocarbons than in hydrocarbons.<sup>8</sup>

It is preferred not to write a mechanism including retardation because so little is known about the retarder. If the retarder concentration is sufficiently low the mechanism approaches that for the unretarded polymerization. This is of more value to the study of the effect of monomer structure on polymerization characteristics, which is our chief interest in pursuing this work. Two arguments can be made to the effect that in Figure 1 the highest value plotted for each set of temperatures and pressures applies to the unretarded polymerization. In the first place, all but one of these values are on an applicable isobar even if one allows less than the usual uncertainty of 5% in  $R_p$  and 1°C. in  $T$ . Such systematic behavior would be observed if the residual concentration of retarder were too low to cause retardation. Alternatively, it could result from an appreciable but common retarder concentration. The second argument bears on this possibility. The intrinsic viscosities listed in Table II increase markedly with polymerization temperature, even up to 230°C. One would think that an active foreign species at a concentration sufficient to cause retardation would undergo transfer reactions and cause decreases in the intrinsic viscosity as the polymerization temperature is raised. A comparison of values of  $[\eta]$  or  $DP_n$  of polymer formed at retarded rates (Table I) at different temperatures suggests that this sometimes happens in our system. Thus the behavior of the data in Table II indicates that the retarder concentration is too low to affect  $R_p$  and  $DP_n$  materially.

In view of the above considerations the isobars drawn in Figure 1 are thought to describe the unretarded polymerization. The mechanism is thought to be the  $\gamma$ -ray-initiated radical chain reaction given in eqs. (1)–(4). The rates for the respective reactions are given in eqs. (1a)–(4a).

Initiation:



Propagation:



Transfer:



Termination:



$$(d[R]/dt) = 1.56 \times 10^{-10} [M] G_i I \quad (1a)$$

$$-(d[M]/dt) = k_2 [M] \sum_1^{\infty} [R_n] \quad (2a)$$

$$(d[P]/dt) = k_3 [M] \sum_1^{\infty} [R_n] \quad (3a)$$

$$-(d[R]/dt) = 2k_4 \left( \sum_1^{\infty} [R_n] \right)^2 \quad (4a)$$



The symbols  $M$ ,  $R_n$ , and  $P_n$  represent monomer, radicals, and polymer, respectively, and values in brackets denote concentrations. The  $k$  are rate constants and  $t$  is time; subscripts indicate the number of monomer units in a chain.  $I$  is the radiation intensity and  $G_i$  is the number of radicals formed per 100 e.v. absorbed. The numerical factor in the equation for step (1) has units such that  $d[R]/dt$  is in mole/liter-hour when  $I$  is in rad/hour.

A free-radical mechanism is postulated because the polymerization rate increases with temperature and as the square root of intensity; otherwise values calculated from other intensities to 47,000 rad/hr. by assuming that  $R_p$  is proportional to  $I^{1/2}$  would not fall on the same isobars in Figure 1. A chain mechanism is postulated because as many as 600,000 monomer units are converted to polymer per 100 e.v. absorbed.

Equations for  $R_p$  and  $DP_n$  are obtained by assuming that all radical concentrations are at their steady-state values. These equations are:

$$R_p = \frac{-d[M]}{[M]dt} = 1.25 \times 10^{-5} \left( \frac{G_i I [M]}{2k_4} \right)^{1/2} k_2 \quad (5)$$

$$DP_n^{-1} = \frac{k_3}{k_2} + \frac{2k_4}{k_2^2 [M]} R_p \quad (6)$$

$$= \frac{k_3}{k_2} + \frac{1.56 \times 10^{-10} G_i I}{R_p} \quad (6a)$$

The second term in eqs. (6) and (6a) is half as large if termination is by combination.

### Effect of Temperature and Pressure on $R_p$

Absolute rate theory offers a straightforward interpretation of the effects of temperature and pressure on  $R_p$ . Each second-order rate constant in eq. 1 is replaced by an expression of the form  $k_j = V(kT/h) \exp \{ -\Delta F^*_j / RT \}$ , where  $k_j$  is the rate constant,  $V$  is the molar volume,  $k$  is the Boltzmann constant,  $h$  is the Planck constant,  $T$  is the absolute temperature,  $R$  is the gas constant, and  $\Delta F^*_j$  is the free energy change in forming the transition complex of reaction  $j$ . It is assumed that  $G_i$  is independent of temperature and pressure. This assumption is in accord with the small temperature dependence of radiation-induced reactions that do not proceed by a chain mechanism. Since  $[M]$  is approximately equal to  $V^{-1}$  the rate equation does not contain  $V$ ; it is:

$$R_p = 1.25 \times 10^{-5} (G_i I k T^{1/2} / 2h) \exp \{ -\Delta F^*_2 + 0.5\Delta F^*_4 \} / RT \quad (7)$$

Equation (7) is transformed by standard methods into equations relating  $\log R_p$  to temperature at constant pressure and to pressure at constant temperature.<sup>9</sup> These equations are:

$$\log 10^5 R_p = 1/2 \log T - (\Delta H^*_2 - 0.5\Delta H^*_4) / 2.3RT + C_1 \quad (8)$$

$$\log 10^5 R_p = -[(\Delta V^*_2 - 0.5\Delta V^*_4) / 2.3RT] P + C_2 \quad (9)$$

TABLE IV  
 Thermodynamic Sums in the Rate Expression<sup>a</sup>

Pres- sure, katm.	Temp., °C.	$\Delta H$ , kcal./mole <sup>b</sup>	$-\Delta V^*$ , cc./mole	$\Delta E^*$ , kcal./mole	$\Delta F^*$ , kcal./mole <sup>c</sup>	$-\Delta S^*$ , cal./mole-°C.
4.5	100	10.0 ± 0.5	9.5 ± 0.5	11.0 ± 0.6	15.4 ± 0.1	14.5 ± 1.5
4.5	130	10.0 ± 0.5	10.1 ± 0.5	11.1 ± 0.6	15.8 ± 0.1	14.4 ± 1.5
10	130	9.6 ± 1.0	10.1 ± 0.5	12.1 ± 1.1	14.5 ± 0.1	12.2 ± 2.7
15	130	8.9 ± 0.2	10.1 ± 0.5	12.6 ± 0.4	13.2 ± 0.1	10.7 ± 0.7
15	225	8.9 ± 0.2	11.2 ± 0.5	12.9 ± 0.5	14.3 ± 0.1	10.8 ± 0.7

<sup>a</sup> Each sum is presumed to be made up of two elements and combined in the form  $\Delta_2 - 0.5\Delta_4$ . The uncertainties in the calculated quantities are our best estimates of the maximum errors based on a consideration of all of the factors in the experiment.

<sup>b</sup> The value of  $G_i$  is assumed to be 10.

<sup>c</sup> 1 kcal. = 4.184 kJ.

In these equations  $\Delta H^*$  and  $\Delta V^*$  are the respective enthalpy and volume changes that occur when the transition state forms,  $P$  is the pressure, and the  $C$ 's are integration constants. In deriving these equations it is assumed that  $\Delta H^*_2 - 0.5\Delta H^*_4$  is independent of temperature at constant pressure and  $\Delta V^*_2 - 0.5\Delta V^*_4$  is independent of pressure at constant temperature. In justification of the second assumption, one finds that values of  $\log R_p$  at constant temperature, as calculated from the intersections of  $10^3/T$  with the isobars of Figure 1, vary linearly with  $P$  for temperatures of 100, 130, and 160°C.

In Table IV are listed values of the  $\Delta H^*$  and  $\Delta V^*$  sums which appear in eqs. (8) and (9). The uncertainties listed result if the uncertainties in  $R_p$ ,  $T$ , and  $\Delta P$  are assumed to be 5%, 1°C., and 100 atm., respectively. The  $\Delta H^*$  sums decrease slightly as pressure increases. The  $\Delta V^*$  sums become more negative as the temperature is increased. The  $\Delta E^*$  term is calculated from the relation  $\Delta E = \Delta H - P\Delta V$ ; it increases with pressure and temperature. All the changes in  $\Delta H$ ,  $\Delta V$ , and  $\Delta E$  are barely significant.

Values of the  $\Delta F^*$  sum in Table IV were calculated from eq. (3) by assuming that  $G_i = 10$ . They are about 1 kcal./mole less if  $G_i = 1$ . Values of the entropy sum,  $\Delta S^*_2 - 0.5\Delta S^*_4$ , were calculated from the relation  $\Delta F^* = \Delta H^* - T\Delta S^*$ . Most of the change in the  $\Delta F^*$  sum with pressure at constant temperature is due to the change in the  $\Delta S^*$  term.

By extrapolating rates previously obtained for propylene and perfluoroheptene-1 to 4,500 atm. and 130°C., one finds that hexafluoropropylene under these conditions polymerizes  $1/15$ th as fast as the former and 100 times as fast as the latter.<sup>7,10</sup> The differences result from a lower activation energy for propylene and a more negative entropy term for perfluoroheptene-1.

### Molecular Weight Effects

In view of the influence of air on the polymers, interpretation will be based on values of the intrinsic viscosity. Values of  $DP_n$  may be affected

by the nonpolymeric products of degradation, since the vapor pressure osmometer responds to such materials. This probably accounts for the instances in Table II in which intrinsic viscosity and  $DP_n$  do not vary in the same direction. In addition, between values of  $DP_n$  of about 60 and 100, concentration dependence becomes significant if one works at concentrations sufficiently large to keep the measurement imprecision at about 5–10%. For this reason values of  $DP_n$  greater than 100 are not listed.

The values of  $[\eta]$  listed in Table II cover the range 0.03–2.0 dl./g. A relation between molecular weight and intrinsic viscosity of polyperfluoropropylene has not been developed. However, such a relation was established for fractions of the somewhat similar polymer of 3,3,3-trifluoropropene.<sup>11</sup> It is used to calculate values in the column headed  $DP_{n_b}$  in Table II. The intent is to establish approximate values of  $DP_n$ . The values listed probably can be looked on as upper limits to the true values because acetone is a poor solvent for poly-3,3,3-trifluoropropene.

The last column in Table II is the reciprocal of the last term of eq. (6a) when  $G_i = 3$ . If the monomer transfer constant,  $k_3/k_2$ , is negligible, these values equal  $DP_n$ . Most of the values are about 30% higher than  $DP_{n_b}$ ; this difference is not interpretable because both  $G_i$  and the relation between  $[\eta]$  and  $DP_n$  have been assumed. However, if transfer were of great importance, values in the last column would greatly exceed values of  $DP_{n_b}$ .

There are three instances in Table II where the values in the two columns differ by a factor of three or more. At 220–230°C. at pressures of both 4,500 and 15,000 atm. these larger differences exist. Thus at 4,500 atm. pressure it is indicated that transfer becomes more important as temperature is increased and controls  $DP_n$  at 220°C. This could be due to an increasing transfer constant, a decrease in the second term of eq. (6a) which obscures any change in the transfer constant, or some combination of both effects. At 15,000 atm. at 230°C. transfer also determines  $DP_n$ . Here the dose rate is very low; since the second term of eq. (6a) increases with  $I$ , it increases relative to  $k_3/k_2$  as intensity is increased. Since  $R_p$  is proportional to  $I^{1/2}$ , one calculates that at 47,000 rad/hr. the value in the last column would be 39,000. This is about the same as the value of  $k_2/k_3$ , i.e.,  $DP_{n_b}$ , at 1,500 rad/hr. Thus transfer and termination would be of equal importance in determining  $DP_n$ . In combination with the result at 4,500 atm. it appears that transfer becomes less important as pressure is increased at constant temperature and intensity.

At 130°C., 10,000 atm. pressure, and 47,000 rad/hr.  $DP_{n_b}$  is one third of  $R_p/4.7I \times 10^{-10}$ . The value of  $[\eta]$  is less than a value found at a higher radiation intensity at nearly the same temperature and pressure. This is contrary to the sense of eqs. (6) or (6a), and probably indicates that a foreign material was present that affected  $DP_n$  without decreasing  $R_p$ . It seems unlikely that attack by air caused the result because the subsequent decrease in intrinsic viscosity observed for this sample was only 0.02 dl./g. in 6 months.

Presumably the observed attack on polyperfluoropropene by air is some kind of hydrolytic oxidation through residual double bonds in the polymer. The air above the polymer of highest intrinsic viscosity (2.0 dl./g.) has yet to develop acidity; presumably there are so few double bonds that the attack is very slow.

This paper is based on research supported by the U.S. Army Office, Durham, North Carolina.

Certain commercial materials are identified in this paper in order to adequately specify the experimental procedure. In no case does such identification imply recommendation or endorsement by the National Bureau of Standards, nor does it imply that the material or equipment identified is necessarily the best available for the purpose.

### References

1. H. S. Eleuterio, U.S. Pat. 2,958,685 (1960).
2. H. S. Eleuterio and E. P. Moore, paper presented at Second International Symposium on Fluorine Chemistry, Estes Park, Colorado, 1962; *Preprints*, p. 344.
3. E. V. Volkova and A. I. Skobina, *Vysokomolekul. Soedin.*, **6**, 984 (1964).
4. B. Manowitz, *Nucleonics*, **11**, No. 10, 18 (1953).
5. M. Hauptschein, A. H. Fainberg, and M. Braid, *J. Am. Chem. Soc.*, **80**, 842 (1958).
6. L. A. Wall, D. W. Brown, and R. E. Florin, paper presented to Division of Polymer Chemistry, 140th Meeting, American Chemical Society, Chicago, Ill., September 1961; *Preprints*, p. 366.
7. D. W. Brown and L. A. Wall, *J. Phys. Chem.*, **67**, 1016 (1963).
8. Y. Kobatake and J. H. Hildebrand, *J. Phys. Chem.*, **65**, 331 (1961).
9. S. D. Hamann, *Physico-Chemical Effects of Pressure*, Academic Press, New York, 1957, p. 162.
10. D. W. Brown and L. A. Wall, *SPE Trans.*, **3**, 300 (1963).
11. D. W. Brown, paper presented at 150th Meeting, American Chemical Society, *Polymer Preprints*, **6** [2], 965 (1965).

### Résumé

La polymérisation de l'hexafluoropropylène induite par irradiation a été étudiée sous presse dans un domaine de pression et de température allant respectivement de 4500 à 15.000 atm. et de 100 à 230°C. Le phénomène de retard constituait un problème difficile. Les résultats supposés être applicables à des polymérisations non-retardées sont résumés ci-dessous. À 1.500 rad/h. la vitesse de polymérisation était de 15%/h. à 230°C et sous 15.000 atm. l'enthalpie d'activation et le volume étaient de 9.5 kcal/mole et -10 cc/mole respectivement. La vitesse varie en fonction de la racine carrée de l'intensité de radiation. La viscosité intrinsèque la plus élevée du polymère était de 2.0 dl/gr.; les valeurs croissent avec la température et la pression. A 130°C et sous 10.000 atm. la viscosité intrinsèque était la même pour deux intensités de radiation différente.

### Zusammenfassung

Die strahlungsinduzierte Polymerisation von Hexafluorpropylen wurde im Druckbereich von 4500 bis 15.000 Atm und im Temperaturbereich von 100 bis 230°C untersucht. Als schwieriges Problem erwies sich die Reaktionsverzögerung; Daten, welche für die unverzögerte Polymerisation charakteristisch sein dürften, werden hier angegeben. Bei 1500 rad/h betrug die Polymerisationsgeschwindigkeit 15%/h, bei 230°C und 15.000 Atm. Die Aktivierungsenthalpie ist 9,5 kcal/Mol und das Aktivierungs-

volumen  $-10 \text{ cm}^3/\text{Mol}$ . Die Geschwindigkeit ist der Wurzel aus der Strahlungsintensität proportional. Die grösste für das Polymere gefundene Viskositätszahl beträgt  $2,0 \text{ dl/g}$ . Die Werte nehmen mit Temperatur und Druck zu, und bei  $130^\circ\text{C}$  und  $10.000 \text{ Atm}$  war die Viskositätszahl bei zwei Strahlungsintensitäten gleich.

Received November 12, 1965

Revised February 7, 1966

Prod. No. 5079A



## Radiation-Induced Solid-State Polymerization in Binary Systems. II. Relationship between Polymerization Rate and Physical Structure of Binary Systems

ISAO KAETSU and NORIO SAGANE, *Central Research Laboratory, Sekisui Chemical Company, Osaka, Japan*, and KOICHIRO HAYASHI and SEIZO OKAMURA, *Department of Polymer Chemistry, Kyoto University, Kyoto, Japan*

### Synopsis

The radiation-induced solid-state polymerization of binary systems consisting of acrylic monomer (acrylamide, acrylic acid) and organic compounds was investigated. In the previous paper on binary systems the authors reported that the rate of polymerization increased in the solid state (eutectic mixture systems). The mechanism of rate increase has been investigated by examination of phase diagrams, viscosities, and surface tension of the binary systems. Viscosity and surface tension are the measure of the molecular interaction of the two-component systems. In addition, the effect of linear crystal growth rate and half maximum width of the x-ray diffraction diagram of the crystallization process were determined. The larger the molecular interaction between the two components, the slower the linear crystal growth rate of monomer. The size of the monomer crystal decreases and the dislocation density of the monomer crystals increases in systems with large molecular interaction. Consequently it can be concluded that the physical structure of a binary solid system is the most important parameter determining the rate increase of solid-state polymerization. Dislocation on the grain boundary is more important than defects inside of the crystal lattice. It was found that the acceleration of polymerization rate is large in binary systems with larger molecular interaction. In some systems such as organic acid-amide systems with strong hydrogen bonds, glassy phases may be formed in which monomer may readily polymerize at very low temperatures.

The authors reported previously<sup>1</sup> that almost all two-component systems containing acrylic monomers are eutectic mixtures and that the polymerization rate was higher in the solid state than in pure monomer crystals. The present work concerns this rate-increasing effect of the solid state. It was assumed that both chemical and physical factors may increase the rate of polymerization in binary solid systems. In the present work, mainly the effects of physical state of two components on the solid-state polymerization is studied, in view of the previous report<sup>2</sup> that polymerization of acrylamide in the solid state is affected by defects in monomer crystals. The boundary area or the crystal grain size is adopted as a physical index

sensitive to polymerization of the mixed solid state, because the grain boundary consists of dislocations which are a kind of facial defect. The crystallization process has been investigated by examining the linear growth rate of crystals and changes in the phase diagram. These have been determined experimentally and compared with the interaction of the two components in the liquid phase, as expressed by viscosity and surface tension. Finally, fairly definite relationships have been found between solid-state polymerization rate, grain size, linear crystallization rate, phase diagram factor, and molecular interaction in the liquid phase. It is concluded that acceleration in the solid-state polymerization of two-component systems is predominantly due to physical effects in the mixed state.

## EXPERIMENTAL

Acrylamide, methacrylamide, acrylic acid, and methacrylic acid monomers were used. Systems containing acrylamide or acrylic acid have been investigated in detail. Systems containing methacrylamide or methacrylic acid showed behavior similar to that of the acrylamide or acrylic acid systems. Experimental methods are explained with the results.

## RESULTS AND DISCUSSION

### Phase Diagram Factor

The phase diagrams of several binary systems were investigated by melting point measurements by differential thermal analysis. As is well known, melting point depression in the phase diagram of a eutectic mixture for monomer component A is expressed thermodynamically by eq. (1):

$$\ln X_A = -\overline{\Delta H}_A \Delta T_A / RT_A T_A^\circ \quad (1)$$

where  $\overline{\Delta H}_A$  is the difference in the partial molar heat of component A in the two phases,  $T_A^\circ$  is the melting point of component A,  $\Delta T_A = T_A^\circ - T_A$ ,  $T_A$  is ambient temperature, and  $X_A$  is the mole fraction of component A.

$$\begin{aligned} \Delta X &= X_{\text{ideal}} - X_{\text{obs}} \\ &= e^{-H_A(T_A^\circ - T_A)/RT_A^\circ T_A} - e^{-(H_A + H_m)(T_A^\circ - T_A)/RT_A^\circ T_A} \\ &= X_{\text{ideal}} (1 - e^{-H_m(T_A^\circ - T_A)/RT_A^\circ T_A}) \end{aligned} \quad (2)$$

where  $H_m$  is the heat of mixing of the two components and  $H_A$  is the heat of fusion of component A.  $\overline{\Delta H}_A$  becomes equal to  $H_A$  (heat of fusion) in eq. (1) for ideal solutions, and the deviation of composition of a nonideal solution from an ideal solution is expressed as shown in eq. (2).  $X_{\text{obs}}$  corresponds to activity and can be estimated experimentally from the phase diagram of the actual mixed system.  $\Delta X_t$ , the composition deviation at a given temperature is related to the heat of mixing and a function of the molecular interaction of the two components, as indicated by the correlation between the molecular interaction and  $\Delta X_t$ , discussed in the following section.  $\Delta X_u$ , the composition deviation at eutectic temperature, is also important, as explained below.  $\Delta X_u$  is the factor determined by

TABLE I  
Physical Parameters and Polymerization Rates in Binary Systems with Acrylamide

Second component	$T_m$ °K.	$\Delta X_f^a$	$X_{ideal}^b$	$\Delta X_u^b$	$\eta$ cp. <sup>c</sup>	$\eta_{sp}$ cp. <sup>d</sup>	$\eta_{AB}^e$	$\eta_{AB}^e$	$\gamma_1$ dyne/ cm. <sup>2g</sup>	$\gamma'$	$V_L$ cm./sec. <sup>f</sup>	$B^g$	$Y^h$
Itaconic acid	315	-0.17	0.44	-0.28	6.62	664.0	33.1	0.77	47.0	1.33	0.0010	12.0	3.0
Crotonic acid	286	-0.14	0.21	-0.31				0.65			0.0026	10.0	2.7
Succinic acid	323	-0.13	0.51	-0.27	3.81	10.32	21.9	0.60	48.8	1.38	0.0090	7.6	1.6
Hydroquinone <sup>i</sup>	328	-0.09	0.57	-0.18	2.93	7.74	8.7	0.38			0.016	5.5	0.4 <sup>i</sup>
Urea	318	-0.10	0.46	-0.17	2.60		10.0	0.60	40.6	1.15	0.017	5.2	1.5
Sorbic acid	326	-0.10	0.60	-0.16	2.96	6.33	8.1	0.35	38.8	1.10	0.013	6.0	1.3
Succinimide	318	-0.08	0.46	-0.16	2.95		8.0	0.30			0.009	4.2	1.4
Thiourea	328	-0.07	0.57	-0.12	2.70	7.59	9.5	0.51			0.03	4.2	1.3
Phthalic anhydride	338	-0.07	0.69	-0.10	1.79	6.38	7.9	0.24	40.6	1.15	0.15	4.0	1.0
Benzoquinone <sup>i</sup>	338	-0.05	0.69	-0.07	1.21		1.1	0.12			1.25	3.2	0.8 <sup>i</sup>
Pure monomer	359	0	—	0	2.08	—	0	0	35.3	1.00	0.29	3.4	1.0

<sup>a</sup> Values at 70°C. calculated by using  $H_A = 4.29$  kcal./mole,  $X_{ideal} = 0.76$ .

<sup>b</sup> Values at eutectic temperature calculated by using  $H_A = 4.29$  kcal./mole.

<sup>c</sup> Values at 90°C., eutectic composition.

<sup>d</sup> Values at eutectic temperature, eutectic composition.

<sup>e</sup> Values at 90°C.

<sup>f</sup> Values at 15°C. except for crotonic acid system at 12°C., eutectic composition.

<sup>g</sup> Measured at  $2\theta = 24.2^\circ$ , eutectic composition; limit is  $1/4$  degree.

<sup>h</sup> Irradiated to total dose of  $0.27$  Mr as the rate of  $9 \times 10^4$  r/hr. at 20°C. excepting for crotonic acid system at 0°C., eutectic composition.

<sup>i</sup> Polymerization inhibitor.

TABLE II  
Physical Parameters and Polymerization Rates in Binary Systems with Acrylic Acid

Second component	$T_w$ °K.	$\Delta X_t^a$	$X_{ideal}^{1b}$	$\Delta X_u^b$	$\eta$ , cp. <sup>c</sup>	$\eta_{AB}^d$	$\gamma$ , dyne/ cm. <sup>2e</sup>	$\gamma'$	$V_{Lr}$ cm./sec. <sup>e</sup>	$B^f$	$Y^g$
Maleic anhydride	255	-0.10	0.56	-0.22	0.97	3.3	50.0	1.41	0.005	2.0	1.2
Benzoic acid	245	-0.09	0.43	-0.20	0.69	2.3	35.9	1.02	0.005	2.3	1.3
Crotonic acid	263	-0.06	0.66	-0.12	0.78	2.2	29.4	0.83	0.006	2.1	1.1
Phenol <sup>h</sup>	268	-0.07	0.73	-0.11	0.85	2.3	38.2	1.08	0.005	1.9	0.9 <sup>h</sup>
Benzene	256	-0.02	0.56	-0.02	0.52	0.8	26.5	0.75	0.003	1.9	1.0
Pure monomer	284	0	---	0	0.58	0	35.3	1.00	0.016	1.9	1.0

<sup>a</sup> Values at 0°C. calculated by using  $H_A = 2.97$  kcal./mole,  $X_{ideal} = 0.81$ .

<sup>b</sup> Values at eutectic temperature calculated by using  $H_A = 2.97$  kcal./mole.

<sup>c</sup> Values at 70°C., eutectic composition.

<sup>d</sup> Values at 70°C.

<sup>e</sup> Values at -20°C. except for benzoic acid system at -30°C., eutectic composition.

<sup>f</sup> Measured at  $2\theta = 23.3$ , eutectic composition; limit is  $1/4$  degree.

<sup>g</sup> Irradiated to total dose of  $0.28 \times 10^4$  Mr at a dose rate of  $9 \times 10^4$  r/hr. at -20°C. except for benzoic acid system at -30°C.

<sup>h</sup> Polymerization inhibitor.

molecular interaction and eutectic temperature. In Tables I and II,  $\Delta X_t$  at 70°C. for acrylamide systems and 0°C. for acrylic acid systems and  $\Delta X_u$  are listed for several two-component systems. It is remarkable that acrylamide-organic acid or acrylic acid-organic amide systems have especially large  $-\Delta X_u$ .

### Viscosity and Surface Tension in the Binary Liquid Phase

The viscosity and surface tension in a binary system are dependent on the molecular interaction in the liquid phase. Viscosity and surface tension have been determined to clarify the relation between  $\Delta X$  and these quantities. The viscosity of liquids in two-component systems was determined with an Ostwald viscometer. Acrylamide and acrylic acid systems were used at 90 and 70°C., respectively, in the presence of trace amounts of inhibitor to inhibit thermal polymerization. The viscosity of the mixed systems is given by eq. (3)

$$\eta = X_A W_A (d/d_A) \eta_A + X_B W_B (d/d_B) \eta_B + 2(X_A X_B W_A W_B d^2/d_A d_B)^{1/2} \eta_{AB} \quad (3)$$

where  $X_A$ ,  $X_B$  denote mole fraction of components A, B;  $W_A$ ,  $W_B$  denote weight fraction of components A, B;  $d_A$ ,  $d_B$  are specific gravity of components A, B;  $\eta_A$ ,  $\eta_B$  are viscosity coefficients of components A, B;  $d$  is the specific gravity of the binary system,  $\eta$  is the viscosity coefficient of the binary system and  $\eta_{AB}$  is a molecular interaction parameter. It is quite obvious that  $\Delta X_t$  and  $\eta_{AB}$  can be satisfactorily correlated, as shown in Tables I and II. According to eq. (3) viscosity consists of the terms related to  $\eta_A$ ,  $\eta_B$ , and  $\eta_{AB}$ .  $\eta_{AB}'$ , the contribution of term  $\eta_{AB}$  to total viscosity  $\eta$ , increases with the increase of  $\Delta X_t$ , as shown in Table I; thus, it can be deduced that  $\eta$  is affected mainly by molecular interaction.  $\eta_u$ , the viscosity at eutectic temperature is also an important factor for the linear crystal growth rate of the eutectic mixture as explained below, and it can be calculated by extrapolation from viscosity measurement as shown in Table I for acrylamide systems.

The surface tension  $\gamma$  was determined by the capillary pressure method at 90°C. for acrylamide systems and at 70°C. for acrylic acid systems in the presence of trace of inhibitor.  $\gamma$  is calculated from eq. (4),<sup>3</sup> and  $\gamma'$ , which is the ratio of the surface tension of the monomer solution at eutectic composition and of pure monomer, is shown in Tables I and II.

$$\gamma = (rg/2) (\rho_1 h_1 - \rho h) + (gr^2/6) \quad (4)$$

where  $\rho$  and  $\rho_1$  are densities of the liquid sample and the standard liquid in the manometer, respectively,  $h_1$  is the difference of the pressure in monomer,  $h$  is the distance between the surface of the sample liquid and the end of capillary, and  $r$  is the radius of the capillary.

Though  $\gamma'$  and  $\Delta X_t$  can not be correlated satisfactorily, the variation of  $\gamma'$  is less than 20–30%, and differences between the systems are significant.



### Linear Crystal Growth Rate

Linear crystal growth rate was investigated as the most important factor in the crystallization process. Rastogi et al.<sup>4,5</sup> reported a method of measurement and theoretical considerations regarding the linear crystal growth rate. They evaluated experimentally the linear crystal growth rate in binary systems by measuring the time for crystal growth from one end to the other end in 0.6–1.0 cm. diameter glass tube. The linear crystal growth rate  $V_L$  can be expressed by eq. (5)

$$V_L = Ce^{-\frac{1}{kT}\left(\Delta u' + \frac{\gamma^2 T u}{4T(T_u - T)}\right)} \quad (5)$$

where  $u'$  is the activation energy of diffusion,  $T_u$  is the eutectic temperature,  $T$  is the crystallization temperature,  $C$  is a constant related to the impact frequency of the liquid molecules on the boundary of crystal, and  $k$  is the Boltzman constant.  $V_L$  of acrylamide and acrylic acid systems obtained by this method are listed in Tables I and II.

According to these results,  $V_L$  is intimately related to  $\Delta X_t$ ,  $\Delta X_u$ ,  $\eta_{AB}$ , and  $\eta_u$ . Equation (5) can be rewritten as follows.

$$\begin{aligned} V_L &= C'De^{-\frac{\gamma^2 T u}{4kT^2(T_u - T)}} \\ &= C''(T/\eta)e^{-\frac{\gamma^2}{4kT^2(T_u - T)}} \end{aligned} \quad (6)$$

Here  $D$  is the diffusion velocity,  $\eta$  is viscosity, and  $C'$ ,  $C''$  are constants.

As shown by eq. (6),  $V_L$  is a function of viscosity, surface tension, and eutectic temperature. Viscosity is affected by molecular interaction and eutectic temperature, and the effect of surface tension is not so significant, as already mentioned.  $V_L$  is mainly influenced by molecular interaction and eutectic temperature, and it decreases with increasing molecular inter-

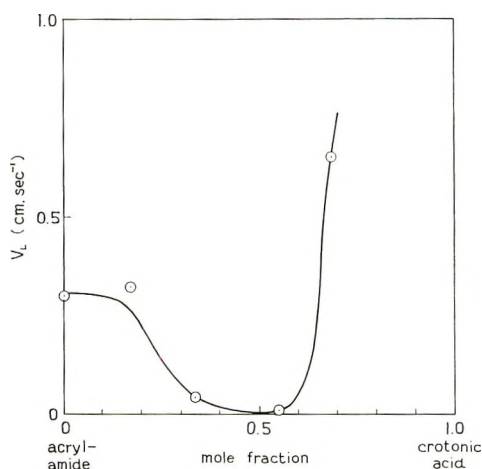


Fig. 1. Relationship between the monomer composition and the linear velocity of crystal growth  $V_L$  in the acrylamide-crotonic acid system.

action and decreasing eutectic temperature. The variation of  $\Delta X_u$  corresponds more closely to the variation of  $V_L$  than does that of  $\Delta X_t$  because  $\Delta X_u$  contains both effects of molecular interaction and eutectic temperature and it increases with the increase of molecular interaction and with the decrease of eutectic temperature, as is obvious from eq. (2). Coefficient  $C$  is related to the impact frequency of the liquid molecules on the crystal boundary and is given no thermodynamical expression at the present time. However, this frequency might be related to molecular interaction between the two components. Figure 1 shows that  $V_L$  reaches a minimum at the eutectic composition because to the left side of this point pure acrylamide crystals grow at a large rate and to the right side crotonic acid crystals grows at a very large rate.

### Size of Crystal Grain

The relation between grain size and linear velocity of crystal growth or molecular interaction of the two components has been studied. The half-maximum width of the x-ray diffraction diagram gives the grain size according to eq. (7):<sup>6</sup>

$$L = \lambda / (B \cos \alpha) \quad (7)$$

where  $L$  is grain size,  $B$  is the half-maximum width, and  $\lambda$  is the x-ray wavelength.

The half-maximum width  $B$  of the monomer crystal reflection in the two-component systems gave the results shown in Tables I and II. A plot of  $B$  against  $V_L$  presents good agreement, as shown in Figure 2. It is found experimentally that grain size decreases with decreasing  $V_L$ , because crystal grain growth in the binary solid system is more frequently interrupted in the case of small growth rate. The effect is not so pronounced

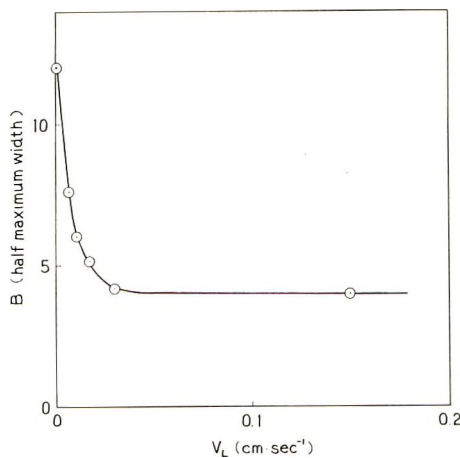


Fig. 2. Relationship between the half-maximum width of the x-ray diffraction diagram  $B$  and the linear velocity of crystal growth  $V_L$  in binary systems with acrylamide. Unit of  $B$  is  $1/4$  degree.

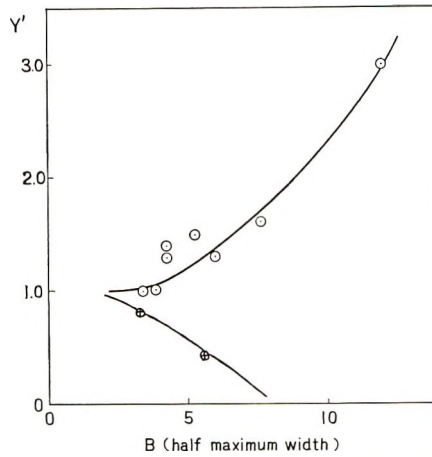


Fig. 3. Relationship between the solid-state polymerization rate  $Y'$  and  $B$  in binary systems with acrylamide: ( $\circ$ ) binary systems with acrylamide; ( $\oplus$ ) acrylamide-inhibitor binary systems. Unit of  $B$  is  $1/4$  degree.

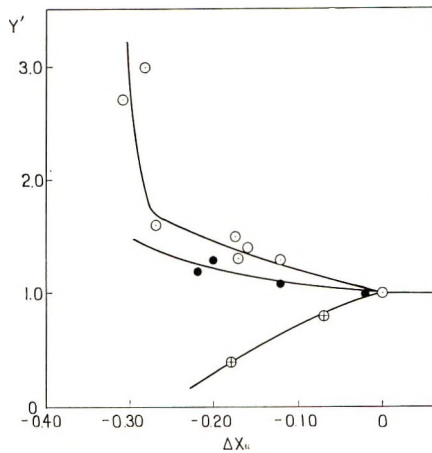


Fig. 4. Relationship between the solid-state polymerization rate  $Y'$  and  $\Delta X_u$ : ( $\circ$ ) binary systems with acrylamide; ( $\bullet$ ) binary systems with acrylic acid; ( $\oplus$ ) acrylamide-inhibitor binary systems.

with acrylic acid systems as with acrylamide systems. Equation (8) relates dislocation density and grain size.<sup>7,8</sup>

$$\rho = \alpha/bL$$

$$\rho \sim (\beta/b)^{1/3} D^{-2/3}$$

or

$$\rho \sim (\alpha/b)^2 \sim \beta^2/9b^2 \quad (8)$$

Here,  $L$  is the grain size,  $\rho$  is the density of the dislocation,  $\beta$  is the observed x-ray width,  $\alpha$  is the angle of inclination between the grains,  $D$  is the distance between the grains, and  $b$  is a constant.

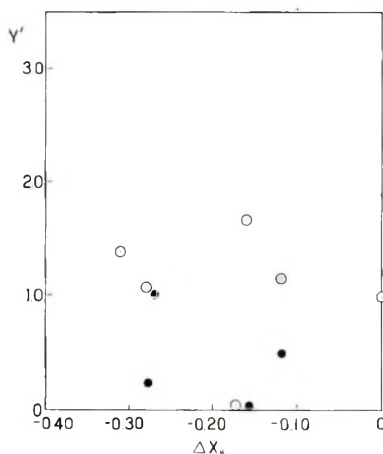


Fig. 5. Relationship between  $Y'$  and  $\Delta X_u$  in the liquid-phase polymerization of acrylamide binary systems: (○) 20% solution in acetone at 15°C.; (●) 10% solution in acetic acid at 15°C.

It may be assumed that smaller grains have more crystal defects.

### Polymerization Rate in the Solid State

Finally the relation between the solid-state polymerization rate and  $\Delta X_u$ ,  $B$  have been clarified. Polymerization rate is expressed by  $Y'$ , which is ratio of conversions of pure monomer to that of a binary system at the same irradiation dose [eq. (9)].

$$Y' = \frac{\text{conversion in the binary systems}}{\text{conversion in pure monomer}} \quad (9)$$

Figures 3 and 4 show the good correlation between  $Y'$  and  $\Delta X_u$ ,  $B$ . When polymerization inhibitors are added, an opposite curve is obtained, as shown in Figures 3 and 4, i.e.,  $Y'$  decreases with increasing  $\Delta X_u$  and with decreasing  $B$ .

### Polymerization Rate in the Liquid Phase

For comparison,  $Y'$  in liquid-phase polymerization has been investigated with the same combination of two components. Acetone and acetic acid were chosen as solvents. The eutectic compositions of several binary systems were dissolved in these solvents at the concentration in which monomer concentration is maintained as described in Figure 5, and the sealed samples were irradiated *in vacuo*. The conversion was determined gravimetrically. As shown in Figure 5,  $Y'$  in the liquid phase is independent of the physical factors already mentioned. This fact suggests that polymerization acceleration in the binary solid phase (eutectic mixture) containing acrylic monomer is not due to chemical effects but mainly to physical effects in the mixed state.

### Conclusions

The acceleration of polymerization rate in solid-state polymerization of binary systems (eutectic mixtures) containing acrylic monomers has been investigated. The following conclusions have been obtained.

(1) Physical differences in mixed solid state is the most important factor determining the polymerization rate of binary systems consisting of acrylic monomer and organic substance.

(2) The physical mixed state is determined by molecular interaction between two components, and polymerization acceleration becomes more pronounced with the increase of such interaction. Systems consisting of one monomer and a highly polar substance having hydrogen bonds are the more effective combinations. In the case of systems with extremely large degrees of association the glassy solid state is easily formed with supercooling. The glassy phase is fairly stable and can be polymerized by irradiation at very low temperatures. Some results on this glassy state polymerization will be published in the near future.

(3) Our results show a correlation between polymerization acceleration or inhibition and grain size or imperfections. Apparently, dislocations in the grain boundary affect the polymerization more strongly than inner imperfections of the crystal lattice.  $Y'$  of the acrylamide-hydroquinone system is 0.4 and  $Y'$  of the acrylamide-urea system is 1.5, though the grain size of the monomer is the same in these systems. If the reduction of  $Y'$  in the former system is due only to inhibition of initiation in the grain boundary, the ratio of initiation in grain boundary is estimated to be

$$\frac{\text{Surface initiation}}{\text{Total (surface + inner) initiation}} = \frac{1.5 - 0.4}{1.5} = 0.73$$

The kinetics of the polymerization is also closely related to the nature of the solid mixed phase in two-component systems. This problem is currently being investigated and will be reported shortly.

### References

1. I. Kaetsu, N. Sagane, K. Hayashi, and S. Okamura, *Kobunshi Kagaku*, **23**, 125 (1966).
2. G. Adler, *J. Chem. Phys.*, **32**, 1698 (1960).
3. A. Ferguson and P. E. Dowson, *Trans. Faraday Soc.*, **17**, 383 (1921).
4. R. P. Rastogi, *J. Phys. Chem.*, **68**, 2398 (1964).
5. R. P. Rastogi, *J. Phys. Chem.*, **59**, 1 (1955).
6. B. D. Cullity, *Elements of X-Ray Diffraction*, Addison-Wesley, Reading, Mass., 1956.
7. A. H. Cottrell, *Dislocations and Plastic Flow in Crystals*, Oxford Univ. Press, London, 1953, p. 101.
8. P. Gay, P. B. Hirsch, and A. Kelly, *Acta Met.*, **1**, 315 (1953).



### Résumé

La polymérisation à l'état solide induite par irradiation de systèmes binaires consistant de monomères acryliques (acrylamide, acide acrylique) et des substances organiques a été étudiée. Dans des publications précédentes sur des systèmes binaires, les auteurs ont rapportés que les vitesses de polymérisation croissaient à l'état solide (système de mélanges eutectiques). Le mécanisme d'accroissement de vitesse a été étudié par l'examen des diagrammes de phases, des viscosités et de la tension superficielle des systèmes binaires. La viscosité et la tension superficielle sont des mesures de l'interaction moléculaire de systèmes de deux composants. En outre, l'effet de la vitesse de croissance linéaire du cristal et la demi-largeur maximum du diagramme de diffraction aux rayons-X au cours de processus de cristallisation ont été déterminés. On a montré que, plus l'interaction moléculaire est grande entre les deux composants, d'autant plus lente est la vitesse linéaire de croissance du cristal des monomères. La grandeur du cristal monomérique décroît et la densité de dislocation des cristaux monomériques croît dans les systèmes avec une grande interaction moléculaire. Conséquemment on a conclu que la structure physique du système solide binaire est le paramètre le plus important qui détermine la vitesse de croissance de la polymérisation à l'état solide. Une dislocation à la séparation de phase est beaucoup plus importante que les défauts intérieurs au sein du réseau cristallin. On a trouvé que l'accélération de la vitesse de polymérisation est grande dans un système binaire avec des grandes interactions moléculaires. Dans certains systèmes tels que des systèmes acide-amide organiques, avec de fortes liaisons hydrogènes, des phases vitreuses peuvent être formées dans lesquelles le monomère peut facilement polymériser à très basses températures.

### Zusammenfassung

Die strahlungsinduzierte Polymerisation binärer Systeme aus Acrylmonomeren (Acrylamid, Acrylsäure) und organischen Substanzen in fester Phase wurde untersucht. In der früheren Arbeit über binäre Systeme berichteten die Autoren, dass die Polymerisationsgeschwindigkeit in fester Phase zunahm (eutektisches Mischungssystem). Der Mechanismus der Geschwindigkeitszunahme wurde durch Bestimmung der Phasendiagramme, der Viskosität und der Oberflächenspannung der binären Systeme untersucht. Viskosität und Oberflächenspannung bilden ein Mass für die molekulare Wechselwirkung in den Zweikomponentensystemen. Ausserdem wurde der Einfluss der linearen Kristallwachstumsgeschwindigkeit sowie der Halbwertsbreite im Röntgendiagramm für den Kristallisationsprozess bestimmt. Es wurde gezeigt, dass die lineare Kristallwachstumsgeschwindigkeit des Monomeren umso kleiner ist, je grösser die Molekülwechselwirkung zwischen den Komponenten ist. In Systemen mit grosser Molekülwechselwirkung nimmt die Grösse der Monomerkristalle ab und ihre Versetzungsdichte zu. Es kann daher geschlossen werden, dass die physikalische Struktur eines binären Feststoffsystems der wichtigste Parameter für die Geschwindigkeitszunahme der Polymerisation in fester Phase ist. Versetzungen an der Kornoberfläche haben grösseren Einfluss als die inneren Fehlstellen des Kristallgitters. Es wurde festgestellt, dass in binären Systemen mit grösser Molekülwechselwirkung eine starke Beschleunigung der Polymerisationsgeschwindigkeit auftritt. In einigen Systemen, wie solchen aus organischer Säure-Amid, mit starken Wasserstoffbindungen können glasartige Phasen gebildet werden, in welchen das Monomere noch bei sehr niedrigen Temperaturen polymerisiert.

Received November 8, 1965

Revised January 31, 1966

Prod. No. 5080A

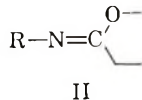
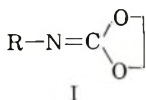
## Homopolymerization of 2-Alkyl- and 2-Aryl-2-Oxazolines

D. A. TOMALIA and D. P. SHEETZ, *Edgar C. Britton Research  
Laboratory, The Dow Chemical Company, Midland, Michigan*

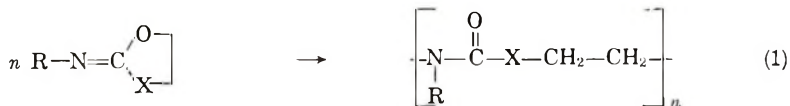
### Synopsis

2-Aryl- and 2-alkyl-2-oxazolines have been polymerized to poly-(*N*-aroyl)aziridines and poly(*N*-acyl)aziridines, respectively, in the presence of boron trifluoride. The polymers obtained were glassy, light yellow resins with molecular weights ranging from 3500 to 7500 (35-50 oxazoline units per chain). The polymerization rates have been determined for several of these monomers. A polymerization mechanism is proposed.

Recently it was shown that a number of *exo*-imino cyclic compounds such as ethylene iminocarbonates (I) and 2-iminotetrahydrofuran (II) undergo a



1,4-addition-type ring-opening polymerization in the presence of cationic catalysts to give polyurethanes and polyamides,<sup>1-4</sup> respectively, as is shown in eq. (1):



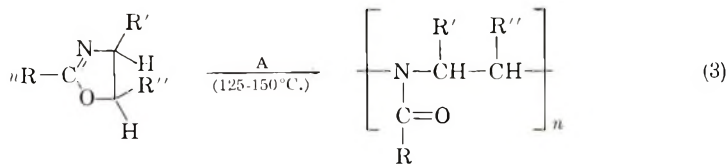
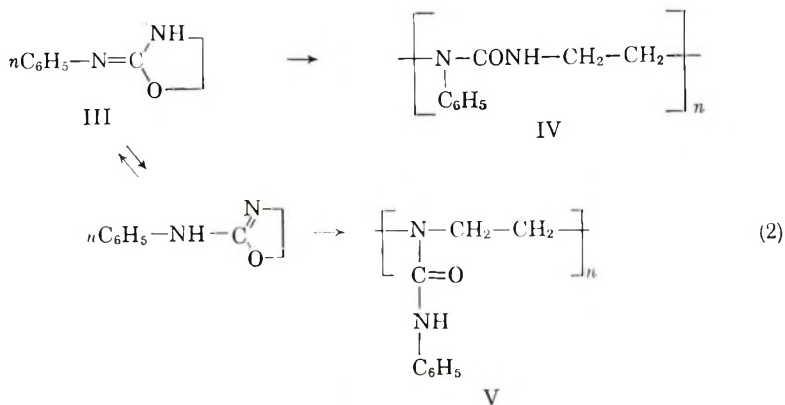
where X is —O— or —CH<sub>2</sub>—.

Mukaiyama and co-workers<sup>1</sup> also reported that the polymerization of 2-phenyliminooxazolidine (III), in the presence of cationic catalysts, gave rise to complex polyureas. Since two tautomeric forms are possible for III, it was suggested by these authors that the polyurea consisted of poly-(ethylene-*N*-phenylurea) (IV) and the polyaziridine-type polymer (V) (see following page).

However, compelling evidence for either polymeric structure was lacking.

In an investigation which we had completed prior to that communication we found that the less complex and analogous 2-alkyl- or 2-aryl-2-oxazoline systems—the *endo* imino cyclic compounds—underwent facile ring opening polymerizations. In the presence of cationic catalysts such as BF<sub>3</sub> or

methyl tosylate, 2-alkyl- and 2-aryl-2-oxazolines were found to polymerize readily to *N*-acyl- or *N*-aroyl-polyaziridines, respectively [eq. (3)].



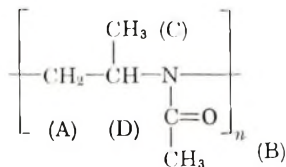
- VI: R = CH<sub>3</sub>—, R' = H, R'' = H  
 VII: R = CH<sub>3</sub>—, R' = CH<sub>3</sub>—, R'' = H  
 VIII: R = C<sub>6</sub>H<sub>5</sub>—, R' = H, R'' = H  
 IX: R = CH<sub>3</sub>—, R' = H, R'' = CH<sub>3</sub>—

In eq. (3) A may be BF<sub>3</sub> etherate, the 2-oxazoline-BF<sub>3</sub> complex, or methyl *p*-toluene-sulfonate.

These polymers were obtained as glassy, light yellow, water-soluble (except for the phenyl derivative) resins with molecular weights ranging from 3500 to 7500 (35–50 oxazoline units per chain).

Evidence supporting the polyimide structure was obtained by acidic or basic hydrolysis of the polymeric product obtained from 2-methyl-2-oxazoline (VI), which in either case leads to substantial amounts of acetic acid.

NMR and infrared analysis provided additional evidence for the proposed structure. The NMR spectrum for poly-2,5-dimethyl-2-oxazoline (IX), (CDCl<sub>3</sub>), consisted of a complex multiplet centered at –3.30 ppm (A), a single peak at –2.10 ppm (B), a doublet at –1.30 ppm (C), and a multiplet centered at –4.20 ppm (D). Integration of these resonance peaks gave proton ratios which were consistent with the structure:



Infrared spectroscopy provided a convenient means for following the conversion of 2-oxazolines to polymers. The oxazoline monomers in all cases displayed intense ( $-\text{C}=\text{N}-$ ) stretching bands<sup>5</sup> at 6.10–6.20  $\mu$  ( $\text{CH}_2\text{Cl}_2$ ) and a medium intensity band at 10.50–10.70  $\mu$  ( $\text{CH}_2\text{Cl}_2$ ) which were characteristic of the oxazoline moiety. Polymerization caused the disappearance of these two bands accompanied by the development of an intense single band at shorter wavelength, 5.95–6.10  $\mu$ . This absorption band was assigned to an imide-type carbonyl stretching. In fact, the infrared spectrum for poly-2-methyl-2-oxazoline exhibited an intense band at 6.04  $\mu$  ( $\text{CH}_2\text{Cl}_2$ ) corresponding exactly with the imide carbonyl band for *N,N'*-diacetylpiperazine which is a cyclic dimer of 1-(acetyl)aziridine. Finally, the infrared spectra for poly-2-methyl-2-oxazoline and poly-1(acetyl)aziridine were found to be virtually identical between 2.5 and 25  $\mu$  ( $\text{CH}_2\text{Cl}_2$ ).

### KINETICS

The polymerizations for the rate study were initiated by the respective  $\text{BF}_3$ -oxazoline complexes in the case of monomers (VI), (VII), and (IX). Due to the insolubility of the 2-phenyl-2-oxazoline- $\text{BF}_3$  complex in the monomer (VIII), it was necessary to use the dimethoxyethane- $\text{BF}_3$  complex as an initiator for this system. It was very essential to exclude atmospheric oxygen from these polymerizations, since it was found that oxygen caused considerable inhibition and inevitably resulted in highly colored low molecular weight polymers.

By following the disappearance of the absorption bands at 10.50–10.70  $\mu$  ( $\text{CH}_2\text{Cl}_2$ ) and by using the Beer-Lambert relationship it was possible to obtain reproducible kinetic data for these polymerizations at 100, 125, and 150°C. Close adherence to Beer's law was observed for standard monomer solutions in the concentration ranges that were used for these polymerizations.

In all cases studied, the polymerizations were found to be first order with respect to monomer concentration during the initial stage of the polymerization. With the exception of 2-phenyl-2-oxazoline (VIII), however, deviations from first-order kinetics appeared as the polymerizations progressed. In the case of VI and VII the deviation was rationalized as being due to the formation of a heterogeneous system which was observed to occur during the latter stages of the polymerization. As polymer concentration built up, a two-phase system resulted, due to the insolubility of the polymer in the monomer. At this point the reaction rate no longer followed a first-order rate expression, but instead showed zero-order kinetics as demonstrated by the linearity in a plot of [monomer] versus time. This can be seen to occur in Figure 1 if one considers those points past the filled triangular points. ( $\blacktriangledown$ ). It is presumed that beyond these points the propagation rate was no longer a function of total monomer concentration, since it was limited by the monomer-polymer solubility relationship.

A very unusual rate curve (Fig. 2) was obtained for the polymerization of 2,5-dimethyl-2-oxazoline (IX). This system was homogeneous and

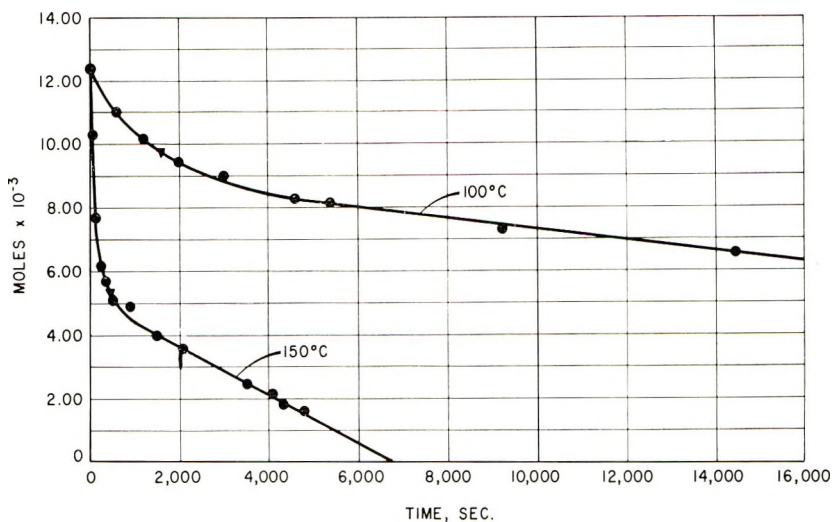


Fig. 1. Polymerization of 2-methyl-2-oxazoline with 1 mole-%  $\text{BF}_3$  at 100 and 150°C.

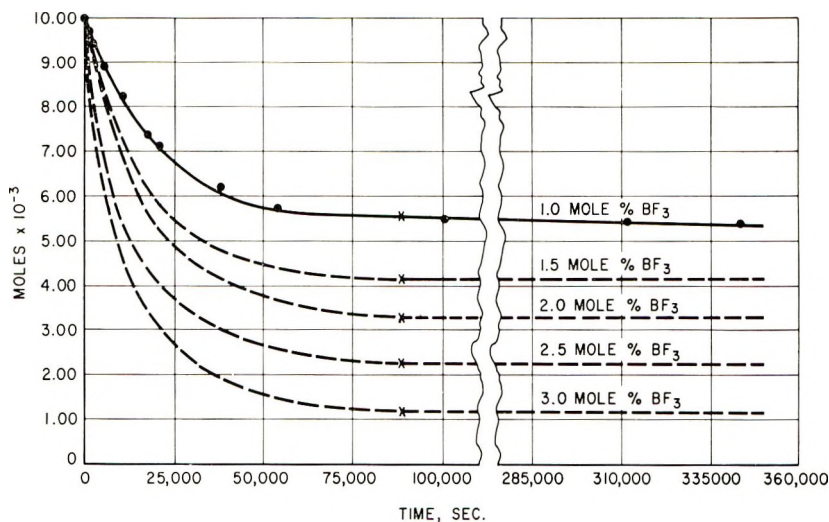


Fig. 2. Polymerization of 2,5-dimethyl-2-oxazoline with various  $\text{BF}_3$  concentrations at 150°C.

appeared to be giving a normal rate plot at the beginning of the polymerization. However, after a polymer concentration of approximately 45% was obtained, the polymerization virtually stopped with the use of 1 mole-% of initiator. The conversion at which polymerization ceased was found to vary with initiator concentration as shown in Figure 2. By using these data in a mathematical analysis, which assumed that active chain sites were being consumed concurrent with propagation, it was possible to calculate propagation and termination rate constants. The calculated propagation



TABLE I  
 Monomer Polymerization Rates

Monomer	$k \times 10^4, \text{sec.}^{-1}$		
	100°C. <sup>a</sup>	125°C. <sup>a</sup>	150°C. <sup>b</sup>
VI	0.63	—	7.2
VII	—	0.21	1.2
VIII	—	—	37
IX	—	—	0.11 <sup>c</sup>
			0.43 <sup>d</sup>

<sup>a</sup> At 100°C. or 125°C.,  $\pm 1^\circ\text{C}$ .

<sup>b</sup> At  $150 \pm 2^\circ\text{C}$ .

<sup>c</sup> Calculated propagation rate constant.

<sup>d</sup> Calculated termination rate constant.

rate constant was found to be consistent with the other propagation rate constants. This analysis will be discussed more fully in the experimental section.

Plots of  $\log [\text{monomer}]$  as a function of time were found to be linear for monomers VI, VII, and VIII. Since transition to a heterogeneous system occurred with monomers VI and VII, only those rate data obtained from the slopes of log plots for the early parts of the polymerizations were considered. These data are summarized in Table I.

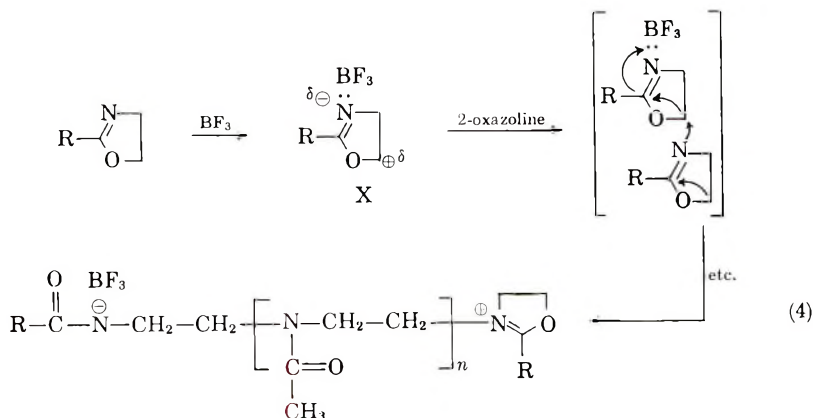
The relative ease of polymerization as measured by the propagation rate constants was found to be in the following order: 2-phenyl-> 2-methyl-> 2,4-dimethyl-> 2,5-dimethyl-2-oxazoline.

It is interesting to note that those monomers with more highly deshielded methylene protons in the five position exhibited larger propagation rate constants. The chemical shifts  $\delta$  for these monomers in  $\text{CDCl}_3$  were found to be as given in Table II.

The ring opening of 2-oxazoline by such reagents as hydrohalides,<sup>6-8</sup> acid chlorides,<sup>9</sup> thiophenols,<sup>10</sup> or thioacids<sup>11</sup> is generally believed to occur by first quaternization of the ring nitrogen followed by nucleophilic attack of the anion at the 5-position. In a similar manner one might postulate that the polymerization of 2-oxazolines first involves coordination of  $\text{BF}_3$  with the ring nitrogen which can then effectively decrease the electron density at the 5-position [eq. (4)]. Since the only potential nucleophile in the reaction medium is the nitrogen on another ring, attachment at this electron-deficient center could occur to generate a quaternary nitrogen on this incoming ring. This, in turn, could inductively decrease the electron den-

TABLE II

Monomer	$\delta, \text{ppm}$	$k_p \times 10^4, \text{sec.}^{-1}$
VIII	-4.37	37
VI	-4.24	7.2
VII	-3.77	1.2



sity at its 5-position. The result would be propagation to an *N*-substituted polyaziridine.

Some evidence supporting this mode of initiation was obtained by comparing the relative deshielding of protons at the five position in the monomer and in the monomer- $\text{BF}_3$  complex. The chemical shift parameter is in general a function of the electron density around the nucleus<sup>12</sup> for comparable protons in a common solvent. If activation of the 5-position in the monomer- $\text{BF}_3$  salts is occurring as illustrated by X, one would expect these protons to be highly deshielded compared to those in the monomer. This does indeed occur. The 5-position protons in 2-methyl-2-oxazoline (VI) had a chemical shift of  $-4.24$  ppm ( $\text{CDCl}_3$ ), whereas comparable protons in the  $\text{BF}_3$  complex were deshielded to  $-4.76$  ppm ( $\text{CDCl}_3$ ). This same trend was also observed for the other oxazolines studied.

## EXPERIMENTAL

Melting points were determined on a Thomas-Hoover capillary melting point apparatus and are uncorrected. Infrared spectra were scanned with a Perkin-Elmer Model 337 grating instrument. Nuclear magnetic resonance spectra were recorded with the Varian A-60 NMR spectrometer, tetramethylsilane being used as an internal standard ( $\delta = 0$ ). The purity of the monomers was ascertained by the use of an F & M programmed vapor-phase chromatograph, Model 500, equipped with a 10 ft.  $\times$  1/4 in. Oronite column (20% on Gas Chrom Z solid support).

### Monomer Synthesis

The 2-oxazoline monomers were synthesized from the appropriate chlorohydrins and nitriles according to a modified version of the method described by Gabriel and Neumann.<sup>13</sup>

2-Methyl-2-oxazoline was prepared by charging equimolar amounts of ethylene chlorohydrin and acetonitrile (3.0 mole) in 300 ml. of methylene chloride into a flask equipped with a stirrer, thermometer, and fritted glass

sparger. All materials were previously dried by passing them through a 3-ft. column containing Dowex 50 ( $K^+$  form) ion-exchange resin. This reaction mixture was cooled to  $5^\circ C.$  while anhydrous HCl was added as rapidly as possible under 3–4 in. Hg. pressure. The temperature was maintained at  $5$ – $10^\circ C.$  during this addition period. After 1.8 mole of HCl/mole of chlorohydrin had been taken up (0.5–1 hr.), the addition was stopped, and the reaction mixture was allowed to stand overnight at  $5^\circ C.$  Sufficient anhydrous methylene chloride was added so that there was 1 liter of solvent per mole of chlorohydrin. This solution was refluxed at  $32^\circ C./575$  mm. for 2 hr. to remove excess HCl. As the HCl was removed, the imidoester·HCl precipitated as small flat plates. This slurry was cooled to  $5^\circ C.$  and 2.3 mole triethylamine/mole imidoester·HCl was added with vigorous stirring over a period of 30 min. An exothermic reaction was observed shortly after all the amine was added. When spontaneous refluxing subsided, heat was applied to maintain reflux for 4 hr. The amine salt was filtered, and methylene chloride was removed from the filtrate by distillation. Periodically, the amine salt which crystallized out in the distillation pot was removed by filtration. After removal of the solvent, fractionation gave a 36% yield of 2-methyl-2-oxazoline, b.p.  $60$ – $62^\circ C./125$  mm.

In a similar manner VIII, IX, and X were prepared in yields of 48, 49, and 33%, respectively.

All of the monomers were redistilled on a  $30 \times 1.5$  cm. glass helix-packed column, and their purity was assured by vapor-phase chromatography before using for the rate studies.

### Preparation of Polymerization Initiators

For the polymerization of VI, VII, or IX, the respective 2-oxazoline- $BF_3$  complex was used as the initiator in the form of a stock solution prepared by using the monomer as a solvent.

The  $BF_3$  complexes of all of the monomers were prepared by charging 1.0 g. of the oxazoline into a flask equipped with a magnetic stirrer. While stirring,  $BF_3$  was allowed to flow over the surface of the liquid to give a slightly exothermic reaction which resulted in the formation of a solid white mass. The reaction flask was flushed with dry nitrogen, weighed and exposed to more  $BF_3$  until a reaction product of constant weight was obtained. Based on a 1:1 complex, the  $BF_3$  uptake corresponded to a conversion of 91–94%. This reaction product consisting of complex and monomer was diluted with sufficient monomer to make a stock solution of desired concentration. These stock solutions were kept cold ( $5$ – $10^\circ C.$ ) and used immediately. Since some of these complexes are fairly hydroscopic, all work was carried out in a nitrogen-filled dry box.

In the case of monomer (VIII), the  $BF_3$  etherate of dimethoxyethane was used as the initiator, since VIII· $BF_3$  was insoluble in the monomer. The etherate stock solutions were prepared by bubbling  $BF_3$  into a freshly distilled sample of the ether in a nitrogen-filled dry box. The  $BF_3$  concentra-

tion was determined according to the method of Walters and Miller.<sup>14</sup> These  $\text{BF}_3$  solutions were diluted with appropriate amounts of dimethoxyethane and used immediately for the rate studies.

### Kinetics

Approximately 1 ml. of the respective monomers was charged into a Carius combustion tube and accurately weighed. Based on the weight of the sample, appropriate amounts of freshly prepared  $\text{BF}_3$  stock solutions were injected with a microsyringe to give the appropriate initiator concentration. The samples were then immediately frozen in a Dry Ice-acetone bath, evacuated, and flushed with dry nitrogen several times followed by flame sealing of the tubes. The samples tubes were immersed in a constant-temperature bath at the desired temperature and withdrawn at specific time intervals. The polymerizations were quenched by cooling in a salt-ice bath followed by dissolution in a minimum of methylene chloride. These solutions were diluted to 25 ml. in a volumetric flask and then scanned in a fixed cell (0.012 cm.) between 10 and 11  $\mu$ . The disappearance of the respective absorption bands ( $\text{CH}_2\text{Cl}_2$ ) shown in Table III was used to follow the polymerization.

TABLE III

Monomer	Wavelength, $\mu$
VI	10.62
VII	10.72
VIII	10.52
IX	10.61

### Derivation of Rate Constants for 2,5-Dimethyl-2-oxazoline

Since homogeneity was observed throughout the course of this polymerization it was assumed that the rates for the propagation and termination [eqs. (5) and (6)] could be expressed by eqs. (7)–(9).

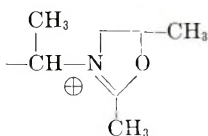


$$-d[\text{M}]/dT = k_p[\text{P}^+][\text{M}] \quad (7)$$

$$-d[\text{P}^+]/dT = k_t[\text{P}^+] \quad (8)$$

$$-\ln [\text{P}^+] = k_t T - \ln [\text{P}_0^+] \quad (9)$$

where,  $\text{P}^+$  denotes the radical



and P is inactive polymer,  $[M]$  is monomer concentration,  $[M_0]$  is initial monomer concentration,  $[P_0^+]$  is  $\text{BF}_3$  concentration,  $k_p$  is the propagation rate constant,  $k_t$  is the termination rate constant, and  $T$  is polymerization time (sec.).

Substituting from the termination rate expression for  $P^+$  gives

$$-d[M]/dT = k_p(e^{-k_t T}[P_0^+])[M] \quad (10)$$

Integration gives

$$-\ln [M] = (-k_p[P_0^+]/k_t, e^{-k_t T} + C \quad (11)$$

When  $T = 0$ , then  $C = -\ln [M_0] + k_p[P_0^+]/k_t$ . Substituting for  $C$  and rearranging yields

$$\ln ([M]/[M_0]) = (k_p[P_0^+]/k_t) e^{-k_t T} - (k_p/k_t) [P_0^+] \quad (12)$$

When  $T = \infty$ , then

$$\ln [M_\infty]/[M_0] = -k_p/k_t [P_0^+] \quad (13)$$

$$\ln [M_\infty] = (-k_p/k_t[P_0^+] + \ln [M_0]) \quad (14)$$

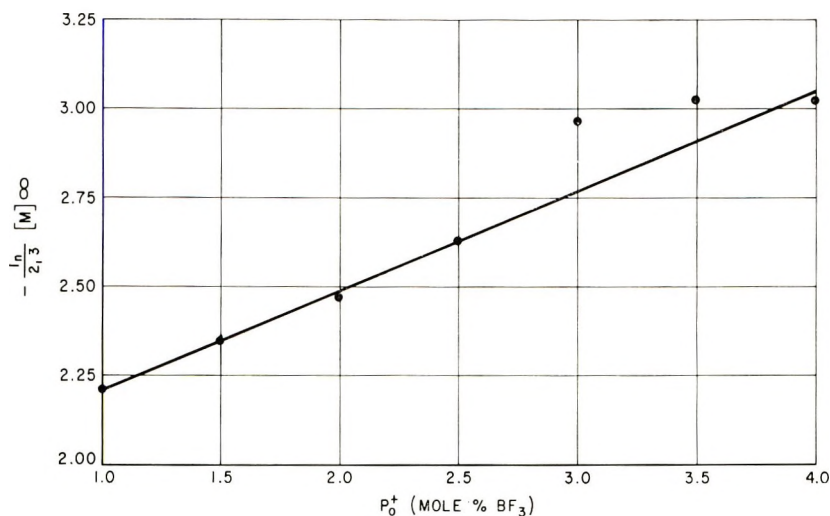


Fig. 3. Polymerization of 2,5-dimethyl-2-oxazoline at  $150^\circ\text{C}$ . Plot of  $\ln [M_\infty]/2.3$  as a function of initiator concentration  $[P_0^+]$ .

Samples of 2,5-dimethyl-2-oxazoline, where  $[P_0^+] = 1.0, 1.5, 2.0, 2.5$  and  $4.0$  mole-% of  $\text{BF}_3$ , were polymerized for an infinite time (Fig. 2), and in this manner it was possible to determine  $[M]$  at  $T = \infty$  for various  $[P_0^+]$ . With these data a plot of  $-\ln [M_\infty]$  versus  $[P_0^+]$  was made, (Fig. 3), which demonstrated that  $\ln [M]$  was a linear function of  $[P_0^+]$  at  $T = \infty$ . The slope of this linear plot is then equal to  $(k_p/k_t)$  and was found to be 0.257.



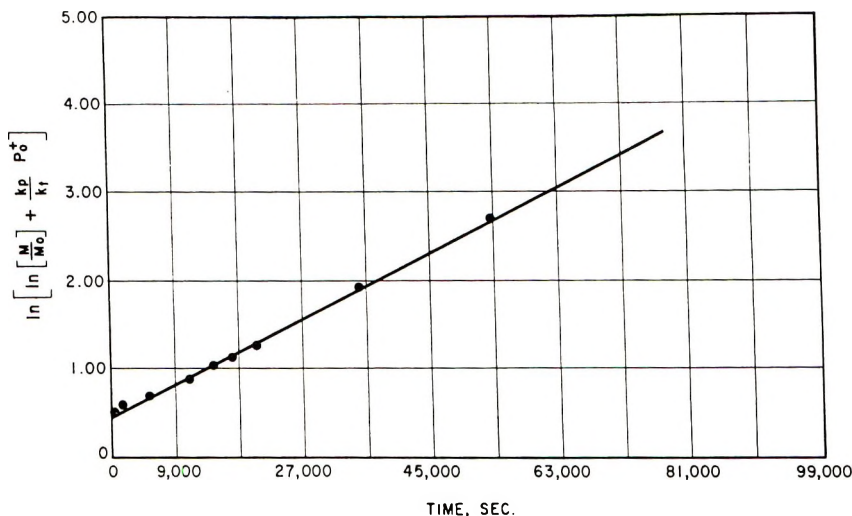


Fig. 4. Polymerization of 2,5-dimethyl-2-oxazoline at 150°C. Plot of  $\ln \left\{ \ln \left( \frac{[M]}{[M_0]} \right) + \left( \frac{k_p}{k_t} \right) [P_0^+] \right\}$  as a function of time.

Rearranging eq. (12), one can obtain

$$\ln \left[ \frac{[M]}{[M_0]} \right] + \left( \frac{k_p}{k_t} \right) [P_0^+] = \left( \frac{k_p}{k_t} \right) [P_0^+] e^{-k_t t} \quad (15)$$

The above expression is then put into a linear form as follows:

$$\ln \left\{ \ln \left[ \frac{[M]}{[M_0]} \right] + \left( \frac{k_p}{k_t} \right) [P_0^+] \right\} = -k_t t + \ln \left( \frac{k_p}{k_t} \right) [P_0^+] \quad (16)$$

If this relationship accurately describes the polymerization rate of 2,5-dimethyl-2-oxazoline, one should obtain a linear plot for the left-hand side of eq. (16) versus time, where the slope ( $-k_t$ ) would be equal to the termination rate constant. Linearity is observed, as shown in Figure 4, and the termination rate constant is easily evaluated and found to be  $0.428 \times 10^{-4} \text{ sec.}^{-1}$ . Since the value of  $(k_p/k_t)$  was determined from the slope of the plot in Figure 3,  $k_p$  can be evaluated.

$$k_p/k_t = 0.257$$

$$\begin{aligned} k_p &= (0.257) (0.428 \times 10^{-4} \text{ sec.}^{-1}) \\ &= 1.10 \times 10^{-5} \text{ sec.}^{-1} \end{aligned}$$

### Bulk Polymerization of 2-Phenyl-2-oxazoline

2-Phenyl-2-oxazoline (1.1322 g.,  $7.69 \times 10^{-3}$  mole) was charged into a Carius combustion tube with  $7.69 \times 10^{-5}$  mole of  $\text{BF}_3$  in the form of a dimethoxyethane solution. After evacuation, flushing with nitrogen, and sealing, the sample was heated at 150°C. for 2 hr. The light yellow glassy polymer that resulted was ground to a fine powder followed by the dissolution of 1.0 g. in 25 ml. of methylene chloride. This solution was added, while stirring vigorously, to 75 ml. of *n*-hexane to give a thick white

precipitate. The material was filtered and reprecipitated two more times in the same manner to yield a fine white powder. The recovery of purified polymer was 80%. The molecular weight of this sample as determined by boiling point elevation in ethanol was 7500.

#### Acid Hydrolysis of Poly-2-methyl-2-oxazoline

A 1.0271 g. sample of poly-2-methyl-2-oxazoline was dissolved in 50.00 ml. of 0.997*N* sulfuric acid. A homogeneous reaction mixture resulted which was heated under reflux for 3.5 hr. The odor of acetic acid was very apparent after this time. Titration of an aliquot of this reaction mixture with standard sodium hydroxide solution (1.00*N*) indicated the hydrolysis was 27% complete. Titration of an aliquot taken after the reaction had refluxed for a total of 21 hr. showed that the hydrolysis was only 38% complete.

#### Basic Hydrolysis of Poly-2-methyl-2-oxazoline

A 1.2900 g. sample of poly-2-methyl-2-oxazoline was added to 50.00 ml. of 0.999*N* sodium hydroxide. The polymer was virtually insoluble in base at room temperature; however, after refluxing 26 hr. the reaction mixture became homogeneous. Cooling to room temperature caused the reaction mixture to gel to a white mass. The reaction mixture was titrated potentiometrically with 1.00*N* hydrochloric acid which indicated the hydrolysis was 65% complete. The odor of acetic acid was apparent at a pH of less than 7; however, the precipitate persisted even at a pH of 4.2. The insoluble matter was presumed to be partially acetylated polyaziridine, however, this material was not isolated and identified.

#### Preparation of 1,4-Diacetylpiperazine

To a stirred solution of 31 g. (0.5 mole) of anhydrous piperazine and 101 g. (1.0 mole) of triethylamine in 1 liter of dry benzene at 10–25°C. was added 78.5 g. (1.0 mole) of acetyl chloride over a period of 30 min. The reaction mixture was allowed to stir for 1 hr. at room temperature, filtered free of amine salt, and washed twice with 15-ml. portions of warm benzene. Sufficient *n*-hexane was added to the filtrate to cause cloudiness. Cooling in an ice bath gave 35.95 g. (49%) of product melting at 131–133°C. One recrystallization from a mixture of benzene and *n*-hexane gave material melting at 133–134°C. A melting point of 134°C. was reported by Herz.<sup>15</sup>

#### Preparation of 1-(Acetyl)aziridine

Acetyl chloride (23.55 g., 0.30 mole) in 225 ml. of anhydrous diethyl ether was stirred at 5–10°C. while a solution of triethylamine (30.70 g., 0.30 + mole) in 50 ml. of ether was added dropwise at such a rate that the temperature did not exceed 10°C. This reaction mixture was stirred vigorously at 0–5°C. while aziridine, (12.90 g., 0.30 mole), in 50 ml. of ether, was added dropwise over a period of 30 min. The reaction temperature was

not allowed to exceed 5°C. After addition was complete, stirring was continued for 30 min. at 0°C. followed by filtration of the amine salt. Removal of the solvent from the filtrate by use of vacuum at room temperature gave a yellow-orange liquid residue. Fractionation of this material on a 12 × 1/4 in. Vigreux column yielded a colorless liquid boiling at 30–32°/6.5 mm. and weighing 8.8 g. (34.6%). A yellow-orange viscous liquid weighing 7.3 g. remained in the distillation flask. The colorless liquid gave an infrared spectrum with a strong carbonyl stretching band at 5.92  $\mu$  (neat). The NMR spectrum consisted of two singlets at –2.21 and –2.14 ppm in a ratio of 3:4, respectively (CDCl<sub>3</sub>).

### Bulk Polymerization of 1-(Acetyl)aziridine

A 1.0-g. sample of 1-(acetyl)-aziridine was charged into a Carius combustion tube with two drops of BF<sub>3</sub> etherate (48%). The tube was thoroughly flushed with nitrogen, flame-sealed, and placed in a tube furnace at 160°C. for 20 hr. An orange-red colored viscous material was formed which was readily soluble in methylene chloride and in water. An infrared spectrum of this polymer in methylene chloride was virtually identical to that obtained for poly-2-methyl-2-oxazoline.

### Bulk Polymerization of 2-Methyl-2-oxazoline

A 1.0-g. sample of oxazoline monomer was polymerized as described above. The polymer was obtained as a glassy, nearly colorless resin with a melting range of 165–175°C. The polymer was readily soluble in methylene chloride and gave an infrared spectrum which was essentially identical to that obtained for poly-1-(acetyl)aziridine.

ANAL. Calcd. for C<sub>4</sub>H<sub>7</sub>NO: C, 56.45%; H, 8.30%; N, 16.46%. Found: C, 56.16%; H, 8.15%; N, 16.13%.

The authors wish to thank Dr. E. C. Steiner and Professor H. Walborsky for helpful discussions. Appreciation is also due to Dr. J. Heeschen for the NMR analyses.

### References

1. T. Mukaiyama, T. Fujisawa, H. Nobira, and T. Hyuaji, *J. Org. Chem.*, **27**, 3337 (1962).
2. T. Mukaiyama and K. Sato, *Bull. Chem. Soc. Japan*, **36**, 99 (1963).
3. T. Fujisawa, Y. Tamura, and T. Mukaiyama, *Bull. Chem. Soc. Japan*, **37**, 793 (1964).
4. H. Nobira, Y. Nishikawa, and T. Mukaiyama, *Bull. Chem. Soc. Japan*, **37**, 797 (1964).
5. A. R. Katrizky, *Physical Methods in Heterocyclic Chemistry*, Vol. II, Academic Press, New York, p. 218.
6. A. A. Goldberg and W. Kelly, *J. Chem. Soc.*, **1948**, 1919.
7. E. M. Fry, *J. Org. Chem.*, **14**, 887 (1949).
8. S. Gabriel and Th. Heymann, *Ber.*, **23**, 2493 (1890).
9. E. M. Fry, *J. Org. Chem.*, **15**, 802 (1950).
10. H. L. Wehrmeister, *J. Org. Chem.*, **28**, 2587 (1963).
11. E. M. Fry, *J. Org. Chem.*, **15**, 438 (1950).

12. J. D. Roberts, *Nuclear Magnetic Resonance*, McGraw-Hill, New York, 1959, p. 22.
13. S. Gabriel and A. Neumann, *Ber.*, **25**, 2383 (1892).
14. S. L. Walters and R. R. Miller, *Ind. Eng. Chem., Anal. Ed.*, **18**, 658 (1946).
15. W. Herz, *Ber.*, **30**, 1585 (1897).

### Résumé

Les 2-aryl et 2-alkyl-2-oxazolines ont été polymérisées en poly(*N*-aroyl) aziridine et poly(*N*-acyl)aziridine respectivement en présence de trifluorure de bore. Les polymères obtenus étaient vitreux sous forme de résine jaune à poids moléculaire variant de 3500 à 7500 (35 à 50 unités oxazolique par chaîne). Les vitesses de polymérisation ont été déterminées pour plusieurs de ces monomères. Un mécanisme de polymérisation est proposé.

### Zusammenfassung

2-Aryl- und 2-Alkyl-2-oxazoline wurden in Gegenwart von Bortrifluorid zu Poly(*N*-aroyl)aziridinen und Poly(*N*-acyl)aziridinen polymerisiert. Die erhaltenen Polymeren waren glasige, leicht gelb gefärbte Harze mit Molekulargewichten im Bereich von 3500 bis 7500 (35-50 Oxazolinbausteine pro Kette). Die Polymerisationsgeschwindigkeit einiger dieser Monomere wurde bestimmt. Ein Polymerisationsmechanismus wird vorgeschlagen.

Received December 22, 1965

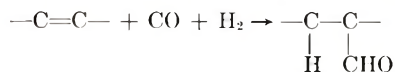
Prod. No. 5088A

## Hydroformylation of High Polymers

FLOYD L. RAMP, ELMER J. DEWITT, and LOUIS E. TRAPASSO,  
*B. F. Goodrich Research Center, Brecksville, Ohio*

### Synopsis

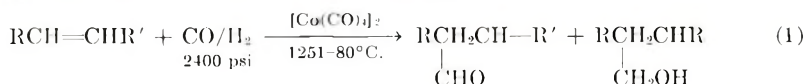
A new class of polymeric materials has been prepared and subjected to preliminary evaluation. These materials were obtained by hydroformylation of diene-based polymers. The olefinic bonds were saturated and aldehyde groups attached:



The extent of reaction may be varied at will up to 100% double bond conversion. The properties of these polymers are dominated by the active aldehyde groups. One of the chief characteristics of simple aldehydes is their ability to polymerize forming mainly aldehyde trimers and tetramers. This same phenomenon has been shown to occur with polymeric aldehydes with consequent gel formation. The gelling tendency has been closely related to the aldehyde content per unit volume which may be conveniently varied by (1) the concentration of the initial polymer, (2) the degree of unsaturation in the polymer, and (3) the extent of double bond conversion. Any combination which gives a free aldehyde concentration in excess of  $1 \times 10^{-4}$  mole/ml. is very prone to gel. The loose gels can be readily reversed by conditions which depolymerize aldehydes. The propensity of the aldehyde polymers to crosslink upon evaporation of the solvent was used to form films. These films were not discolored by ultraviolet light but under such treatment became quite brittle. The products may be stabilized by conversion of the aldehyde groups to more stable derivative, in particular the acetal. The extent of acetal formation has been shown to be controlled by steric factors. Complete polyacetal formation was possible only when the aldehyde groups were well dispersed along the polymer chain. Certain aldehyde derivatives (acetals, oximes) are thermoplastic. They soften at lower temperature than commercial plastics.

### INTRODUCTION

The oxo reaction converts olefins to aldehydes by a catalytic reaction with carbon monoxide and hydrogen [eq. (1)].

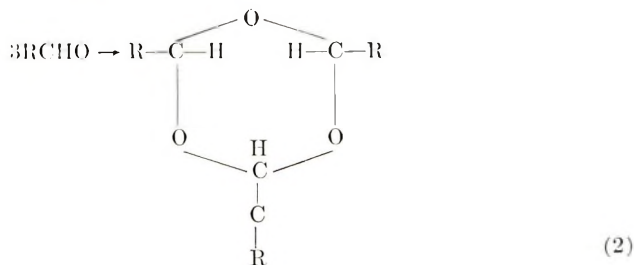


The catalyst (dicobalt octacarbonyl) is oil-soluble; hence oxo reaction mixtures are homogeneous. This process is, therefore, particularly applicable to diene-based polymers. There has been little mention of the hydroformylation of olefinic polymers in the literature.<sup>1-3</sup> The process may be considered as an alternative method to oxygenate polymers.

The oxo reaction has a long history and has been used industrially for



a number of years to make the so-called oxo alcohols by subsequent catalytic hydrogenation. When operating under optimum conditions, a very rapid reaction takes place and yields of simple aldehydes as high as 90% have been reported. The by-products formed by side reactions are predictable from the chemistry of aldehydes. The principal high-molecular weight by-products come from the polycondensation of aldehydes, e.g., acetaldehyde to paraldehyde<sup>4</sup> [eq. (2)].



The aldol condensation takes place under oxo conditions and directly or indirectly accounts for other high-boiling by-products present in the aldehyde distillation bottoms. Ketones are a by-product of importance in the hydroformylation of ethylene [eq. (3)], but have been reported to be of little importance with higher olefins.<sup>5-7</sup>



Alcohols are present due to reductive hydroformylation, and the aldehydes and alcohols react to form acetals. The alcohols may undergo homologation to form alcohols having one more carbon atom than the original alcohol.<sup>8,9</sup>



Various diene polymers, copolymers, and terpolymers, among them 1,4-polybutadiene, styrene-butadiene copolymer, and acrylonitrile-butadiene copolymers, have been evaluated under oxo conditions.

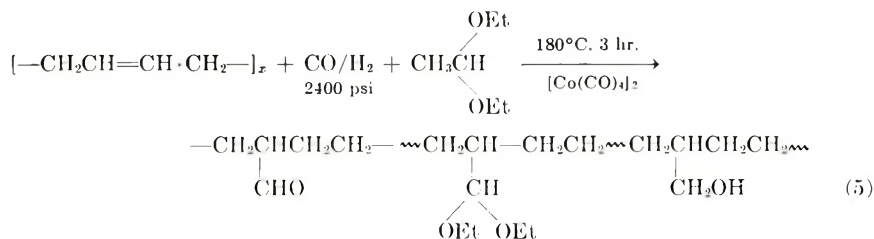
## DISCUSSION

### Oxo Reaction on 1,4-Polybutadiene

When a solution of polybutadiene (emulsion, free radically polymerized) was subjected to the oxo reaction at 145°C. for 3 hr. with an initial synthesis gas ( $\text{H}_2:\text{CO}$ , 1:1) pressure of 2400 psi, charged at room temperature a gel (crosslinking) was formed. However, under milder conditions, i.e., 125°C., 2 hr., 2400 psi gas, an oxo product of low double-bond conversion was obtained in solution. Free-radical crosslinking was suspected. It was found that the addition of certain free-radical inhibitors prevented gelation of polybutadiene in benzene at 145°C. Some antioxidants, such as phenyl  $\beta$ -naphthylamine and *tert*-butyl catechol, completely inhibited the oxo reaction. The free-radical inhibitor used with most success was *p*-

methoxyphenol. Phenolthiazine was also effective. However, free-radical inhibitors alone did not prevent gels in the oxo products.

Initial data indicated that with increasing aldehyde concentration in the polymer molecule, the polymer became more susceptible to gelling. Reagents were then added to the reaction mixture which would react with the aldehyde groups without preventing the oxo reaction. Reagents such as malonic ester, paraformaldehyde, and formalin inhibited the oxo reaction completely. Reagents which formed acetals on interaction with the aldehyde groups were effective to varying degrees. Methanol and ethyl orthoformate did not inhibit the oxo reaction, but they lost their effectiveness as the conversion of the double bonds became high, probably because of their slow rate in producing the acetal. Other acetal-forming agents (2,2-dimethoxypropane, 2,3-butanediol, 1,1-diethoxyethane, and other 1,2- and 1,3-glycols), although inhibiting the hydroformylation at 145°C., prevented gels at nearly quantitative double bond conversion at 180°C. Ethers and almost any reagent with electronegative atoms in a 1,2 or 1,4 position, i.e., 1,1-diethoxyethane, ethylene glycol, etc., showed an inhibitory influence under the usual oxo conditions, presumably due to interaction with the cobalt atom of the catalyst. This inhibition can be overcome in most cases by raising the temperature. As just noted, higher temperature (180°C. or higher), is required, and then two reactions proceed simultaneously. These are reduction of the aldehyde groups to alcohols and acetal formation. The final polymer, therefore, contains three different groups as shown by the infrared spectrum: aldehyde, hydroxyl, and acetal. The overall reaction with 1,1-diethoxyethane as condensing agent may be illustrated in eq. (5).



With acetal (1,1-diethoxyethane) as a condensing agent, other limiting conditions were also found. A catalyst concentration of 1.5% by weight of polymer gave almost complete conversion of the double bonds and no further beneficial effect may be derived by adding a larger quantity. A carbon monoxide to hydrogen ratio greater than one slows the rate of hydroformylation, while a ratio much less than one causes gel. The gel formation at higher hydrogen pressure is probably due to an increase in the rate of hydroformylation relative to the rate of acetal formation. Higher hydrogen pressures are known to speed up the rate of the oxo reaction,<sup>8</sup> but there is no report on its influence upon acetal formation. In actual practice it was found most convenient to use synthesis gas (CO:H<sub>2</sub> = 1:1) and this was employed extensively throughout the investigation. Furthermore, an

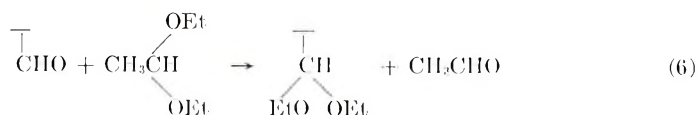
acetal (1,1-diethoxyethane) to olefin ratio of 1:3 gave a gel while a ratio of 3:1 gave a fluid solution. Under otherwise optimum conditions, a polymer solution above 4% resulted in a gel.

Upon standing at room temperature, many of the fluid oxo products prepared with acetal as a condensing agent also gelled. Those gels which developed on standing and many of those obtained directly from the autoclave were broken by adding more acetal and bubbling HCl gas through the gel. Hence, it was concluded that crosslinking occurred chiefly by a mechanism similar to that for the formation of paraldehyde from acetaldehyde.

This hypothesis was further strengthened by the fact that no condensing agent was necessary to produce a free polyaldehyde with a high conversion of the double bonds provided that a 6:1 ratio of a monofunctional, low molecular weight, aldehyde to olefin was used in place of the acetal forming reagent. Presumably, the monoaldehyde (acetaldehyde or *n*-heptaldehyde) minimized the interaction between polymer chains by itself becoming involved in the aldehyde polymerization. The concentration of the initial polymer solution using such aldehyde stabilizers, however, could not be increased beyond 5.5% since loose gels were otherwise obtained.

One may, therefore, conclude with a reasonable degree of certainty that the principal crosslinking reaction under the established experimental conditions is aldehyde polymerization. It is possible, however, that inter-chain acetal formation and ketone formation as well as aldol condensation and free-radical additions, involving unreacted double bonds, become more prevalent when concentrated cements are used or in the absence of a condensing agent or stabilizer. These additional crosslinking reactions probably do occur to a significant extent at higher temperatures since some gels, especially those formed in concentrated cements and/or at temperatures greater than 180°C., cannot be broken by the usual techniques for opening aldehyde trimers.

It was also found that when the more oil-soluble, nonvolatile alcohols and glycols, such as  $\beta$ -phenylethyl alcohol, 2,3-butanediol, and hexylene glycol, were employed as condensing agents, fluid reaction products were obtained which were less prone to gel on standing than the products prepared with 1,1-diethoxyethane as the acetal-forming reagent. A glycol to olefin ratio of 6:1 was usually required. Yet as indicated above only one-half as much acetal (1,1-diethoxyethane) is ordinarily required to obtain a gel-free product under the same reaction conditions. That this particular condensing agent was twice as effective as either the low molecular weight aldehydes or the glycols but were more gel-prone on standing may be due to its twofold activity. The 1,1-diethoxyethane reacts with the polyaldehyde by *trans*-acetal formation, producing a diethyl acetal on the polymer chain [eq. (6)]. Acetaldehyde produced as a by-product enters



into aldehyde cyclization, acting to limit the effective attached aldehyde concentration available for crosslinking. The tendency for these polymer solutions to gel upon standing may then be due to evaporation of the acetaldehyde (b.p. 20°C.) stabilizer.

Other condensing agents were also tried and were found to be effective. Benzene-insoluble glycols (ethylene glycol and glycerol) did not prevent gelling unless a cosolvent (usually tetrahydrofuran) was used to produce a homogeneous reaction mixture or one that would be homogeneous at the oxo reaction temperature.

Attempts were made to drive the acetal formation to high conversion under oxo conditions by adding a large excess of condensing agent and using anhydrous benzene as solvent. Since acetal formation is an equilibrium process [eq. (7)], both an increase in glycol concentration and a decrease in the concentration of water should drive the reaction to completion.



Even though high conversion of the double bonds was realized, incomplete conversion of the aldehyde groups to acetals was evident in the infrared spectra. There were always strong carbonyl peaks as well as the hydroxyl and acetal peaks. Several further attempts to prepare the complete polyacetal were carried out by a subsequent treatment varying the solvent (benzene, toluene, xylene), the catalyst (*p*-toluenesulfonic acid, sulfosalicylic acid), and the condensing agent (ethylene glycol, glycerol, 2,3-butanediol, hexylene glycol). All were performed with the use of a water separator to remove water by azeotropic distillation from the reaction mixture as it was formed in order to drive the reaction to completion. Such a technique has been reported to give excellent yields of acetals from monomeric aldehydes. In all cases the infrared spectra showed a substantial carbonyl absorption band which, although reduced in intensity, could never be eliminated completely.<sup>10a,11</sup>

Simple aldehydes are reported to react with hexylene glycol giving acetals in very high conversion because the equilibrium, eq. (7), lies far to the right. The oxo reaction mixture of 1,4-polybutadiene (1,4-PBX) with hexylene glycol can be concentrated, and the polymer is soluble in the glycol. The infrared spectrum of this solution showed no carbonyl band and an extremely small amount of unsaturation. Upon precipitation by addition of methanol, the polymer dissolved in fresh benzene with difficulty, and the resulting partially gelled solution gave a large infrared carbonyl band. The aldehyde groups in the former case were apparently present as the unstable hemiacetals due to excess glycol. Azeotropic distillation of water from the acidified polymer glycol solution failed to produce any alteration in the physical or chemical properties of the polymer. Water was collected which probably resulted from acid-catalyzed dehydration of



hexylene glycol. A similar experiment was carried out with the use of neopentyl glycol, which does not dehydrate, at least not by any simple mechanism. As with hexylene glycol, a substituted six-membered cyclic acetal should also be sterically favored. The polymer was not soluble in the melted glycol, but both glycol and polymer were soluble in refluxing xylene. No water was produced from this system, and the infrared spectrum still showed a very large carbonyl band. It was later found that completion of acetal formation is readily achieved when using a base polymer with fewer aldehyde groups on the polymer chain as in the case of hydroformylated high-styrene SBR. The difficulty in obtaining a high conversion to a polyacetal may, therefore, be attributed to steric hindrance which increases with increasing acetal formation.

### Oxo Reaction on High-Styrene SBR

Olefinic polymers hydroformylated to low conversion tended to be more soluble and less prone to gel. Thus, as the aldehyde concentration is diminished, the polyaldehyde oxo products from 1,4-polybutadiene became less susceptible to crosslinking via aldehyde polymerization. Reducing the ultimate aldehyde concentration may also be accomplished by hydroformylating base polymers with fewer double bonds. It was particularly desirable to obtain the oxo polyaldehyde acetal that was soluble once isolated and dried. The oxo process with ethylene glycol as condensing agent on styrene-butadiene copolymer (SBR, styrene:butadiene mole ratio = 1:6) still gives a rubbery material which is insoluble after drying. Hydroformylation of high-styrene SBR (styrene:butadiene mole ratio = 1:1) in the presence of ethylene glycol, glycerol, and 2,3-butanediol all gave polymers which were soluble in tetrahydrofuran after drying. A more detailed investigation of this base polymer was therefore initiated.

As with 1,4-PBN, the oxo reaction on high-styrene SBR required acetal-forming reagents to prevent gels at quantitative double bond conversion, also polymer concentrations greater than 4% resulted in gelled-material. A cosolvent, miscible with benzene (usually THF), was also necessary to solubilize the oil-insoluble glycol condensing agents. The glycol condensing agents inhibited the oxo reaction at 145°C., but at 180°C. quantitative conversion of the double bonds was realized with a reaction time of 3 hr. A minimum ratio of glycol to olefin bond of 4.5:1 was necessary to prevent gel formation via aldehyde polymerization. The amount of glycol used also affected the solubility as well as the dynamic extrusion temperatures of the dried polymers. Thus, as the ratio of ethylene glycol to olefinic bond is increased from 4.5:1 to 6:1, the dynamic extrusion temperatures ( $T_1$  and  $T_2$ ) decreased, and solubility in THF and benzene increased (Table I). This is probably due to an increase in cyclic acetal formation with a greater concentration of ethylene glycol. A further increase in the amount of glycol, however, does not produce any further effect. These materials were thermoplastics softening at low temperatures.

Under milder conditions (150°C. 3 hr.) it is also possible to obtain the



TABLE I  
Dynamic Extrusion Temperatures of the Oxo Product of High-Styrene SBR with Increasing Amounts of Ethylene Glycol

Ratio $\frac{\text{HOCH}_2\text{CH}_2\text{OH}}{\text{—CH=CH—}}$	Solubility (room temp.), time to dissolve	Dynamic extrusion temperatures <sup>a</sup>	
		$T_1$ , °C.	$T_2$ , °C.
Base polymer	Soluble	6	61
No glycol (free aldehyde)	Insoluble (—)	45	180
4.5	3 days	39	104
5	24 hr.	42.1	96.6
6	15 min.	31	78.5

<sup>a</sup> Dynamic extrusion values  $T_1$ , roughly the second-order transition temperature and  $T_2$ , the melt flow temperature, were estimated by using a dynamic extrusion rheometer. In the operation of this instrument the (granular) polymer sample is placed in a chamber under a plunger comprising a load of 3263 psi. The sample is gradually heated to effect its ultimate extrusion through a 0.0625-in. diameter orifice. Plunger advance and temperature increase are measured. A plot of these values provides a curve from which  $T_1$  and  $T_2$  can be obtained.

free polyaldehyde of high-styrene SBR in high double bond conversion. The infrared spectrum shows very little residual unsaturation in addition to a very large carbonyl band. The maximum possible concentration was not determined, but the experiment was repeated several times with an initial 2.5% solution. The dry, free polyaldehyde was a crosslinked material. By addition of a high-boiling alcohol as stabilizer (ethanol  $\beta$ -phenylethyl alcohol) concentrations up to 10% can be obtained without gelling. Acetaldehyde and *n*-heptaldehyde were also found to be very effective stabilizers.

### Reductive Hydroformylation

As the temperature and/or the time of reaction is increased, a correspondingly larger number of the aldehyde groups become reduced to hydroxymethyl groups. At 150°C. for 3 hr. without a condensing agent, a solution of the free polyaldehyde results from an initial 2.5% solution. At 180°C. for 3 hr. a gel results which is probably due to both aldehyde polymerization and chain-chain acetal or hemiacetal formation. At 240°C. for 3 hr. a partially gelled polymer solution results whose infrared spectrum shows a large aldehyde band but also a well-distinguished hydroxyl band. In the presence of isopropyl alcohol (alcohol to olefin ratio = 6:1) at 225°C. for 5 hr., a solution of the hydroxymethyl polymer results. This hydroxylic polymer was a low-softening plastic ( $T_1 = 45^\circ\text{C.}$ ,  $T_2 = 75^\circ\text{C.}$ ) readily soluble in THF and benzene. It is significant to note, however, that the attempted oxo reduction of SBR and 1,4-polybutadiene produced only gelled material.

Complete acetal formation, which was found impossible with the oxo product from 1,4-PBN because of molecular overcrowding, was readily achieved with high-styrene SBR. The benzene solutions of the polyalde-

hyde-acetals from the hydroformylation were mixed with additional glycol and an acid catalyst, and the acetal formation was driven to completion by azeotropic distillation of water. The polyacetals from ethylene glycol and glycerol have been prepared which have infrared spectra with very weak or no carbonyl peaks. These products were rubbery materials and very soluble in THF. The polyaldehyde acetals resulting from the oxo process on high-styrene SBR in the presence of glycols were more plastic and much more insoluble than the polyacetals resulting from their further reaction with addition glycols. This is probably because the free aldehyde groups of the former provide crosslinks via aldehyde polymerization which causes the material to be less soluble. This explanation is consistent with the gradation in properties obtained by increasing the glycol concentration in the oxo reaction mixture.

The polyaldehyde acetals were moldable. Since the  $T_1$  increased with increasing aldehyde concentration, it seemed possible that the free polyaldehyde might also be moldable and provide a harder, higher-softening plastic with essentially thermally reversible crosslinks. However, the insoluble, dried polyaldehyde showed a considerable memory upon molding, even with an acid (*p*-toluenesulfonic acid) present which might have been expected to catalyze cleavage of the crosslinks similar to acid-catalyzed monoaldehyde formation from paraldehydes. That the crosslinking is due to aldehyde polymerization was verified by the fact that removal of the last traces of aldehyde by sodium borohydride reduction gave a readily soluble polymer.

#### Oxo Reaction on Other Olefinic Polymers

The standard conditions established for the oxo process on 1,4-PBN and high-styrene SBR in the presence of glycols and other condensing agents (180°C., 3 hr., 2400 psi gas, 2.5–4.0% cements) were applied to other diene polymers. Thus, ethyl acrylate–butadiene copolymer (mole ratio 1:1), methyl methacrylate–butadiene copolymer (mole ratio 1:1), Neoprene (type W), Hycar 1041 (39–42% bound VCN), Hycar 1577 (34% BN, 35% styrene, 31% VCN), Hycar 1010 × 25 (6% BN, 17% styrene, 16% VCN), isoprene–butadiene copolymer (mole ratio 1:1), natural rubber (pale crepe), Balata, SBR, an SBR with 3.0% bound acrylic acid, and styrene–butadiene copolymer (25% BN) all gave polyaldehyde acetals with nearly quantitative double-bond conversion. Experiments employing benzene-insoluble glycols required a cosolvent (usually THF) in order to obtain a completely miscible reaction mixture. In all cases, the ratio of glycol to olefinic bond of 6:1 or greater was required to prevent gels. All but styrene–butadiene copolymer (25% BN) and the SBR with 3.0% bound acrylic acid gave rubbery products. The two exceptions were plastic materials. Attempts to produce a free polyaldehyde from each of these materials with the use of 2.3–3.0% cements resulted in gels.

#### Decobalting

A number of patents have been issued involving catalyst removal from monomeric aldehydes prepared by hydroformylation.<sup>4</sup> A number of these

methods have been tried to suit our particular circumstances. It was found, however, that decobalting became increasingly difficult with an increase in the aldehyde content of the polymer since these polymers with high aldehyde content were more gel prone. Hence, the oxo products from 1,4-PBN were more difficult to decobalt than the oxo products from high-styrene SBR. Similarly, it was more difficult to remove the cobalt catalyst from the free polyaldehydes than from the polyaldehyde-acetals.

Decomposition of the dicobalt octacarbonyl was usually effected by bubbling HCl gas through the reaction mixture. A blue or green solution would result due to anhydrous or hydrated  $\text{CoCl}_2$ . If an insufficient amount of condensing agent were present, the solution would gel since aldehyde polymerization is an acid-catalyzed process. The cyclic acetal derivatives showed less propensity to gel probably because they were more stable and because the glycol condensing agents were not volatile. Decomposing the cobalt carbonyl in the presence of the free polyaldehyde of high-styrene SBR was effectively accomplished by heating the dark reaction mixture in the presence of oxalic acid dihydrate crystals. Presumably, the cobalt oxalate which is formed becomes occluded onto the surface of the larger insoluble (in benzene) oxalic acid crystals. The decobalted polyaldehyde solution may then be decanted from the solid material.

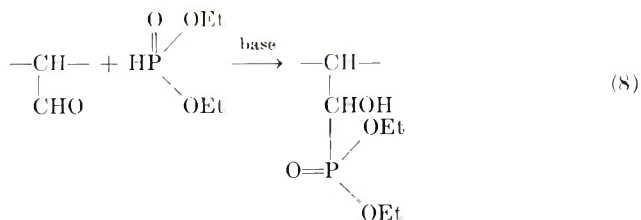
### Preparation of Aldehyde Derivatives

It has previously been stated that the polyacetals from high-styrene SBR can be readily obtained by running the hydroformylation in the presence of glycols followed by a subsequent step to complete the acetal formation. Since the free polyaldehyde of high-styrene SBR was also obtained, other aldehyde derivatives were prepared.

With the use of a cosolvent and a base to liberate the free hydroxylamine, the polyoxime was prepared. It was a low-softening thermoplastic ( $T_1 = 52.5^\circ\text{C}$ .,  $T_2 = 107^\circ\text{C}$ .), whose infrared spectrum showed that the carbonyl band had been completely eliminated.

As previously stated, the polyhydroxy methylene derivative has also been prepared by sodium borohydride reduction. It also is a low-softening thermoplastic ( $T_1 = 45^\circ\text{C}$ .,  $T_2 = 75^\circ\text{C}$ .).

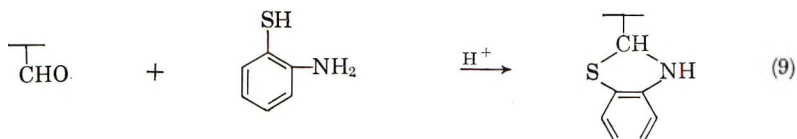
The base-catalyzed reaction of an aldehyde with diethyl phosphite [eq. (8)] proceeds exothermically.<sup>12,13</sup>



The polymer derivative so prepared still showed a moderate carbonyl band in its infrared spectrum, but the dry polymer was a tough material soluble in THF and benzene.

Several attempts at peracetic acid oxidation of the polyaldehyde consistently gave a material which when dry was tough but insoluble. The freshly precipitated polymer, however, was soluble in THF and benzene. A silver oxide oxidation was also tried but the aldehyde groups failed to oxidize.

The condensation product of the aldehyde groups with *o*-aminothiophenol was also prepared [eq. (9)]. The carbonyl band was reduced not



eliminated. The product was a low-softening plastic with a rough appearance when molded ( $T_1 = 70^\circ\text{C}$ .,  $T_2 = 166^\circ\text{C}$ ).<sup>10b</sup>

These same reactions as described above on high styrene SBR were also tried on the polyaldehyde acetals from 1,4-PBN. With basic reactants or under basic conditions, the acetals on the polymer chain should be stable permitting only the residual free aldehyde groups to react. These attempts were unsuccessful, due probably to steric hindrance, as in the case of the failure to obtain complete polyacetal formation with hydroformylated 1,4-PBN.

TABLE II  
Hydroformylated High-Styrene SBR

	No. 2070	No. 2080	2081
Condensation agent	Ethylene glycol	Glycerol	2,3-Butanediol
Infrared spectrum	St. $\begin{array}{c} \text{O} \\ // \\ \text{C} \\   \end{array}$ and ether bands, little unsaturation	St. $\begin{array}{c} \text{O} \\ // \\ \text{C} \\   \end{array}$ and ether bands; little unsaturation	St. $\begin{array}{c} \text{O} \\ // \\ \text{C} \\   \end{array}$ and ether bands, little unsaturation
Dynamic extrusion temp., °C.			
$T_1$	33	26	31
$T_2$	95	85	91
Izod impact, ft.-lb./in. thickness	10.8	9.6	11.2
Tensile strength			
Avg. yield point, psi	1133	—	1021
Avg. ultimate tensile, psi	1300	1125	1096
Avg. ultimate elongation, %	218	95	322
Rotary flex			
Avg. no. of flexures	3,504	960	9,444
Avg. time, min.	49.2	8	78.7



### Physical Evaluation as Thermoplastic Materials

Oxo products from 1,4-PBN in the presence of acetal-forming reagents are rubbery, crosslinked materials. The polyaldehyde-acetals resulting from the hydroformylation of high-styrene SBR in the presence of ethylene glycol, glycerol, and 2,3-butanediol appeared to be stiff and hard enough to be evaluated as thermoplastics. Some of the more important information is summarized in Table II.

**Heat Aging.** These tests were conducted at 190°C. for 15, 30, 45, 60, 75, and 90 min. This heat treatment was rather severe but the result may still be significant. The samples became progressively more brittle and darker with time. The clear sheets shrunk and became light brown after 90 min. The amount of shrinkage after 90 min. of exposure appeared to be the same as after 15 min.

**Weatherometer Tests.** The materials were subjected to ultraviolet light under standard Weatherometer test conditions at 156°F. for 3 days. The treatment resulted in very little discoloration but all three samples became quite brittle and broke under mild pressure. Brittleness due to curing is probably due to the free aldehyde content, since acetal linkages are known to be relatively stable to ultraviolet light (i.e., Butyral). All three samples contained a considerable amount of free aldehyde units which were not converted to acetals as indicated by their infrared spectra.

## EXPERIMENTAL

### Materials

All polymers were either commercial materials or were prepared by standard techniques. Cobalt octacarbonyl was prepared from cobalt carbonate by reaction with synthesis gas.

### Hydroformylation of Olefinic Polymers

A 6.0% solution of each of the base polymers in benzene or tetrahydrofuran was prepared and stored until ready for use. The appropriate amount of each 6.0% solution was weighed out and mixed with benzene and/or tetrahydrofuran. A condensing agent or stabilizer (glycol, alcohol, or aldehyde) was also usually added. The final concentration of polymer was ordinarily 2.5–4.0% with the glycol condensing agents, although concentrations up to 6.0% can be used without gel formation using aldehyde stabilizers. A minimum catalyst concentration of 1.5% by weight on polymer was generally used. These materials were then placed into an autoclave, charged with synthesis gas ( $\text{CO}:\text{H}_2 = 1:1$ ) and heated at 125–225°C. for 1–5 hr. The following reactions are typical.

**Oxo Reaction on 1,4-Polybutadiene.** The charge was 1,4-PBN (6% benzene solution), 85 g. (0.1 mole  $\text{CH}=\text{CH}$ ); benzene, 280 ml.; 1,1-diethoxyethane, 44 g. (0.37 mole); cobalt carbonyl (0.353*M*) 2 ml. The autoclave (850 ml.) was purged with  $\text{N}_2$  and charged to 2400 psi gas at room temperature. The reaction was run at 180°C. for 3 hr.



Other oxo products from 1,4-PBN may be obtained by adding 0.6 mole of other condensing agents (2,3-butanediol, hexylene glycol, neopentyl glycol, etc.) in place of the 1,1-diethoxyethane. Alternately, 0.6 mole of a monoaldehyde stabilizer or 1.2 mole of a benzene-soluble monohydric alcohol which does not precipitate the polymer (e.g., benzyl alcohol) may also be used.

**Oxo Reaction on 1,4-PBN with a Benzene-Insoluble Glycol.** The charge was 1,4-PBN (6% benzene solution), 445 g. (0.5 mole —CH=CH—); tetrahydrofuran, 800 ml.; ethylene glycol, 198 g. (3.2 mole); benzene, 800 ml.; cobalt carbonyl (0.353*M*) 10 ml. The autoclave (2960 ml.) was purged with N<sub>2</sub> and charged to 2400 psi gas at room temperature. The reaction was run at 180°C. for 3 hr.

The use of tetrahydrofuran as a mutually miscible cosolvent is imperative when benzene-insoluble glycols such as ethylene glycol and glycerol are used, since gels otherwise result. It may, however, be used as a standard cosolvent for hydroformylation of olefinic polymers.

### References

1. L. F. Hatch, *Higher Oxo Alcohols*, Wiley, New York, 1957.
2. M. Orchin, *Advan. Catal.*, **5**, 385 (1953).
3. I. Wender and M. Orchin, *Advan. Catal.*, **9**, 594 (1957).
4. M. Orchin and L. S. Kirch, Ph.D. Dissertation, University of Cincinnati, 1958; University Microfilms, Inc., Ann Arbor, Michigan.
5. D. L. Cottle and D. W. Young, U.S. Pat. 2,787,644 (1957).
6. D. L. Cottle, A. J. Moreway, and D. W. Young, U.S. Pat. 2,844,534 (1958).
7. J. P. Jones and W. M. Axe, U.S. Pat. 2,544,555 (1951).
8. O. Roelen, U.S. Pat. 2,327,066 (1943).
9. G. Natta, P. Pino, and R. Ercoli, *J. Am. Chem. Soc.*, **74**, 4496 (1952).
10. E. E. Royals, *Advanced Organic Chemistry*, Prentice-Hall, New York, 1954, (a) p. 629; (b) p. 649.
11. R. E. Dunbar and H. Adkins, *J. Am. Chem. Soc.*, **56**, 442 (1934).
12. E. K. Fields, *J. Am. Chem. Soc.*, **74**, 1528 (1952).
13. G. M. Kosolapoff, *Organophosphorus Compounds*, Wiley, New York, 1950, p. 128.

### Résumé

Une nouvelle classe de matériaux polymériques ont été préparés et soumis à une évaluation préliminaire. Ces matériaux ont été obtenus par hydroformylation de polymères à base de diène. Les liaisons oléfiniques ont été saturées et des groupes aldéhydiques introduits suivants l'équation: —C=C— + CO + H<sub>2</sub> → —C—C—.



Le degré d'avancement de la réaction peut être variable mais peut atteindre jusqu'à 100% de double soudure consommée. Les propriétés de ces polymères sont dominées par des groupes aldéhydiques actifs. L'une des caractéristiques principales des aldéhydes simples est leur capacité à polymériser en formant des aldéhydes trimères et tétramères. Ce même phénomène se passe avec ces aldéhydes polymériques avec conséquemment la formation d'un gel. La tendance à gélifier a été étroitement liée à la teneur en groupe aldéhyde par unité de volume qui peut être varié soit (1) en variant la concentration en polymère initial; (2) le degré de la saturation dans le polymère et (3) en variant le degré de conversion de la double soudure. Chaque combinaison qui donne une concentration

d'aldéhyde libre excédant  $4 \times 10^{-4}$  mole/ml. est très apte à se gélifier. Les gels plus ou moins lâches peuvent être facilement dissous dans des conditions qui dépolymérisent les aldéhydes. La propension des polymères aldéhydiques à se ponter par évaporation des solvants peut être utilisée en fin de formation de films. Ces films ne se colorant pas par la lumière ultraviolette mais deviennent sous l'effet de ce traitement plutôt fragiles. Les produits peuvent être stabilisés en transformant des groupes aldéhydiques en groupes dérivés plus stables tels que des groupes acétaliques. Le degré de formation d'acétal est contrôlé par des facteurs stériques. La formation complète en polyacétal était possible uniquement lorsque des groupes aldéhydiques étaient bien dispersés le long de la chaîne polymérique. Certains dérivés de ces aldéhydes tels que acétals et oximes sont thermoplastiques. Ils se ramolissent à la température plus basse que les plastiques commerciaux.

### Zusammenfassung

Eine neue Klasse polymerer Stoffe wurde dargestellt und einer vorläufigen Auswertung unterzogen. Diese Stoffe wurden durch Hydroformylierung von Polymeren auf Diengrundlage erhalten. Die olefinischen Bindungen wurden gesättigt und Aldehydgruppen angebracht:

$$-C=C- + CO + H_2 \rightarrow -\underset{\text{H}}{C}-\underset{\text{CHO}}{C}-$$

Der Reaktion kann willkürlich bis zu 100% Doppelbindungsumsatz gebracht werden. Die Eigenschaften dieser Polymeren werden durch die aktiven Aldehydgruppen bestimmt. Eines der Hauptmerkmale einfacher Aldehyde ist ihre Fähigkeit, unter bevorzugter Bildung von Aldehydtrimeren und -tetrameren zu polymerisieren. Die gleiche Erscheinung mit darauffolgender Gelbildung konnte an den polymeren Aldehyden nachgewiesen werden. Die Gelbildungstendenz steht in enger Beziehung zum Aldehydgehalt pro Volumseinheit, welche in einfacher Weise durch (1) die Konzentration des Ausgangspolymeren, (2) den Un sättigungsgrad in Polymeren und (3) das Ausmass des Doppelbindungsumsatzes variiert werden kann. Jede Kombination, welche eine Konzentration an freiem Aldehyd oberhalb  $1 \cdot 10^{-4}$  Mol/ml liefert, neigt stark zur Gelbildung. Die lockeren Gele können unter Bedingungen, welche zur Depolymerisation von Aldehyden führen, leicht zerstört werden. Die Fähigkeit der Aldehydpolymeren, bei Verdampfung des Lösungsmittels zu vernetzen, wurde zur Bildung von Filmen benützt. Diese Filme wurden durch UV-Licht nicht verfarbt, wurden aber bei dieser Behandlung recht spröde. Die Produkte können durch Umwandlung der Aldehydgruppen in stabile Derivate, besonders in das Acetal, stabilisiert werden. Das Ausmass der Acetalbildung wird durch sterische Faktoren kontrolliert. Eine vollständige Polyacetal-Bildung war nur bei einer guten Verteilung der Aldehydgruppen über die Polymerkette möglich. Gewisse Aldehydderivate (Acetale, Oxime) sind Thermoplaste. Sie erweichen bei niedrigeren Temperaturen als handelsübliche Plastomere.

Received March 30, 1965

Prod. No. 5089A

## Studies on Polymers Containing Functional Groups.

### III. Charge-Transfer Interaction between Quinone and Aza Polymers

HIROKO SUGIYAMA and HIROYOSHI KAMOGAWA, *Textile Research Institute, Kanagawa, Yokohama, Japan*

#### Synopsis

Absorption maxima and equilibrium constants for charge-transfer complexes between quinone and aza polymers, such as poly-2-vinylpyridine, poly-4-vinylpyridine, poly-2-methyl-5-vinylpyridine, and poly-*N*-dimethylaminomethylacrylamide, were determined spectrophotometrically. For comparison, those for charge-transfer complexes between quinone and aza compounds, such as pyridine, methyl-substituted pyridines, quinoline, triethylamine, and dimethylaniline were also presented. It was found that the equilibrium constants for polymer complexes are always larger than those for the corresponding monomer complexes, while the time required for attaining the equilibrium was longer for polymer complexes than for monomer complexes. In the interaction between quinone and poly-*N*-dimethylaminomethylacrylamide, two absorption maxima which gradually shifted towards each other were observed. The same phenomenon was found in the interaction between quinone and the corresponding monomer, triethylamine.

Pronounced changes in absorption spectra are often observed to accompany the reaction of two substances to form a charge-transfer complex. This effect is generally attributed to a loose reversible association between electron donor and electron acceptor.

Detailed spectroscopic investigations concerning these charge-transfer complexes have been carried out by several groups of workers,<sup>1-7</sup> but much less is known about charge-transfer complex formation in which one of the components is polymer.<sup>8,9</sup>

The present investigation was undertaken to obtain some information on the mechanism of complex formation between a donor-type polymer, aza-polymer, and a monomer acceptor, quinone, and to see if there are peculiarities in polymer interaction as compared with interaction between monomers.

#### EXPERIMENTAL

##### Materials

**Donors.** Pyridine,  $\alpha$ -picoline,  $\beta$ -picoline,  $\gamma$ -picoline, 2,6-lutidine, 2,4,6-collidine, quinoline, triethylamine, and dimethylaniline were purified by distillation just before use.

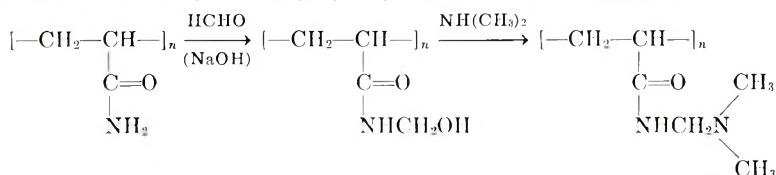
**Acceptors.** Reagent-grade quinone was used without further treatment.

**Solvent.** Reagent-grade ethyl alcohol, chloroform, and ion-exchanged water were used without further purification. It was confirmed that they were spectroscopically pure in the measuring range.

**Donor-Type Polymer.** Poly-2-vinylpyridine (PVP-2), poly-4-vinylpyridine (PVP-4), and poly-2-methyl-5-vinylpyridine (2M-PVP-5) were obtained through the azobisisobutyronitrile-initiated polymerization of the respective vinylpyridines. In a typical preparation, 5 g. of 2-vinylpyridine free from inhibitor and 0.05 g. of azobisisobutyronitrile as initiator in 5 ml. ethyl alcohol were put into a sealed tube. The tube was cooled with Dry Ice, evacuated, and warmed to room temperature. This operation was repeated twice, after which the tube was evacuated and sealed.

Polymerization was carried out at 80°C. for 48 hr. After about 1 hr. the solution changed in color to light yellow. The polymer solution thus produced was diluted with a small amount of ethyl alcohol and poured into a large quantity of water. The precipitated polymer was finally obtained in white and fluffy form by freeze-drying from *tert*-butyl alcohol.

Poly-*N*-dimethylaminomethylacrylamide (PDA) was obtained by reaction between methylolated polyacrylamide and dimethylamine.



A mixture of 5.0 g. of acrylamide and 0.05 g. of potassium persulfate as initiator in 100 ml. water containing 20% methyl alcohol, was heated at 90°C. for 50 min. (Methyl alcohol was used to decrease the degree of polymerization.) The polyacrylamide solution obtained was heated at 50°C. for 1 hr. with 40% excess paraformaldehyde, the medium being kept basic with sodium hydroxide. The resulting solution of methylolated polyacrylamide was heated with 40% excess dimethylamine at 50°C. for 1 hr.

The polymer solution thus prepared was poured into an excess of acetone to precipitate the polymer. The polymer was dissolved in a small amount of water and then precipitated in a large quantity of acetone. The operation was repeated until the smell of dimethylamine disappeared. Finally the precipitated polymer was obtained in white and fluffy form by freeze-drying from *tert*-butyl alcohol containing some water. This polymer is soluble in ethyl alcohol as easily as in water. Upon standing in the air, it gradually turns light pink.

The infrared spectrum of this polymer was essentially identical with that of polyacrylamide except for an absorption peak at about 1550  $\text{cm}^{-1}$  which is assignable to the amide II band. The purity of this polymer was

calculated to be 67.7% by the titration with HCl. The intrinsic viscosity of the polymer was 0.7 dl./g. at 25°C. in water.

### Method

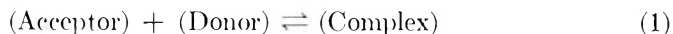
The absorption spectra and optical density measurements were made on a Hitachi photoelectric spectrophotometer EPU-2A and a Hitachi recording spectrophotometer EPS-2 with the use of 1-cm. quartz cells at room temperature.

Quinone solutions and mixed solutions of quinone and aza compounds were always protected from light.

The optical density for either quinone or the aza compound alone was always subtracted from the result to afford that of the charge-transfer complex.

The equilibrium constant  $K$  and the molecular extinction coefficient  $\epsilon$  were calculated by the method of Benesi and Hildebrand.<sup>1</sup>

If the complex is assumed to contain one mole each of donors and acceptor, the association equilibrium may be written as



$K$  is given by then

$$K = [C] / \{([A] - [C]) \cdot ([D] - [C])\} \quad (2)$$

where  $[A]$ ,  $[D]$ , and  $[C]$  are molar concentrations of acceptor, donor, and complex, respectively.

For the experimental conditions employed,  $[D] \gg [A]$ ,  $[D] - [C] \approx [D]$ . Substituting the optical density,  $\delta = \log I_0/I$ , for  $[C]$  and rearranging eq. (2), we obtained the expression,

$$[A] \cdot l / \delta = (1/K\epsilon[D]) + (1/\epsilon) \quad (3)$$

where  $l$  is the cell length.

A plot of  $[A]l/\delta$  against  $1/[D]$  should be linear and yield  $\epsilon$  as the reciprocal of the intercept and the product  $K\epsilon$  as the reciprocal of the slope.

## RESULTS AND DISCUSSION

For all complexes in this study, fairly good straight lines of optical density plots were obtained, so that it is evident that 1:1 type complexes were formed. Figure 1 shows optical density plots for the complex of quinone and PDA. The absorption maximum  $\lambda_{\max}$ , equilibrium constant  $K$ , and molecular extinction coefficient  $\epsilon$  for all complexes are summarized in Table I.

### Charge-Transfer Interaction between Quinone and Pyridine

**Change of Spectra with Time.** An aqueous solution of quinone and pyridine is strongly colored in the visible wavelength region, while a solution containing either quinone or pyridine alone is comparatively light in color in this wavelength region.



The color intensity of this solution increases with reaction time. At first the absorption maximum appears at 430  $m\mu$ , and the absorption intensity at the maximum increases rapidly within 1 hr. (Fig. 2). Then the maximum at 430  $m\mu$  disappears gradually and at last the absorption maximum shifts to 360  $m\mu$  after 24 hr. The color intensity of the solution of either quinone or pyridine alone scarcely changed after 24 hr.

TABLE I  
 $\lambda_{\max}$ ,  $K$ , and  $\epsilon$  for Quinone-Donor Systems

Donor	Solvent	$\lambda_{\max}$ , $m\mu$	$K$	$\epsilon$
Pyridine	H <sub>2</sub> O	430	9.0	1500
"	H <sub>2</sub> O-EtOH, 80:20	420	4.0	1200
"	H <sub>2</sub> O-EtOH, 60:40	420	3.4	700
"	H <sub>2</sub> O-EtOH, 40:60	430	0.6	900
"	H <sub>2</sub> O-EtOH, 20:80	430	—	—
"	EtOH	438	0.1	40
"	Chloroform	445	—	—
$\alpha$ -Picoline	H <sub>2</sub> O	430	4.8	1700
$\beta$ -Picoline	H <sub>2</sub> O	430	11.7	1400
$\gamma$ -Picoline	H <sub>2</sub> O	370	5.6	3400
2,6-Lutidine	H <sub>2</sub> O	430	8.6	800
2,4,6-Collidine	H <sub>2</sub> O	405	6.9	2000
Dimethylaniline	EtOH	470	0.5	400
Triethylamine	EtOH	480	2.0	200
		360	24.5	200
Quinoline	EtOH	500	0.5	700
		390	—	—
PVP-2	H <sub>2</sub> O-EtOH, 20:80	360	18.9 <sup>a</sup>	400
PVP-4	H <sub>2</sub> O-EtOH, 20:80	360	91.7 <sup>a</sup>	140
2M-PVP-5	H <sub>2</sub> O-EtOH, 20:80	360	15.5 <sup>a</sup>	220
PDA	H <sub>2</sub> O	510	86. <sup>b</sup>	1250
PDA	H <sub>2</sub> O	325	48. <sup>a</sup>	2300

<sup>a</sup> Optical density measured 2 hr. after the solution was prepared.

<sup>b</sup> Optical density measured 10 min. after the solution was prepared.

Readings of absorption intensity were taken 1 hr. after the preparation of the solution for the complexes with aza compounds in order to eliminate the effect of secondary reaction.

**Effect of Solvent on Equilibrium Constant.** In water, ethyl alcohol, and water-ethyl alcohol mixtures equilibrium constants increased with increasing water content in mixed-solvent media. In chloroform the opti-

cal density was so weak that the equilibrium constant could not be calculated.

It was also noticed that there is a strong blue shift when the polarity of solvent is increased, suggesting that in these systems pyridine behaves as a *n*-donor.

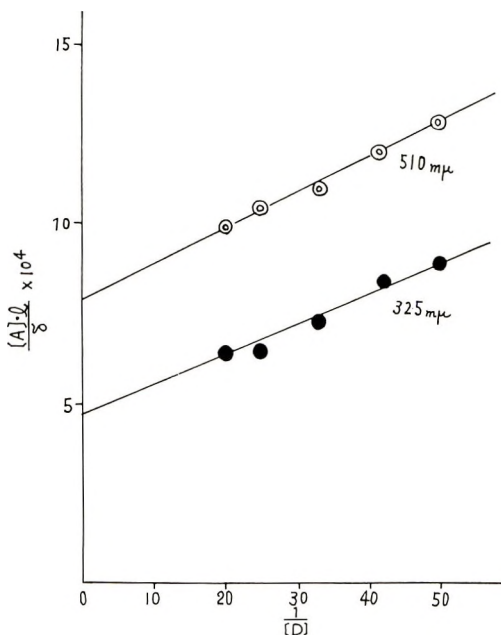


Fig. 1. Complex formation of quinone with PDA.

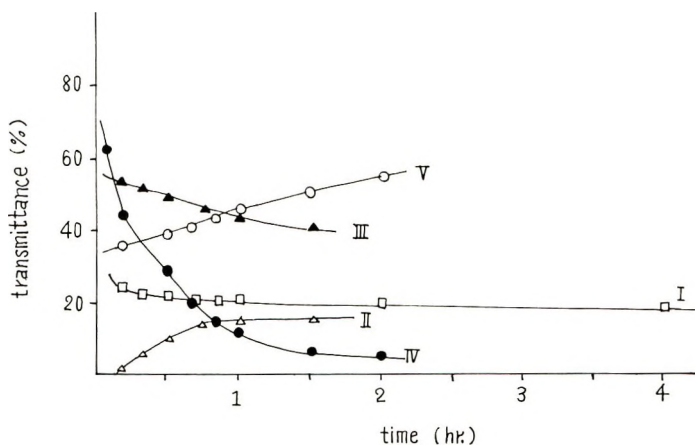


Fig. 2. Change of absorption intensity with time: (I) quinone-pyridine system, 430  $m\mu$  ( $H_2O$ ); (II) quinone-triethylamine system, 360  $m\mu$  ( $EtOH$ ); (III) quinone-triethylamine system, 480  $m\mu$  ( $EtOH$ ); (IV) quinone-PDA system, 325  $m\mu$  ( $H_2O$ ); (V) quinone-PDA system, 510  $m\mu$  ( $H_2O$ ).

### Charge-Transfer Interaction between Quinone and Methyl-Substituted Pyridine

Except for  $\gamma$ -picoline, the absorption maxima for these complexes are not too far from 430  $m\mu$ . The stability of the complexes might be determined by the steric effect and hyperconjugation of methyl groups of substituted pyridines. That the equilibrium constants for  $\alpha$ -picoline, 2,6-lutidine, and 2,4,6-collidine are less than that for pyridine can be explained by the conjecture that the methyl groups at the 2 or 6 position will effectively shield the nitrogen atom at the 1 position. It can also be understood that the equilibrium constant for  $\beta$ -picoline is larger than that for  $\alpha$ -picoline as a result of reduced steric hindrance. But  $\gamma$ -picoline, which is free from steric hindrance and should have a positive effect owing to hyperconjugation, gives a much smaller equilibrium constant than expected.

It can be seen from the above results that the steric hindrance of methyl groups is more effective in modifying the stability of complexes than hyperconjugation and that the geometrical structures for the complexes are not simple.

### Charge-Transfer Interaction between Quinone and Other Aza Compounds (Dimethylaniline, Triethylamine, and Quinoline)

In alcoholic solution of quinone and dimethylaniline, a new absorption band appeared at 470  $m\mu$ . The intensity at maximum and the spectral curve did not change with reaction time. It seemed that formation of the charge-transfer complex proceeds instantaneously, while all other aza compounds, such as pyridine, triethylamine, and quinoline, need about 1 hr. to attain the equilibrium state.

In the quinone-triethylamine system, a new strong absorption maximum appears at 360  $m\mu$  within 10 min. after preparation of the solution. The intensity at 360  $m\mu$  gradually diminishes with time and a weak absorption maximum appears at 480  $m\mu$  showing a sharp isosbestic point at 440  $m\mu$ . After 1 day the peak at 360  $m\mu$  remains at a weaker level and the peak at 480  $m\mu$  is deepened. The changes of color intensity with time at 360 and 480  $m\mu$  are shown in Figure 2.

In the quinone-quinoline system, two absorption maxima, a stronger one at 390  $m\mu$ , and a weaker one located at 500  $m\mu$ , were observed. For the complex with quinoline having an absorption maximum at 390  $m\mu$ , the intercept of the optical density plots was negative, so that the equilibrium constant and molecular extinction coefficient could not be calculated.

This fact might suggest that the two peaks have different origins; for instance, one of them might be due to a  $\pi$ -donor and the other a  $n$ -donor.

### Charge-Transfer Interaction between Quinone and Polyvinylpyridine

When one of the components of the complexes is a polymer, there are many difficulties in measuring optical density. For instance, the presence of some insoluble residue greatly affects apparent optical density of the complex.

According to Zwick,<sup>9</sup> the age of the polymer solution also affects the optical density of the complex. In our study, the polymer solution was mixed with a quinone solution 2 hr. after the polymer was dissolved.

In complex formations between quinone and the three types of polyvinylpyridine in ethyl alcohol, absorption maxima appeared at 360  $m\mu$  except for 2M-PVP-5, where the absorption intensity was increased but a distinct absorption maximum could not be observed. In these systems, it seems that a 2-hr. period is required to attain the equilibrium state.

Optical densities for the quinone-PVP-2 system at 360  $m\mu$  2 hr. after the two components were mixed were 0.390 in ethyl alcohol, and 1.732 in 80% ethyl alcohol-20% water, respectively. The tendency for a small concentration of water to increase the absorption intensity was also observed in the quinone-pyridine system.

The equilibrium constants are much larger than those for the corresponding monomer complexes. It seems that, although a longer period is required for quinone to approach to the donor groups of the polymer, the complex, once formed, is not so easily dissociated. The equilibrium constant for complex formation with PVP-4 is larger than that for PVP-2. This fact might be explained by steric hindrance of the polymer chain.

### Charge-Transfer Interaction between Quinone and Poly-*N*-dimethylaminomethylacrylamide

In alcoholic solution of quinone and PDA, just as in the quinone-triethylamine system, the new absorption band appeared at first at 360  $m\mu$ , and deepened up to 1.5 hr. after preparation of the solution. The strength of the absorption then diminished and at the same time, a weak absorption band appeared at 480  $m\mu$ , with an isosbestic point at 450  $m\mu$ .

As summarized in Table II, under the same conditions, the color intensity of the complex of quinone and PDA is much stronger than that of the complex between quinone and triethylamine.

When water is employed as solvent, a sharp isosbestic point is observed just as in ethyl alcohol, but the absorption maxima are shifted to 325 and 510  $m\mu$ . A remarkable difference between water and ethyl alcohol is that in the former, the peak at longer wavelength appears at first and then it shifts to shorter wavelength, while in the latter, the peak shifts from shorter

TABLE II  
Absorption Intensity for the Quinone-Triethylamine System and the Quinone-PDA System<sup>a</sup>

Donor	Transmittance, %	
	At 360 $m\mu$	At 480 $m\mu$
Triethylamine	1	54
PDA	Scale out	5

<sup>a</sup> Solvent: EtOH, quinone concn.:  $5 \times 10^{-3}$  mole/l., donor concn.:  $5 \times 10^{-1}$  mole/l., reaction time: 10 min.

to longer wavelength. Figure 2 shows the change of color intensity at 325 and 510  $m\mu$  in this system.

From the above results, it can be concluded that in this system, two different types of complexes are formed, that one may be transformed into the other, and that their relative stability depends on the solvent. The nature of the complexes is under investigation.

### References

1. H. A. Benesi and J. H. Hildebrand, *J. Am. Chem. Soc.*, **71**, 2703 (1949).
2. R. S. Mulliken, *J. Am. Chem. Soc.*, **74**, 811 (1952).
3. L. J. Andrews, *Chem. Rev.*, **54**, 713 (1954).
4. S. P. McGlynn, *Chem. Rev.*, **58**, 1113 (1958).
5. J. N. Chaudhuri and S. Basu, *Trans. Faraday Soc.*, **55**, 898 (1959).
6. M. Chowdhury and S. Basu, *Trans. Faraday Soc.*, **56**, 335 (1960).
7. M. Chowdhury, *Trans. Faraday Soc.*, **57**, 1482 (1961).
8. H. Kamogawa, Y. H. C. Giza, and H. G. Cassidy, *J. Polymer Sci. A*, **2**, 4647 (1964).
9. M. M. Zwick, *J. Appl. Polymer Sci.*, **9**, 2393 (1965).

### Résumé

Des maxima d'absorption et des constantes d'équilibre pour des complexes de transfert de charges entre la quinone et des aza-polymères tels que le polyvinylpyridine-2, polyvinylpyridine-4, 2-méthylpolyvinylpyridine-5 et le poly-*N*-diméthylaminoéthylacrylamide ont été déterminés spectrophotométriquement. Par comparaison, les complexes de transfert de charges entre les quinones et les composés aza tels que la pyridine, les pyridines alcoylées, la quinoline, la triéthylamine et la diméthylaniline ont également été présentés. On a trouvé que les constantes d'équilibre pour les complexes polymériques sont toujours plus grands que ceux pour les complexes monomériques correspondants, alors que le temps requis pour atteindre l'équilibre était plus long pour les complexes polymériques que pour les complexes monomériques. Dans l'interaction entre la quinone et le poly-*N*-diméthylaminométhylacrylamide, deux maxima d'absorption ont été observés, qui glissent progressivement les uns vers les autres. Ces mêmes phénomènes ont été trouvés au cours de l'interaction entre la quinone et le monomère correspondant à la triéthylamine.

### Zusammenfassung

Absorptionsmaxima und Gleichgewichtskonstante wurden für Ladungsübergangskomplexe zwischen Chinon und Azapolymere, wie Polyvinylpyridin-2, Polyvinylpyridin-4, 2-Methylpolyvinylpyridin-5 und Poly(*N*-dimethylaminomethylacrylamid) spektrophotometrisch bestimmt. Zum Vergleich wurden auch die entsprechenden Grössen für Ladungsübergangskomplexe zwischen Chinon und Azaverbindungen wie Pyridin, methylsubstituierte Pyridine, Chinolin, Triäthylamin und Dimethylanilin angegeben. Es wurde gefunden, dass die Gleichgewichtskonstanten für Polymerkomplexe immer grösser als diejenigen für die entsprechenden Monomerkomplexe sind, während die Zeit zur Gleichgewichtseinstellung für Polymerkomplexe länger war als für Monomerkomplexe. Bei der Wechselwirkung zwischen Chinon und Poly(*N*-dimethylaminomethylacrylamid) wurden zwei Absorptionsmaxima beobachtet, welche sich allmählich gegeneinander verschoben. Die gleiche Erscheinung trat bei der Wechselwirkung von Chinon und den entsprechenden Monomeren, Triäthylamin auf.

Received November 3, 1965

Revised February 10, 1966

Prod. No. 5090A



## Fluorodienes. V. Copolymerization of 1,1,4,4-Tetrafluoro-1,3-butadiene with Oxygen and Nitric Oxide\*

R. E. PUTNAM and W. H. SHARKEY, *Central Research  
Department, E. I. du Pont de Nemours and Company Inc.,  
Wilmington, Delaware*

### Synopsis

1,1,4,4-Tetrafluoro-1,3-butadiene reacts with oxygen to form a polyperoxide containing 1.0-1.1 peroxide groups for each diene unit. This polymer behaves like a typical peroxide. It explodes violently when heated to 120°C. or when subjected to shock, and it initiates polymerization of vinyl monomers at temperatures of 90°C. or higher. The tetrafluorobutadiene also copolymerizes with nitric oxide to give a highly cross-linked polymer containing three molecules of diene for each two molecules of nitric oxide.

The reaction of 1,3-butadiene and related conjugated dienes with oxygen is known to lead to polymeric peroxides.<sup>2</sup> We have found that 1,1,4,4-tetrafluoro-1,3-butadiene is also easily converted to a polymeric peroxide and that this product differs in a number of important ways from the polyperoxides formed by the hydrocarbon dienes.

In contrast to 1,3-butadiene, which reacts very slowly below 75°C., 1,1,4,4-tetrafluoro-1,3-butadiene (TFBD) reacts with oxygen at room temperature to give excellent yields of a polyperoxide. The physical properties of the polymer depend in part on the oxygen pressure used in its preparation. Thus, products formed using an oxygen pressure of about 2500 psi are tough and leathery, while those formed at 50 psi are quite elastomeric. Both have the same composition as judged by infrared, elemental, and peroxide analyses. Although the reasons for the difference in properties have not been established, the most likely causes are variation in molecular weight and degree and length of chain branches.

Elemental analyses and iodometric peroxide titrations showed the polymer to contain 1.0-1.1 mole of peroxide per mole of diene. The peroxide content in excess of 1.0 mole is almost certainly due to chain branching rather than crosslinking. This belief is supported by the fact that the polymer is readily soluble in acetone. In addition, an infrared spectrum of the polymer showed an appreciable concentration of difluorovinyl groups (3125  $\text{cm}^{-1}$  for  $-\text{CH}=\text{C}(\text{F})_2$  and 1745  $\text{cm}^{-1}$  for  $\text{CF}_2$ ) formed by 1,2-polymeriza-

\* For Paper IV in this series, see Putnam et al.<sup>1</sup>

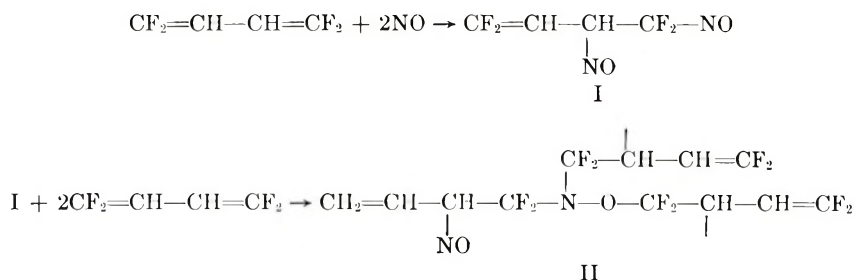
tion of the diene. These groups would be expected to participate in peroxide formation.

Preparation and handling of the polyperoxide can be quite hazardous. The polymer explodes violently when heated to 120–125°C. or when subjected to shock. Although quite stable at –80°C., it very slowly liberates carbonyl fluoride on standing at room temperature. In addition, it behaves like a typical peroxide in its ability to initiate polymerization of vinyl monomers, exhibiting reasonable activity at about 90°C.

Nitric oxide is akin to oxygen in that it also is a paramagnetic molecule. We have found that it copolymerizes with TFBD to give, insofar as we are aware, the first example of a nitric oxide copolymer. Best results were obtained by using perfluorodimethylcyclohexane solvent at 100°C., although polymer could be prepared at temperatures from –40 to +100°C. in the absence of a solvent.

Elemental analysis showed the polymer to have an empirical formula  $(C_4F_4H_2)_3(NO)_2$ . Infrared absorptions at 3100 and 1750  $cm^{-1}$  indicated the presence of difluorovinyl groups. The presence of nitroso groups is supported by an infrared band at 1600  $cm^{-1}$ .

It is thought that the polymer is formed in two steps, the first of which involves addition of nitric oxide to the diene to give a compound (I) containing nitroso groups. The second step is visualized as copolymerization of this intermediate with TFBD to form a very highly crosslinked polymer of structure II. The sequence is illustrated for a 1,2-polymerization only. Undoubtedly, 1,4-polymerization also takes place.



The TFBD/NO copolymer is an insoluble, infusible, white solid. Freshly prepared polymer does not appear to decompose noticeably unless heated to 320°C. However, the polymer slowly loses carbonyl fluoride and nitrogen dioxide when it is stored for a long time at room temperature. Pyrolysis of an aged sample *in vacuo* at 260°C. yields gaseous products, including carbonyl fluoride, nitrous oxide, nitrogen dioxide, dinitrogen tetroxide, and carbon dioxide. We were not able to isolate identifiable, high-boiling products.

This, then, appears to be another example of the copolymerization of a fluorine-containing nitroso compound with a fluoroolefin. Previously reported polymers of this type include those from trifluoronitrosomethane and tetrafluoroethylene<sup>3-5</sup> and  $O_2NCF_2CF_2NO$  and tetrafluoroethylene.<sup>6</sup>

## EXPERIMENTAL DETAILS

### Copolymers of TFBD and Oxygen

An 80-ml., stainless-steel, shaker tube containing 7 g. of TFBD was connected to an oxygen cylinder, and oxygen was admitted until the total pressure in the tube was 2410 psi. The tube was shaken for 16 hr. at room temperature and then vented to release the excess oxygen. The product was a white polymer<sup>7</sup> present as a tough, leathery film on the wall of the shaker tube. Because of the hazards connected with recovering the polymer, only 7 g. (80%) was isolated. It is soluble in acetone, explodes when heated to 120–125°C., and explodes when struck with a hammer. Analytical data were obtained on portions of the film that did not adhere to the walls of the shaker tube.

ANAL. Calcd. for  $C_4F_4H_2O_2$ : C, 30.4%; H, 1.3%; F, 48.1%. Found: C, 30.48%; H, 1.62%; F, 48.41%.

Peroxide content (1.0–1.1 mole/mole of diene) was determined by digesting 0.25-g. samples of the polymer in a mixture of 20 ml. of acetone, 10 ml. of glacial acetic acid, and 5 ml. of 55% HI and titrating liberated iodine in the usual manner.

Copolymers identical in composition were obtained by reaction of 1,1,4,4-tetrafluoro-1,3-butadiene with oxygen at pressures as low as 50 psi. At the lower pressures, the products formed were less tough and stiff and more rubberlike in character. Reaction between the diene and oxygen also occurred at low temperatures, but the product formed is dangerous. A shaker tube containing diene was cooled to  $-40^\circ\text{C}$ . and oxygen admitted until the total pressure was 500 psi. It was shaken 16 hr. at  $-40^\circ\text{C}$ . and then allowed to warm. Before room temperature was reached, the contents of the tube exploded. Because of the danger of explosions, it is essential that the shaker tubes used be fitted with safety disks that will rupture and release unusually high pressures.

### Polymerization Initiation by the Copolymer of 1,1,4,4-Tetrafluoro-1,3-butadiene and Oxygen

The copolymer (0.5 g., cut into very small pieces), 10 g. of acrylonitrile, and 25 ml. of *tert*-butyl alcohol were heated to  $90^\circ\text{C}$ . in an atmosphere of nitrogen. Polymer formed immediately. After 2 hr. the polymerization mixture was almost solid and was poured into 100 ml. of water. The solid precipitate that formed was washed first with methanol, then with acetone and finally with ether. The polymer (3 g., 30%) gave an infrared spectrum typical of that for polyacrylonitrile except that it contained a weak absorption at  $1725\text{ cm.}^{-1}$  which is believed to be associated with difluorovinyl endgroups from the initiator. The inherent viscosity of this polyacrylonitrile in 0.1% solution in dimethylformamide was 2.4.

### Copolymers of 1,1,4,4-Tetrafluoro-1,3-butadiene and Nitric Oxide

To an 80-ml., stainless-steel, shaker tube containing 5 g. of 1,1,4,4-tetrafluoro-1,3-butadiene was added 0.1 g. of nitric oxide. The tube was shaken at room temperature for several hours and then opened. It contained 1.4 g. of white polymer. This polymer was insoluble in acetone and did not melt or degrade at temperatures up to 290°C. It burned slowly when placed in a flame.

ANAL. Calcd. for  $C_{12}F_{12}H_6N_2O_2$ : C, 32.8%; H, 1.4%; N, 6.4%. Found: C, 32.57%; H, 1.72%; N, 5.86%.

The infrared spectrum of this polymer had bands at 3100  $cm^{-1}$  (medium) ( $=CH$ ); 2925 and 2990  $cm^{-1}$  (weak) (saturated CH); 1750  $cm^{-1}$  (strong) and 1832  $cm^{-1}$  (medium) ( $CF_2=CH$ ); 1600  $cm^{-1}$  (strong) (in the range for  $N=O$  absorption); and very strong absorption in the 1000–1250  $cm^{-1}$  region (consistent with C—F and C—O).

Polymer of slightly higher nitrogen content was obtained at higher temperatures. A shaker tube containing 7 g. of 1,1,4,4-tetrafluoro-1,3-butadiene and 20 ml. of perfluorodimethylcyclohexane was pressured to 100 psi with nitric oxide. The tube was heated to 100°C. and shaken for 16 hr. A white polymer that contained 6.73% nitrogen was formed in quantitative yield.

A 6.2-g. sample of the copolymer from 1,1,4,4-tetrafluoro-1,3-butadiene and nitric oxide was placed in a glass tube. The tube was connected to a trap cooled with liquid nitrogen, which was attached to a vacuum pump. The system was evacuated to 4 mm. Hg, and the tube was heated to 260°C. Decomposition occurred, and volatile products were condensed in the trap. A sample of the trap contents was evaporated into an infrared sample tube. The spectrum shows bands at 953, 962, 976, 1940, and 1965  $cm^{-1}$ . From the intensity of the 1965  $cm^{-1}$  band, it was estimated that about 10% of the sample was  $COF_2$ . Bands also were present at 1600 and 1633  $cm^{-1}$  ( $NO_2$ ), at 1795  $cm^{-1}$  ( $N_2O_4$ ), at 2220 and 2265  $cm^{-1}$  ( $N_2O$ ), at 1032 and 1038  $cm^{-1}$  ( $SiF_4$ ), and at 2340  $cm^{-1}$  ( $CO_2$ ).

The authors are pleased to acknowledge the assistance of Dr. J. L. Anderson with whom many helpful conversations were held.

### References

1. R. E. Putnam, R. J. Harder, and J. E. Castle, *J. Am. Chem. Soc.*, **83**, 391 (1961).
2. C. T. Handy and H. S. Rothrock, *J. Am. Chem. Soc.*, **80**, 5306 (1958).
3. D. A. Barr and R. N. Haszeldine, *J. Chem. Soc.*, **1955**, 1881.
4. J. B. Rose, Brit. Pat. 789,254 (January 15, 1958).
5. G. H. Crawford, D. E. Rice, and J. C. Montermoso, paper presented at 137th Meeting of the American Chemical Society, Cleveland, Ohio, April 1960; *Abstracts of Papers*, p. 7L.
6. G. H. Crawford, *J. Polymer Sci.*, **45**, 259 (1960).
7. J. L. Anderson and R. E. Putnam, U.S. Pat. 2,971,949 (February 14, 1961).

### Résumé

Le butadiène 1,3-tétrafluoré-1,1,4,4, réagit avec l'oxygène pour former un polyperoxyde contenant 1,0 à 1,1 peroxyde par unité diénique. Ce polymère se comporte comme un peroxyde typique. Il explose violemment lorsqu'il est chauffé jusqu'à 120°C ou soumis à un choc qui initie la polymérisation de monomères vinyliques à des températures de 90°C ou supérieures. Le tétrafluorobutadiène copolymérise également avec les oxydes d'azote pour former un polymère hautement ponté contenant 3 molécules de diène pour 2 molécules d'oxyde d'azote.

### Zusammenfassung

1,1,4,4-Tetrafluor-1,3-butadien reagiert mit Sauerstoff unter Bildung eines Polyperoxyds mit 1,0-1,1 Peroxydgruppen pro Dienbaustein. Dieses Polymere verhält sich wie ein typisches Peroxyd. Es explodiert beim Erhitzen auf 120°C oder bei Schlageinwirkung heftig und startet die Polymerisation von Vinylmonomeren bei Temperaturen von 90°C oder höher. Tetrafluorobutadien copolymerisiert auch mit Stickoxyd unter Bildung eines hochvernetzten Polymeren mit drei Dienmolekülen auf je zwei Moleküle Stickoxyd.

Received March 1, 1966

Prod. No. 5091A



## **$\gamma$ -Radiation-Induced Ionic Polymerization of Pure Liquid Styrene. II**

R. C. POTTER, R. H. BRETTON,\* and D. J. METZ, *Brookhaven  
National Laboratory, Upton, New York*

### **Synopsis**

In this second paper of the series we present additional evidence that the  $\gamma$ -radiation-induced polymerization of very pure, ultradry styrene exhibits kinetics that can best be explained as due to one or more ionic processes, depending on the dryness of the sample. We have shown the effect of the various steps in the drying procedure on the observed kinetics, and we have described a preparative procedure which yields good reproducibility among independently prepared samples. Under these conditions, the rate of polymerization is proportional to the 0.70 power of the dose rate at 0°C.; there appears to be no wall effect; and the temperature coefficient for the process appears to be a complicated function, most probably a small negative value over the range of temperature (0–50°C.) and dose rates ( $\sim 10^3$ – $10^5$  rad/hr.) covered in this study. The maximum  $G$  value for disappearance of monomer which we have observed is of the order of  $6 \times 10^5$  molecules of monomer/100 e.v. at 0°C. and a dose rate of  $2 \times 10^3$  rad/hr.

### **Introduction**

Subsequent to the oral presentations<sup>1,2</sup> of very preliminary data on the unexpected behavior of pure, dry styrene in a radiation field, Okamura and his co-workers<sup>3,4</sup> have published more extensive data on this system, confirming the original findings and further extending our knowledge in this area. The first paper<sup>5</sup> of this present series demonstrated that the kinetic effects observed are uniquely associated with the radiation-induced process. It appears that the kinetic behavior observed by both us and Okamura is not the "classical" free-radical polymerization process.<sup>6</sup> All previous work in this relatively new area has indicated a lack of reproducibility, and it is a major function of the present paper to demonstrate a technique of sample preparation that yields reproducible kinetic results.

In addition, we would like to present our findings regarding the effect of various steps in the preparation technique, the absence of any wall effects, and also some preliminary data we have obtained in an investigation of the temperature coefficient of the polymerization process.

### **Experimental Procedure**

We employed the same method of monomer purification, irradiation, dosimetry and dilatometric determination of the rate of polymerization as

\* Address: Department of Engineering and Applied Science, Yale University, New Haven, Connecticut.

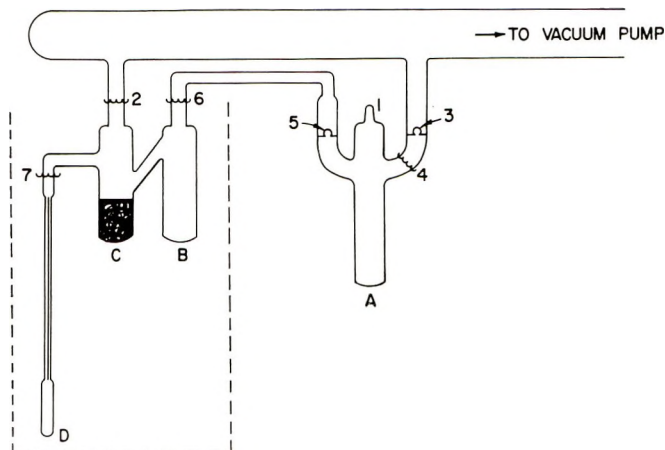


Fig. 1. Schematic arrangement of apparatus used to prepare samples according to procedure II.

was previously described.<sup>5</sup> However, we modified the previous method of sample preparation to eliminate some of its obvious shortcomings, and the new method will be described. Where necessary to differentiate, in what follows, the older method of sample preparation will be designated procedure I and the new, modified version, procedure II.

As in procedure I, the ampule A is filled from the purification still and removed from it at point I (Fig. 1) by the same steps as previously described. This vessel is then sealed onto the remainder of the apparatus, as shown, and the monomer is kept frozen during the subsequent bake-out steps. Vessels B and C, containing silica gel, and D (a dilatometer) fit within an electrically heated oven (shown schematically by broken lines). The operating temperature of the oven is 500°C. The remainder of the glassware, with the exception of vessel A, is wound with heater tape. The system is baked out at  $10^{-7}$ – $10^{-8}$  torr for approximately 40 hr. (After this treatment above there remains a detectable background of oxygen and water vapor, as registered on a Consolidated Electro-dynamics Corporation Model 21-614 residual gas analyzer).

After bake-out, the oven is removed and vessel B and its appendages are sealed off the vacuum line at point 2. The conditioned glassware and drying agent are thus completely isolated from both the vacuum system and the monomer-containing ampule, and remain thus until the monomer has been completely degassed.

The breakseal at point 3 is then broken, and the monomer is degassed by successive freeze–pump–thaw cycles until there is no evidence of gas release. The monomer is then frozen, and ampule A is removed, by flame sealing, from the manifold at point 4.

Monomer is next transferred from vessel A to vessel B by first fracturing the breakseal at point 5 and then placing an ice–water mixture around vessel B. When sufficient monomer has been transferred to B, both A and

B are frozen, and B and its attachments are separated from the remainder of the monomer by flame sealing at point 6.

The silica gel in C is transferred, by pouring into vessel B, and monomer is allowed to equilibrate with the drying agent. When this is accomplished, sufficient monomer to fill the dilatometer is directly distilled from B to D by surrounding the latter with an ice-water bath. After the dilatometer has been filled, methanol-Dry Ice baths are placed around vessels C and D, and vessel D is removed by flame sealing at point 7.

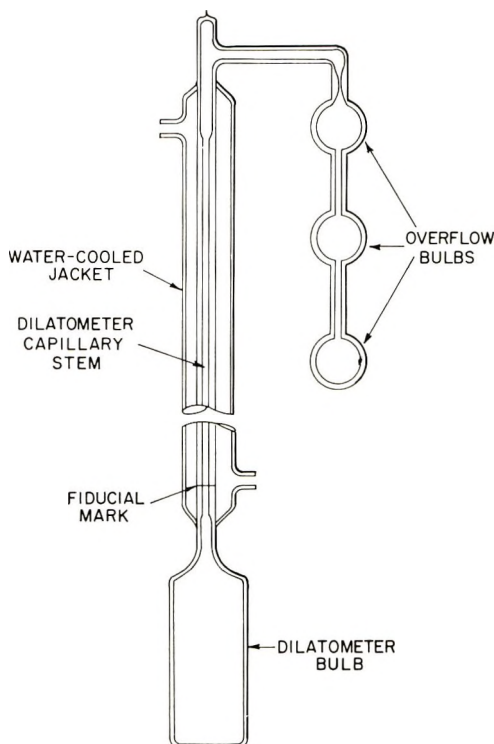


Fig. 2. Dilatometer with water-cooled jacket and overflow bulbs used for temperature studies.

The elaborateness of this procedure (procedure II) is believed necessary to overcome two serious shortcomings in procedure I. In the first place, the baked-out glassware and drying agent are not allowed to remain attached to the vacuum line during the monomer degassing operation, thereby preventing their contamination by water, residual gas, or monomer that might backstream along the vacuum manifold during this operation. Secondly, no monomer is included in the final sample that was frozen in the presence of the silica gel. We believe this point to be important. Observation has indicated to us that in the freezing and thawing of silica gel (with the use of Dry Ice or liquid nitrogen) a certain amount of fracturing of the silica gel occurs. We believe that some water might be released to the dried mono-

mer either by the exposure of previously unexposed surfaces of the silica gel or by a temperature-dependent water distribution coefficient.

From a very pragmatic point of view, the elaborate procedure has been justified since, as will be seen, it has led to reproducible kinetics.

For the temperature coefficient studies we had constructed dilatometers of a special design shown in Figure 2. Firstly, in order to minimize the problem of monomer vaporization in the stem of the dilatometer, the stem is surrounded by a condenserlike jacket through which cooling water may be circulated. Secondly, the dilatometer stem is connected at its upper end to a series of small, spherical bulbs, so designed that after the completion of a run at a given temperature, sufficient monomer can be distilled into one of the bulbs so that the meniscus of the residual styrene will fall toward the upper end of the capillary stem at the next higher temperature to be investigated. The monomer removed from the dilatometer stem is eliminated completely by freezing both dilatometer bulb and disposable storage bulb, and the latter is removed by flame sealing.

### Experimental Results

Prior to adopting procedure II, we were interested in obtaining a feeling for the importance of the two "drying" steps employed in procedure I, namely the baking of the glassware and the use of baked silica gel as a bulk drying agent for the monomer. Figure 3 shows the results we obtained.

In Figure 3 we have plotted the rate of polymerization measured at 40°C. versus the dose rate for three dilatometers. The upper curve refers to a sample that had been subjected to the full treatment: baked drying agent and glassware. The experimental dose rate dependence is 1.1. The next curve depicts the behavior of a sample in which the monomer was subjected to all the distillation steps as before, the glassware was baked out, but no silica gel was present. The experimental dose rate dependence is 0.86, and the absolute values of the rates of polymerization are lower than in all previous samples. The next experimental curve refers to a sample in which only the initial purification and on-line distillation steps were followed, but there was no drying agent present in vessel C and the glassware was not baked. The experimental dose rate dependence is 0.60, and the data lie very close to the values calculated for the "classical" behavior of styrene under free radical-propagated radiation-induced polymerization.<sup>6</sup>

When this last sample was stored for 8 days and reirradiated, the same dose rate dependence was obtained but, interestingly, the absolute value of the rates of polymerization fell somewhat below the "classical" curve. After another two weeks of storage under water, this sample reproduced the previous data.

Qualitatively, then, it appears that the bake-out of the glassware plays an even greater role in our system than does the drying agent. It should be remembered, however, that our "undried" monomer is considerably drier than might be suspected, due to its method of purification and sample isolation from the still (see Part I.<sup>5</sup>).

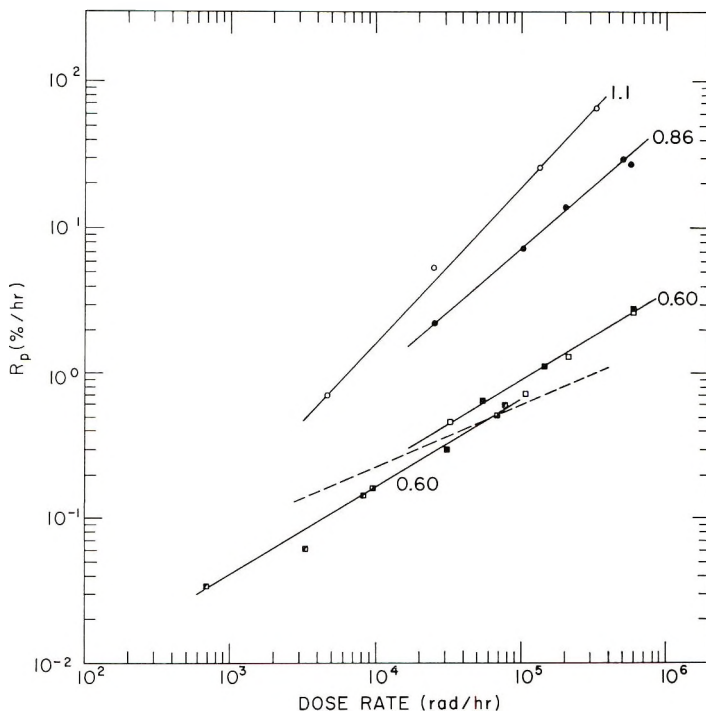


Fig. 3. Effect of various steps in the drying process on the observed rates of polymerization and their dependence on the dose rate: (O) baked glassware and baked silica gel; (●) baked glassware, no silica gel; (□) no baking of glassware, no silica gel; (■) above sample after 1 day storage; (▣) above sample after additional 8 days storage; (▤) above sample after additional 12 days storage submerged in water. Reaction temperature 40°C.

Having partially satisfied our curiosity concerning the above facet of the investigation, we decided to apply the more rigorous sample preparation technique (procedure II) to styrene. The first indication that procedure II might yield the long sought-for reproducibility was developed during a parallel study<sup>7</sup> of the radiation-induced polymerization of  $\alpha$ -methylstyrene, another project of long standing in this laboratory.<sup>8</sup>

Figure 4 presents data obtained with five dilatometric samples. These represent three entirely independent preparations, two of which yielded two (duplicate) dilatometers, and the third a single dilatometer. Two of the dilatometers (the single dilatometer and one of the paired dilatometers) had been packed with spherical glass beads in order to increase surface-to-volume ratio in the dilatometer bulb. In Figure 4 a single line is readily drawn through the points for the two pairs of duplicate samples (four samples) and a second line passes through the data obtained on the fifth sample. At one and the same time this figure demonstrates several interesting points.

Firstly, the least-squares line drawn through the data on the four samples and the very small spread of the data around this line both demonstrate the level of reproducibility which can be achieved by using our procedure II,



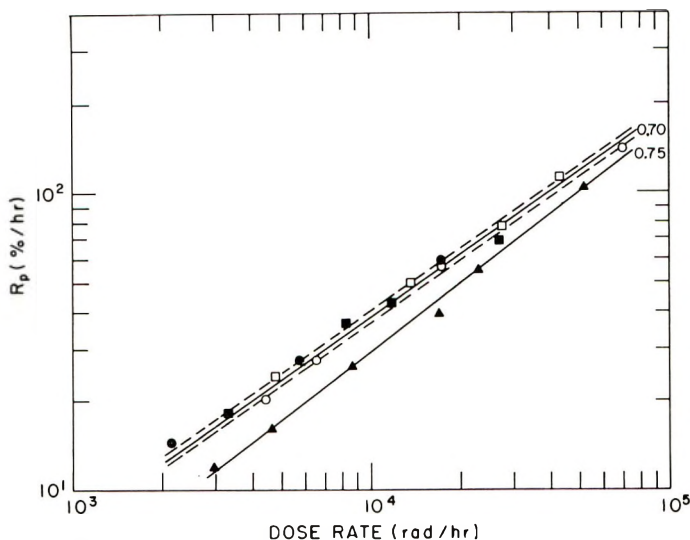


Fig. 4. Radiation polymerization of styrene at 0°C. with the use of preparative procedure II. The broken lines on either side of the upper line are drawn at  $\pm 2\sigma$  (standard deviation). (O), (●) surface/volume = 6 (duplicate samples from single preparation); (□) surface/volume = 12, (■) surface/volume = 6 (duplicate samples from single preparation); (▲) surface/volume = 12.

Secondly, the departure of the data on the fifth sample from the above line indicates that one does not always achieve this level of reproducibility. However, we tend to regard the upper curve as a "standard" rate curve and to consider data which do not fall close enough to it to be representative of an inferior sample. At its worst point the lower curve in this figure lies approximately eight times the standard deviation of the "standard" curve from that curve; at its best point, it lies five standard deviations away.

Thirdly, the rates of polymerization of all these samples at any dose rate studied are higher by a factor of at least five than previously reported rates.<sup>3-5</sup>

Fourthly, the observed dose rate dependence of the standard curve has decreased from the previously reported values of 1.0<sup>5</sup> and 0.80<sup>4</sup> to a value of  $0.70 \pm 0.02$  (standard deviation of 0.012).

Finally, a twofold increase in the surface-to-volume ratio does not seem to have any measurable effect on either the value of the rate of polymerization, at a given dose rate, or the dose rate dependence of the rate of polymerization.

The two points (401%/hr., 10<sup>6</sup> rad/hr.; 349%/hr.,  $7.17 \times 10^5$  rad/hr.) of the fastest dilatometric run from the previous paper<sup>5</sup> may be compared to Figure 4. An extension of the two curves in this figure will pass well above either of the values.

In Figure 5 we have presented the data obtained in our temperature studies. The symbols employed here to denote samples are the same as used in Figure 4. Several points are apparent from this figure.

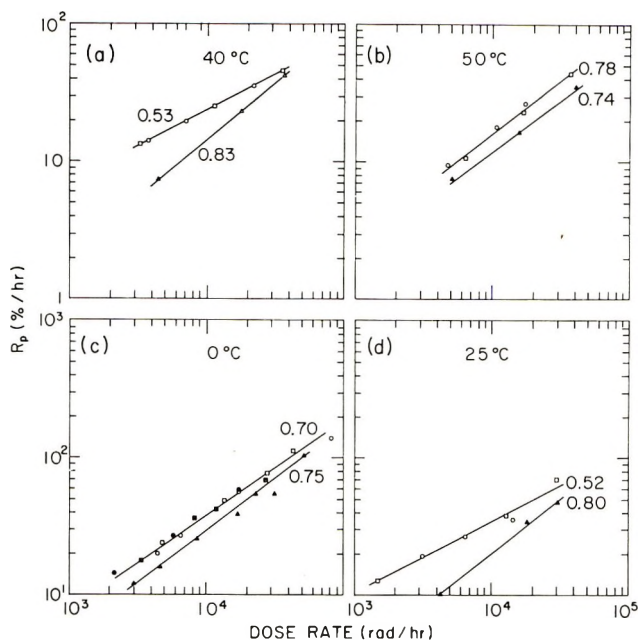


Fig. 5. Dose rate dependence of rate of polymerization of styrene at several temperatures: (a) 40°C.; (b) 50°C.; (c) 0°C.; (d) 25°C. The symbols used here denote the same samples as in Fig. 4.

In the first place, the 0°C. data here are a replot of the data in Figure 4. At each of the four temperatures, the data for the two samples that yielded our standard curve in the previous figure all fall along reasonable straight lines. Moreover, the sample that deviates from the standard curve samples at 0°C. also deviates from them at the other three temperatures, being, in general, lower than the latter.

Secondly, the dose rate dependence of the rates for the standard samples appears to vary with temperature, while that of the other sample is reasonably constant; also the variation of this dependence of the former two samples is not a monotonic function of the temperature. Thus, a temperature coefficient for the reaction calculated on the basis of these data will appear to be a function of the dose rate.

In general, it appears from either set of data, taken independently, that the algebraic sign of the temperature coefficient is negative. From the complexity of the data, however, it is obvious that a single numerical value of this function cannot be specified.

### Discussion

We have previously demonstrated<sup>5</sup> that the careful, exhaustive drying of styrene drastically alters its behavior in a radiation field while not affecting its polymerization initiated by either ultraviolet radiation or heat, both of

which are accepted as proceeding via a free-radical mechanism. This leads inevitably to the conclusion that the reduction of the water content of styrene to extremely low levels affects uniquely its behavior in a radiation field, and also leads us to postulate the existence of one or more ionic propagating species, whose presence are manifest only when the water content of the sample has been reduced sufficiently.

The immediate consequences of this hypothesis have been stated in our previous paper but, for the sake of completeness, are repeated here. Under the conditions of sample preparation on which the "classical" behavior<sup>6</sup> of styrene was established, apparently insufficient care was employed to remove the last traces of water from the monomer. Thus, the radical-ions directly formed both by Compton scattering from a monomer and electron capture by a monomer molecule and the normal ions produced by heterolytic dissociation of excited monomer molecules were "killed" by the water impurity. Hence, only radical fragments, formed by homolytic rupture of an excited monomer molecule, remained to initiate a free radical-propagated polymerization.

Anything which is done to reduce the water content of the styrene should, below a certain critical water level, increase the rate of the polymerization by allowing an additional initiation and propagation process to occur. Once we have entered this region of enhanced rate, the dose rate dependence of the rate of polymerization should be different from the classical square-root value. As we proceed to more and more exhaustive drying, these two experimentally observed values—rate of polymerization and its dose rate dependence—should pass through a succession of values. We believe that the data presented in Figure 3 demonstrate this.

In reply to the question of why our undried monomer shows slightly higher rates and a slightly higher dose rate dependence than the "classical" values, we reply that our starting monomer is considerably drier than those samples on which the "classical" data were obtained.

Another obvious question arises when one looks at our data on the undried monomer. Why, after the sample stands for 8 days, do the absolute values of the rate decrease? We consider that this happens because, on standing, additional water was leached from the walls of the glass vessel. The importance of the water adhering to the glass is, we believe, demonstrated by comparing the relative decrease in rates of polymerization caused by elimination of the drying agent and the elimination of the bake-out of the glassware. Similar results regarding the necessity of baking the glassware are reported by Okamura et al.<sup>4</sup>

To see if this decrease was due to diffusion of water from the outside of the sample, through the glass wall, we stored the same sample for an additional 12 days while the dilatometer bulb was completely submerged in water. Upon reirradiation, no further change in the rate was observed, indicating either that no water diffused through the glass or that a water content had been achieved in the sample beyond which small additions of water would have no further effect.

We are at a loss to explain why our actual rates of polymerization after the first 8 days of storage are below the classical values.

As the drying process is made more efficient, we have observed several phenomena. Firstly, the absolute values of the rates of polymerization increase. Secondly, at these higher rates, the dose rate dependence of the rate becomes appreciably less than unity. How can these results be explained in a self-consistent manner?

A detailed kinetic analysis of the process under consideration is impossible at this stage of our knowledge of what intermediates are formed when ionizing radiation interacts with pure, dry styrene. We do know that several detectable species are formed, and that these have half lives ranging from several microseconds to several hundred milliseconds.<sup>9</sup> (These data have resulted from pulse radiolysis studies which we are currently performing at the Argonne National Laboratory.) Therefore, it is a gross oversimplification to assume that a single species, whether it be assumed to be a normal cation, normal anion, radical cation, or radical anion, is responsible for the polymerization we observe under these conditions. The most that can be safely offered to explain these data is that, on assuming the concentration of "active" species is proportional to the dose rate and invoking the usual concept of the steady state, the termination reaction must be first-order in the propagating species in order for the overall rate of polymerization to exhibit a linear dependence on dose rate. This type of behavior is similar to that reported for both the cationic, stannic chloride-initiated polymerization of styrene in ethylene dichloride<sup>10</sup> and the anionic, potassium amide-initiated polymerization of styrene in liquid ammonia.<sup>11</sup>

When we consider the higher rates of polymerization obtained at even lower water concentrations, and the fact that the dose rate dependence is significantly less than unity under those conditions, we are again led to an oversimplified kinetic picture. It appears that under the usual kinetic assumptions concerning the proportionality of the concentration of active species to the dose rate and the steady-state assumption, the termination reaction is being contributed to by a process which is second-order in the propagating species and, at the same time, the overall propagation process is enhanced by the presence of a second type of propagation reaction.

Recognizing the shortcomings of any such overly simplified picture as that which we hinted at in our previous publication,<sup>5</sup> we note that such a simple picture provides us a convenient point of departure. It also allowed us to correctly predict the increase in overall rate and the decrease in the order dependence of the rate on dose rate as the drying procedure was improved. This view can best be summarized as shown in Table I.

The rationale behind this picture is that both carbonium ions and carbanions will be rendered ineffective by any reasonable amounts of water. As the water level is reduced, first the carbonium ions will make their presence evident in a change in the kinetic behavior of the system. At even lower water levels, carbanions can have an appreciable life time and contribute to both the overall rate of polymerization and also the termination



TABLE I  
 Probable Relative Importance of Active Species in the Radiation  
 Polymerization of Liquid Styrene under Different Conditions of Dryness

Relative water content	Relative overall rate of polymerization	Dose rate dependence of rate of polymerization ( $n$ )	Kinetic scheme	
			Propagating species	Termination
High	Low	$n = 1/2$	$R\cdot$	$R\cdot + R\cdot \rightarrow \text{Prod.}$
Low	High	$n \approx 1$	$R^+ (\gg R\cdot)$	$R^+ + ? \rightarrow \text{Prod.}$
Very low	Very high	$1/2 < n < 1$	$R^+$ and $R^-$	$R^+ + ? \}$ $R^- + ? \}$ $R^+ + R^- \}$ $\rightarrow \text{Prod.}$

process. We believe this to be a naïve view and one which may well be refined by future work, especially when a more exact assignment of the structures of the initiating species in this system can be made. At the moment, however, it appears futile to draw any more definitive picture of the process.

From our data on the absence of a strong surface-to-volume ratio effect on the kinetics of the process, we tentatively conclude that we are dealing with a process which occurs principally in the bulk liquid phase. On the basis of present data, it would appear that the only role played by the glass surface is to provide some fraction of the Compton recoil electrons which then irradiate the bulk liquid. We do not believe that the glass surface provides traps for electrons ejected from monomer molecules, preferential sites of initiation, or termination sites. In brief, we do not believe that any significant wall effects are present in this system.

Finally, with respect to our investigation of the temperature coefficient of the polymerization process, we are not in a position yet to quote a numerical value nor to present a complete analysis of the data shown in Figure 5. In fact, the complexities indicated in these data show that the complete description of the process under investigation will involve a considerable amount of additional work. At this point, all we can say is that our data indicate a small negative temperature coefficient. A more detailed investigation of this will be reported in a subsequent publication.

We would like to conclude this paper by drawing some comparisons between the results we have obtained in this laboratory and those published by Okamura and his co-workers.<sup>3,4</sup> Okamura reports a maximum rate of polymerization at a dose rate of  $6 \times 10^4$  rad/hr. and  $10^\circ\text{C}$ . of 24% conversion/hr.,<sup>4</sup> with a reproducibility that runs between a factor of 2 and 3; under nearly the same conditions,  $6 \times 10^4$  rad/hr. and  $0^\circ\text{C}$ ., we find a maximum rate of 120% conversion/hr., with a 10% reproducibility. Okamura reports a  $G$  value for the disappearance of monomer of 34,400 at  $1.9 \times 10^5$  rad/hr. and at  $24^\circ\text{C}$ .; we find a value of 150,000 at the same dose rate and  $20^\circ\text{C}$ . Okamura finds no dependence of  $\bar{M}_n$  on dose rate; we previously reported similar behavior.<sup>1,2</sup> Okamura gives, for the dose rate



dependence of the polymerization, 0.80 for  $\gamma$ -rays and 1.0 for accelerated electrons; we find, for  $\gamma$ -rays, a variation between 0.60 and 1.1, depending on the dryness of the sample and the temperature. For our standard curve, the value is 0.70 at 0°C. Between -20 and 85°C., Okamura reports a temperature coefficient which is approximately zero; we find behavior, very complex when viewed in detail, but pointing towards a fairly small negative value.

We feel that both studies point to the importance of a rigorous preparative technique. Both Okamura's technique, involving Na-K drying agent and flaming of glassware, and our technique, with the use of baked silica gel and high temperature bake-out of glassware, are sufficient to demonstrate the existence of this novel effect. However, in terms of reproducibility of data and absolute values of rates, we feel that the technique described here, procedure II, is somewhat superior.

### Conclusions

Based on the data presented here and also that previously reported by us<sup>5</sup> and others,<sup>3,4</sup> we conclude that the radiation-induced polymerization of pure, very dry liquid styrene is principally propagated by one or more ionic reactions over the temperature range of 0-50°C. The relative contributions of the several propagation reactions, generically referred to as free radicals, cationic and anionic, are governed by the chemical purity of the styrene and the dryness of both the styrene and all the glassware employed.

We suspect that this type of behavior can be observed in other vinyl monomers, the critical water levels being a function of the particular system. We believe that it is also quite possible that ionic reactions, and hence, a different distribution of radiolysis products, can be developed in the radiolysis of simple liquid organic compounds. In brief, the previously held belief that ionic reactions are highly improbable in organic liquids under irradiation because of the low dielectric constants of the media probably should be modified drastically. We believe that the presence of impurities such as water, oxygen, etc., that are highly reactive toward carbonium ions and carbanions can be of even greater importance in masking the radiolytically formed ions, and hence, favoring free-radical reactions.

This work was performed under the auspices of the U. S. Atomic Energy Commission.

This work is taken in part from the doctoral dissertation of R. C. Potter to be written and submitted to the Graduate Faculty of Engineering and Applied Science, Yale University.

### References

1. C. L. Johnson and D. J. Metz, Am. Chem. Soc., Div. Polymer Chem., New York, September, 1963, *Polymer Preprints*, **4**, 440 (1963).
2. D. J. Metz, *Trans. Am. Nuc. Soc.*, **7**, 313 (1964), San Francisco, November, 1964.
3. K. Ueno, K. Hayashi, and S. Okamura, *J. Polymer Sci. B*, **3**, 363 (1965).
4. K. Ueno, K. Hayashi, and S. Okamura, *Polymer*, in press.
5. R. C. Potter, R. H. Bretton, C. L. Johnson, and D. J. Metz, *J. Polymer Sci.*, **4**, 430 (1966).

6. A. Chapiro, *Radiation Chemistry of Polymeric Systems*, Interscience, New York, 1962, p. 164.
7. D. J. Metz and C. L. Johnson, unpublished results.
8. C. G. Baumann and D. J. Metz, *J. Polymer Sci.*, **62**, S141 (1962).
9. D. J. Metz, J. K. Thomas, and R. C. Potter, unpublished results.
10. D. C. Pepper, *Trans. Faraday Soc.*, **45**, 404 (1949).
11. W. C. E. Higginson and N. S. Wooding, *J. Chem. Soc.*, **1952**, 760.

### Résumé

Dans ce second manuscrit de cette série, nous présentons une évidence supplémentaire que les polymérisations induites par radiation- $\gamma$  de styrène très pur et ultra-sec présentent une cinétique qui peut le mieux être expliquée par un ou plusieurs processus ioniques suivant le degré de siccité de l'échantillon. Nous avons montré l'effet des différentes étapes dans le procédé de séchage sur les cinétiques observées et nous avons décrit le procédé de préparation qui fournit des résultats reproductibles entre les différents échantillons préparés indépendamment. Dans ces conditions de préparation la vitesse de polymérisation est proportionnelle à la puissance 0.7 de la vitesse de dose à 0°C; il n'y a pas d'effet de parois et le coefficient de température pour le processus semble être une fonction compliquée et s'élève plus que probablement à une valeur faiblement négative dans le domaine de température de 0° à 50°C et des vitesses de dose de  $\sim 10^3$  à  $10^5$  rad/h. La valeur maximum de  $G$  pour la disparition du monomère qui a été observée est de l'ordre de  $6 \times 10^5$  molécules de monomère par 100 ev à 0°C et une vitesse de dose de  $2 \times 10^3$  rad/h.

### Zusammenfassung

In der vorliegenden Mitteilung der Reihe werden zusätzliche Belege dafür angegeben, dass die  $\gamma$ -strahlinduzierte Polymerisation von sehr reinem ultratrockenem Styrol eine Kinetik aufweist, welche am besten je nach der Trockenheit der Probe als durch einen oder mehrere ionische Prozesse bedingt verstanden werden kann. Der Einfluss der verschiedenen Schritte beim Trocknungsverfahren auf die beobachtete Kinetik wurden nachgewiesen und ein Darstellungsverfahren, welches eine gute Reproduzierbarkeit bei unabhängig dargestellten Proben liefert, beschrieben. Unter diesen Darstellungsbedingungen ist die Polymerisationsgeschwindigkeit der 0,7. Potenz der Dosisleistung bei 0°C proportional. Es scheint kein Wandeffluss zu bestehen, und der Temperaturkoeffizient der Reaktion scheint eine komplizierte Funktion, am wahrscheinlichsten ein kleiner negativer Wert im hier untersuchten Temperatur- (0–50°C) und Dosisleistungs- ( $\sim 10^3$ – $10^5$  rad/h) Bereich zu sein. Der höchste beobachtete  $G$ -Wert für den Monomerverbrauch ist von der Grössenordnung von  $6 \cdot 10^5$  Monomermoleküle/100 eV bei 0°C und einer Dosisleistung von  $2 \cdot 10^3$  rad/h.

Received March 8, 1966  
Prod. No. 5101A

## Preparation and Thermal Stability of Organometallosiloxanes and Organometallic Compounds

A. D. DELMAN, A. A. STEIN, B. B. SIMMS, AND R. J. KATZEN-  
STEIN, *U.S. Naval Applied Science Laboratory, Naval Base,  
Brooklyn, New York 11251*

### Synopsis

This study covers the results of synthesis and investigation of thermal stabilities of several organometallosiloxanes and organometal compounds containing Group IV elements. Investigations indicate, in general, that heat resistance is related to the dissociation energies of the M—O bonds, the number of organic groups connected to the metal atom, and the structure of the molecule as a whole. More specifically, the substitution of Ge—O and Sn—O bonds for some Si—O linkages in organosiloxanes produces a reduction in heat stability. The influence of the Ge—O bond to decrease the resistance of siloxanes is less than that of the Sn—O linkage; an increase in the number of Sn—O linkages producing a corresponding decrease in heat stability of the organosiloxane. The resistances of the germoxysiloxanes to heat degradation are less than that which would be expected from indications given by the relative stabilities of more simple organometallic compounds.

### INTRODUCTION

Recent technological developments have given impetus to the search for new useful polymeric products that are more heat resistant than are conventional organic macromolecules based on a framework of carbon-carbon bonds. The very broad front on which these investigations are being conducted has resulted in the production of a wide variety of new substances, of which only a comparatively small number can be fabricated into end-products for use at moderately high temperatures. Of these synthetic polymers, the most widely employed are the polysiloxanes. However, these materials readily undergo radical structural rearrangements to form volatile, low molecular weight, cyclic products when heated in the absence of air at temperatures in excess of 300°C. At these temperatures in air, silicon-methyl bond cleavage of polydimethylsiloxane occurs with subsequent crosslinking of the polymer.

Various lines of investigation have been undertaken to improve the resistance of polysiloxanes to thermal and oxidative degradation. Murphy and co-workers<sup>1</sup> determined that phenyl in place of methyl substituent groups on silicon improves the heat stability of the polymer. Numerous

additives have been suggested for extending the useful life of polysiloxanes at elevated temperatures under oxidative conditions.<sup>2-4</sup> More recently, increased thermal resistance of polysiloxanes has been sought through modification of the electronic character of the polymer by substitution of metal atoms for some or all of the silicon.<sup>5-8</sup>

Andrianov<sup>9,10</sup> investigated the stability of a variety of polymetallo-siloxanes by differential thermal analysis. Foster and Koenig<sup>11,12</sup> prepared stannosiloxanes with methyl and or phenyl pendant groups that were less thermally stable than polydiphenylsiloxane. The heat resistance of this polymer decreased with increased tin content, when exposed for prolonged time intervals at 245°C. Stavitskii and co-workers<sup>8</sup> reported that the thermal stability of polydimethylgermanosiloxanes are not affected by the concentrations of germanium atoms in the siloxane structure.

All of these studies are significant contributions toward understanding the effects on thermal stability of metal atoms in polysiloxane structures. To further augment such information, this paper presents the results of heat-resistance studies of structurally related aryl group-substituted organometallosiloxanes containing germanium or tin atoms. Results are compared to the thermal stabilities of less complex organometallic compounds containing germanium, silicon, or tin atoms.

## APPARATUS AND METHODS

### Infrared Spectra

The spectra from Nujol suspensions or films prepared by evaporation of benzene solutions of the products were recorded over the 2.5-15  $\mu$  range with a Perkin-Elmer Model 21 double-beam spectrophotometer equipped with sodium chloride optics.

### Thermogravimetric Analysis

The residual weight and temperature of 200-mg. samples of the products were recorded continuously on an Ainsworth, two-pen, Type BYR-AU-A, semimicro recording balance while being heated in air in a Kanthal wire-wound furnace<sup>13</sup> at 180°C./hr. Temperature measurements were made with a Pt/Pt-10% Rh thermocouple.

### Elemental Analysis and Molecular Weight

Analyses and molecular weight determinations, following the isothermal distillation procedure developed by Signer<sup>14</sup> and Barger,<sup>15</sup> were made by the Schwarzkopf Microanalytical Laboratory, Woodside, N.Y.

## MATERIALS

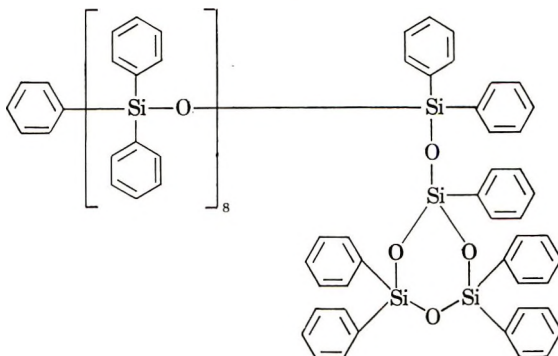
### Organometallic Substances

Diphenylsilanediol and triphenylsilanol were purchased from Peninsular ChemResearch, Inc., Gainesville, Fla. A sample of triphenyltin

hydroxide was provided by M & T Chemicals Inc., Rahway, N.J., for which kindness the authors are grateful. The procedure developed by Brook and Gilman<sup>16</sup> was used to synthesize triphenylgermanium hydroxide, m.p. (uncorr.) 133–135°C. (lit.<sup>17</sup>: 134.2°C.), yield 63.5%, from triphenylbromogermane, m.p. (uncorr.) 136.5–138°C., (lit.<sup>17</sup>: 138.7°C.), yield 64%, which was prepared by the method of Kraus and Foster.<sup>18</sup> Hexaphenyl-disiloxane, m.p. (uncorr.) 223–224°C. (lit.<sup>19</sup>: 222–224.5°C.), yield 81.3%, was synthesized by the method of Rochow and Gingold.<sup>20</sup>

It has long been known that electrophilic agents may be used to induce cleavage of aryl groups from silicon. For example, Clark<sup>21</sup> produced resinous products by heating mixtures of phenylchlorosilanes and aluminum chloride. Thus, to study the effects of metal atoms on the thermal resistance of higher molecular weight organosiloxanes, efforts were directed to synthesize such materials through aryl group cleavage reactions by similar treatment of mixtures of organosilanols and organometal hydroxides. The organosilanols were also heated in the absence of organometal hydroxides, as follows.

**Triphenylsilanol and Aluminum Chloride.** A mixture consisting of 100 g. (0.362 mole) of triphenylsilanol and 0.89 g. (0.0067 mole) of anhydrous aluminum chloride was heated to 225–250°C. in 1 hr. and maintained at that temperature for an additional 2 hr. The volatile products were removed by applying a vacuum to the system, and the residue was cooled to room temperature and dissolved in benzene. The solution was filtered and the solvent evaporated to recover 69.5 g. (94.5% yield) of a clear, colorless, hard, brittle resinous product which starts to soften at about 70°C. (uncorr.). The infrared absorption spectrum of a film of the material exhibits a doublet at 8.89 and 8.95  $\mu$  which suggests the presence of (C<sub>6</sub>H<sub>5</sub>)Si— linkages in the molecule.<sup>22</sup> Also present in the spectrum is an absorption band at 9.39  $\mu$  and a weak vibration frequency at 9.82  $\mu$ , which may be assigned to Si—O—Si bonding in branched open-chain and cyclic trimer siloxanes, respectively.<sup>23</sup> The structure I for the product is suggested.



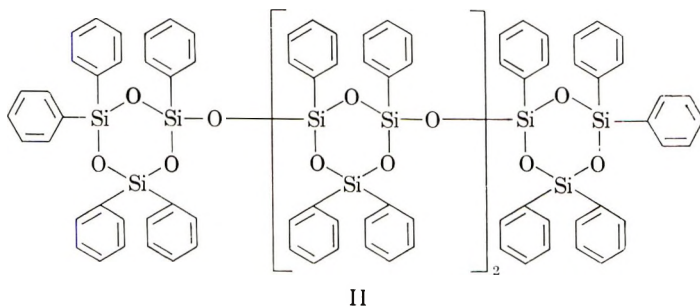
I

ANAL. Calcd. for C<sub>144</sub>H<sub>120</sub>O<sub>12</sub>Si<sub>12</sub>: C, 70.80%; H, 4.96%; Si, 13.80%; mol. wt., 2442.7. Found: C, 71.52%; H, 5.25%; Si, 13.45%; mol. wt., 2385.



**Diphenylsilanediol and Aluminum Chloride.** Similar treatment of a mixture comprised of 100.78 g. (0.466 mole) of diphenylsilanediol and 1.39 g. (0.01 mole) of anhydrous aluminum chloride produced 75.9 g. of a clear, hard resinous material, which starts to soften at about 80°C. (uncorr.). This product is soluble in benzene, chloroform, and ethyl ether. Except for the absence of a vibration mode at 9.39  $\mu$ , which indicates that the molecule probably does not contain branched open-chain Si—O—Si bonding, the infrared spectrum of a film of this material is very similar to that obtained, from the product prepared from triphenylsilanol.

A possible structural formula for the product is II.



ANAL. Calcd. for  $C_{108}H_{90}O_{15}Si_{12}$ : C, 66.01%; H, 4.63%; Si, 17.15%; mol. wt., 1965. Found: C, 66.19%; Y, 4.92%; Si, 17.20%; mol. wt., 1860.

**Bis(triphenylgermanium) Oxide.** By the same general procedure as above, a mixture of 5.0 g. (0.0156 mole) of triphenylgermanium hydroxide and 0.039 g. (0.00029 mole) of anhydrous aluminum chloride produced 4.75 g. (97.7% yield) of a white crystalline material, m.p. (uncorr.) 183–184°C. (lit.:<sup>24</sup> 183–185°C.).

ANAL. Calcd. for  $C_{36}H_{30}Ge_2O$ : C, 69.30%; H, 4.86%; Ge, 23.27%; mol. wt., 623.86. Found: C, 69.16%; H, 4.91%; Ge, 22.96%; mol. wt., 633.

The digermanoxane compound was also obtained in 95.1% yield when attempts were made to recrystallize triphenylgermanium hydroxide from a solvent mixture comprised of ligroine (b.p. 100–115°C.)–chloroform (50:1). The infrared spectrum of a Nujol mull of the substance corresponds to that reported in the literature.<sup>25</sup>

**Bis(triphenyltin) Oxide.** A mixture containing 10 g. (0.027 mole) of triphenyltin hydroxide and 0.067 g. (0.0005 mole) of anhydrous aluminum chloride was heated as above. After cooling to room temperature, the reaction products were washed in turn with chloroform and ethyl alcohol. The residue was separated by filtration and dried to produce 5.5 g. (56.4% yield) of a white crystalline substance, m.p. (uncorr.) 125°C. (lit.:<sup>19</sup> 123–124°C.).

ANAL. Calcd. for  $C_{36}H_{30}OSn_2$ : C, 60.38%; H, 4.23%; Sn, 33.15%. Found: C, 60.14%; H, 4.52%; Sn, 33.01%.

The infrared spectrum of a Nujol mull of the compound showed absorption bands corresponding to that reported by Poller.<sup>26</sup> Since bis(triphenyltin) oxide is known to disproportionate to tetraphenyltin and diphenyltin oxide when heated at the temperature used in this study,<sup>27</sup> the isolation of the product in this case was unexpected. This suggests that anhydrous aluminum chloride affects the disproportionation reaction.

### Organometallosiloxanes

The same general method described above was followed for the reactions shown below.

**Triphenylgermanium Hydroxide and Triphenylsilanol.** After similar treatment of a mixture consisting of 5.0 g. (0.0156 mole) of triphenylgermanium hydroxide, 4.3 g. (0.0156 mole) of triphenylsilanol and 0.077 g. (0.00058 mole) of anhydrous aluminum chloride, the product was extracted with petroleum ether and the insoluble fraction was dried under vacuum at 60°C. to produce, after recrystallization from petroleum ether-chloroform, 4.9 g. (61.7% yield) of white, waxlike tetraphenylbis[(triphenylgermyl)oxy] disiloxane, softening point (uncorr.) 90–97°C.

ANAL. Calcd. for  $C_{60}H_{50}Ge_2O_3Si_2$ : C, 70.61%; H, 4.95%; Ge, 14.23%; Si, 5.51%; mol. wt., — 1020.48. Found: C, 70.60%; H, 5.19%; Ge, — 15.26%; Si, 5.75%; mol. wt., 1031.

The infrared spectrum shows bands at 8.95 and 9.15  $\mu$  which are assigned to  $C_6H_5-Si$  and  $C_6H_5-Ge$  vibrations, respectively.<sup>28</sup> Absorption modes are also exhibited at 9.35 and 10.11  $\mu$  which are attributed to  $Si-O-Si$  and  $Si-O-Ge$  bonds, respectively.<sup>29</sup> A broad band at 11.65  $\mu$ , which is in the same range as similar modes in the spectra of triphenylgermanium hydroxide and bis(triphenylgermanium) oxide, is tentatively assigned to the  $(C_6H_5)_3GeO$  structure.

**Triphenylgermanium Hydroxide and Diphenylsilanediol.** To 5.0 g. (0.0156 mole) of triphenylgermanium hydroxide and 3.37 g. (0.0156 mole) of diphenylsilanediol was added 0.077 g. (0.00058 mole) of anhydrous aluminum chloride. The mixture was then treated as above. The reaction products were washed with petroleum ether and the residue was dried at 60°C. under vacuum and recrystallized from petroleum ether-chloroform to give 4.5 g. (57.0% yield) of a clear, hard resinous material, softening point (uncorr.) about 50°C. A film of this material produces an infrared spectrum which contains a doublet absorbing at 8.95 and 8.97  $\mu$  that may be attributed to  $(C_6H_5)_2Si$  bonding. Other vibration modes at 9.17, 9.42, 10.11, and 11.76  $\mu$  are assignable to  $C_6H_5-Ge$ ,  $Si-O-Si$ ,  $Si-O-Ge$ , and  $(C_6H_5)_3GeO$  structures, respectively.

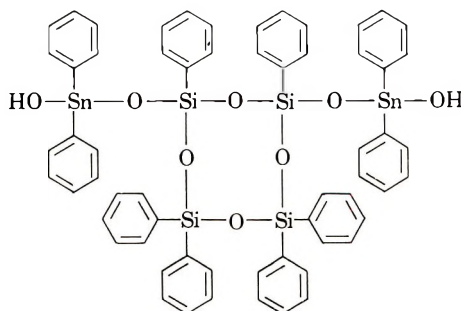
These data, together with molecular weight determinations and elemental analyses, support the structure III suggested.



ANAL. Calcd. for  $C_{48}H_{40}O_{3.5}SiSn_{2.5}$ : C, 57.72%; H, 4.15%; Si, 2.81%; Sn, 29.71%; mol. wt., 998.7. Found: C, 58.14%; H, 4.30%; Si, 2.83%; Sn, 29.17%; mol. wt., 968.

**Triphenyltin Hydroxide and Diphenylsilanediol.** A mixture consisting of 5.00 g. (0.0136 mole) of triphenyltin hydroxide, 2.93 g. (0.0136 mole) of diphenylsilanediol, and 0.66 g. (0.00049 mole) of anhydrous aluminum chloride was treated according to the general procedure above. After heating the mixture, the neck of the flask contained a white crystalline deposit which was removed and recrystallized from hot benzene solution to recover 2.5 g. (86.2% yield based on triphenyltin hydroxide) of tetraphenyltin, m.p. (uncorr.)  $224^{\circ}C$ . (lit.<sup>19</sup>  $225^{\circ}C$ .). The remainder of the reaction product was dissolved in benzene and worked up by addition of petroleum ether to the solution. The precipitate was separated by filtration and dried in the usual manner to give 4.9 g. of a hard, brittle, resinous product, softening point (uncorr.) about  $70^{\circ}C$ . The infrared spectrum from a film of the material contains a band at  $2.75\ \mu$  which is shown by substances containing Sn—OH bonds.<sup>32</sup> Vibration modes are also present at 8.89, 9.29, and  $10.20\ \mu$  which are derived from  $C_6H_5-Si$ ,  $C_6H_5-Sn$ , and Si—O—Sn bonding, respectively. In addition, the spectrum contains a shoulder  $9.20\ \mu$ , which emanates from the  $9.29\ \mu$  band, that may be assigned to Si—O—Si bonding in cyclic tetramers.<sup>23</sup>

A structural formula V, derived from the above data suggested is V.



V

ANAL. Calcd. for  $C_{60}H_{52}O_8Si_4Sn_2$ : C, 57.61%; H, 4.20%; Si, 8.98%; Sn, 18.98%; mol. wt., 1250.9. Found: C, 56.84%; H, 4.25%; Si, 8.32%; Sn, 19.21%; mol. wt., 1015.

The product may be similar to one reported by Foster and Koenig.<sup>12</sup>

### THERMAL STABILITY

Although the limitations of thermogravimetric analysis are well known, the method is widely accepted as a useful research tool for assessing and comparing the resistance of materials to degradation at elevated temperatures, under the same experimental conditions. The thermograms of the products reported in this paper are presented in Figures 1-4.

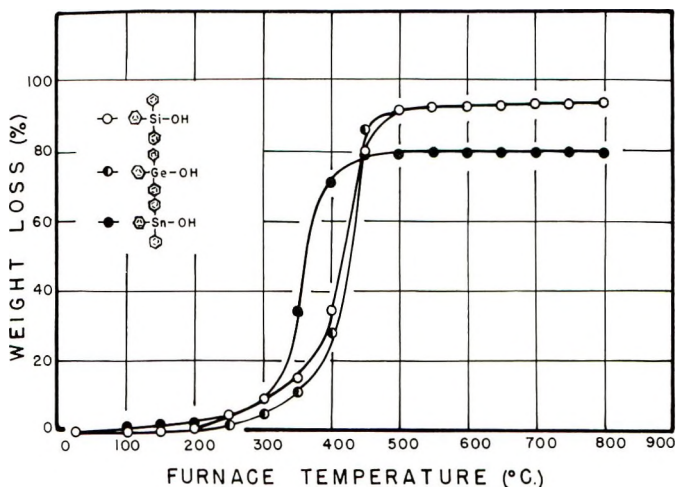


Fig. 1. TGA thermograms of organometal hydroxides.

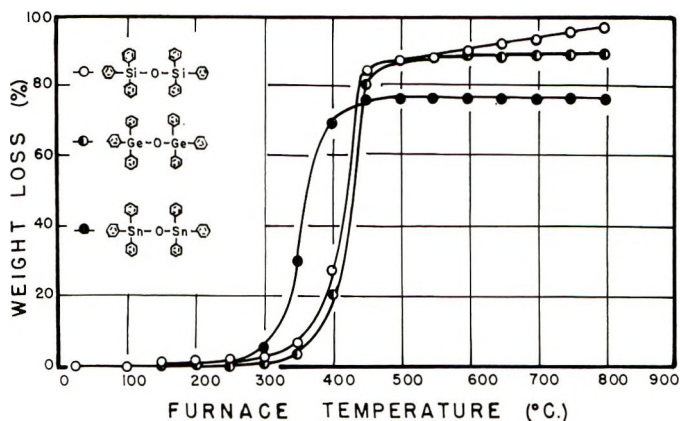


Fig. 2. TGA thermograms of organometal oxanes.

The heat resistances of the organometal hydroxides are shown in Figure 1. It is apparent from the thermograms that triphenylgermanium hydroxide is just slightly more heat-stable than triphenylsilanol which in turn, is much more resistant than triphenyltin hydroxide.

The thermograms of the dimetalloxanes are presented in Figure 2. Comparison of these data with results given in Figure 1 indicate that the dimetalloxane compounds are somewhat more heat stable than their corresponding organometal hydroxides. In terms of relative heat resistance, the results obtained with the dimetalloxanes closely parallel the order of stability observed with the organometal hydroxides.

Figure 3 shows the thermograms of the products obtained by heating triphenylsilanol alone or in mixture with triphenylgermanium hydroxide or triphenyltin hydroxide in the presence of anhydrous aluminum chloride.



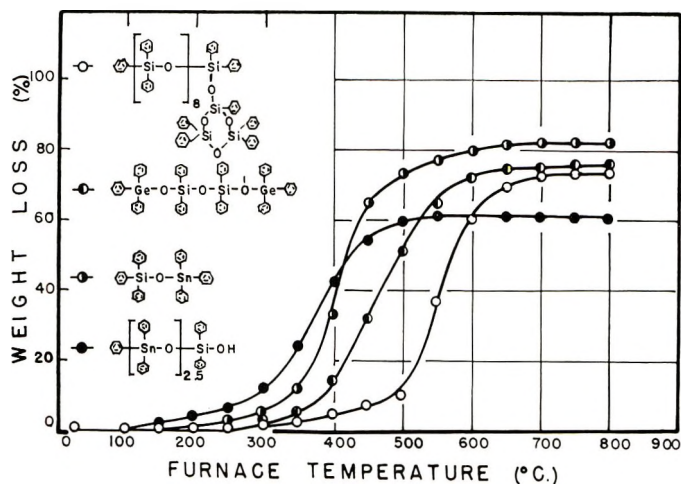


Fig. 3. TGA thermograms of organometallosiloxanes from triphenylsilanol and organometal hydroxides.

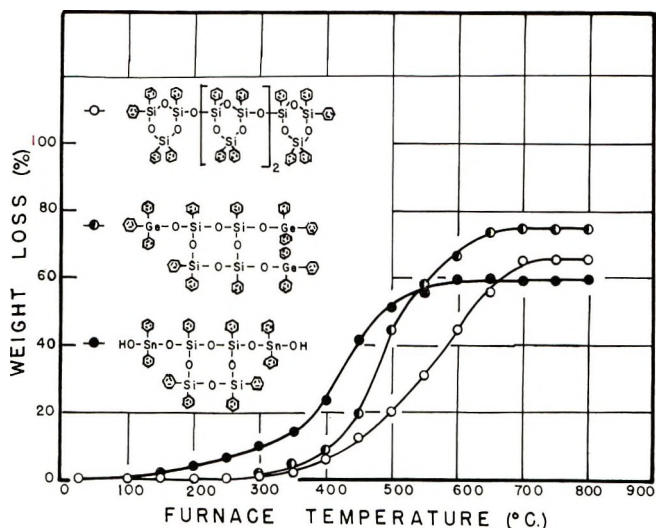


Fig. 4. TGA thermograms of organometallosiloxanes from diphenylsilanediol and organometal hydroxides.

Results indicate that the polysiloxane is definitely more heat stable than any of the metallosiloxanes. In addition, the heat resistance of tetraphenylbis[(triphenylgermyl)oxy]disiloxane is superior to the organostannyloxysilane products. Comparison of the thermograms given by the materials containing tin shows that thermal stability decreases as the ratio of tin to silicon atoms increases.

The thermograms of 1,3,5-tris[(triphenylgermyl)oxy]-1,3,5,7,7-pentaphenylcyclotetrasiloxane (III), 1,3-bis[(diphenylhydroxystannyl)oxy]-

1,3,5,5,7,7-hexaphenylcyclotetrasiloxane (V), and the product prepared by heating diphenylsilanediol in the presence of anhydrous aluminum chloride are shown in Figure 4. Comparison of these data with results presented in Figure 3 indicate that the products derived from diphenylsilanediol are somewhat more heat resistant than corresponding materials obtained from triphenylsilanol. The relative heat stability shown by the former products is in the same order as that exhibited by the latter materials.

Summarizing the results of thermal stability measurements, it may be said that: In general, all of the organometallosiloxanes investigated are more heat-resistant than the organometallic compounds. The thermal stabilities of the germoxysiloxanes, however, are less than that which might be expected from results obtained with the more simple germanium compounds. In fact, replacement of some of the Si—O bonds in organosiloxanes with Ge—O or Sn—O produces a reduction of the heat resistance of siloxanes. The capacity of the Sn—O unit to lower the thermal stability is greater than that of Ge—O. In the case of Si—O bond substitution by Sn—O linkages, an increase in the number of Sn—O units produces a corresponding decrease in the heat stability of the organosiloxane.

## DISCUSSION

To reduce the number of parameters that may contribute to heat stability, we have limited this study to substances having only phenyl substituent groups. While the nature of such pendent groups exert a great influence, the backbone structure of siloxanes is the controlling factor of its thermal stability. When linear polysiloxanes are heated at about 300°C., the polymer degrades through Si—O bond cleavage and cyclic products are formed. At more elevated temperatures, rupture of Si—C bonds occur. In branched and crosslinked polymers, heating induces only destruction of Si—C bonds and not Si—O linkages.<sup>33</sup> Since all of the products investigated in this study are soluble in several organic solvents, they are not considered to be crosslinked. If it can be assumed, therefore, that the decomposition of organometallosiloxanes proceeds along lines similar to that of the more conventional siloxanes, then the bond dissociation energies of the M—O links may provide a means for predicting their relative heat stabilities.

Representative values given in the literature<sup>34</sup> for the dissociation energies of Si—O, Ge—O, and Sn—O bonds are 185, 157, and 132 kcal./mole, respectively. On this basis, one might predict that the heat resistance of polysiloxanes would be lowered as some of the silicon atoms are replaced by germanium or tin; the latter metal producing the largest stability decrease. In fact, the relative thermal resistances of the organometallosiloxanes reported in this study and of the stannosiloxanes described by Foster and Koenig<sup>11,12</sup> support this general postulation. It would seem from this that the M—O bond dissociation energies may be a contributing factor in the resistance of the organometallosiloxanes to thermal degradation.

However, the stabilities of the more simple organometallic compounds do not appear to follow the relative order of dissociation energy values for the M—O bonds; the organogermanium products exhibit resistances that are at least equal to if not better than corresponding organosilicon substances. It is possible that this apparent anomaly may be attributed to differences in their behavior when heated.

An outstanding characteristic of the silanols is the ease with which they condense to siloxanes. Diphenylsilanediol dehydrates readily, when heated above its melting point (201–202°C.), to produce simple cyclic siloxanes and more complex polymers.<sup>35</sup> Results of these studies indicate that diphenylsilanediol undergoes Si—C<sub>6</sub>H<sub>5</sub> bond cleavage when heated at 250°C. These studies and research described in the literature<sup>36</sup> show that triphenylsilanol also is subject to similar fission reactions at 250°C., accompanied by the formation of benzene. Hexaphenyldisiloxane is probably formed as an intermediate product.<sup>37</sup>

As in the case of the silanols, triphenylgermanium hydroxide loses water at temperatures above its melting point (134.2°C.) to produce bis(triphenylgermanium) oxide. However, these studies show that the digermanoxane compound does not undergo M—C<sub>6</sub>H<sub>5</sub> bond cleavage when heated at 250°C. as does the analogous disiloxane. This suggests that phenyl groups attached to germanium atoms are more resistant to cleavage by heat than when attached to silicon. Similar findings have been reported by Gilman and Gerow<sup>38</sup> in their investigations of the relative thermal stabilities of aryl-substituted digermanes and disilanes. The superior heat resistance of the Ge—C<sub>6</sub>H<sub>5</sub> bond over that of the Si—C<sub>6</sub>H<sub>5</sub> bond probably explains why the more simple germanium compounds show better thermal resistance than corresponding organosilicon products.

The literature<sup>37</sup> indicates that the thermal stability of the Si—O bond decreases with increasing number of organic groups attached to the silicon atom. Each of the organometallosiloxanes containing germanium atoms that are reported in this study probably only have one or at most two phenyl radicals attached to a silicon atom, whereas there are three benzene rings attached to the silicon atoms of triphenylsilanol and hexaphenyldisiloxane. The difference in number of phenyl radicals attached to the silicon atoms may be a contributing factor as to why the organogermanosiloxanes are more heat stable than the more simple organosilicon compounds.

The stability of specific bonds to cleavage by heat also is known to be dependent on the spacial arrangement of such bonds in the molecule. Infrared spectroscopy data indicate that the organometallosiloxanes prepared from diphenylsilanediol contain Si—O bonds in a cyclic arrangement, while the molecules of the materials made from triphenylsilanol have Si—O linkages in all or predominantly linear configurations. Andrianov<sup>39</sup> shows that linear organosiloxanes are more susceptible to thermooxidation cleavage reactions than corresponding cyclic or crosslinked polymers. Rupture of the Si—O backbone in cyclic organosiloxanes is not observed at 550°C., regardless of the type of organic pendent group present. This

may explain the superior thermal stability of the products derived from diphenylsilanediol when compared to analogous materials prepared from triphenylsilanol.

In conclusion, the heat stability of the organometallosiloxanes and the more simple Group IV organometallic compounds studied seem to be influenced by factors such as the M—O bond dissociation energy, the number of organic groups bound to the metal atom, and the spatial arrangement of the M—O linkages. Additional studies along these lines are necessary to determine whether these findings are applicable in a general way to other organometallosiloxane and organometallic systems.

The authors are grateful to E. A. Bukzin and W. B. Shetterly, Bureau of Ships, Washington, D.C., for sponsoring this study and to J. M. McGreevy, Associate Technical Director, U.S. Naval Applied Science Laboratory, Brooklyn, N.Y., for his interest and encouragement.

The opinions or assertions contained in this paper are the private ones of the authors and are not to be construed as official or reflecting the views of the Naval Service at large.

### References

1. C. M. Murphy, C. E. Saunders, and D. C. Smith, *Ind. Eng. Chem.*, **42**, 2462 (1950).
2. R. R. McGregor and E. L. Warrick, U.S. Pat. 2,389,802 (1945).
3. A. R. Gilbert (to General Electric Co.), U.S. Pat. 2,717,902 (1955).
4. J. Swiss, U.S. Pat. 2,465,296 (1949).
5. K. A. Andrianov and A. A. Zhdanov, *J. Polymer Sci.*, **30**, 513 (1958).
6. K. A. Andrianov and E. Z. Asnovich, *Vysokomol. Soedin.*, **2**, 136 (1960).
7. S. M. Atlas and H. F. Mark, *Angew. Chem.*, **72**, 249 (1960).
8. I. K. Stavitskii, S. N. Borisov, N. G. Ponomarenko, N. G. Sviridova, and G. Ya. Zueva, *Vysokomol. Soedin.*, **1**, 1502 (1959).
9. K. A. Andrianov, *Khim. Tekhnol. Polimerov*, **1960**, 26.
10. K. A. Andrianov, "High-Temperature Resistance and Thermal Degradation of Polymers," Monograph No. 13, Society of Chemical Industry, Plastics and Polymer Group, London, 1961.
11. W. E. Foster and P. E. Koenig, U.S. Pat. 2,998,407 (1956).
12. W. E. Foster and P. E. Koenig, U.S. Pat. 2,998,440 (1956).
13. A. Reisman and F. Holtzberg, *J. Am. Chem. Soc.*, **77**, 2115 (1955).
14. R. Signer, *Ann.*, **478**, 246 (1930).
15. G. Barger, *J. Chem. Soc.*, **85**, 286 (1904).
16. A. G. Brook and H. Gilman, *J. Am. Chem. Soc.*, **76**, 77 (1954).
17. *Handbook of Chemistry and Physics*, 42nd Ed., Chemical Rubber Publishing Co., Cleveland, 1960–1961.
18. C. A. Kraus and L. S. Foster, *J. Am. Chem. Soc.*, **49**, 457 (1927).
19. H. C. Kaufman, *Handbook of Organometallic Compounds*, D. Van Nostrand Co., Princeton, N.J., 1961.
20. E. G. Rochow and K. Gingold, *J. Am. Chem. Soc.*, **76**, 4852 (1954).
21. A. H. Clark, U.S. Pat. 2,557,782 (1951).
22. C. W. Young, P. C. Servais, C. C. Currie, and M. J. Hunter, *J. Am. Chem. Soc.*, **70**, 3758 (1948).
23. L. J. Bellamy, *The Infra-red Spectra of Complex Molecules*, 2nd Ed., Wiley, New York, 1958.
24. H. Gilman and C. W. Gerow, *J. Am. Chem. Soc.*, **79**, 342 (1957).
25. N. A. Chumakovskii, *Opt. Spektroskopiya*, **13**, 68 (1962).
26. R. C. Poller, *J. Inorg. Nucl. Chem.*, **24**, 593 (1963).



27. W. T. Reickle, *J. Polymer Sci.*, **49**, 521 (1961).
28. M. C. Henry and J. G. Noltes, *J. Am. Chem. Soc.*, **82**, 555 (1960).
29. H. Schmidbaur, J. Hussek, *J. Organometal. Chem.*, **1**, 235 (1964).
30. S. Papetti and H. W. Post, *J. Org. Chem.*, **22**, 526 (1957).
31. M. C. Henry and J. G. Noltes, *J. Am. Chem. Soc.*, **82**, 558 (1960).
32. R. West and H. Baney, *J. Phys. Chem.*, **64**, 822 (1960).
33. K. A. Andrianov and N. N. Sokolov, *Khim. Prom.*, **1953**, 329.
34. T. L. Cottrell, *The Strengths of Chemical Bonds*, Academic Press, New York, 1965.
35. C. A. Burkhard, *J. Am. Chem. Soc.*, **67**, 2173 (1945).
36. A. K. McCloskey, W. G. Woods, R. J. Brothers, G. W. Willcockson, H. Goldsmith, M. L. Iverson, K. Kitasaki, H. M. Manasevit, H. C. Newsom, and L. L. Petterson, Research on Inorganic Polymer Systems, Wright Air Development Division Tech. Report 60-911, Wright Patterson Air Force Base, Ohio (1961).
37. K. A. Andrianov, *Organosilicon Compounds*, Goskhimizdat, Moscow, 1955.
38. H. Gilman and C. W. Gerow, *J. Am. Chem. Soc.*, **77**, 5509 (1955).
39. K. A. Andrianov, *Metalorganic Polymers*, Interscience, New York, 1965.

### Résumé

Ce travail rapporte les résultats de synthèses et de déterminations de stabilité thermique de nombreux organométallosiloxanes et de composés organométalliques contenant des éléments du groupe IV. En général, ces études indiquent que la résistance thermique est liée aux énergies de dissociation des liens métal-oxygène, du nombre de groupes organiques attachés à l'atome métallique et de la structure de la molécule dans son entièreté. Plus spécifiquement la substitution de liens de germanium-oxygène et d'étain-oxygène à certains liens silicium-oxygène dans les organosiloxanes produit une diminution de stabilité thermique. L'influence du lien germanium-oxygène dans le sens de la diminution de la résistance des siloxanes est inférieure à celle du lien étain-oxygène: un accroissement du nombre de liens étain-oxygène produisant une diminution correspondante de stabilité thermique de l'organo-siloxane. Les résistances des germoxysiloxanes à la dégradation thermique sont inférieures à celles que l'on s'attendrait obtenir au départ des stabilités relatives de composés organo-métalliques plus simples.

### Zusammenfassung

Die vorliegende Untersuchung bringt die Ergebnisse von Versuchen, über Synthese und Hitzebeständigkeit einiger Organometallsiloxane und Organometallverbindungen mit Elementen der Gruppe IV. Die Hitzebeständigkeit wird im allgemeinen durch die Dissoziationsenergie der M—O-Bindung, die Anzahl der an das Metallatom gebundenen organischen Gruppen und die Struktur des Moleküls als ganzes bedingt. Genauer gesagt führt die Substitution einiger Si—O-Bindungen in Organosiloxanen durch Ge—O- und Sn—O-Bindungen zu einer Herabsetzung der Hitzebeständigkeit. Der Einfluss der Ge—O-Bindung auf die Herabsetzung der Beständigkeit von Siloxanen ist geringer als derjenige der Sn—O-Bindung; eine Zunahme der Zahl der Sn—O-Bindungen führt zu einer entsprechenden Abnahme der Hitzebeständigkeit des Organosiloxans. Die Beständigkeit der Germoxysiloxane gegen Hitzeabbau ist geringer als man nach der relativen Stabilität einfacherer organometallischer Verbindungen erwarten würde.

Received January 26, 1966

Revised March 18, 1966

Prod. No. 5114A





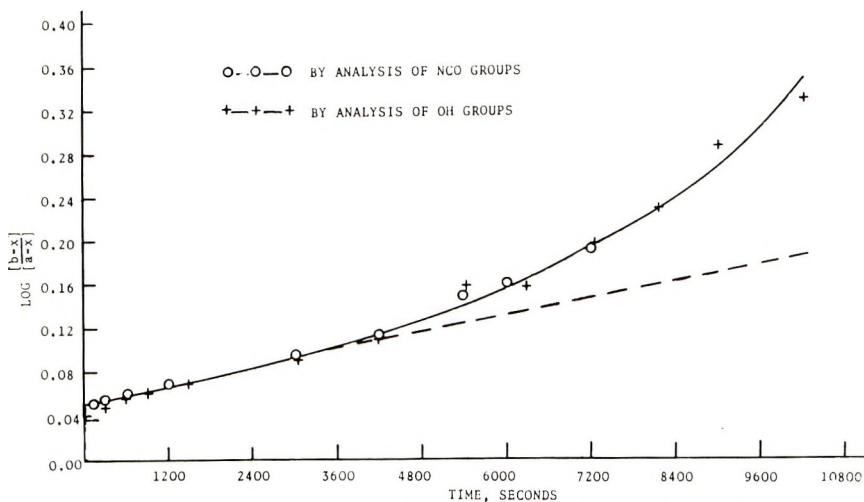


Fig. 1. Reaction of phenyl isocyanate and 1-methoxy-2-propanol;  $1 \times 10^{-4}$  mole/l. dibutyltin dilaurate, toluene,  $30^{\circ}\text{C}$ .

#### References

1. K. C. Frisch and S. L. Reegen, paper delivered at the International Symposium on Macromolecular Chemistry, IUPAC, Prague, Czechoslovakia, August 1965.
2. L. Rand, B. Thir, S. L. Reegen, and K. C. Frisch, *J. Appl. Polymer Sci.*, **9**, 1787 (1965).
3. J. W. Baker and J. B. Holdsworth, *J. Chem. Soc.*, **1947**, 713.
4. H. Okada and Y. Iwakura, *Makromol. Chem.*, **64**, 91 (1963).
5. M. Sato, *J. Org. Chem.*, **27**, 819 (1962).
6. I. C. Kogon, *J. Org. Chem.*, **26**, 3004 (1961).
7. G. Gutnikov and G. N. Schenk, *Anal. Chem.*, **34**, 1316 (1962).

S. L. REEGEN  
K. C. FRISCH

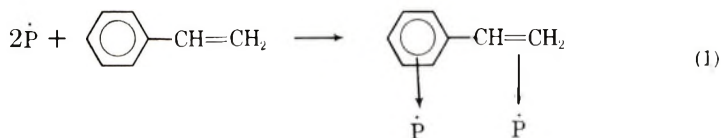
Research Laboratories  
Wyandotte Chemicals Corporation  
Wyandotte, Michigan

Received February 1, 1966

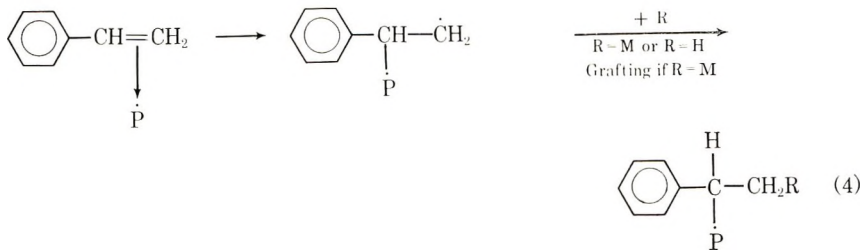
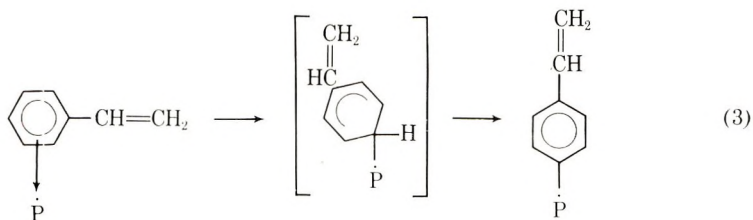
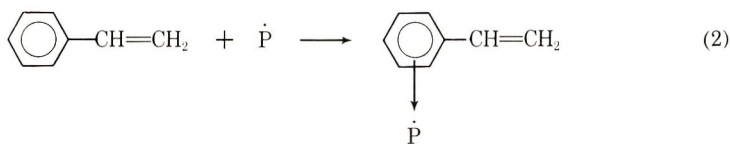
***A Charge-Transfer Theory for the Interpretation of  
Radiation-Induced Grafting of Monomers to Cellulose***

The results of radiation-induced grafting experiments have demonstrated the importance of the adsorption characteristics of monomers and solvents in cellulose copolymerization studies.<sup>1</sup> EPR investigations have shown that radiation-induced trapped radical formation, involving sites "inaccessible" to chemical entities, may occur during the grafting.<sup>1,2</sup> The problem in this system and also in grafting initiated by analogous methods<sup>3,4</sup> is the nature of the bonding in the copolymer.

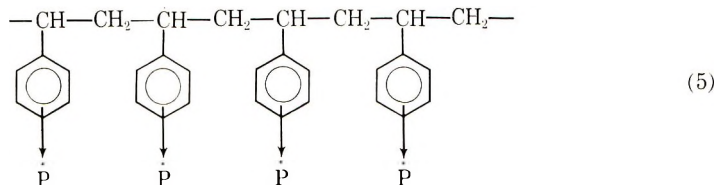
By using styrene-cellulose as a model system, in the present paper it is intended to show how adsorption phenomena and "inaccessible" radical sites may both contribute to the nature of the bonding if the concept of a charge-transfer interaction<sup>5-7</sup> is invoked. In the simplest example, styrene is adsorbed on the cellulose surface as a charge-transfer complex involving the delocalization of the styrene  $\pi$ -electrons into the free valencies of the irradiated cellulose [eq. (1), where  $\dot{P}$  is a radical site either on the surface or within the bulk].



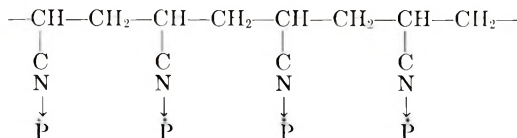
Because of the ease of accessibility of radical sites at the surface of the cellulose, further reaction ( $\pi$ - $\sigma$  conversion)<sup>6</sup> may occur only in this instance to give a stable  $\sigma$ -bonded species [eqs. (2) and (3)]. The examples of  $\pi$ -bonding through the ring [eqs. (2) and (3)] and through the side-chain [eq. (4)] will be illustrated separately.



For grafting within the bulk of the cellulose, the mobility of polystyrene chains and radicals would be impeded, and a mechanism analogous to the  $\pi$ - $\sigma$  conversion would be difficult to apply, although the following modified form of eq. (2) may be envisaged



Bonding of this type would be extremely strong and would tend to keep homopolymer locked between the chains as "graft" polymer. Similar charge-transfer bonding may be used to interpret grafting between cellulose and monomers such as acrylonitrile, where the functional group may now act as the donor.



It is stressed at this time that the present concept is essentially an hypothesis which may be of help in interpreting grafting reactions rather than a theory established on extensive experimental work. Grafting studies supporting the charge-transfer theory will be published in the near future.

We thank Australian Paper Manufacturers Ltd. for the award of a fellowship (S. D.), the Australian Institute for Nuclear Science and Engineering and the Australian Atomic Energy Commission for the irradiations and the Wool Research Trust Fund for financial support.

### References

1. S. Dilli and J. L. Garnett, unpublished data.
2. I. T. Ernst and J. L. Garnett, unpublished data.
3. N. Geacintov, V. Stannett, E. W. Abrahamson, and J. J. Hermans, *J. Appl. Polymer Sci.*, **3**, 54 (1960).
4. H. Yasuda, J. A. Wray, and V. Stannett, in *Fourth Cellulose Conference (J. Polymer Sci., C, 2)*, R. H. Marchessault, Ed. Interscience, New York, 1963, p. 387.
5. W. R. McClellan, H. H. Hoehn, H. N. Cripps, E. L. Muettterties, and B. W. Howk, *J. Am. Chem. Soc.*, **83**, 1601 (1961).
6. J. L. Garnett and W. A. Sollich-Baumgartner, *J. Phys. Chem.*, **69**, 1850 (1965).
7. I. T. Ernst, J. L. Garnett, and W. A. Sollich-Baumgartner, *J. Catal.*, **3**, 568 (1964).

S. DILLI  
J. L. GARNETT

Department of Physical Chemistry  
The University of New South Wales  
Kensington, New South Wales, Australia

Received December 14, 1965  
Revised February 4, 1966





of the siloxane linkages. Measurements of the hydroxy equivalent did not show any appreciable change in molecular weight on the reduction; however, a lowering of the inherent viscosity of the diol compared to the diacid strengthened the view that cleavage of the polysiloxane had occurred.

The disiloxane monomer with carboxyl endgroups was synthesized by the method of Marvel and Mulvaney.<sup>3</sup>

## EXPERIMENTAL

### Materials

*Diethyl ether* "A. R. Grade" was obtained from Mallinckrodt Chemical Works.

*Lithium aluminum hydride* was obtained from Metal Hydrides, Inc.

*Methylmagnesium bromide* was supplied by Arapahoe Chemical Co. as a 3.8 mole/l. solution in diethyl ether.

$\gamma$ -Cyanopropyl-dichlorosilane was the gift of Dr. E. W. Bennet of the Silicones Division of Union Carbide Corp.

*Dimethylcyanopropylchlorosilane* was the gift of Dr. J. R. Elliott of The General Electric Co.

*Octamethylcyclotetrasiloxane* was obtained from K & K Laboratories, Inc. and used without any further purification.

### Polymerizations

Polymerizations were performed in a manner similar to that described by Sorenson and Campbell.<sup>1</sup>

**Preparation of  $\alpha,\omega'$ -Bis( $\delta$ -hydroxybutyl)dimethyl Polysiloxane [Redistribution reaction of Tetramethyl-1,3-bis( $\delta$ -hydroxybutyl)disiloxane and Octamethylcyclotetrasiloxane].** A mixture of 5.4 g. (0.02 mole) of tetramethyl-1,3-bis( $\delta$ -hydroxybutyl)disiloxane (II) and 36 g. (0.12 mole) of octamethylcyclotetrasiloxane were placed in a pressure bottle with 1 ml. of concentrated sulfuric acid and shaken for 24 hr. After this time, 50 ml. of diethyl ether and 20 ml. of water were added and the mixture shaken for 1 hr. further. The ether layer was separated, washed three times with 20 ml. of water, and dried over anhydrous magnesium sulfate. The solvent was removed under reduced pressure, leaving the clear liquid polysiloxane (91% yield), which had an inherent viscosity of 0.098 at 30°C. in toluene. The molecular weight determined from the hydroxy equivalent was 12,246, compared to the theoretical value of 2,323 assuming a perfect equilibration between the two compounds.

ANAL. Calcd. for experimental molecular weight: C, 32.80%; H, 8.15%; Si, 37.51%. Found: C, 33.21%; H, 8.08%; Si, 38.07%.

When 6.74 g. (0.0228 mole) of tetramethyl-1,3-bis( $\delta$ -hydroxy-*n*-butyl)disiloxane and 35.9 g. (0.129 mole) of the cyclic tetramer were equilibrated in 60 ml. of dry diethyl ether for three days with 1.5 ml. of concentrated sulfuric acid catalyst, a polysiloxane having an experimental molecular weight of 6656 was formed (theoretical molecular weight 1956). The inherent viscosity at 30°C. in toluene was 0.093.

**Preparation of  $\alpha,\omega$ -Bis( $\gamma$ -carboxy-*n*-propyl)dimethyl Polysiloxane [Redistribution Reaction of Octamethylcyclotetrasiloxane and Tetramethyl-1,3-bis( $\gamma$ -carboxy-*n*-propyl)disiloxane].** A 6 $\frac{1}{2}$ -g. portion (0.212 mole) of tetramethyl-1,3-bis( $\gamma$ -carboxy-*n*-propyl)disiloxane was added to 35 g. (0.118 mole) of cyclic tetramer in a pressure bottle together with 1.1 ml. of concentrated sulfuric acid and shaken for 24 hr. The polysiloxane was worked up as described above, giving 37 g. (89% yield) of clear, fluid liquid with an inherent viscosity of 0.05 at 30°C. in toluene. The experimental molecular weight (2090) agreed very well with the theoretical value of 1955.

ANAL. Calcd. for experimental molecular weight: C, 34.52%; H, 8.155%; Si, 35.06%. Found: C, 34.67%; H, 8.10%; Si, 35.13%.

**Reduction of  $\alpha,\omega$ -Bis( $\gamma$ -carboxy-*n*-propyl)dimethyl Polysiloxane.** A 10-g. portion of the carboxyl-terminated polysiloxane (mol. wt. 2090) was dissolved in 50 ml. of diethyl ether and added dropwise to an ice-cold solution of lithium aluminum hydride (4 g., 0.105 mole) in 150 ml. of ether. The solution was stirred vigorously and refluxed for 2 hr. after completion of the addition, and then left overnight. The excess hydride was destroyed with 10% hydrochloric acid and the ether layer separated. The aqueous layer was extracted three times with 30 ml. of ether and the combined ether solution dried over anhydrous sodium sulfate. The ether was removed on a rotary evaporator, leaving a colorless fluid (6.5 g.) with an inherent viscosity at 30°C. in toluene of 0.033. The molecular weight as determined from hydroxy equivalent measurements was 2275. The infrared spectrum of the compound showed the presence of hydroxyl groups with an absorption band at 3350  $\text{cm}^{-1}$  but also an absorption at 2120  $\text{cm}^{-1}$  due to the formation of Si-H.

ANAL. Calcd. for molecular weight of 2275: C, 34.76%; H, 8.425%. Found: C, 35.14%; H, 8.58%.

**Preparation of Tetramethyl-1,3-bis( $\delta$ -hydroxy-*n*-butyl)disiloxane (II).** A suspension of 8.2 g. (0.22 mole) of lithium aluminum hydride in 300 ml. of ether was placed in a one-liter flask equipped with a reflux condenser, dropping funnel, and mechanical stirrer. Through the dropping funnel, 29.4 g. (0.097 mole) of 5,5,7,7-tetramethyl-5,6-sila-6-oxaundecanedioic acid in 100 ml. of diethyl ether was introduced at a rate such as to produce gentle reflux. After 5 hr. the excess lithium aluminum hydride was decomposed by cautious addition of dilute hydrochloric acid, and the ether layer separated. The aqueous layer was extracted with 100 ml. of ether twice and the combined ether solution dried over anhydrous magnesium sulfate, before vacuum distillation, to yield 7.5 g. (28.2% yield) of tetramethyl-1,3-bis( $\delta$ -hydroxy-*n*-butyl)disiloxane, b.p. 62–63°C./0.2 mm.,  $n_D^{27}$ , 1.4495.

ANAL. Calcd. for  $\text{C}_{12}\text{H}_{30}\text{O}_3\text{Si}_2$ : C, 48.50%; H, 10.85%; Si, 21.89%. Found: C, 51.64%; H, 10.74%; Si, 19.61%.

The financial support of the Textile Fibers Department of E. I. du Pont de Nemours and Company is gratefully acknowledged.

#### References

1. W. Sorenson and T. W. Campbell, *Preparative Methods of Polymer Chemistry*, Interscience, New York, 1961, p. 259.
2. C. L. Ogg, W. L. Porter, and C. O. Willis, *Ind. Eng. Chem., Anal. Ed.*, **17**, 394 (1945).
3. C. S. Marvel and J. E. Mulvaney, *J. Polymer Sci.*, **50**, 541 (1961).

K. KOJIMA\*  
C. R. GORE†  
C. S. MARVEL

Department of Chemistry  
University of Arizona  
Tucson, Arizona

Received March 8, 1966

\* Post-doctoral Research Associate supported by Textile Fibers Department of E. I. du Pont de Nemours and Company, 1963–65.

† Post-doctoral Research Associate supported by Textile Fibers Department of E. I. du Pont de Nemours and Company, 1964–65.

### Improved Method of Polymer Purification

In this laboratory, removal of emulsifiers and polymer solvents when polymers are precipitated into water has often proved difficult. This is a report of a method that accomplishes both tasks quickly with results superior to mechanical stirring or to blending. The apparatus used is shown in Figure 1.

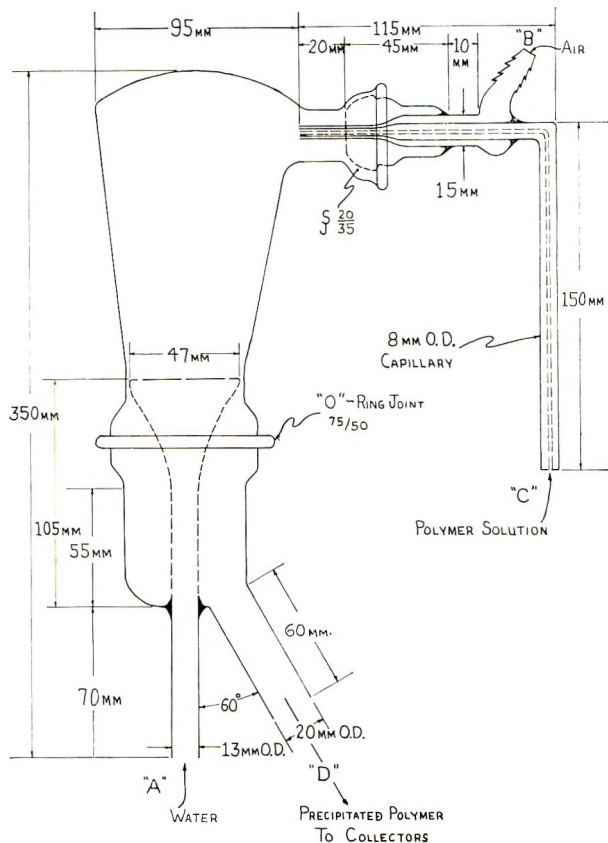


Figure 1.

In operation, water is supplied from the top to the precipitator at A. When air, under pressure, is introduced at B, the polymer solution is drawn up the capillary at C and atomized into a torrent of water. In the case of acrylic-type polymers, the precipitated polymer issuing from D is collected in two 4-l. beakers in series with a 15 mm. O.D. spout on the bottom of each. The beakers act as a series of settling tanks. The first beaker arrests the turbulence from the precipitator, empties into the second (the top of which is covered by a piece of 100-mesh screen or suitable material) and as the effluent from the second is discarded, a precipitation run is accomplished unattended. Certainly other methods of collecting the precipitated polymer are possible, e.g., collecting the entire effluent from a run in a large container and subsequent retrieval of the coagulated polymer.

This method offers several advantages over previous techniques: (1) The large excess of water (water:polymer solution approximately 150:1) thoroughly removes all water-soluble impurities from the small precipitated polymer particles; (2) complete removal

of polymer solvent makes the purified sample easier to filter; (3) the sample is uniform; (4) no explosion hazard from an electrical motor in the presence of a flammable solvent exists; (5) further testing of the purified sample is easy because the particles are fine; (6) a nondestructive means of coagulation.

In a typical run, we were able to precipitate 30–45 ml. of dilute (1–5%) polymer solution per minute in a shower of 120–150 ml. of water per second. The coagulated polymer particles are very small because the dilute polymer solution is introduced into the precipitating chamber in the form of a fine mist. Thorough washing is insured by the large, constantly changing, volume of water used. The method is safe and nondestructive chemically, since only water and air are employed.

The author gratefully acknowledges the help, suggestions,<sup>1</sup> and support of Professor C. S. Marvel. This is a partial report of work done under contract with the Southern and Western Utilization Research and Development Divisions, Agricultural Research Service, U. S. Department of Agriculture and authorized by the Research and Marketing Act of 1946. The contract is supervised by Dr. T. H. Applewhite of the Western Division's Field Crops Laboratory.

#### Reference

1. C. S. Marvel, G. D. Jones, T. W. Mastin, and G. L. Shertz, *J. Am. Chem. Soc.*, **64**, 2356 (1942).

RALPH W. MAGIN  
HARRY G. NUNNAMAKER

Department of Chemistry  
University of Arizona  
Tucson, Arizona

Received March 16, 1966

### *Solid-State Polymerization of Diacetone Acrylamide*

The polymerization of diacetone acrylamide both in the liquid state and in solution has been reported recently.<sup>1</sup> Free-radical and ionic catalysts have been shown to give satisfactory polymerization. On the basis of structural similarities between this monomer and acrylamide, we compared the radiation-induced, solid-state polymerization of diacetone acrylamide to that of acrylamide. The two monomers have been shown to be essentially equivalent in their polymerization behavior.

The solid-state polymerization of acrylamide has been investigated thoroughly<sup>2,3</sup> and is probably the best understood of all such polymerizations. The crystal lattice of this monomer has been shown to superimpose very little order on the final polymer. Evidence points toward a random, diffusion-controlled polymerization. The resultant random polymer contrasts to the more ordered polymers obtained from the solid-state polymerization of cyclic monomers such as trioxane,<sup>4,5</sup> trithiane,<sup>6,7</sup> and  $\beta$ -propiolactone.<sup>8</sup>

In the present investigation, we irradiated diacetone acrylamide both in the solid and liquid state. In the solid state, irradiation could be conducted at a lower temperature and then the major part of the polymerization accomplished at a higher temperature with the monomer still in the solid state. With decreasing monomer purity, as evidenced by the lower melting point, the percentage conversion to polymer increased in the solid state. This increase in conversion can be explained by the partial destruction of the crystalline monomer structure with a consequent increase in the ease of monomer diffusion. Both for pure and impure monomer, the final solid-state prepared polymer did not replicate the crystalline structure of the initial monomer. In the liquid state, the polymer conversion under similar radiation conditions was higher than that in the solid state. These initial results for both the solid and liquid states are in accord with the findings for acrylamide polymerization.<sup>2,3</sup>

## EXPERIMENTAL

### Preparation and Irradiation Polymerization

Diacetone acrylamide was prepared by a procedure<sup>1</sup> involving the reaction of acrylonitrile, sulfuric acid, and acetone. Recrystallization of the monomer from benzene-petroleum ether gave crystals about 1 mm. in length, m.p. 53–54°C. (literature m.p. 52.0–53.5°C.). Samples for irradiation were prepared by sealing 1.0 g. of this material in 10-mm. o.d. glass tubes at 25°C. and at 0.3 mm. pressure. In a few cases, the monomer was carefully melted and resolidified to permit determination of the effect of this procedure on the polymerization. This procedure has been shown to modify markedly the solid-state polymerization of trioxane.<sup>9</sup>

The sealed samples were then irradiated with the use of a 2.0 M.e.v. Van de Graaff electron accelerator with a sample pass rate of 18.4 in./min. under a 12-in. scanned beam. The dose per pass was controlled by varying the beam current. Temperature control during the irradiation was achieved by using a slotted plate for the samples. The slotted plate in turn was placed on a rectangular box through which water was continuously pumped from a controlled-temperature bath.

After the irradiation, the sample tubes were either (1) kept at  $-80^{\circ}\text{C}$ . until analyzed or (2) placed in a constant temperature bath for the stated time and then cooled to  $-80^{\circ}\text{C}$ . until analyzed. The sample was then transferred to a tared, glass vial, weighed, and added to water. The monomer dissolved over a period of 2 days, and the polymer remaining was filtered through a tared, sintered-glass crucible. Drying was accomplished by 4 days of heating at  $50^{\circ}\text{C}$ . and at 50 mm. pressure under a continuous air flush. No molecular weight determinations could be made on the final polymer since it did not dissolve but only swelled in dimethylformamide, a known viscosity solvent for the polymer.<sup>1</sup>

## RESULTS

Some preliminary runs on percentage polymerization as a function of dose, of temperature of irradiation, and of temperature after irradiation are presented in Table I.



TABLE I  
Preliminary Results on Polymerization of Diacetone Acrylamide

Radiation dose, Mrad	Dose per pass, Mrad	Irradiation temperature, °C.	Treatment After irradiation		Polymer, %
			Time, hr.	Temp., °C.	
0.5	0.5	25		None	0.0
					0.0
0.5	0.5	39		None	0.8
					1.2
0.5	0.5	39	6		6.4
				39	10.0
1.0	1.0	25		None	8.7
					10.8
1.0	1.0	25	6		19.5
				39	24.0
1.0	0.2	39		None	34.1
					36.3
1.0	1.0	39		None	95.9
					97.8
2.0	1.0	25		None	20.2
					25.8
			0.5		39
			1.0		39
					31.6
					31.6
			2.0		39
					44.5
2.0	0.2	39		None	99.9
					97.8
2.0	1.0	39			100.0
None			6		39
0.1	0.1	68		None	99.8
					93.7
0.2	0.1	68		None	99.9
					99.8
0.4	0.1	68		None	99.9
					100.0
0.7	0.1	68		None	99.9
					100.1
1.0	0.1	68		None	99.9
					100.0

Table I shows the following: (1) conversion increases with increasing dose; (2) conversion increases when the sample is held at an elevated temperature after irradiation; (3) conversion increases with increasing temperature of irradiation; and (4) conversion increases with increasing dose per pass close to the melting point of the monomer.

A series of samples was then irradiated at 15°C. and subsequently heated at 35 or 45°C. to determine if the conventional<sup>9</sup> linear relationship of logarithm of aging time versus percentage polymerization is found for the pure monomer, m.p. 53–54°C. These results are collected in Table II. For the 35°C. heating subsequent to irradiation, the values gave a linear plot of aging time versus percentage conversion (Fig. 1). For the 45°C. heating subsequent to irradiation, the values appeared to be best fitted into the standard plot of logarithm of aging time versus percentage conversion (Fig. 2). The difference between the relationship found for subsequent heating at 35 and 45°C. may be re-

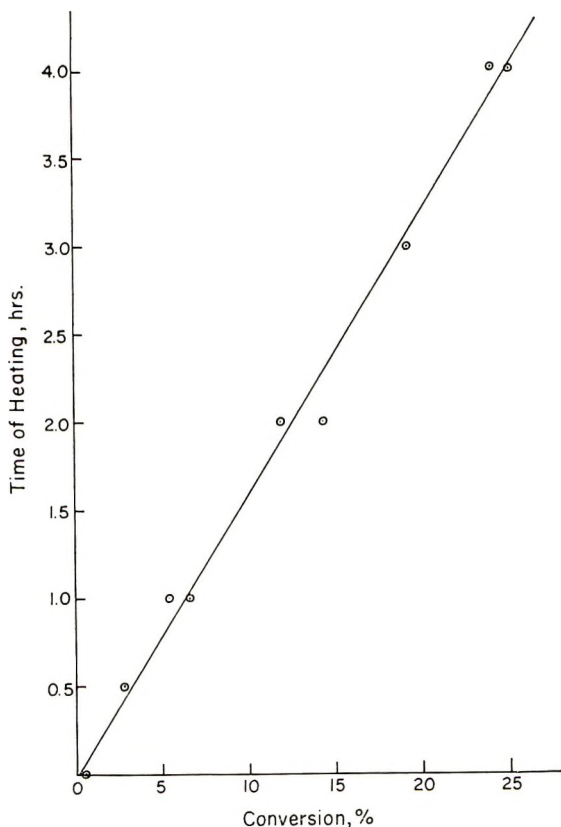


Fig. 1. Conversion as a function of aging time at 35°C. Monomer m.p. 52–53°C.

lated to the level of conversion. Thus, for the 35°C. runs, where unlimited monomer is still available to the propagating chain in the solid state, we would expect different kinetics than for the 45°C. runs, where only a small amount of monomer is left to react after irradiation and aging for 0.5 hr. at 45°C.

Another series of samples was then run with impure monomer. After standing for several months, the melting point of one preparation of monomer had decreased from 53–54°C. to 42–45°C. The nature of the impurity was not determined. However, the monomer did not contain polymer as proven by its complete water solubility.

TABLE II  
Conversion as a Function of Heating After Irradiation<sup>a</sup>

Time of subsequent heating, hr.	Conversion, % <sup>b</sup>	
	35°C.	45°C.
0.5	2.8	74.5, 75.2
1.0	6.6, 5.4	78.3, 77.9
2.0	11.9, 14.3	79.3, 79.9
3.0	19.3	81.0, 80.6
4.0	24.0, 25.1	81.3, 81.7

<sup>a</sup> Radiation dose: 1.0 Mrad at 15°C., melting point of monomer 53–54°C.

<sup>b</sup> Conversion without heating subsequent to irradiation, 0.5, 0.6, 0.6%.

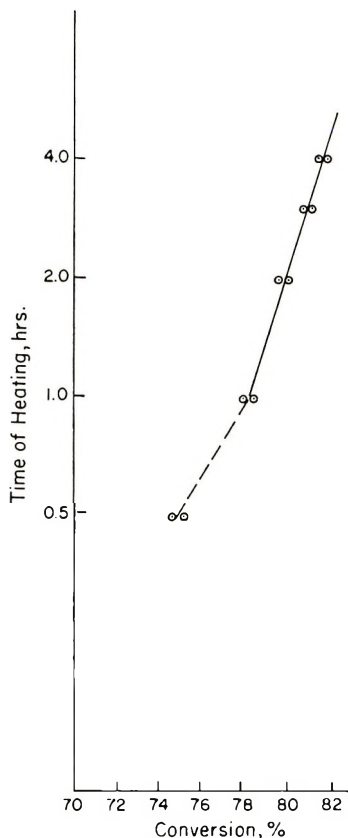


Fig. 2. Conversion as a function of aging time at 45°C. Monomer m.p. 52–53°C.

In accord with the previous series, a 15°C. irradiation temperature and a 35°C. subsequent aging temperature were employed. However, to permit a study of the polymerization kinetics after irradiation, the radiation dose was reduced to 0.5 Mrad. Without heating after irradiation, polymerization percentages of 12.7 and 13.4% were obtained on fine crystalline monomer and 14.3% on a thick monomer film prepared by melting and re-solidification. With heating afterwards, the percentage conversion was shown to be a linear function of the log of aging time (Fig. 3). This is the classical relationship for

TABLE III  
Conversion as a Function of Heating After Irradiation<sup>a</sup>

Heating time at 35°C., hr.	Conversion, %	
	Crystalline monomer	Resolidified monomer
0.5	28.4	24.8
1.0	25.3	29.0
2.0	31.6, 29.0	35.3
3.0	34.2, 39.1	40.4
4.0	38.9	42.6

<sup>a</sup>Radiation dose: 0.5 Mrad; radiation temperature, 15°C.; monomer m.p., 43–45°C.

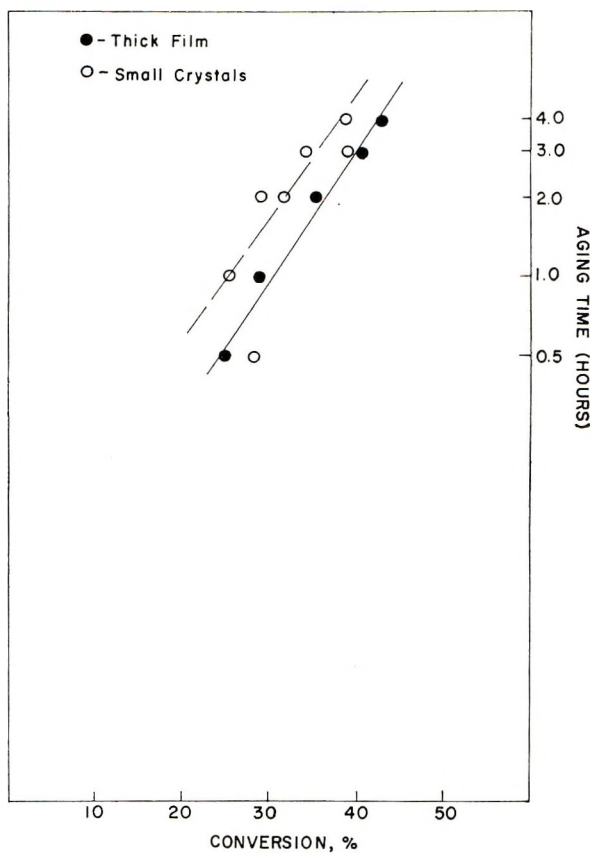


Fig. 3. Polymerization of diacetone acrylamide.

TABLE IV  
Conversion as a Function of Polymerization Variables

Monomer	Atmosphere (both irradiation and aging)	Time of subsequent heating at 39°C., hr.	Conversion to polymer, %
As is (fine crystals)	Vacuum	0	98.9
		0.5	98.4
		1.0	97.5
		1.0	97.4
		3.0	96.5
		3.0	99.0
		4.0	97.6
Melt, resolidified into 2-mm. thick film	Air	0.0	14.4
		2.0	13.7
	Vacuum	0.0	83.1
		0.5	81.6
		1.0	91.5
		2.0	56.3
		4.0	56.9

solid-state polymerization, as a function of heating after irradiation. The results are collected in Table III and show that under the same polymerization conditions the lower-melting monomer gives higher conversions than the pure monomer, m.p. 53–54°C.

A final series of monomer samples, m.p. 42–45°C., was irradiated at 1.0 Mrad at 18°C. Under these conditions, we found that the conversion was essentially quantitative either without or with heating afterwards at 39°C. However by modification of two of the variables, the polymer conversion was reduced: (1) when the monomer sample was melted and resolidified into a continuous film prior to irradiation and (2) when air was present during the irradiation and heating thereafter.

These results are collected in Table IV. The reduction in conversion in the presence of air is an expected phenomenon for a free radical-induced polymerization, this effect being less marked for a solid film than for fine crystals.

We thank Mr. S. Olfky for the irradiations and dosimetry.

### References

1. L. E. Coleman, J. F. Bork, D. P. Wyman, and D. I. Hoke, *J. Polymer Sci. A*, **3**, 1601 (1965).
2. R. B. Mesrobian, P. Ander, D. S. Ballantine, and G. J. Dienes, *J. Chem. Phys.*, **22**, 565 (1954).
3. B. Baysal, G. Adler, D. Ballantine, and A. Glines, *J. Polymer Sci. B*, **1**, 247 (1963).
4. S. Okamura, K. Hayashi, and Y. Nakamura, *Doitai To Hoshasen*, **3**, 416 (1960).
5. G. Carazzolo, S. Leghissa, and M. Mammi, *Makromol. Chem.*, **60**, 171 (1963).
6. L. B. Lando and V. Stannett, *J. Polymer Sci. B*, **2**, 375 (1964).
7. G. Carazzolo and M. Mammi, *J. Polymer Sci. B*, **2**, 1957 (1964).
8. S. Okamura, K. Hayashi, Y. Kitanishi, and M. Nishii, *Doitai To Hoshasen*, **3**, 510 (1960).
9. N. Marans and F. Wessells, *J. Appl. Polymer Sci.*, **9**, 3681 (1965).

N. S. MARANS  
R. J. EHRIG

W. R. Grace Research Division  
Clarksville, Maryland

Received December 28, 1965  
Revised March 22, 1966



### Anionic Polymerizations in Dimethyl Sulfoxide

Recently, Corey and Chaykovsky<sup>1</sup> described the preparation of methyl sulfinyl carbanion by reaction of dimethyl sulfoxide with sodium hydride. Since they reported this new anion to be sufficiently basic to convert triphenyl methane into the deep-red triphenyl methyl anion which is known<sup>2</sup> to initiate the polymerization of some vinyl monomers in liquid ammonia or in diethyl ether, it seemed attractive to explore the possibility of using methyl sulfinyl carbanion as an initiator for the polymerization of vinyl monomers in dimethyl sulfoxide (DMSO) as a reaction medium. Because of its high solubility parameter (13.0) and its high dielectric constant (48.9 at 20°C.), DMSO dissolves many monomers and polymers which are not readily soluble in the solvents conventionally used for anionic polymerizations.

Solutions (0.5*M*) of methyl sulfinyl carbanion were prepared according to Corey and Chaykovsky<sup>1</sup> by reaction of sodium hydride (Metal Hydrides, Inc.) with dimethyl sulfoxide (Crown-Zellerbach) which was purified by distillation from sodium hydride *in vacuo*. The initiator solution contained a small amount of triphenyl methane as an indicator. The polymerizations were carried out at room temperature under nitrogen by dropping 200 g. of monomer (undiluted or dissolved in DMSO) slowly into 300 g. of DMSO containing so much initiator solution that the red color of the indicator just persisted. If the red color disappeared, indicating termination by impurities present in the monomer, the polymerization was re-initiated by adding more initiator solution. After the reaction was complete, the formed polymer was isolated by precipitation with methanol or water and drying *in vacuo*. Polymers of low molecular weight ( $\bar{M}_w \leq 20,000$ ) were obtained from styrene, sodium styrene sulfonate, acrylonitrile, methyl methacrylate, and 4-vinylpyridine. No polymers were isolated from the attempted reactions with vinylchloride, vinylidene chloride, and *N*-vinyl-5-methyl-2-oxazolidinone. Excessive amounts of initiator used to re-initiate terminated polymerizations can be considered to be the major reason for the low molecular weights of the polymers formed under the above conditions. However, a decrease in molecular weight because of termination of polymerizing chains by chain transfer with the DMSO might also be expected.

#### References

1. E. J. Corey and M. Chaykovsky, *J. Am. Chem. Soc.*, **84**, 866 (1962).
2. N. S. Wooding and W. C. E. Higginson, *J. Chem. Soc.*, **1952**, 774.

G. E. MOLAU\*

J. E. MASON†

\* Plastics Department Research

† Polymer and Chemicals Research

The Dow Chemical Company

Midland, Michigan

Received February 1, 1966

Revised March 29, 1966

### *Aromatic Polyamides Containing the 4,4'-Oxydiphenylene Group*

Recently, the synthesis and properties of wholly aromatic polyamides were reported.<sup>1-8</sup> Aromatic polyamides are usually high melting, slightly soluble, and possess high thermal stability. The properties of these polymers are influenced by features of the chemical structure such as the hydrogen bond of the amide group, the symmetry of benzene ring, and the chain stiffening resulting from conjugation of the carbonyl groups with the ring. It appeared of interest, therefore, to introduce the 4,4'-oxydiphenylene group which enhances thermal stability of the polymer and flexibility of the molecule into the recurring unit of the aromatic polyamides. The present paper is concerned with aromatic polyamides as part of the investigation<sup>9,10</sup> of preparations and properties of condensation polymers containing the 4,4'-oxydiphenylene group.

#### Experimental

4,4'-Diaminodiphenyl ether was recrystallized from ethanol. Terephthaloyl and isophthaloyl chlorides were purified by distillation under a nitrogen atmosphere and recrystallization from *n*-hexane. Aromatic polyamides were prepared by interfacial polycondensation. 4,4'-Diaminodiphenyl ether was dissolved in a water-tetrahydrofuran (THF) mixture (1:1 by volume) at a given concentration containing 2 moles of sodium hydroxide per mole of diamine. The acid chlorides were dissolved in benzene, tetrachloroethane, and THF at various molar concentrations. The acid chloride solution was added to the diamine solution kept at the reaction temperature below 10°C. with vigorous

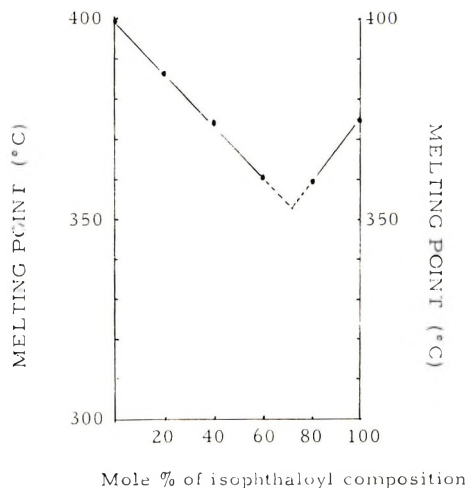


Fig. 1. Melting points of aromatic copolyamides.

stirring. Polymers were filtered and washed with hot water and methanol. Aromatic copolyamides of isophthaloyl and terephthaloyl chlorides with diamine were also obtained by the same method.

The reduced viscosity was measured at a concentration of 0.5 g./100 ml. of dimethylformamide containing lithium chloride (5 wt.-%) at 30°C. Melting point determinations were made by differential thermal analysis, and thermal stability was measured by thermogravimetric analysis.

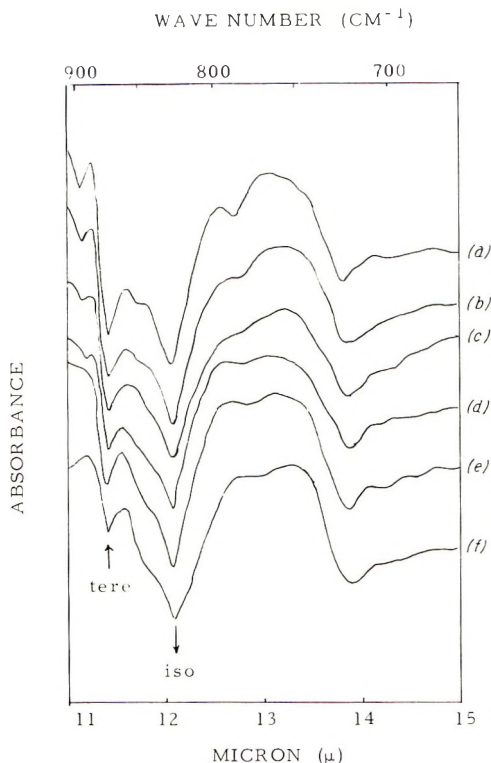


Fig. 2. Infrared spectra of aromatic polyamides from terephthaloyl (tere) and isophthaloyl (iso) chlorides: (a) 100% tere; (b) tere/iso = 80/20; (c) tere/iso = 60/40; (d) tere/iso = 40/60; (e) tere/iso = 20/80; (f) 100% iso.

### Results

Interfacial polycondensation was carried out in water-tetrahydrofuran mixture and a variety of water-immiscible organic solvents. In the case of isophthaloyl chloride, benzene, tetrachloroethane, and tetrahydrofuran were used as organic solvents, but these solvents (except THF) did not yield polyamides of a high molecular weight. The results for polyamides obtained from 4,4'-diaminodiphenyl-ether and terephthaloyl or isophthaloyl chloride with the use of THF as solvent for the acid chloride are listed in Table I.

As shown in Table I the viscosity of poly-4,4'-oxydiphenylene-isophthalamide was influenced by the monomer concentration. The molar ratio of diamine to acid chloride giving polyamide with a high molecular weight was about 1.2 and the concentration of acid chloride was 0.050 mole/l. In the case of poly-4,4'-oxydiphenyleneterephthalamide, viscosities at the same concentration were in range of 0.38–0.49 and did not increase specifically with a variety of the molar ratios between the two components.

On the basis of these data, aromatic copolyamides of 4,4'-diaminodiphenyl ether with terephthaloyl and isophthaloyl chloride in tetrahydrofuran solvent were prepared. The concentrations of acid chloride and diamine were 0.050 and 0.060 mole/l., respectively. The polymerization products and their characteristics are presented in Table II.

The copolyamides were insoluble in acetic acid, formic acid, *m*-cresol, and pyridine but were soluble in dimethylformamide, dimethylacetamide, and dimethyl sulfoxide containing 5% dissolved LiCl. The polyamide from terephthaloyl chloride melts with decomposition. A graphical presentation of the melting points versus the proportion of iso-

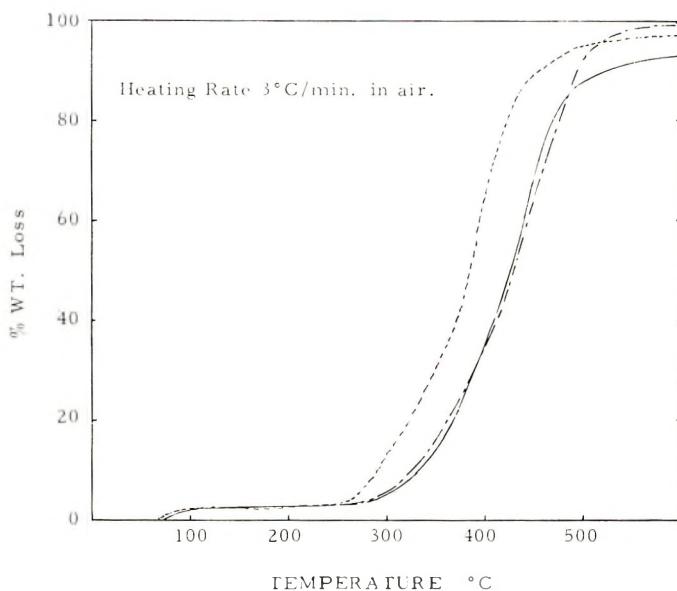


Fig. 3. Thermal stability of polyamides: (—) polymer from terephthaloyl chloride; (- -) copolymer (tere/iso = 60/40); (- · -) polymer from isophthaloyl chloride.

phthaloyl units is given in Figure 1. This shows the usual V-shaped curve of copolymer melting points plotted as a function of composition. The maximum depression of its curve is at about 73 mole-% of isophthaloyl units. These copolyamides were crystalline, and the degree of crystallinity increased with increase in the proportion of terephthaloyl units. The x-ray diffraction angles were in the range of 25.4–25.7° and 34.0–34.2°. However, the polyamide from isophthaloyl chloride alone was not crystalline.

The difference between the feed ratio of acid chlorides and that of the condensation products was determined from the infrared spectra. The spectra of copolyamides are

TABLE I  
Polyamide from 4,4'-Diaminodiphenyl Ether and Terephthaloyl or Isophthaloyl Chloride

Acid chloride	Acid chloride concn., mole/l.	Diamine concn., mole/l.	$\eta_{sp}/c$	Yield, %
Isophthaloyl chloride	0.020	0.020	0.22	78.8
		0.024	0.24	80.0
		0.028	0.20	81.8
Isophthaloyl chloride	0.050	0.020	0.04	39.5
		0.040	0.17	91.3
		0.050	0.29	99.2
		0.060	0.68	99.4
		0.070	0.51	98.4
Isophthaloyl chloride	0.100	0.080	0.08	55.1
		0.100	0.36	80.0
		0.110	0.39	86.0
		0.120	0.40	91.5
Terephthaloyl chloride	0.050	0.050	0.48	90.8
		0.060	0.49	90.6
		0.070	0.38	88.9

TABLE II  
Aromatic Copolyamides of 4,4'-Diaminodiphenyl Ether with  
Terephthalic and Isophthaloyl Chlorides

Acid chloride		Yield, %	$n_{sp}/c$	Melting point, °C.	Crystallinity
Terephthalic acid, mole-%	Isophthalic acid, mole-%				
100	0	90.6	0.49	376	High
80	20	66.6	0.38	359	High
60	40	67.8	0.44	362	Intermediate
40	60	79.9	0.46	376	Low
20	80	65.7	0.48	387	Low
0	100	99.4	0.68	398	—

distinguishable from the aromatic carbon-hydrogen out-of-plane deformations in the region of 700–900  $\text{cm}^{-1}$ . Characteristic bands due to *para* and *meta* aromatic dibasic acid appeared at 875 and 826  $\text{cm}^{-1}$ , respectively. As shown in Figure 2, these examinations revealed that the acid composition of the copolyamides changed quantitatively in proportion to that of feed acid chloride.

The thermal stability of the copolyamides is comparable to that of the homopolyamides from terephthaloyl or isophthaloyl chloride, as shown in Figure 3. Polyamides and copolyamides prepared in this work showed an initial weight loss of approximately 3% which was due to adsorbed water at temperatures above 70°C., and they began to decompose slowly at above 250°C. The 60:40 copolyamide lost 30% by weight at 350°C.; a poly-4,4'-oxydiphenyleneisophthalamide, 16%; and poly-4,4'-oxydiphenylene-terephthalamide, 13%. All of them degraded almost completely below 500°C. The thermal stability of copolyamide was lower in comparison with those of polyamide.

#### References

1. H. W. Hill, S. L. Kwolek, and P. W. Morgan, French Pat. 1,199,460 (June 6, 1959); U.S. Pat. 3,006,899 (February 28, 1957).
2. S. L. Kwolek, P. W. Morgan, and W. R. Sorenson, U.S. Pat. 3,063,966 (February 5, 1958).
3. V. M. Savinov and L. B. Sokolov, *J. Appl. Chem. USSR (Eng. Transl.)*, **34**, 2021 (1961).
4. L. B. Sokolov and T. V. Kudin, *Vysokomolekul. Soedin.*, **2**, 698 (1960).
5. H. F. Mark, S. M. Atlas, and N. Ogata, *J. Polymer Sci.*, **61**, 549 (1962).
6. R. A. Dine-Hart, B. J. C. Moore, and W. W. Wright, *J. Polymer Sci. B*, **2**, 369 (1964).
7. J. Preston and E. Dobinson, *J. Polymer Sci. B*, **2**, 1171 (1964).
8. P. W. Morgan, *Condensation Polymers by Interfacial and Solution Methods*, Interscience, New York, 1965, pp. 180, 190.
9. S. Nishizaki and Y. Kuruu, *Kogyo Kagaku Zasshi*, **68**, 249 (1965).
10. S. Nishizaki and A. Fukami, *Kogyo Kagaku Zasshi*, **68**, 1955 (1965).

S. NISHIZAKI  
A. FUKAMI

Central Research Laboratories  
Mitsubishi Electric Corporation  
Amagasaki-shi, Japan

Received February 24, 1966  
Revised April 4, 1966

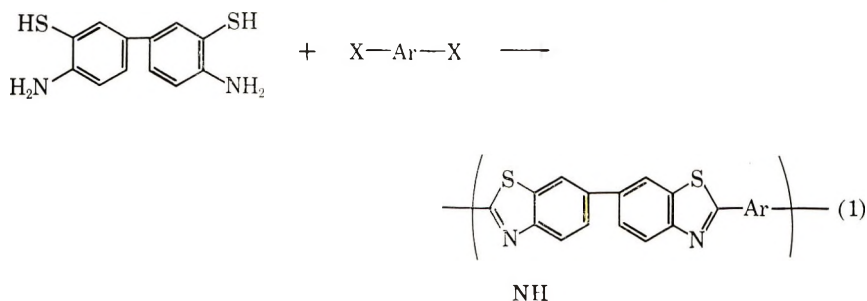


## Polybenzothiazoles. II. A New Synthetic Approach and Preliminary Stability Evaluation

### Introduction

In recent years, a variety of organic heterocyclic polymers such as the benzimidazoles,<sup>1</sup> benzoxazoles,<sup>2</sup> oxadiazoles,<sup>3</sup> imides,<sup>4</sup> and quinoxalines,<sup>5</sup> possessing excellent thermal stability have been prepared. Recently the polybenzothiazoles have been added to this list.

The first successful preparation of completely aromatic linear high molecular weight polybenzothiazoles (PBT) was first reported in 1964.<sup>6</sup> The synthetic approach involved the condensation of 3,3'-dimercaptobenzidine (DMB) with an aromatic dicarboxylic acid, or benzothiazole-forming derivative thereof, according to equation (1).



where Ar = arylene, X = CO<sub>2</sub>H, CO<sub>2</sub>R, CONH<sub>2</sub>, C(=NH)<sub>2</sub>, CN, etc.

In 1965, Imai and coworkers<sup>7</sup> also reported the preparation of PBT by the same method in polyphosphoric acid. Our work describes a new approach to the preparation of PBT.

### Experimental Results and Discussion

High molecular weight polybenzoxazoles were prepared in 1964 by Kubota and Nakanishi<sup>2</sup> through the reaction of 3,3'-dihydroxybenzidine with an aromatic diacid halide to initially form a high molecular weight polyamide precursor polymer, which subsequently underwent thermal cyclodehydration to yield an aromatic polybenzoxazole. About the same time, we were investigating the preparation of benzothiazole polymers by the same route. The reaction of DMB with isophthaloyl chloride was investigated and found to yield a high molecular weight precursor polymer which underwent cyclodehydration to yield the aromatic PBT according to equation (2). As indicated in the equation, it was anticipated that two different precursor polymers, a polyamide or a polythioester, could be obtained under certain experimental conditions. The first approach to be discussed will be that concerning the preparation of the polyamide precursor.

The general experimental conditions involved the addition of a solution of freshly distilled isophthaloyl chloride to a cold (-5° to 0°C.) solution of DMB under argon. A number of solvents and solvent mixtures, which had been thoroughly dried, were investigated such as *N,N*-dimethylformamide (DMF), pyridine, and *N,N*-dimethylacetamide (DMAC). Various acid acceptors, both organic and inorganic bases such as trialkylamines, pyridine, sodium bicarbonate, and sodium acetate were used. After the addition of the diacid halide solution, the reaction mixture was stirred at ambient temperature; in most cases the viscosity of the reaction mixture increased tremendously, stopping the stirrer in many experiments. The precursor polymer was isolated by quenching with water or methanol to precipitate a yellow solid which was generally soluble in *m*-cresol, DMF, DMAC, and formic and sulfuric acid. Tough flexible trans-

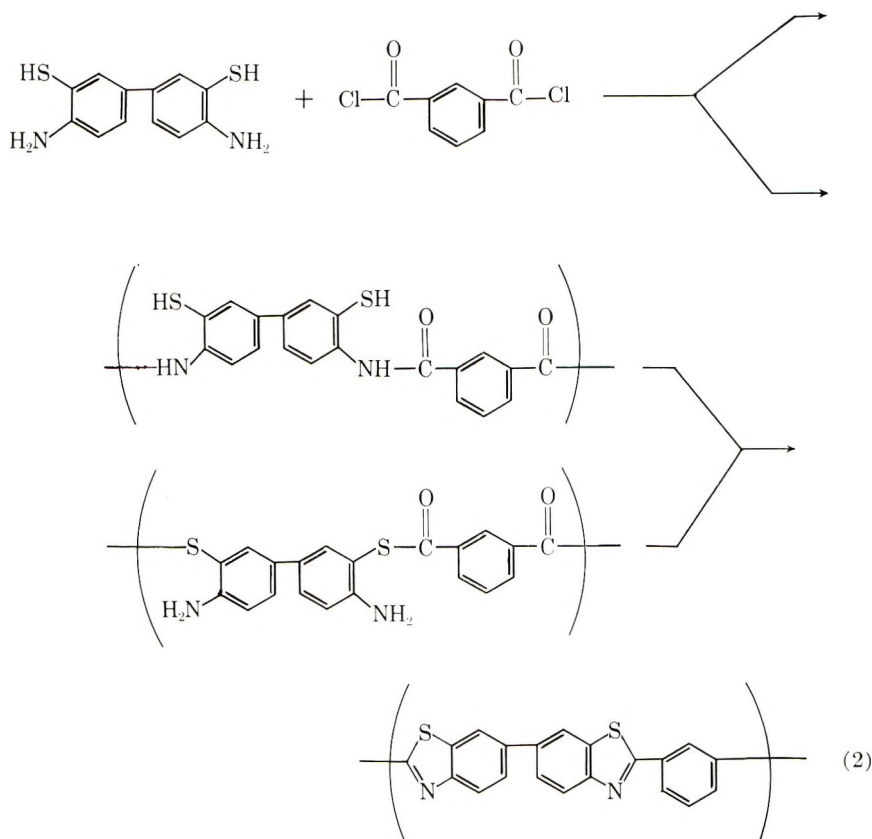


TABLE I  
Characterization Summary

Polymer	$\eta_{inh}^a$	Elemental analysis <sup>b</sup>				Infrared spectrum Figure no.
		% C	% H	% N	% S	
Polyamide precursor	0.50	63.61	3.87	7.70	17.06	1a
PBT from polyamide	0.60	69.57	2.93	7.85	18.61	1b
PBT after 250 hr. at 700°F. in air	—	62.49	2.71	7.06	14.06	—
Polythioester precursor	0.21	61.09	4.44	8.42	16.53	1c
PBT from polythioester	—	69.89	2.86	8.21	18.43	same as 1b

<sup>a</sup>  $\eta_{inh}$  = inherent viscosity (0.5%  $H_2SO_4$  solution at 25°C.)

	% C	% H	% N	% S
<sup>b</sup> for precursor, calculated for $(C_{20}H_{14}N_2O_2S_2)_n$ :	63.47	3.73	7.40	16.94
for final PBT, calculated for $(C_{20}H_{10}N_2S_2)_n$ :	70.14	2.94	8.19	18.73

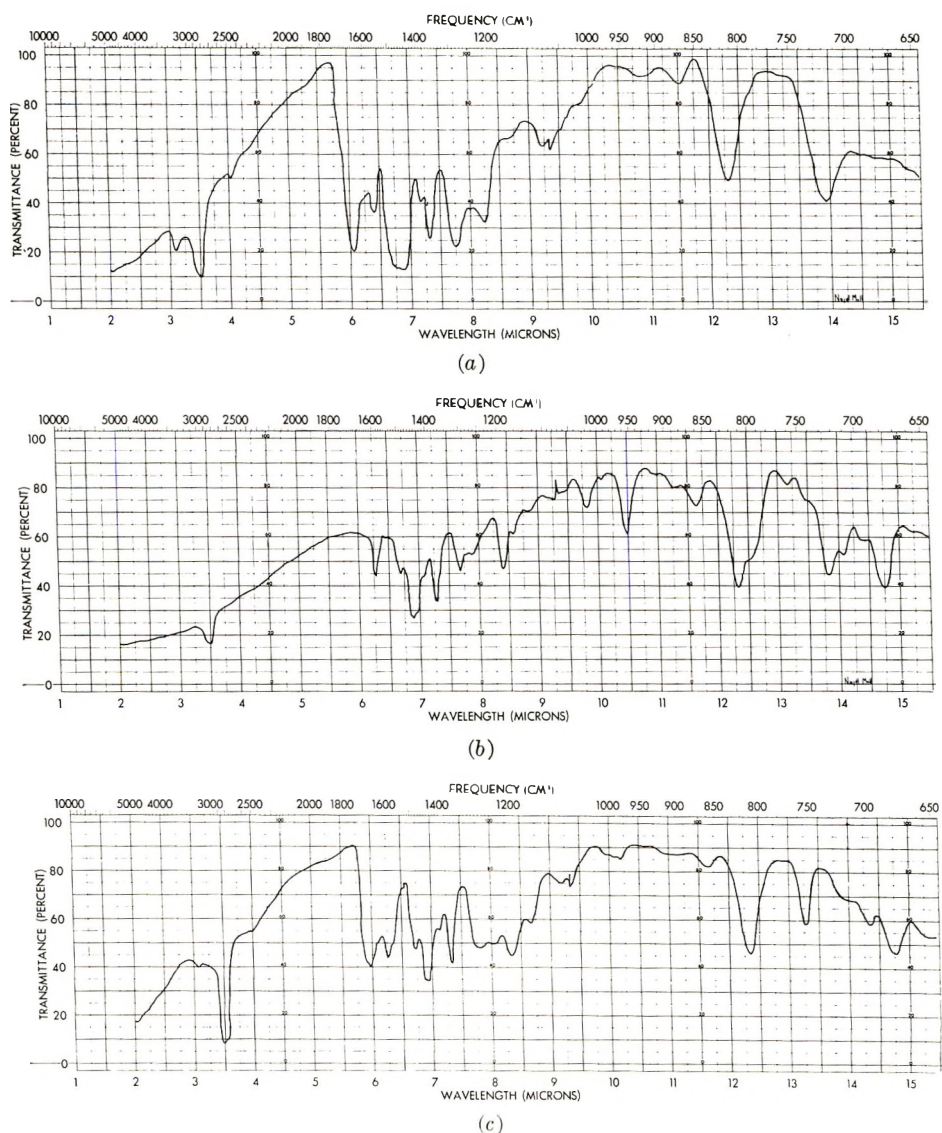


Fig. 1. Infrared spectra: (a) polyamide from the reaction of 3,3'-dimercaptobenzidine and isophthaloyl chloride; (b) poly-2,2'-(*m*-phenylene)-6,6'-bibenzothiazole; (c) precursor polymer from the reaction of the disodium salt of DMB with isophthaloyl chloride.

lucent films were cast from *m*-cresol and formic acid solutions. Acidification of a dilute aqueous sodium hydroxide solution of the precursor polymer gave a yellow solid having physical properties essentially identical to the original material. The inherent viscosity of 0.5% sulfuric acid solution at 25°C. was as high as 0.50. The elemental analysis of the precursor polymers agreed well with the theoretical. A representative example is shown in Table I.

The infrared spectrum of a nujol mull of the polyamide precursor shown in Figure 1a, was consistent with the proposed structure of the polyamide.

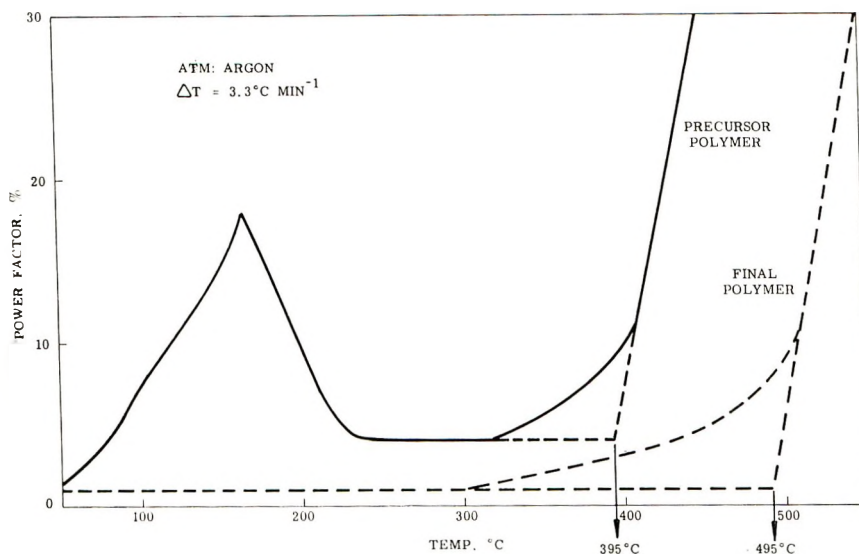


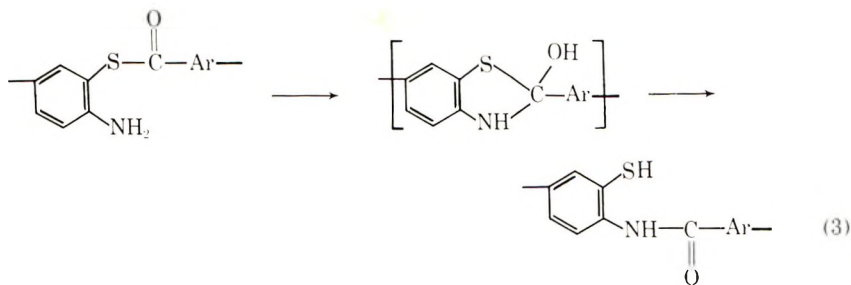
Fig. 2. Dielectric properties as a function of temperature.

Experiments were conducted to determine the temperature for cyclization to the final polymer, with evolution of water. This temperature was found to be 160°C., which agreed well with that determined by observing changes in the dielectric properties of the precursor polymer when the percent change in power factor was plotted versus temperature, as shown in Figure 2. Transitions observed at 165°C. suggest the cyclization step while the transition at 395°C. represents the glass transition temperature ( $T_g$ ) of the polymer. However, when the precursor polyamide was heated at 400°C. for 1 hr. under argon, the  $T_g$  of the resulting yellowish brown polymer was 495°C.

The elemental analysis of the polymer is given in Table I. The inherent viscosities (0.5%  $H_2SO_4$  solution at 25°C.) were as high as 0.60. The infrared spectrum of the final polymer, as a nujol mull, was consistent with that expected for the desired polymer and is shown in Figure 1b.

The ultraviolet spectrum of the precursor polymer and of the final polymer are illustrated in Figure 3. As shown by the ultraviolet spectra, a bathochromic shift of 9 m $\mu$  occurred when the precursor polymer was converted to final polymer while the specific extinction coefficient remained essentially the same.

The second approach to obtaining a precursor polymer, a thioester type, involved adding a solution of isophthaloyl chloride to DMB in an aqueous solution of sodium hydroxide or sodium sulfide under argon, in an attempt to obtain preferential reaction through the very nucleophilic thio anion to yield a polythioester. Only a moderate



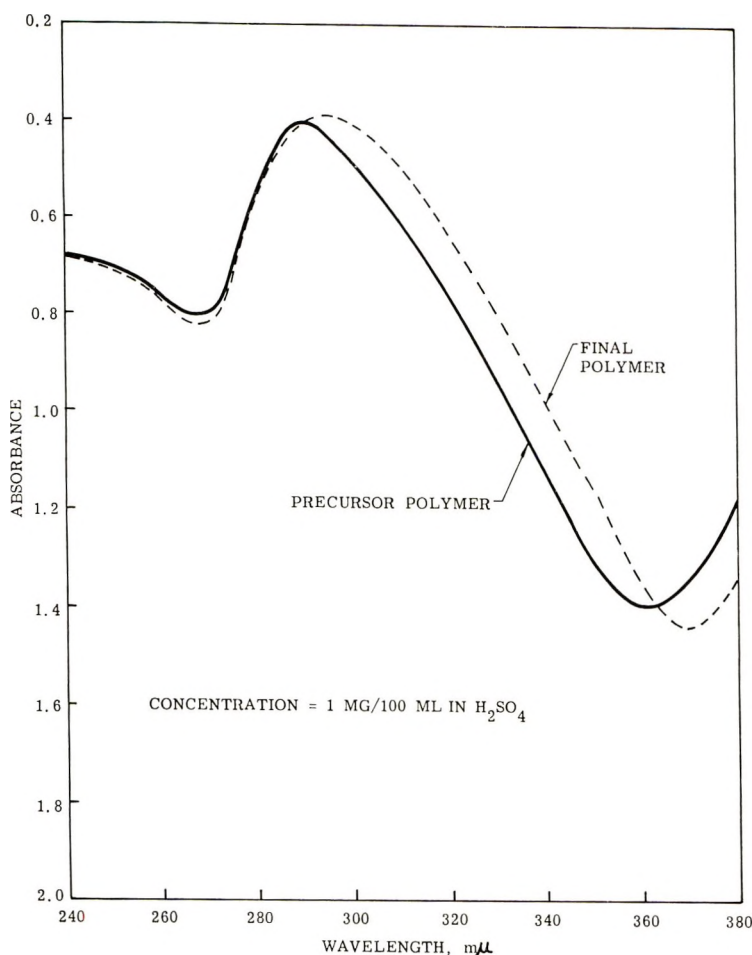


Fig. 3. Ultraviolet spectrum.

amount of success was attained as indicated by solubility tests and the infrared spectrum of the precursor polymer as shown in Figure 1c. Two distinct carbonyl absorptions are present which suggested the presence of both thioester and secondary amide groups. Apparently under alkaline conditions, partial rearrangement of the thioester to amide occurred. A number of researchers<sup>8</sup> have substantiated acyl migration of this type and suggested that rearrangement occurred through a cyclic intermediate thiazoline as indicated in equation (3). The elemental analysis of the precursor polymer is given in Table I. The yellow polymer was soluble in *m*-cresol, DMF, DMAC, and sulfuric acid. Inherent viscosities (0.5% H<sub>2</sub>SO<sub>4</sub> at 25°C.) were only as high as 0.21. A solution of the precursor in aqueous potassium hydroxide, after stirring for 1 hr. in argon, gave a yellow solid (after precipitation with acetic acid) whose infrared spectrum indicated essentially complete rearrangement to the polyamide. Regardless of the presence of thioester and amide links, cyclization should yield a PBT, as experiments showed. The final polymers from the polythioester approach failed to dissolve completely in sulfuric acid but exhibited physical properties (TGA, *T<sub>g</sub>*) comparable to the final polymer made via the polyamide. The elemental analysis of a representative final polymer made via the polythioester approach is shown in Table I.



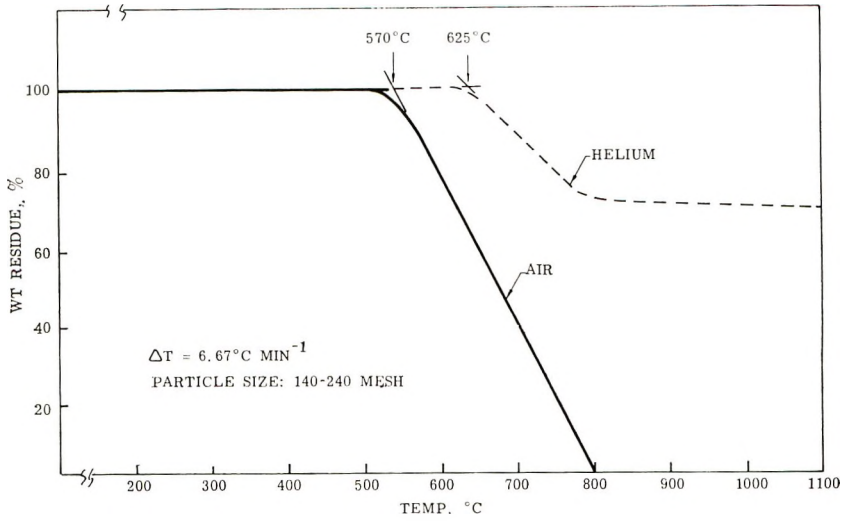


Fig. 4. Thermogram of poly-2,2'-(*m*-phenylene)-6,6'-bibenzothiazole.

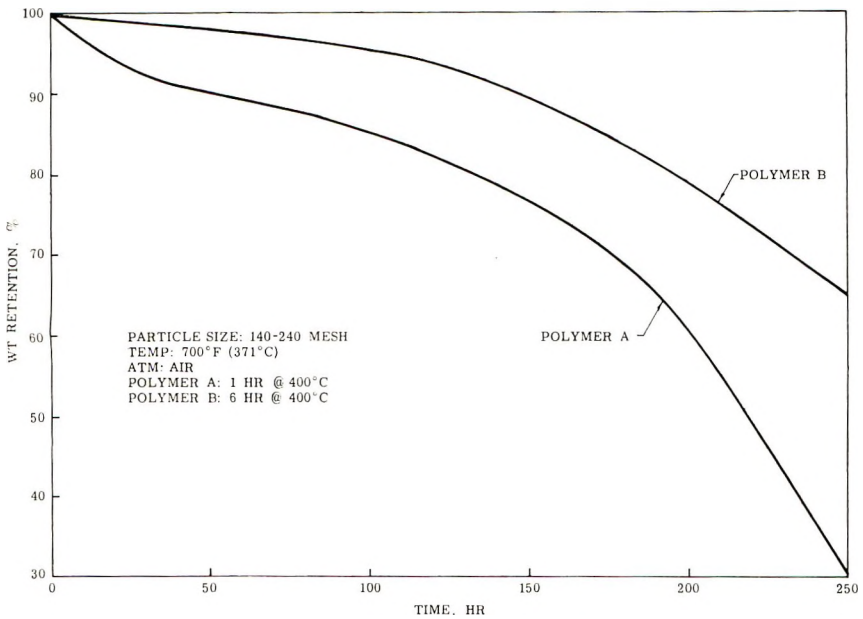


Fig. 5. Isothermal weight loss curve of poly-2,2'-(*m*-phenylene)-6,6'-bibenzothiazole.

### Stability

Poly-2,2'-(*m*-phenylene)-6,6'-bibenzothiazole from the polyamide precursor of 140-240 mesh size was refluxed for 3 hr. in 40% aqueous potassium hydroxide. The polymer was recovered in quantitative yield and exhibited no change in its inherent viscosity, elemental analysis, or infrared spectrum.

The thermogram of the final polymer (Polymer A) is represented in Figure 4 and gave the following thermogravimetric analysis\* data.

Atm. <sup>a</sup>	PDT, °C. <sup>a</sup>	MRWL <sup>a</sup>	<i>T</i> of MRWL, °C. <sup>a</sup>
Air	570	3.32	650-700
Helium	625	1.13	700-750

<sup>a</sup> Atm. = atmosphere; PDT = polymer decomposition temperature,  $\pm 10^\circ\text{C}$ .; MRWL = maximum rate of weight loss,  $\% \text{ min.}^{-1}$ ; *T* of MRWL = temperature of MRWL, °C.

Two polymer samples of 140-240 mesh size were subjected to an isothermal weight loss study at 371°C. in air as illustrated in Figure 5. Polymer A was cured for 1 hr. at 400°C. in argon while polymer B, a portion of polymer A, was cured for an additional 5 hr. at 400°C. in argon. As indicated in the curve, the additional cure had a pronounced effect upon the polymer's isothermal aging. The elemental analysis of polymer A after 250 hr. at 700°F. in air is given in Table I.

\* TGA performed using a Stanton Thermobalance.

#### References

1. H. Vogel and C. S. Marvel, *J. Polymer Sci.*, **50**, 511 (1961).
2. T. Kubota and R. Nakanishi, *J. Polymer Sci. B*, **2**, 655 (1964).
3. A. H. Frazer, W. Sweeny, and F. T. Wallenberger, *J. Polymer Sci. A*, **2**, 1157 (1964).
4. G. M. Bower and L. W. Frost, *J. Polymer Sci. A*, **1**, 3135 (1963).
5. J. K. Stille, J. R. Williamson, and F. E. Arnold, *J. Polymer Sci. A*, **3**, 1013 (1965).
6. P. M. Hergenrother, W. Wrasidlo, and H. H. Levine, *ACS Polymer Preprints*, **5**, [1], 153 (1964); P. M. Hergenrother, W. Wrasidlo, and H. H. Levine, *J. Polymer Sci. A*, **3**, 1665 (1965).
7. Y. Imai, I. Taoka, K. Uno, and Y. Jwakura, *Makromol. Chem.*, **83**, 167 (1965).
8. R. B. Martin, S. Lowey, E. L. Elson, and J. T. Edsall, *J. Am. Chem. Soc.*, **81**, 5089 (1959); R. B. Martin and A. Purcell, *J. Am. Chem. Soc.*, **83**, 4830 (1961).

PAUL M. HERGENROTHER  
HAROLD H. LEVINE

Narmco Research & Development Division  
Whittaker Corporation  
San Diego, California

Received March 17, 1966

## ERRATA

### **Relationship Between the Ionic Nature of Some Organoaluminum-Transition Metal Catalysts and the Rate of Polymerization**

(article in *J. Polymer Sci. A-1*, **4**, 215-232, 1966)

By R. D. BUSHICK and R. S. STEARNS

*Research and Development, Sun Oil Company, Marcus Hook, Pennsylvania*

The formula given on pages 215, 219, and 221 should read  $\text{Al}(n\text{-C}_{10}\text{H}_{21})_3$  rather than  $\text{Al}(n\text{-C}_{10}\text{H}_{19})_3$ .

The caption for Figure 6 on page 223 should read: (B) heptane (70%), benzene (30%); (C) heptane (30%), benzene (70%).

### **Polybenzoylenebenzimidazoles**

(article in *J. Polymer Sci. A-1*, **4**, 59-70, 1966)

By J. G. COLSON, R. H. MICHEL, and R. M. PAUFLER

*Film Department, E. I. du Pont de Nemours & Company, Inc.,  
Buffalo, New York*

The first sentence of the last paragraph, page 60, should read, "The amino acid amide IV was heated at 140-160°C. for 1/2 hr., either as a solid or a DMAc solution to give *N*-(*o*-aminophenyl)phthalimide (V)."

INFORMATION FOR CONTRIBUTORS

1. Manuscripts should be submitted to H. Mark, Polytechnic Institute of Brooklyn, 333 Jay Street, Brooklyn, New York 11201. In Europe, manuscripts may be submitted to Professor G. Smets, University of Louvain, Louvain, Belgium; and in the United Kingdom to Sir Harry W. Melville, Department of Scientific and Industrial Research, 5-11 Regent Street, London, S.W.1, England. Address all other correspondence to Periodicals Division, Interscience Publishers, John Wiley & Sons, Inc., 605 Third Avenue, New York, New York 10016.
2. It is the preference of the Editors that papers be published in the English language. However, if the author desires that his paper be published in French or German, it is necessary that a particularly complete and comprehensive synopsis be furnished.
3. Manuscripts should be submitted in triplicate (one *original*, two carbon copies), typed *double space* throughout and on one side of each sheet only, on a *heavy* grade of paper with margins of at least one inch on all sides.
4. A short synopsis (maximum length 200 words) is required for papers in Parts A. No synopsis is published for Part B or for "Notes" in Parts A. This synopsis should be carefully prepared, for it will appear in English, in French, and in German, and is automatically the source of most abstracts. The Synopsis should be a summary of the entire paper; not the conclusions alone.
5. The paper should be reasonably subdivided into sections and, if necessary, subsections. Please refer to any issue of this *Journal* for examples.
6. The references should be numbered consecutively in the order of their appearance and should be complete, including authors' initials and—for unpublished lectures or symposia—the title of the paper, the date, and the name of the sponsoring society. Please compile references on a separate sheet at the end of the manuscript. Abbreviations of journal titles should conform to the practices of *Chemical Abstracts*.
7. Please supply numbers and titles for all tables. All table columns should have an explanatory heading.
8. It is particularly important that all figures be submitted in a form suitable for reproduction. Good glossy photographs are required for halftone reproductions. For line drawings (graphs, etc.), the figures must be drawn clearly with India ink on heavy white paper, Bristol board, drawing linen, or coordinate paper with a very light blue background. The India ink lettering of graphs must be large, clear, and "open" so that letters and numbers do not fill in when reduced for publication. It is the usual practice to submit drawings that are twice the size of the final engravings; the maximum final size of figures for this *Journal* is  $4\frac{1}{2} \times 7\frac{1}{2}$  inches.  
It is the author's responsibility to obtain written permission to reproduce material which has appeared in another publication.  
If in doubt about the preparation of illustrations suitable for reproduction, please consult the publisher at the address given above in paragraph 1 and ask for a sample drawing.
9. Please supply legends for all figures and compile these on a separate sheet.
10. Authors are cautioned to type—wherever possible—all mathematical and chemical symbols, equations, and formulas. If these must be handwritten, please print clearly and leave ample space above and below for printer's marks; please use only ink. All Greek or unusual symbols should be identified in the margin the first time they are used. Please distinguish in the margins of the manuscript between capital and small letters of the alphabet wherever confusion may arise (e.g., k, K, κ). Please underline with a wavy line all vector quantities. Use fractional exponents to avoid root signs.  
The nomenclature sponsored by the International Union of Chemistry is requested for chemical compounds. Chemical bonds should be correctly placed, and double bonds clearly indicated. Valence is to be indicated by superscript plus and minus signs.

JOURNAL OF POLYMER SCIENCE

11. Authors will receive 50 reprints of their articles without charge. Additional reprints can be ordered and purchased by filling out the form attached to the galley proof. Page proofs will not be supplied.
12. No manuscript will be returned following publication unless a request for return is made when the manuscript is originally submitted.

**Manuscripts and illustrations not conforming to the style of the *Journal* will be returned to the author for reworking, thus delaying their appearance.**